Netherlands Enterprise Agency

# Geotechnical Report

## Geological Ground Model Borssele Wind Farm Site III

>> *Sustainable. Agricultural. Innovative. International.*

DNV·GL

Netherlands Enterprise Agency (RVO.nl)
Croeselaan 15 | 3521 BJ | Utrecht
P.O. Box 8242 | 3503 RE| Utrecht
Netherlands

Det Norske Veritas, Danmark A/S
Energy
Technical
Tuborg Parkvej 8, 2nd Floor
DK2900 Hellerup
Denmark
Tel: +45 39 45 48 00
Fax: +45 39 45 48 01

| **Date**: | **Our reference**: | **Your reference**: |
|---|---|---|
| 2015-01-26 | DNV GL Doc. No:<br>1KI2TUA-15<br>Sign: MICWAG<br>Corresp. No.: | |

**Zone Borssele Site Data – Geological Ground Model**

The following reports produced by Fugro Engineers B.V. have been reviewed by DNV GL:

1. Geological Ground Model / Wind Farm Site III / Borssele Wind Farm Zone / Dutch Sector, North Sea / Report No. N6083/05 Issue 3 / 2015-12-22
2. Geological Ground Model / Wind Farm Site IV / Borssele Wind Farm Zone / Dutch Sector, North Sea / Report No. N6083/06 Issue 3 / 2015-12-22

Comments to the documents listed above have been given in the referenced Verification Comment Sheet (Reference /A/).

DNV GL has found that the above referenced reports provide proper geological models of the corresponding wind farm sites which can be relied upon to establish general geologic conditions, including discussions on site variability, in order to establish future geotechnical investigation campaigns. The data in this report can be used for establishing a Design Basis for Offshore Wind Turbine Structures in accordance with DNV-OS-J101.

Please note that detailed geotechnical investigations will need to be performed in order to address potential data gaps in the preliminary investigations, in particular the lack of a specific wind farm layout.

References:

/A/: Verification Comment Sheet “VCS-644235-12”
Revision 01, dated 08.01.2016
Doc-ID: 644235-VCS-12-rev01-Geological Ground Model WFS III and IV

Sincerely
for Det Norske Veritas, Danmark A/S


Erik Asp Hansen
Principal Engineer

Mobile: +45 20 27 38 71
Direct: +45 39 45 48 71
Erik.Asp@dnvgl.com

Michael Wagner
Senior Engineer

Direct: +49 40 36149 7914
Michael.Wagner@dnvgl.com

**Geological Ground Model**
**Wind Farm Site III**
**Borssele Wind Farm Zone**
**Dutch Sector, North Sea**

Client Reference No. WOZ1500010

Fugro Report No. N6083/05

Issue 3

Rijksdienst voor Ondernemend Nederland (RVO)

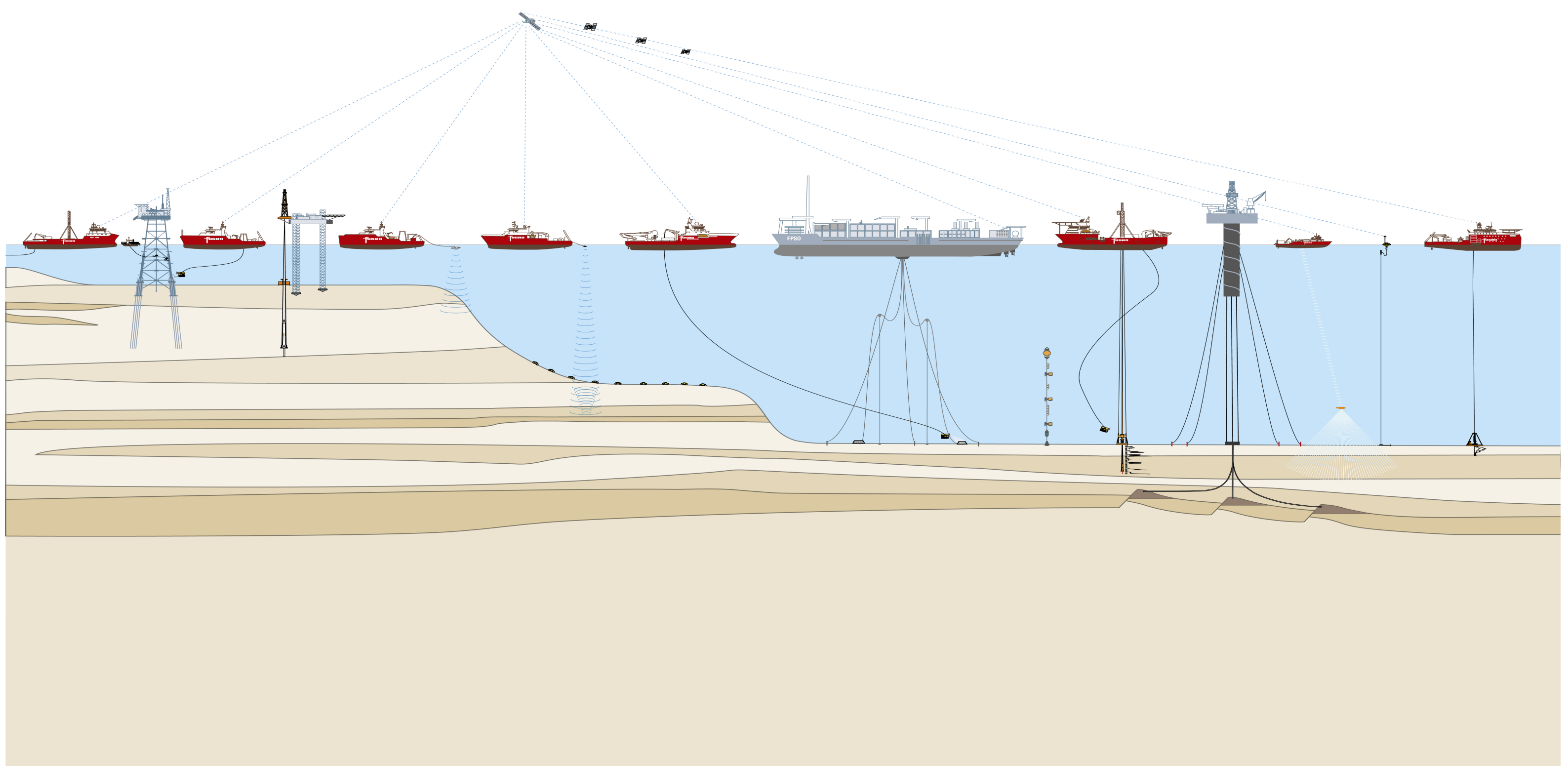

# Geological Ground Model
# Wind Farm Site III
# Borssele Wind Farm Zone
# Dutch Sector, North Sea

| | |
|---|---|
| Client | Rijksdienst voor Ondernemend Nederland (RVO) |
| Client Address | Croeselaan 15<br>3521 BJ Utrecht<br>The Netherlands |
| Client Reference No. | WOZ1500010 |
| Fugro Report No. | **N6083/05 (3)** |

| Report Issue No. | Date | Report Status | Approved |
|---|---|---|---|
| 3 | 22-Dec-2015 | Revised Final | |
| 2 | 11-Dec-2015 | Final | LJP |
| 1 | 19-Nov-2015 | Fugro approved draft | LJP |

Prismastraat 4, P.O. Box 130, 2630 AC Nootdorp, The Netherlands
Phone: +31 (0)70 311 1444, Fax: +31 (0)70 320 3640 Trade Register: 27114149 / VAT: 005621409B07

Prismastraat 4
P.O. Box 130
2630 AC Nootdorp
The Netherlands
Phone: 31-70-3111444
E-Mail: febvinfo@fugro.nl

Rijksdienst voor Ondernemend Nederland (RVO)
Croeselaan 15
3521 BJ Utrecht
The Netherlands

**Attention: Mr R. de Bruijne**

Our ref: N6083/05 (3)/BBK/EMG

Nootdorp, 22 December 2015

**Geological Ground Model - Wind Farm Site III**
**Borssele Wind Farm Zone - Dutch Sector, North Sea**

This report presents a geological ground model. The report was prepared in accordance with Contract WOZ1500010 between Rijksdienst voor Ondernemend Nederland (RVO) and Fugro Engineers B.V., dated 20 August 2015.

The principal team members for report preparation were Dr B. Klosowska, Dr B. Meijninger and Mr W. van Kesteren (Geologists). We acknowledge the valuable assistance of Mr R. de Bruijne, who acted as Client contact for this project.

Thank you for the opportunity to be of service. Please do not hesitate to contact us if you require any additional information.

Yours faithfully
**FUGRO ENGINEERS B.V.**

for
**E. Schoute**
Senior Project Engineer

CONTENTS

**LIST OF PLATES FOLLOWING MAIN TEXT:** Plate

## REPORT ISSUE CONTROL

| Section | Page No. | Plate No. | Issue No. | Revision |
|---|---|---|---|---|
| Summary / Samenvatting | All | - | 3 | Reference to plate numbers have been updated |
| Summary / Samenvatting | - | All | 3 | Summary plates renumbered |
| Main Text | All | - | 3 | Editorial corrections in text and Table 3.2 |
| Main Text | All | - | 2 | Editorial corrections and additions |
| Plates following Main Text | - | 2-1 | 2 | Transformation parameters updated |
| | - | 3-7 to 3-32 | 2 | Plates updated |
| | - | 5-1 | 2 | Plate updated |
| Section A | All | All | 2 | Plates updated |
| Section B | All | All | 2 | Plates updated |
| Appendix 1 | - | - | 2 | Two documents added |
| | | | | |
| | | | | |
| | | | | |
| | | | | |
| | | | | |
| | | | | |
| | | | | |
| | | | | |

**Notes:**

1) The definitive copy of this report is held in Fugro's information system
2) Report distribution is restricted to project participants approved by the Client
3) The *report* issue number is the same as the highest issue number of any individual page
4) Pages of this report are at Issue 1, except those pages listed above
5) The number at the bottom left-hand corner of each page shows the Fugro report number and page issue number. The number in brackets indicates the issue number of the page

**QUALITY MANAGEMENT RECORD**

Project Lead: B. Klosowska - Project Geologist
Report Review: W. van Kesteren – Senior Geologist
Report Approval: L.J. Peuchen – Principal Geotechnical Engineer

| Report Section | Prepared By | Checked By |
|---|---|---|
| Main Text | BBK/BLM | BBK/WVK |
| Plates following Main Text | LHT/BLM | BBK/WVK |
| Section A | BBD | JLI/MKL |
| Section B | BBD | JLI/MKL |
| | | |
| | | |
| | | |
| | | |
| | | |
| | | |
| | | |
| | | |
| | | |
| | | |

**Person(s):**
BBK: B. Klosowska
BLM: B. Meijninger
JLI: J. Marçal Liça
BBD: B. Brand
LHT: L. van der Horst
LJP: J. Peuchen
MKL: M. Klein
WVK: W. van Kesteren

## SUMMARY


The Dutch Government has developed a systematic framework under which offshore wind farm zones are designated. Within the designated wind farm zones the government decides the specific sites where wind farms can be constructed. Site development will be tendered. Winners of these site development tenders will be granted a permit to build a wind farm, a SDE+ grant, and will be offered a grid connection to the main land. The Ministry of Economic Affairs provides site data, which can be used for the preparation of bids for these tenders. This system is expected to contribute to cost savings.

As part of the tender preparations, the Netherlands Enterprise Agency (RVO), henceforth referred to as ‘Client’, has requested Fugro to perform a geotechnical investigation of Wind Farm Site WFS III & IV of the Borssele Wind Farm Zone (WFZ). The Borssele Wind Farm Zone is located in the Dutch Sector of the North Sea, approximately 36 km from the coastline (refer to Page vii of xi, “Vicinity Map”).

The objective of the geotechnical investigation and associated laboratory testing programme for WFS III and WFS IV is to:

- Improve the geological and geotechnical understanding;
- Update an earlier geological and geophysical model;
- Provide a detailed geological ground model;
- Determine the vertical and lateral variation in seabed conditions;
- Provide relevant geotechnical data to progress the design of windfarm foundation elements, including, but not limited to foundations and cables.

The offshore phase of the geotechnical investigation included geotechnical borehole drilling with downhole sampling and in situ testing, seafloor in situ testing and geotechnical laboratory testing. An office programme of geotechnical laboratory testing and reporting of results followed the offshore phase.

This report is one of a set of Fugro reports (refer to Page viii of xi, “List of Fugro Reports”). This particular report presents a concise and coherent geological ground model for WFS III (Page vii of xi), which takes account of geotechnical and geophysical data specifically acquired for WFS III and WFS IV. The geological ground model provides an integrated framework that links (1) geophysical data interpretation, (2) geotechnical parameters and (3) site suitability, particularly geological features and processes which can be potential hazards (geohazards) for windfarm development, including but not limited to support structures (foundations) and cables.

Plates following this summary text provide key information, as follows:

- Page ix of xi shows bathymetry. It highlights major sand banks and associated seabed erosion and sediment deposition processes;
- Page x of xi presents an example cross section of geophysical data with interpreted geotechnical unit boundaries and cone penetration test (CPT) data at the geotechnical locations superimposed;
- Page xi of xi presents the subcrop of the Tertiary geotechnical units below the Quaternary geotechnical units (i.e. Units A and B). This map illustrates the truncation of the dipping Tertiary geotechnical units against the base of the Quaternary sediments and, as a consequence, the absence of younger geotechnical units in the stratigraphic profiles towards the southwest. In this respect, the subcrop map can be regarded as a zonation map (i.e. indicating zones with similar stratigraphy). Note that geotechnical Units A and B are

present over the entire WFS III. Unit E1 is the youngest Tertiary unit at WFS III. Unit F1 (i.e. Sub-unit F1c) is the oldest geotechnical unit that subcrops below the Quaternary units, within the depth coverage of the geological ground model. The depth to the top of these geotechnical units increases to northeast.

The depth coverage of the geological ground model and geotechnical parameter values is to approximately 115 m relative to Lowest Astronomical Tide (LAT). This depth coverage corresponds broadly with the maximum geotechnical investigation depth for WFS III and WFS IV. The source data from geophysical survey extend below 115 m relative to LAT.

The available geotechnical and geophysical data align well. They provide a robust basis for the geological ground model. The geological ground model fits published regional frameworks. The geotechnical data set further enhances and refines the understanding of the identified soil units.

The geotechnical parameters include CPT data, water content and Atterberg limits, soil unit weight, particle size distribution, relative density, undrained shear strength and shear wave velocity. The parameter values indicate that spatial soil variability is limited for a majority of the ten soil units. Exceptions are geotechnical Units E1 to E3.

Geotechnical assessment of suitability of possible foundation elements indicates that the more commonly used types are feasible, particularly multiple pile and monopile foundations.

## SAMENVATTING

De Nederlandse overheid heeft een systematisch kader ontwikkeld waarin zones voor windparken op zee zijn aangewezen. De overheid bepaalt in welke specifieke gebieden binnen deze aangewezen zones windparken kunnen worden aangelegd. Ontwikkeling van de gebieden zal volgens subsidie- en vergunningstenders worden gegund. Winnaars van deze tenders zullen een vergunning ontvangen voor de bouw en exploitatie van een windpark, een SDE+ subsidie, en kunnen gebruik maken van een verbinding naar het elektriciteitsnet op het vaste land. Het Ministerie van Economische Zaken stelt locatiegegevens beschikbaar welke gebruikt kunnen worden bij het opstellen van biedingen voor de subsidie- en vergunningstenders. Dit systeem zal naar verwachting bijdragen aan kostenreductie.

T.b.v. de voorbereiding van de inschrijvingen heeft de Rijksdienst Voor Ondernemend Nederland (RVO) Fugro gecontracteerd voor een geotechnisch onderzoek in de kavels WFS III & IV van windgebied Borssele (WFZ). Het windgebied Borssele ligt in het Nederlandse deel van de Noordzee, ongeveer 36 km voor de kust (zie Page vii of xi, “Vicinity Map”).

Het doel van het geotechnisch onderzoek en bijbehorend programma van laboratoriumproeven is om:

- Inzicht te verkrijgen in de geologische en geotechnische omstandigheden;
- Het bestaande geofysische en geologische model te verfijnen;
- Een gedetailleerd geologisch grondmodel te genereren;
- De verticale en laterale variabiliteit van de grond te bepalen;
- Relevante geotechnische data voor de ontwikkeling van het ontwerp van windpark funderingsconstructies beschikbaar te stellen, inclusief maar niet gelimiteerd tot funderingen en kabels.

Het geotechnisch onderzoek op locatie bestond uit geotechnische boorgaten met monsternames en in situ testen, sonderingen vanaf de zeebodem en geotechnische laboratoriumproeven. Vervolgens zijn op kantoor een geotechnisch laboratorium testprogramma en rapportage van de resultaten uitgevoerd.

Dit rapport is er één uit een reeks Fugro rapporten (zie Page viii of xi, “List of Fugro Reports”). Dit specifieke rapport presenteert een coherent geologisch grondmodel voor WFS III (Page vii of xi), op basis van gegevens van geotechnische en geofysische onderzoeken die specifiek zijn uitgevoerd voor WFS III en WFS IV. Het geologisch grondmodel geeft een kader met integrale verbanden tussen (1) interpretatie van geofysische gegevens, (2) geotechnische parameters en (3) geotechnische geschiktheid van het windgebied, met name geologische kenmerken en processen met potentiële risico’s voor ontwikkeling van een windpark, inclusief maar niet gelimiteerd tot funderingen en kabels.

Kerninformatie is weergegeven door middel van afbeeldingen (plates) volgend op de tekst van deze samenvatting:

- Page ix of xi laat de waterdiepte zien. Significante zandbanken zijn zichtbaar en de daarmee samenhangende processen van erosie en afzetting van sedimenten;
- Page x of xi laat een voorbeeld zien van een doorsnede van het grondmodel, met onder andere, geofysische interpretatie, overgangen van geotechnische lagen en sondeergegevens (CPT) van de geselecteerde geotechnische meetlocaties;

- Page xi of xi presenteert geotechnische lagen van het Tertiair, waar ze grenzen met de bovenliggende geotechnische lagen (Units A en B) van het Kwartair. Deze kaart illustreert de dip van Tertiaire grond lagen t.o.v. de ondergrens van de Kwartaire sedimenten. Daarnaast laat het de afwezigheid zien van de jongere geotechnische lagen in het zuidwestelijke deel van het grondmodel. Deze informatie kan worden beschouwd als een zonekaart, die zones aangeeft met overeenkomstige laagopbouw. Hierbij kan worden opgemerkt dat Units A en B aanwezig zijn in het gehele windgebied WFS III. Unit E1 is de jongste geotechnische laag van het Tertiair van WFS III. Unit F1 (i.e. Sub-unit F1c) is de oudste geotechnische laag die grenst aan de Kwartaire lagen, binnen het verticale bereik van het geologisch grondmodel. De diepte tot de top van deze geotechnische lagen neemt toe in noordoostelijke richting.

Het verticale bereik van het geologisch grondmodel en de geotechnische parameters is tot ongeveer 115 m beneden LAT (Lowest Astronomical Tide). Dit niveau komt globaal overeen met de maximale diepte van het geotechnisch onderzoek voor WFS III and WFS IV. Data van geofysisch onderzoek zijn beschikbaar vanaf de zeebodem tot dieper dan 115 m beneden LAT.

De beschikbare geotechnische en geofysische data laten een goede correlatie zien. De data zijn een geschikte basis voor het geologische grondmodel. Dit model past binnen het kader van de gepubliceerde regionale geologie. De geotechnische gegevens verhogen en verfijnen de kennis van de geïdentificeerde grondlagen.

De presentatie van geotechnische parameters omvat gegevens van sonderingen (CPT), Atterbergse grenzen, korrelverdeling, volumiek gewicht, relatieve dichtheid, ongedraineerde schuifsterkte en schuifgolfsnelheid. De geotechnische parameters van de meeste grondlagen laten een beperkte laterale variabiliteit zien. Van de tien grondlagen zijn geotechnische Units E1 tot E3 de uitzonderingen.

De geotechnische evaluatie van de geschiktheid van mogelijke funderingsoplossingen geeft aan dat de veel voorkomende typen kunnen worden toegepast, met name (mono) paalfunderingen.

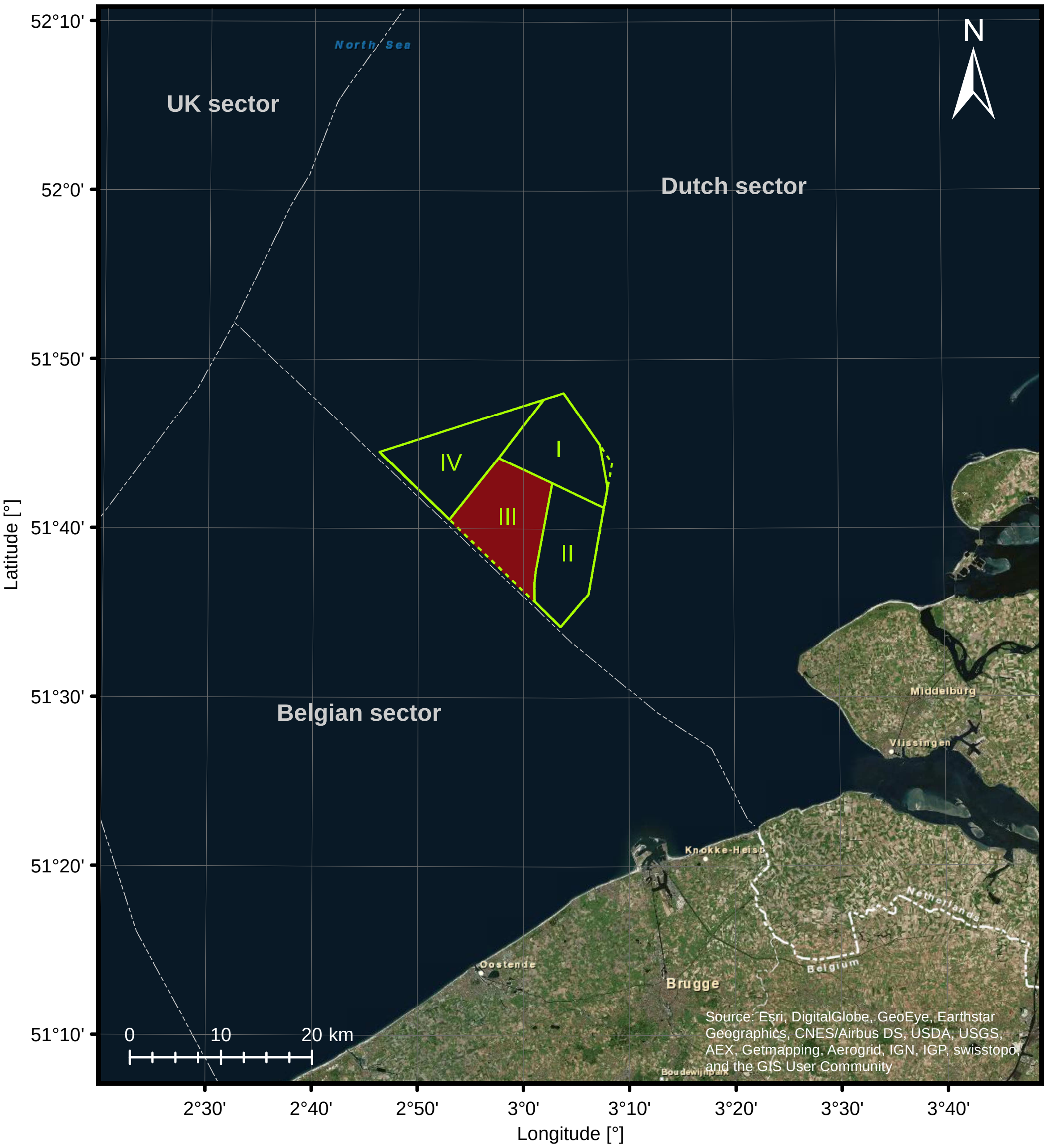


Investigation Area III (subject of this report)

Outline of Borssele Wind Farm Zone

Outline Borssele Investigation Area (Roman numeral indicates area number)

Maritime Boundary

Ellipsoid: GRS 1980
Datum: ETRS 1989

Printed: 11/16/2015 8:43:27 AM

**VICINITY MAP**

BORSSELE WIND FARM ZONE, WFS III – DUTCH SECTOR, NORTH SEA

| Report Number | Title | Contents |
|---|---|---|
| N6083/01 | Geotechnical Report - Investigation Data - Geotechnical Borehole Locations<br>Wind Farm Site III<br>Borssele Wind Farm Zone - Dutch Sector, North Sea | Geotechnical data including geotechnical logs, results from downhole (seismic) cone penetration tests and results from geotechnical laboratory tests. |
| N6083/02 | Geotechnical Report - Investigation Data - Seafloor In Situ Test Locations<br>Wind Farm Site III<br>Borssele Wind Farm Zone - Dutch Sector, North Sea | Geotechnical data including interpreted geotechnical logs and results from seafloor cone penetration tests. |
| N6083/03 | Geotechnical Report - Investigation Data - Geotechnical Borehole Locations<br>Wind Farm Site IV<br>Borssele Wind Farm Zone - Dutch Sector, North Sea | Geotechnical data including geotechnical logs, results from downhole (seismic) cone penetration tests and results from geotechnical laboratory tests. |
| N6083/04 | Geotechnical Report - Investigation Data - Seafloor In Situ Test Locations<br>Wind Farm Site IV<br>Borssele Wind Farm Zone - Dutch Sector, North Sea | Geotechnical data including interpreted geotechnical logs and results from seafloor cone penetration tests. |
| N6083/05 | Geological Ground Model<br>Wind Farm Site III<br>Borssele Wind Farm Zone - Dutch Sector, North Sea | Geological ground model including, stratigraphy, lateral soil variability, geohazards, basic geotechnical parameter values and assessment of geotechnical suitability of selected types of structures. |
| N6083/06 | Geological Ground Model<br>Wind Farm Site IV<br>Borssele Wind Farm Zone - Dutch Sector, North Sea | Geological ground model including, stratigraphy, lateral soil variability, geohazards, basic geotechnical parameter values and assessment of geotechnical suitability of selected types of structures. |
| N6083/07 | Geotechnical Report - Laboratory Test Data<br>Wind Farm Sites III & IV<br>Borssele Wind Farm Zone - Dutch Sector, North Sea | Results of advanced static and cyclic laboratory tests. |

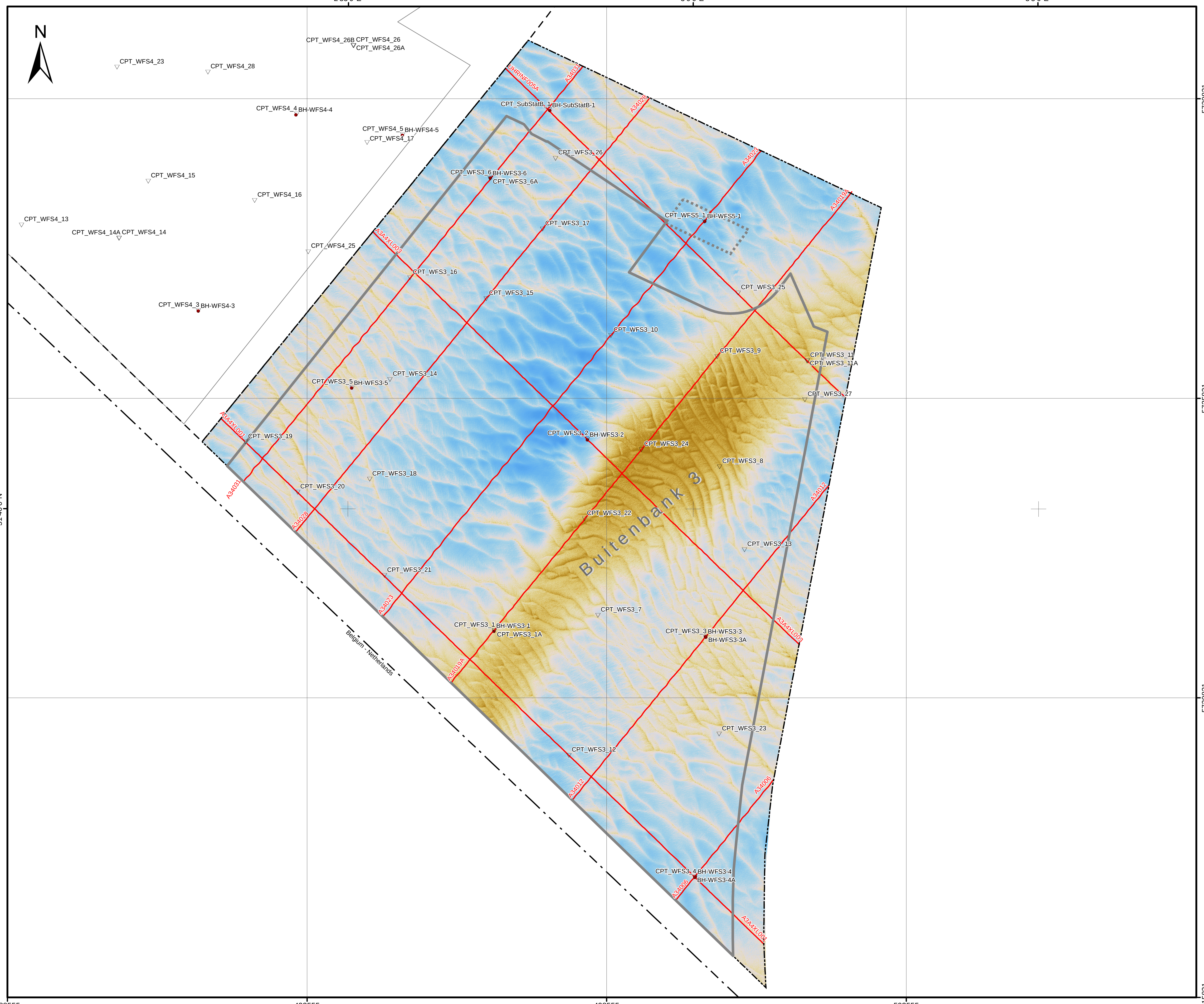


**LEGEND:**

- CPT location
- BH location
- Outline of WFS III
- Outline of WFS IV
- Outline of WFS V
- Investigation Area III
- Investigation Area IV
- Maritime boundary
- Section line of cross-section presented in the report

**Bathymetry [m below LAT]**

13, 17, 21, 25, 29, 33, 37, 41, 43

**NOTES:**

- Reproduced from Fugro (2015a and 2015b)
- Resolution cells 0.5 m x 0.5 m
- Data acquired by Multi-Beam Echo Sounder (MBES)

**GEODETIC PARAMETERS:**

| | |
|---|---|
| DATUM | ETRS89 |
| Ellipsoid | GRS80 |
| Semi major axis | a = 6 378 137.000 |
| Inverse flattening | 1/f = 298.257222101 |
| PROJECTION | UTM, Zone 31 North |
| Central Meridian (CM) | 3°00' 00" E |
| Latitude of Origin | 0°00' 00" N |
| False Easting | 500 000 m |
| False Northing | 000 000 m |
| Scale factor | 0.9996 |
| Units | metres/degrees |

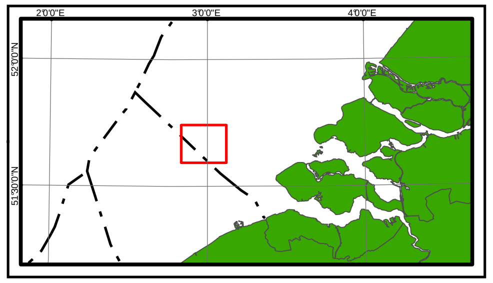



Rijksdienst voor Ondernemend Nederland (RVO)
Croeselaan 15, 3521 BJ, Utrecht - THE NETHERLANDS

Fugro
Prismastraat 4, 2631 RT, Nootdorp - THE NETHERLANDS


**BATHYMETRY**

**BORSSELE WIND FARM ZONE, WFS III**
**DUTCH SECTOR, NORTH SEA**

1:60,000
at original A3 page size

0 500 1,000 1,500 2,000 metres

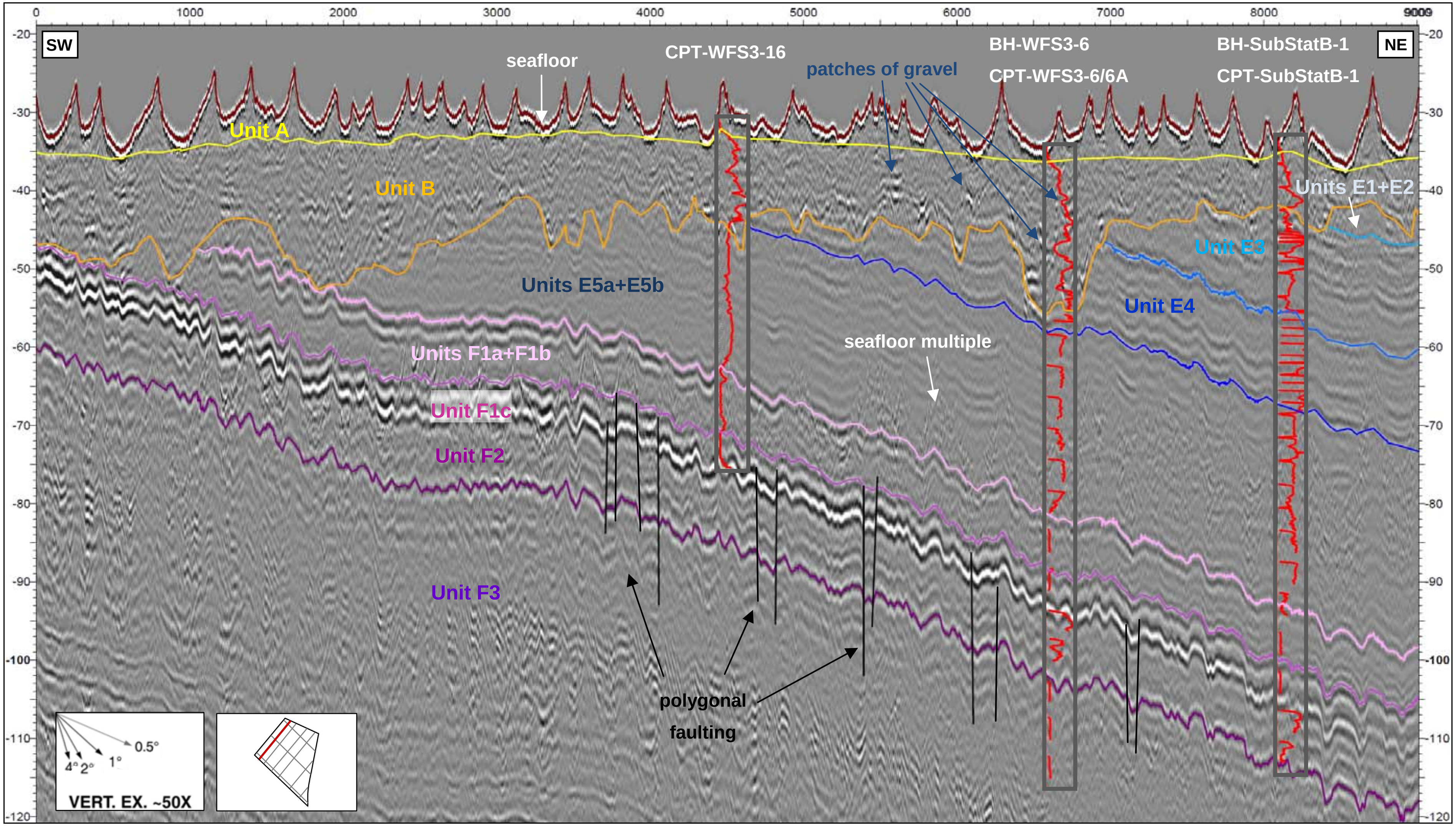


NOTE: Example of MCS line. Vertical scale is depth in metres below LAT. Horizontal scale is distance in metres. CPT cone resistance data (red line) for the geotechnical locations are projected on the cross section. Left side of the grey box marks the geotechnical location. The width of the box marks cone resistance values to 50 MPa. Location of the cross section is shown on Plate 3-6.

**CROSS SECTION – SECTION LINE A34031**

BORSSELE WIND FARM ZONE, WFS III – DUTCH SECTOR, NORTH SEA

ISSUE 01

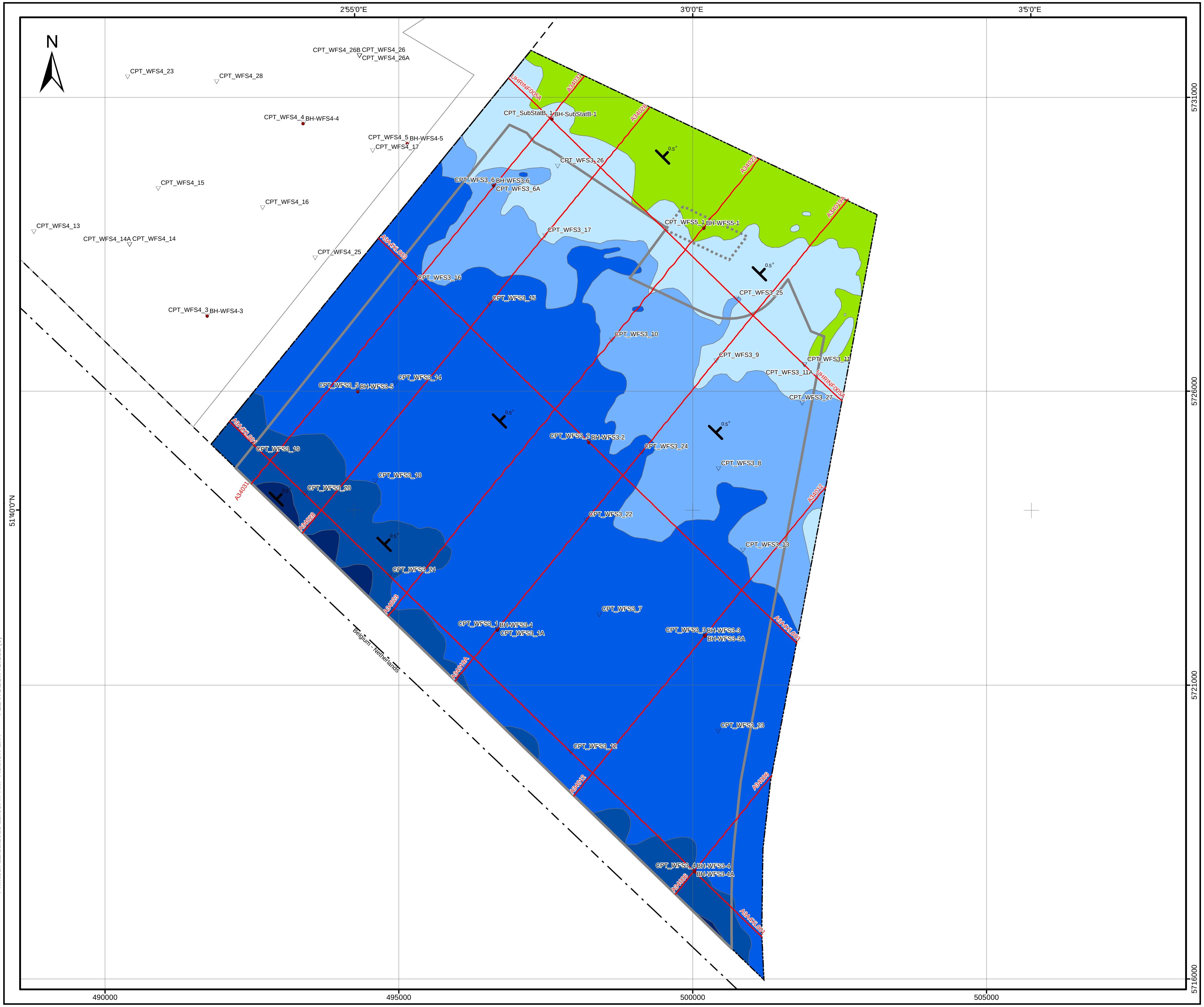




**LEGEND:**

- CPT location
- BH location
- Outline of WFS III
- Outline of WFS IV
- Outline of WFS V
- Investigation Area III
- Investigation Area IV
- Maritime boundary
- Section line of cross-section presented in the report

**Subcrop of Tertiary Units**

- Units E1 + E2 (Ruisbroek Sand Mb. + Watervliet Clay Mb.)
- Unit E3 (Bassevelde 3 Sand Mb.)
- Unit E4 (Bassevelde 2 Sand Mb.)
- Unit E5 (Bassevelde 1 Sand Mb.)
- Units F1a + F1b (Onderdijke Mb.)
- Units F1c + F2 (Onderdijke Mb. + Buisputten Mb.)

0.5° Orientation of layers (long line is layer azimuth; short line represents dip direction; value is approximate dip angle)

**NOTES:**

- Base of Unit B (Pleistocene) represents an erosional surface truncating underlying dipping Tertiary strata
- Tertiary units subcropping at base of Unit B are represented, i.e. intersection of unit boundaries with base of Unit B
- Outline of units based on interpretation from MCS data
- The Tertiary strata below Unit B are gently dipping (0.5 degrees) to NE (refer to main text)

**GEODETIC PARAMETERS:**

| | |
|---|---|
| DATUM | ETRS89 |
| Ellipsoid | GRS80 |
| Semi major axis | a = 6 378 137.000 |
| Inverse flattening | 1/f = 298.257222101 |
| PROJECTION | UTM, Zone 31 North |
| Central Meridian (CM) | 3°00' 00" E |
| Latitude of Origin | 0°00' 00" N |
| False Easting | 500 000 m |
| False Northing | 000 000 m |
| Scale factor | 0.9996 |
| Units | metres/degrees |

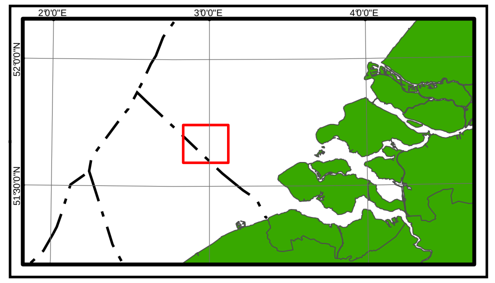


Rijksdienst voor Ondernemend Nederland (RVO)
Croeselaan 15, 3521 BJ, Utrecht - THE NETHERLANDS

Fugro
Prismastraat 4, 2631 RT, Nootdorp - THE NETHERLANDS

**TERTIARY UNITS BELOW UNIT B**

**BORSSELE WIND FARM ZONE, WFS III, DUTCH SECTOR, NORTH SEA**

Scale 1:60,000
at original A3 page size

0 500 1,000 1,500 2,000 metres

FUGRO

Fugro Report No. N6083/05 | Issue 3 | 

# 1. INTRODUCTION

## 1.1 Purpose of Report

The Dutch Government has developed a systematic framework under which offshore wind farm zones are designated. Within the designated wind farm zones the government decides the specific sites where wind farms can be constructed. Site development will be tendered. Winners of these site development tenders will be granted a permit to build a wind farm, a SDE+ grant, and will be offered a grid connection to the main land. The Ministry of Economic Affairs provides site data, which can be used for the preparation of bids for these tenders. This system is expected to contribute to cost savings.

As part of the tender preparations, the Netherlands Enterprise Agency (RVO), henceforth referred to as 'Client', has requested Fugro to perform a geotechnical investigation of Wind Farm Site WFS III & IV of the Borssele Wind Farm Zone (WFZ). The Borssele Wind Farm Zone is located in the Dutch Sector of the North Sea, approximately 36 km from the coastline (refer to Plate 1-1 "Vicinity Map").

The objective of the geotechnical investigation and associated laboratory testing programme for WFS III and WFS IV is to:

- Improve the geological and geotechnical understanding;
- Update an earlier geological and geophysical model;
- Provide a detailed geological ground model;
- Determine the vertical and lateral variation in seabed conditions;
- Provide relevant geotechnical data to progress the design of windfarm foundation elements, including, but not limited to foundations and cables.

The offshore phase of the geotechnical investigation included geotechnical borehole drilling with downhole sampling and in situ testing, seafloor in situ testing and geotechnical laboratory testing. An office programme of geotechnical laboratory testing and reporting of results followed the offshore phase.

This particular report presents a concise and coherent geological ground model for WFS III (Plate 1-1), which takes account of geotechnical and geophysical data specifically acquired for WFS III and WFS IV. The geological ground model provides an integrated framework that links (1) geophysical data interpretation, (2) geotechnical parameters and (3) site suitability, particularly geological features and processes which can be potential hazards (geohazards) for windfarm development, including but not limited to support structures (foundations) and cables.

## 1.2 Scope of Report

This report comprises the following:

- Geological ground model;
- Geotechnical parameters versus depth per investigated geotechnical location;
- Geotechnical parameters versus depth per geotechnical unit;

- Assessment of geotechnical suitability of selected types of structures, including an inventory of (geo)hazards and constraints that may affect design and installation of the planned structures, including cables and temporary structures such as jack-up platforms.

The geological ground model applies to an area demarcated as Investigation Area III on the Vicinity Map (Plate 1-1). This area includes an innovation site WFS V for wind turbine generator foundations. Investigation Area III also includes the planned Substation Beta Substation Betatransformer station of transmission system operator TenneT. WFS V and Substation Beta are presented on Plate 3-4. The boundaries of WFS III and WFS V may be subject to change.

For practical reasons, the information obtained at the WFS V and Substation Beta locations will be reported along with WFS III data. No further distinction or separation (other than location name) will be made in this report. The text sections of the report and the plates (i.e. Plates 1-1, 3-1 to 3-32 and 5-1) refer to WFS III, WFS V and Substation Beta as defined at the start of this investigation. The entire Investigation Area III is meant where the report text refers to WFS III.

The depth coverage of the geological ground model and geotechnical parameter values is to approximately 115 m relative to Lowest Astronomical Tide (LAT). This depth coverage corresponds broadly with the maximum geotechnical investigation depth (i.e. approximately 80 m below seafloor (bsf)) for WFS III and WFSIV. The source data from geophysical survey extend below 115 m relative to LAT.

## 1.3 Project Responsibilities and Use of Report

This report presents information according to a project specification determined and monitored by the Client.

This report must be read in conjunction with “Guide for use of Report”, Section C.

Fugro understands that this report will be used for the purpose described in this “Introduction” section. That purpose was a significant factor in determining the scope and level of the services. Results must not be used if the purpose for which the report was prepared or the Client’s proposed development or activity changes. Results may possibly suit alternative use. Suitability must be verified.

## 1.4 Report Format

This report is one in a series of reports. Refer to Plate 1-2 for a list of Fugro reports which were prepared as part of this project.

This report uses and summarises information from sources listed in Section 2. The reader should consult the source information for details, particularly for topics with an indirect link to the geological ground model, e.g. morphodynamic and metocean desk studies. Understanding of site conditions improves upon further data acquisition and interpretation. This means that some of the source interpretations may be superseded by information presented in this report. Also, source information may be updated after publication of this report.

The principal sections of this report are the Summary, Main Text, Plates following the Main Text, and Sections A and B. Comments are as follows:

- The Summary section allows a quick-scan management overview. It includes a selection of plates. The selected plates are duplicates from a larger set of Plates following the Main Text;
- Section 2 of the Main Text focuses on methodology;
- Sections 3 to 5 provide the principal information as described in Section 1.2 Scope of Report. These text sections should be read in conjunction with the Plates following the Main Text, where applicable;
- Each of the Sections 3 to 5 starts with primary information, which may consist of links to Plates following the Main Text. Plate numbering starts with a Section number, e.g. Plate 3-2 belongs to Section 3;
- Sections A and B summarise geotechnical parameter values presented and explained in Fugro Reports N6083/01 and N6083/02 titled "Geotechnical Report – Investigation Data – Wind Farm Site III" (Plate 1-2);
- Section C and Appendix 1 provide general practice statements and terminology. This background information supports the Main Text. It will be familiar to expert users of the type of information presented in this report.

# 2. STUDY OVERVIEW

## 2.1 Sources of Information

Client-supplied information included the following:

- Boundaries and coordinates of WFS III, including WFS V and Substation Beta (RVO, 2015; Periplus, 2015);
- Information available on the RVO-website for Borssele Wind Farm Zone: (http://offshorewind.rvo.nl)

  This information includes (but not exclusively) the following studies (i.e. reports and accompanying data in GIS-format):
  - Geological Desk Study (CRUX Engineering, 2014);
  - UXO Desk Study (REASeuro, 2014);
  - Morphodynamical Desk Study (Deltares, 2014);
  - Archaeological Desk Study (Vestigia, 2014);
  - Metocean Desk Study (Deltares, 2015);
  - Geophysical Site Survey (Fugro, 2015a and b);
  - Geological Ground Model Reports for WFS I and WFS II (Fugro, 2015c and d);
  - Geological Ground Model GIS database for WFS I and WFS II (Fugro, 2015e).

  Data from geophysical site survey in digital file format (e.g. *.SEGY, *.XYZ-format):
  - Multi-Beam Echo Sounder (MBES) data;
  - Side Scan Sonar (SSS) data;
  - Magnetometer (MAG) data;
  - 2D UHR Multi-Channel Seismic (MCS) reflection data;
  - Pinger data, Sub-bottom Profiler seismic reflection (SBP).

Section 3 includes details about the geophysical site survey data, i.e. data resolution and data coverage, particularly Plates 3-1 and 3-2 titled: 'Design Basis for Site Characterisation'.

Geotechnical investigation data for WFS III (refer to Reports N6083/01 and N6083/02, listed on Plate 1-2, which include:

- Geotechnical logs for boreholes at eight locations which include results from downhole sampling and cone penetration testing;
- Geotechnical logs for additional boreholes at four of the eight locations which include interpreted results of downhole Cone Penetration Tests (CPTs);
- Results of downhole CPTs from all boreholes at these eight locations;
- Results of downhole seismic cone penetration testing at two of the eight locations;
- Results of geotechnical laboratory tests on a selection of samples;
- Geotechnical logs for 25 locations, which include interpreted results of seafloor CPTs;
- Results of 27 seafloor CPTs at 25 locations, including one additional test to match stop criteria and one additional test at Client request.

Fugro's database provided additional information, including:

- Information about the regional geology;
- General geotechnical data;
- Previous geotechnical investigation data applicable to nearby sites;
- Electronic Navigation Charts (ENC).

### 2.2 Data Interpretation and Geotechnical Analysis

The following data analysis steps were taken:

- Compilation of geotechnical, geophysical and geological data in a Geographic Information System (i.e. ArcGIS) and seismic and geological interpretation software (i.e. Kingdom Suite), including information from the Fugro database;
- Independent verification of data interpretations (e.g. site use, seafloor conditions and seismostratigraphy) given in previous studies (i.e. geological desk study, UXO desk study, morphodynamic desk study, archaeological desk study, metocean desk study and geophysical site survey ), where possible;
- Identification of geotechnical units using geological and geotechnical engineering criteria, including composition, geotechnical properties and behaviour as determined by laboratory tests and interpretation of CPT results;
- Assessment of a lithostratigraphic framework based on interpreted geotechnical unit boundaries and geotechnical unit descriptions, and correlation of the geotechnical units with the lithostratigraphy for the Quaternary and Tertiary of both the Netherlands and Belgium;
- Assessment of a seismostratigraphic framework based on the geophysical character of the available MCS data and reference to previous investigations and studies (i.e. WFS I and WFS II);
- Ground truthing of seismostratigraphic units based on geotechnical logs, results from (seismic) cone penetration tests (CPT) and results from geotechnical laboratory tests;
- Correlation of the lithostratigraphic unit boundaries with the seismostratigraphic unit boundaries and (re)interpretation of seismic horizons (i.e. tracing seismic reflections or unconformable surfaces on MCS data) to extrapolate the geotechnical unit boundaries at the geotechnical locations to the entire site, where possible;
- Gridding of geotechnical unit boundaries and assessing the depth and the thickness variation of the geotechnical units;
- Characterisation of the interpreted geotechnical units in view of their geotechnical parameters (i.e. parameters relevant to the geological ground model) and the lateral variation;
- Assessment of suitability of a selection of permanent and temporary foundation types and of cables in view of the geological ground model;
- Iteration of analysis steps, where required to improve interpretation.

The presented geological ground model is for Investigation Area III and takes account of geotechnical and geophysical data specifically acquired for both Investigation Areas III and IV. Geotechnical and geophysical data acquired for WFS I and WFS II were used to tie-in the seismostratigraphic framework.

Subdivision into geotechnical units and sub-units considers:

- Geological formations and formation members' boundaries interpreted from seismic reflection data;
- Thicknesses of soil layers (i.e. main soil types) and their lateral continuity across the site.

The Quaternary lithostratigraphy according to Rijsdijk et al. (2005) applies, with adjustments as explained in Section 3.

The presented lithostratigraphy of the Tertiary is based on Dutch onshore nomenclature (TNO, 2013a to c). This report further differentiates the Dutch nomenclature according to the Belgium lithostratigraphy (Vandenberghe et al., 2004), where appropriate. Section 3 provides details.

The interpretation of the seismic reflection data is based on the data as processed and provided by Fugro (2015a and b). Comments are as follows:

- The MCS data were corrected for tide effects by matching the seismically derived seafloor (i.e. seafloor pick) with the MBES data (referenced to LAT). This matching process introduced some differences between the MCS seafloor and the MBES seafloor of about 1.0 m to 1.5 m (Fugro, 2015a and b).
- The MCS data are affected by seafloor multiples at approximately twice the water depth below sea level. As a consequence, the continuation of the seismic reflections is obscured at the depth interval where the seafloor multiples appear. The interpretations of the seismic horizons are inferred from the relation with the trend of the seismic reflections within the same seismostratigraphic unit.
- The MCS data are affected by a zone with acoustic transparency below the wide, elongated sandbank area, i.e. Buitenbank 3. The interpretation of the continuation of the horizons in this zone has been inferred from the general trend of relevant horizons from adjacent seismic reflection lines.
- The geophysical reflectors underneath major sand dunes appear at slightly higher elevations than where sand dunes do not occur at seafloor. This "pull-up" effect is probably artificial and a result of steep-sided slopes of the sand dunes and/or preferential deposition of coarser-grained material at the sand dunes compared to finer-grained material in the troughs. Preferential deposition can result in small seismic velocity variations within Unit A.
- The integration of the different datasets incorporated a best match of seismic response with geotechnical changes. In most cases this was possible. Comparison of the geotechnical and geophysical data shows good agreement between datasets.
- Small differences in geotechnical unit depth and depths of corresponding seismic reflectors do occur and may be attributed among others to the conversion of (geophysical) data to LAT, time-depth conversion. The effects of time-depth conversion increase with depth below LAT.

Jacobs and De Batist (1996) correlated seismostratigraphy to Palaeogene lithostratigraphy. They compared the seismic facies with the lithofacies for the Maldegem Formation and showed that seismic facies do not always correlate with lithological facies.

Gridding of the horizon interpretations considers the MCS track lines. The interpolation between the track lines is based on a flex grid routine (2D/3D PAK, Kingdom Suite software), which combines minimum curvature and minimum tension algorithms in a single routine. The grids have a 50 m cell size. For these grids, interpolation considers a minimum curvature value of 0.5 (from 1 – minimum tension, to 0 – minimum curvature) to fit the data and a value of 10 (out of 11) for smoothing.

Contour lines of the gridded data were prepared in Kingdom Suite software using contour version 7.5. Contour intervals were either 5 m or 1 m. Contour smoothing level was low, with grid smoothing minimum tension of 0.9, and smoothness of 1.

The subcrops of geotechnical units were determined from where they truncate against the base of Unit B on MCS lines. Interpolation and interpretative smoothing were applied for areas between the MCS lines.

Geotechnical data coverage is limited for soils between approximately 80 m and 115 m LAT. This is because of variable penetration depths at geotechnical locations. Soil conditions and geotechnical parameters within this depth interval were interpreted from the acoustic character of the geophysical data. Changes in acoustic properties were approximately correlated with the ground-truth data to assess changes in soil conditions and laterally extrapolated to areas with no geotechnical data. More uncertainty applies to interpretation of the soil conditions for the deeper geotechnical units, where no geotechnical ground-truth data is available.

The identification of geohazards from the MCS data is limited by the track line spacing (i.e. minimum 400 m). Geological features between track lines will remain undetected.

### 2.3 Geodetic Parameters

The geodetic parameters for horizontal positioning are presented on Plate 2-1.

Lowest Astronomical Tide (LAT) and seafloor were used as vertical reference levels for water depth measurement and geotechnical sampling and testing depth, respectively. The depth references of the unit boundaries of the geological model (i.e. cross sections and depth maps) refer to LAT.

The use of the geodetic information presented must consider the accuracy of measurements, particularly where use may differ from original intentions.

## 3. GEOLOGICAL GROUND MODEL

### 3.1 Overview

The geological ground model is mainly presented by plates providing the following principal information:

- Plates 3-1 and 3-2 present design basis information for site characterisation;
- Plate 3-3 presents a lithostratigraphic framework, reproduced after De Lugt (2007). It provides background information to selection of the lithostratigraphic framework for the Borssele Wind Farm Zone. The selected lithostratigraphic framework is presented in Section 3.3 and Table 3.1 below;
- Plates 3-4 and 3-5 show bathymetry and the derived seafloor gradient;
- Plate 3-6 presents MCS track lines and section lines of selected cross sections;
- Plates 3-7 to 3-15 present cross sections of MCS data with the interpreted geotechnical unit boundaries and cone resistance (CPT) data at the geotechnical locations superimposed;
- Plate 3-16 presents the subcrop of the Tertiary geotechnical units below the Quaternary geotechnical units (i.e. Units A and B). This map illustrates the truncation of the dipping Tertiary geotechnical units against the base of the Quaternary sediments and, as a consequence, the absence of younger geotechnical units in the stratigraphic sequence towards the southwest. In this respect, the subcrop map can be regarded as a zonation map (i.e. indicating zones with similar stratigraphic profile). Note that geotechnical Units A and B are present over the entire Investigation Area III. Unit E1 is the youngest geotechnical unit and Unit F1 (i.e. Sub-unit F1c) is the oldest geotechnical unit that subcrops below the Quaternary units. The depth to the base of the Tertiary geotechnical units increases to northeast;
- Plates 3-17 to 3-24 present the depths (relative to LAT) of the geotechnical units (Units A to F3). Note that geotechnical Units E2 and F1b are too thin to be reliably identified from MCS data. These units have been combined with geotechnical Unit E1 and Unit F1a, respectively. Blank areas within the boundary of Investigation Area III on the above plates represent the areas where the considered geotechnical units do not occur;
- Plates 3-25 to 3-32 present the thickness of geotechnical Units A to F2. Note that geotechnical Units E2 and F1b are too thin to be reliably derived from MCS data. These units have been combined with geotechnical Unit E1 and Unit F1a, respectively. The base of geotechnical Unit F3 is below the depth considered for the geological ground model.

The following naming convention applies:

- An uppercase letter indicates a geological formation (Fm.);
- A number indicates a geological formation member (Mb.);
- A lowercase letter indicates a soil layer of considerable thickness (i.e. thicker than 2 m) that is laterally continuous across the site and which shows distinct geotechnical characteristics.

Sections 3.2 to 3.6 provide supplementary information.

### 3.2 Geological Setting

The Borssele WFZ is part of the Southern Bight, i.e. the area of the southern North Sea between the Netherlands, Belgium and the United Kingdom. The Southern Bight is situated on the London-Brabant Massif, which has been a major structural high since Triassic time.

The North Sea Basin is an extensional basin that developed at the beginning of the Cenozoic as the result of post-rift thermal relaxation of the lithosphere, isostatic adjustment and sediment loading (Ziegler, 1990). Thermal subsidence was interrupted by occasional compressional tectonic events.

In Cretaceous times, the area was set in a shallow water environment. Sediments from this period consist mainly of marls and chalk. In the Late Cretaceous, crustal movements resulted in thermal uplift of the British Isles and Central Europe (Ziegler, 1990). These movements are attributed to the Alpine orogeny (i.e. mountain building). Large land masses became exposed to sub-aerial erosion. The crustal movements caused a sudden and substantial increase in supply of siliciclastic material into the North Sea basin throughout the Tertiary period. During this period, the area experienced different rates of thermal subsidence, in response to the gradual lithospheric cooling of an underlying Mesozoic rift dome, dominated by broad synclinal downwarping towards a depositional axis to the north-east. The Borssele WFZ is located approximately at the south-western edge of this broad syncline.

Throughout the Palaeogene (i.e. Palaeocene, Eocene, and Oligocene), a shallow shelf sea environment persisted at the Borssele WFZ. Water depth during high stand periods probably never exceeded 100 m (Cameron et al., 1992). During Eocene times, the shallow sea extended westwards, well into the English Channel. During the Pyrenean and Savian tectonic phases at the end of the Eocene and Oligocene, respectively, large areas of the North Sea basin, including the Borssele WFZ, became sub-aerially exposed as a result of uplift in combination with sea level fall (Ziegler, 1990; De Jager, 2007). This resulted in erosion across the area.

The Neogene (i.e. Miocene and Pliocene) was a period of sediment starvation. The depocentre shifted northwards into the main North Sea Basin (Balson, 1989; Cameron et al., 1989). From the end of the Miocene onwards, a complex fan delta system developed, which gradually evolved into an alluvial plain prograding from the east, from a large Baltic River System (Overeem, 2002).

In Quaternary times, the area of the Borssele WFZ was subject to global sea level fluctuations due to Pleistocene glaciations (Laban, 1995) and partially by glacio-isostacy. This resulted in shallow marine to fluvial deposition during the interglacial periods and extended erosion during the glacial periods. The relatively deep erosion features at the base of the Quaternary (i.e. Unit B) are referred to as scour hollows (Liu et al., 1993). The Holocene sea level rise led to flooding of the continental shelf, which has remained essentially sediment starved (Jacobs and De Batist, 1996). Holocene deposits occur mainly in the form of sand banks (Liu et al., 1993).

## 3.3 Lithostratigraphic Framework

Table 3.1 presents the lithostratigraphic framework selected for the Borssele Wind Farm Zone.

**Table 3.1 Lithostratigraphic Framework for Borssele WFZ**

<table>
<tr><th colspan="2">Geotechnical</th><th colspan="2">Lithostratigraphy</th><th>Seismo-stratigraphy Fugro (2015a,b)</th><th colspan="3">Time Scale</th></tr>
<tr><th>Unit</th><th>Sub-Unit</th><th>Member</th><th>Formation</th><th>Unit</th><th>Age</th><th>Epoch</th><th>Period</th></tr>
<tr><td>A</td><td></td><td></td><td>Southern Bight</td><td>A</td><td></td><td>Holocene</td><td rowspan="2">Quaternary</td></tr>
<tr><td>B</td><td></td><td></td><td>Kreftenheye/Eem</td><td>B</td><td>Weichselian/ Eemian</td><td>Pleistocene</td></tr>
<tr><td>C1</td><td></td><td></td><td rowspan="2">Westkapelle Ground (Brielle Ground)</td><td rowspan="2">C</td><td rowspan="2"></td><td rowspan="2">Pliocene</td><td rowspan="14">Tertiary</td></tr>
<tr><td>C2</td><td></td><td></td></tr>
<tr><td>D</td><td></td><td>Rupel Clay</td><td>Rupel</td><td>D</td><td rowspan="4">Rupelian</td><td rowspan="4">Oligocene</td></tr>
<tr><td>E1</td><td></td><td>Ruisbroek Sand</td><td rowspan="6">Tongeren</td><td>E1</td></tr>
<tr><td>E2</td><td></td><td>Watervliet Clay</td><td rowspan="5">E2</td></tr>
<tr><td>E3</td><td></td><td>Bassevelde 3 Sand</td></tr>
<tr><td>E4</td><td></td><td>Bassevelde 2 Sand</td><td rowspan="3">Priabonian</td><td rowspan="8">Eocene</td></tr>
<tr><td rowspan="2">E5</td><td>E5a</td><td rowspan="2">Bassevelde 1 Sand</td></tr>
<tr><td>E5b</td></tr>
<tr><td rowspan="3">F1</td><td>F1a</td><td rowspan="3">Onderdijke</td><td rowspan="5">Dongen</td><td rowspan="2">F1 (Onderdijke Member) F2 (Buisputten Member)</td><td rowspan="4">Bartonian</td></tr>
<tr><td>F1b</td></tr>
<tr><td>F1c</td><td rowspan="2">F3 (Zomergem Member)</td></tr>
<tr><td>F2</td><td></td><td>Buisputten</td></tr>
<tr><td>F3</td><td></td><td>Zomergem</td><td>F4 (Onderdale Member)</td><td>Lutetian</td></tr>
</table>

The lithostratigraphy of the Quaternary used in this report is according to Rijsdijk et al. (2005). It is assessed to be more applicable than the onshore lithostratigraphy for the Quaternary proposed by TNO (2013a to c).

The lithostratigraphy of the Tertiary used in this report is according to Dutch onshore nomenclature (TNO, 2013a to c). The report further differentiates the Dutch onshore nomenclature according to the Belgian lithostratigraphy (Vandenberghe et al., 2004; Maréchal, 1993), where appropriate. Comments are as follows:

- The Tertiary lithostratigraphy has been defined separately for the Dutch onshore and offshore. The Dutch onshore nomenclature is more detailed and assessed to be more applicable than the Dutch offshore nomenclature for the Tertiary (TNO, 2013d; Van Adrichem Boogaert and Kouwe, 1997). Note that the onshore and offshore lithostratigraphic unit names show differences, as shown in Table 3.2;
- The main difference between the Dutch onshore and offshore Tertiary lithostratigraphy is that the onshore Tongeren Formation is part of the offshore Vessem Member and named thereafter, i.e. the Tongeren Formation is omitted from the offshore Tertiary lithostratigraphic nomenclature. Note

that the offshore Vessem Member represents the lower part of the offshore Rupel Formation (below the Rupel Clay Member), and that the offshore Rupel Formation therefore correlates with both the onshore Rupel Formation and the onshore Tongeren Formation;

- The lithostratigraphic unit names defined by the Dutch onshore nomenclature for the Tertiary are almost the same as the corresponding Belgian lithostratigraphic unit names. The Belgian Sector of the North Sea is adjacent to the Borssele WFZ;
- The Bassevelde Sand Member (Tongeren Formation) and the Asse Member (i.e. Dongen Formation) have been further subdivided based on Belgian lithostratigraphy (Vandenberghe et al., 2004). The lithostratigraphy according to Vandenberghe et al. (2004) differentiates the Bassevelde Sands in three separate units (based on micro-fauna);
- The Dutch Asse Member correlates with the Belgium Maldegem Formation. The Maldegem Formation has been further differentiated in the Onderdijke Member (clay), Buisputten Member (sand), Zomergem Member (clay), Onderdale Member (sand), Ursel Member (clay) and Asse Member (clay). The clay of the Zomergem Member is the deepest lithostratigraphic unit encountered above 115 m LAT;
- Plate 3-3 presents a comparison between the Belgian and the Netherlands offshore lithostratigraphic nomenclature for the Tertiary (modified after De Lugt, 2007). Differences are significant. Particularly, the Netherlands offshore Rupel Formation correlates with both the Belgian Rupel Group and the Tongeren Group.

**Table 3.2 Lithostratigraphic Correlation for The Netherlands – Tertiary**

<table>
<tr><th colspan="2">Lithostratigraphy used in this Report</th><th colspan="3">Lithostratigraphy Dutch Onshore</th><th colspan="2">Lithostratigraphy Dutch Offshore</th><th colspan="3">Time Scale</th></tr>
<tr><th>Unit</th><th>Stratigraphy</th><th>Formation</th><th colspan="2">Member</th><th>Formation</th><th>Member</th><th>Age</th><th>Epoch</th><th>Period</th></tr>
<tr><td>C</td><td>Westkapelle Ground/ Brielle Ground</td><td>Westkapelle Ground/ Brielle Ground</td><td colspan="2"></td><td>Westkapelle Ground/ Brielle Ground</td><td></td><td></td><td>Pliocene</td><td rowspan="10">Tertiary</td></tr>
<tr><td>D</td><td>Rupel Clay</td><td>Rupel</td><td colspan="2">Rupel Clay</td><td rowspan="3">Rupel</td><td>Rupel Clay</td><td rowspan="4">Rupelian</td><td rowspan="4">Oligocene</td></tr>
<tr><td>E1</td><td>Ruisbroek Sand</td><td rowspan="5">Tongeren</td><td rowspan="5">Zelzate</td><td>Ruisbroek</td><td rowspan="3">Vessem</td></tr>
<tr><td>E2</td><td>Watervliet Clay</td><td>Watervliet</td></tr>
<tr><td>E3</td><td>Bassevelde 3 Sand</td><td rowspan="3">Bassevelde</td><td rowspan="3">Undifferentiated</td></tr>
<tr><td>E4</td><td>Bassevelde 2 Sand</td><td rowspan="2"></td><td rowspan="2">Priabonian</td><td rowspan="5">Eocene</td></tr>
<tr><td>E5</td><td>Bassevelde 1 Sand</td></tr>
<tr><td>F1</td><td>Onderdijke</td><td rowspan="3">Dongen</td><td colspan="2" rowspan="3">Asse</td><td rowspan="3">Dongen</td><td rowspan="3">Asse</td><td rowspan="2">Bartonian</td></tr>
<tr><td>F2</td><td>Buisputten</td></tr>
<tr><td>F3</td><td>Zomergem</td><td>Lutetian</td></tr>
</table>

The Tertiary strata below Unit B are gently dipping (0.5°) to NE and form an angular relationship with the base of Unit B, i.e. the Tertiary strata are truncated. As a consequence, the Tertiary strata subcropping below the base of Unit B become progressively older to the southwest and the younger geotechnical units become absent in the stratigraphic profiles towards the southwest. The angular relationship is probably due to tilting during the Savian (Alpine) tectonic phase at the transition from Rupelian to Chattian (middle to late Oligocene).

Plate 3-16 presents the subcrop of the Tertiary geotechnical units below the Quaternary geotechnical units (i.e. Units A and B). This map illustrates the termination of the dipping Tertiary geotechnical units to the base of the Quaternary sediments. In this respect, the subcrop map can be regarded as a zonation map (i.e. indicating zones with similar stratigraphy).

The subcrop map is based on the integration of geotechnical and geophysical data and, as such, shows a projected distribution of the Tertiary Members (units) in areas where geotechnical data are absent. The results show that geotechnical Units A and B are present over the entire Investigation Area III. Unit E1 is the youngest Tertiary unit and Unit F1 (i.e. Sub-unit F1c) is the oldest geotechnical unit that subcrops below the Quaternary units, within the depth coverage of the geological ground model.

Unit C and Unit D are not present in Investigation Area III.

## 3.4 Seismostratigraphic Framework

For the Borssele Wind Farm Zone, including Investigation Area III, the description and thickness of most geotechnical units correlate well with the identified seismostratigraphic units.

In general, differences occur between the measured unit boundary depths at the geotechnical locations and the derived horizon depths (associated with the geotechnical unit boundaries) from the geophysical data. This mainly results from inevitable uncertainties associated with processing of geophysical data, e.g. time/depth conversion. The difference in depths between the interpreted geotechnical unit boundaries and the interpreted seismic horizons can be up to 2 m over the investigated depth range.

Table 3.1 includes a comparison of the selected lithostratigraphic framework for Borssele WFZ and seismostratigraphy interpreted by Fugro (2015a and b). The seismostratigraphy presented in Fugro (2015a and b) for Units F1 to F4, differs from the seismostratigraphy adopted for the Borssele WFZ and used in this report. Comments are as follows:

- The seismostratigraphic boundary between Unit A and Unit B cannot be clearly resolved from the MCS data. The small compositional differences between Units A and B do not result in a clear seismic reflection response (i.e. reflector);
- The seismostratigraphic unit boundaries between Unit B and the Tertiary units are erosion surfaces. They correlate well with the geotechnical unit boundaries;
- The base of Unit E2 appears as strong amplitude reflections on MCS data within the lithostratigraphic Tongeren Formation. They are concordant (i.e. layered, without erosive cross-cutting of strata). This boundary may coincide with the Pyrenean tectonic phase;
- Units E1 and E2 correlate to one seismostratigraphic unit. They are combined and mapped together (Plate 3-27);
- The transition between Unit E5 and the underlying Sub-unit F1a is gradual and not characterised by a distinct geophysical response (i.e. reflector). The nearest seismic reflector was taken as the geophysical boundary between these units. As a result, the depth of the boundary may differ between geotechnical and geophysical data. The depth to base of Unit 5 map (Plate 3-22) and

thickness maps of Unit 5 and Sub-units F1a and F1b (Plates 3-30 to 3-31) can deviate from the geotechnical data;

- Unit F relates to the top of an intensely faulted interval within the lithostratigraphic Dongen Formation. These faults are polygonal faults, have small displacement and are intra-formational. As a result, the faults do not reach the seafloor. The shallowest occurrence of the polygonal faults is in the west and south of Investigation Area IV, and roughly follows the area where Units F1 and F2 truncate against Unit B (Plate 3-16). This fault pattern has been described for polygonal fault systems in the Rupel Clay Member (Rupel Formation) and the Ieper Clay Member (Dongen Formation) (Dehandschutter et al., 2002; Horseman et al., 1987). The MCS data show that the polygonal faulting system is especially distinct in Sub-unit F1c and the upper part of Unit F3 (see Plates 3-7 to 3-15). The faulted interval shows fissures in the geotechnical clay samples. The fissures provide some indication for deformation within this interval;
- Sub-unit F1c and Unit F2 correlate to one seismostratigraphic unit in most of the Investigation Area III and the base of Sub-unit F1c is not always distinct in MCS data. Therefore the units are combined and mapped together (Plate 3-32).

Table 3.3 presents a description of seismic character of the geotechnical units, i.e. acoustic parameters (amplitude, frequency), internal configuration, continuity and character of the boundaries as identified from the MCS data. It should be noted that seismostratigraphic boundaries result from changes in physical properties in the soil (e.g. seismic velocity and soil density) and may not necessarily be interpreted in lithostratigraphical terms. Moreover, lateral variations in geotechnical properties (e.g. cone resistance) within a unit do not necessarily give rise to a seismostratigraphical boundary (e.g. seismic reflection).

**Table 3.3: Seismic Character of Geotechnical Units – Investigation Area III**

| Unit | Image | Seismic Character | Comments |
|---|---|---|---|
| A | 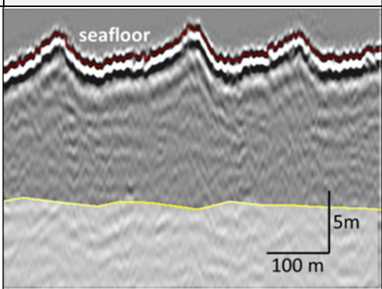  | Semi-transparent, homogenous character with no or minor internal seismic reflectors. Where present, internal reflectors are discontinuous, display low to medium amplitudes and high frequency. | ▪ The boundary with the underlying unit (Unit B) can often not be clearly differentiated, however considered to be an undulating surface semi-parallel to seafloor<br>▪ <5m-thick, locally thicker below crests of major sand dunes and Buitenbank 3 |
| B | 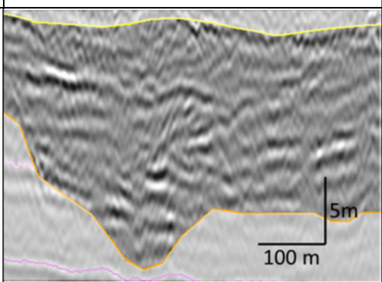  | Semi-transparent to chaotic character, discontinuous reflectors with low to high amplitudes and variable frequency.<br>High amplitude reflections occur locally and correlate to gravelly or clayey, organic-rich intervals (see e.g. Plates 3-7, 3-8, 3-10 for location of high amplitude reflections). | ▪ The base of this unit is a distinct, irregular erosion surface<br>▪ In general, this unit can be easily distinguished from the units below<br>▪ Thickness is highly variable due to channels and scour hollows incised into underlying units and filled in with deposits of this unit |

| Unit | Image | Seismic Character | Comments |
|---|---|---|---|
| E1 & E2 | 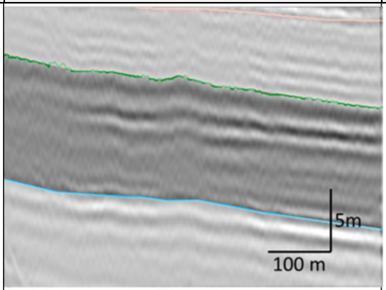  | Heterogeneous character. Locally vertical succession of two seismic facies/sub-units:<br>1) upper part - often regular continuous to discontinuous parallel reflectors of medium to high amplitude;<br>2) lower part - often transparent, locally high amplitude, discontinuous and limited lateral extent. | ▪ Geotechnically heterogeneous unit.<br>▪ The base of geotechnical Unit E2 correlates with strong continuous seismic reflector<br>▪ The boundary between geotechnical Units E1 and E2 has no clear seismic expression<br>▪ The transparent and structureless character of the lower part may reflect the more clayey character of Unit E2 |
| E3 | 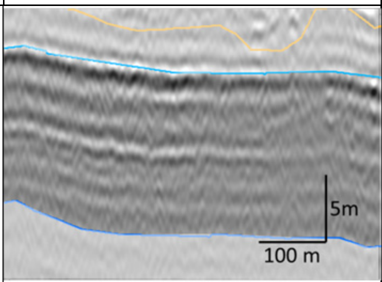  | Heterogeneous character. Semi-transparent to transparent character. Parallel low amplitude and low frequency seismic reflectors present locally. | ▪ Geotechnically heterogeneous unit<br>▪ Internal seismic reflectors do not correlate with geotechnical data |
| E4 | 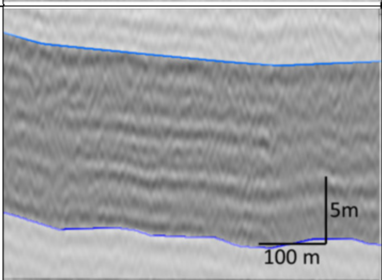  | Semi-transparent to transparent character. Parallel, low to medium amplitude and low frequency seismic reflectors present locally. | ▪ Geotechnically homogenous unit<br>▪ The upper and lower boundaries not always clear, especially below Buitenbank 3<br>▪ The unit is slightly thicker, up to approximately 14 m, in the north-central part of Investigation Area III |
| E5 | 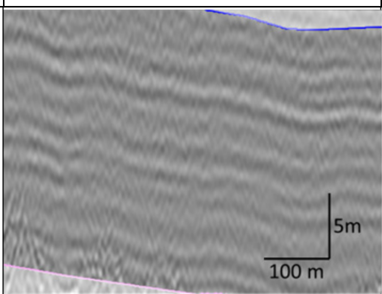  | Semi-transparent to transparent character. Semi-parallel to parallel, low to medium amplitude continuous to discontinuous internal reflectors are present locally. Some seismic reflectors at the base show onlap on the underlying Dongen Formation. | ▪ Geotechnically homogenous unit<br>▪ The base correlates with moderately strong continuous reflector |
| F1 | 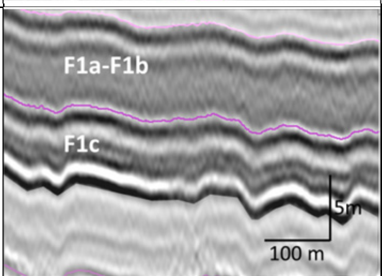  | Variable across the Investigation Area III. Vertical succession of three seismic facies/sub-units:<br>1) upper part - continuous, parallel weak reflectors;<br>2) middle part - seismically transparent to very weak parallel reflectors ;<br>3) lower part - regular sequence of strong continuous parallel reflectors in the western part and weak continuous parallel reflectors in the eastern part. | ▪ Geotechnically heterogeneous unit, subdivided into three sub-units<br>▪ The base of Unit F1b correlates with the onset of strong continuous, parallel reflectors<br>▪ Polygonal faulting |

| Unit | Image | Seismic Character | Comments |
|---|---|---|---|
| F2 | 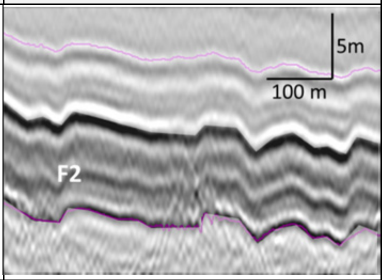  | Semi-transparent to transparent character. Locally parallel, discontinuous, low amplitude reflectors. | ▪ Not distinguishable from the overlying Unit F1c in the eastern part of the Investigation Area III<br>▪ Maximum thickness in the western part of Investigation Area III |
| F3 | 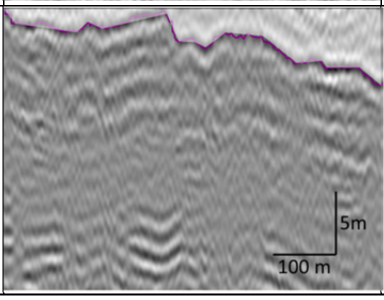  | Semi-transparent to transparent character. Locally parallel, discontinuous, low amplitude reflectors. | ▪ Polygonal faulting in the upper part<br>▪ The top correlates with strong continuous reflector |

**Notes:**
- Presented images are for guidance only. The annotated cross sections on Plates 3-7 to 3-15 present further information on seismic character in relation to geotechnical units.
- Frequency (high or low) gives a qualitative indication of the number of distinct seismic reflectors over a given depth interval, i.e. high frequency indicates a large(r) number of seismic reflectors within a unit.
- Amplitude (high, intermediate, low) gives an indication of reflector strength, which in turn is related to physical properties such as density and seismic velocity of soil.
- The geotechnical description of the units and unit thickness are presented in Table 3-4.

## 3.5 Geotechnical Units

Table 3.4 summarises stratigraphy interpreted for Investigation Area III (i.e. to approximately 115 m below LAT) in terms of geotechnical units.

**Table 3.4: Stratigraphy – Investigation Area III**

| Unit | Sub-Unit | Depth to Base of Unit[1)] [m LAT] | Vertical Thickness Range[2)] [m] | Soil Description | Comments |
|---|---|---|---|---|---|
| A | - | 27 to 44 | >0 to 16 | Very loose to very dense fine to medium SAND, locally (slightly) gravelly and with beds of (slightly) gravelly clayey sand or clay | ▪ At base locally a thin to medium bed of gravelly clayey sand or clay<br>▪ Base of Unit A generally follows trend of sandbanks<br>▪ Variable thickness due to bedforms (i.e. sand waves) at seafloor |
| B | - | 36 to 68 | >0 to 29 | Medium dense to very dense fine to medium SAND, locally (slightly) gravelly | ▪ Irregular surface at base - erosional<br>▪ Channels and scour hollows present mostly in central part of Investigation Area III<br>▪ Thickness largest at sandbank and major sand dunes |

| Unit | Sub-Unit | Depth to Base of Unit[1)] [m LAT] | Vertical Thickness Range[2)] [m] | Soil Description | Comments |
|---|---|---|---|---|---|
| E1 | - | - | 0 to 14 | Medium dense to dense fine SAND, locally silty, locally (very) clayey, locally with beds of glauconitic sand | ▪ Present in the most northern part of Investigation Area III<br>▪ Dipping gently (0.5°) to NE<br>▪ Unit truncated by Unit B within Investigation Area III<br>▪ Unit spatially varies in soil conditions<br>▪ Unit contains locally beds with high CPT friction ratio, indicating glauconite content |
| E2 | - | 41 to 52 | | Medium dense clayey fine SAND | ▪ Present in the northern part of Investigation Area III<br>▪ Dipping gently (0.5°) to NE<br>▪ Unit truncated by Unit B within Investigation Area III<br>▪ Unit spatially varies in soil conditions<br>▪ Soil conditions of Unit E2 are comparable with Units E1 and E3 |
| E3 | - | 43 to 66 | 0 to 16 | Medium dense to very dense silty fine to medium SAND, locally clayey, locally with beds of glauconitic sand | ▪ Present in northern half of Investigation Area III<br>▪ Dipping gently (0.5°) to NE<br>▪ Unit truncated by Unit B within Investigation Area III<br>▪ Unit spatially varies in soil conditions<br>▪ Unit contains locally beds with high CPT friction ratio, indicating glauconite content |
| E4 | - | 40 to 82 | 0 to 18 | Very dense fine to medium SAND | ▪ Present in northern half of Investigation Area III<br>▪ Dipping gently (0.5°) to NE<br>▪ Unit truncated by Unit B within Investigation Area III<br>▪ Scour hollow removed locally part of unit<br>▪ Maximum thickness in central and northern part of Investigation Area III<br>▪ Unit characterised by high CPT $q_c$ values (low penetration or refusals) |
| E5 | E5a | - | 0 to 34 | Dense to very dense (slightly) silty fine SAND, locally very silty | ▪ Present over almost entire Investigation Area III<br>▪ Dipping gently (0.5°) to NE<br>▪ Unit truncated by Unit B within Investigation Area III |
| | E5b | 40 to 113 | | Medium dense to dense silty fine SAND, locally with beds of glauconitic sand | ▪ Present over almost entire Investigation Area III<br>▪ Dipping gently (0.5°) to NE<br>▪ Unit truncated by Unit B within Investigation Area III<br>▪ Unit contains locally beds with high CPT friction ratio, indicating glauconite content |

| Unit | Sub-Unit | Depth to Base of Unit[1)] [m LAT] | Vertical Thickness Range[2)] [m] | Soil Description | Comments |
|---|---|---|---|---|---|
| F1 | F1a | - | 0 to 11 | Very stiff to hard (slightly/very) sandy CLAY with thin to medium beds of (very) sandy clay or (very) clayey sand, locally with pockets of sand | ▪ Present over almost entire Investigation Area III<br>▪ Dipping gently (0.5°) to NE<br>▪ Unit truncated by Unit B within Investigation Area III |
| | F1b | 46 to 119 | | Hard very sandy CLAY; Locally SILT | ▪ Present over almost entire Investigation Area III<br>▪ Dipping gently (0.5°) to NE<br>▪ Unit truncated by Unit B within Investigation Area III |
| | F1c | - | 10 to 16 | Stiff to very stiff (sandy) CLAY, fissured | ▪ Present over entire Investigation Area III<br>▪ Dipping gently (0.5°) to NE<br>▪ Unit truncated by Unit B within Investigation Area III<br>▪ Fissures coincide with faulted interval on MCS data |
| F2 | - | 58 to 133 | | Dense to very dense becoming medium dense to dense clayey or silty SAND, locally with a bed of very clayey sand | ▪ Present over entire Investigation Area III<br>▪ Dipping gently (0.5°) to NE |
| F3 | - | - | - | Very stiff to hard CLAY, fissured at top, locally with pockets of sand | ▪ Present over entire Investigation Area III<br>▪ Dipping gently (0.5°) to NE<br>▪ Fissures coincide with faulted interval on MCS data |

**Notes:**
- LAT = relative to LAT
- 1) Depths and thicknesses based on geophysical and geotechnical data
- 2) Thickness range can be influenced by dipping strata, where unit is truncated by base of Unit B

<u>Geotechnical Unit A</u> is interpreted as the Southern Bight Formation (Holocene). The Southern Bight Formation consists of the Bligh Bank Member and the Buitenbanken Member (Balson et al., 1991a). The older Buitenbanken Member has been reworked and incorporated in the Bligh Bank Member. The geotechnical data do not allow distinguishing the Southern Bight Formation. The Holocene sediments are interpreted to be deposited over a relatively flat surface (possibly a tidal flat of Pleistocene age). This surface appears as a semi-planar seismic reflection on MCS data. A thin layer of gravelly lag deposits can be locally present at the base of Unit A. The unit is generally thin (less than 5 m) but is locally thicker below the crests of the major sand dunes and below Buitenbank 3. The maximum thickness of Unit A is approximately 16 m. The depth to base and thickness maps of Unit A (refer to Plates 3-17 and 3-25) show apparent linear morphological structures indicating that this top unit is highly influenced by seafloor topography, especially the Buitenbank 3.

<u>Geotechnical Unit B</u> is interpreted to represent Pleistocene sediments. The expected Pleistocene formations at Borssele WFZ are the Eem Formation and probably locally the Kreftenheye Formation on top. The Kreftenheye Formation is generally coarser grained than the Eem Formation, while the Eem Formation is more clayey and contains marine shells and shell fragments (Rijsdijk, 2013). The

fluvial deposits of the Kreftenheye Formation have been interpreted to reach the Borssele WFZ just in the north (i.e. WFS I and IV) and an isolated patch within the Investigation Area III (Rijsdijk, 2013). The sediments of the marine Eem Formation can be partially reworked and incorporated in the Kreftenheye Formation. The available geotechnical data do not allow for distinguishing between the Eem and Kreftenheye Formations.

Unit B in the Borssele Wind Farm Zone is thin in comparison to the Pleistocene strata further north on the Dutch shelf of the North Sea. This is due to the relative position of the Borssele WFZ at the margin of the North Sea Basin. Therefore, eustatic sea level fluctuation during the Pleistocene glaciations resulted in erosion and non-deposition. The base of Unit B (Pleistocene) is an erosion surface, which locally incises deeply in the underlying strata. These local incisions are referred to as scour hollows (Le Bot et al., 2005; Liu et al., 1993). The scour hollows are probably associated with marine currents, rather than fluvial processes. The infill of these scour hollows results in much thicker (up to tens of metres) Pleistocene strata. The Pleistocene infill of the scour hollows and paleo-channels contains (marine) shells and shell fragments.

Geotechnical Unit B shows diffraction hyperbola in the SBP data. This might be indicative for local accumulation of coarse material, e.g. boulders. Boulders, however, are not expected as ice sheets did not reach the Borssele Wind Farm Zone during the Pleistocene glaciations and there are no nearby sources for the boulders. The hyperbola might reflect patches of gravel that act as a larger body.

Geotechnical Units C and Unit D are absent in Investigation Area III.

Geotechnical Unit E is interpreted as the Tongeren Formation (Upper Eocene to Lower Oligocene) and consists of several Members (i.e. Geotechnical Units E1 to E5). The unit consists of fine sand, interbedded with silty (or clayey) sand, locally with thin to medium beds of (sandy) clay. Unit E is interpreted as deposited on the shelf in a shallow marine sedimentary environment in water depths of maximum few tens of meters (De Man, 2006; De Lugt, 2007). Vertical changes in sediment properties and composition (sand versus clay content) through the unit are related to sea level fluctuations in the marginal (restricted) marine setting of the southern North Sea Basin.

Geotechnical Unit E contains glauconite, with locally increased proportions (described as beds of glauconitic sand). Glauconitic grains are sand-size clay aggregates, which can easily deform under mechanical stress (Van Alboom et al., 2012). The glauconite content was examined and confirmed by visual inspection of the soil samples. Glauconite may also be inferred from high sleeve friction values in the CPT data.

Unit E is subdivided into Units E1 to E5, based on their geotechnical properties. Units E1 to E3 display a large range of cone resistance values with no apparent lateral continuity. This underlines the spatial heterogeneity of the deposits. Units E1 and E2 are characterised in general by a higher fines fraction, represented by a mixture of sand and clay with no apparent lateral continuity. The MCS seismic reflection data show a strong, laterally continuous seismic reflector that correlates with base of laterally continuous layer of sandy clay to locally clayey sand. This layer has been interpreted as Geotechnical Unit E2.

Geotechnical Unit E2 (Watervliet Clay Member) is known to include local lignite or brown coal (TNO, 2013b). The lignite probably marks the onset of a transgressive phase. Seismic amplitude anomalies on MCS data may be interpreted as lignite or shallow gas within the Tongeren Formation.

Units E3, E4 and E5 represent the Bassevelde Sand Member (Bassevelde 3 Sand, Bassevelde 2 Sand, and Bassevelde 1 Sand). These units show significant mica content. Unit E3 is characterised by internal spatial (lateral and vertical) variability in CPT cone resistance. The changes in CPT cone resistance are not always correlated with the MCS seismic reflection data. Unit E4 can be easily identified from CPT cone resistance, which is high (with frequent CPT refusals).

Internal seismic reflections can be observed within Unit E5 (Plates 3-7 to 3-12 and 3-15). Locally, the internal seismic reflections have a positive correlation with changes in CPT character, e.g. increased friction ratio. In other areas, similar seismic reflections occur without associated changes in CPT character. This situation precludes clear differentiation of Unit E5 based on seismic character. The unit is divided into Sub-units E5a and E5b based on geotechnical properties alone, with Sub-unit E5b containing a higher fines fraction (silt and clay) and including beds interpreted as glauconitic sand.

Unit E shows medium amplitude reflections towards the base of the seismostratigraphic unit. Some seismic reflection at the base shows onlap on the underlying Dongen Formation. The transition from the Dongen Formation to the Tongeren Formation (i.e. from Unit E to Unit F) probably coincided with the Pyrenean orogeny at the transition from Bartonian to Priabonian (late Eocene).

Geotechnical Unit F is interpreted as the Dongen Formation (Eocene). It consists of very stiff to hard clay (Units F1 and F3, Onderdijke and Zomergem Members, respectively), interrupted by a layer of clayey sand (Unit F2, Buisputten Member). Unit F is considered to have been deposited on the shelf in an open marine sedimentary environment with a shallowing-up sequence (Le Bot, 2005; De Lugt, 2007). Changes in sediment composition and properties between the sub-units are probably related to sea level fluctuations in the marginal marine setting of the southern North Sea Basin.

Sub-unit F1c and Unit F3 consist predominantly of fat clay and Sub-unit F1b consists typically of lean clay. Sub-unit F1a and, locally, transition intervals between the (sub)units (i.e. gradual unit boundaries) comprise more sand fraction. As a result, Sub-unit F1a, and locally, base of Sub-unit F1c and upper part of Unit F3 consist of lean clay.

Unit F shows higher amplitude reflections than the overlying Tongeren Formation (Unit E), characterising a clay-dominated unit. The base of Sub-unit F1b can be easily traced in the MCS reflection seismic data over the entire Investigation Area III. The base of Sub-unit F1c does not always correlate with the seismic boundary.

Unit F corresponds with the top of a zone of small-scale faulting inferred from the MCS data (Plates 3-7 to 3-15). Sub-unit F1c (Onderdijke Member) and the upper part of Unit F3 (Zomergem Member) show platy/fissured structures. The platy/fissured structures disappear at depth within Unit F3.

### 3.6 Seafloor Conditions and Site Use

Within Investigation Area III, the water depth and seafloor morphology will change over time as a result of seabed mobility. The reader should consult Deltares (2014) for detailed information. Comments are as follows:

- Sand dunes and sandbanks form prominent seabed features in the Borssele WFZ. Three scales of bedforms can be distinguished for the Borssele WFZ: (tidal) sand banks, sand waves and mega ripples. The largest sand bank in Investigation Area III is referred to as Buitenbank 3. Refer to Appendix 1, document titled Site Characterisation, for general descriptions of these bedforms;
- The migration rate of sand waves varies within the Borssele WFZ. In addition, the overall tidal current direction varies in the Borssele WFZ resulting in bed load parting, e.g. scour zones due to divergent patterns in sediment transport;
- Existing and future windfarms can act as hydraulic obstructions, which can contribute to changing conditions and hence changes in the general scheme of scour and deposition;
- The Borssele WFZ can be subject to multi-year fluvial sediment starvation or surplus.

The reader should consult Fugro (2015a and b), REASeuro (2014), Vestigia (2014) for detailed information about site use. Site use refers to past and/or present activities that can put constraints on the development of the wind farm site. Examples of site use are seafloor objects and activities having led to disturbance of soil. Comments are as follows:

- Seafloor objects within the Borssele WFZ include cables and pipelines, wrecks and other debris. Not all cables and pipelines are in service;
- The cables and pipelines may be partially or completely buried by the mobile bedforms. Fugro has no information on trenching and whether mattresses or rock dumps have been used locally for stabilisation of the cables and pipelines. Trenching and post-lay stabilising activities cause disturbance of the seabed;
- Trawl fishing and UXO clearance activities have been documented for the Borssele WFZ. This will have caused local disturbance of the seabed;
- There is evidence of prehistoric human activities in the southern North Sea (Hijma et al., 2011). This relates to the last ice age (Weichselian glacial). Sea level was much lower than today and a land bridge existed between the British Isles and mainland Europe. The archaeological desk study showed a low probability of encountering well-preserved early prehistoric sites with in situ remains within Borssele Wind Farm Zone (Vestigia, 2014). The probability of soil disturbance due to prehistoric human activities is assessed negligible for Investigation Area III;
- The geotechnical site investigation (Plate 1-2) used intrusive geotechnical investigation techniques (i.e. borehole drilling and in situ testing). These activities cause local soil disturbance.

## 4. GEOTECHNICAL PARAMETER VALUES

Sections A and B summarise geotechnical parameter values reported and explained in Fugro Report Nos. N6083/01 and N6083/02 (refer to Plate 1-2). Appendix 1 also includes explanations of these parameter values. Note that the presented information represents measured values and derived values, as defined in Appendix 1, document titled Geotechnical Analysis.

Section A presents location-specific parameter values versus depth:

- Normalized CPT parameters;
- CPT net cone resistance;
- Water content and Atterberg limits;
- Soil unit weights;
- Particle size distribution;
- Relative density;
- Undrained shear strength;
- Shear wave velocity and shear modulus at small strain.

Section B presents the same parameter values but grouped versus depth per geotechnical unit. A single plate presents data for a maximum of 12 geotechnical locations. Locations have been grouped on a geographical basis and divided over four plates (a to d). The geographical basis follows the north-east dipping Tertiary strata, with increasingly older sediments subcropping below Unit B towards the SW. This geographical approach aims for a particular unit within one group to be presented at approximately the same depths. Several locations that terminated within Unit B were grouped together and presented on one plate (d).

## 5. COMMENTS ON SITE SUITABILITY

### 5.1 Potential Site-specific Hazards

Table 5.1 and Plate 5-1 present identified geological features and processes, which can be potential hazards (geohazards) for structures, i.e. windfarm support structures (foundations) and cables. Sections 5.2 to 5.6 provide supplementary information for consideration. The information is high level (indicative) and not intended to be complete or comprehensive.

Table 5.1 includes approximate and subjective probability indicators for hazards: Negligible (N), Low (L) and High (H) probability. Appendix 1, document titled “Geotechnical Analysis”, explains these expressions. An indicator between brackets, e.g. [L], refers to a situation considering appropriate measures for countering the hazard, such as source elimination, avoidance, implementation of a barrier, minimising consequences and design for the hazard (ISO, 2015).

The following example illustrates how to read Table 5.1 and Sections 5.2 to 5.6.

Adverse metocean conditions can change an initially flat seafloor to an uneven seafloor. This situation is assessed to have High probability H (no brackets) for affecting placement of a gravity base foundation (GBS), if no appropriate measures for countering the hazard are implemented. The example situation is assigned Negligible probability [N] (with brackets) when appropriate measures for countering the hazard are implemented, such as scour-resistant seabed preparation and availability of equipment for removal of loose sediments immediately before GBS placement.

**Table 5.1: Potential Site-specific Hazards and Constraints for Structures – Investigation Area III**

| Geological Feature / Hazard Type | Occurrence Area | Constraints on Structure | Constraint/ Hazard Probability | | | | |
|---|---|---|---|---|---|---|---|
| | | | Pile Foundations (PL) | Jack-up Platforms (JU) | Gravity Base Foundations (GB) | Suction Caisson Foundations (SC) | Cables (CB) |
| Bedforms (sand waves and mega ripples) / uneven seafloor | Entire Investigation Area III | ▪ JU: uneven seafloor causing high and non-uniform VHM loading on legs<br>▪ GB: seabed preparation required for foundation stability/ stiffness<br>▪ SC: installation requires initial embedment before applying suction (hydraulic leaks)<br>▪ CB: trenching on locally steep slope | N [N] | L [N] | H [N] | L [N] | L [N] |
| Migrating bedforms / mobile seabed sediments | Entire Investigation Area III | ▪ All: exposure or burial of structure due to local, general and regional scour or sedimentation affecting structure stability, structure stiffness<br>▪ CB: exposure or burial of cable affecting thermal characteristics; spanning of cable leading to snagging from trawling or anchoring | H [L] | L [N] | H [N] | H [L] | L [N] |

| Geological Feature / Hazard Type | Occurrence Area | Constraints on Structure | Constraint/ Hazard Probability | | | | |
|---|---|---|---|---|---|---|---|
| | | | Pile Foundations (PL) | Jack-up Platforms (JU) | Gravity Base Foundations (GB) | Suction Caisson Foundations (SC) | Cables (CB) |
| Loose to medium dense sand | Locally in Unit A | ▪ All: cyclic loading of seabed and structure can affect structure stability and structure stiffness<br>▪ CB: liquefaction of sand can affect cable flotation and thermal characteristics | H [N] | L [N] | H [N] | L [N] | L [N] |
| Alternation of sand and clay (inferred from depositional environment) | Infill of paleo-channels and scour hollows (Unit B) | ▪ JU: possibility of leg punch through followed by jack-up instability<br>▪ SC: installation may not be feasible | N [N] | L [N] | N [N] | H [L] | N [N] |
| Very dense sand/ hard clay | ▪ Unit E4 – very dense sands<br>▪ Unit F- stiff to hard clays and very dense sands | ▪ PL: early refusal of pile installed by impact driving<br>▪ SC: limited penetration<br>▪ CB: trenching difficulties | L [N] | N [N] | N [N] | L [L] | L [N] |
| Gravels and cobbles | ▪ Base of Unit A and Unit B – locally with gravels and cobbles | ▪ PL: possibly early refusal or damage and pile verticality issues during pile driving<br>▪ SC: limited penetration<br>▪ CB: trenching difficulties | L [N] | N [N] | N [N] | L [L] | L [N] |
| Glauconitic sands | Units E1, E3 and E5 - locally present | GB: differential settlement of foundation due to compressibility of glauconitic grains in sand | N [N] | N [N] | L [N] | N [N] | N [N] |
| Fissured clay structures | Units F1c and F3 | GB: low foundation bearing/sliding resistance compared to soil with no fissures | N [N] | N [N] | L [N] | N [N] | N [N] |
| Swelling clays | Unit F | None | N [N] | N [N] | N [N] | N [N] | N [N] |
| Lignite (brown coal), | Unit E1 and E2 (not proven) | None | N [N] | N [N] | N [N] | N [N] | N [N] |
| Shallow gas, Biogenic gas charged sediments | Unit B (not proven) | ▪ GB: possible migration of shallow gas into skirted compartment, affecting foundation performance<br>▪ SC: possible migration of shallow gas into caisson, affecting foundation performance | N [N] | N [N] | L [N] | L [N] | N [N] |
| Polygonal faulting | Units F1 and F3 | GB: low foundation bearing/sliding resistance compared to soil with no faulting | N [N] | N [N] | L [N] | N [N] | N [N] |

| Geological Feature / Hazard Type | Occurrence Area | Constraints on Structure | Constraint/ Hazard Probability | | | | |
|---|---|---|---|---|---|---|---|
| | | | Pile Foundations (PL) | Jack-up Platforms (JU) | Gravity Base Foundations (GB) | Suction Caisson Foundations (SC) | Cables (CB) |
| Existing structures, e.g. pipeline and cable | Refer to Section 3.6 | ▪ All: avoid immediate area around object for structures<br>▪ All: potentially disturbed ground compared to areas away from object<br>▪ All: potential interruption in hydraulic flow regime affecting scour and soil deposition processes<br>▪ CB: avoidance may not be practicable; windfarm power/communication cables will require crossings | H [N] | H [N] | H [N] | H [N] | H [L] |
| Future structures, e.g. wind farm itself (wind turbines, transformer station, cables) and structures in region | Entire Investigation Area III | All: potential interruption in hydraulic flow regime affecting scour and soil deposition processes | L [N] | N [N] | L [N] | L [N] | L [N] |

N : Negligible probability
L : Low probability
H : High probability

- Descriptor (without brackets): approximate and subjective probability for a situation with no specific measures countering the hazard
- Descriptor between brackets [...]: approximate and subjective probability for a situation considering appropriate measures for countering the hazard

## 5.2 Pile Foundations

Pile foundations are assessed feasible at Investigation Area III.

Design and installation should take account of the constraints given in Table 5.1.

The assessment considers monopiles, jacket piles and piles for tripod support structures installed by impact driving.

Where applicable, driven pile installation should be sufficiently robust for penetration of very dense sand layers and/or concentrations of gravels and cobbles in the subsurface.

## 5.3 Jack-up Platforms

Use of jack-up platforms for temporary works is assessed feasible at Investigation Area III.

Jack-up placement and operation should take account of the constraints given in Table 5.1. Particularly, scour and soil deposition around spudcans should be allowed for:

- Scour can make periodic re-levelling of the jack-up necessary, can increase required leg length and can reduce spudcan soil resistance after jack-up placement;
- Risk assessments for jack-up siting should consider structural integrity for a scenario of strongly non-uniform soil support of a spudcan, i.e. moment loading;
- Soil deposition around and on a spudcan will affect required extraction forces.

## 5.4 Gravity Base Foundations

Gravity base foundations are assessed feasible at Investigation Area III.

Design and installation should take account of the constraints given in Table 5.1.

Design should consider seabed preparation to allow for potentially uneven and sloping seafloor and to allow for loose to medium dense sands that can show significant loss of strength upon cyclic loading.

Any seabed preparation (levelling, ground improvement) prior to foundation installation should consider potential disruption by rapid scour and sedimentation processes.

It is assessed that scour protection will be required, except if the foundation base or skirt tip can be positioned below long-term scour levels.

High mechanical stresses applied to glauconitic sands can cause significant deformation and compression of the glauconitic grains, compared to quartz-type particles. Increased differential settlement of a gravity base foundation may result.

## 5.5 Suction Caisson Foundations

Suction caisson foundations are assessed marginally feasible at Investigation Area III.

Design considerations should include:

- Constraints given in Table 5.1;
- Sloping and uneven seafloor conditions that can affect caisson penetration and required sealing for initial suction application;
- Relatively shallow water depths that will limit allowable suction pressures, in particular at Buitenbank 3;
- Scour protection, except if the caisson skirt tip can be positioned well below long-term scour levels;
- Measures for caisson penetration taking account of interbedded sand/clay layers, concentrations of gravels and cobbles.

It may be possible to design for difficult conditions for caisson penetration. Tjelta (2015) provides guidance.

## 5.6 Cables

Installation and operation of cables are assessed feasible at Investigation Area III.

Design and installation should take account of the constraints given in Table 5.1.

Design should consider long-term scour and soil deposition processes for thermal response and any minimum cable burial requirements.

Activities for cable burial should consider potential disruption by rapid scour and sedimentation processes.

## 6. REFERENCES

Balson, P.S. (1989), “Neogene Deposits of the UK Sector of the Southern North Sea (51°-53° N), in Henriet, J.P., De Moor, G. and De Batist, M. (Eds.), The Quaternary and Tertiary Geology of the Southern Bight, North Sea, Ministry of Economic Affairs. Belgian Geological Survey, Brussels, pp. 119-135.

Balson, P.S., Laban, C., Schüttenhelm, R.T.E., Paepe, R. and Baeteman, C. (1991a), “Ostend, Sheet 51˚N - 02˚E, Sea Bed Sediments and Holocene Geology”, British Geological Survey, Keyworth and Rijks Geologische Dienst, Haarlem, 1:250,000 Series.

Balson, P.S., Laban, C., Frantsen, P.J., Parker, N., Henriet, J.P., de Batist, M. and Mostaert, F. (1991b), “Ostend, Sheet 51˚N - 02˚E, Solid Geology”, British Geological Survey, Keyworth, Rijks Geologische Dienst, Haarlem and Belgische Geologische Dienst, Brussels, 1:250,000 Series.

Cameron, T.D.J., Laban, C. and Schüttenhelm, R.T.E. (1989), "Upper Pliocene and Lower Pleistocene Stratigraphy in the Southern Bight of the North Sea", in Henriet, J.P., De Moor, G. and De Batist, M. (Eds.), The Quaternary and Tertiary Geology of the Southern Bight, North Sea, Ministry of Economic Affairs,. Belgian Geological Survey, Brussels, pp. 119-135.

Cameron, T.D.J., Crosby, A., Balson, P.S., Jeffery, D.H., Lott, G.K., Bulat, J. and Harrison, D.J. (1992), "The Geology of the Southern North Sea", London, HMSO, British Geological Survey United Kingdom Offshore Regional Report.

CRUX Engineering BV, ediGEO, GisSense (2014), “Borssele Wind Farm Zone - Geological Desk Study”, Report No. RE14254a4, Rev 4.

Dehandschutter, B., Sintubin, M., Vandenberghe, N., Vandycke, S., Gaviglio, P. and Wouters, L. (2002), "Fracture Analysis in the Boom Clay (URF, Mol, Belgium)", Degryse, P.; Sintubin, M. (Eds.), Contributions to the Geology of Belgium and Northwest Europe: Proceedings of the first Geologica Belgica International Meeting, Leuven, 11-15 September 2002, Leuven University Press, Leuven, Aardkundige Mededelingen, 12, pp. 245-248.

De Jager, J. (2007), “Geological Development”. In: Wong, T.E., Batjes, D.A.J. & Jager, J. de (eds.). Geology of the Netherlands, Royal Netherlands Academy of Arts and Sciences, Amsterdam, pp. 5-26.

De Lugt, I.R. (2007), “Stratigraphical and Structural Setting of the Palaeogene Siliciclastic Sediments in the Dutch Part of the North Sea Basin”, PhD Thesis, Utrecht University, the Netherlands, 112 pp.

De Man, E. (2006), “Benthic Foraminifera Biofacies Analysis and Stable Isotopes of the Middle Eocene to Oligocene Successions in the Southern North Sea Basin. Tools for Stratigraphy and for Reconstruction of Extreme Climate Changes. Unpublished PhD Thesis, University of Leuven, Belgium, 375 pp.

Deltares (2014), "Site Studies Wind Farm Zone Borssele: Morphodynamics of Borssele Wind Farm Zone", Report Number 1210520-000.

Deltares (2015), "Metocean Studies for the Borssele Wind Farm Zone, Site I", Report Number 1210467-000.

Fugro (2015a), “Geophysical Site Investigation Survey, Dutch Continental Shelf, North Sea, Borssele Wind Farm Development Zone, Wind Farm Site III”, Fugro Report No. GH157-R1, Revision A, dated 14 August 2015.

Fugro (2015b), “Geophysical Site Investigation Survey, Dutch Continental Shelf, North Sea, Borssele Wind Farm Development Zone, Wind Farm Site IV”, Fugro Report No. GH157-R2, Revision A, dated 14 August 2015.

Fugro (2015c), “Geological Ground Model, Wind Farm Site I, Borssele Wind Farm Zone, Dutch Sector North Sea”, Fugro Report No. N6016/05, Issue 3, dated 15 July 2015.

Fugro (2015d), “Geological Ground Model, Wind Farm Site II, Borssele Wind Farm Zone, Dutch Sector North Sea”, Fugro Report No. N6016/06, Issue 4, dated 3 August 2015.

Fugro (2015e),”Geological Ground Model, Wind Farm Site I & II, Borssele Wind Farm Zone, Dutch Sector North Sea”, GIS database and metadata files, dated 19 August 2015.

Horseman, S.T., Winter, M.G. and Entwistle, D.C. (1987), "Geotechnical Characterization of Boom Clay in relation to the Disposal of Radioactive Waste", Office for Official Publications of the European Communities, Luxembourg, VIII, 86 pp. (Report / Commission of the European Communities - Nuclear Science and Technology ; EUR 10987).

Hijma, M.P., Cohen, K.M., Roebroeks, W., Westerhoff, W.E., Busschers, F.S. (2011), “Pleistocene Rhine–Thames Landscapes: Geological Background for Hominin Occupation of the Southern North Sea Region”, Journal of Quaternary Science, Vol. 27, No. 1, pp. 17-39.

ISO International Organization for Standardization (2015), “General Principles on Reliability for Structures”, International Standard ISO 2394:2015.

Jacobs, P. and De Coninck, F. (1992), “Qualitative Clay Mineralogy of the Middle and Upper Eocene in the North-Western Belgium”, Tertiary Research, Vol. 14, No. 2, pp. 61-72.

Jacobs, P. and De Batist, N. (1996), “Sequence Stratigraphy and Architecture on a Ramp-type Continental Shelf: the Belgian Palaeogene”, in De Batist, N. and Jacobs, P. (Eds.), Geology of Siliciclastic Shelf Seas, Geological Society Special Publications, No. 117, pp. 23-48.

Laban, C., Schüttenhelm, R.T.E., Balson, P.S., Baeteman, C. and Paepe, R. (1992), “Ostend, Sheet 51˚N - 02˚E, Quaternary Geology”, British Geological Survey, Keyworth, Rijks Geologische Dienst, Haarlem and Belgische Geologische Dienst, Brussels, 1:250,000 Series.

Laban, C. (1995), “The Pleistocene Glaciations in the Dutch Sector of the North Sea: A Synthesis of Sedimentary and Seismic Data”, PhD Thesis, University of Amsterdam.

Le Bot, S., Van Lancker, V., Deleu, S., De Batist, M., Henriet, J. and Haegeman, W. (2005), "Geological Characteristics and Geotechnical Properties of Eocene and Quaternary Deposits on the Belgian Continental Shelf: Synthesis in the Context of Offshore Wind Farming." Netherlands Journal of Geosciences – Geologie en Mijnbouw, Vol. 84, No. 2, pp. 147-160.

Liu, A.C., De Batist, M., Henriet, J.P. and Missiaen, T. (1993), “Plio-Pleistocene Scour Hollows on the Southern Bight of the North Sea”, Netherlands Journal of Geosciences – Geologie en Mijnbouw, Vol. 71, No. 3, pp. 195-204.

Maréchal, R. (1993), “A New Lithostratigraphic Scale for the Palaeogene of Belgium”. Bulletin de la Societé Belge de Geologie, Vol. 102, No. 1-2, pp. 215-229.

Overeem, I. (2002), “Process-Response Simulation of Fluvio-deltaic Stratigraphy”, PhD Thesis, Delft University of Technology, Department of Applied Earth Sciences.

Periplus (2015), Email titled “20150828 Borssele Sector 5 – coordinates”, dated 28 August 2015 from J.W. van Etten (Periplus) to F. Ruhs and W. Sotthewes (Fugro) containing confirmation on locations of WFS III, WFS IV, WFS V and Substation Beta.

REASeuro (2014), “Site Data Borssele Wind Farm Zone - Unexploded Ordnance (UXO) - Desk Study”, Project No. 71992, 9 December 2014.

Rijksdienst voor Ondernemend Nederland (2015), “Site Studies Borssele Wind Farm Zone – Boundaries & Coordinates Wind Farm Zone”, Final Issue, 23 July 2015.

Rijsdijk, K.F., Passchier, S., Weerts, H.J.T., Laban, C., Van Leeuwen, R.J.W., and Ebbing, J.H.J. (2005), “Revised Upper Cenozoic Stratigraphy of the Dutch Sector of the North Sea Basin: towards an Integrated Lithostratigraphic, Seismostratigraphic and Allostratigraphic Approach”, Netherlands Journal of Geosciences – Geologie en Mijnbouw, Vol. 84, No. 2, pp. 129-146.

Rijsdijk, K.F. (2013), “Reconstructing Quaternary Rhine–Meuse Dynamics in the Southern North Sea: Architecture, Seismolithofacies Associations and Malacological Biozonation”, Journal of Quaternary Science, Vol. 28, No. 5, pp. 1-14.

Schittekat, J., Henriet, J.P. and Vandenberghe, N. (1983), “Geology and Geotechnique of the Scheldt Surge Barrier. Characteristics of an Overconsolidated Clay”, Proceedings of 8th International Harbour Congress, KVIV.

Tjelta, T.I. (2015) “The Suction Foundation Technology”, Meyer, V. (ed.), Frontiers in Offshore Geotechnics III: proceedings of the Third International Symposium on Frontiers in Offshore Geotechnics (ISFOG 2015), Oslo, Norway, 10-12 June 2015, CRC Press, Boca Raton, pp. 85-93.

TNO (2013a), “Rupel Formatie”, in: Lithostratigrafische Nomenclator van de Ondiepe Ondergrond, https://www.dinoloket.nl/rupel-formatie (accessed April 30, 2015).

TNO (2013b), “Formatie van Tongeren”, in Lithostratigrafische Nomenclator van de Ondiepe Ondergrond, https://www.dinoloket.nl/formatie-van-tongeren (accessed 30 April 2015).

TNO (2013c), “Formatie van Dongen”, in Lithostratigrafische Nomenclator van de Ondiepe Ondergrond. https://www.dinoloket.nl/formatie-van-dongen (accessed 30 April 2015).

TNO (2013d), Lithostratigrafische Nomenclator van de Diepe Ondergrond, versie 2013, https://www.dinoloket.nl/nomenclature-deep (Accessed 30 April 2015).

TNO (2014), “Geological and Geohydrological Characterization of the Boom Clay and its Overburden”, OPERA-PU-TNO411.

Van Adrichem Boogaert, H.A., Kouwe, W.F.P. (Eds.), (1997), “Stratigraphic Nomenclature of the Netherlands”, Revision and Update by RGD and NOGEPA. Mededelingen Rijks Geologische Dienst 50. NITG-TNO, Haarlem.

Van Alboom, G., Dupont, H., Maertens, J. and Haelterma, K. (2012), "Glauconiethoudende Zanden", Geotechniek, Vol. 16, No. 2, pp. 32-37.

Vandenberghe, N., Van Simaeys, S., Steurbaut, E., Jagt, J.W.M. and Felder, P.J. (2004), “Stratigraphic Architecture of the Upper Cretaceous and Cenozoic along the Southern Border of the North Sea Basin in Belgium”, Netherlands Journal of Geosciences - Geologie en Mijnbouw, Vol. 83, No. 3, pp.155-171.

Vestigia (2014), “Borssele Wind Farm Zone, North Sea, The Netherlands - Archaeological Desk Study, Risk Assessment and Recommendations”, Report No. V1199, Final Version 2.0, dated 28 November 2014.

Ziegler, P.A. (1990), “Geological Atlas of Western and Central Europe”, 2nd and compl. rev. ed., Shell Internationale Petroleum Maatschappij, The Hague.

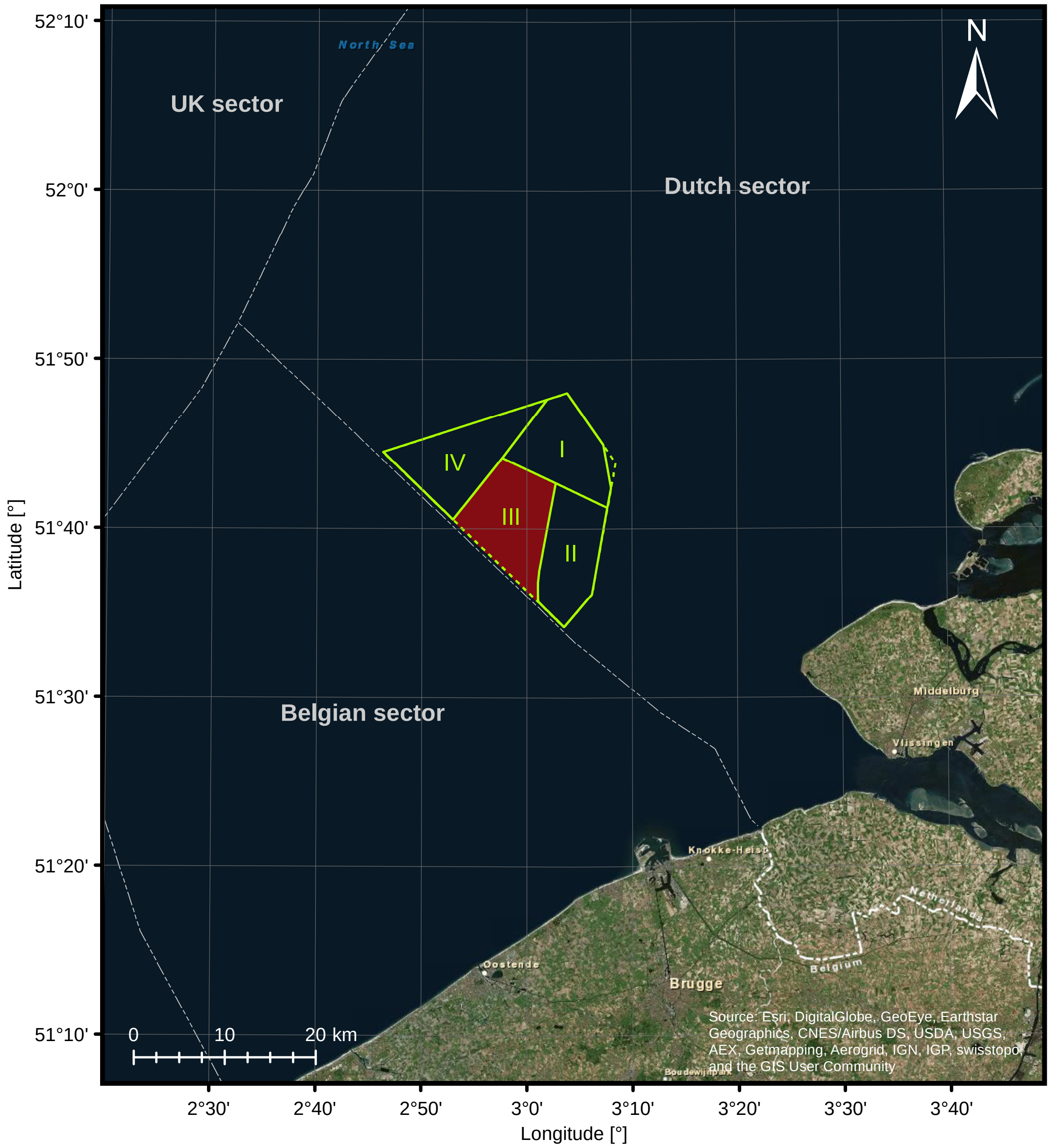


Investigation Area III (subject of this report)

Outline of Borssele Wind Farm Zone

Outline Borssele Investigation Area (Roman numeral indicates area number)

Maritime Boundary

Ellipsoid: GRS 1980
Datum: ETRS 1989

Printed: 11/16/2015 8:43:27 AM

**VICINITY MAP**

BORSSELE WIND FARM ZONE, WFS III – DUTCH SECTOR, NORTH SEA

| Report Number | Title | Contents |
|---|---|---|
| N6083/01 | Geotechnical Report - Investigation Data - Geotechnical Borehole Locations<br>Wind Farm Site III<br>Borssele Wind Farm Zone - Dutch Sector, North Sea | Geotechnical data including geotechnical logs, results from downhole (seismic) cone penetration tests and results from geotechnical laboratory tests. |
| N6083/02 | Geotechnical Report - Investigation Data - Seafloor In Situ Test Locations<br>Wind Farm Site III<br>Borssele Wind Farm Zone - Dutch Sector, North Sea | Geotechnical data including interpreted geotechnical logs and results from seafloor cone penetration tests. |
| N6083/03 | Geotechnical Report - Investigation Data - Geotechnical Borehole Locations<br>Wind Farm Site IV<br>Borssele Wind Farm Zone - Dutch Sector, North Sea | Geotechnical data including geotechnical logs, results from downhole (seismic) cone penetration tests and results from geotechnical laboratory tests. |
| N6083/04 | Geotechnical Report - Investigation Data - Seafloor In Situ Test Locations<br>Wind Farm Site IV<br>Borssele Wind Farm Zone - Dutch Sector, North Sea | Geotechnical data including interpreted geotechnical logs and results from seafloor cone penetration tests. |
| N6083/05 | Geological Ground Model<br>Wind Farm Site III<br>Borssele Wind Farm Zone - Dutch Sector, North Sea | Geological ground model including, stratigraphy, lateral soil variability, geohazards, basic geotechnical parameter values and assessment of geotechnical suitability of selected types of structures. |
| N6083/06 | Geological Ground Model<br>Wind Farm Site IV<br>Borssele Wind Farm Zone - Dutch Sector, North Sea | Geological ground model including, stratigraphy, lateral soil variability, geohazards, basic geotechnical parameter values and assessment of geotechnical suitability of selected types of structures. |
| N6083/07 | Geotechnical Report - Laboratory Test Data<br>Wind Farm Sites III & IV<br>Borssele Wind Farm Zone - Dutch Sector, North Sea | Results of advanced static and cyclic laboratory tests. |



**LIST OF FUGRO REPORTS**

BORSSELE WIND FARM ZONE, WFS III – DUTCH SECTOR, NORTH SEA

| | | |
|---|---|---|
| **DGPS Geodetic Parameters** | | |
| Datum | | WGS84 (World Geodetic System 1984) |
| Ellipsoid | | WGS84 (World Geodetic System 1984) |
| Semi-Major Axis, a | | 6378137.000 m |
| Inverse Flattening, 1/f | | 298.257223563 |
| **Transformation Parameters** (from WGS84 to Local Grid) | | For transformation parameter details refer to:<br>N6083/01 (see Plate 1-2);<br>N6083/02 (see Plate 1-2), and;<br>Fugro (2015a) |
| **Local Grid Geodetic Parameters** | | |
| Datum | | ETRS89 (European Terrestrial Reference System 1989) |
| Ellipsoid | | GRS80 (Geodetic Reference System 1980) |
| Semi-Major Axis, a | | 6378137.000 m |
| Inverse Flattening, 1/f | | 298.257222101 |
| **Local Projection Parameters** | | |
| Projection | | Universal Transverse Mercator |
| UTM Zone | | 31 North |
| Central Meridian (CM) | | 03° 00’ 00” E |
| Latitude of Origin | | 00° 00’ 00” N |
| False Easting | | 500 000 m |
| False Northing | | 000 000 |
| Scale Factor on CM | | 0.9996 |
| Units | | metres |
| **Example Coordinates** | | |
| Local grid coordinates | Easting | 503819.64 m |
| | Northing | 5738442.18 m |
| Local geographical coordinates | Latitude | 51° 47’ 48.5644” N |
| | Longitude | 03° 03’ 19.3986” E |
| WGS84 geographical coordinates | Latitude | 51° 47’ 48.5803” N |
| | Longitude | 03° 03’ 19.4204” E |



**GEODETIC PARAMETERS**

BORSSELE WIND FARM ZONE, WFS III – DUTCH SECTOR, NORTH SEA

**DESIGN APPROACH**

| | |
|---|---|
| General Procedure: | – Refer to documents titled "Site Characterisation" and "Geotechnical Analysis" presented in Appendix 1<br>– According to ISO 19900 (2013) Section 5 |
| Premise(s): | – Design basis verification required; site characterisation is for conceptual phase and suitable for use in FEED, subject to a separate verification of the design basis |
| Type of Structure(s) and Purpose: | Multiple foundation concepts are considered (e.g. pile(s), caisson, gravity base), jack-up and cable; final foundation design to be selected at later stage |
| Location: | – Dutch Sector of the North Sea<br>– Refer to Plate 1-1 for site location |

**DATA COVERAGE**

| | |
|---|---|
| Met-ocean Data: | Not considered: outside scope of Project Specification |
| Environmental Baseline: | Not considered: outside scope of Project Specification |
| UXO Information: | Refer to Section 3.6 of Main Text, titled Seafloor Conditions and Site Use |
| Archaeological Information: | Not considered: outside scope of Project Specification |
| Geological Data: | Refer to Section 3 of Main Text, titled Geological Ground Model and to Plate 3-4 |
| Geophysical Survey Data: | – Single- and Multi-Beam Echo Sounder (SBES and MBES), Side Scan Sonar (SSS), Magnetometer (MAG); line spacing: approximately 100 m between main lines and 500 m or 1000 m between cross lines<br>– Sub-Bottom Profiler (SBP), pinger source; penetration: approximately 20 m bsf; line spacing: approximately 100 m between main lines and 500 m or 1000 m between cross lines<br>– 2D UHR Multi-Channel Seismic reflection data (MCS), sparker source; penetration: approximately 170 m bsf; line spacing: approximately 400 m between main lines and 500 m or 1000 m between cross lines; vertical resolution: 2 m, horizontal (along-line) resolution: 4 m |
| Geotechnical Data: | Refer to Section 3 of Main Text titled Geological Ground Model, Section 4 of Main Text titled Geotechnical Parameter Values and to Plate 3-4 |
| Monitoring Data: | None available for study |
| Physical Modelling Data: | None available to the authors of this document |

**SITE USE**

| | |
|---|---|
| Historic and Current Site Use: | Refer to Section 3.6 of Main Text, titled Seafloor Conditions and Site Use |
| Changes in Site Conditions since Data Acquisition: | Not known at time of issue of this report |



**DESIGN BASIS FOR SITE CHARACTERISATION**

BORSSELE WIND FARM ZONE, WFS III – DUTCH SECTOR, NORTH SEA

## SEAFLOOR CONDITIONS AND (SITE) HAZARDS

| | |
|---|---|
| Seafloor: | – Variable elevations, including potential for mobile seabed sediments, disturbance by geotechnical site investigation<br>– Structure(s) to be designed and positioned to suit as-found seafloor conditions<br>– Refer to Main Text for details |
| Local Scour: | Refer to Sections 3 and 5 of Main Text, titled Geological Ground Model and Comments on Site Suitability, respectively |
| General Scour: | Refer to Sections 3 and 5 of Main Text, titled Geological Ground Model and Comments on Site Suitability, respectively |
| Regional Scour: | To be considered |
| Low-Strength Seabed Soils: | Very loose SAND can be present at seafloor |
| Other (Site)Hazards: | Refer to Section 5 of Main Text, titled Comments on Site Suitability |
| Interpretive Limit(s): | – Assessment of seafloor conditions and (site) hazards results from interpretation of data available at the time of study<br>– Hazard identification can be based on reasonably-inferred understanding<br>– A hazard may remain undetected because of partial data coverage or detection limits of deployed tools |

## STRATIGRAPHIC SCHEMATISATION

| | |
|---|---|
| Ground Type(s): | Interbedded medium dense to very dense SAND and stiff to hard CLAY |
| Lateral Correlation of Ground Strata: | Refer to Section 3 of Main Text, titled Geological Ground Model |
| Vertical Correlation of Ground Strata: | Implicitly incorporated in stratigraphic schematisation and selection of other parameter values |
| Interpretive Limit(s): | – Stratigraphic schematisation results from interpretation of data available at the time of study<br>– Schematisation can be approximate because of partial data coverage or detection limits of deployed tools and an interface between strata may be more gradual than indicated |

## GEOTECHNICAL PARAMETERS

| | |
|---|---|
| Ground Description: | – According to document titled “Soil Description” presented in Appendix 1<br>– Based on BSI (1999) |
| Groundwater Pressure: | Assumed hydrostatic |
| Basic Physical Properties: | Refer to Sections A and B, titled Geotechnical Parameters |
| Stress/Strain Parameters: | Refer to Sections A and B, titled Geotechnical Parameters |
| Geo-thermal Parameters: | Not considered, geo-thermal setting assumed according to seasonal equilibrium |
| Interpretive Limit(s): | Level of detail and accuracy in interpretation of geotechnical parameter values depend on factors such as test data, sample size, quality, coverage, and availability of supplementary information such as geological understanding |



## REFERENCES


– BSI British Standards Institution (1999), "Code of Practice for Site Investigations", British Standard BS 5930:1999.

– ISO International Organization for Standardization (2013), “Petroleum and Natural Gas Industries - General Requirements for Offshore Structures”, International Standard ISO 19900:2013.

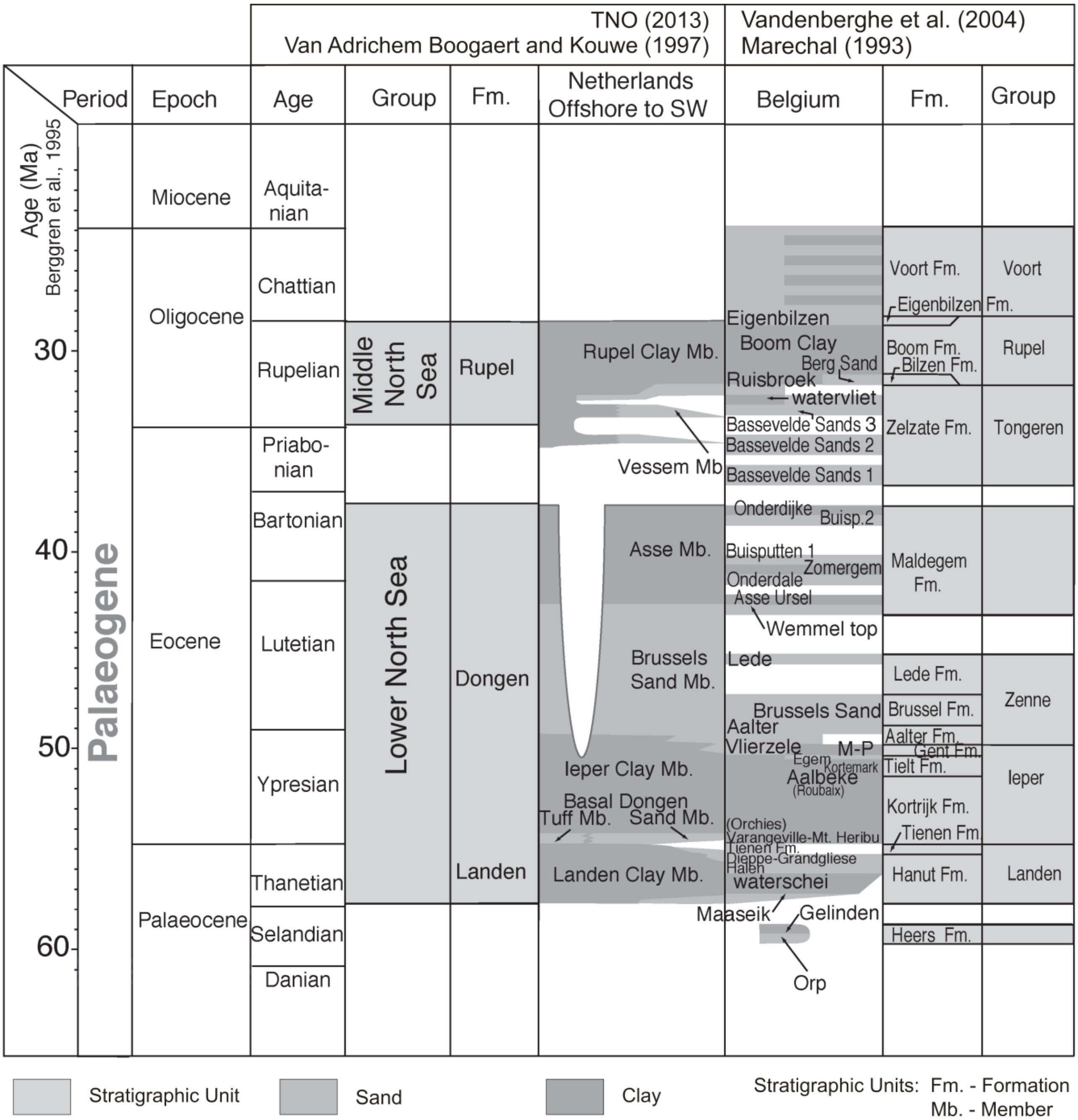


Simplified lithological correlation between the Netherlands offshore and Belgium.
Modified after De Lugt (2007).



**LITHOSTRATIGRAPHIC FRAMEWORK**
BORSSELE WIND FARM ZONE, WFS III – DUTCH SECTOR, NORTH SEA

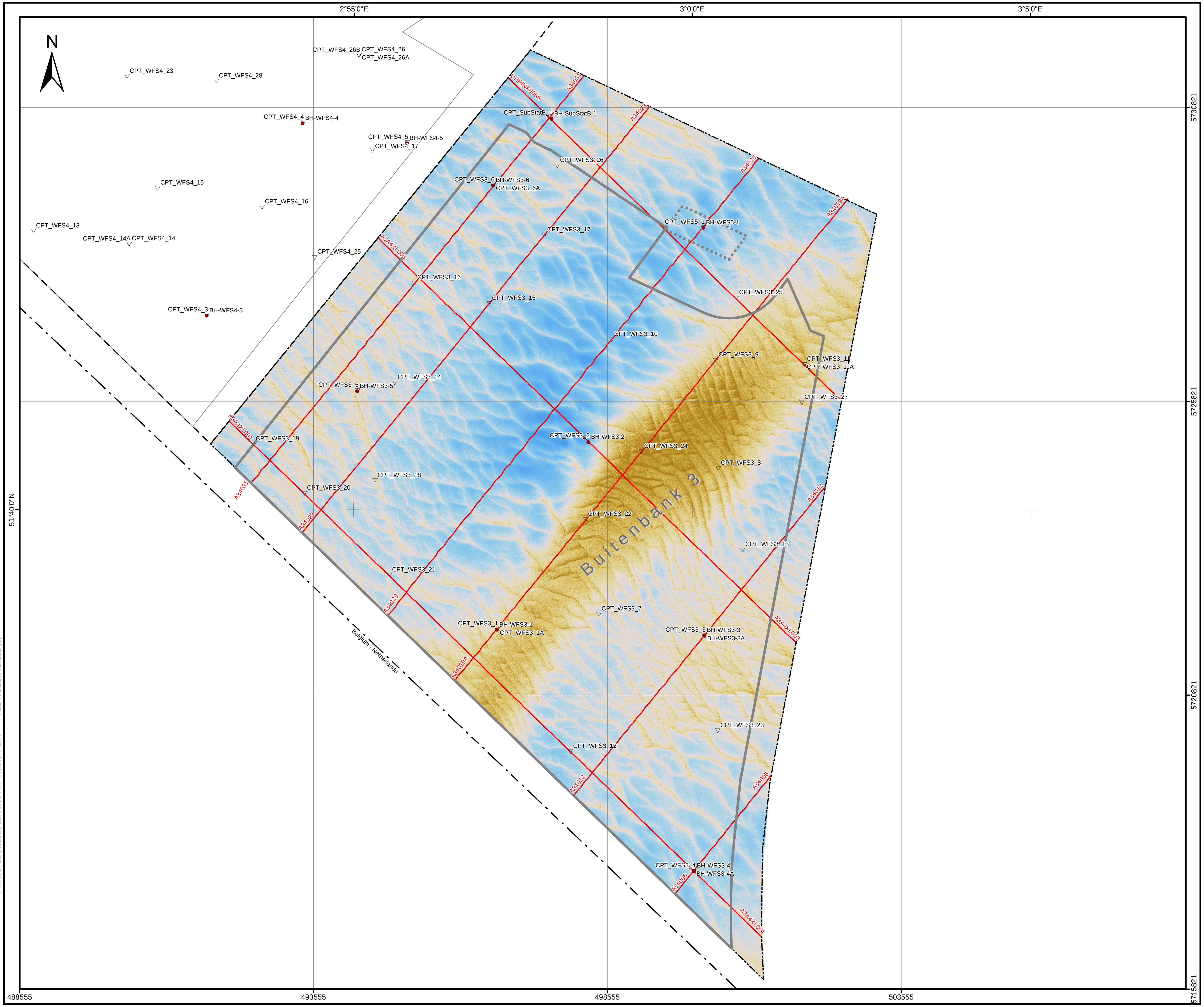


**LEGEND:**

- CPT location
- BH location
- Outline of WFS III
- Outline of WFS IV
- Outline of WFS V
- Investigation Area III
- Investigation Area IV
- Maritime boundary
- Section line of cross-section presented in the report

**Bathymetry [m below LAT]**

13, 17, 21, 25, 29, 33, 37, 41, 43

**NOTES:**
- Reproduced from Fugro (2015a and 2015b)
- Resolution cells 0.5 m x 0.5 m
- Data acquired by Multi-Beam Echo Sounder (MBES)

**GEODETIC PARAMETERS:**

| | |
|---|---|
| DATUM | ETRS89 |
| Ellipsoid | GRS80 |
| Semi major axis | a = 6 378 137.000 |
| Inverse flattening | 1/f = 298.257222101 |
| PROJECTION | UTM, Zone 31 North |
| Central Meridian (CM) | 3° 00' 00" E |
| Latitude of Origin | 0° 00' 00" N |
| False Easting | 500 000 m |
| False Northing | 000 000 m |
| Scale factor | 0.9996 |
| Units | metres/degrees |

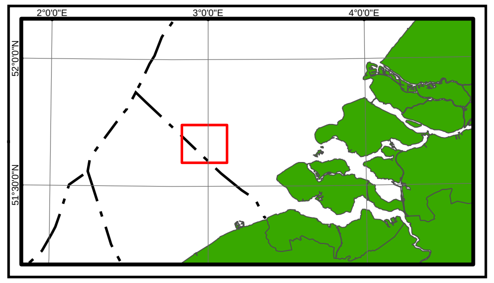

Rijksdienst voor Ondernemend Nederland (RVO)
Croeselaan 15, 3521 BJ, Utrecht - THE NETHERLANDS

Fugro
Prismastraat 4, 2631 RT, Nootdorp - THE NETHERLANDS

**BATHYMETRY**

**BORSSELE WIND FARM ZONE, WFS III**
**DUTCH SECTOR, NORTH SEA**

1:60,000
at original A3 page size
0 500 1,000 1,500 2,000 metres

FUGRO

Fugro Report No. N6083/05 | Issue 1 | Plate 3-4

Printed: 11/19/2015 11:00:09 AM Author: LHT FEBV/GEO/FIG/152 (0)

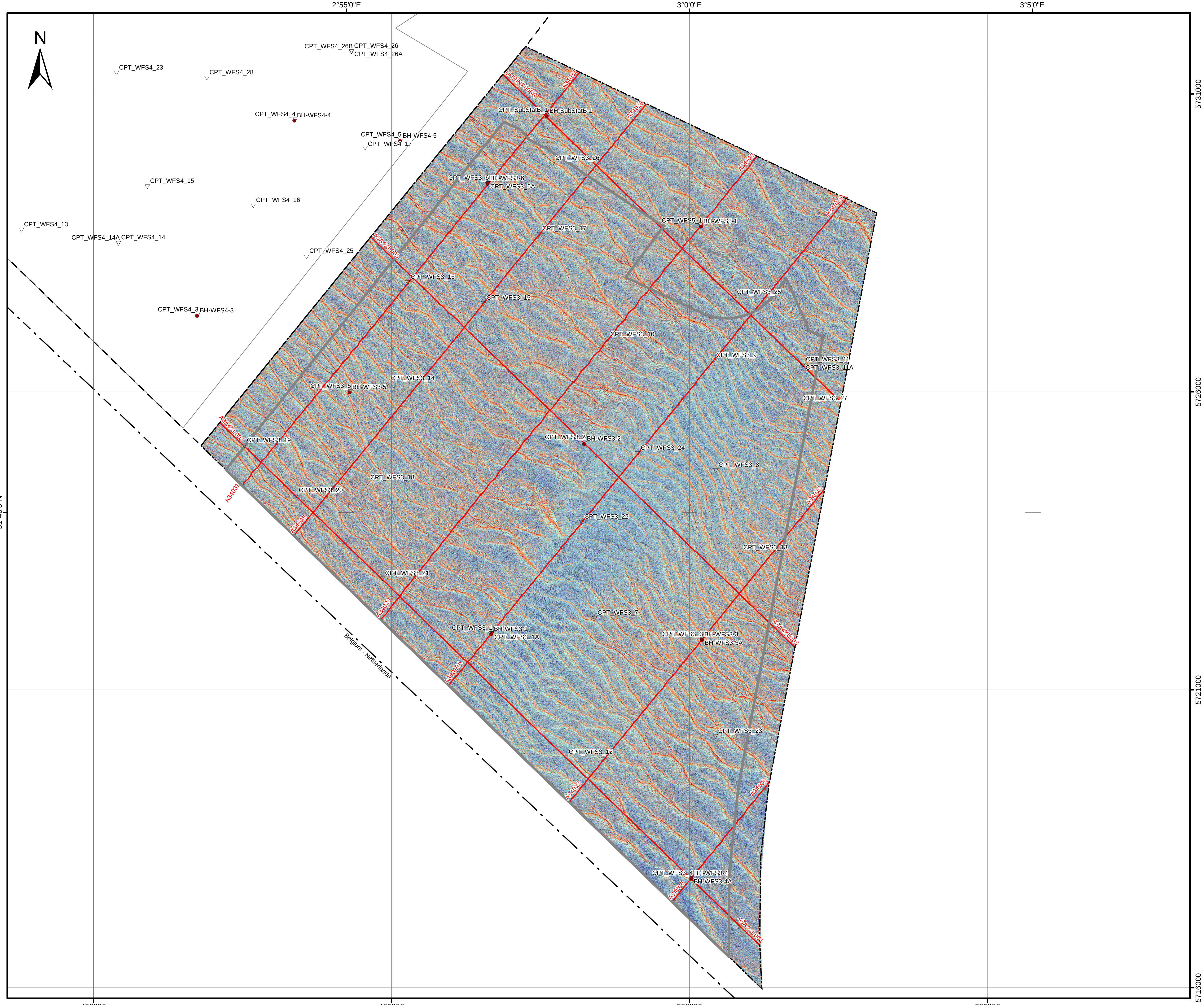


**LEGEND:**

- CPT location
- BH location
- Outline of WFS III
- Outline of WFS IV
- Outline of WFS V
- Investigation Area III
- Investigation Area IV
- Maritime boundary
- Section line of cross-section presented in the report

**Seafloor gradient [deg]**

- 0 - 2
- 2 - 5
- 5 - 8
- 8 - 15
- 15 - 60

**NOTES:**

- Seafloor gradient derived from bathymetry data
- Survey data acquired in 2015

**GEODETIC PARAMETERS:**

| | |
|---|---|
| DATUM | ETRS89 |
| Ellipsoid | GRS80 |
| Semi major axis | a = 6 378 137.000 |
| Inverse flattening | 1/f = 298.257222101 |
| PROJECTION | UTM, Zone 31 North |
| Central Meridian (CM) | 3° 00' 00" E |
| Latitude of Origin | 0° 00' 00" N |
| False Easting | 500 000 m |
| False Northing | 000 000 m |
| Scale factor | 0.9996 |
| Units | metres/degrees |

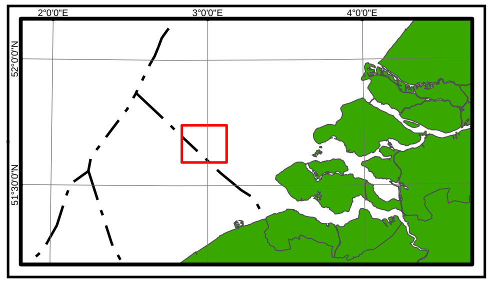


Rijksdienst voor Ondernemend Nederland (RVO)
Croeselaan 15, 3521 BJ, Utrecht - THE NETHERLANDS

Fugro
Prismastraat 4, 2631 RT, Nootdorp - THE NETHERLANDS

**SEAFLOOR GRADIENT**

**BORSSELE WIND FARM ZONE, WFS III, DUTCH SECTOR, NORTH SEA**

Scale 1:60,000
at original A3 page size

0 500 1,000 1,500 2,000 metres

| Fugro Report No. N6083/05 | Issue 1 | Plate 3-5 |
|---|---|---|

Printed: 11/19/2015 11:03:44 AM Author: LBH FEBV/GEO/FIG/152 (0)

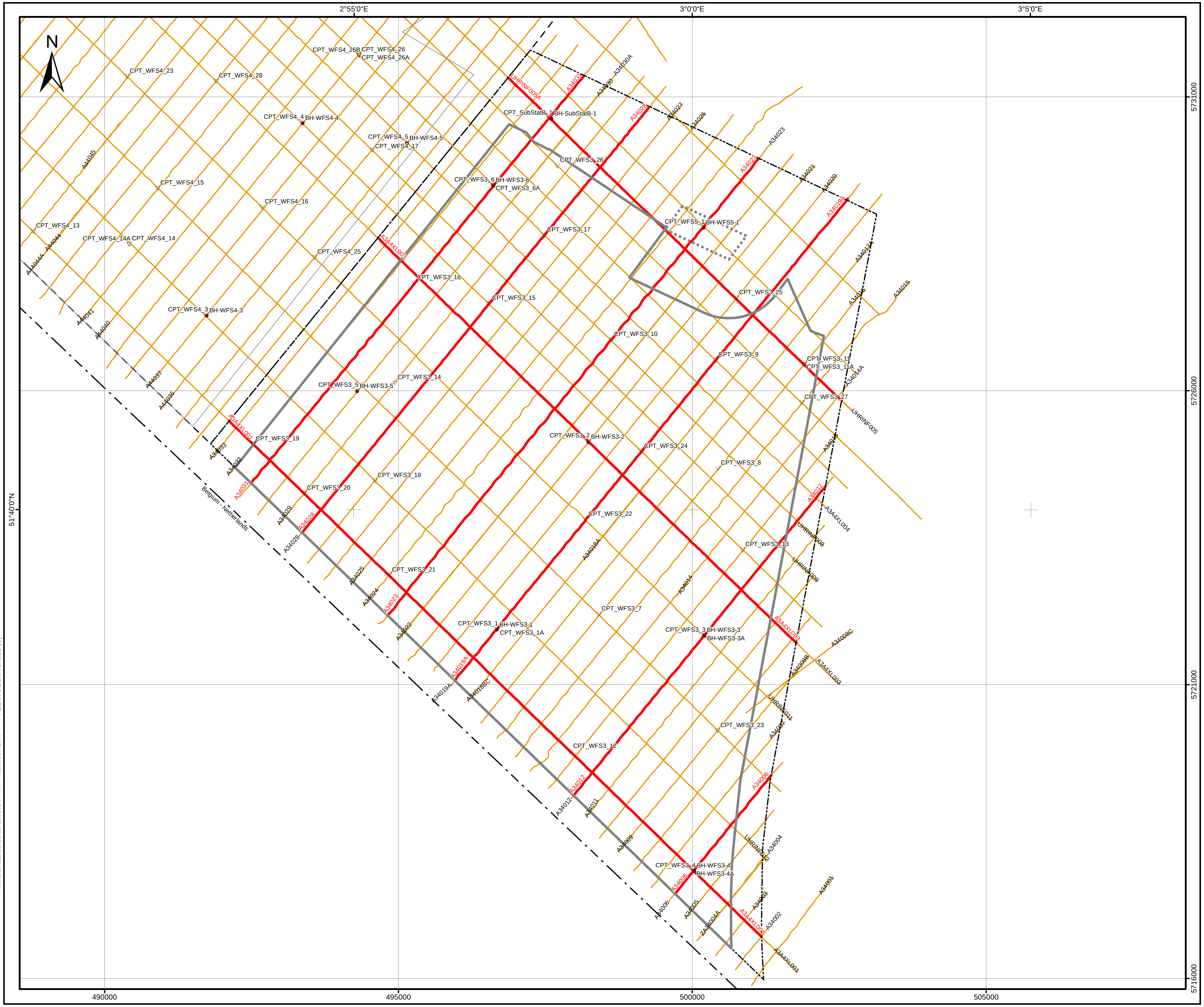


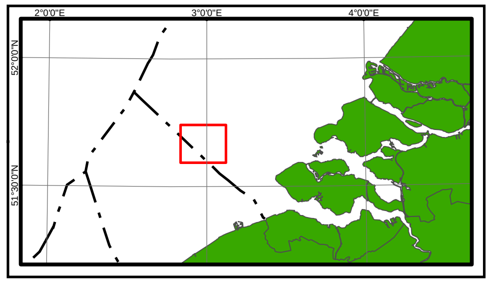


**LEGEND:**

- CPT location
- BH location
- Outline of WFS III
- Investigation Area III
- Outline of WFS IV
- Investigation Area IV
- Outline of WFS V
- Maritime boundary
- Line of cross-section as presented in the report
- 2D Ultra High Resolution Seismic (2DUHR) track line

**NOTES:**

- Data acquired by Fugro (2015a and 2015b)
- Section lines present part of track lines presented as cross-sections

**GEODETIC PARAMETERS:**

| | |
|---|---|
| DATUM | ETRS89 |
| Ellipsoid | GRS80 |
| Semi major axis | a = 6 378 137.000 |
| Inverse flattening | 1/f = 298.257222101 |
| PROJECTION | UTM, Zone 31 North |
| Central Meridian (CM) | 3° 00' 00" E |
| Latitude of Origin | 0° 00' 00" N |
| False Easting | 500 000 m |
| False Northing | 000 000 m |
| Scale factor | 0.9996 |
| Units | metres/degrees |

Rijksdienst voor Ondernemend Nederland (RVO)
Croeselaan 15, 3521 BJ, Utrecht - THE NETHERLANDS

Fugro
Prismastraat 4, 2631 RT, Nootdorp - THE NETHERLANDS

**2D UHR MULTI-CHANNEL SEISMIC TRACK LINES AND SECTION LINES**

**BORSSELE WIND FARM ZONE, WFS III, DUTCH SECTOR, NORTH SEA**

Scale 1:60,000
at original A3 page size

0 500 1,000 1,500 2,000 metres

| Fugro Report No. N6083/05 | Issue 1 | Plate 3-6 |
|---|---|---|

Printed: 11/18/2015 2:39:54 PM Author: LHT FEBV/GEO/FIG/152 (0)

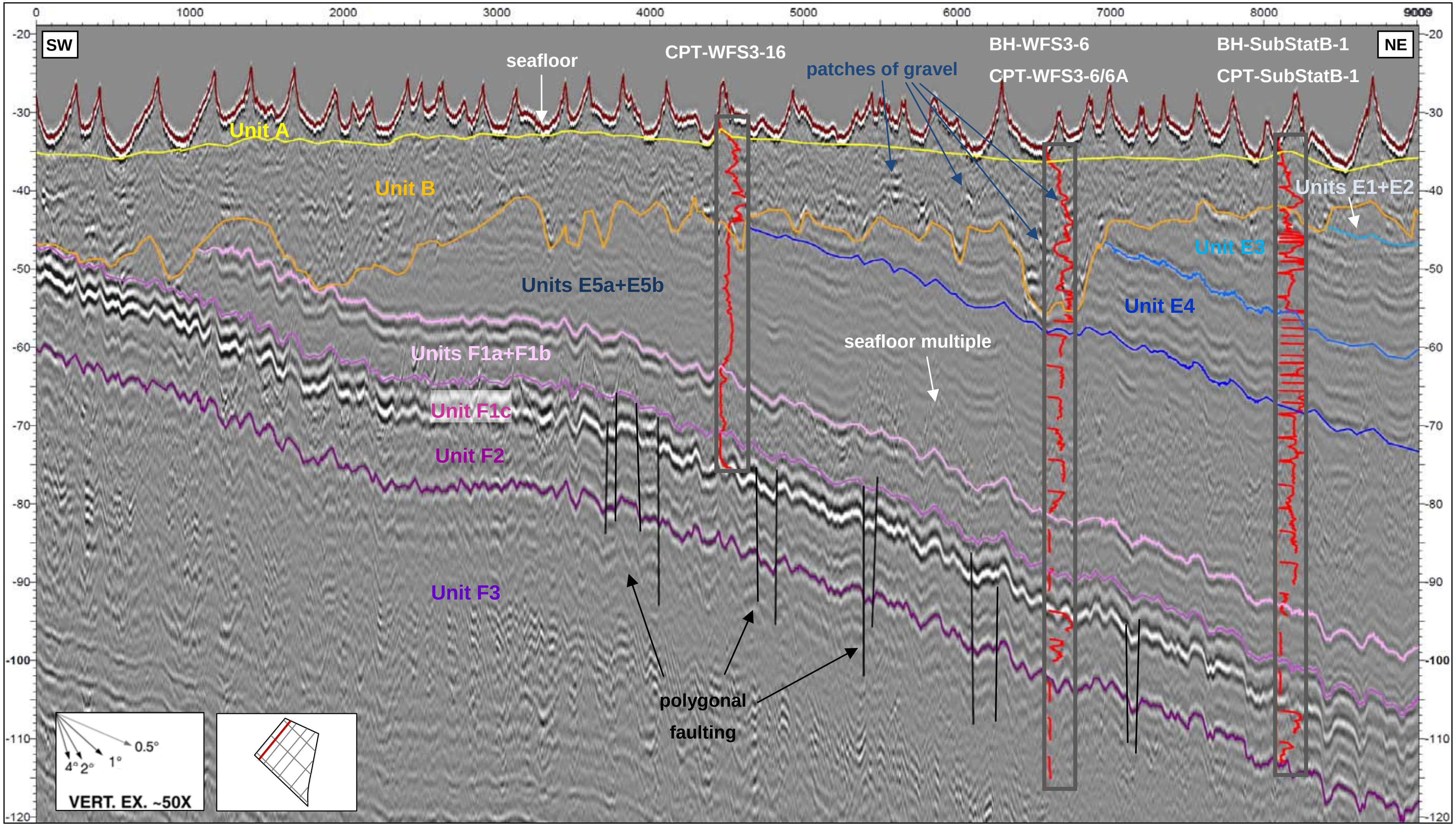


NOTE: Example of MCS line. Vertical scale is depth in metres below LAT. Horizontal scale is distance in metres. CPT cone resistance data (red line) for the geotechnical locations are projected on the cross section. Left side of the grey box marks the geotechnical location. The width of the box marks cone resistance values to 50 MPa. Location of the cross section is shown on Plate 3-6.

**CROSS SECTION – SECTION LINE A34031**

BORSSELE WIND FARM ZONE, WFS III – DUTCH SECTOR, NORTH SEA

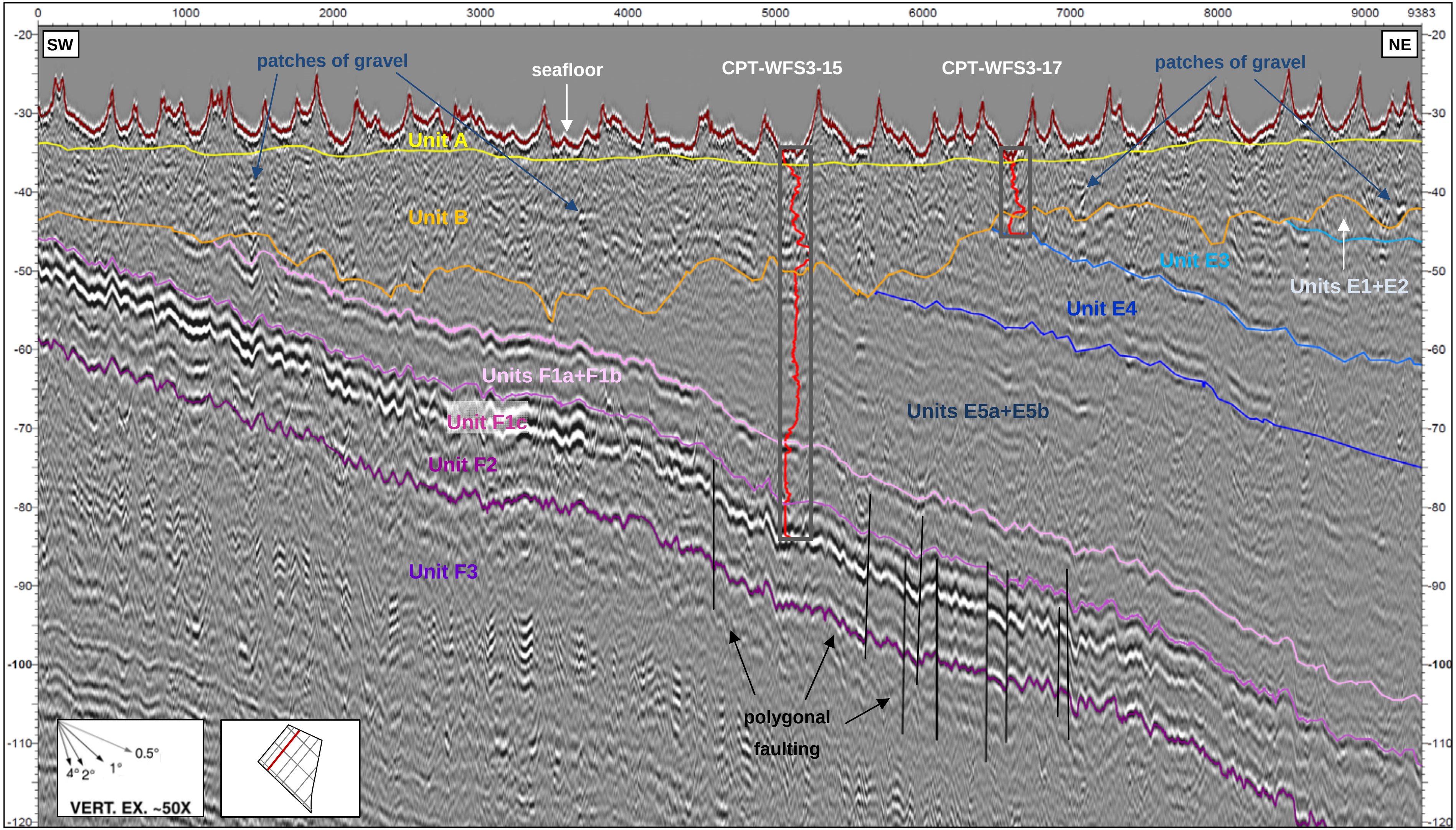


NOTE: Example of MCS line. Vertical scale is depth in metres below LAT. Horizontal scale is distance in metres. CPT cone resistance data (red line) for the geotechnical locations are projected on the cross section. Left side of the grey box marks the geotechnical location. The width of the box marks cone resistance values to 50 MPa. Location of the cross section is shown on Plate 3-6.

**CROSS SECTION – SECTION LINE A34028**

BORSSELE WIND FARM ZONE, WFS III – DUTCH SECTOR, NORTH SEA

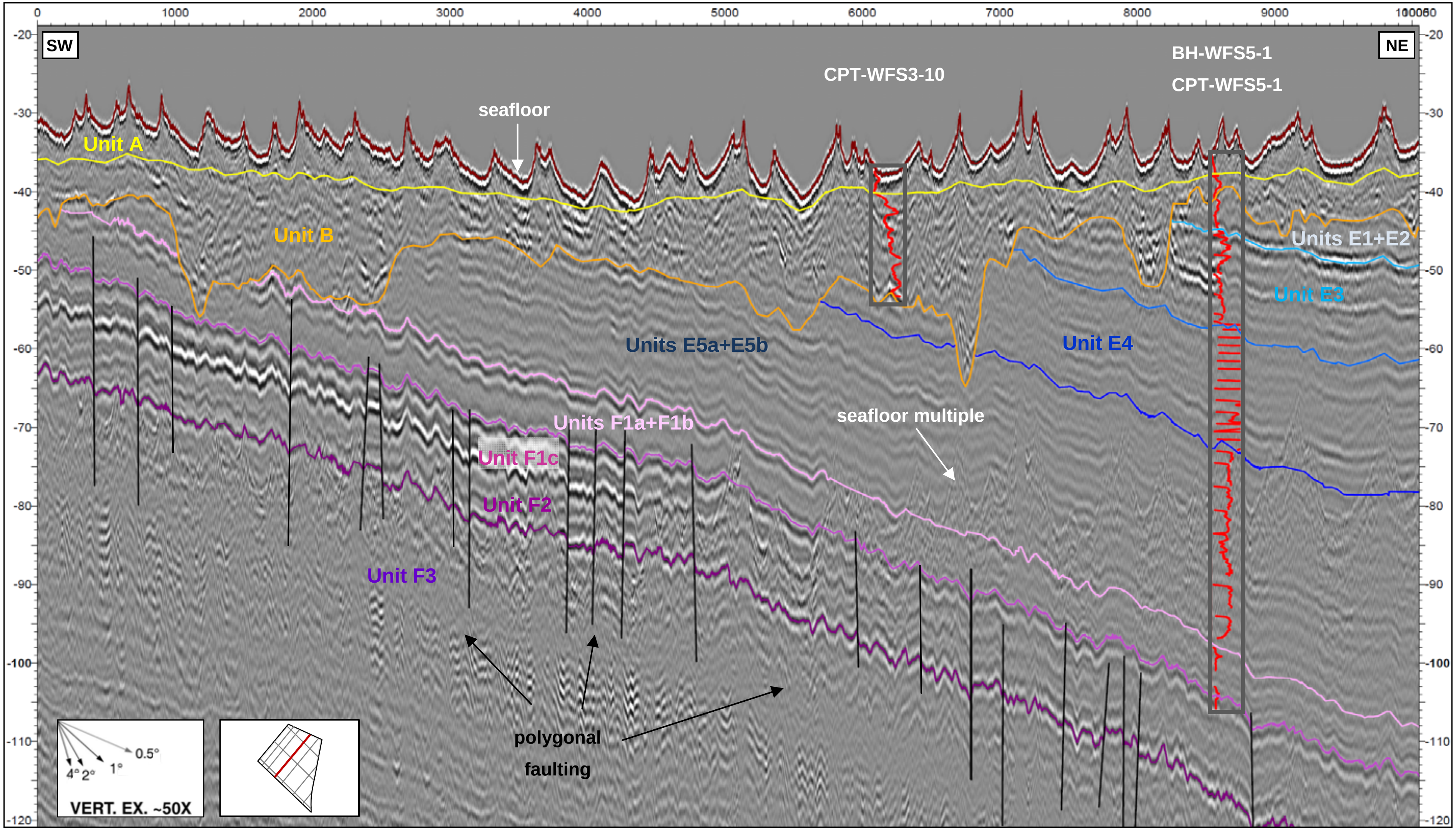


NOTE: Example of MCS line. Vertical scale is depth in metres below LAT. Horizontal scale is distance in metres. CPT cone resistance data (red line) for the geotechnical locations are projected on the cross section. Left side of the grey box marks the geotechnical location. The width of the box marks cone resistance values to 50 MPa. Location of the cross section is shown on Plate 3-6.

**CROSS SECTION – SECTION LINE A34023**

BORSSELE WIND FARM ZONE, WFS III – DUTCH SECTOR, NORTH SEA

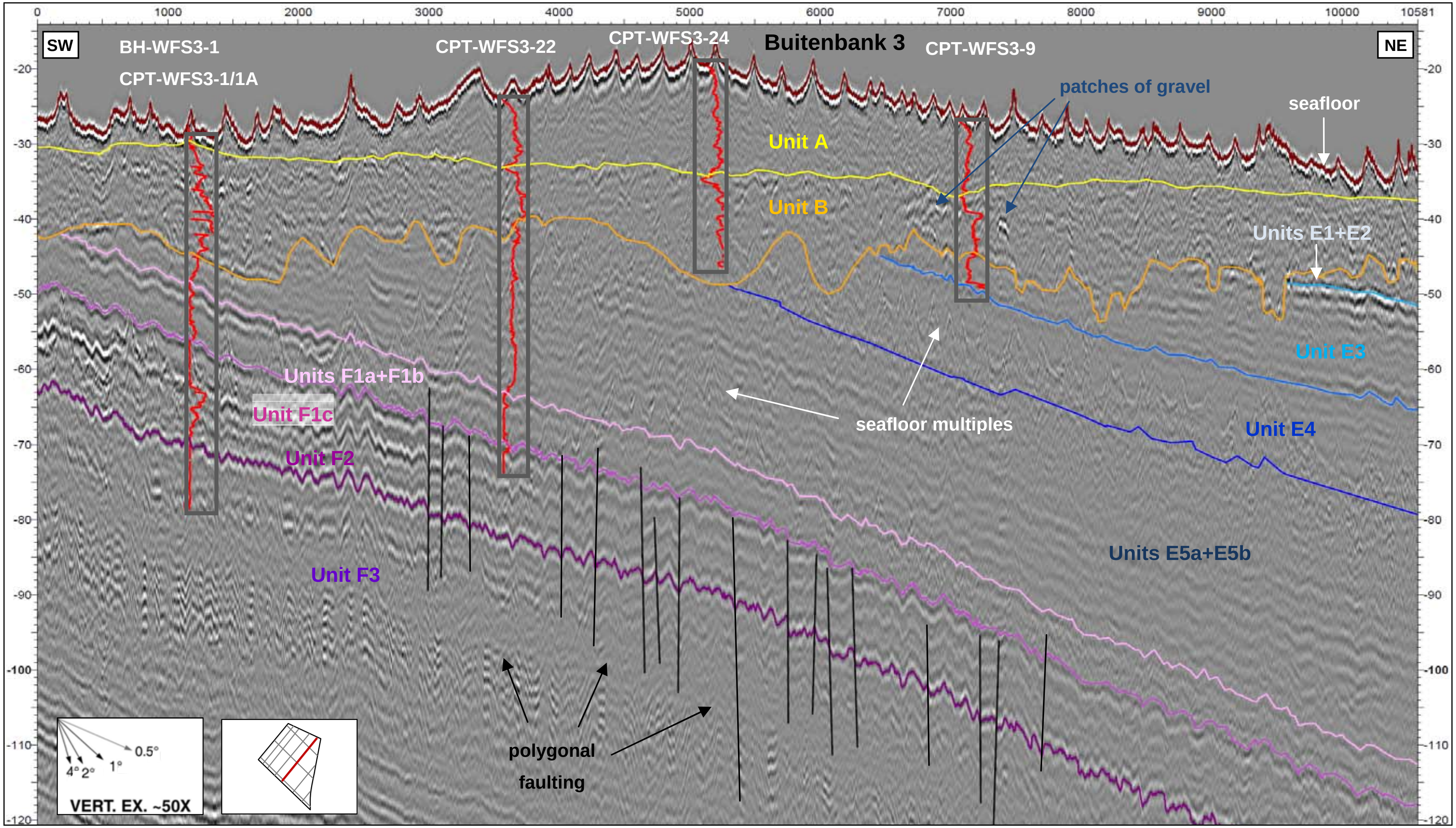


NOTE: Example of MCS line. Vertical scale is depth in metres below LAT. Horizontal scale is distance in metres. CPT cone resistance data (red line) for the geotechnical locations are projected on the cross section. Left side of the grey box marks the geotechnical location. The width of the box marks cone resistance values to 50 MPa. Location of the cross section is shown on Plate 3-6.

**CROSS SECTION – SECTION LINE A34019A**

BORSSELE WIND FARM ZONE, WFS III – DUTCH SECTOR, NORTH SEA

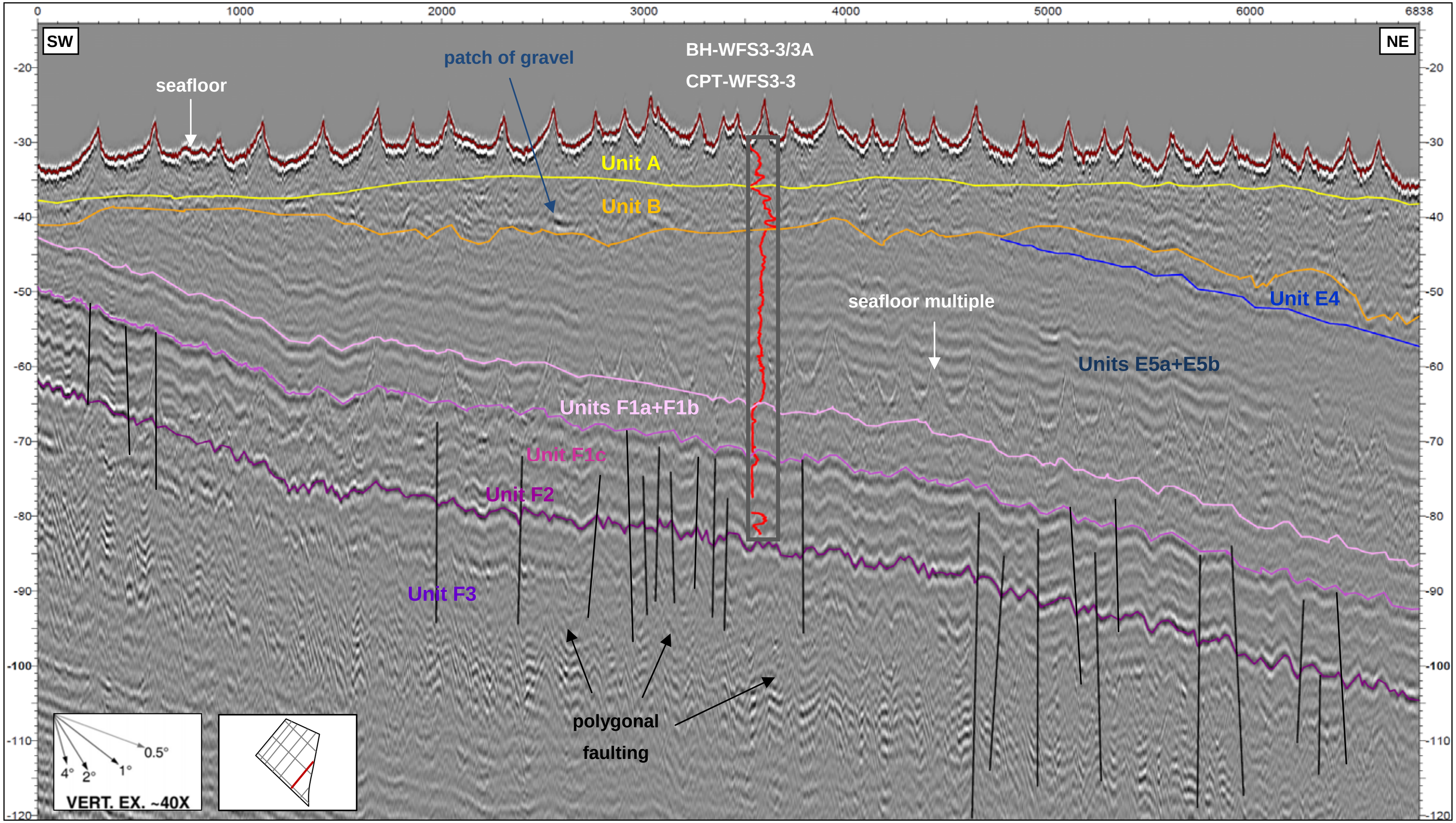


NOTE: Example of MCS line. Vertical scale is depth in metres below LAT. Horizontal scale is distance in metres. CPT cone resistance data (red line) for the geotechnical locations are projected on the cross section. Left side of the grey box marks the geotechnical location. The width of the box marks cone resistance values to 50 MPa. Location of the cross section is shown on Plate 3-6.

**CROSS SECTION – SECTION LINE A34012**

BORSSELE WIND FARM ZONE, WFS III – DUTCH SECTOR, NORTH SEA

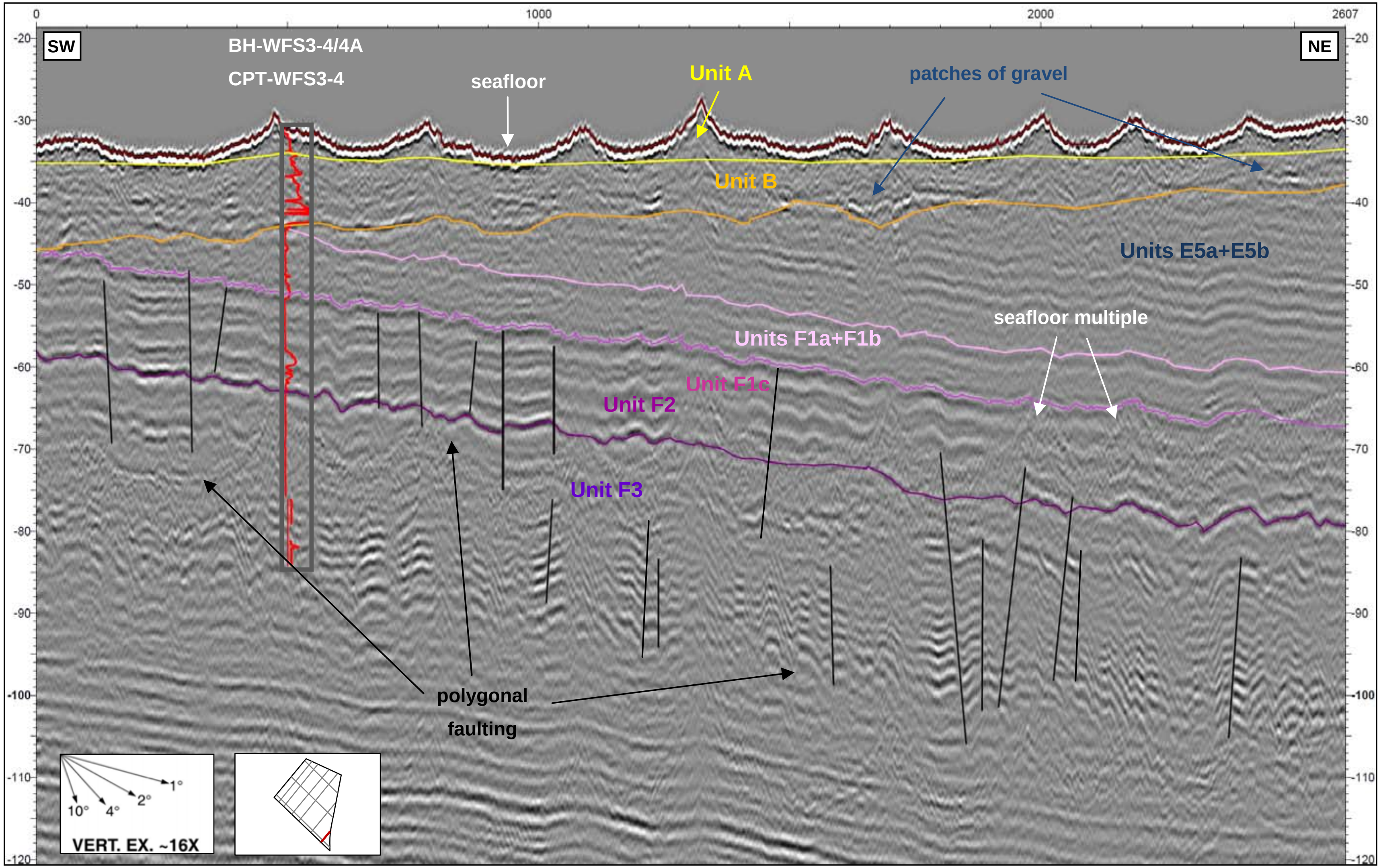


NOTE: Example of MCS line. Vertical scale is depth in metres below LAT. Horizontal scale is distance in metres. CPT cone resistance data (red line) for the geotechnical locations are projected on the cross section. Left side of the grey box marks the geotechnical location. The width of the box marks cone resistance values to 50 MPa. Location of the cross section is shown on Plate 3-6.

**CROSS SECTION – SECTION LINE A34006**

BORSSELE WIND FARM ZONE, WFS III – DUTCH SECTOR, NORTH SEA

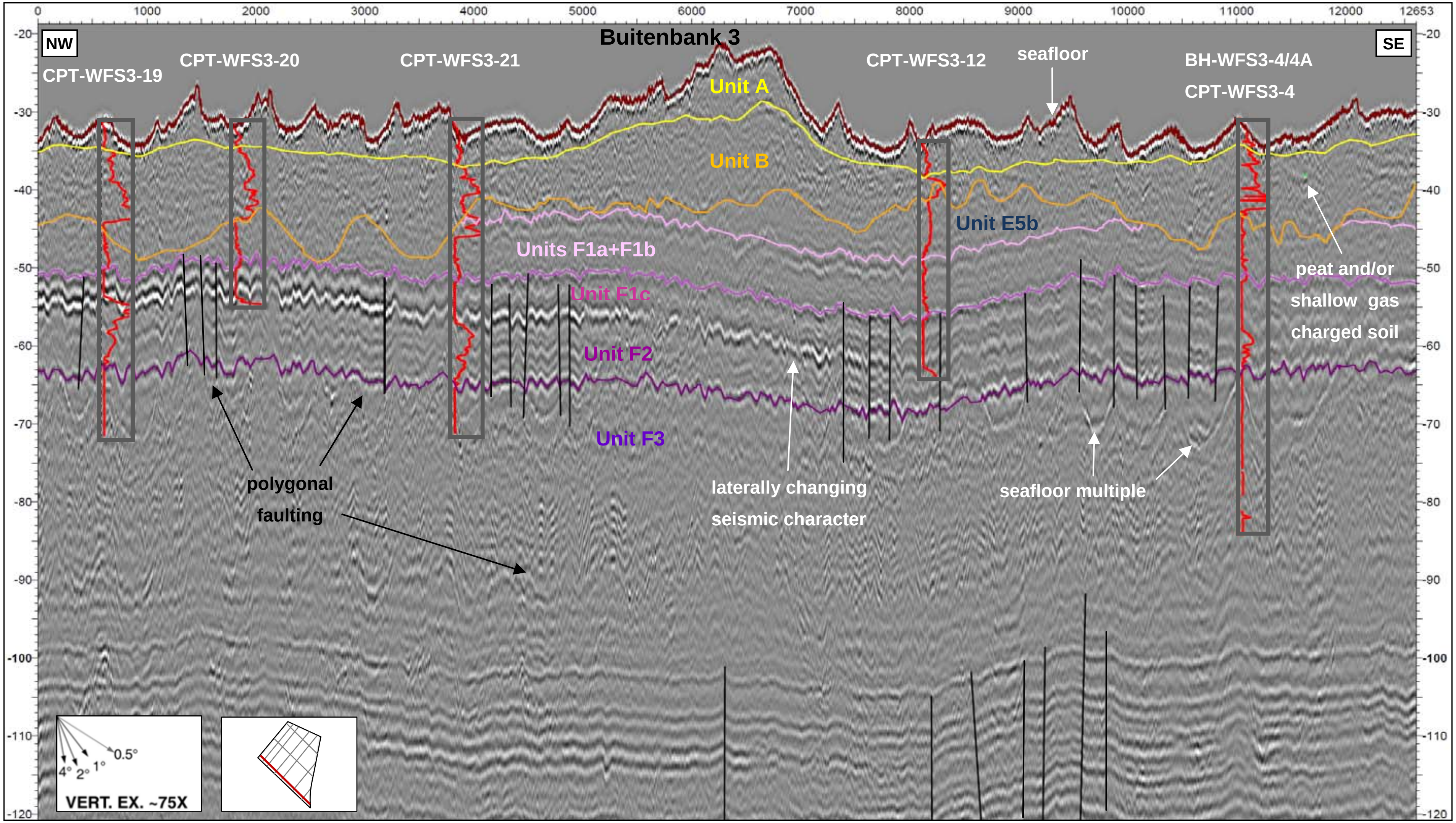


NOTE: Example of MCS line. Vertical scale is depth in metres below LAT. Horizontal scale is distance in metres. CPT cone resistance data (red line) for the geotechnical locations are projected on the cross section. Left side of the grey box marks the geotechnical location. The width of the box marks cone resistance values to 50 MPa. Location of the cross section is shown on Plate 3-6.

**CROSS SECTION – SECTION LINE A3A4XL001**

BORSSELE WIND FARM ZONE, WFS III – DUTCH SECTOR, NORTH SEA

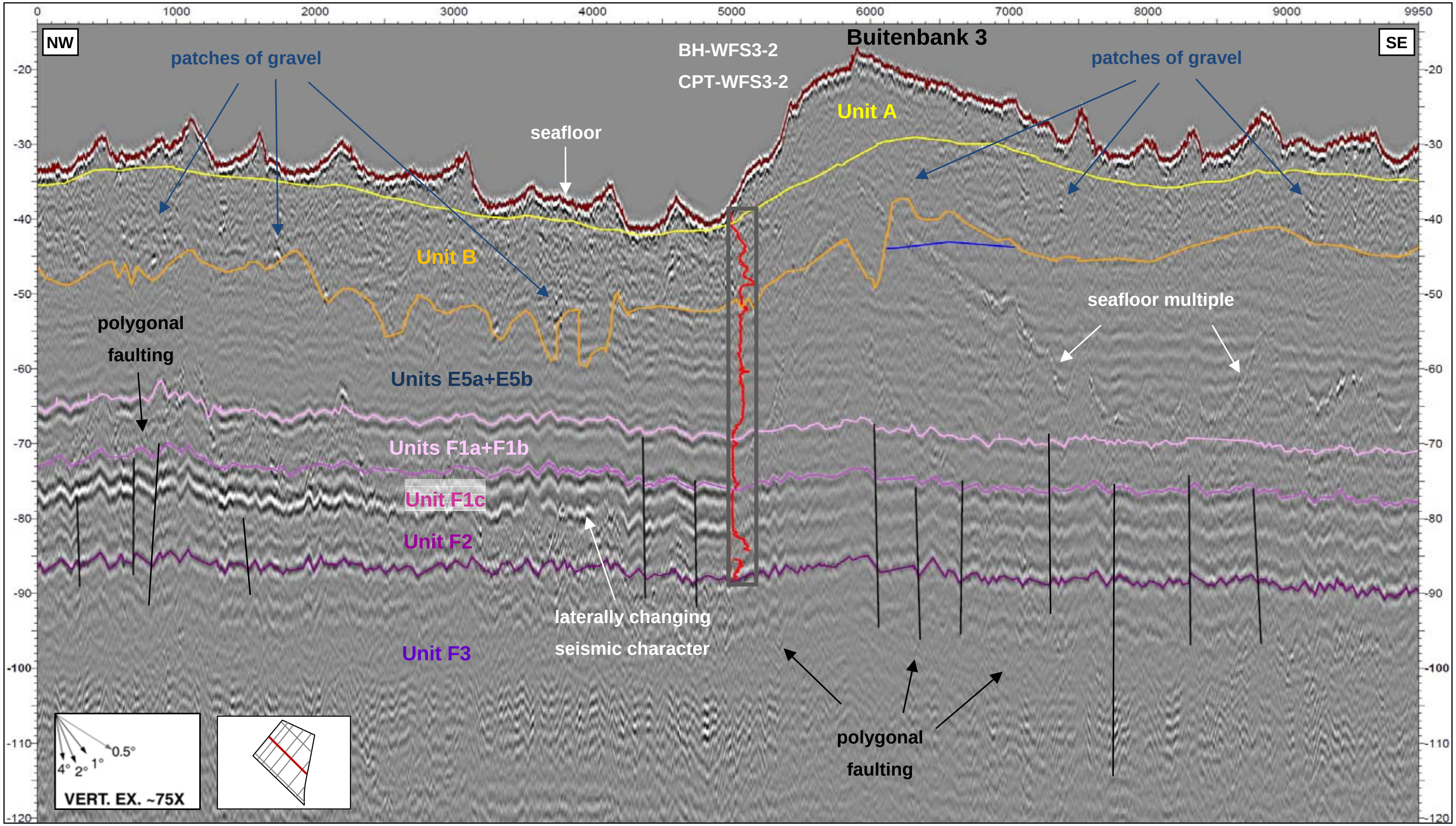


NOTE: Example of MCS line. Vertical scale is depth in metres below LAT. Horizontal scale is distance in metres. CPT cone resistance data (red line) for the geotechnical locations are projected on the cross section. Left side of the grey box marks the geotechnical location. The width of the box marks cone resistance values to 50 MPa. Location of the cross section is shown on Plate 3-6.

**CROSS SECTION – SECTION LINE A3A4XL003**

BORSSELE WIND FARM ZONE, WFS III – DUTCH SECTOR, NORTH SEA

ISSUE 01

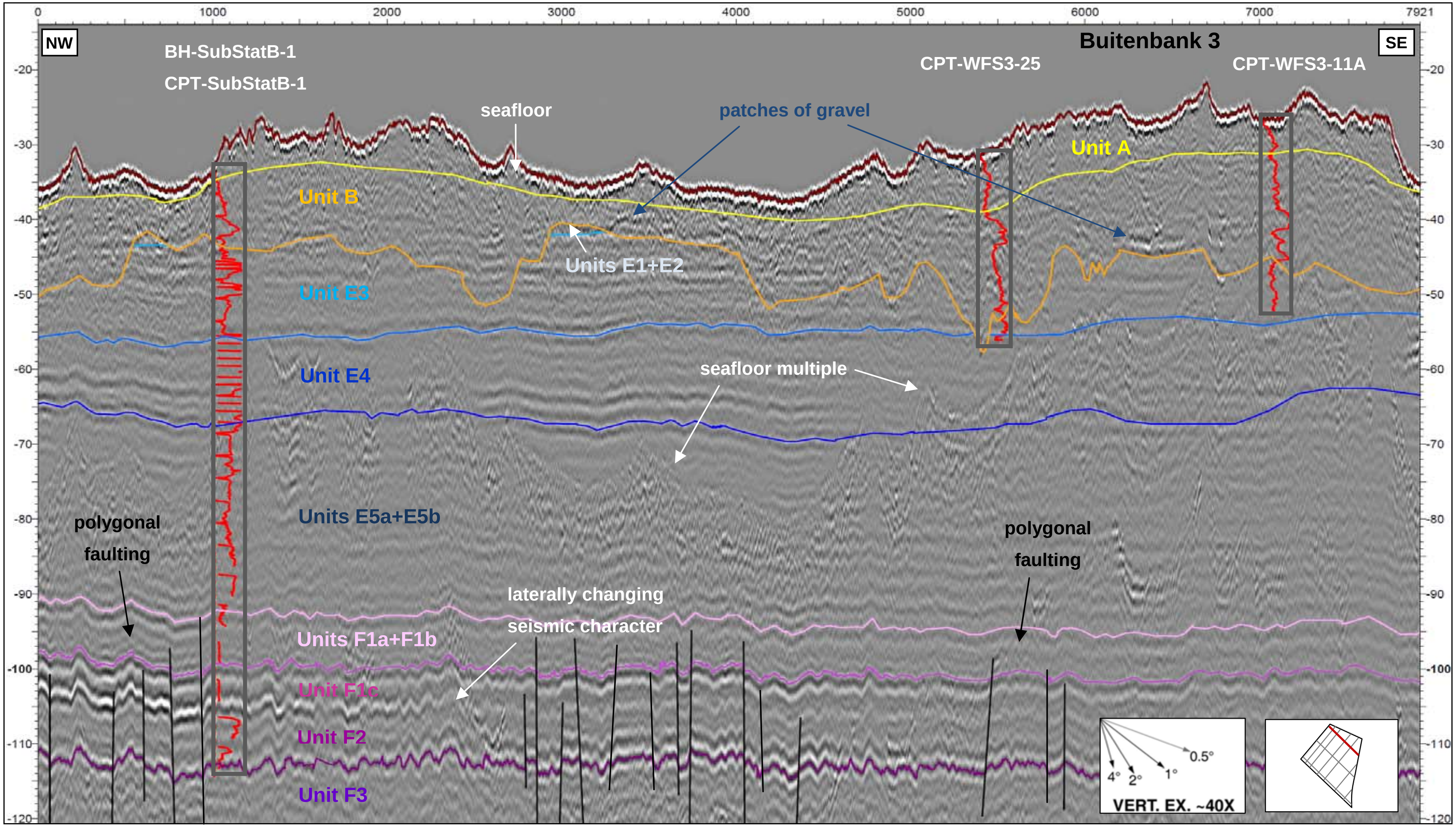


NOTE: Example of MCS line. Vertical scale is depth in metres below LAT. Horizontal scale is distance in metres. CPT cone resistance data (red line) for the geotechnical locations are projected on the cross section. Left side of the grey box marks the geotechnical location. The width of the box marks cone resistance values to 50 MPa. Location of the cross section is shown on Plate 3-6.

**CROSS SECTION – SECTION LINE UHRINF005A**

BORSSELE WIND FARM ZONE, WFS III – DUTCH SECTOR, NORTH SEA

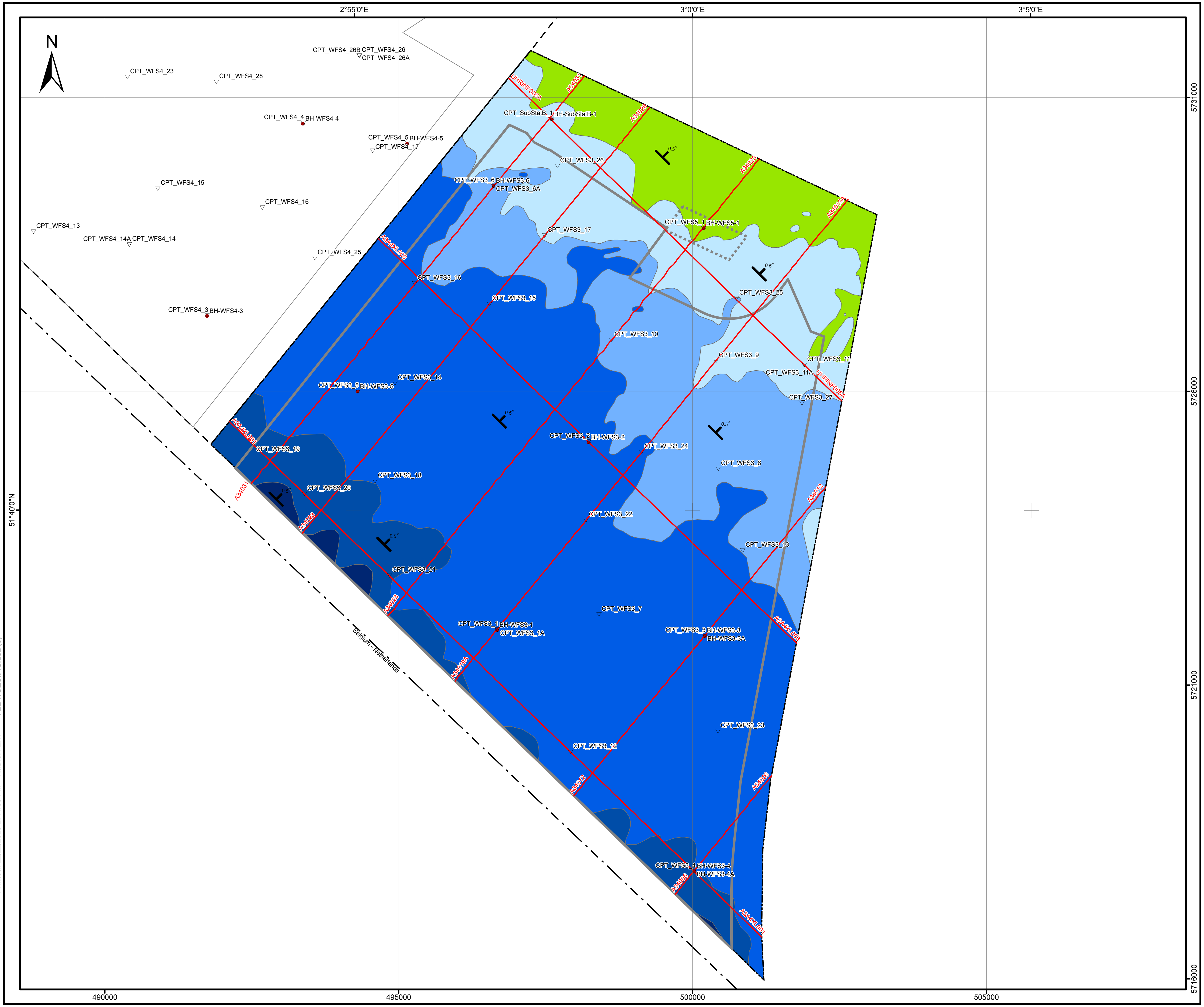


**LEGEND:**

- CPT location
- BH location
- Outline of WFS III
- Outline of WFS IV
- Outline of WFS V
- Investigation Area III
- Investigation Area IV
- Maritime boundary
- Section line of cross-section presented in the report

**Subcrop of Tertiary Units**

- Units E1 + E2 (Ruisbroek Sand Mb. + Watervliet Clay Mb.)
- Unit E3 (Bassevelde 3 Sand Mb.)
- Unit E4 (Bassevelde 2 Sand Mb.)
- Unit E5 (Bassevelde 1 Sand Mb.)
- Units F1a + F1b (Onderdijke Mb.)
- Units F1c + F2 (Onderdijke Mb. + Buisputten Mb.)

0.5° Orientation of layers (long line is layer azimuth; short line represents dip direction; value is approximate dip angle)

**NOTES:**

- Base of Unit B (Pleistocene) represents an erosional surface truncating underlying dipping Tertiary strata
- Tertiary units subcropping at base of Unit B are represented, i.e. intersection of unit boundaries with base of Unit B
- Outline of units based on interpretation from MCS data
- The Tertiary strata below Unit B are gently dipping (0.5 degrees) to NE (refer to main text)

**GEODETIC PARAMETERS:**

| | |
|---|---|
| DATUM | ETRS89 |
| Ellipsoid | GRS80 |
| Semi major axis | a = 6 378 137.000 |
| Inverse flattening | 1/f = 298.257222101 |
| PROJECTION | UTM, Zone 31 North |
| Central Meridian (CM) | 3° 00' 00" E |
| Latitude of Origin | 0° 00' 00" N |
| False Easting | 500 000 m |
| False Northing | 000 000 m |
| Scale factor | 0.9996 |
| Units | metres/degrees |

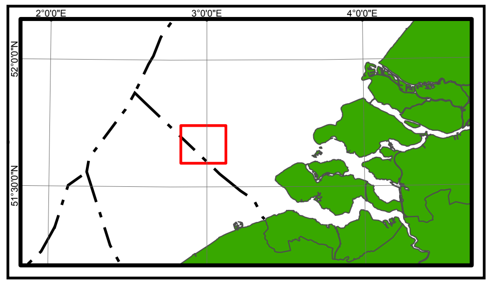



Rijksdienst voor Ondernemend Nederland (RVO)
Croeselaan 15, 3521 BJ, Utrecht - THE NETHERLANDS

Fugro
Prismastraat 4, 2631 RT, Nootdorp - THE NETHERLANDS


**TERTIARY UNITS BELOW UNIT B**

---

**BORSSELE WIND FARM ZONE, WFS III, DUTCH SECTOR, NORTH SEA**

Scale 1:60,000
at original A3 page size

0 500 1,000 1,500 2,000 metres

Fugro Report No. N6083/05 | Issue 2 | Plate 3-16

Printed: 12/11/2015 2:44:05 PM Author: LHT FEBV/GEO/FIG/152 (0)

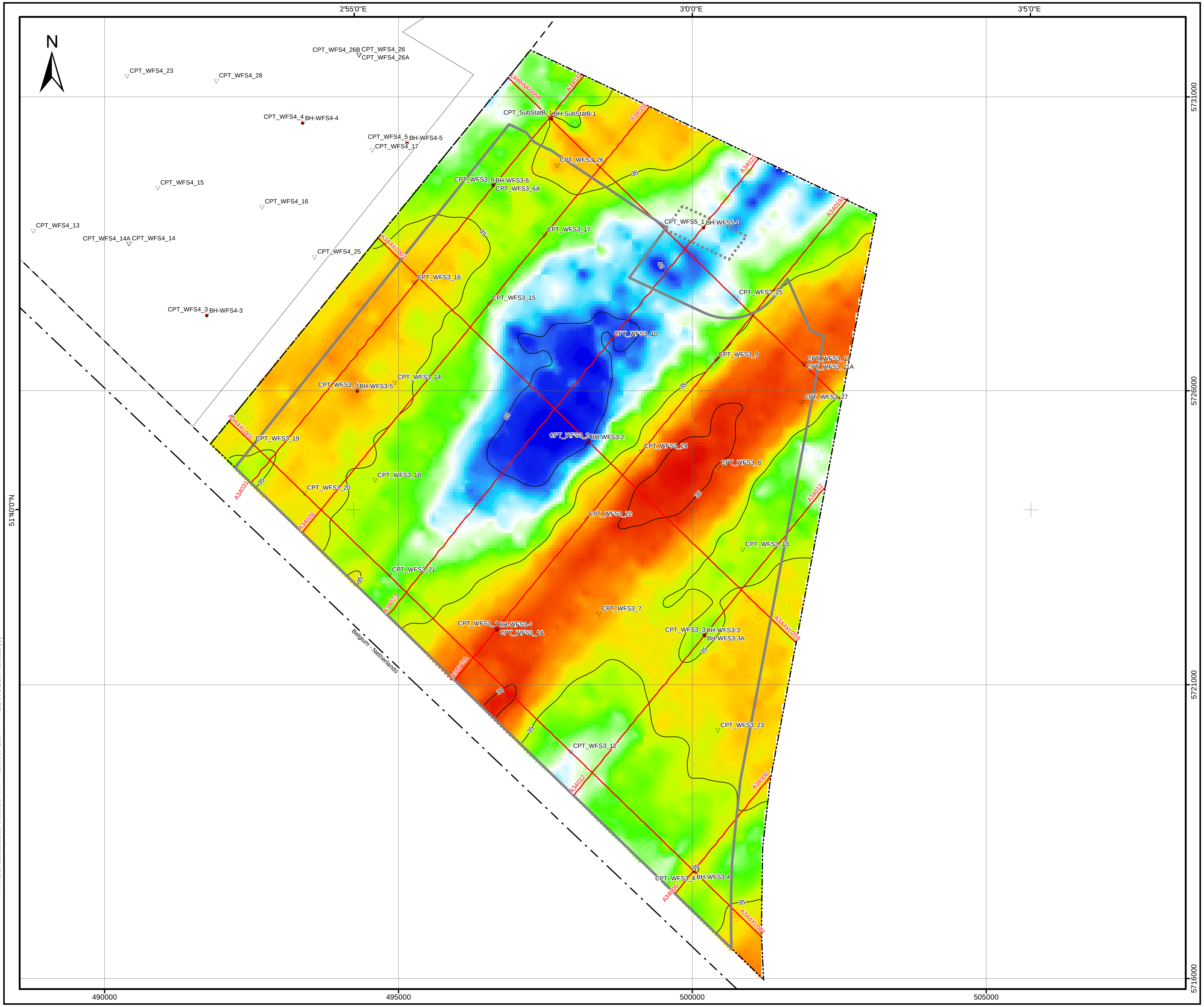


**LEGEND:**

- CPT location
- BH location
- Outline of WFS III
- Investigation Area III
- Section line of cross-section presented in the report
- Contour line of depth to base [m below LAT]
- Outline of WFS V
- Investigation Area IV
- Outline of WFS IV
- Maritime boundary

**Depth to base [m below LAT]**

-27
-35
-44

**NOTES:**

**GEODETIC PARAMETERS:**

| | |
|---|---|
| DATUM | ETRS89 |
| Ellipsoid | GRS80 |
| Semi major axis | a = 6 378 137.000 |
| Inverse flattening | 1/f = 298.257222101 |
| PROJECTION | UTM, Zone 31 North |
| Central Meridian (CM) | 3°00' 00" E |
| Latitude of Origin | 0°00' 00" N |
| False Easting | 500 000 m |
| False Northing | 000 000 m |
| Scale factor | 0.9996 |
| Units | metres/degrees |

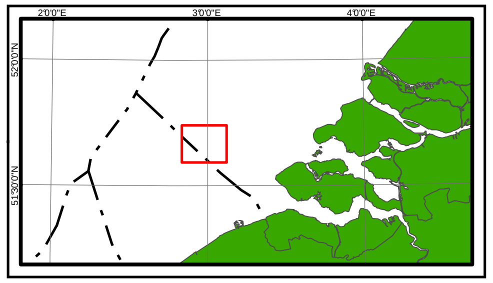



Rijksdienst voor Ondernemend Nederland (RVO)
Croeselaan 15, 3521 BJ, Utrecht - THE NETHERLANDS

Fugro
Prismastraat 4, 2631 RT, Nootdorp - THE NETHERLANDS


**DEPTH TO BASE OF UNIT A (SOUTHERN BIGHT FM.)**

**BORSSELE WIND FARM ZONE, WFS III, DUTCH SECTOR, NORTH SEA**

Scale 1:60,000
at original A3 page size

0 500 1,000 1,500 2,000 metres

| | | |
|---|---|---|
| Fugro Report No. N6083/05 | Issue 2 | Plate 3-17 |

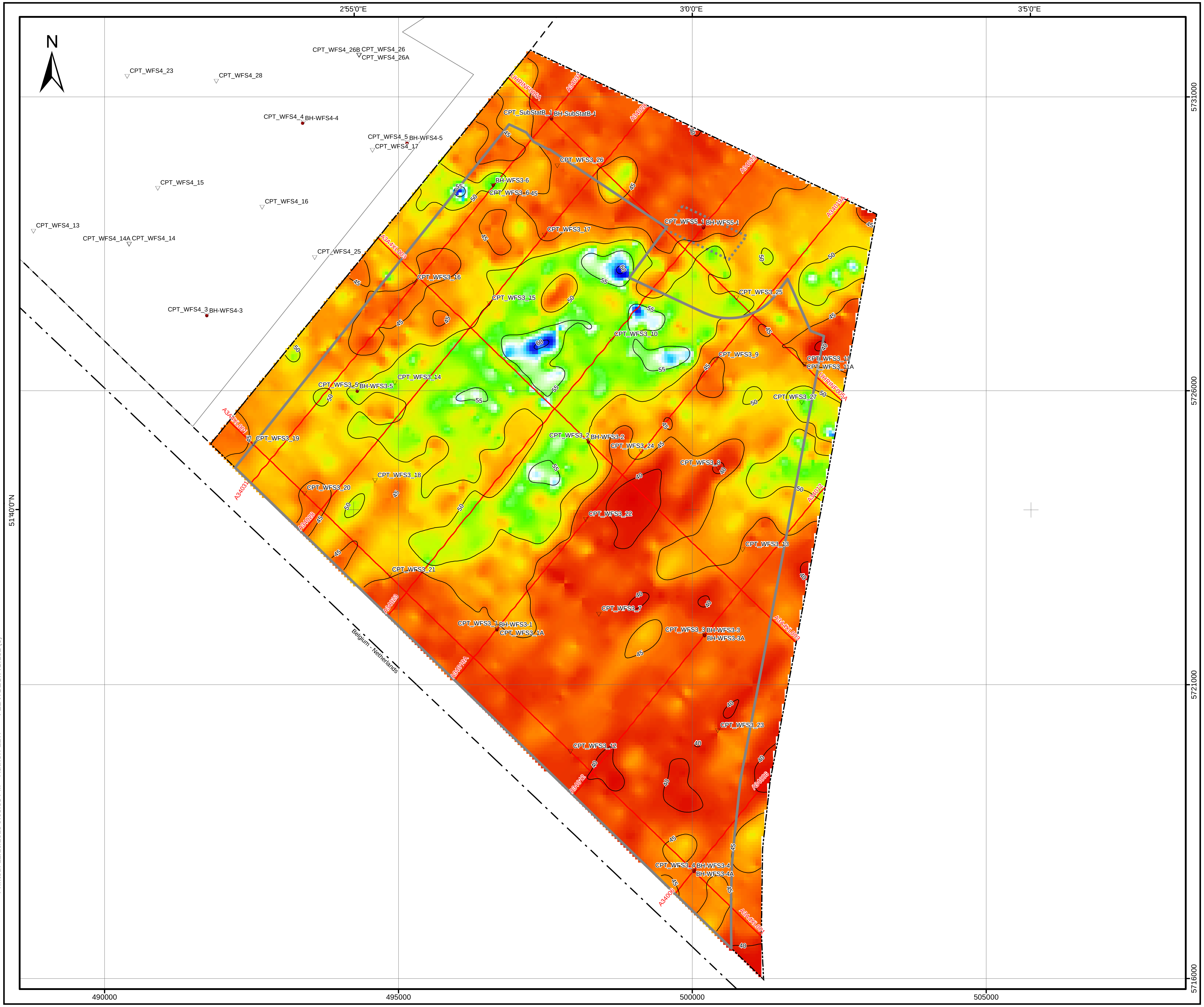


**LEGEND:**

- CPT location
- BH location
- Outline of WFS III
- Outline of WFS V
- Outline of WFS IV
- Investigation Area III
- Investigation Area IV
- Maritime boundary
- Section line of cross-section presented in the report
- Contour line of depth to base [m below LAT]

**Depth to base [m below LAT]**

36

-52

-68

**NOTES:**

**GEODETIC PARAMETERS:**

| | |
|---|---|
| DATUM | ETRS89 |
| Ellipsoid | GRS80 |
| Semi major axis | a = 6 378 137.000 |
| Inverse flattening | 1/f = 298.257222101 |
| PROJECTION | UTM, Zone 31 North |
| Central Meridian (CM) | 3°00' 00" E |
| Latitude of Origin | 0°00' 00" N |
| False Easting | 500 000 m |
| False Northing | 000 000 m |
| Scale factor | 0.9996 |
| Units | metres/degrees |

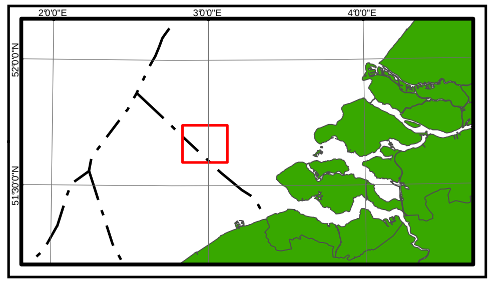



Rijksdienst voor Ondernemend Nederland (RVO)

Croeselaan 15, 3521 BJ, Utrecht - THE NETHERLANDS

Fugro

Prismastraat 4, 2631 RT, Nootdorp - THE NETHERLANDS


**DEPTH TO BASE OF UNIT B (KREFTENHEYE FM. / EEM FM.)**

**BORSSELE WIND FARM ZONE, WFS III, DUTCH SECTOR, NORTH SEA**

Scale 1:60,000
at original A3 page size

0 500 1,000 1,500 2,000 metres

| Fugro Report No. N6083/05 | Issue 2 | Plate 3-18 |
|---|---|---|

Printed: 12/10/2015 9:03:53 PM Author: LBH FEBV/GEO/FIG/152 (0)

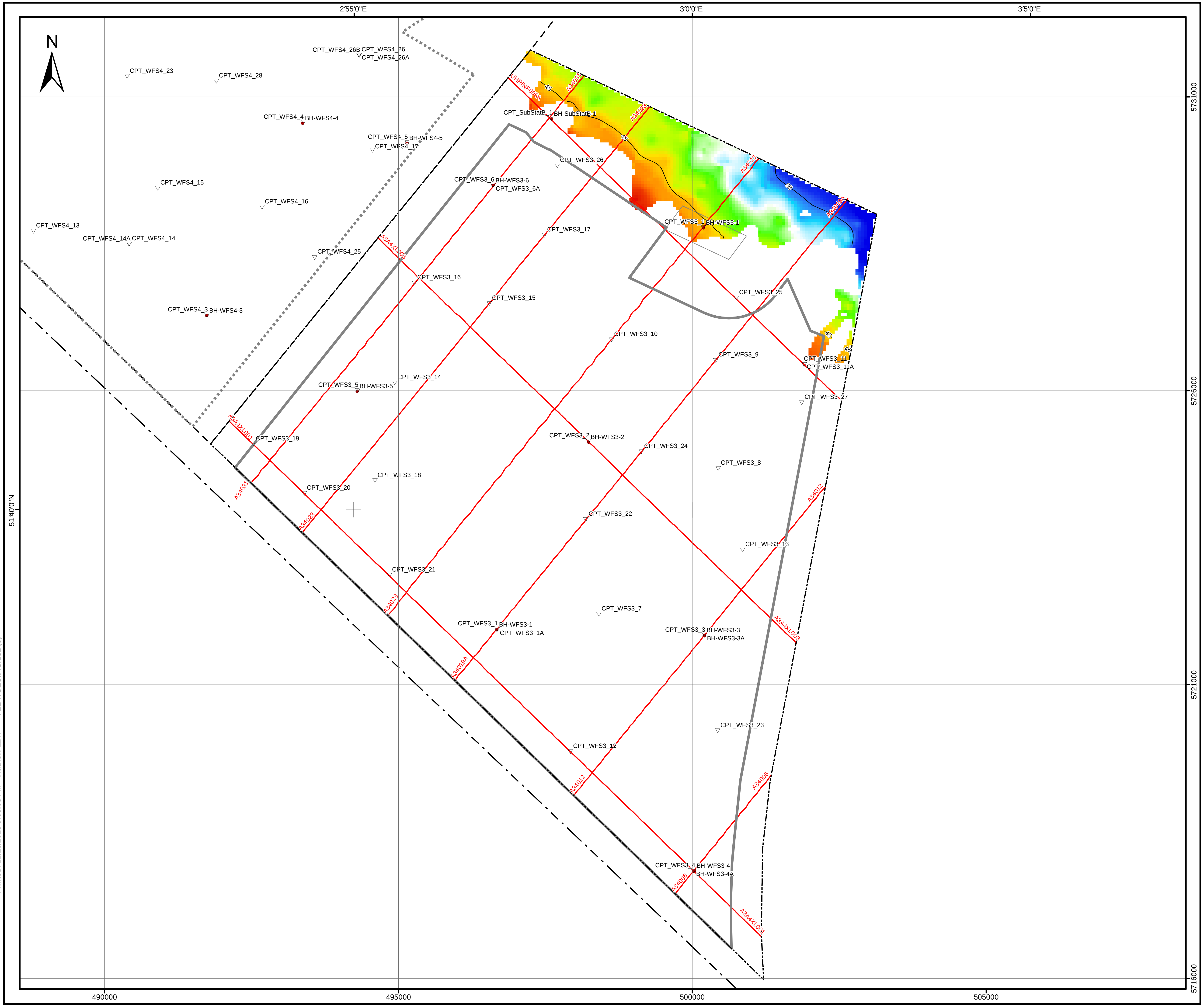


**LEGEND:**

- CPT location
- BH location
- Outline of WFS III
- Outline of WFS IV
- Outline of WFS V
- Investigation Area III
- Investigation Area IV
- Maritime boundary
- Section line of cross-section presented in the report
- Contour line of depth to base [m below LAT]

**Depth to base [m below LAT]**

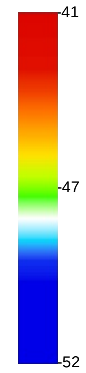


**NOTES:**
- Unit is absent at blank area within Investigation Area III

**GEODETIC PARAMETERS:**

| | |
|---|---|
| DATUM | ETRS89 |
| Ellipsoid | GRS80 |
| Semi major axis | a = 6 378 137.000 |
| Inverse flattening | 1/f = 298.257222101 |
| PROJECTION | UTM, Zone 31 North |
| Central Meridian (CM) | 3°00' 00" E |
| Latitude of Origin | 0°00' 00" N |
| False Easting | 500 000 m |
| False Northing | 000 000 m |
| Scale factor | 0.9996 |
| Units | metres/degrees |

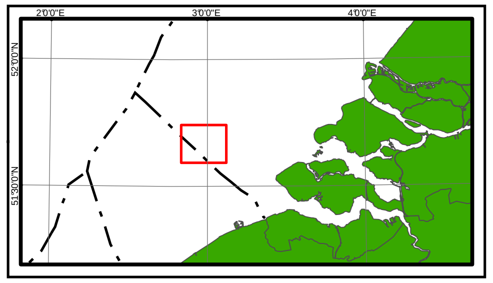


Rijksdienst voor Ondernemend Nederland (RVO)
Croeselaan 15, 3521 BJ, Utrecht - THE NETHERLANDS

Fugro
Prismastraat 4, 2631 RT, Nootdorp - THE NETHERLANDS

**DEPTH TO BASE OF UNIT E2 (WATERVLIET CLAY MB.)**

**BORSSELE WIND FARM ZONE, WFS III, DUTCH SECTOR, NORTH SEA**

Scale 1:60,000
at original A3 page size

0 500 1,000 1,500 2,000 metres

Fugro Report No. N6083/05 | Issue 2 | Plate 3-19

Printed: 12/10/2015 9:05:03 PM Author: LBH FEBV/GEO/FIG/152 (0)

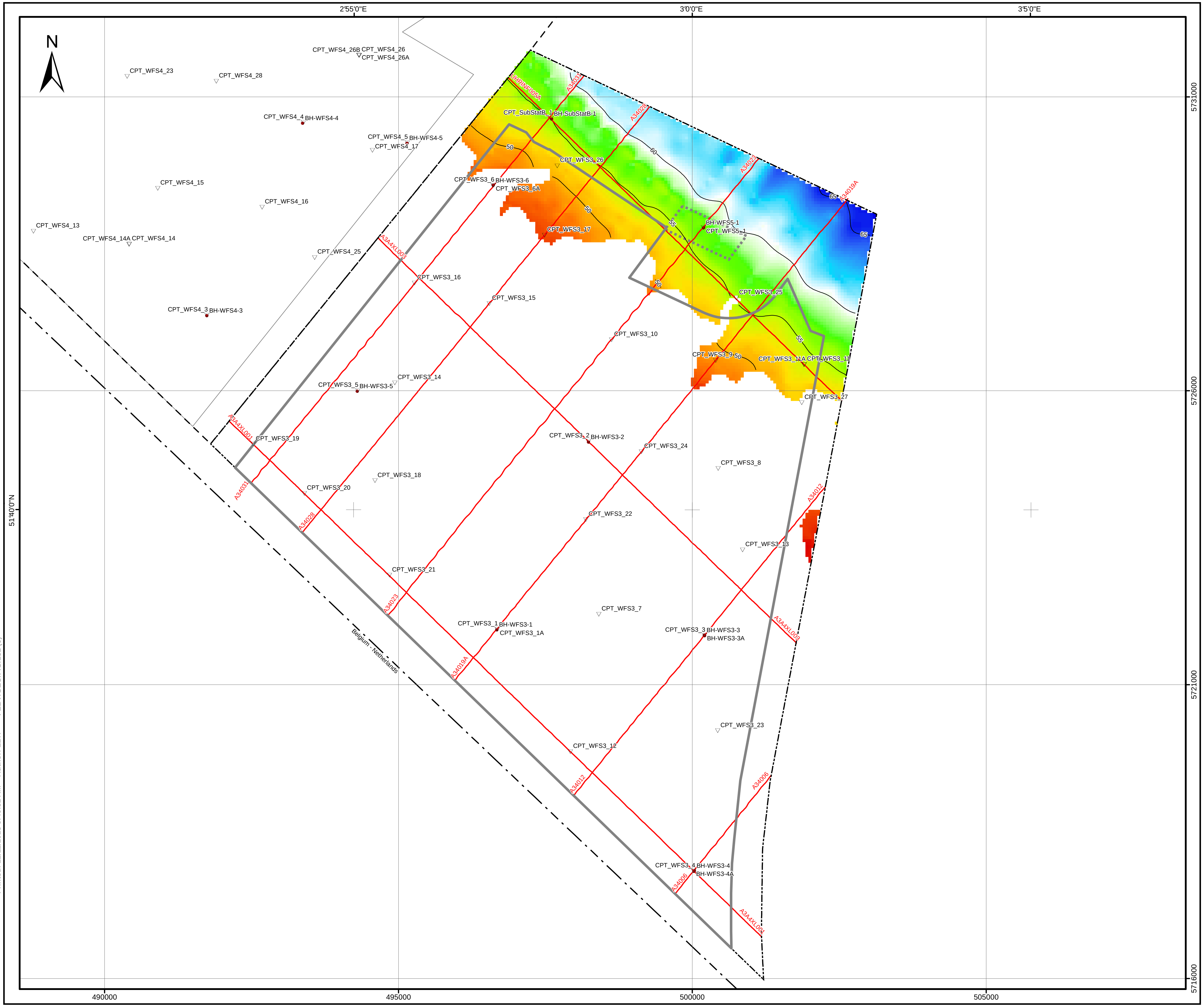


**LEGEND:**

- CPT location
- BH location
- Outline of WFS III
- Investigation Area III
- Section line of cross-section presented in the report
- Contour line of depth to base [m below LAT]
- Outline of WFS V
- Investigation Area IV
- Outline of WFS IV
- Maritime boundary

**Depth to base [m below LAT]**

41

55

66

**NOTES:**

- Unit is absent at blank area within Investigation Area III

**GEODETIC PARAMETERS:**

| | |
|---|---|
| DATUM | ETRS89 |
| Ellipsoid | GRS80 |
| Semi major axis | a = 6 378 137.000 |
| Inverse flattening | 1/f = 298.257222101 |
| PROJECTION | UTM, Zone 31 North |
| Central Meridian (CM) | 3°00' 00" E |
| Latitude of Origin | 0°00' 00" N |
| False Easting | 500 000 m |
| False Northing | 000 000 m |
| Scale factor | 0.9996 |
| Units | metres/degrees |

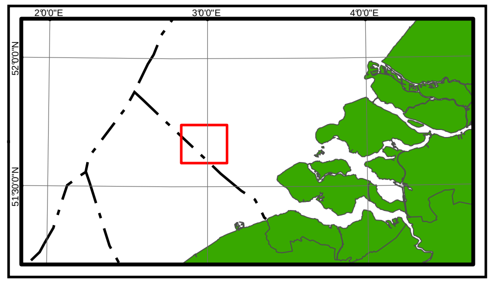


Rijksdienst voor Ondernemend Nederland (RVO)

Croeselaan 15, 3521 BJ, Utrecht - THE NETHERLANDS

Fugro

Prismastraat 4, 2631 RT, Nootdorp - THE NETHERLANDS

**DEPTH TO BASE OF UNIT E3 (BASSEVELDE 3 SAND MB.)**

**BORSSELE WIND FARM ZONE, WFS III, DUTCH SECTOR, NORTH SEA**

Scale 1:60,000
at original A3 page size

0 500 1,000 1,500 2,000 metres

Fugro Report No. N6083/05 | Issue 2 | Plate 3-20

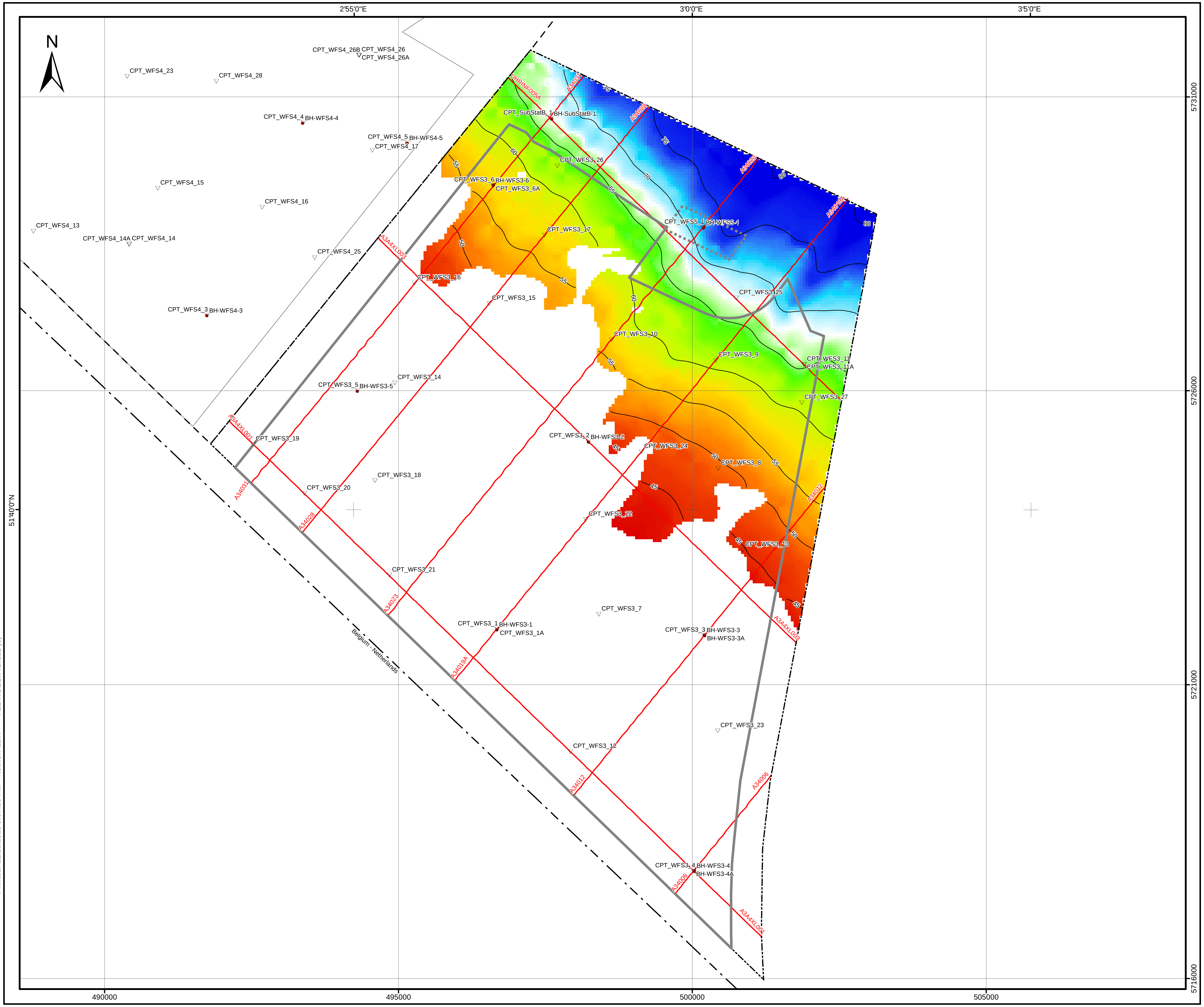


Printed: 12/10/2015 9:07:29 PM Author: LBH FEBV/GEO/FIG/152 (0)

**LEGEND:**

- CPT location
- BH location
- Outline of WFS III
- Outline of WFS IV
- Outline of WFS V
- Investigation Area III
- Investigation Area IV
- Section line of cross-section presented in the report
- Maritime boundary
- Contour line of depth to base [m below LAT]

**Depth to base [m below LAT]**

40
61
82

**NOTES:**
- Unit is absent at blank areas within Investigation Area III

**GEODETIC PARAMETERS:**

| | |
|---|---|
| DATUM | ETRS89 |
| Ellipsoid | GRS80 |
| Semi major axis | a = 6 378 137.000 |
| Inverse flattening | 1/f = 298.257222101 |
| PROJECTION | UTM, Zone 31 North |
| Central Meridian (CM) | 3°00' 00" E |
| Latitude of Origin | 0°00' 00" N |
| False Easting | 500 000 m |
| False Northing | 000 000 m |
| Scale factor | 0.9996 |
| Units | metres/degrees |

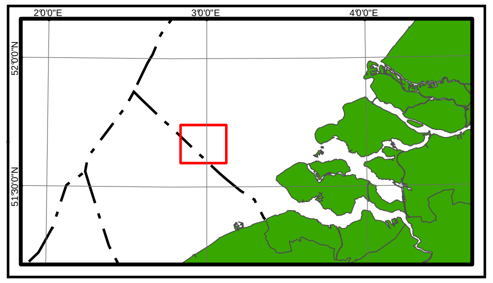

Rijksdienst voor Ondernemend Nederland (RVO)
Croeselaan 15, 3521 BJ, Utrecht - THE NETHERLANDS

Fugro
Prismastraat 4, 2631 RT, Nootdorp - THE NETHERLANDS

**DEPTH TO BASE OF UNIT E4 (BASSEVELDE 2 SAND MB.)**

**BORSSELE WIND FARM ZONE, WFS III, DUTCH SECTOR, NORTH SEA**

Scale 1:60,000
at original A3 page size

0 500 1,000 1,500 2,000 metres

FUGRO

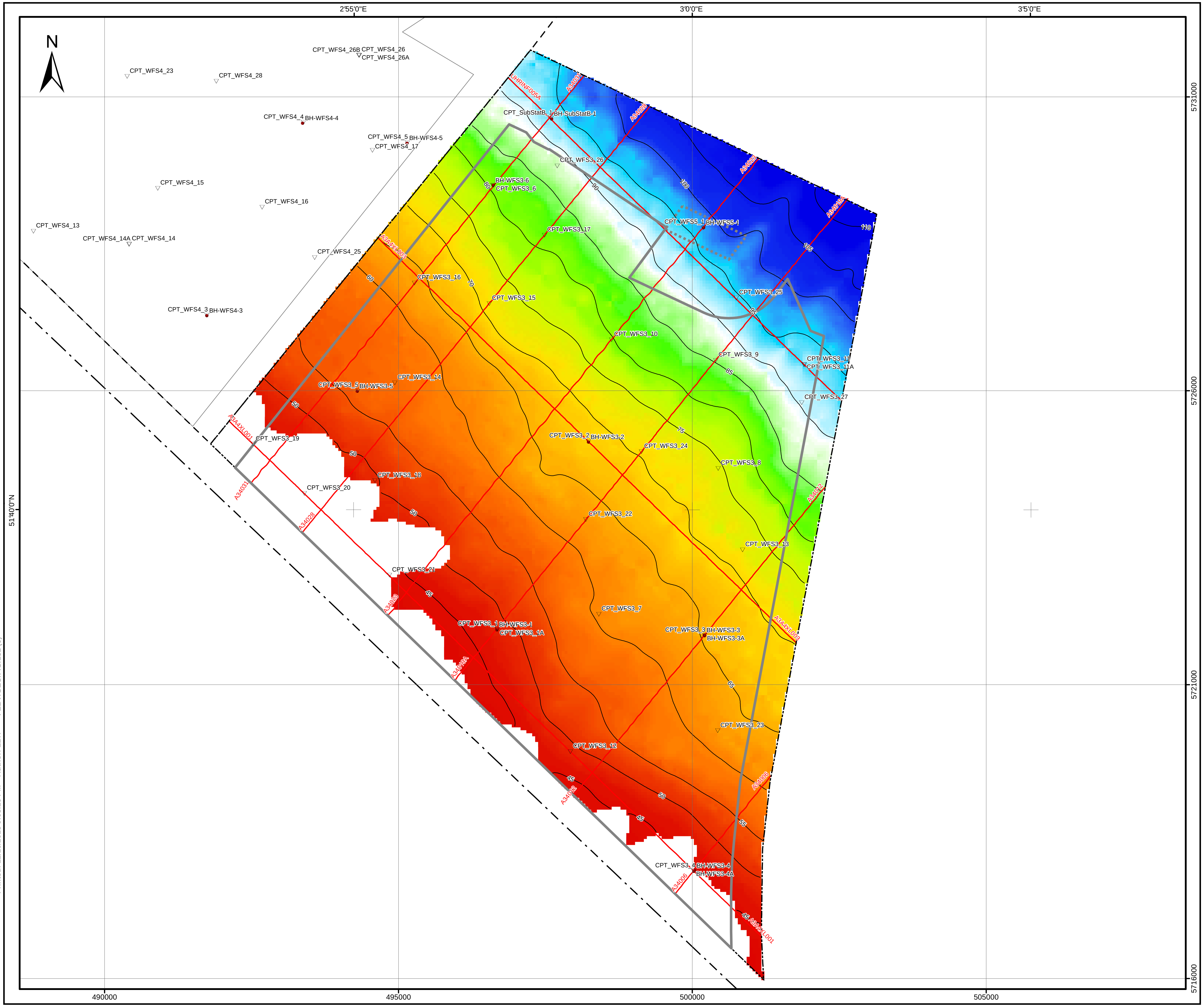


LEGEND:

- CPT location
- BH location
- Outline of WFS III
- Outline of WFS IV
- Outline of WFS V
- Investigation Area III
- Investigation Area IV
- Section line of cross-section presented in the report
- Maritime boundary
- Contour line of depth to base [m below LAT]

Depth to base [m below LAT]

40

76

113

NOTES:

- Unit is absent at blank areas within Investigation Area III
- The depth of the boundary between Unit E5 and Sub-unit F1a may differ between geotechnical and geophysical data (refer to main text for details)

GEODETIC PARAMETERS:

| | |
|---|---|
| DATUM | ETRS89 |
| Ellipsoid | GRS80 |
| Semi major axis | a = 6 378 137.000 |
| Inverse flattening | 1/f = 298.257222101 |
| PROJECTION | UTM, Zone 31 North |
| Central Meridian (CM) | 3°00' 00" E |
| Latitude of Origin | 0°00' 00" N |
| False Easting | 500 000 m |
| False Northing | 000 000 m |
| Scale factor | 0.9996 |
| Units | metres/degrees |

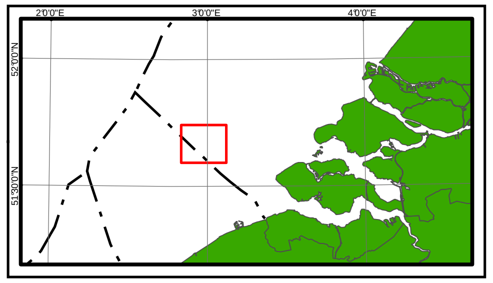

Rijksdienst voor Ondernemend Nederland (RVO)

Croeselaan 15, 3521 BJ, Utrecht - THE NETHERLANDS

Fugro

Prismastraat 4, 2631 RT, Nootdorp - THE NETHERLANDS

**DEPTH TO BASE OF UNIT E5 (BASSEVELDE 1 SAND MB.)**

**BORSSELE WIND FARM ZONE, WFS III, DUTCH SECTOR, NORTH SEA**

Scale 1:60,000
at original A3 page size

0 500 1,000 1,500 2,000 metres

FUGRO

| Fugro Report No. N6083/05 | Issue 2 | Plate 3-22 |
|---|---|---|

Printed: 12/10/2015 9:08:29 PM Author: LBH FEBV/GEO/FIG/152 (0)

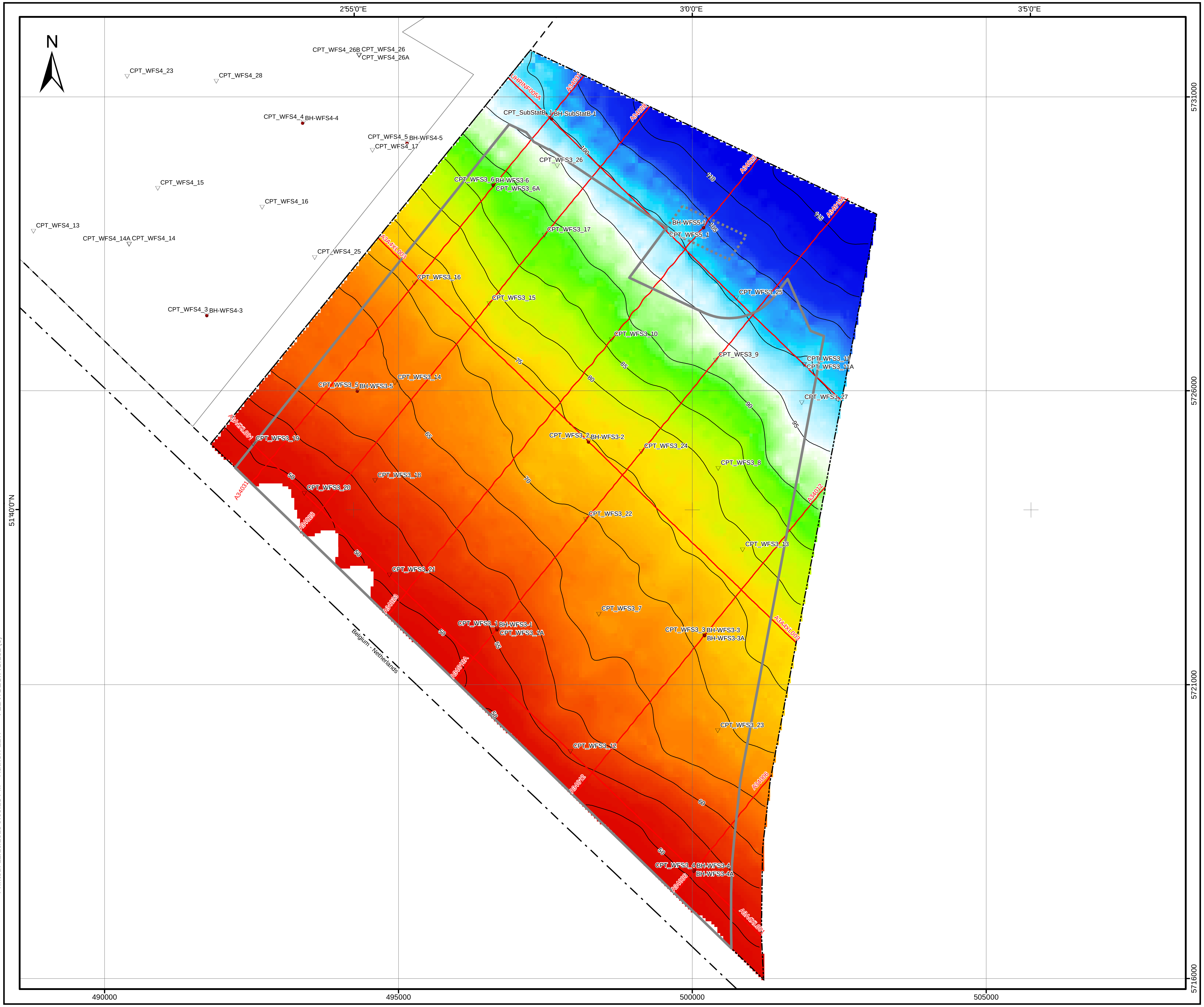


**LEGEND:**

- CPT location
- BH location
- Outline of WFS III
- Outline of WFS IV
- Outline of WFS V
- Investigation Area III
- Investigation Area IV
- Section line of cross-section presented in the report
- Maritime boundary
- Contour line of depth to base [m below LAT]

**Depth to base [m below LAT]**

46

82

119

**NOTES:**
- Unit is absent at blank areas within Investigation Area III

**GEODETIC PARAMETERS:**

| | |
|---|---|
| DATUM | ETRS89 |
| Ellipsoid | GRS80 |
| Semi major axis | a = 6 378 137.000 |
| Inverse flattening | 1/f = 298.257222101 |
| PROJECTION | UTM, Zone 31 North |
| Central Meridian (CM) | 3°00' 00" E |
| Latitude of Origin | 0°00' 00" N |
| False Easting | 500 000 m |
| False Northing | 000 000 m |
| Scale factor | 0.9996 |
| Units | metres/degrees |

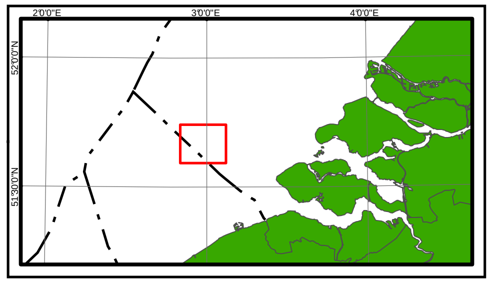

Rijksdienst voor Ondernemend Nederland (RVO)
Croeselaan 15, 3521 BJ, Utrecht - THE NETHERLANDS

Fugro
Prismastraat 4, 2631 RT, Nootdorp - THE NETHERLANDS

**DEPTH TO BASE OF UNIT F1b (ONDERDIJKE MB.)**

**BORSSELE WIND FARM ZONE, WFS III, DUTCH SECTOR, NORTH SEA**

Scale 1:60,000
at original A3 page size

0 500 1,000 1,500 2,000 metres

| Fugro Report No. N6083/05 | Issue 2 | Plate 3-23 |
|---|---|---|

Printed: 12/10/2015 9:09:23 PM Author: LBH FEBV/GEO/FIG/152 (0)

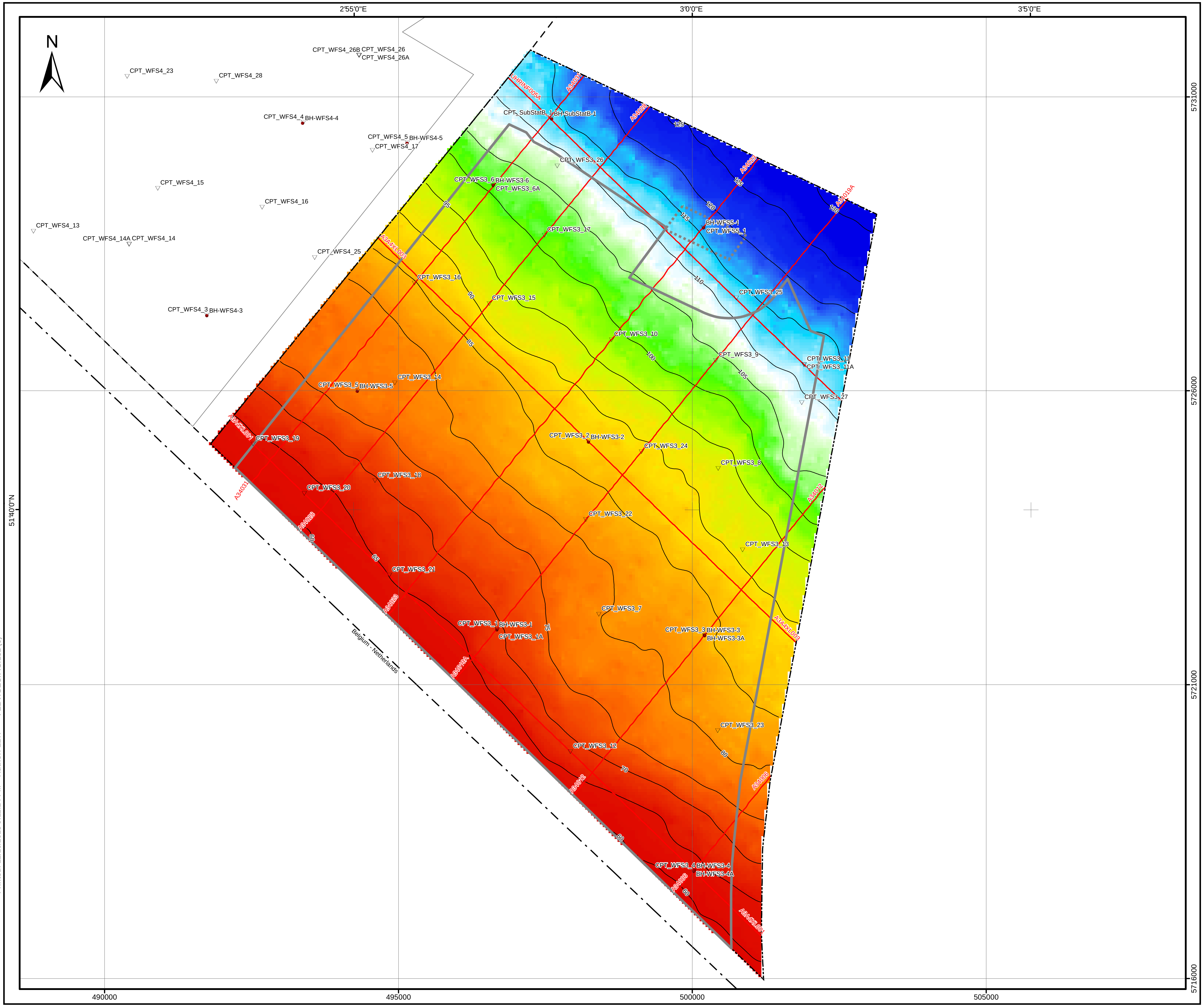


**LEGEND:**

- CPT location
- BH location
- Outline of WFS III
- Investigation Area III
- Outline of WFS V
- Investigation Area IV
- Outline of WFS IV
- Maritime boundary
- Section line of cross-section presented in the report
- Contour line of depth to base [m below LAT]

**Depth to base [m below LAT]**

58

95

133

**NOTES:**

**GEODETIC PARAMETERS:**

| | |
|---|---|
| DATUM | ETRS89 |
| Ellipsoid | GRS80 |
| Semi major axis | a = 6 378 137.000 |
| Inverse flattening | 1/f = 298.257222101 |
| PROJECTION | UTM, Zone 31 North |
| Central Meridian (CM) | 3°00' 00" E |
| Latitude of Origin | 0°00' 00" N |
| False Easting | 500 000 m |
| False Northing | 000 000 m |
| Scale factor | 0.9996 |
| Units | metres/degrees |

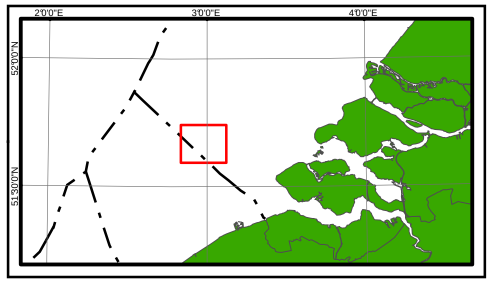


Rijksdienst voor Ondernemend Nederland (RVO)

Croeselaan 15, 3521 BJ, Utrecht - THE NETHERLANDS

Fugro

Prismastraat 4, 2631 RT, Nootdorp - THE NETHERLANDS

**DEPTH TO BASE OF UNIT F2**
**(BUISPUTTEN MB.)**

**BORSSELE WIND FARM ZONE, WFS III,**
**DUTCH SECTOR, NORTH SEA**

Scale 1:60,000
at original A3 page size

0 500 1,000 1,500 2,000 metres

Fugro Report No. N6083/05 | Issue 2 | Plate 3-24

Printed: 12/10/2015 9:11:24 PM Author: LBH FEBV/GEO/FIG/152 (0)

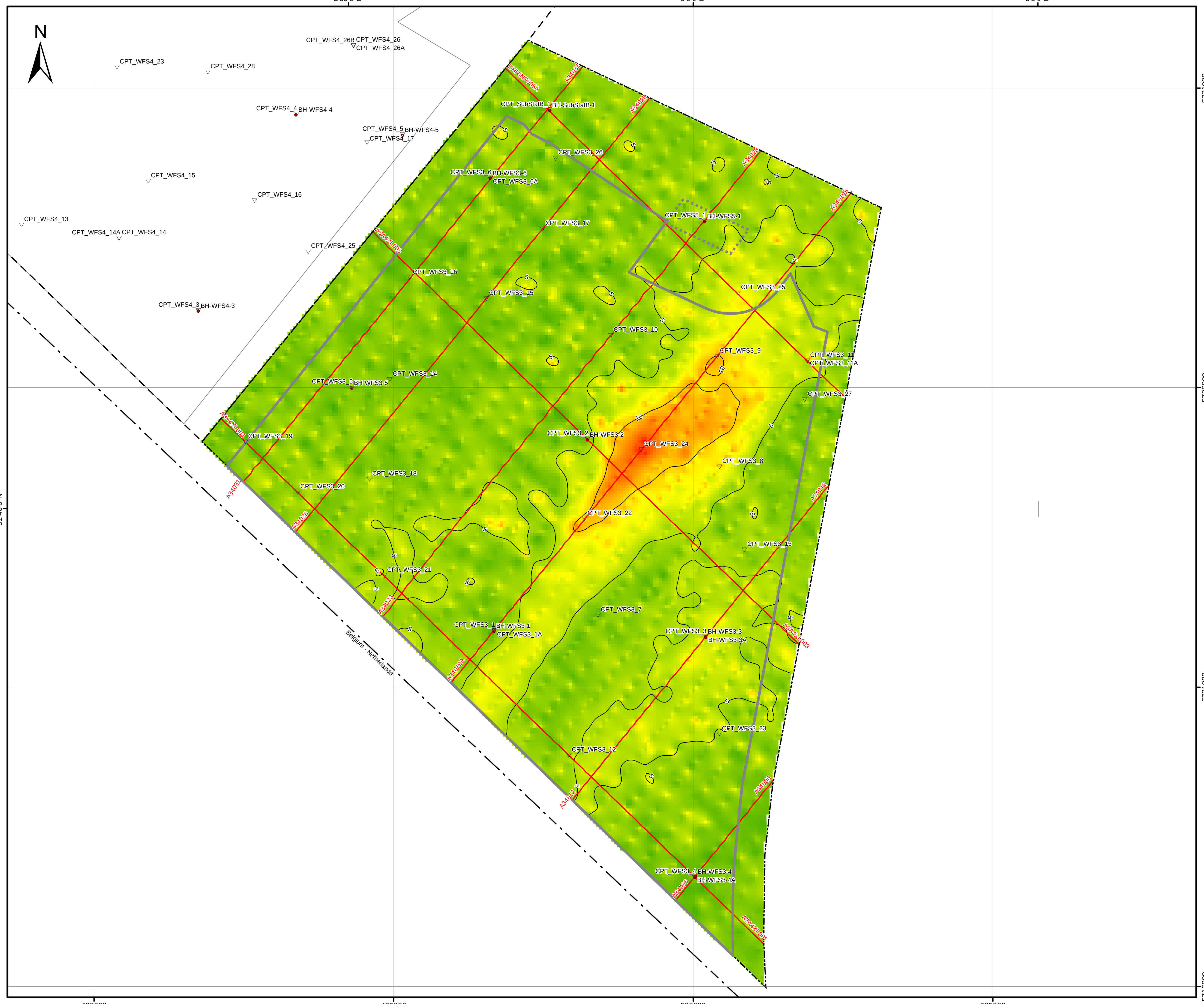


**LEGEND:**

- CPT location
- BH location
- Outline of WFS III
- Outline of WFS IV
- Outline of WFS V
- Investigation Area III
- Investigation Area IV
- Maritime boundary
- Section line of cross-section presented in the report
- Contour line of thickness [m]

**Thickness [m]**

17

8

>0

**NOTES:**

**GEODETIC PARAMETERS:**

| | |
|---|---|
| DATUM | ETRS89 |
| Ellipsoid | GRS80 |
| Semi major axis | a = 6 378 137.000 |
| Inverse flattening | 1/f = 298.257222101 |
| PROJECTION | UTM, Zone 31 North |
| Central Meridian (CM) | 3°00' 00" E |
| Latitude of Origin | 0°00' 00" N |
| False Easting | 500 000 m |
| False Northing | 000 000 m |
| Scale factor | 0.9996 |
| Units | metres/degrees |

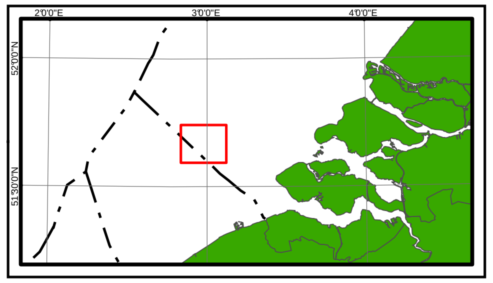


Rijksdienst voor Ondernemend Nederland (RVO)
Croeselaan 15, 3521 BJ, Utrecht - THE NETHERLANDS

Fugro
Prismastraat 4, 2631 RT, Nootdorp - THE NETHERLANDS

**THICKNESS OF UNIT A (SOUTHERN BIGHT FM.)**

**BORSSELE WIND FARM ZONE, WFS III, DUTCH SECTOR, NORTH SEA**

Scale 1:60,000
at original A3 page size

0 500 1,000 1,500 2,000 metres

| Fugro Report No. N6083/05 | Issue 2 | Plate 3-25 |
|---|---|---|

Printed: 12/10/2015 8:38:11 PM Author: LHT FEBV/GEO/FIG/152 (0)

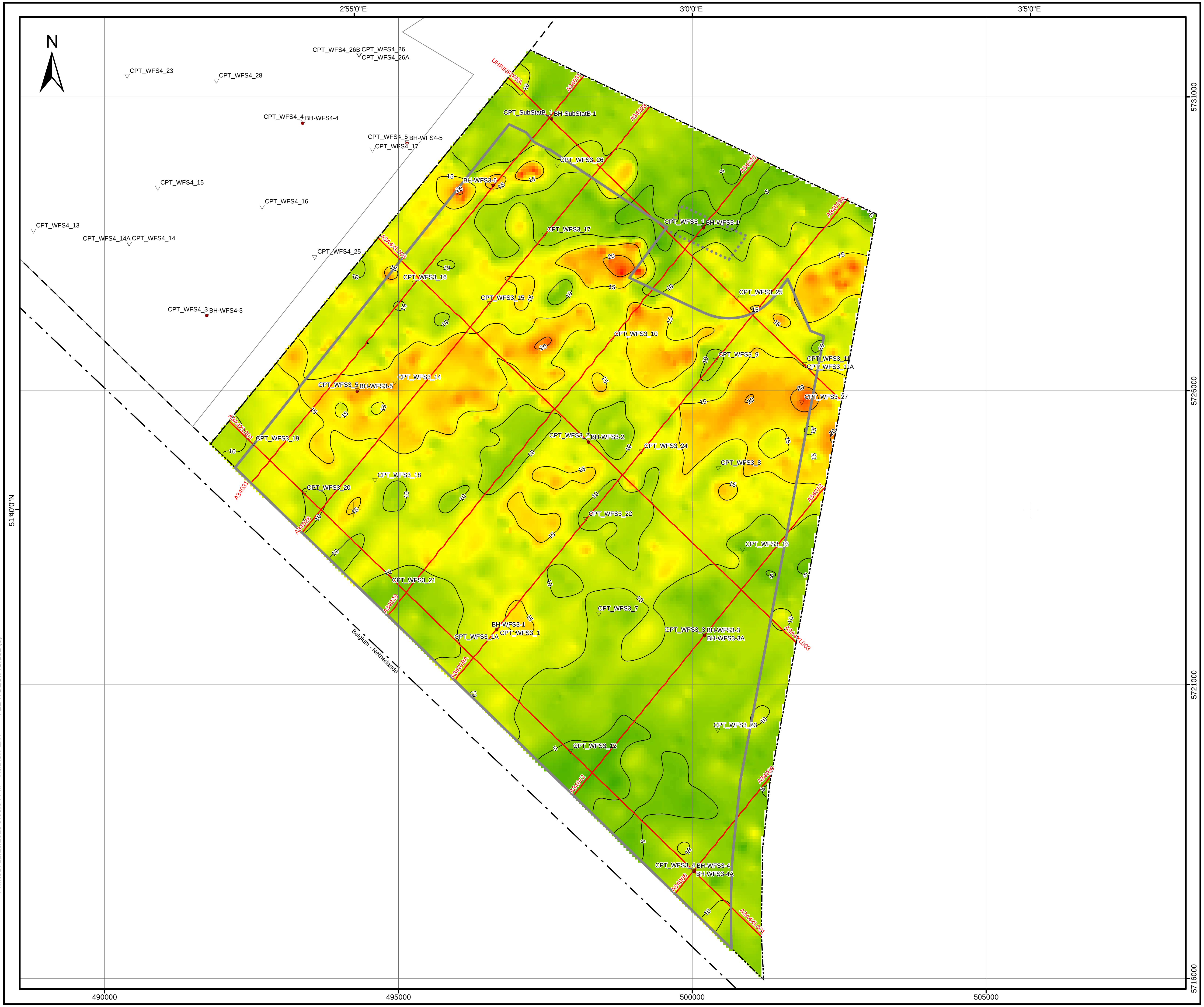


**LEGEND:**

- CPT location
- BH location
- Outline of WFS III
- Outline of WFS IV
- Outline of WFS V
- Investigation Area III
- Investigation Area IV
- Maritime boundary
- Section line of cross-section presented in the report
- Contour line of thickness [m]

**Thickness [m]**

29

14

>0

**NOTES:**

**GEODETIC PARAMETERS:**

| | |
|---|---|
| DATUM | ETRS89 |
| Ellipsoid | GRS80 |
| Semi major axis | a = 6 378 137.000 |
| Inverse flattening | 1/f = 298.257222101 |
| PROJECTION | UTM, Zone 31 North |
| Central Meridian (CM) | 3°00' 00" E |
| Latitude of Origin | 0°00' 00" N |
| False Easting | 500 000 m |
| False Northing | 000 000 m |
| Scale factor | 0.9996 |
| Units | metres/degrees |

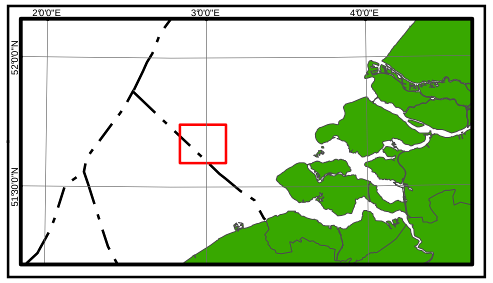



Rijksdienst voor Ondernemend Nederland (RVO)
Croeselaan 15, 3521 BJ, Utrecht - THE NETHERLANDS

Fugro
Prismastraat 4, 2631 RT, Nootdorp - THE NETHERLANDS


**THICKNESS OF UNIT B (KREFTENHEYE FM./ EEM FM.)**

BORSSELE WIND FARM ZONE, WFS III, DUTCH SECTOR, NORTH SEA

Scale 1:60,000
at original A3 page size

0 500 1,000 1,500 2,000 metres

Fugro Report No. N6083/05 | Issue 2 | Plate 3-26


Printed: 12/10/2015 9:00:04 PM Author: LHT FEBV/GEO/FIG/152 (0)

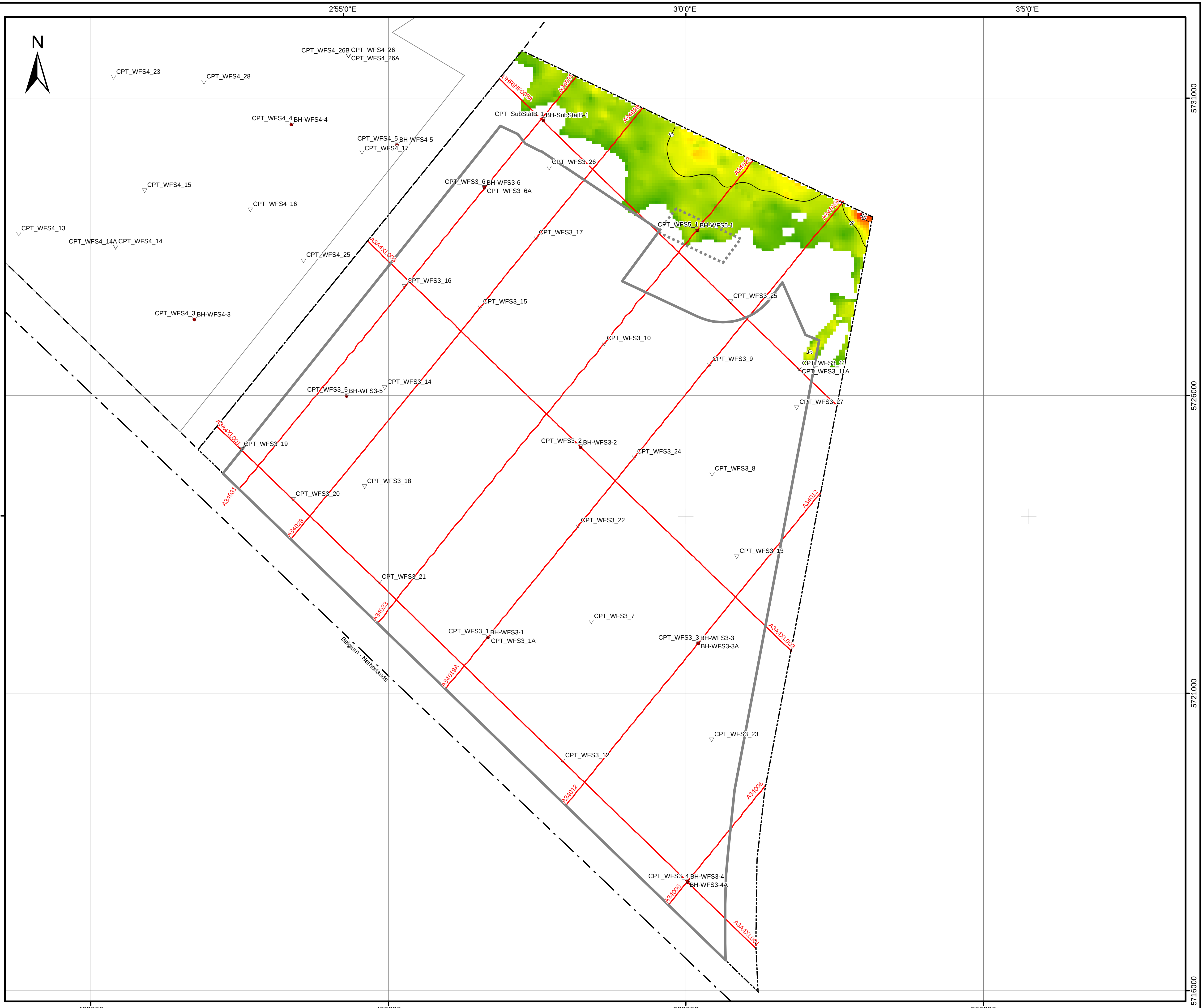


**LEGEND:**

- CPT location
- BH location
- Outline of WFS III
- Outline of WFS IV
- Outline of WFS V
- Investigation Area III
- Investigation Area IV
- Maritime boundary
- Section line of cross-section presented in the report
- Contour line of thickness [m]

**Thickness [m]**

14

7

>0

**NOTES:**
- Unit is absent at blank area with Investigation Area III

**GEODETIC PARAMETERS:**

| | |
|---|---|
| DATUM | ETRS89 |
| Ellipsoid | GRS80 |
| Semi major axis | a = 6 378 137.000 |
| Inverse flattening | 1/f = 298.257222101 |
| PROJECTION | UTM, Zone 31 North |
| Central Meridian (CM) | 3°00' 00" E |
| Latitude of Origin | 0°00' 00" N |
| False Easting | 500 000 m |
| False Northing | 000 000 m |
| Scale factor | 0.9996 |
| Units | metres/degrees |

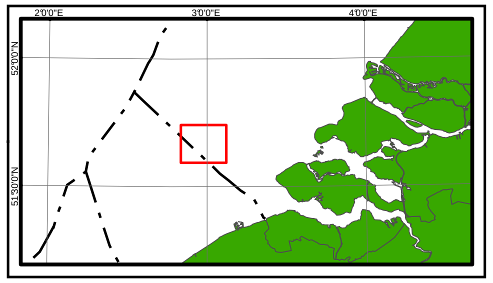


Rijksdienst voor Ondernemend Nederland (RVO)
Croeselaan 15, 3521 BJ, Utrecht - THE NETHERLANDS

Fugro
Prismastraat 4, 2631 RT, Nootdorp - THE NETHERLANDS

**THICKNESS OF UNIT E1 AND E2 (RUISBROEK SAND MB. + WATERVLIET CLAY MB.)**

**BORSSELE WIND FARM ZONE, WFS III, DUTCH SECTOR, NORTH SEA**

Scale 1:60,000
at original A3 page size

0 500 1,000 1,500 2,000 metres

FUGRO

Fugro Report No. N6083/05 | Issue 2 | Plate 3-27

Printed: 12/10/2015 9:16:03 PM Author: LHT FEBV/GEO/FIG/152 (0)

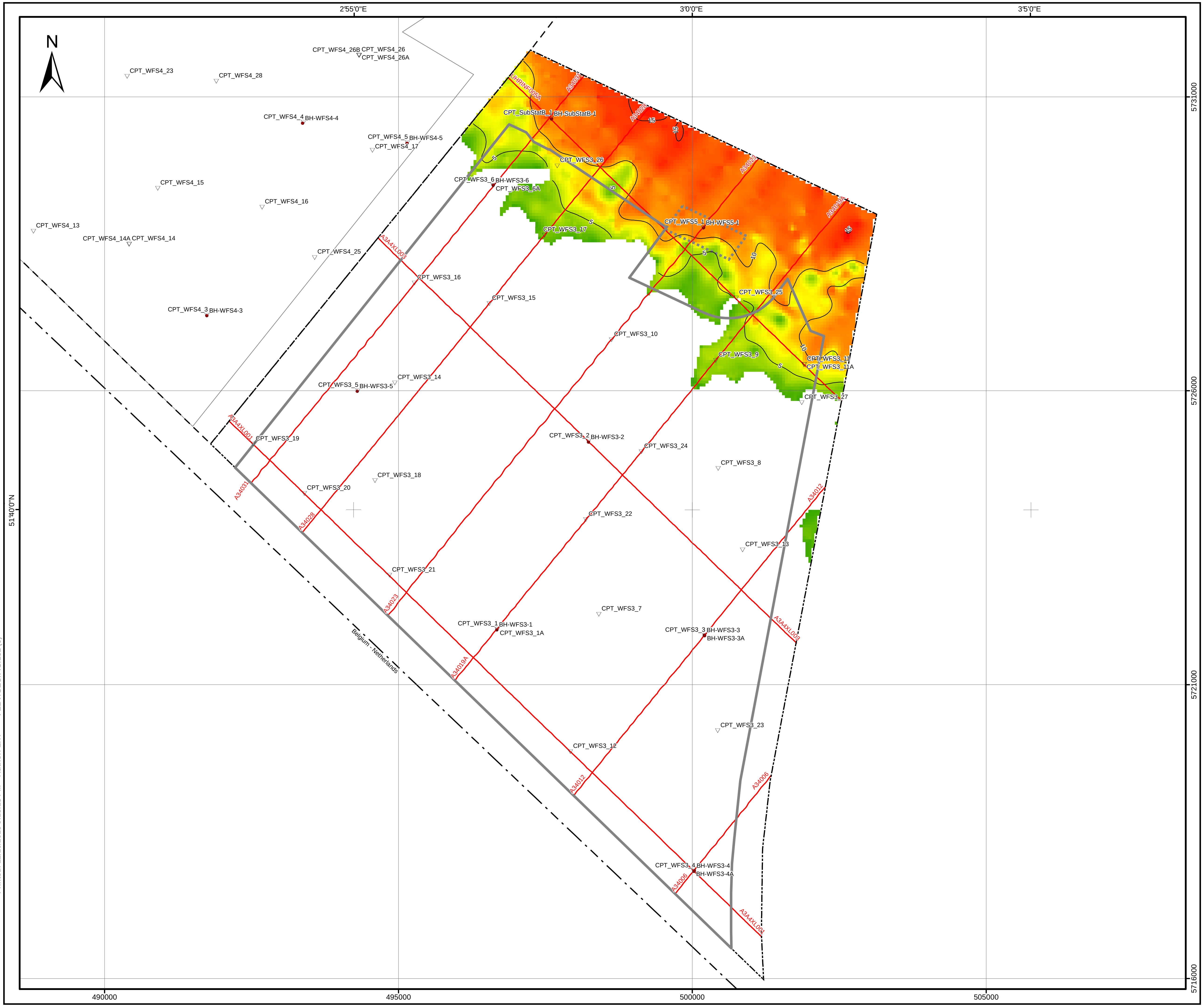


**LEGEND:**

- CPT location
- BH location
- Outline of WFS III
- Outline of WFS IV
- Outline of WFS V
- Investigation Area III
- Investigation Area IV
- Maritime boundary
- Section line of cross-section presented in the report
- Contour line of thickness [m]

**Thickness [m]**

16

8

<0

**NOTES:**
- Unit is absent at blank area within Investigation Area III

**GEODETIC PARAMETERS:**

| | |
|---|---|
| DATUM | ETRS89 |
| Ellipsoid | GRS80 |
| Semi major axis | a = 6 378 137.000 |
| Inverse flattening | 1/f = 298.257222101 |
| PROJECTION | UTM, Zone 31 North |
| Central Meridian (CM) | 3°00' 00" E |
| Latitude of Origin | 0°00' 00" N |
| False Easting | 500 000 m |
| False Northing | 000 000 m |
| Scale factor | 0.9996 |
| Units | metres/degrees |

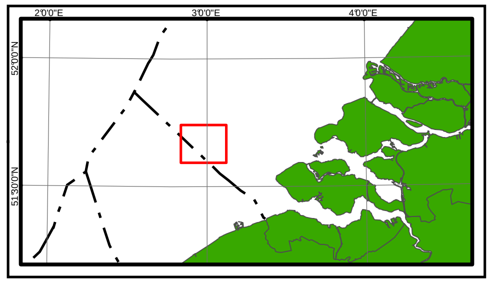


Rijksdienst voor Ondernemend Nederland (RVO)
Croeselaan 15, 3521 BJ, Utrecht - THE NETHERLANDS

Fugro
Prismastraat 4, 2631 RT, Nootdorp - THE NETHERLANDS

**THICKNESS OF UNIT E3 (BASSEVELDE 3 SAND MB.)**

**BORSSELE WIND FARM ZONE, WFS III, DUTCH SECTOR, NORTH SEA**

Scale 1:60,000
at original A3 page size

0 500 1,000 1,500 2,000 metres

FUGRO

Fugro Report No. N6083/05 | Issue 2 | Plate 3-28

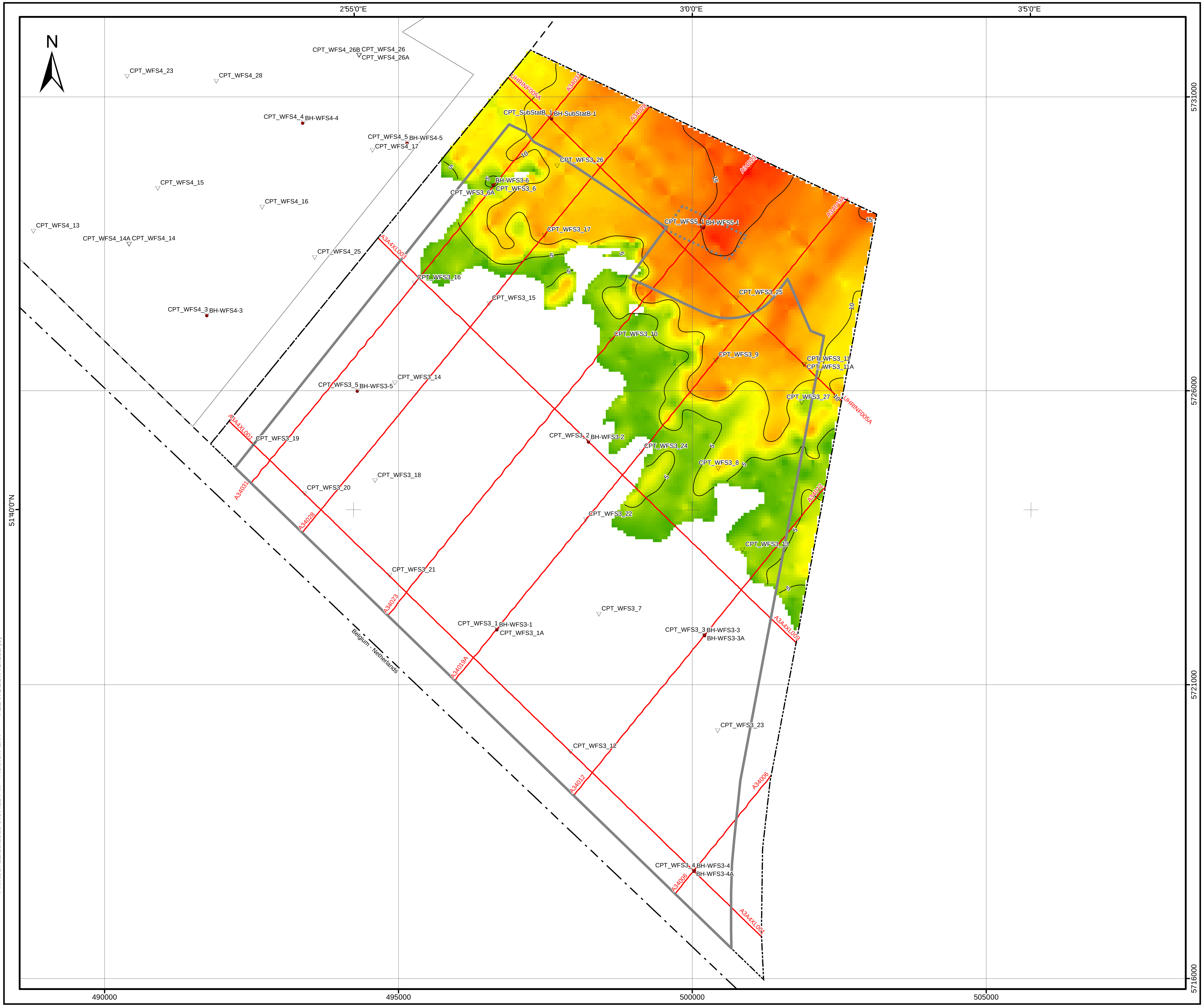


**LEGEND:**

- CPT location
- BH location
- Outline of WFS III
- Outline of WFS IV
- Outline of WFS V
- Investigation Area III
- Investigation Area IV
- Maritime boundary
- Section line of cross-section presented in the report
- Contour line of thickness [m]

**Thickness [m]**

18

9

>0

**NOTES:**
- Unit is absent at blank areas within Investigation Area III

**GEODETIC PARAMETERS:**

| | |
|---|---|
| DATUM | ETRS89 |
| Ellipsoid | GRS80 |
| Semi major axis | a = 6 378 137.000 |
| Inverse flattening | 1/f = 298.257222101 |
| PROJECTION | UTM, Zone 31 North |
| Central Meridian (CM) | 3°00' 00" E |
| Latitude of Origin | 0°00' 00" N |
| False Easting | 500 000 m |
| False Northing | 000 000 m |
| Scale factor | 0.9996 |
| Units | metres/degrees |

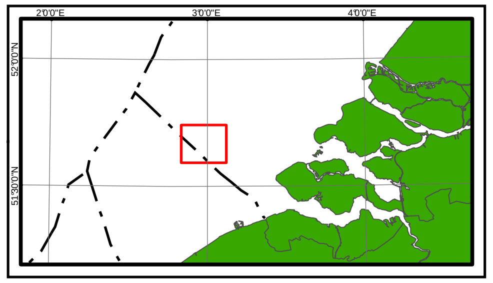


Rijksdienst voor Ondernemend Nederland (RVO)
Croeselaan 15, 3521 BJ, Utrecht - THE NETHERLANDS

Fugro
Prismastraat 4, 2631 RT, Nootdorp - THE NETHERLANDS

**THICKNESS OF UNIT E4 (BASSEVELDE 2 SAND MB.)**

**BORSSELE WIND FARM ZONE, WFS III, DUTCH SECTOR, NORTH SEA**

Scale 1:60,000
at original A3 page size

0 500 1,000 1,500 2,000 metres

| Fugro Report No. N6083/05 | Issue 2 | Plate 3-29 |
|---|---|---|

Printed: 12/10/2015 9:37:12 PM Author: LHT FEBV/GEO/FIG/152 (0)

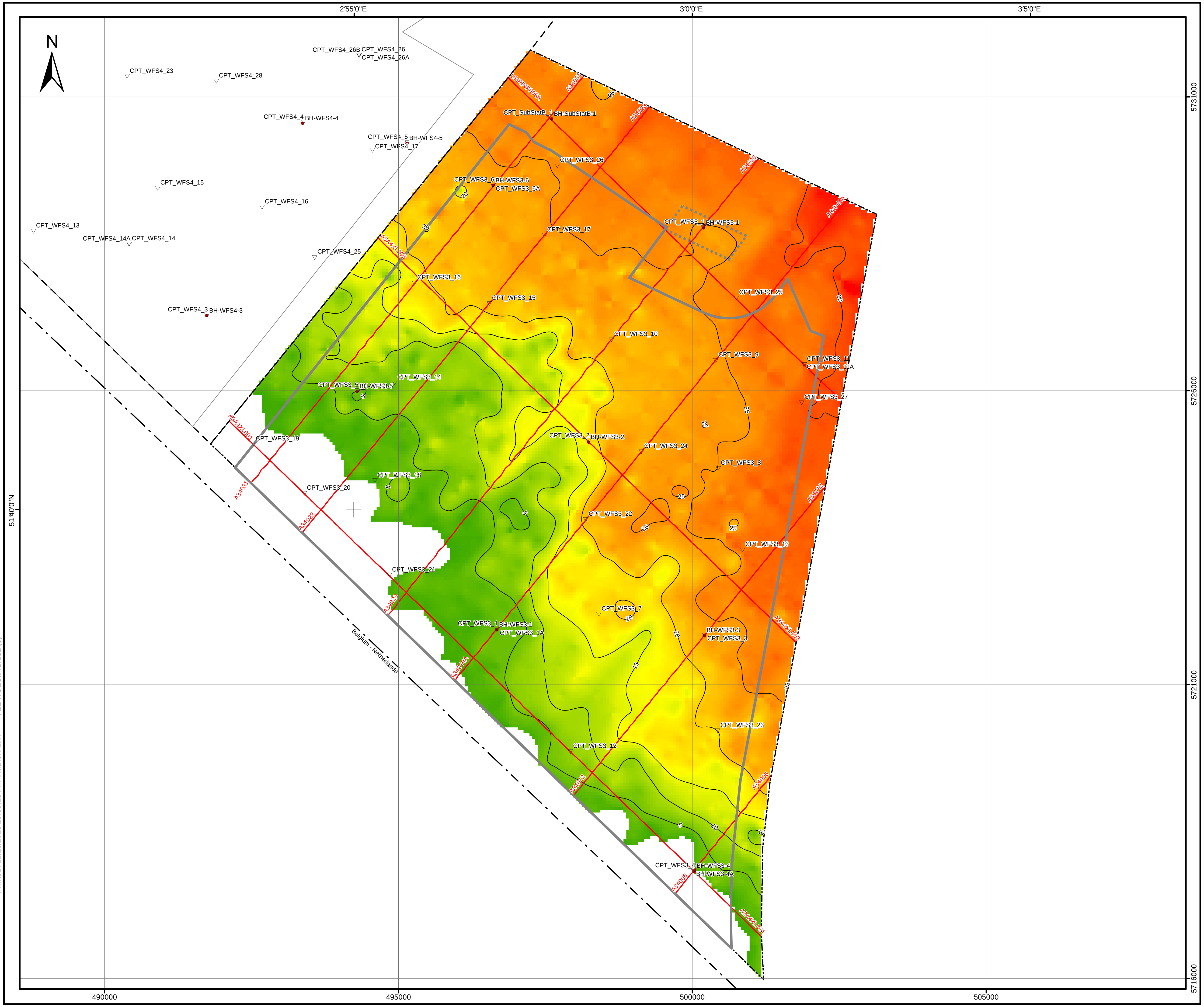


**LEGEND:**

- CPT location
- BH location
- Outline of WFS III
- Outline of WFS IV
- Outline of WFS V
- Investigation Area III
- Investigation Area IV
- Maritime boundary
- Section line of cross-section presented in the report
- Contour line of thickness [m]

**Thickness [m]**

34

17

>0

**NOTES:**

- Unit is absent at blank areas within Investigation Area III
- The thickness of Unit E5 may differ between geotechnical and geophysical data (refer to main text for details).

**GEODETIC PARAMETERS:**

| | |
|---|---|
| DATUM | ETRS89 |
| Ellipsoid | GRS80 |
| Semi major axis | a = 6 378 137.000 |
| Inverse flattening | 1/f = 298.257222101 |
| PROJECTION | UTM, Zone 31 North |
| Central Meridian (CM) | 3°00' 00" E |
| Latitude of Origin | 0°00' 00" N |
| False Easting | 500 000 m |
| False Northing | 000 000 m |
| Scale factor | 0.9996 |
| Units | metres/degrees |

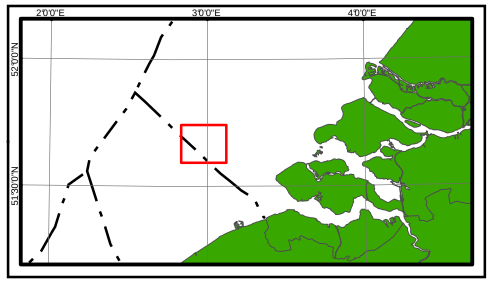



Rijksdienst voor Ondernemend Nederland (RVO)
Croeselaan 15, 3521 BJ, Utrecht - THE NETHERLANDS

Fugro
Prismastraat 4, 2631 RT, Nootdorp - THE NETHERLANDS


**THICKNESS OF UNIT E5 (BASSEVELDE 1 SAND MB.)**

**BORSSELE WIND FARM ZONE, WFS III, DUTCH SECTOR, NORTH SEA**

Scale 1:60,000
at original A3 page size

0 500 1,000 1,500 2,000 metres

Fugro Report No. N6083/05 | Issue 2 | Plate 3-30

FEBV/GEO/FIG/152 (0)
Printed: 12/10/2015 10:06:18 PM Author: LHT

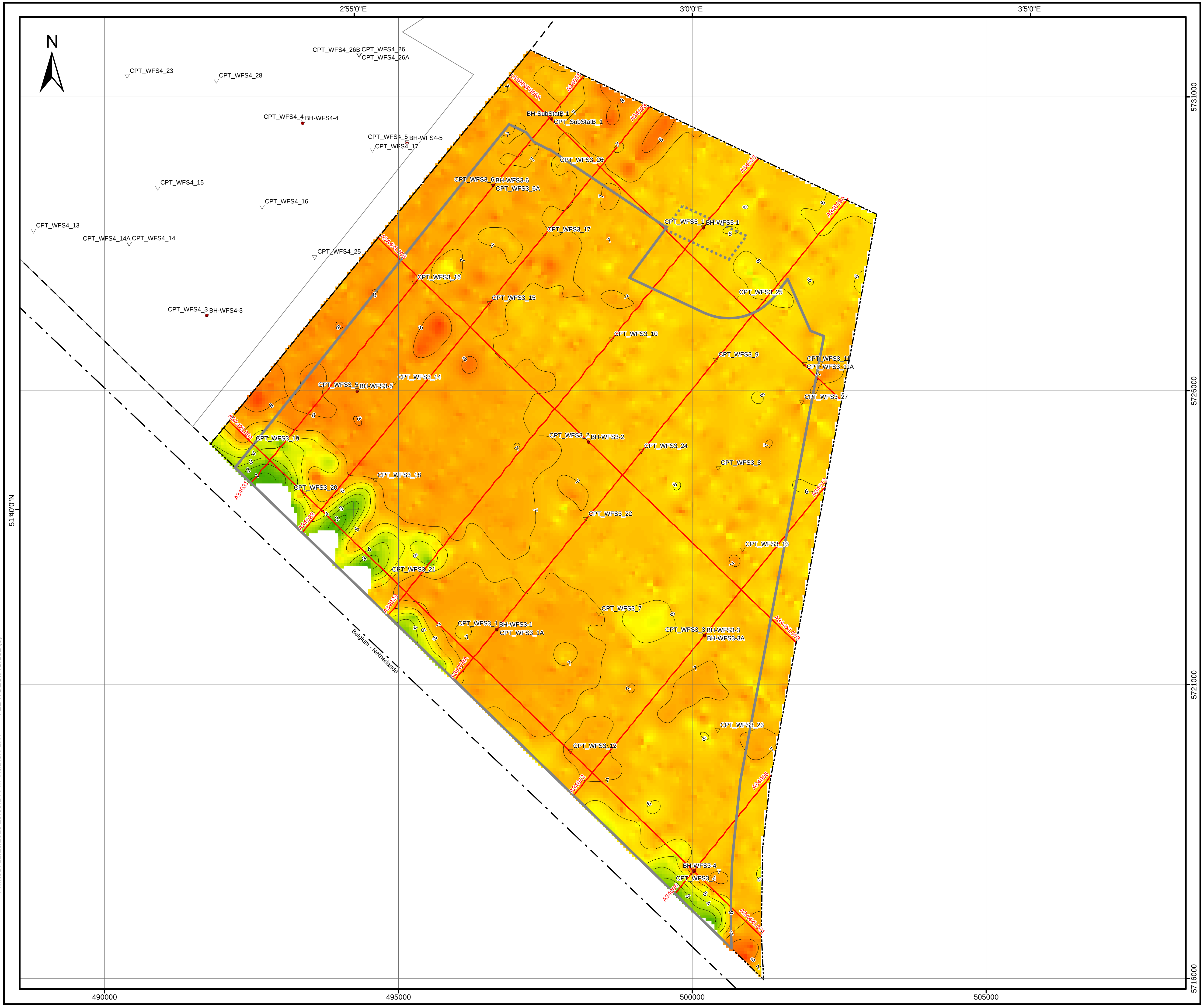


Printed: 12/10/2015 10:06:24 PM Author: LHT FEBV/GEO/FIG/152 (0)

**LEGEND:**

- CPT location
- BH location
- Outline of WFS III
- Outline of WFS IV
- Outline of WFS V
- Investigation Area III
- Investigation Area IV
- Maritime boundary
- Section line of cross-section presented in the report
- Contour line of thickness [m]

**Thickness [m]**

11

5

>0

**NOTES:**

- Unit is absent at blank areas within Investigation Area
- The thickness of Sub-units F1a and F1b may differ between geotechnical and geophysical data (refer to main text for details).

**GEODETIC PARAMETERS:**

| | |
|---|---|
| DATUM | ETRS89 |
| Ellipsoid | GRS80 |
| Semi major axis | a = 6 378 137.000 |
| Inverse flattening | 1/f = 298.257222101 |
| PROJECTION | UTM, Zone 31 North |
| Central Meridian (CM) | 3°00' 00" E |
| Latitude of Origin | 0°00' 00" N |
| False Easting | 500 000 m |
| False Northing | 000 000 m |
| Scale factor | 0.9996 |
| Units | metres/degrees |

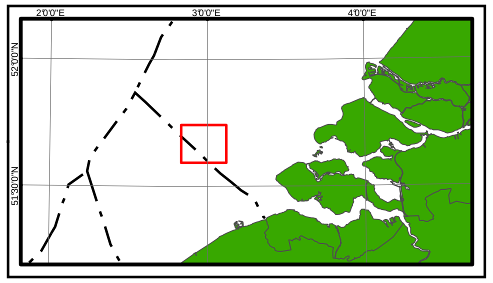


Rijksdienst voor Ondernemend Nederland (RVO)

Croeselaan 15, 3521 BJ, Utrecht - THE NETHERLANDS

Fugro

Prismastraat 4, 2631 RT, Nootdorp - THE NETHERLANDS

**THICKNESS OF UNITS F1a AND F1b (ONDERDIJKE MB.)**

**BORSSELE WIND FARM ZONE, WFS III, DUTCH SECTOR, NORTH SEA**

Scale 1:60,000
at original A3 page size

0 500 1,000 1,500 2,000 metres

Fugro Report No. N6083/05 | Issue 2 | Plate 3-31

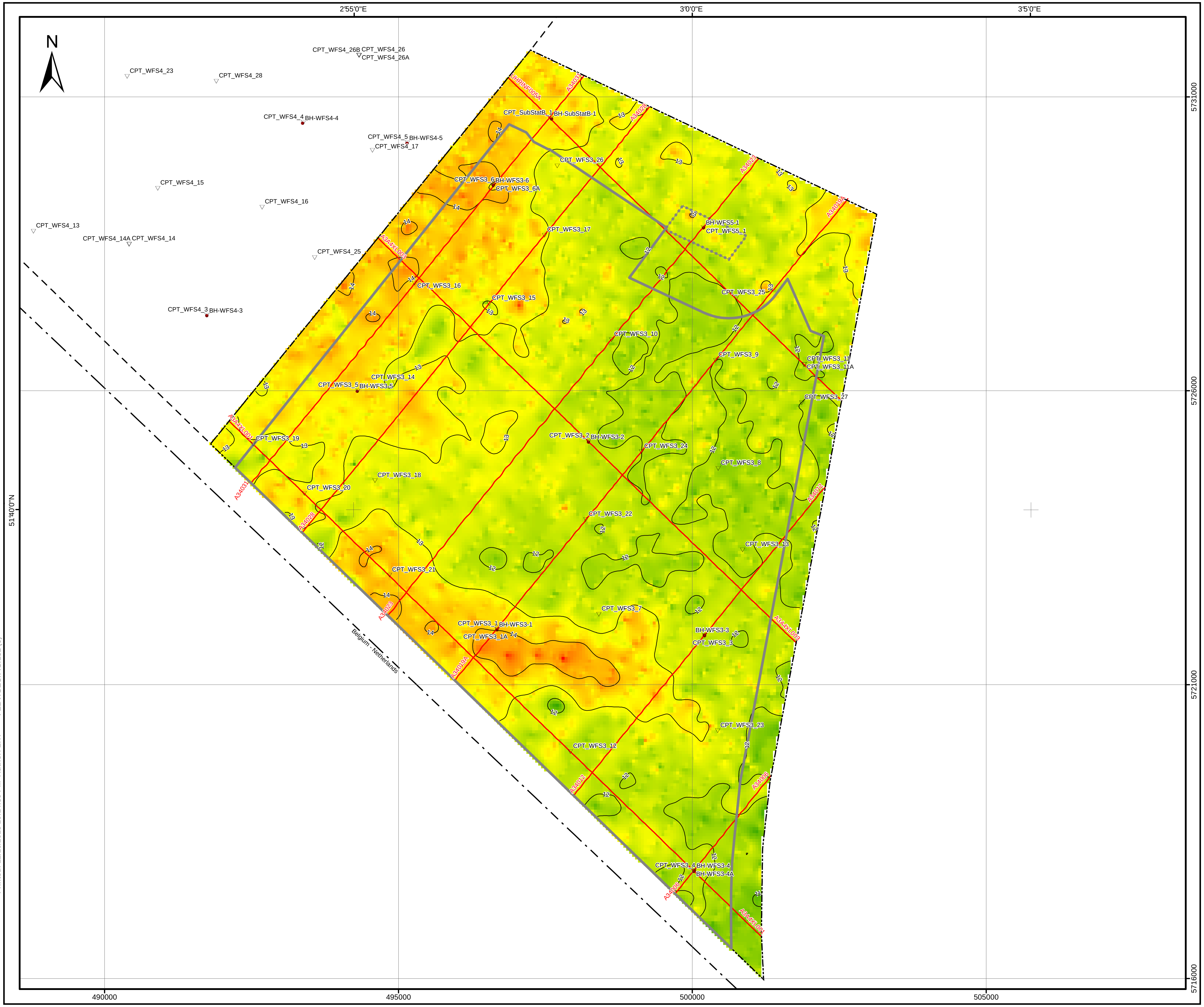


**LEGEND:**

- CPT location
- BH location
- Outline of WFS III
- Investigation Area III
- Outline of WFS V
- Investigation Area IV
- Outline of WFS IV
- Maritime boundary
- Section line of cross-section presented in the report
- Contour line of thickness [m]

**Thickness [m]**

16

13

10

**NOTES:**

**GEODETIC PARAMETERS:**

| | |
|---|---|
| DATUM | ETRS89 |
| Ellipsoid | GRS80 |
| Semi major axis | a = 6 378 137.000 |
| Inverse flattening | 1/f = 298.257222101 |
| PROJECTION | UTM, Zone 31 North |
| Central Meridian (CM) | 3°00' 00" E |
| Latitude of Origin | 0°00' 00" N |
| False Easting | 500 000 m |
| False Northing | 000 000 m |
| Scale factor | 0.9996 |
| Units | metres/degrees |

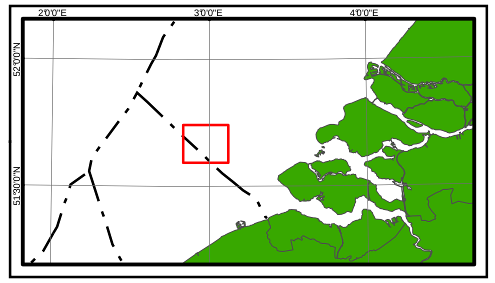


Rijksdienst voor Ondernemend Nederland (RVO)
Croeselaan 15, 3521 BJ, Utrecht - THE NETHERLANDS

Fugro
Prismastraat 4, 2631 RT, Nootdorp - THE NETHERLANDS


**THICKNESS OF UNITS F1c AND F2 (ONDERDIJKE MB. + BUISPUTTEN MB.)**

**BORSSELE WIND FARM ZONE, WFS III, DUTCH SECTOR, NORTH SEA**

Scale 1:60,000
at original A3 page size

0 500 1,000 1,500 2,000 metres

| Fugro Report No. N6083/05 | Issue 2 | Plate 3-32 |
|---|---|---|

Printed: 12/10/2015 10:14:39 PM Author: LHT FEBV/GEO/FIG/152 (0)

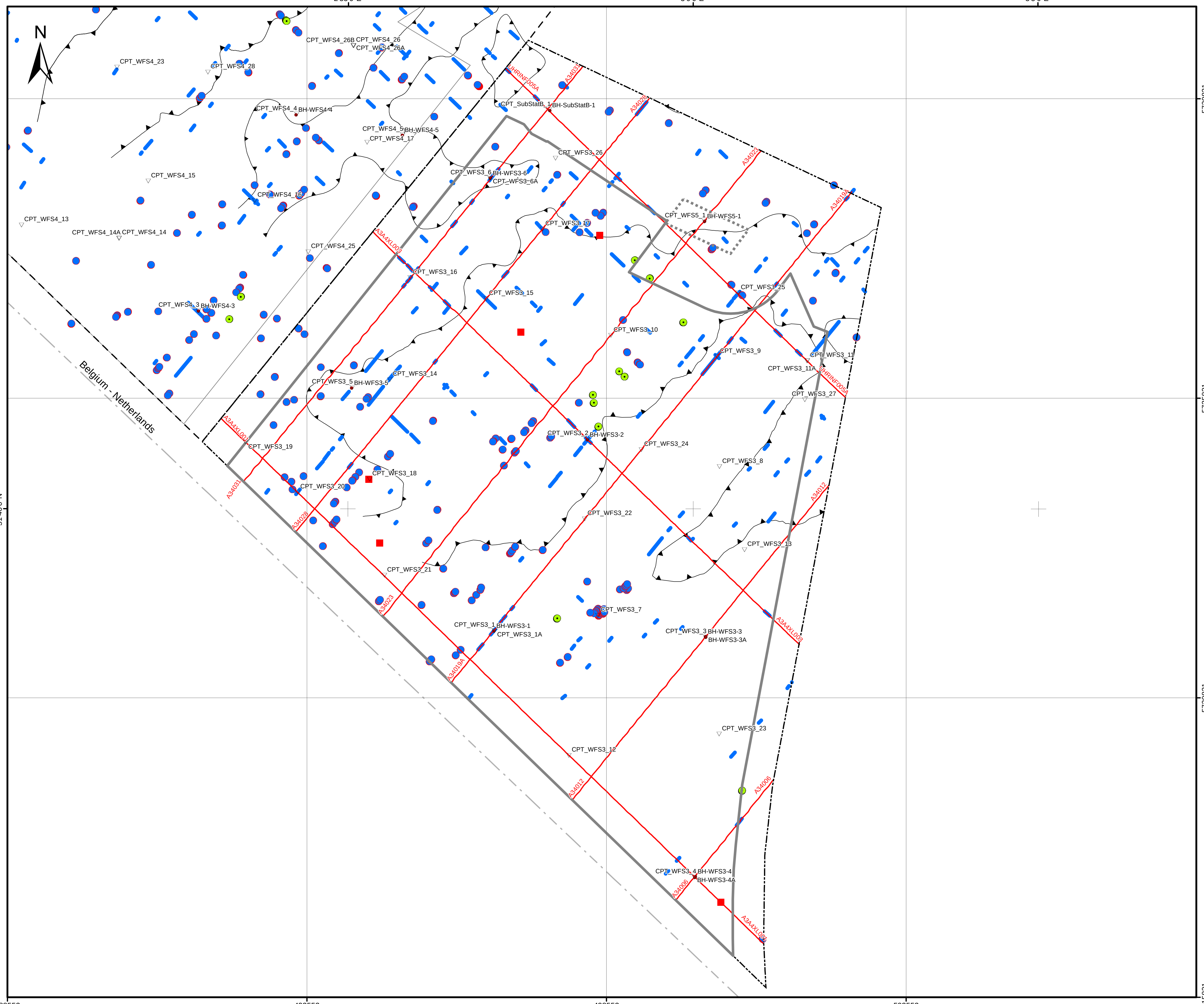


**LEGEND:**

- CPT location
- BH location
- Outline of WFS III
- Outline of WFS IV
- Outline of WFS V
- Investigation Area III
- Investigation Area IV
- Maritime boundary
- Section line of cross-section presented in the report

**Geological features**

- Possible gas and peat layers (seismic anomaly on MCS data)
- Possible boulder (seismic anomaly on SBP data)
- Accumulation of coarse sediment, gravel and cobbles within Unit A and B (based on SBP data)
- Accumulation of coarse sediment, gravel and cobbles within Unit A and B (based on MCS data)
- Edge of erosive sequence filled with Unit A and B

**NOTES:**
- Modified from Fugro (2015a and 2015b)
- Presented information applies to SBP and MCS track lines
- Arrows on "edge of erosive sequence"-feature point to direction of increased incision and increased thickness of Unit B

**GEODETIC PARAMETERS:**

| | |
|---|---|
| DATUM | ETRS89 |
| Ellipsoid | GRS80 |
| Semi major axis | a = 6 378 137.000 |
| Inverse flattening | 1/f = 298.257222101 |
| PROJECTION | UTM, Zone 31 North |
| Central Meridian (CM) | 3°00' 00" E |
| Latitude of Origin | 0°00' 00" N |
| False Easting | 500 000 m |
| False Northing | 000 000 m |
| Scale factor | 0.9996 |
| Units | metres/degrees |

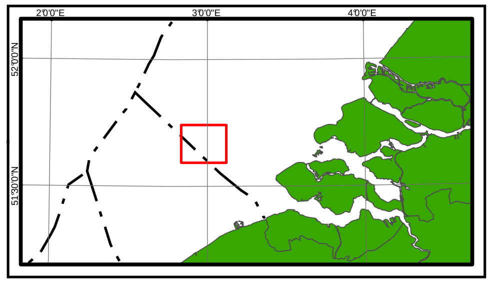


Rijksdienst voor Ondernemend Nederland (RVO)

Croeselaan 15, 3521 BJ, Utrecht - THE NETHERLANDS

Fugro

Prismastraat 4, 2631 RT, Nootdorp - THE NETHERLANDS

**GEOLOGICAL FEATURES**

**BORSSELE WIND FARM ZONE, WFS III**
**DUTCH SECTOR, NORTH SEA**

Scale 1:60,000
at original A3 page size

0 500 1,000 1,500 2,000 metres

| Fugro Report No. N6083/05 | Issue 3 | Plate 5-1 |
|---|---|---|

Printed: 12/21/2015 3:38:24 PM Author: LHT FEBV/GEO/FIG/152 (0)

## SECTION A: GEOTECHNICAL PARAMETERS – LOCATION SPECIFIC

**LIST OF PLATES IN SECTION A:**

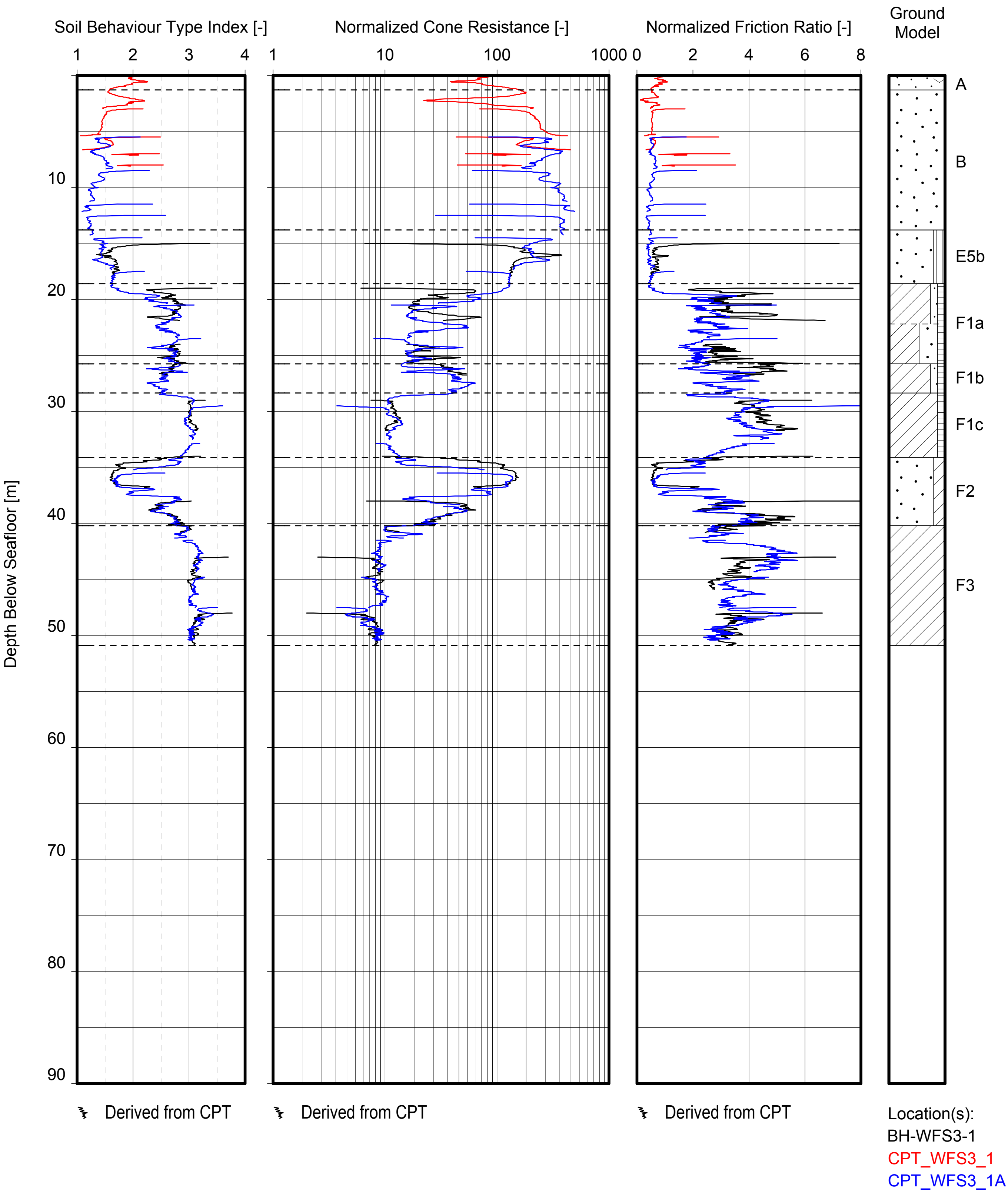


Note(s):
- Soil Behaviour Type Index is according to Robertson (2009), refer to Appendix 1, document titled "Cone Penetration Test Interpretation"

GeODin/1.Normalized CPT Parameters versus Depth (all UNITS, incl. GM).GLO/2015-12-09 10:46:38

## NORMALIZED CPT PARAMETERS VERSUS DEPTH

BORSSELE WIND FARM ZONE, WFS III - DUTCH SECTOR, NORTH SEA

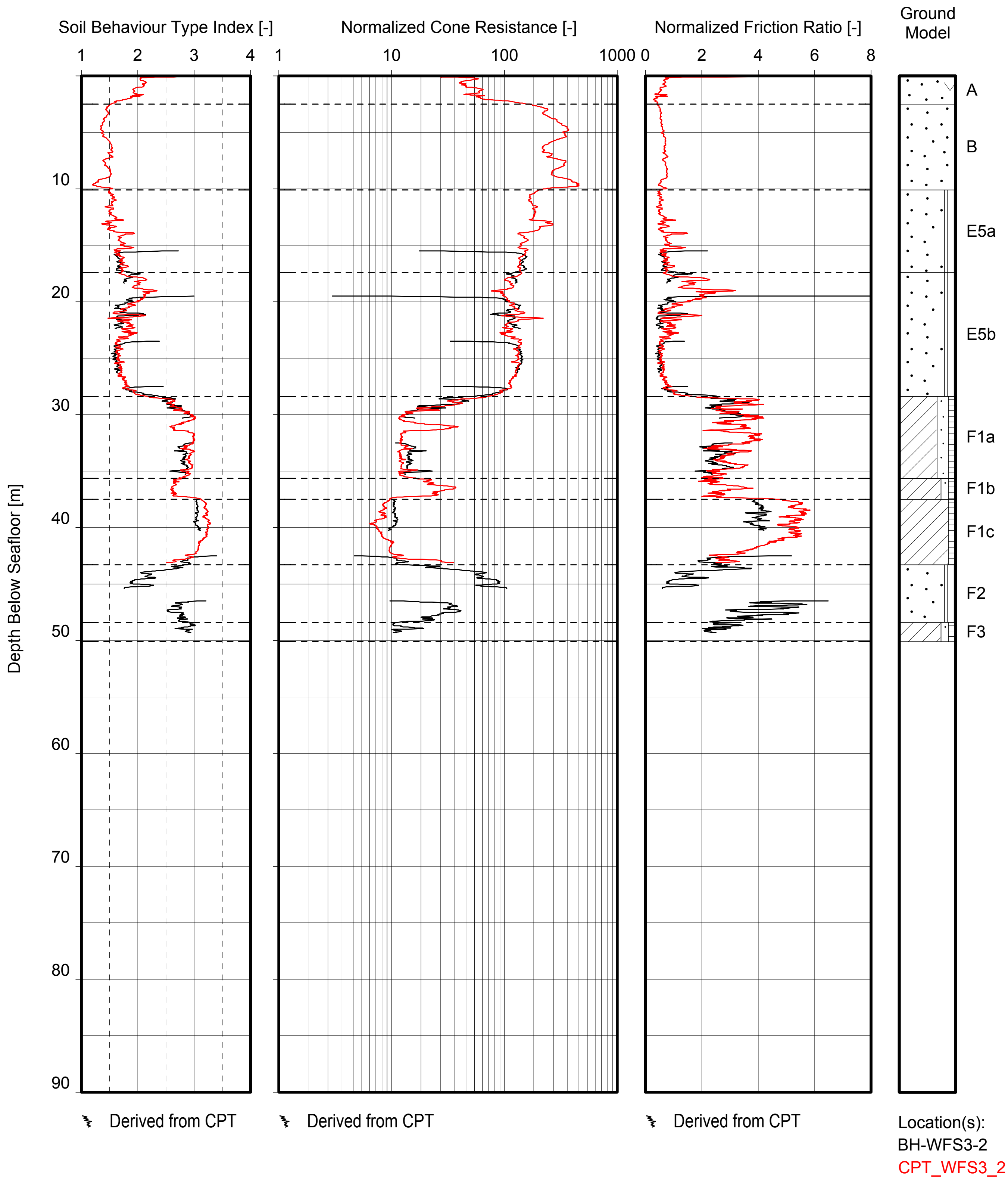


Note(s):
- Soil Behaviour Type Index is according to Robertson (2009), refer to Appendix 1, document titled "Cone Penetration Test Interpretation"

GeODin/1.Normalized CPT Parameters versus Depth (all UNITS, incl. GM).GLO/2015-12-09 10:49:33

**NORMALIZED CPT PARAMETERS VERSUS DEPTH**

BORSSELE WIND FARM ZONE, WFS III - DUTCH SECTOR, NORTH SEA

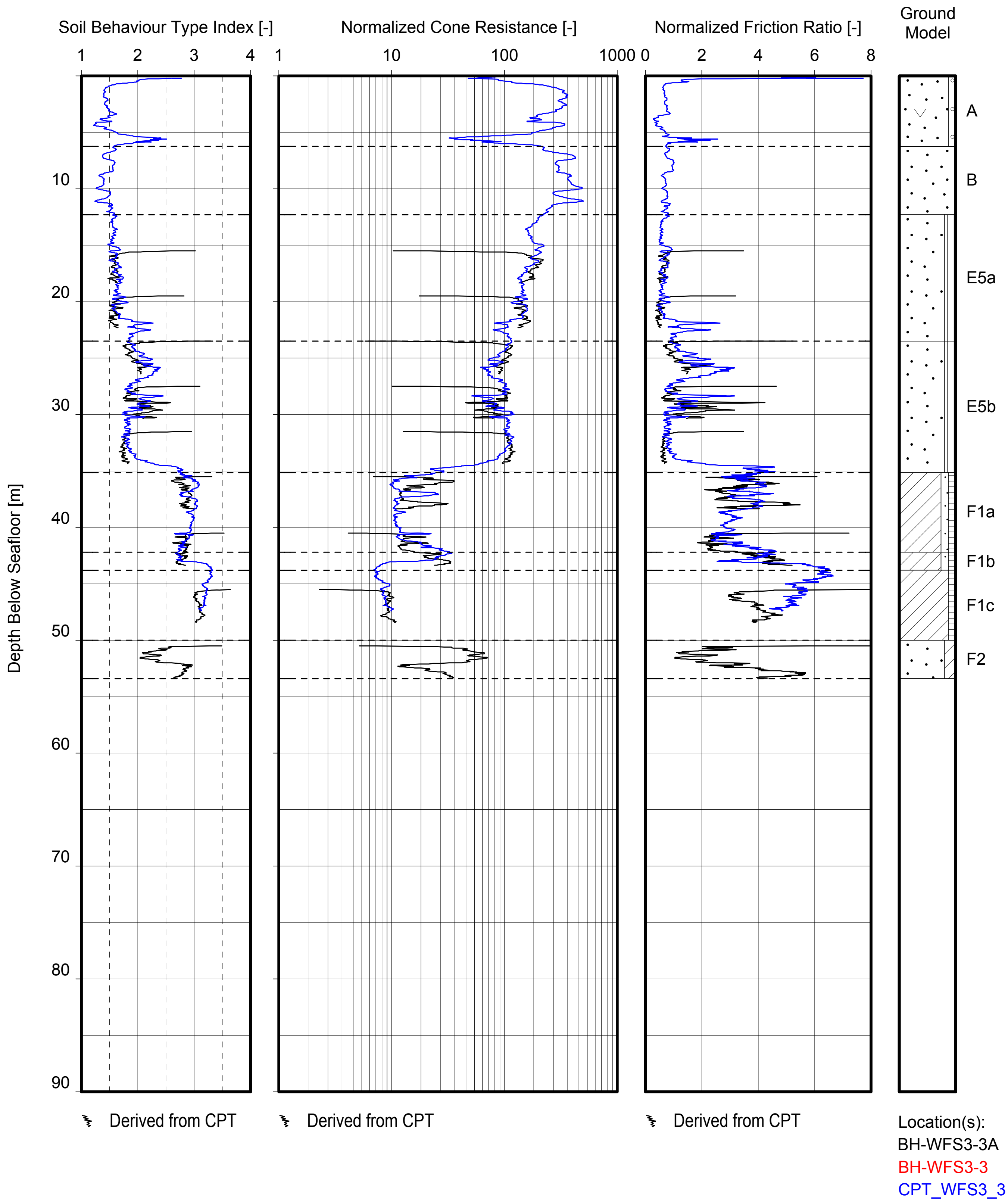


Note(s):
- Soil Behaviour Type Index is according to Robertson (2009), refer to Appendix 1, document titled "Cone Penetration Test Interpretation"

GeODin/1.Normalized CPT Parameters versus Depth (all UNITS, incl. GM).GLO/2015-12-09 10:52:35

## NORMALIZED CPT PARAMETERS VERSUS DEPTH

BORSSELE WIND FARM ZONE, WFS III - DUTCH SECTOR, NORTH SEA

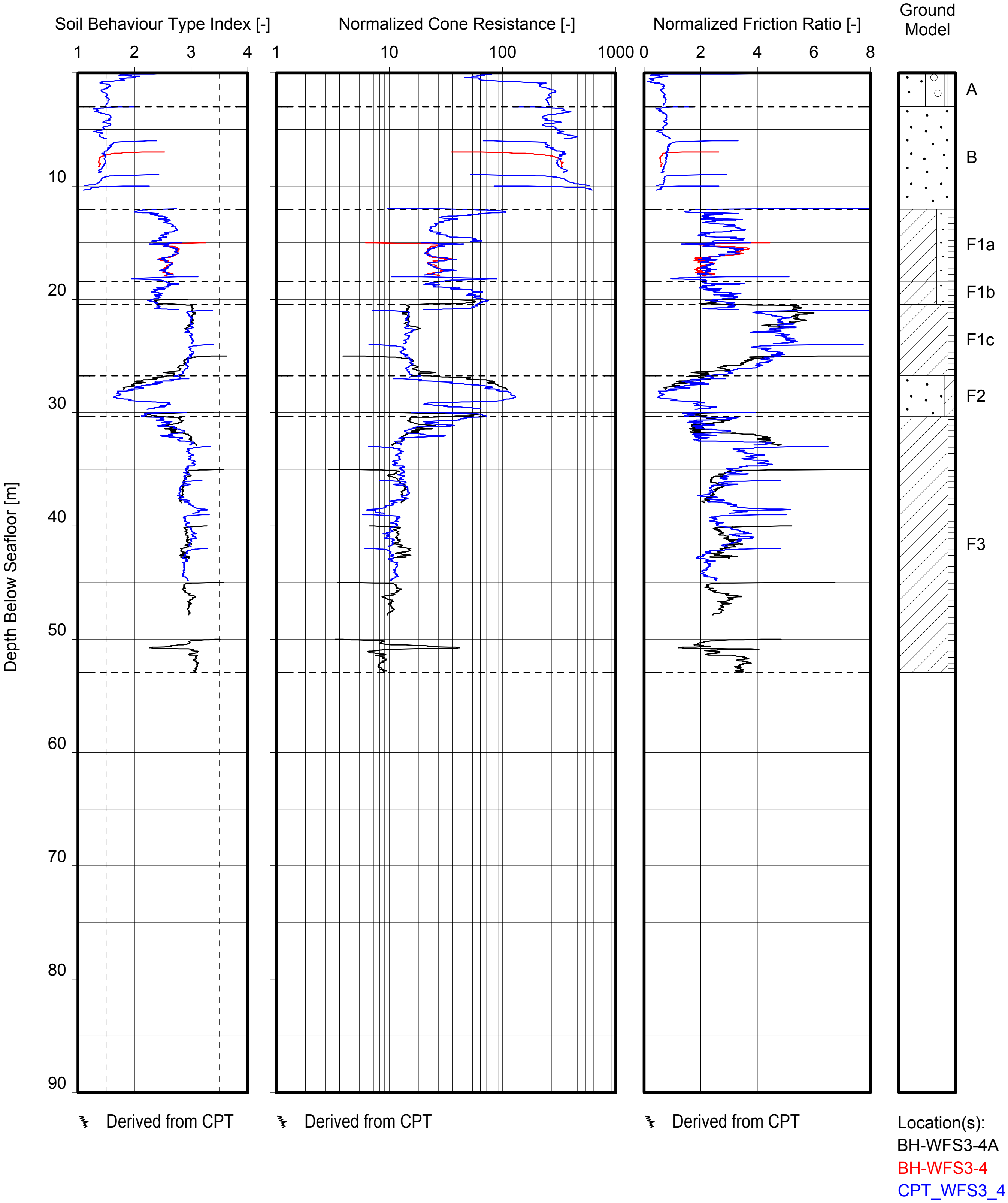


Note(s):
- Soil Behaviour Type Index is according to Robertson (2009), refer to Appendix 1, document titled "Cone Penetration Test Interpretation"

**NORMALIZED CPT PARAMETERS VERSUS DEPTH**

BORSSELE WIND FARM ZONE, WFS III - DUTCH SECTOR, NORTH SEA

GeODin/1.Normalized CPT Parameters versus Depth (all UNITS, incl. GM).GLO/2015-12-09 10:54:53

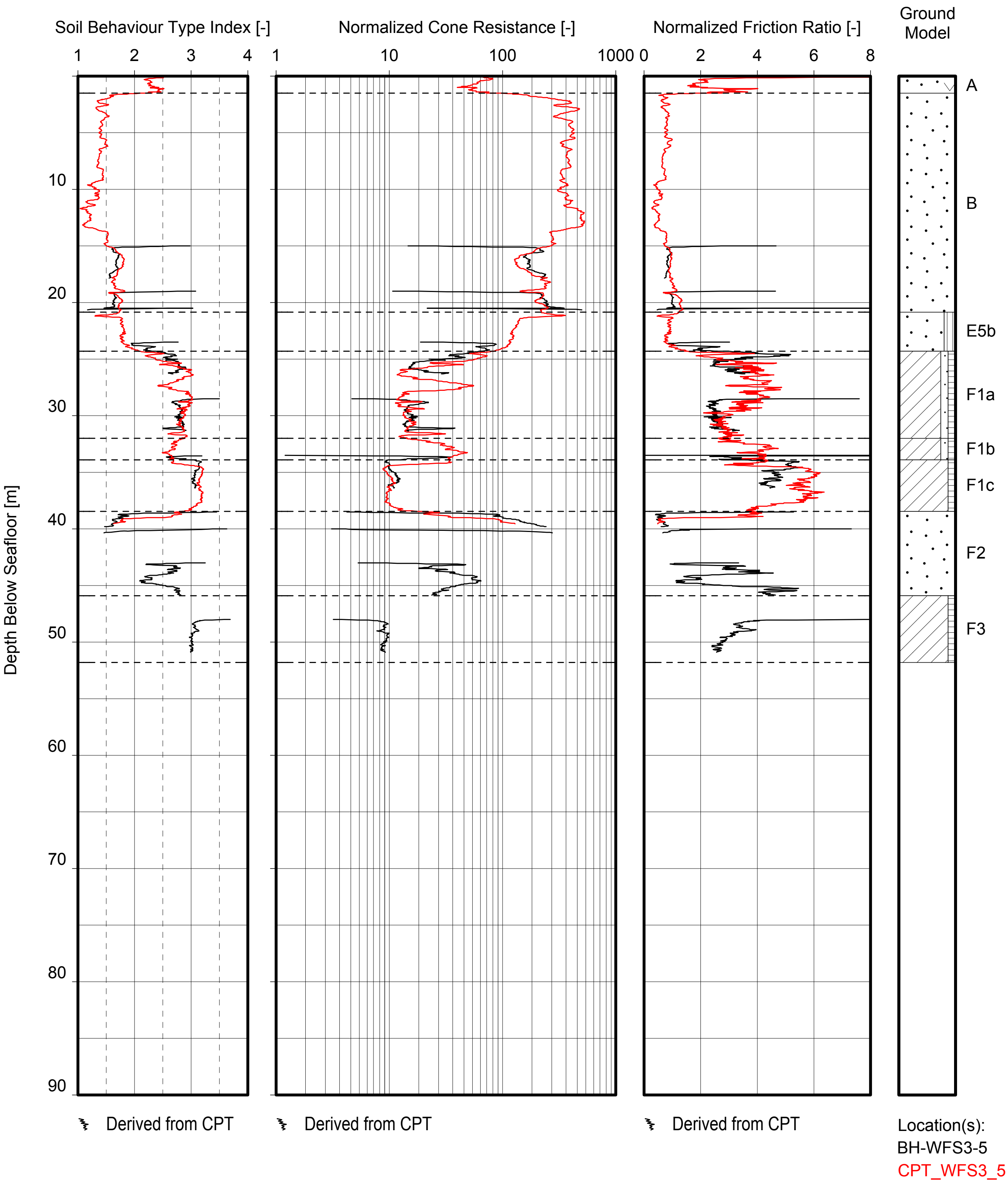


Note(s):
- Soil Behaviour Type Index is according to Robertson (2009), refer to Appendix 1, document titled "Cone Penetration Test Interpretation"

GeODin/1.Normalized CPT Parameters versus Depth (all UNITS, incl. GM).GLO/2015-12-09 10:57:03

**NORMALIZED CPT PARAMETERS VERSUS DEPTH**

BORSSELE WIND FARM ZONE, WFS III - DUTCH SECTOR, NORTH SEA

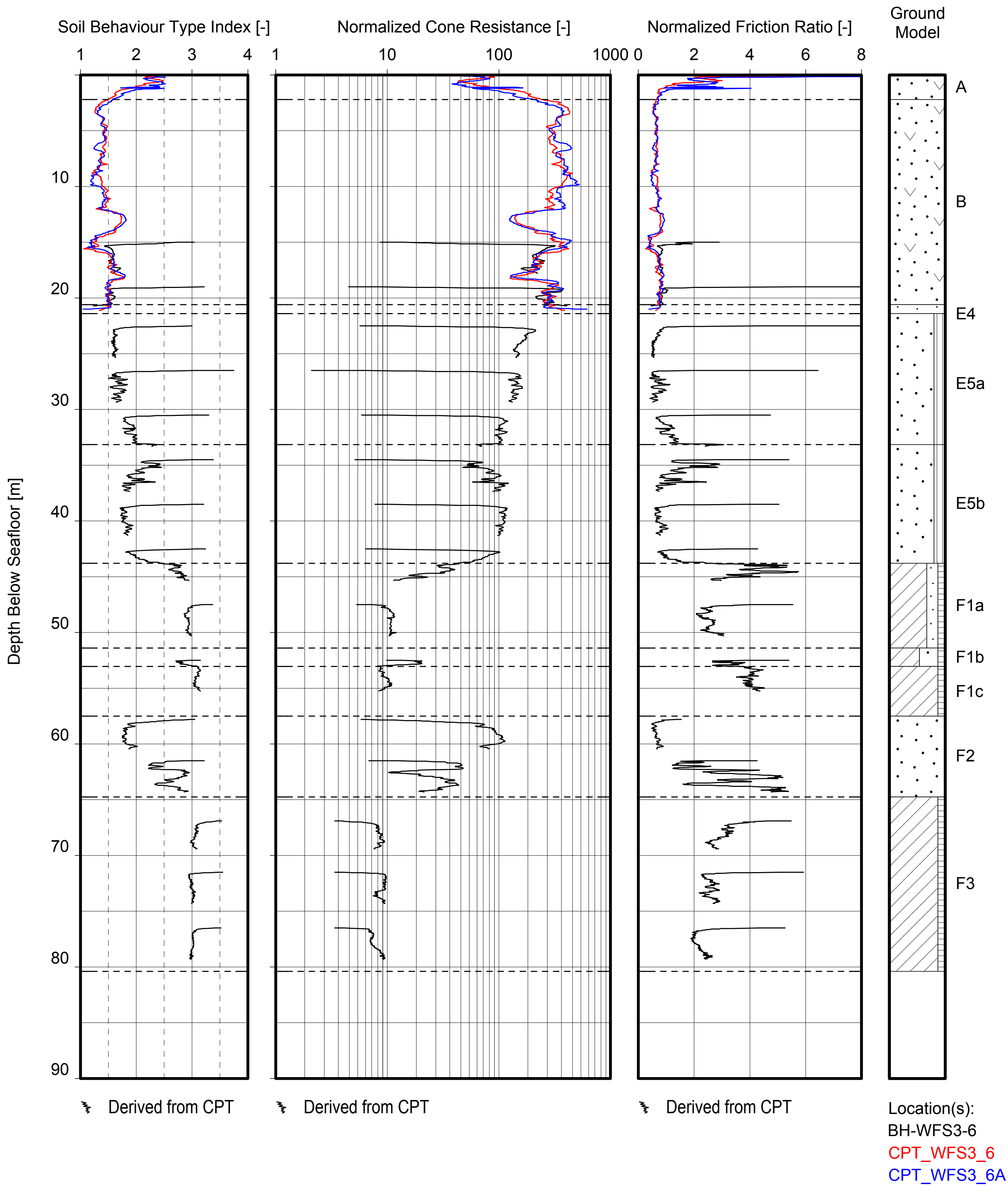


GeODin/1.Normalized CPT Parameters versus Depth (all UNITS, incl. GM).GLO/2015-12-09 11:18:43

Note(s):
- Soil Behaviour Type Index is according to Robertson (2009), refer to Appendix 1, document titled "Cone Penetration Test Interpretation"

**NORMALIZED CPT PARAMETERS VERSUS DEPTH**

BORSSELE WIND FARM ZONE, WFS III - DUTCH SECTOR, NORTH SEA

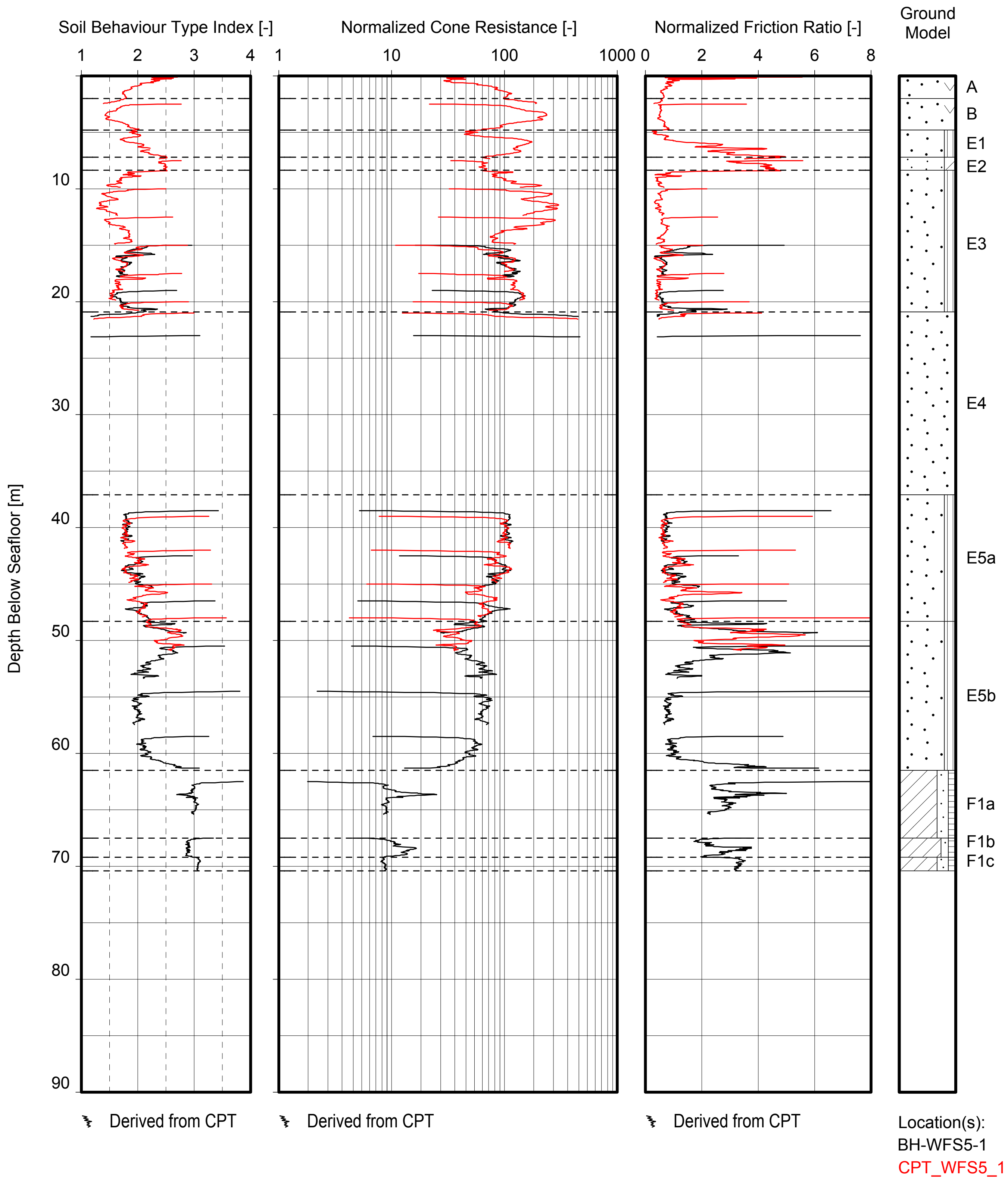


GeODin/1.Normalized CPT Parameters versus Depth (all UNITS, incl. GM).GLO/2015-12-09 11:21:20

Note(s):
- Soil Behaviour Type Index is according to Robertson (2009), refer to Appendix 1, document titled "Cone Penetration Test Interpretation"

**NORMALIZED CPT PARAMETERS VERSUS DEPTH**

BORSSELE WIND FARM ZONE, WFS III - DUTCH SECTOR, NORTH SEA

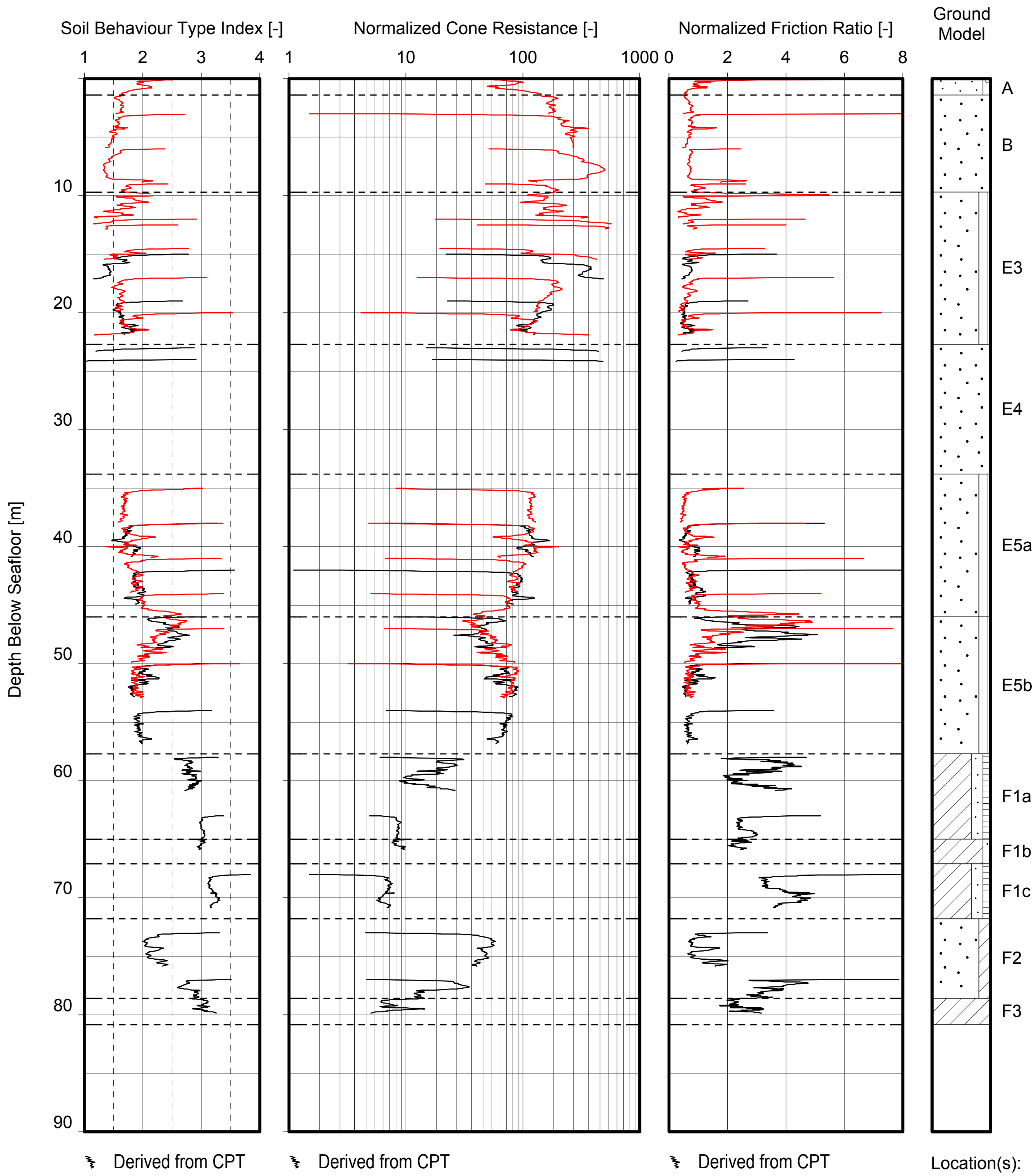


Location(s):
BH-SubStatB-1
CPT_SubStatB_1



Note(s):
- Soil Behaviour Type Index is according to Robertson (2009), refer to Appendix 1, document titled "Cone Penetration Test Interpretation"

**NORMALIZED CPT PARAMETERS VERSUS DEPTH**

BORSSELE WIND FARM ZONE, WFS III - DUTCH SECTOR, NORTH SEA

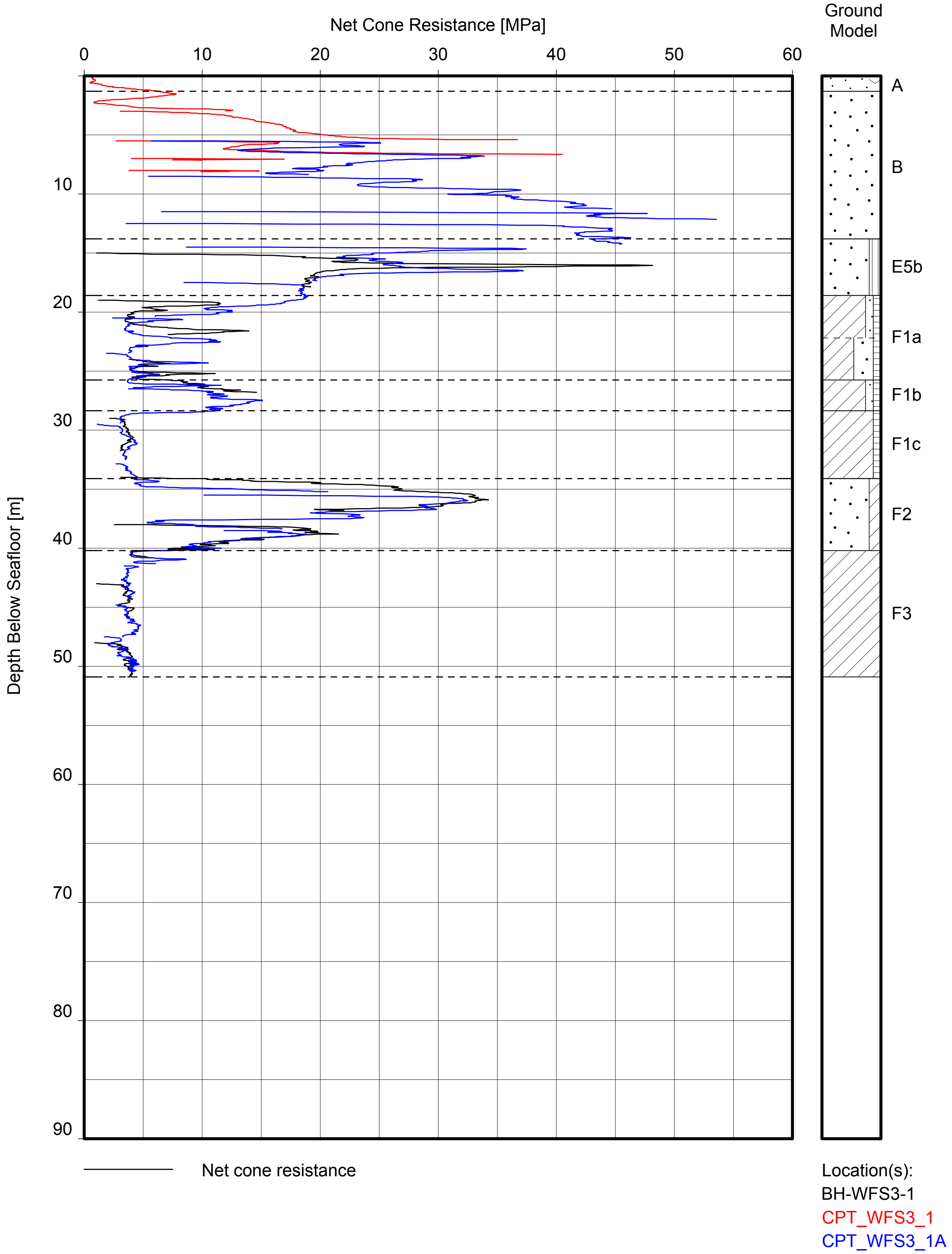


GeODin/2.Net Cone Resistance versus Depth (all UNITS, incl. GM).GLO/2015-12-09 10:47:07

## NET CONE RESISTANCE VERSUS DEPTH

BORSSELE WIND FARM ZONE, WFS III - DUTCH SECTOR, NORTH SEA

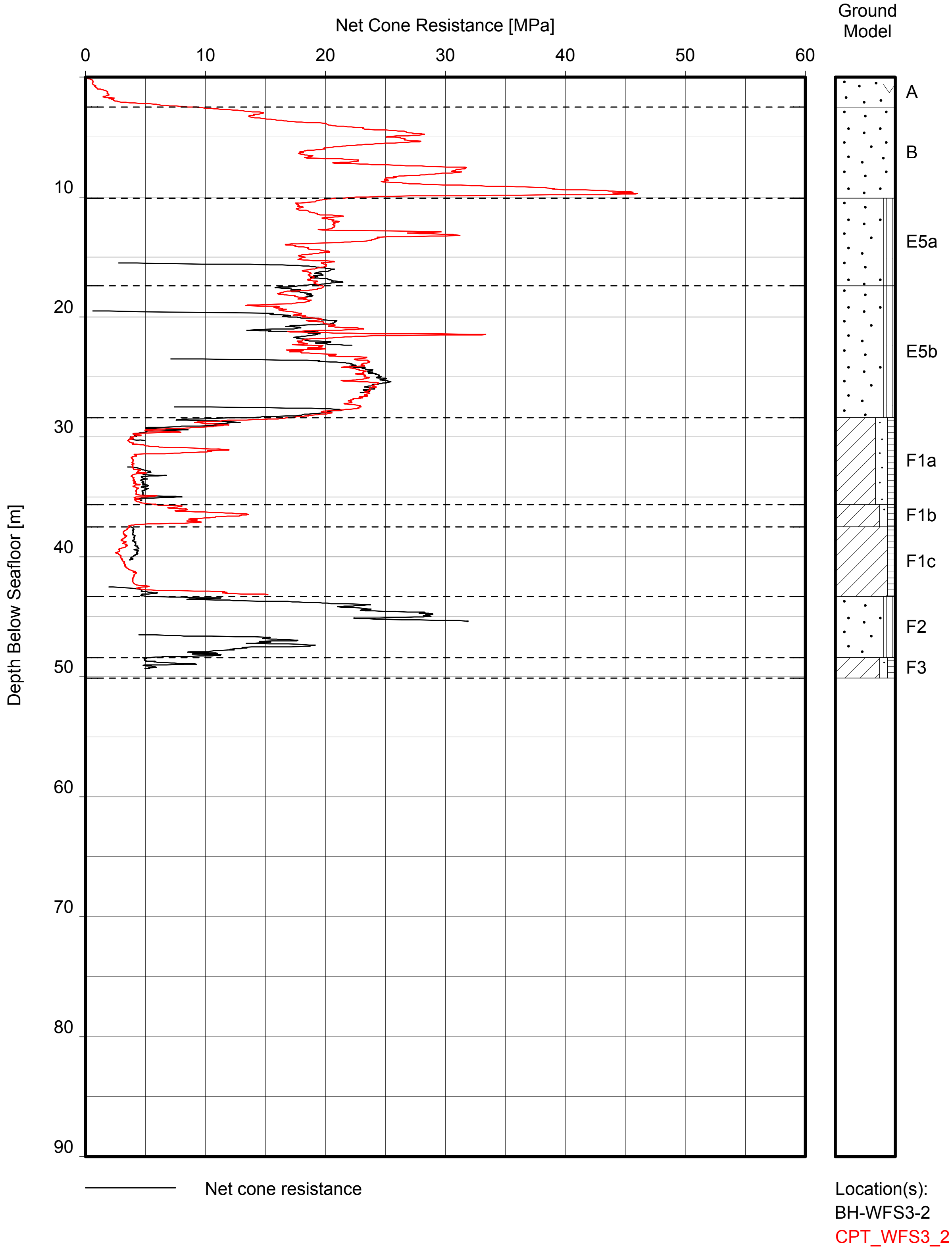


GeODin/2.Net Cone Resistance versus Depth (all UNITS, incl. GM).GLO/2015-12-09 10:49:55

**NET CONE RESISTANCE VERSUS DEPTH**

BORSSELE WIND FARM ZONE, WFS III - DUTCH SECTOR, NORTH SEA

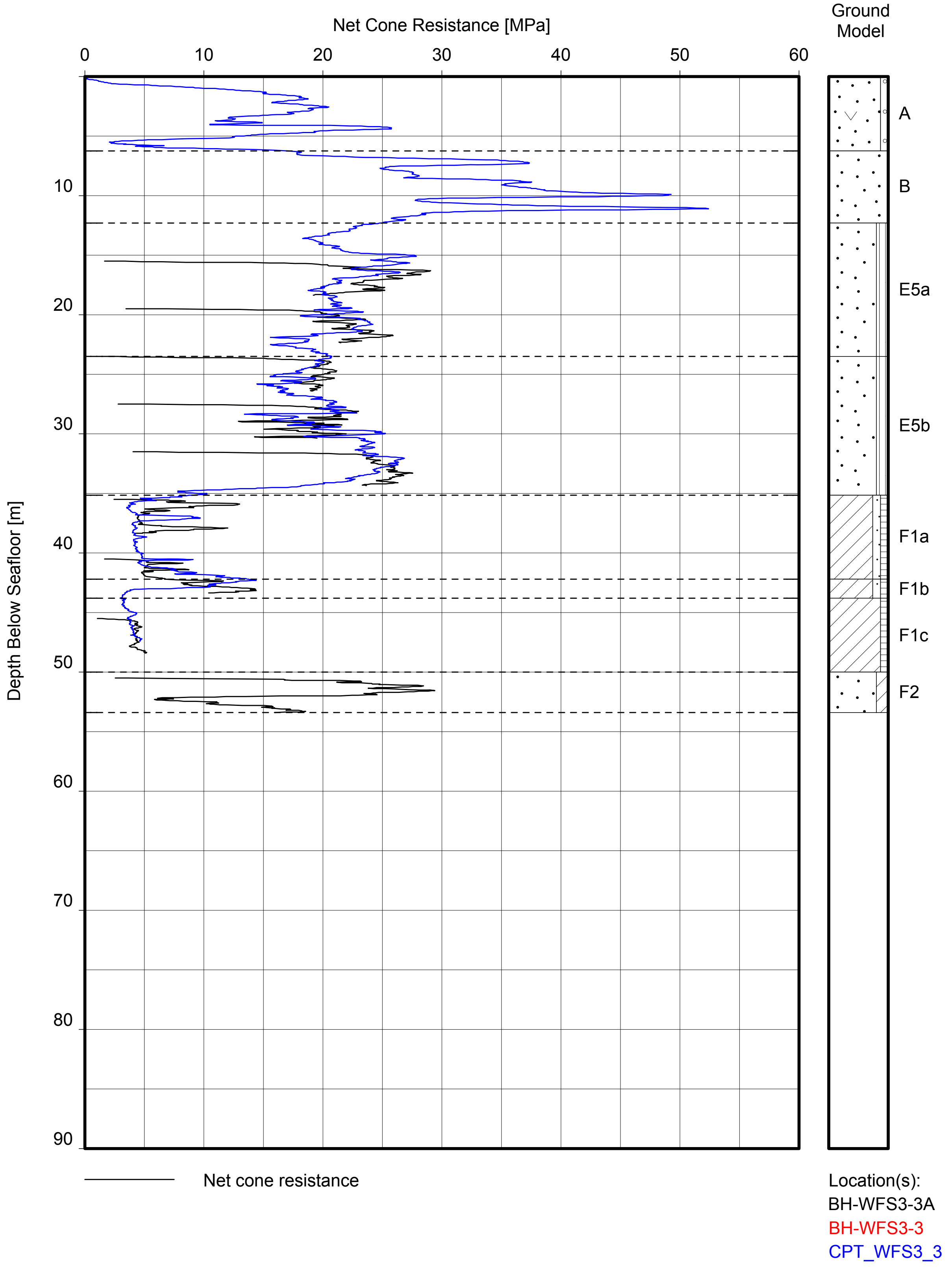


GeODin/2.Net Cone Resistance versus Depth (all UNITS, incl. GM).GLO/2015-12-09 10:52:53

## NET CONE RESISTANCE VERSUS DEPTH

BORSSELE WIND FARM ZONE, WFS III - DUTCH SECTOR, NORTH SEA

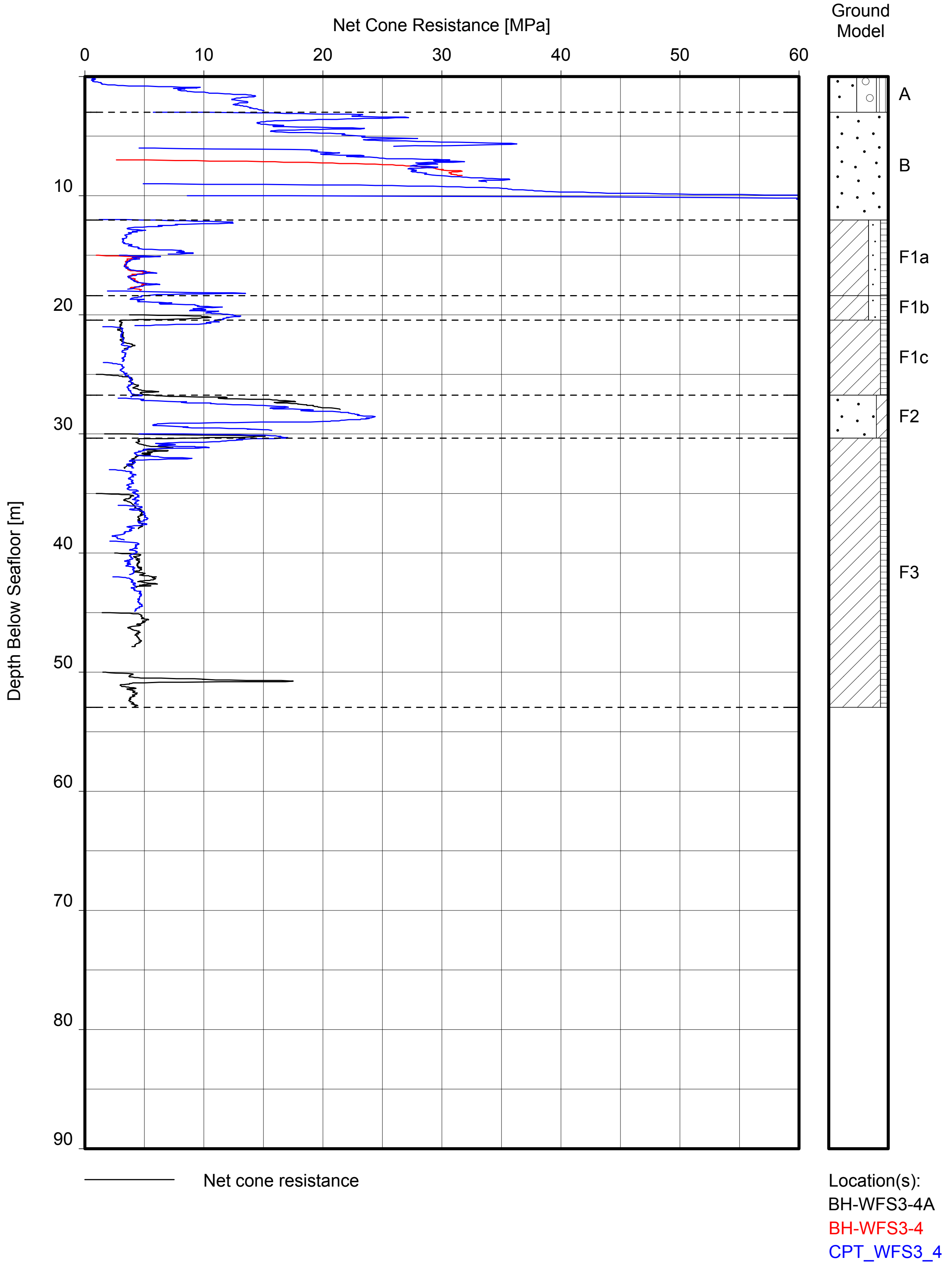


GeODin/2.Net Cone Resistance versus Depth (all UNITS, incl. GM).GLO/2015-12-09 10:55:04

**NET CONE RESISTANCE VERSUS DEPTH**

BORSSELE WIND FARM ZONE, WFS III - DUTCH SECTOR, NORTH SEA

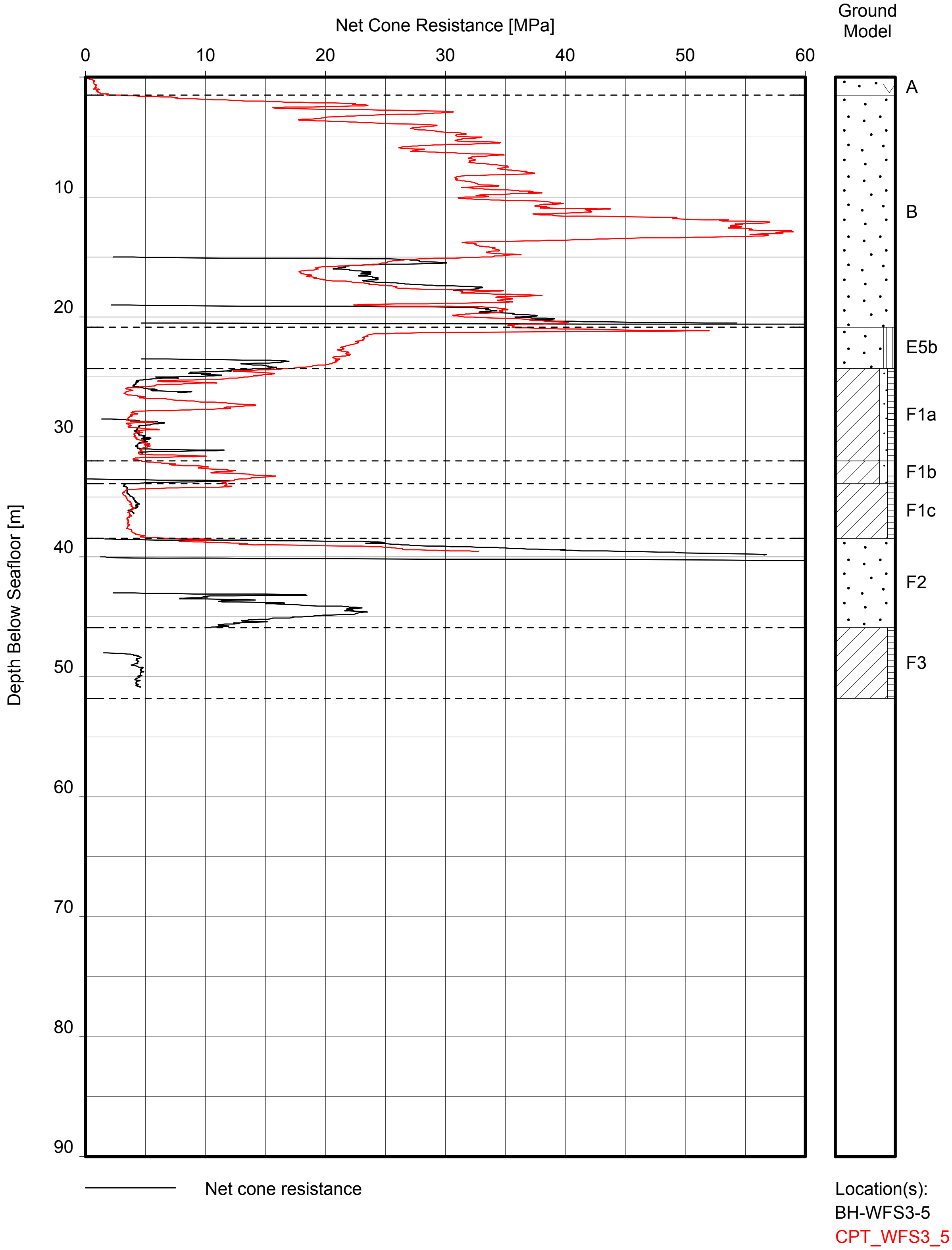


GeODin/2.Net Cone Resistance versus Depth (all UNITS, incl. GM).GLO/2015-12-09 10:57:17

**NET CONE RESISTANCE VERSUS DEPTH**

BORSSELE WIND FARM ZONE, WFS III - DUTCH SECTOR, NORTH SEA

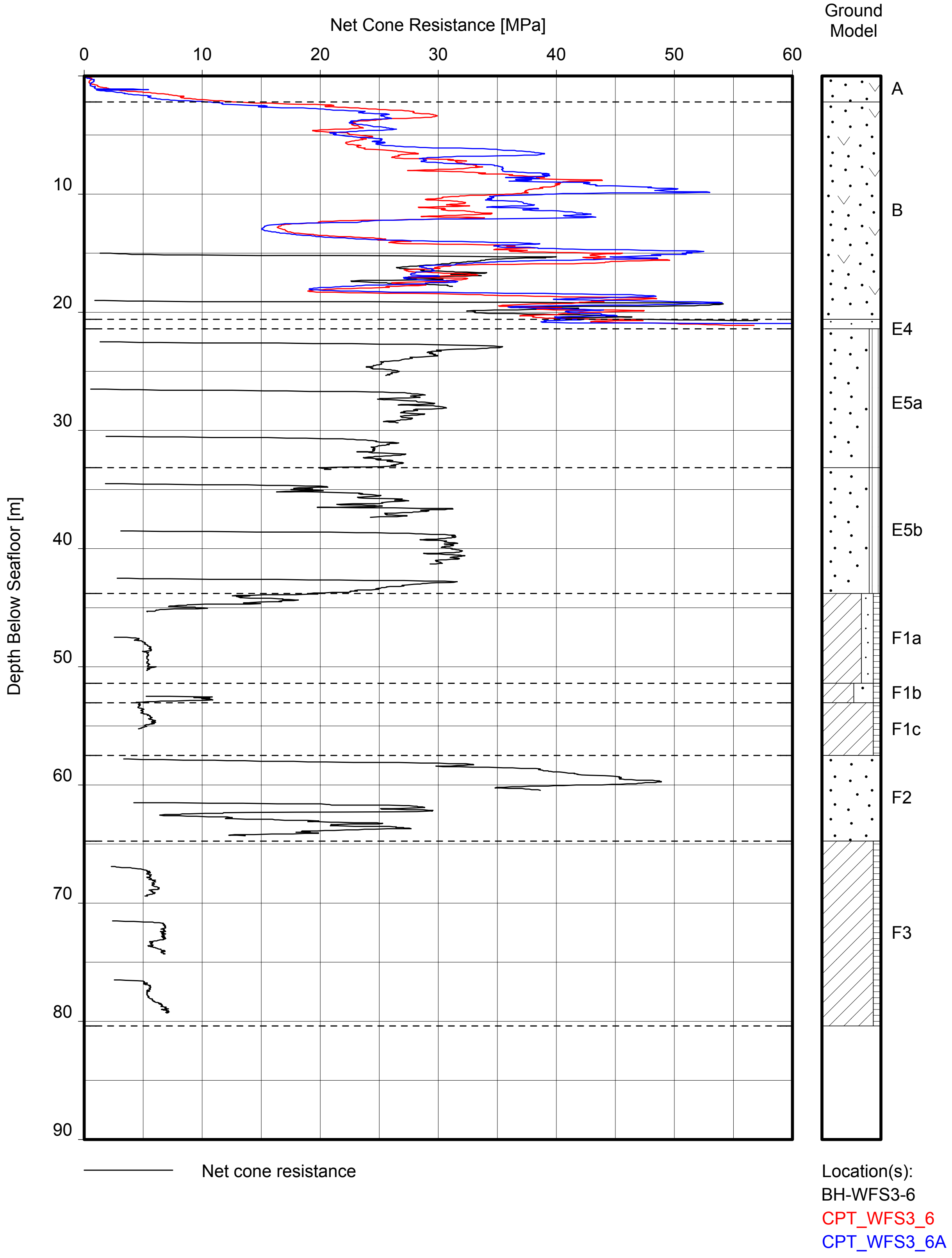




**NET CONE RESISTANCE VERSUS DEPTH**

BORSSELE WIND FARM ZONE, WFS III - DUTCH SECTOR, NORTH SEA

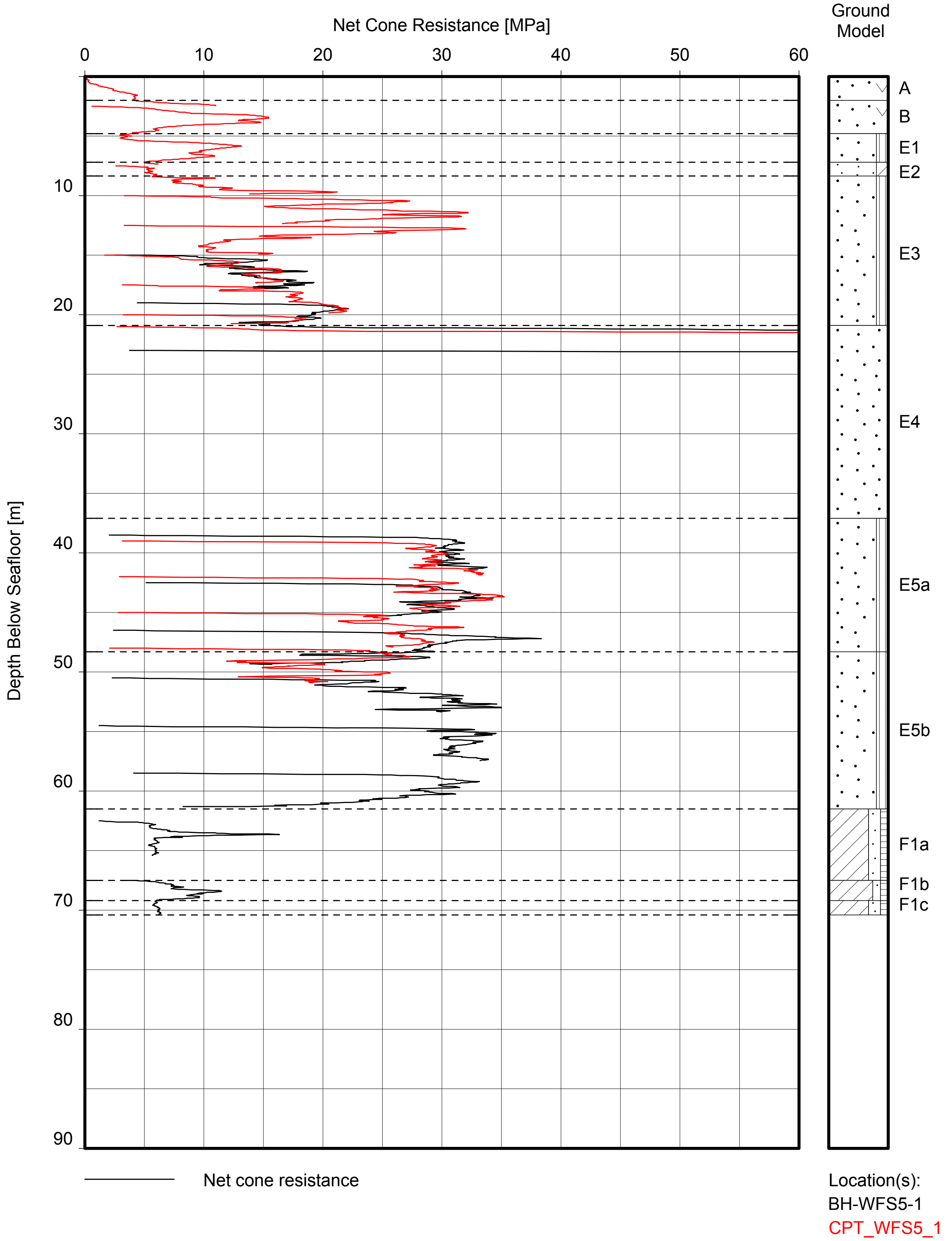


GeODin/2.Net Cone Resistance versus Depth (all UNITS, incl. GM).GLO/2015-12-09 11:21:37

## NET CONE RESISTANCE VERSUS DEPTH

BORSSELE WIND FARM ZONE, WFS III - DUTCH SECTOR, NORTH SEA

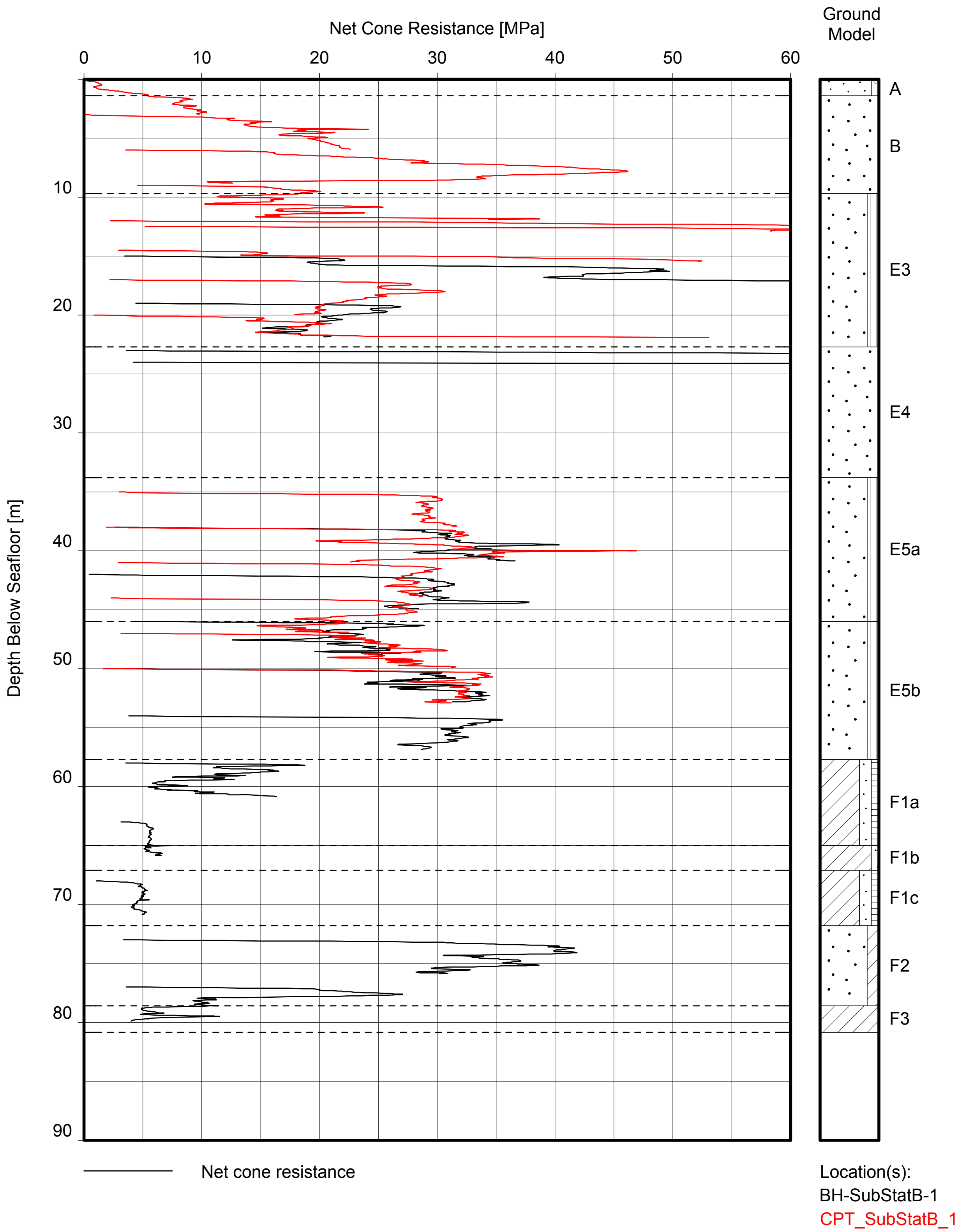


GeODin/2.Net Cone Resistance versus Depth (all UNITS, incl. GM).GLO/2015-12-09 11:24:10

# NET CONE RESISTANCE VERSUS DEPTH

BORSSELE WIND FARM ZONE, WFS III - DUTCH SECTOR, NORTH SEA

Fugro

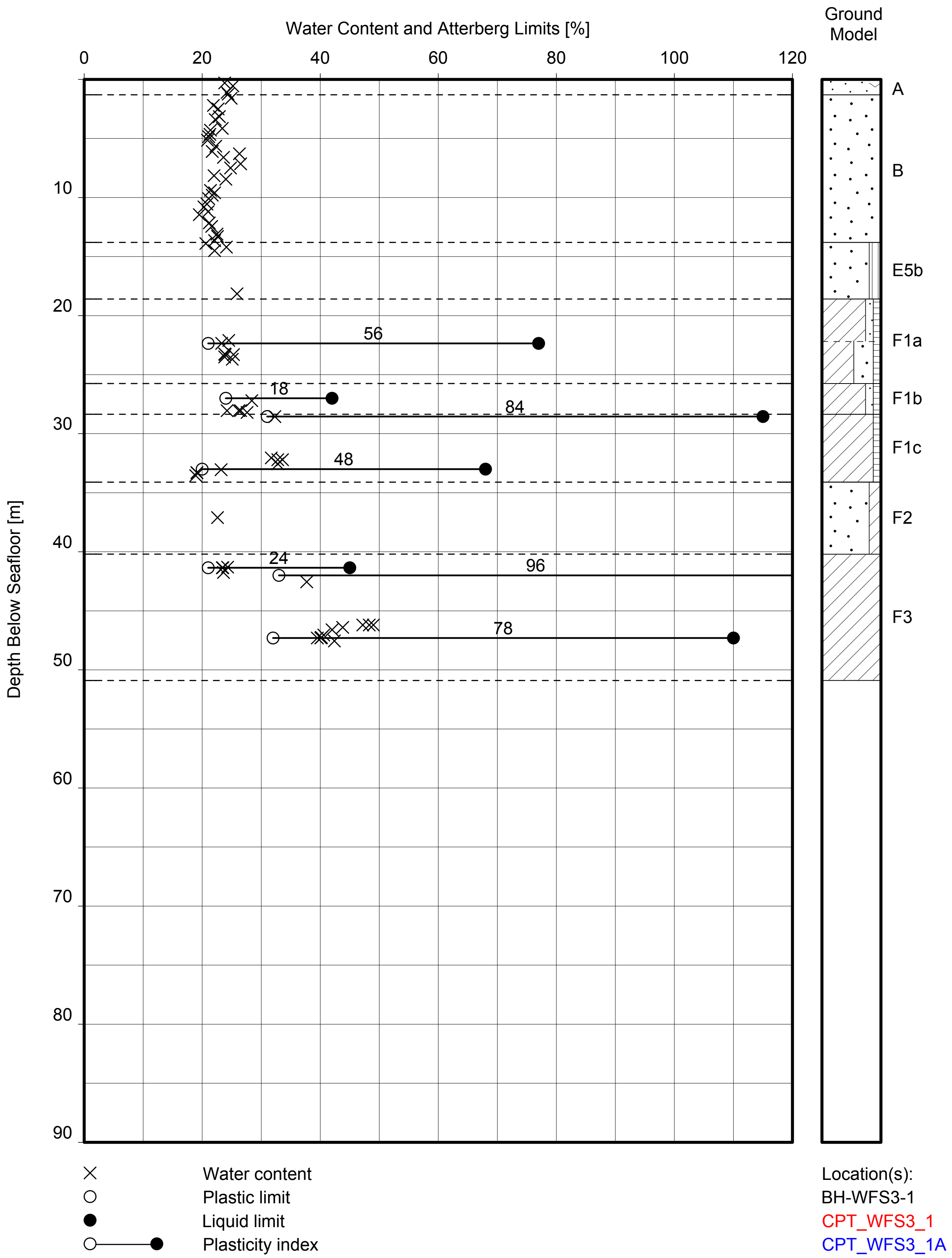


GeODin/3.Water Content and Atterberg limits vs Depth (all UNITS, incl. GM).GLO/2015-12-09 10:47:20

**WATER CONTENT AND ATTERBERG LIMITS VERSUS DEPTH**

BORSSELE WIND FARM ZONE, WFS III - DUTCH SECTOR, NORTH SEA

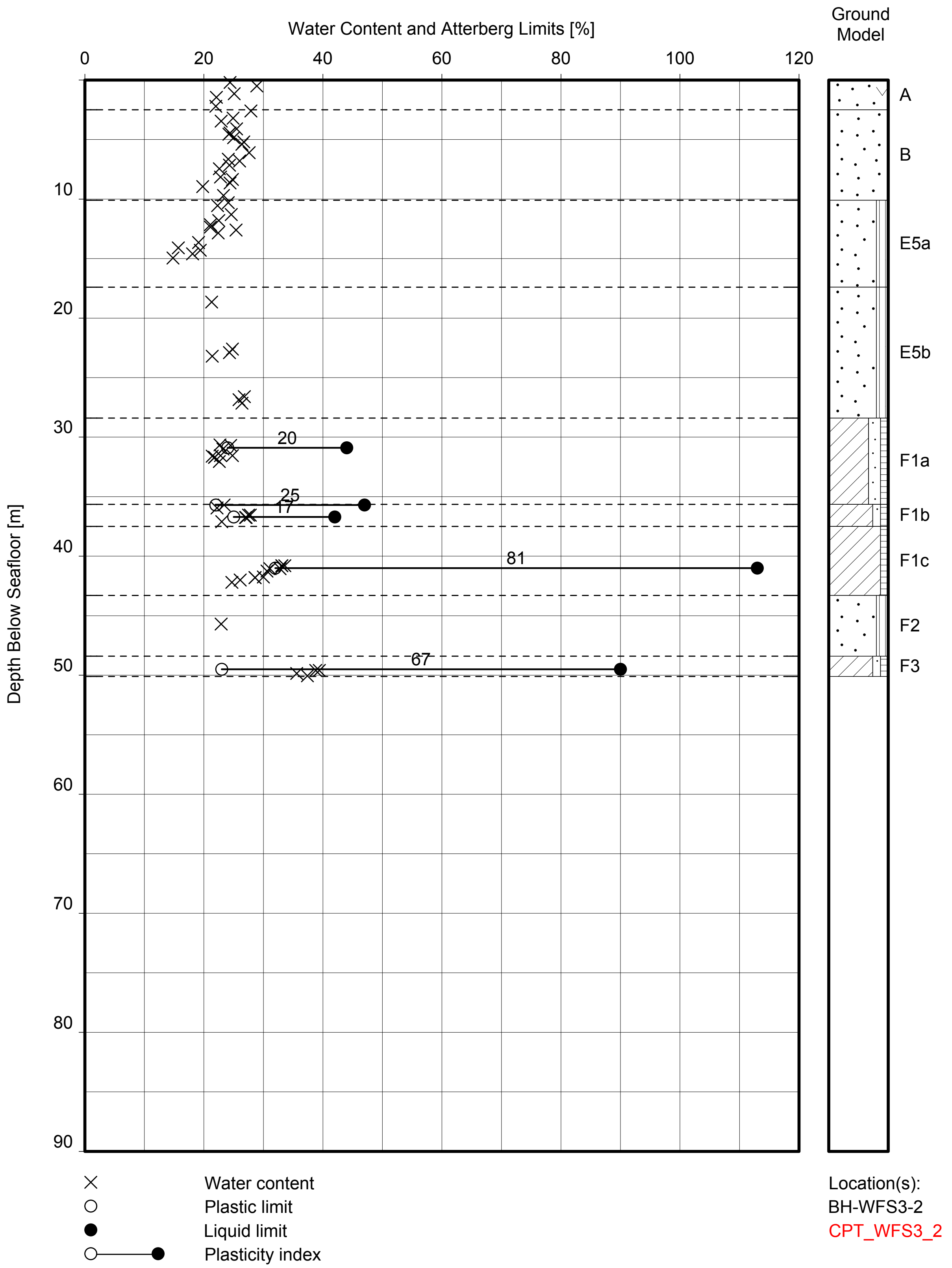


GeODin/3.Water Content and Atterberg limits vs Depth (all UNITS, incl. GM),GLO/2015-12-09 10:50:14

**WATER CONTENT AND ATTERBERG LIMITS VERSUS DEPTH**

BORSSELE WIND FARM ZONE, WFS III - DUTCH SECTOR, NORTH SEA

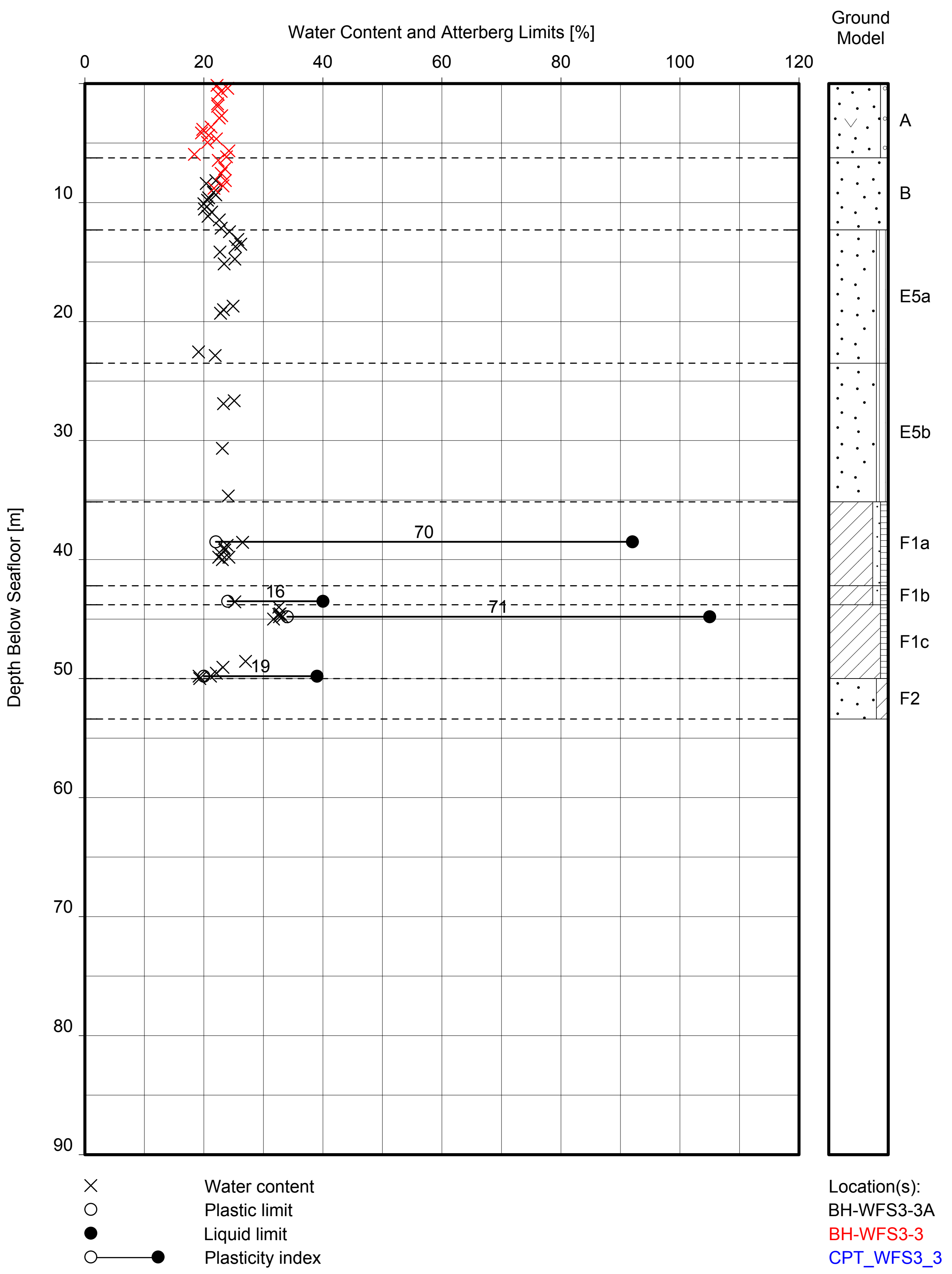


GeODin/3.Water Content and Atterberg limits vs Depth (all UNITS, incl. GM).GLO/2015-12-09 10:53:09

**WATER CONTENT AND ATTERBERG LIMITS VERSUS DEPTH**

BORSSELE WIND FARM ZONE, WFS III - DUTCH SECTOR, NORTH SEA

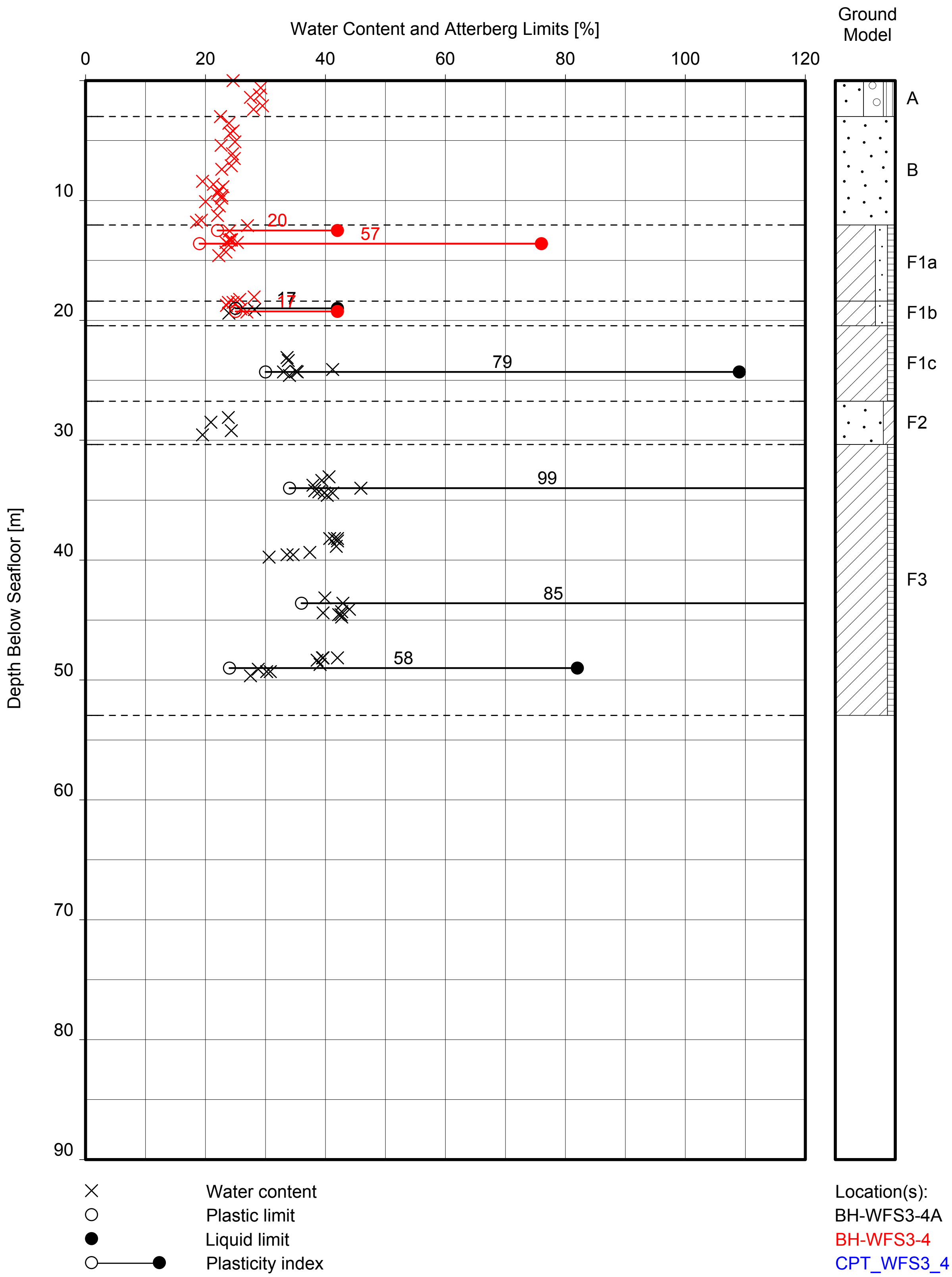


GeODin/3.Water Content and Atterberg limits vs Depth (all UNITS, incl. GM),GLO/2015-12-09 10:55:19

**WATER CONTENT AND ATTERBERG LIMITS VERSUS DEPTH**

BORSSELE WIND FARM ZONE, WFS III - DUTCH SECTOR, NORTH SEA

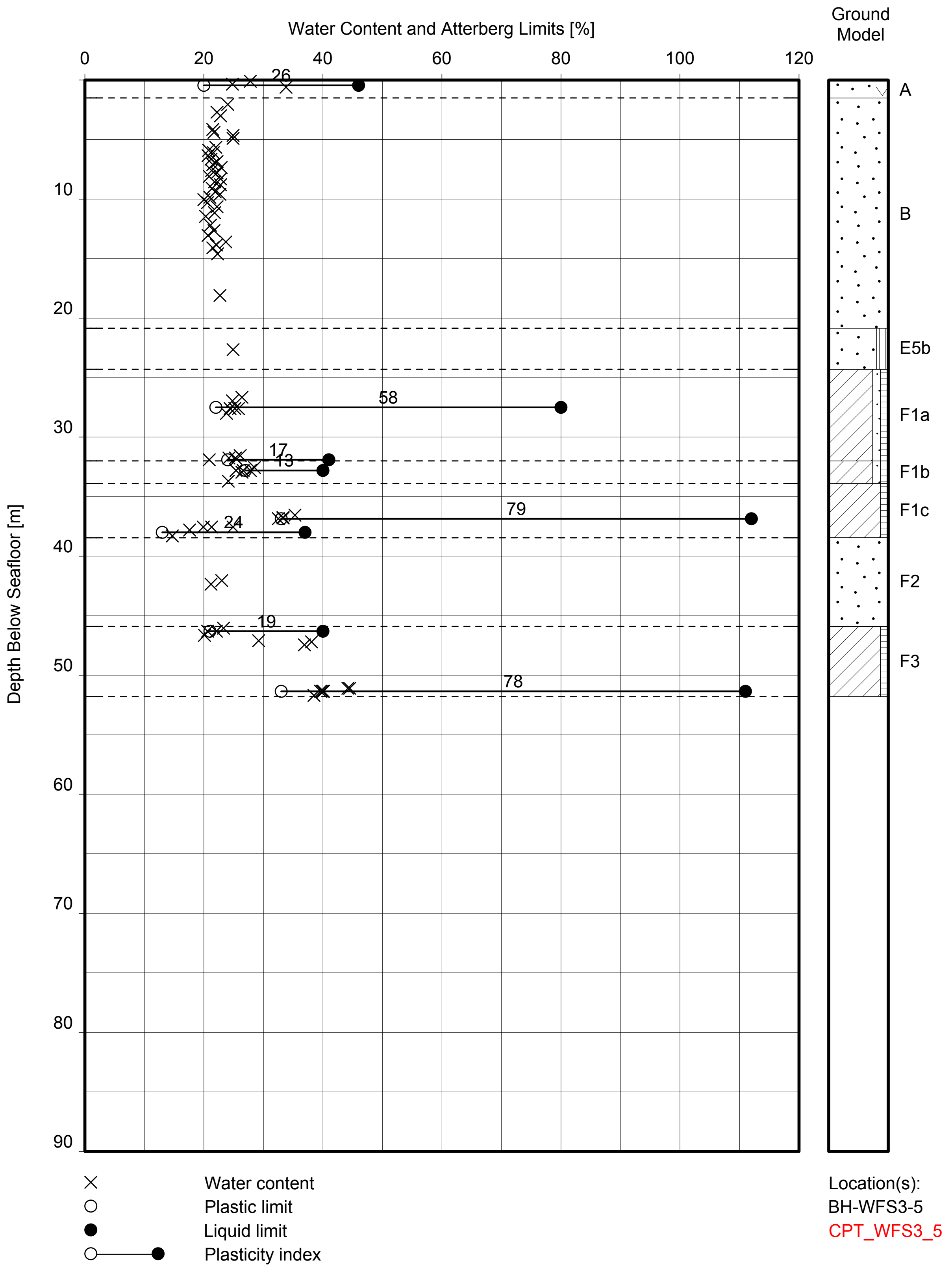


GeODin/3.Water Content and Atterberg limits vs Depth (all UNITS, incl. GM).GLO/2015-12-09 10:57:31

**WATER CONTENT AND ATTERBERG LIMITS VERSUS DEPTH**

BORSSELE WIND FARM ZONE, WFS III - DUTCH SECTOR, NORTH SEA

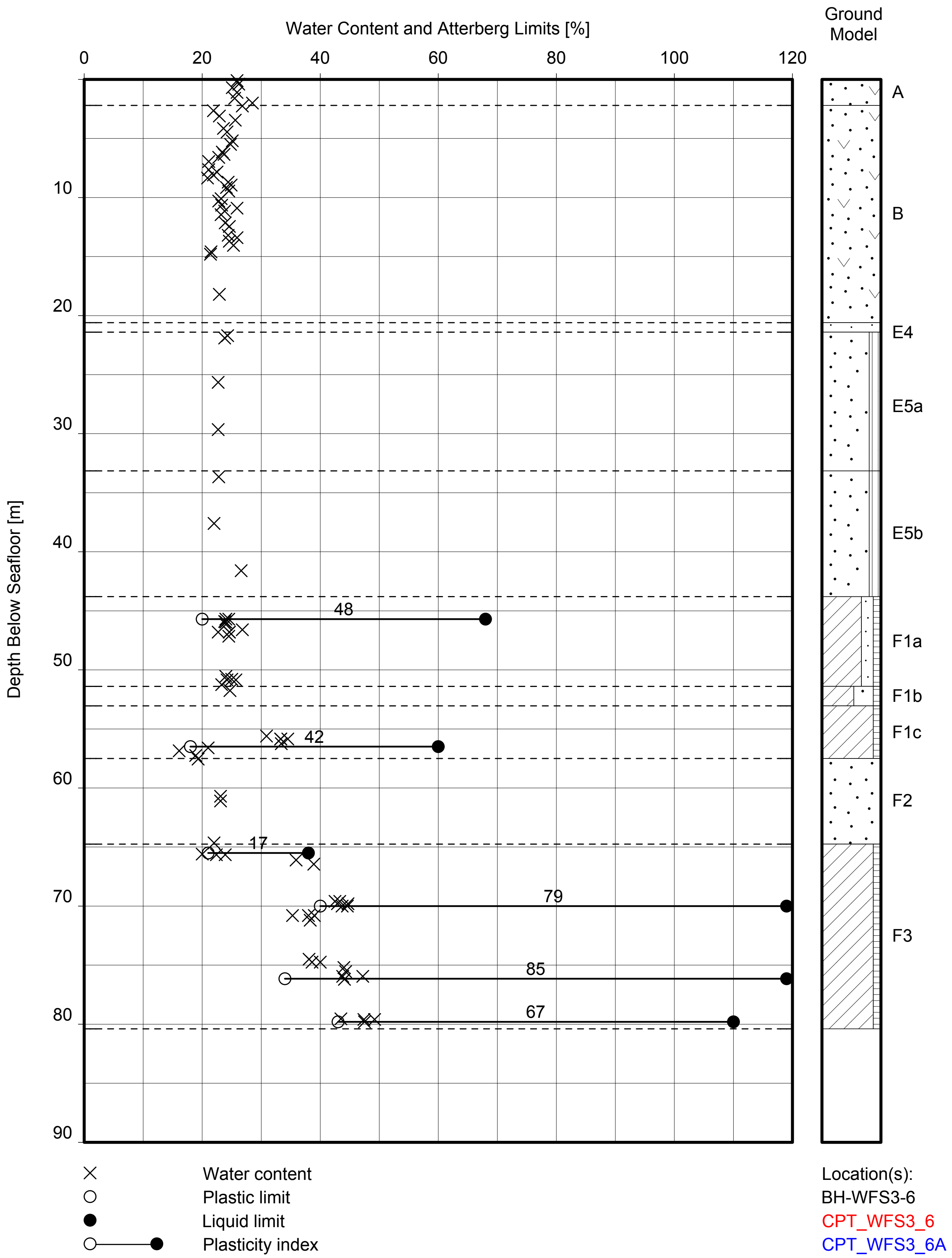


GeODin/3.Water Content and Atterberg limits vs Depth (all UNITS, incl. GM).GLO/2015-12-09 11:19:10

**WATER CONTENT AND ATTERBERG LIMITS VERSUS DEPTH**

BORSSELE WIND FARM ZONE, WFS III - DUTCH SECTOR, NORTH SEA

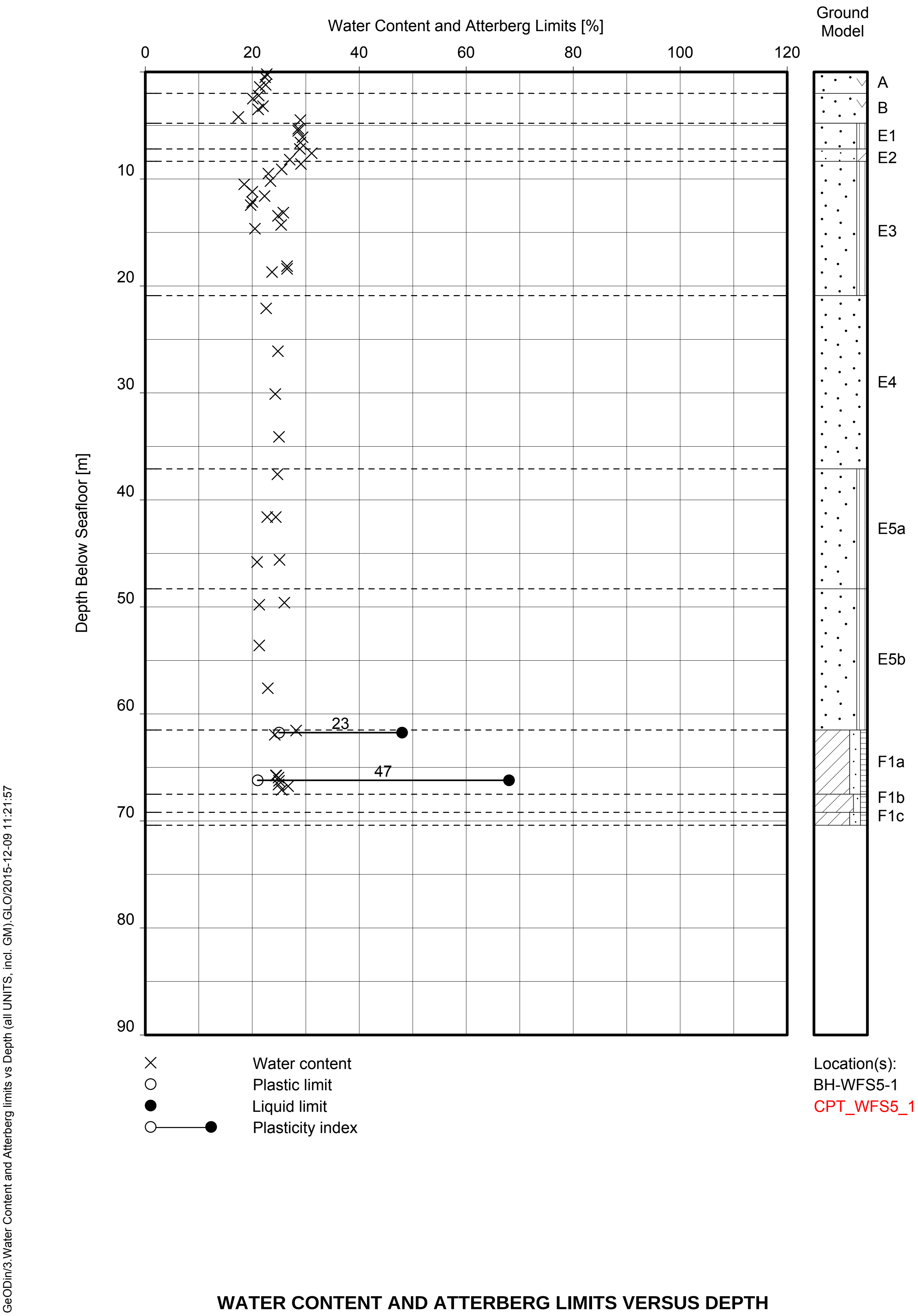


**WATER CONTENT AND ATTERBERG LIMITS VERSUS DEPTH**

BORSSELE WIND FARM ZONE, WFS III - DUTCH SECTOR, NORTH SEA

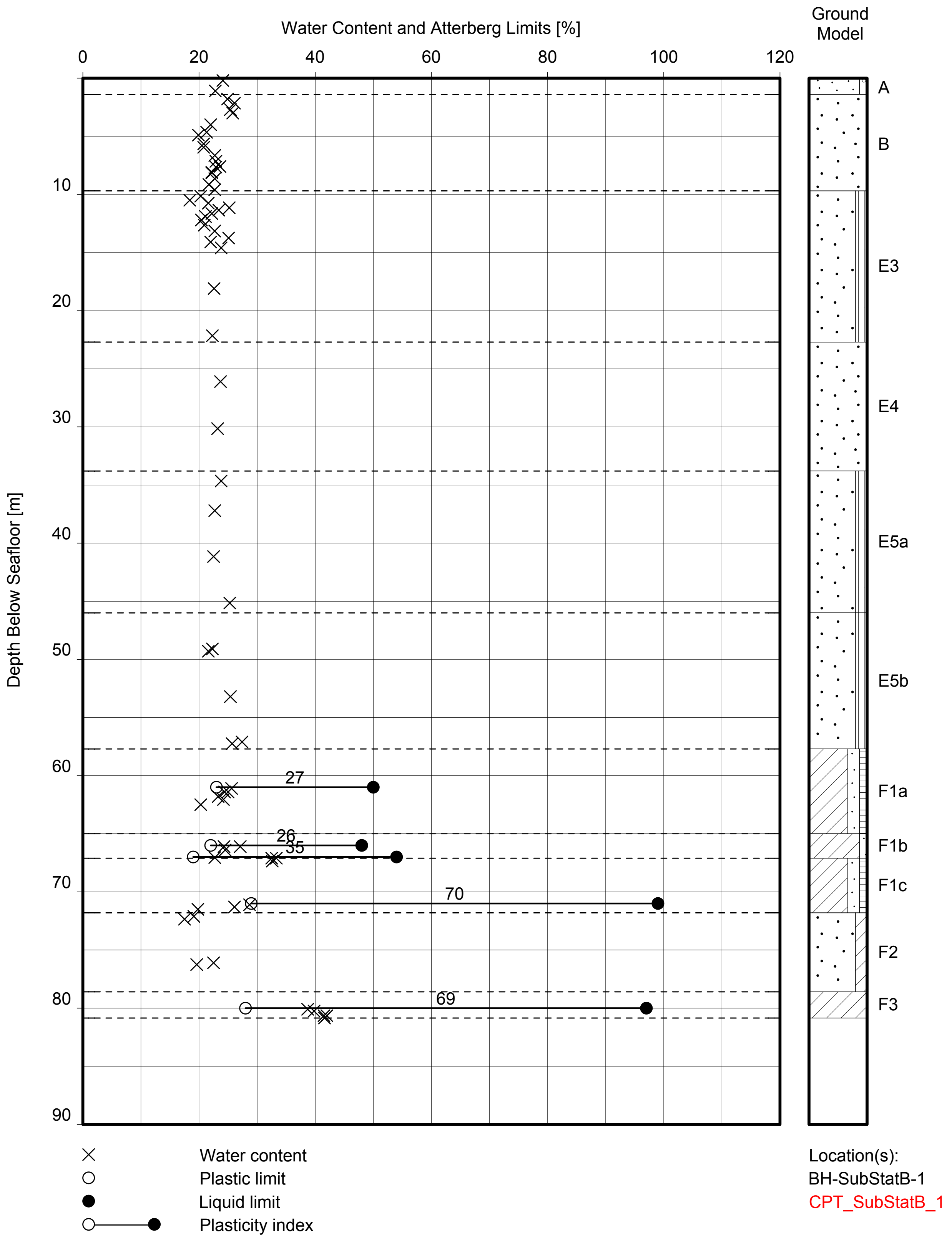


GeODin/3.Water Content and Atterberg limits vs Depth (all UNITS, incl. GM).GLO/2015-12-09 11:24:22

**WATER CONTENT AND ATTERBERG LIMITS VERSUS DEPTH**

BORSSELE WIND FARM ZONE, WFS III - DUTCH SECTOR, NORTH SEA

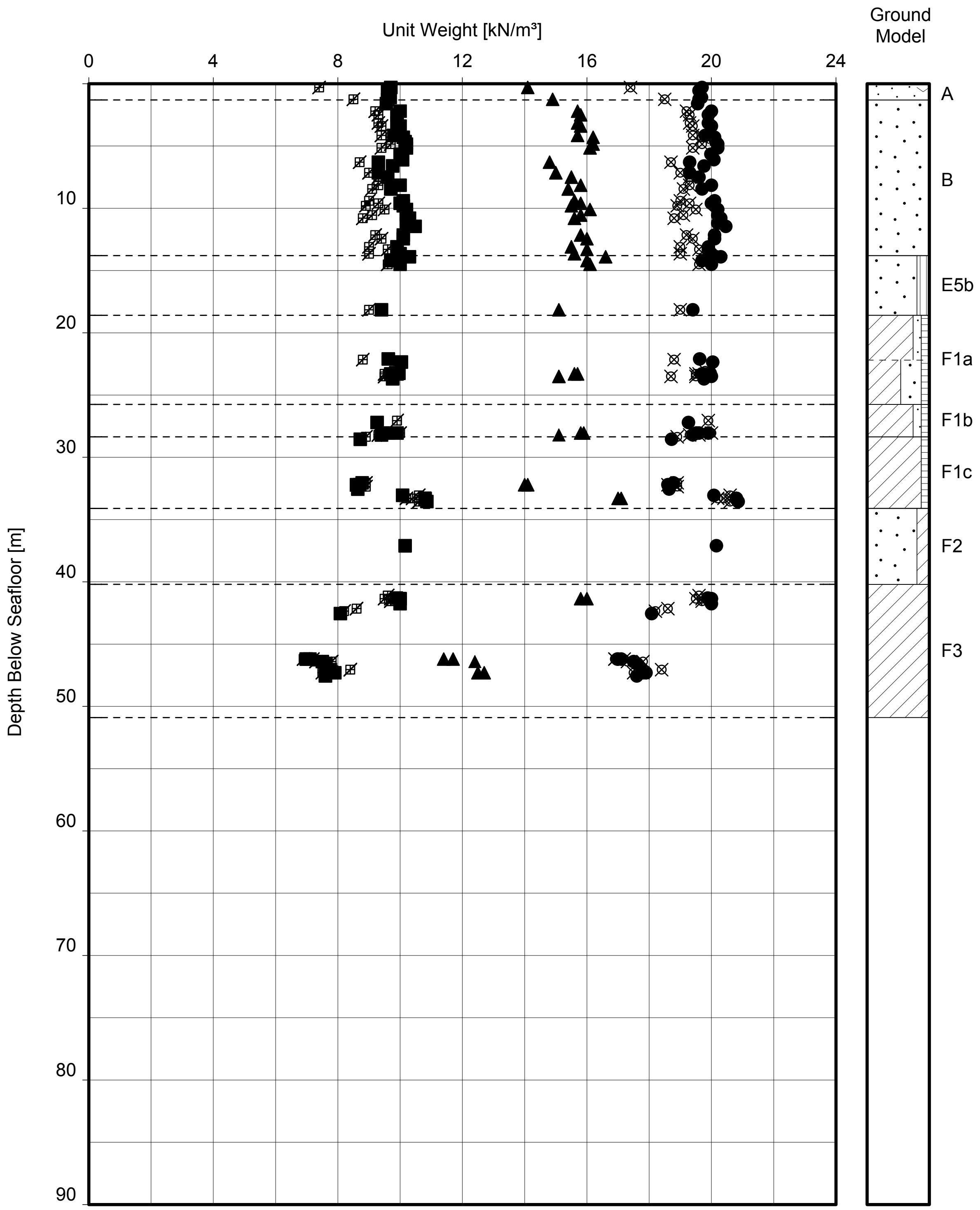


● Unit weight derived from water content and particle density
⊠ Unit weight derived from volume mass calculation
■ Submerged unit weight derived from water content and particle density
⊠ Submerged unit weight derived from volume mass calculation
▲ Dry unit weight derived from volume mass calculation

Location(s):
BH-WFS3-1
CPT_WFS3_1
CPT_WFS3_1A

Note(s):
- No dry unit weight available for unit weight measurements by volume mass calculation on WAX samples.

GeODin/4.Unit Weight, Dry Unit Weight and Submerged Unit Weight versus Depth(all UNITS, incl. GM).GLO/2015-12-09 10:47:35

**UNIT WEIGHT, DRY UNIT WEIGHT AND SUBMERGED UNIT WEIGHT VERSUS DEPTH**

BORSSELE WIND FARM ZONE, WFS III - DUTCH SECTOR, NORTH SEA

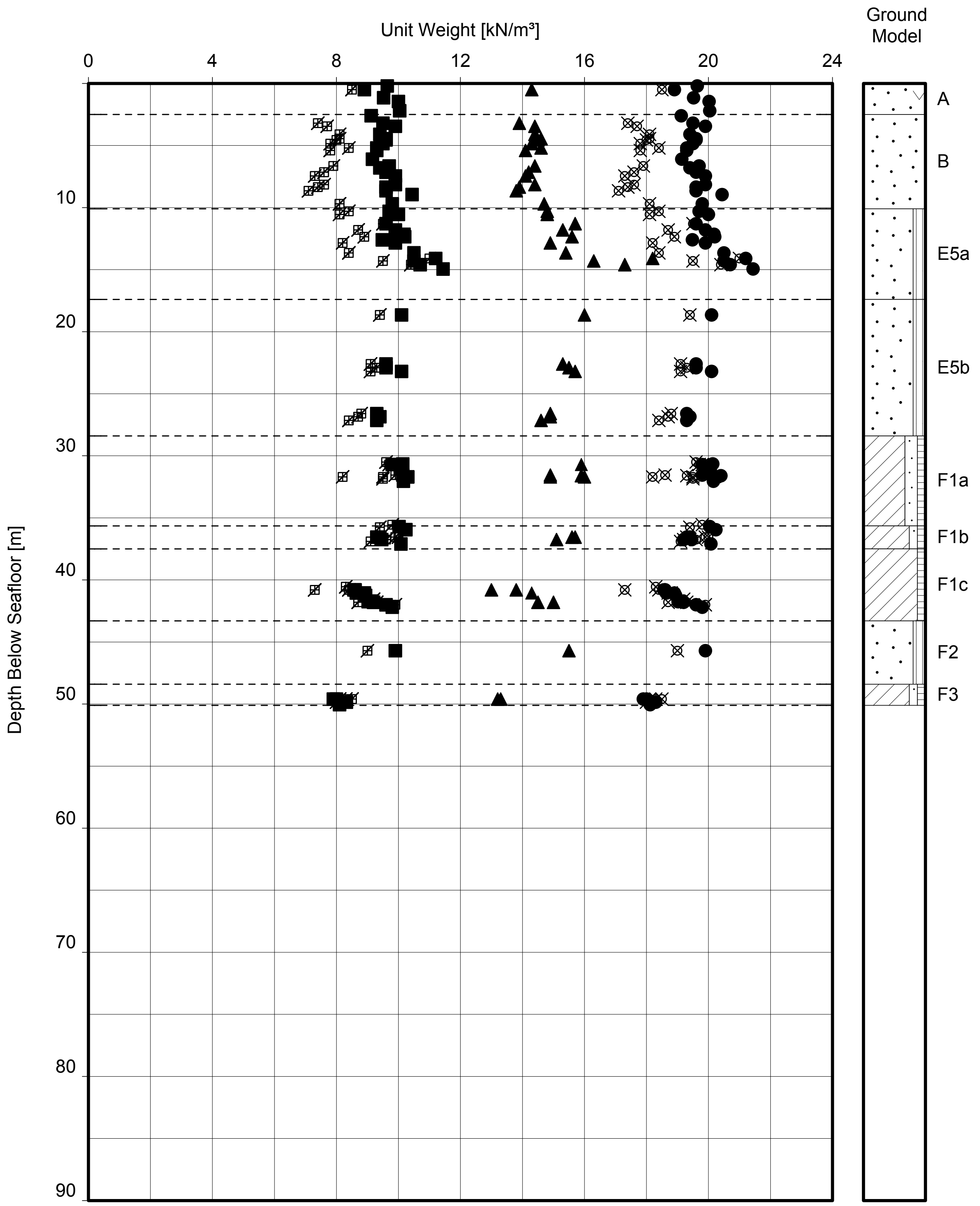


● Unit weight derived from water content and particle density
⊠ Unit weight derived from volume mass calculation
■ Submerged unit weight derived from water content and particle density
⊠ Submerged unit weight derived from volume mass calculation
▲ Dry unit weight derived from volume mass calculation

Location(s):
BH-WFS3-2
CPT_WFS3_2

Note(s):
- No dry unit weight available for unit weight measurements by volume mass calculation on WAX samples.

GeODin/4.Unit Weight, Dry Unit Weight and Submerged Unit Weight versus Depth(all UNITS, incl. GM).GLO/2015-12-09 10:50:35

**UNIT WEIGHT, DRY UNIT WEIGHT AND SUBMERGED UNIT WEIGHT VERSUS DEPTH**

BORSSELE WIND FARM ZONE, WFS III - DUTCH SECTOR, NORTH SEA

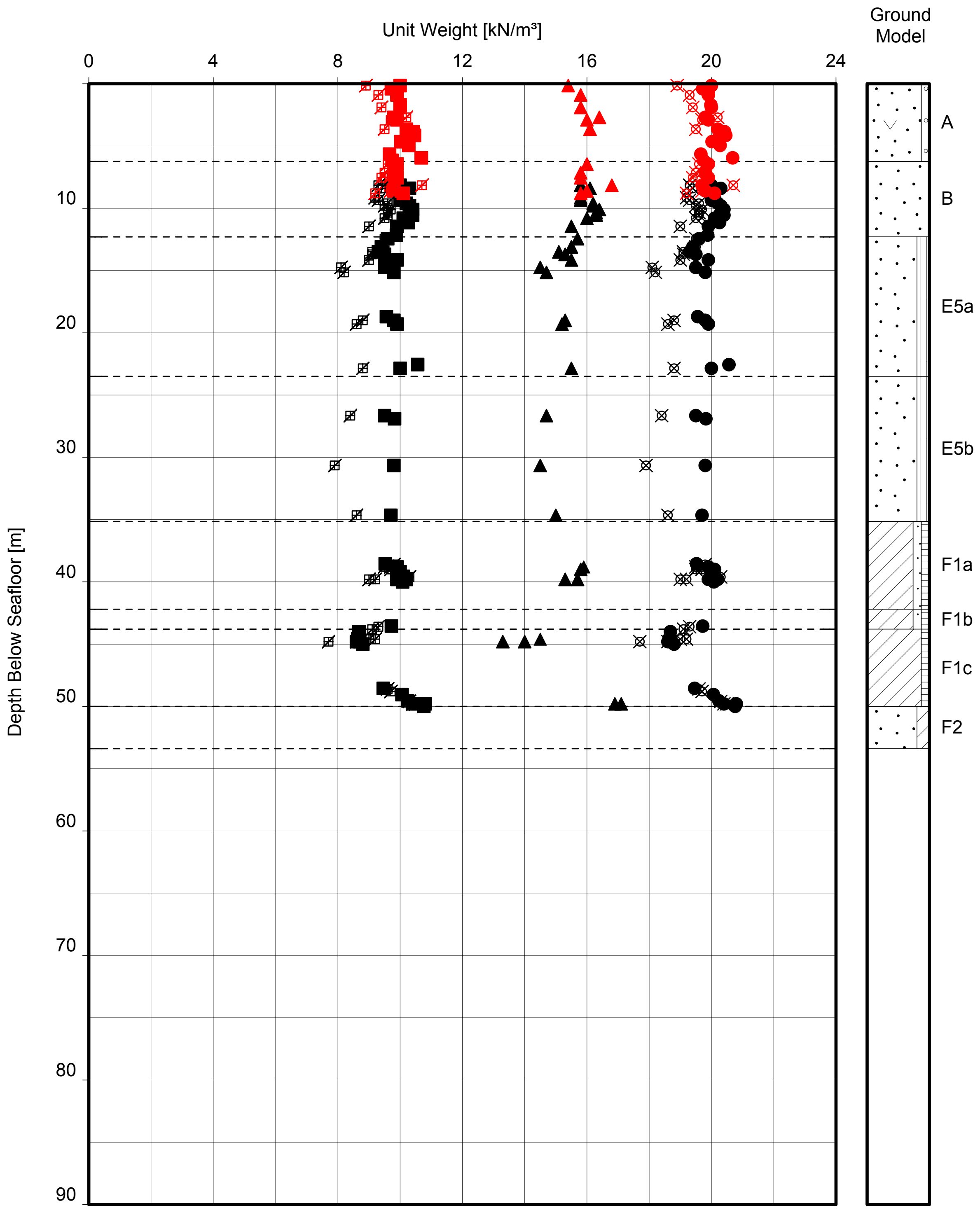


● Unit weight derived from water content and particle density
⊠ Unit weight derived from volume mass calculation
■ Submerged unit weight derived from water content and particle density
⊠ Submerged unit weight derived from volume mass calculation
▲ Dry unit weight derived from volume mass calculation

Location(s):
BH-WFS3-3A
BH-WFS3-3
CPT_WFS3_3

Note(s):
- No dry unit weight available for unit weight measurements by volume mass calculation on WAX samples.

GeODin/4.Unit Weight, Dry Unit Weight and Submerged Unit Weight versus Depth(all UNITS, incl. GM).GLO/2015-12-09 10:53:23

**UNIT WEIGHT, DRY UNIT WEIGHT AND SUBMERGED UNIT WEIGHT VERSUS DEPTH**

BORSSELE WIND FARM ZONE, WFS III - DUTCH SECTOR, NORTH SEA

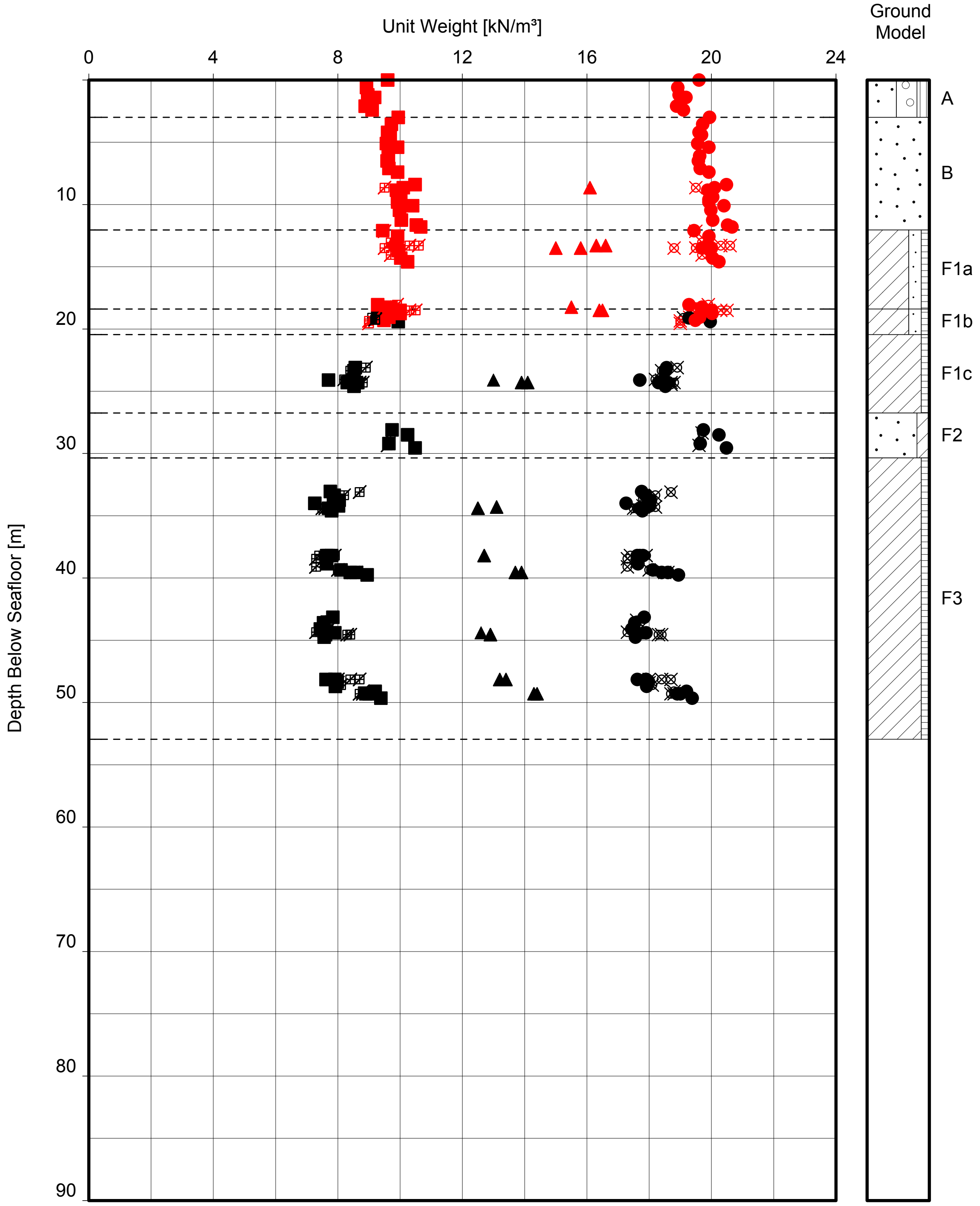


- ● Unit weight derived from water content and particle density
- ☒ Unit weight derived from volume mass calculation
- ■ Submerged unit weight derived from water content and particle density
- ☒ Submerged unit weight derived from volume mass calculation
- ▲ Dry unit weight derived from volume mass calculation

Location(s):
BH-WFS3-4A
BH-WFS3-4
CPT_WFS3_4

Note(s):
- No dry unit weight available for unit weight measurements by volume mass calculation on WAX samples.

GeODin/4.Unit Weight, Dry Unit Weight and Submerged Unit Weight versus Depth(all UNITS, incl. GM).GLO/2015-12-09 10:55:34

**UNIT WEIGHT, DRY UNIT WEIGHT AND SUBMERGED UNIT WEIGHT VERSUS DEPTH**

BORSSELE WIND FARM ZONE, WFS III - DUTCH SECTOR, NORTH SEA

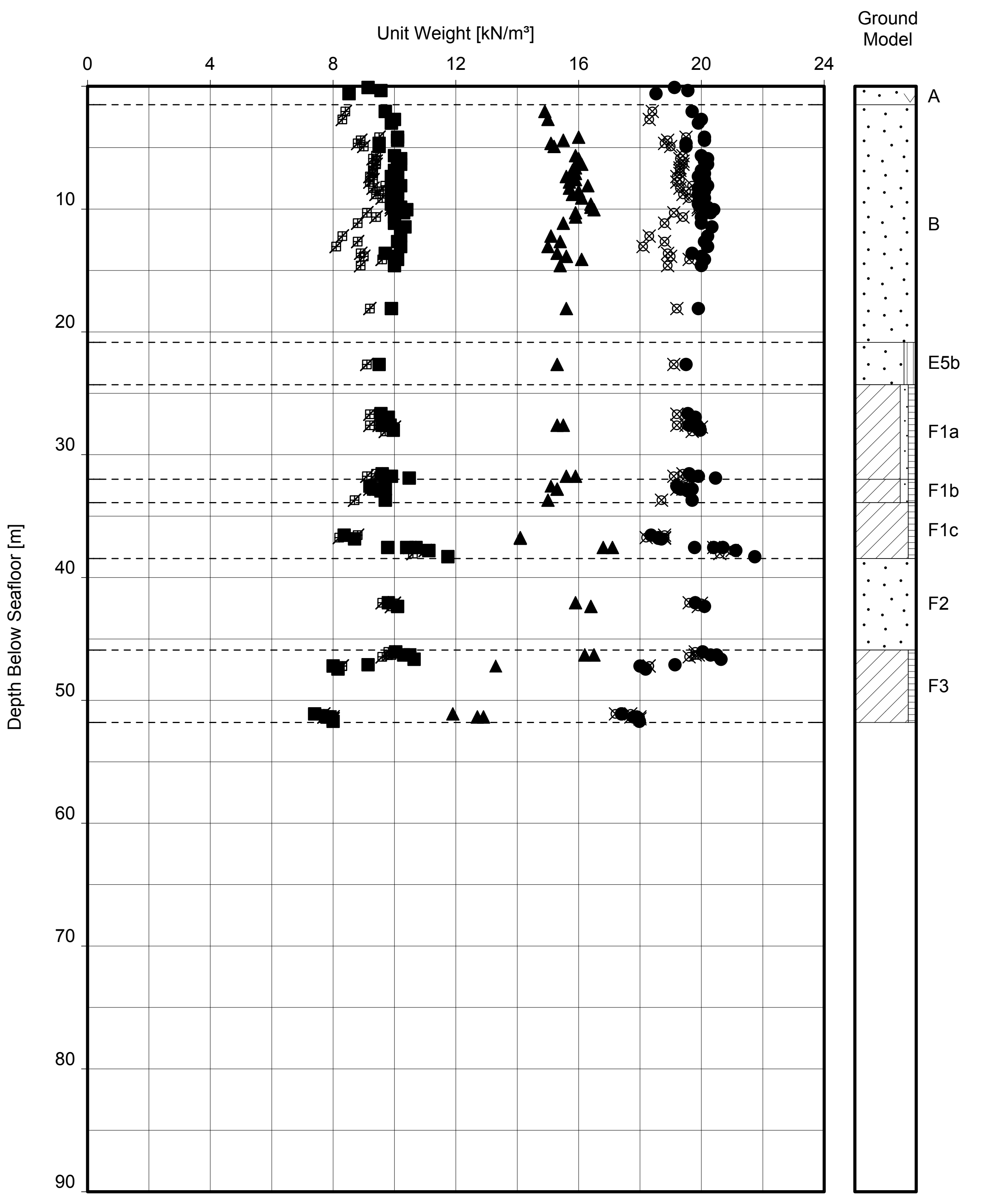


● Unit weight derived from water content and particle density
⊠ Unit weight derived from volume mass calculation
■ Submerged unit weight derived from water content and particle density
⊠ Submerged unit weight derived from volume mass calculation
▲ Dry unit weight derived from volume mass calculation

Location(s):
BH-WFS3-5
CPT_WFS3_5

Note(s):
- No dry unit weight available for unit weight measurements by volume mass calculation on WAX samples.

GeODin/4.Unit Weight, Dry Unit Weight and Submerged Unit Weight versus Depth(all UNITS, incl. GM).GLO/2015-12-09 10:57:44

**UNIT WEIGHT, DRY UNIT WEIGHT AND SUBMERGED UNIT WEIGHT VERSUS DEPTH**

BORSSELE WIND FARM ZONE, WFS III - DUTCH SECTOR, NORTH SEA

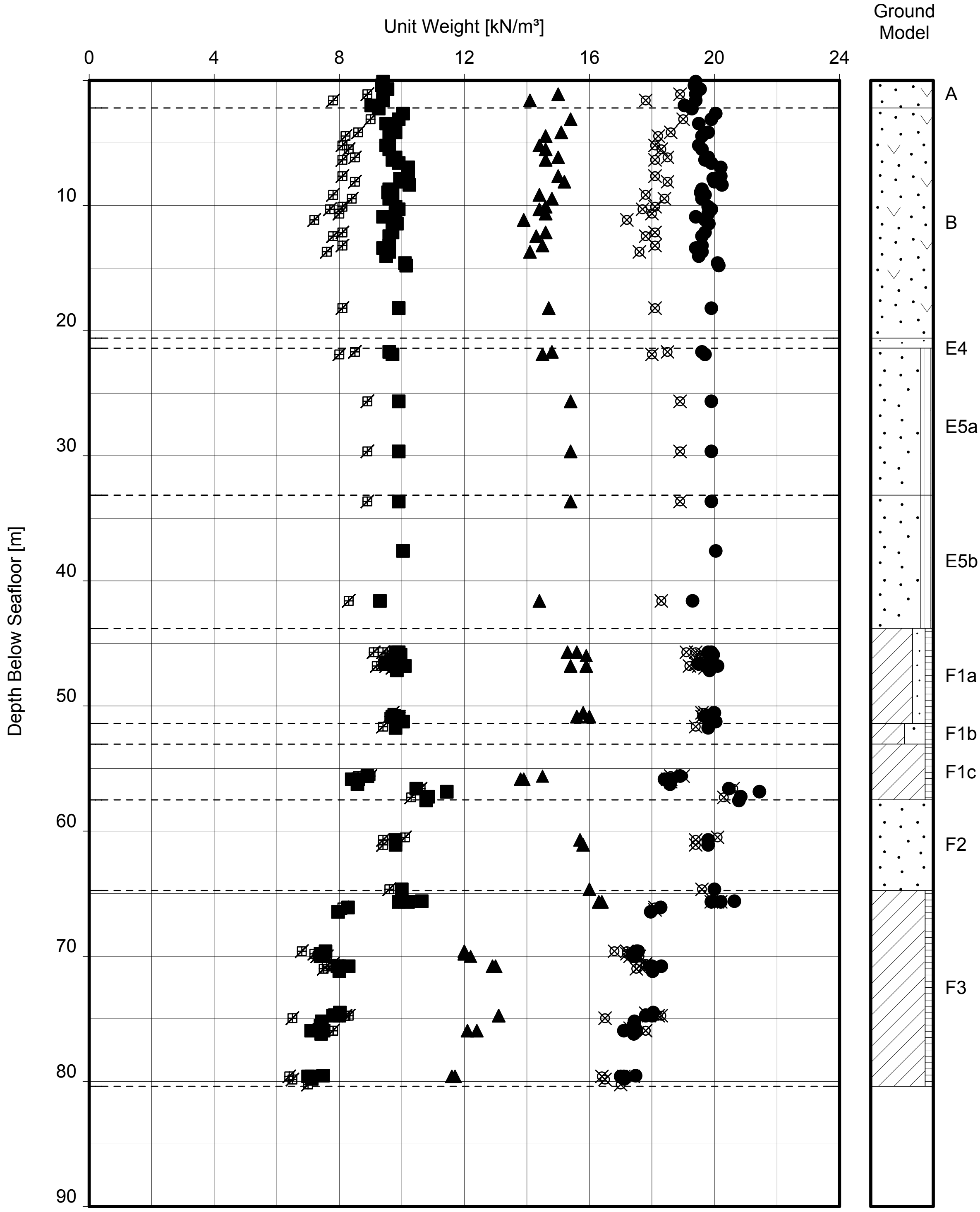


● Unit weight derived from water content and particle density
⊠ Unit weight derived from volume mass calculation
■ Submerged unit weight derived from water content and particle density
⊠ Submerged unit weight derived from volume mass calculation
▲ Dry unit weight derived from volume mass calculation

Location(s):
BH-WFS3-6
CPT_WFS3_6
CPT_WFS3_6A

Note(s):
- No dry unit weight available for unit weight measurements by volume mass calculation on WAX samples.

GeODin/4.Unit Weight, Dry Unit Weight and Submerged Unit Weight versus Depth(all UNITS, incl. GM).GLO/2015-12-09 11:19:25

## UNIT WEIGHT, DRY UNIT WEIGHT AND SUBMERGED UNIT WEIGHT VERSUS DEPTH

BORSSELE WIND FARM ZONE, WFS III - DUTCH SECTOR, NORTH SEA

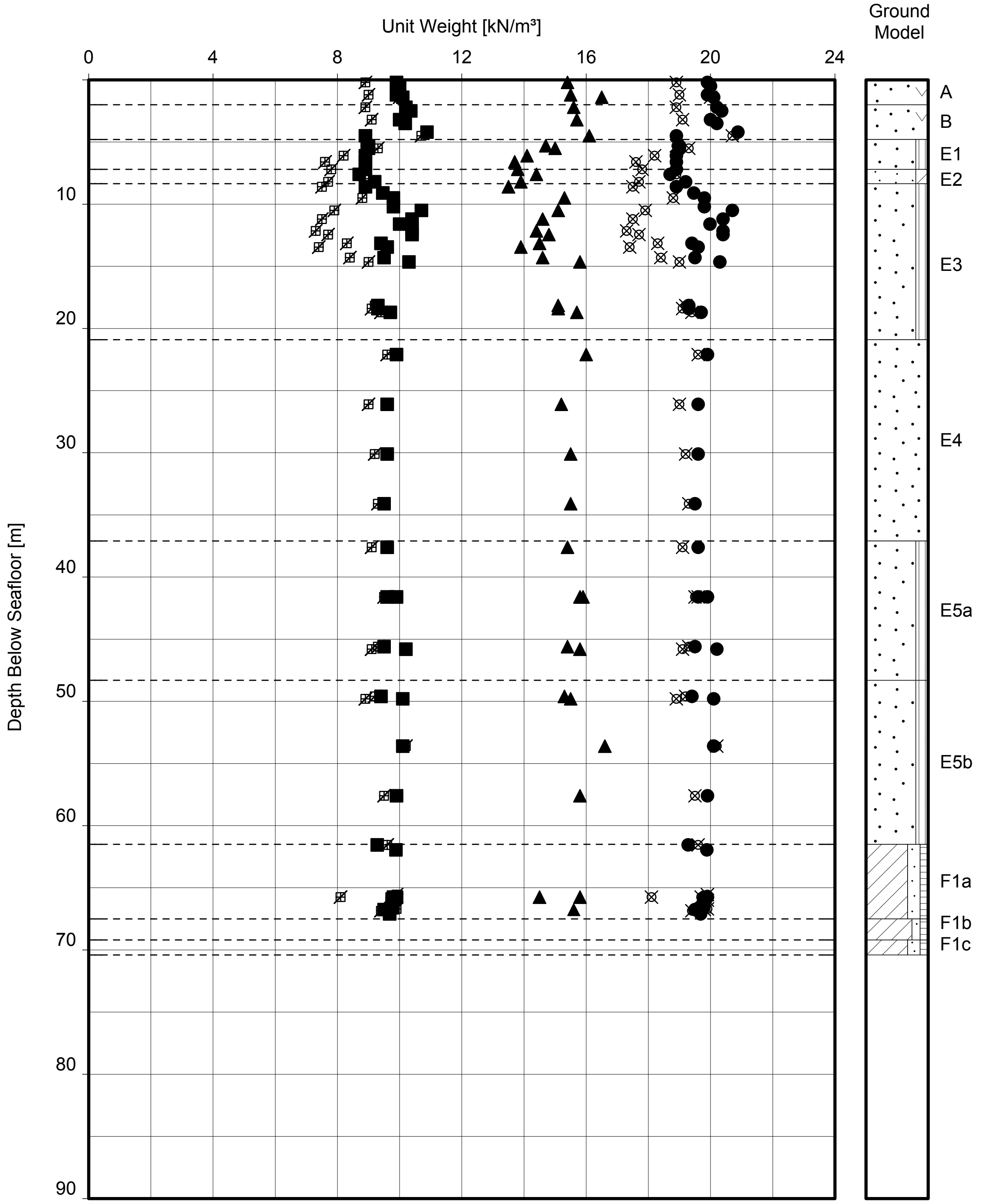


● Unit weight derived from water content and particle density
⊠ Unit weight derived from volume mass calculation
■ Submerged unit weight derived from water content and particle density
⊠ Submerged unit weight derived from volume mass calculation
▲ Dry unit weight derived from volume mass calculation

Location(s):
BH-WFS5-1
CPT_WFS5_1

Note(s):
- No dry unit weight available for unit weight measurements by volume mass calculation on WAX samples.

GeODin/4.Unit Weight, Dry Unit Weight and Submerged Unit Weight versus Depth(all UNITS, incl. GM).GLO/2015-12-09 11:22:11

## UNIT WEIGHT, DRY UNIT WEIGHT AND SUBMERGED UNIT WEIGHT VERSUS DEPTH

BORSSELE WIND FARM ZONE, WFS III - DUTCH SECTOR, NORTH SEA

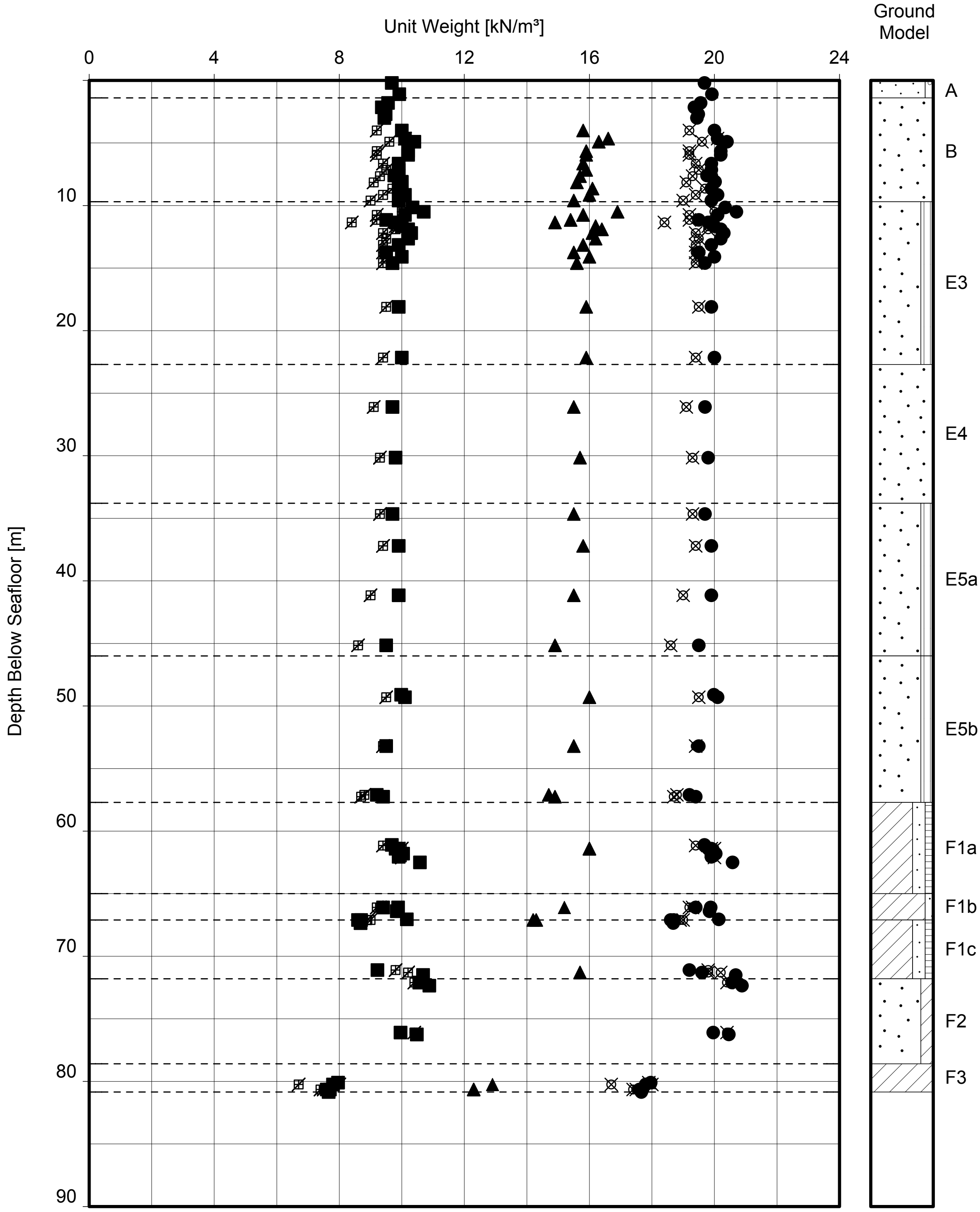


● Unit weight derived from water content and particle density
⊠ Unit weight derived from volume mass calculation
■ Submerged unit weight derived from water content and particle density
⊠ Submerged unit weight derived from volume mass calculation
▲ Dry unit weight derived from volume mass calculation

Location(s):
BH-SubStatB-1
CPT_SubStatB_1

Note(s):
- No dry unit weight available for unit weight measurements by volume mass calculation on WAX samples.

GeODin/4.Unit Weight, Dry Unit Weight and Submerged Unit Weight versus Depth(all UNITS, incl. GM).GLO/2015-12-09 11:24:35

**UNIT WEIGHT, DRY UNIT WEIGHT AND SUBMERGED UNIT WEIGHT VERSUS DEPTH**

BORSSELE WIND FARM ZONE, WFS III - DUTCH SECTOR, NORTH SEA

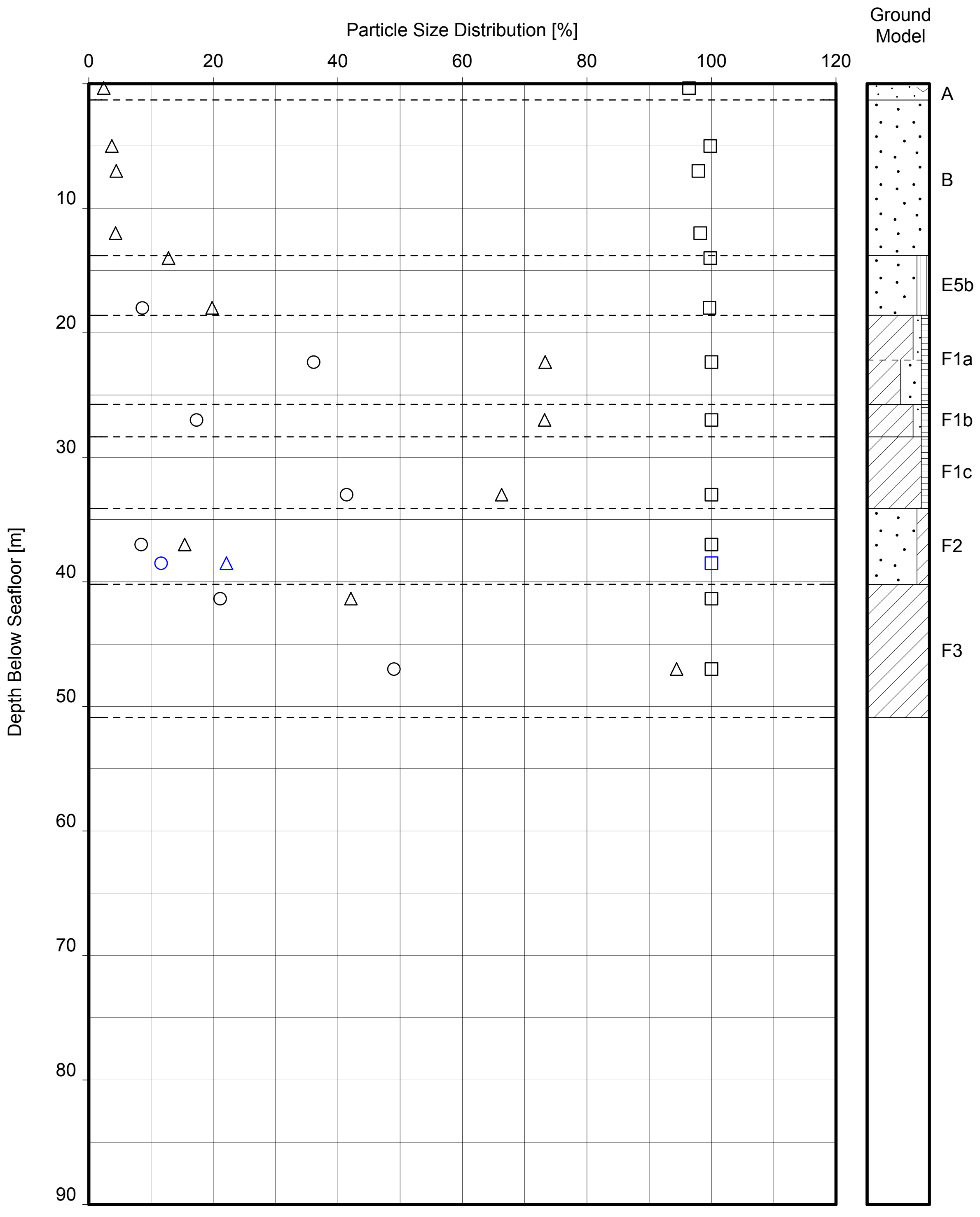


○ Particle size by mass percentage < 2 µm
△ Particle size by mass percentage < 60 µm
□ Particle size by mass percentage < 2000 µm

Location(s):
BH-WFS3-1
CPT_WFS3_1
CPT_WFS3_1A

GeODin/5.Particle Size Distribution versus Depth (all UNITS, incl. GM),GLO/2015-12-09 10:47:50

## PARTICLE SIZE DISTRIBUTION VERSUS DEPTH

BORSSELE WIND FARM ZONE, WFS III - DUTCH SECTOR, NORTH SEA

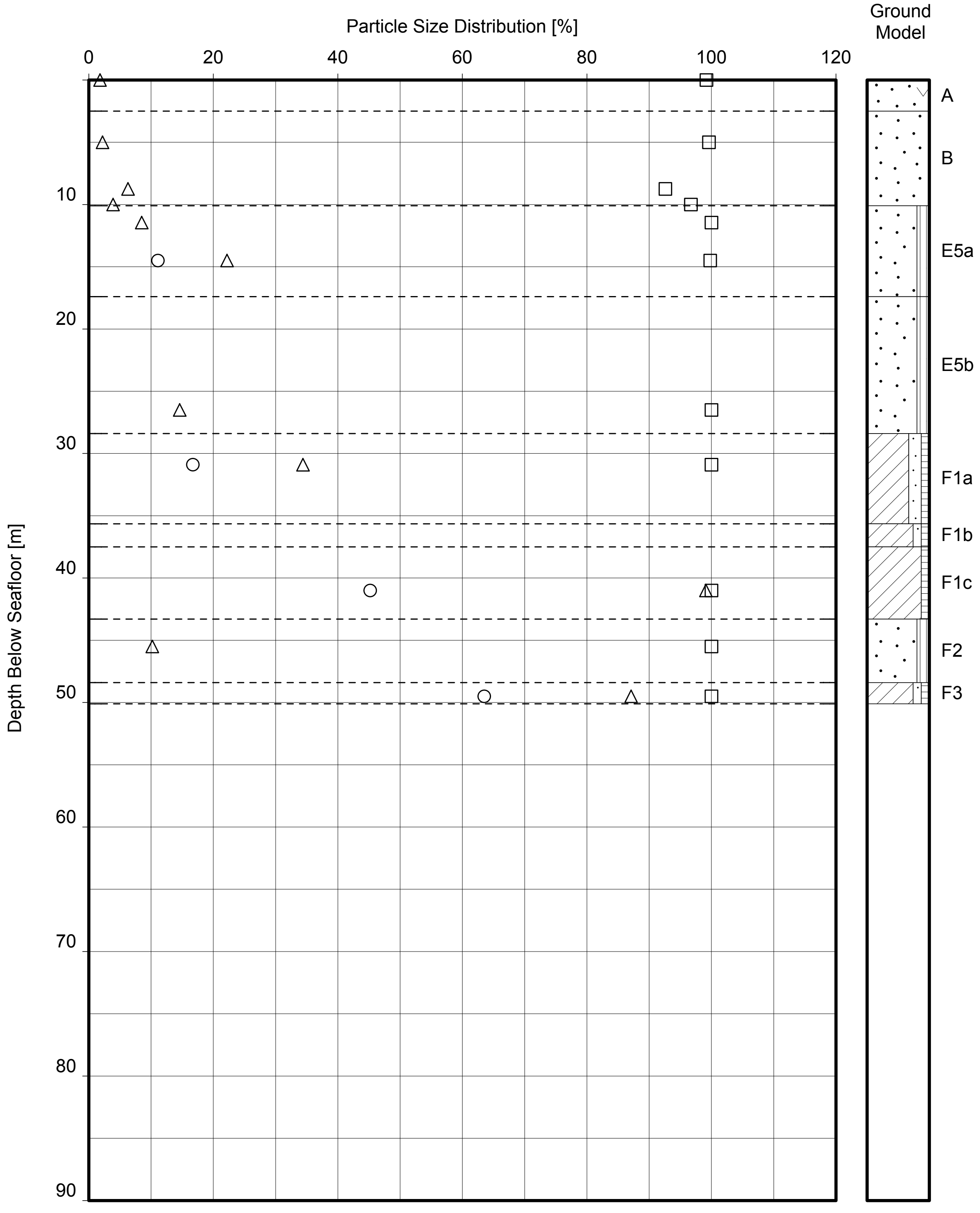


○ Particle size by mass percentage < 2 µm
△ Particle size by mass percentage < 60 µm
□ Particle size by mass percentage < 2000 µm

Location(s):
BH-WFS3-2
CPT_WFS3_2

GeODin/5.Particle Size Distribution versus Depth (all UNITS, incl. GM),GLO/2015-12-09 10:50:50

**PARTICLE SIZE DISTRIBUTION VERSUS DEPTH**

BORSSELE WIND FARM ZONE, WFS III - DUTCH SECTOR, NORTH SEA

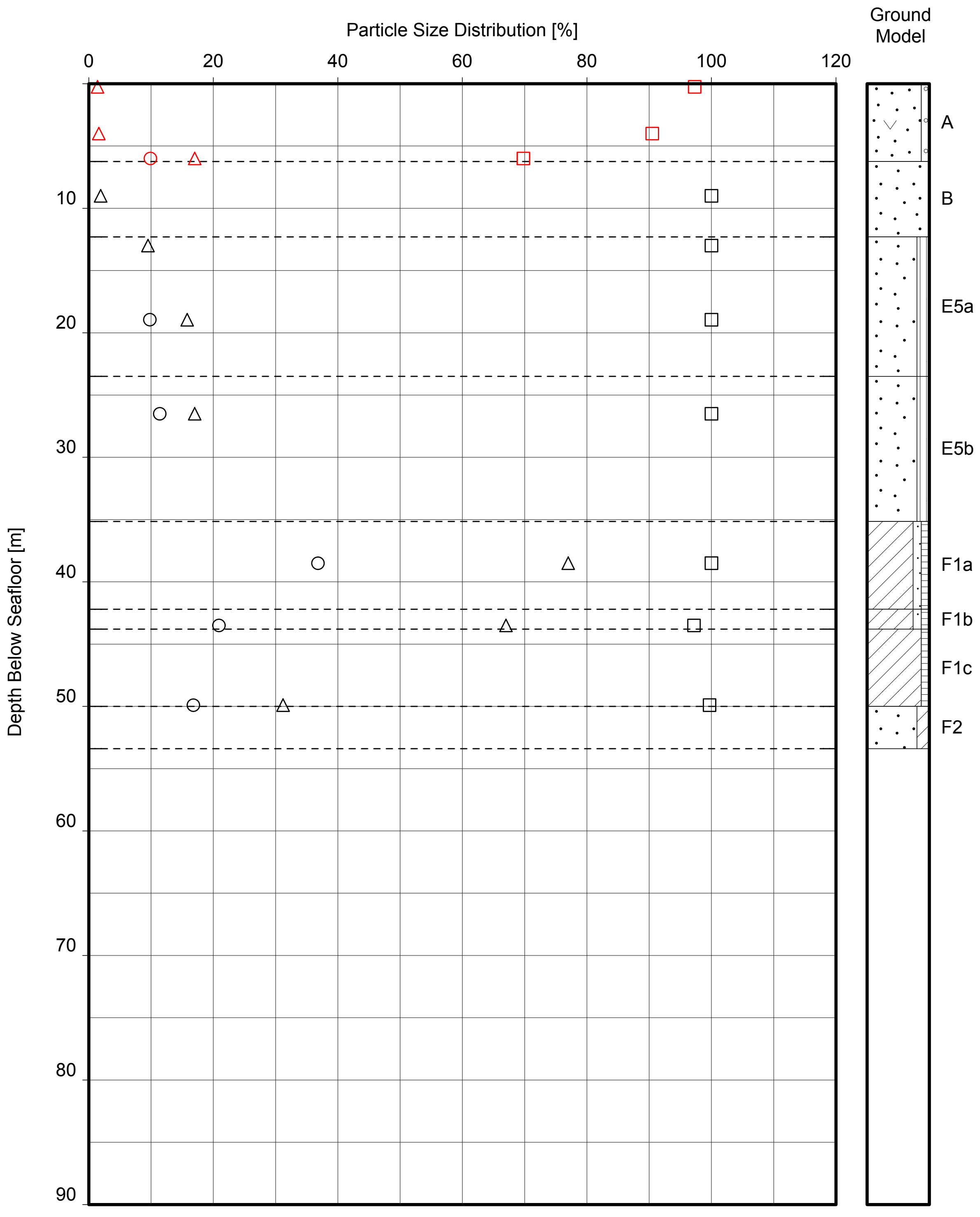


○ Particle size by mass percentage < 2 µm
△ Particle size by mass percentage < 60 µm
□ Particle size by mass percentage < 2000 µm

Location(s):
BH-WFS3-3A
BH-WFS3-3
CPT_WFS3_3

GeODin/5.Particle Size Distribution versus Depth (all UNITS, incl. GM),GLO/2015-12-09 10:53:39

**PARTICLE SIZE DISTRIBUTION VERSUS DEPTH**

BORSSELE WIND FARM ZONE, WFS III - DUTCH SECTOR, NORTH SEA

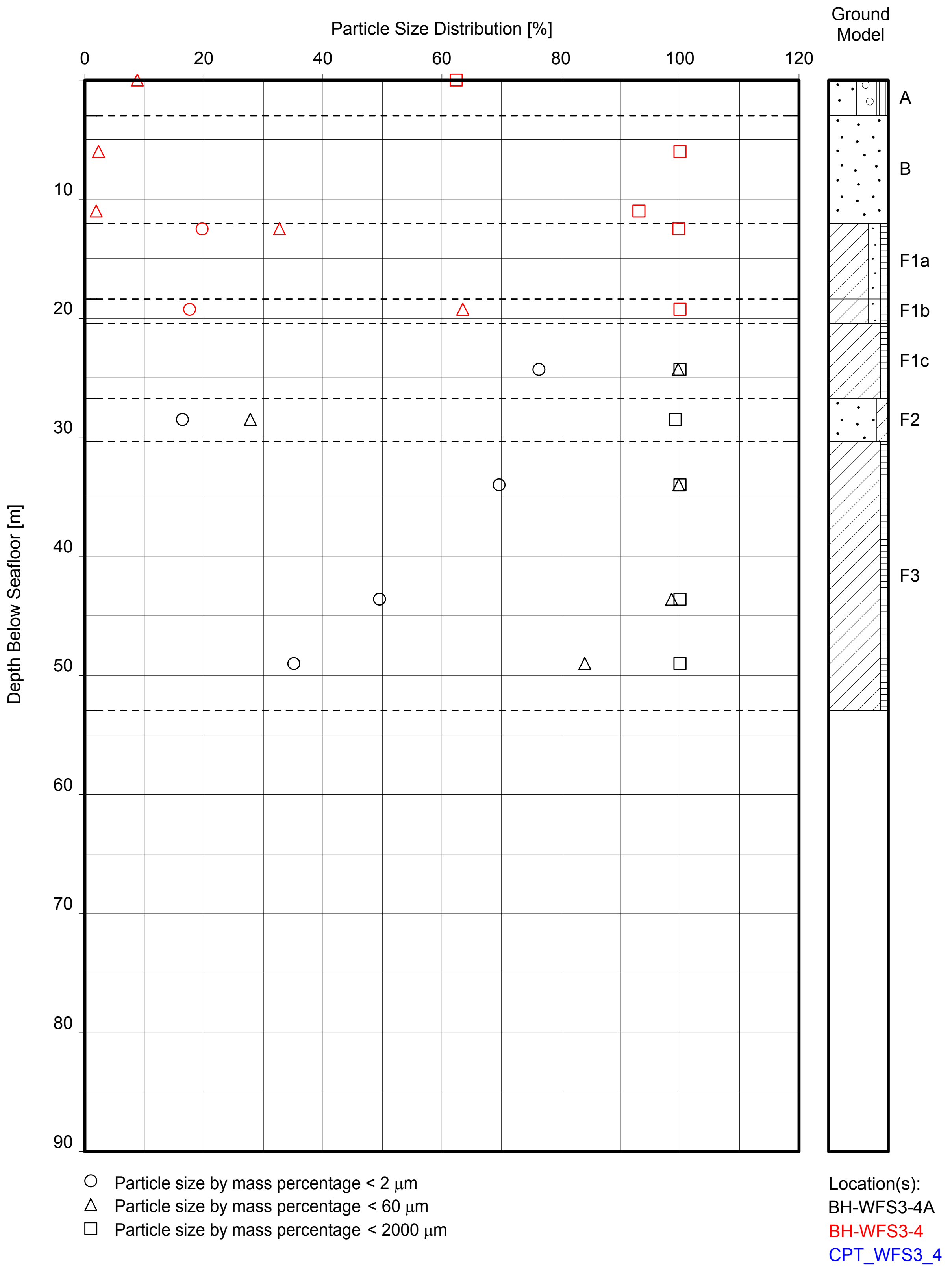


GeODin/5.Particle Size Distribution versus Depth (all UNITS, incl. GM),GLO/2015-12-09 10:55:47

**PARTICLE SIZE DISTRIBUTION VERSUS DEPTH**

BORSSELE WIND FARM ZONE, WFS III - DUTCH SECTOR, NORTH SEA

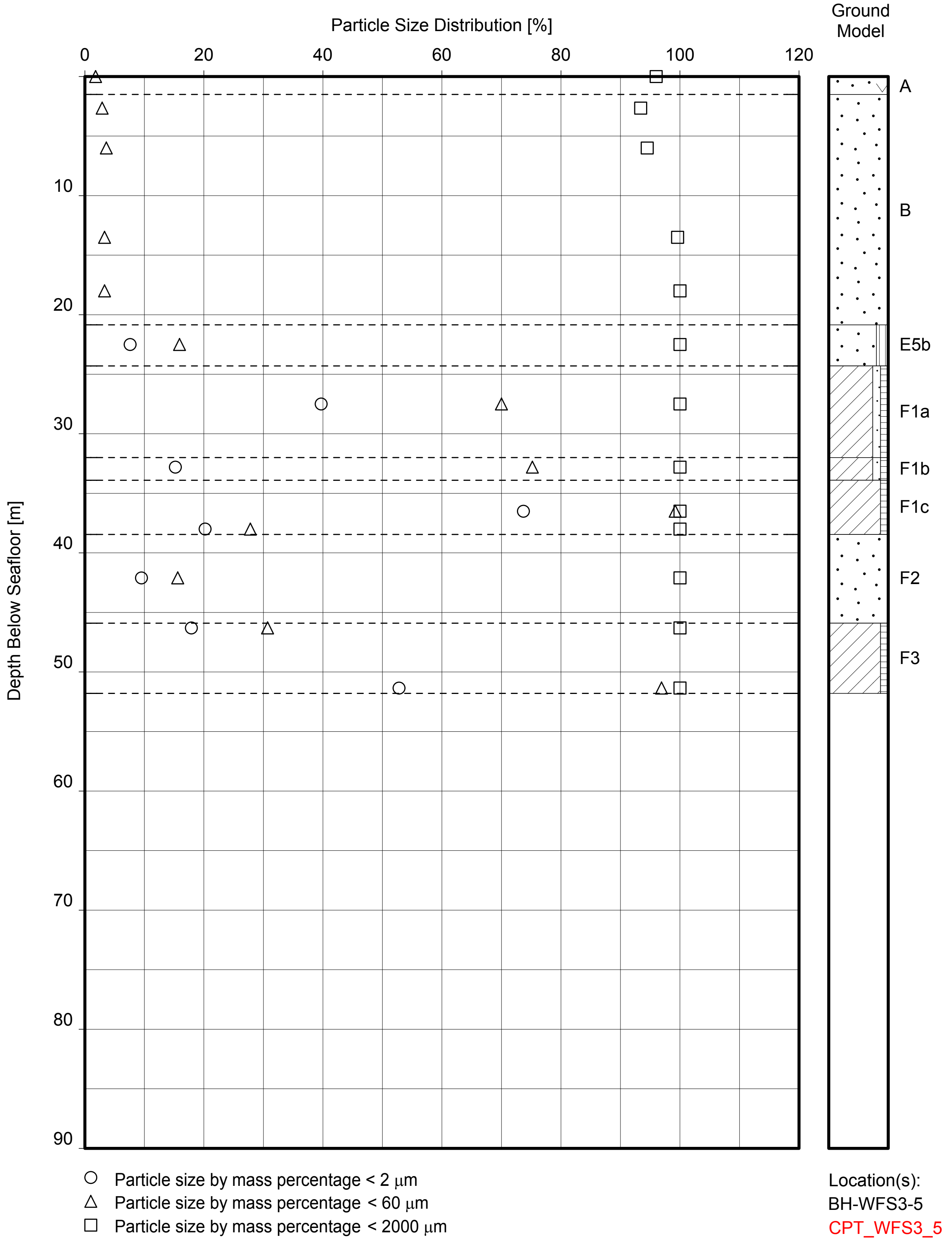


GeODin/5.Particle Size Distribution versus Depth (all UNITS, incl. GM),GLO/2015-12-09 10:58:01

**PARTICLE SIZE DISTRIBUTION VERSUS DEPTH**

BORSSELE WIND FARM ZONE, WFS III - DUTCH SECTOR, NORTH SEA

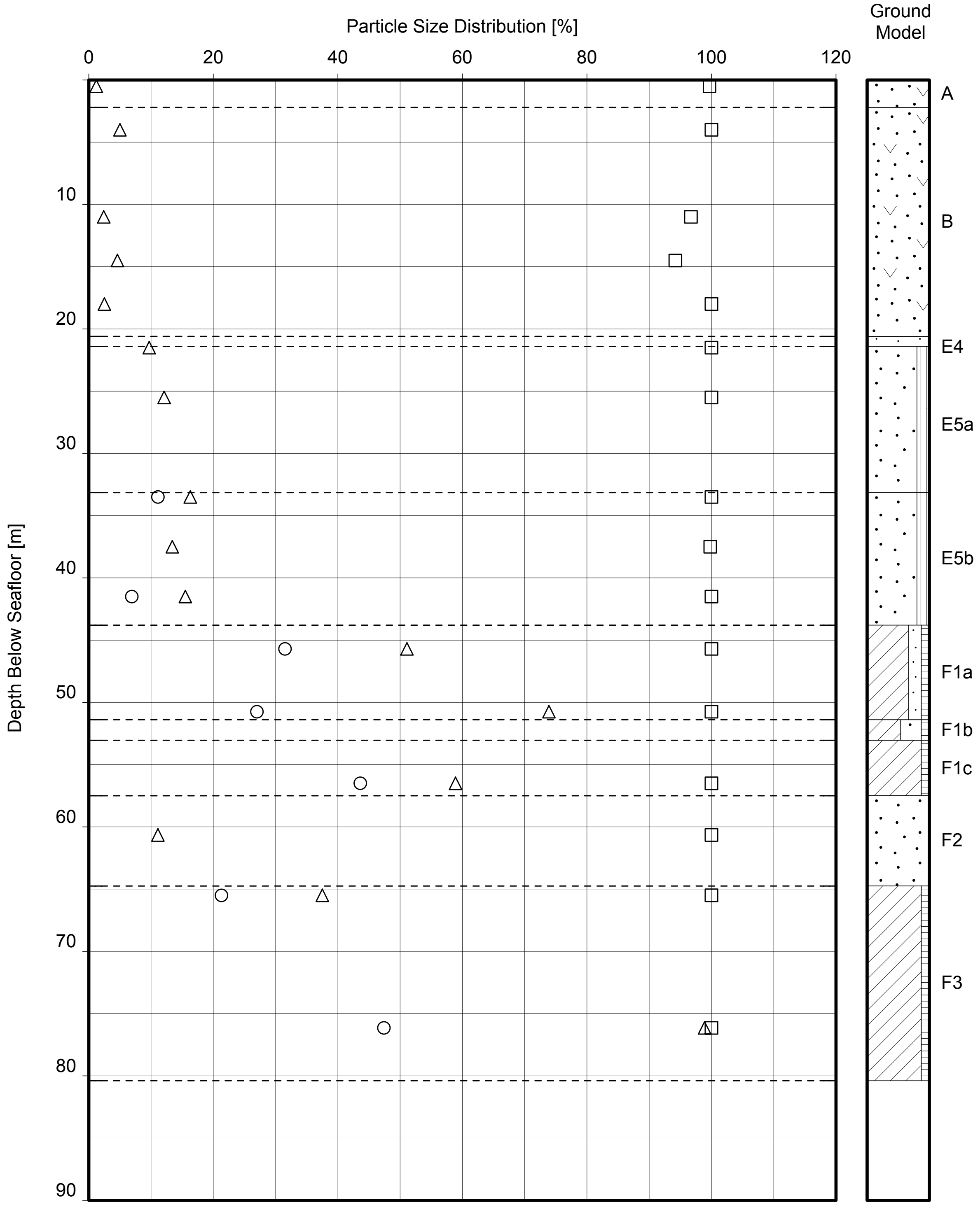


○ Particle size by mass percentage < 2 μm
△ Particle size by mass percentage < 60 μm
□ Particle size by mass percentage < 2000 μm

Location(s):
BH-WFS3-6
CPT_WFS3_6
CPT_WFS3_6A

GeODin/5.Particle Size Distribution versus Depth (all UNITS, incl. GM),GLO/2015-12-09 11:19:57

**PARTICLE SIZE DISTRIBUTION VERSUS DEPTH**

BORSSELE WIND FARM ZONE, WFS III - DUTCH SECTOR, NORTH SEA

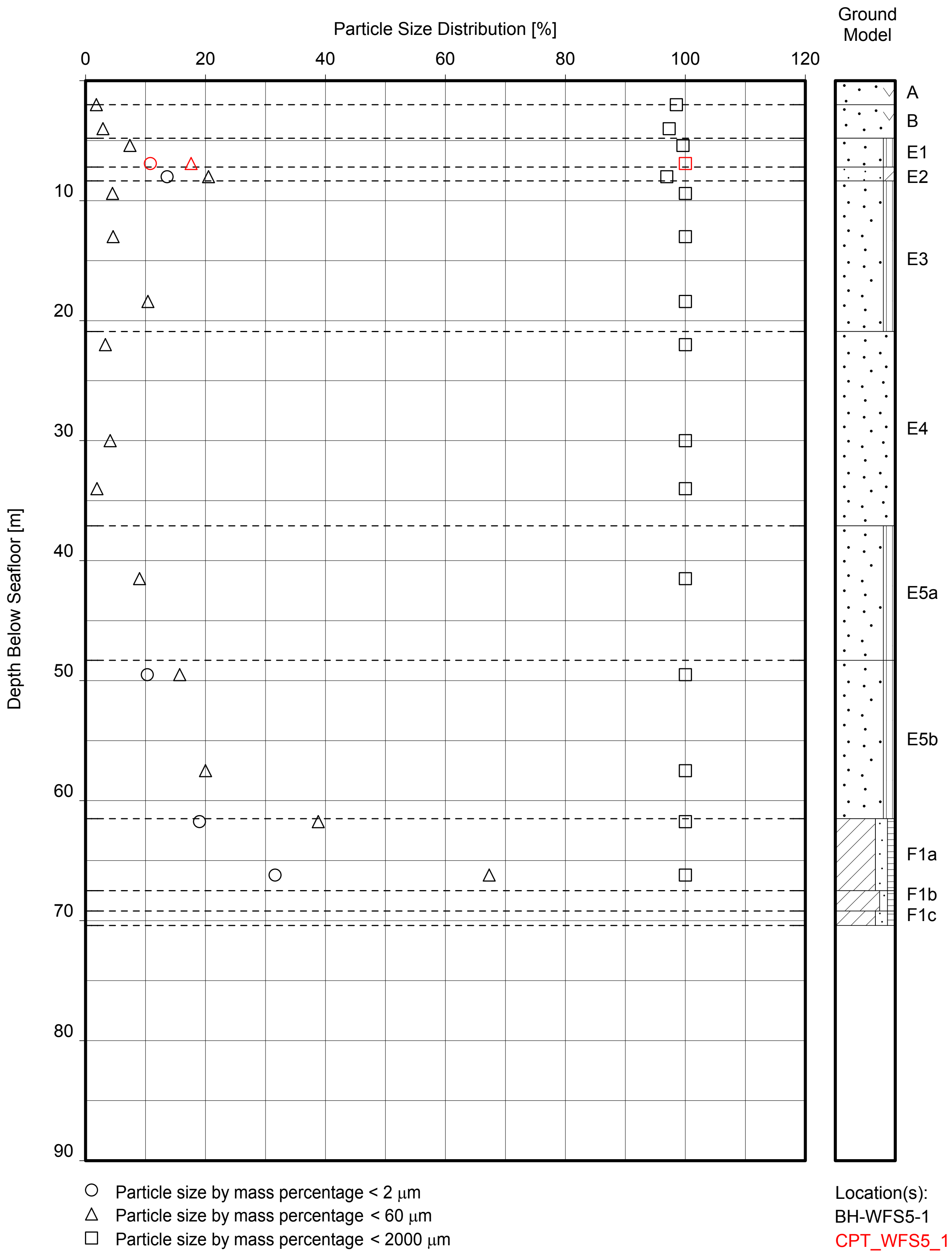


GeODin/5.Particle Size Distribution versus Depth (all UNITS, incl. GM),GLO/2015-12-09 11:22:24

**PARTICLE SIZE DISTRIBUTION VERSUS DEPTH**

BORSSELE WIND FARM ZONE, WFS III - DUTCH SECTOR, NORTH SEA

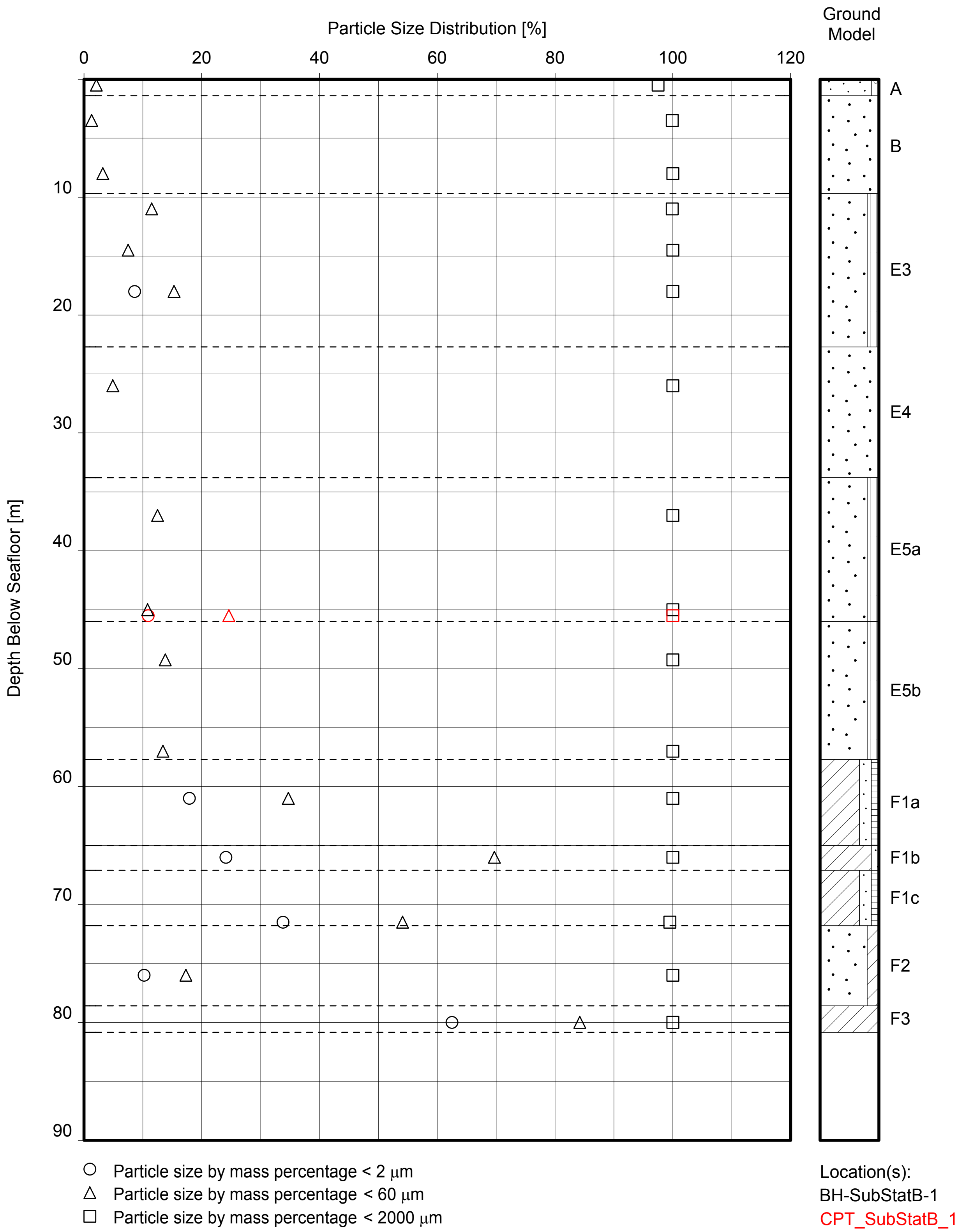


GeODin/5.Particle Size Distribution versus Depth (all UNITS, incl. GM),GLO/2015-12-09 11:24:59

## PARTICLE SIZE DISTRIBUTION VERSUS DEPTH

BORSSELE WIND FARM ZONE, WFS III - DUTCH SECTOR, NORTH SEA

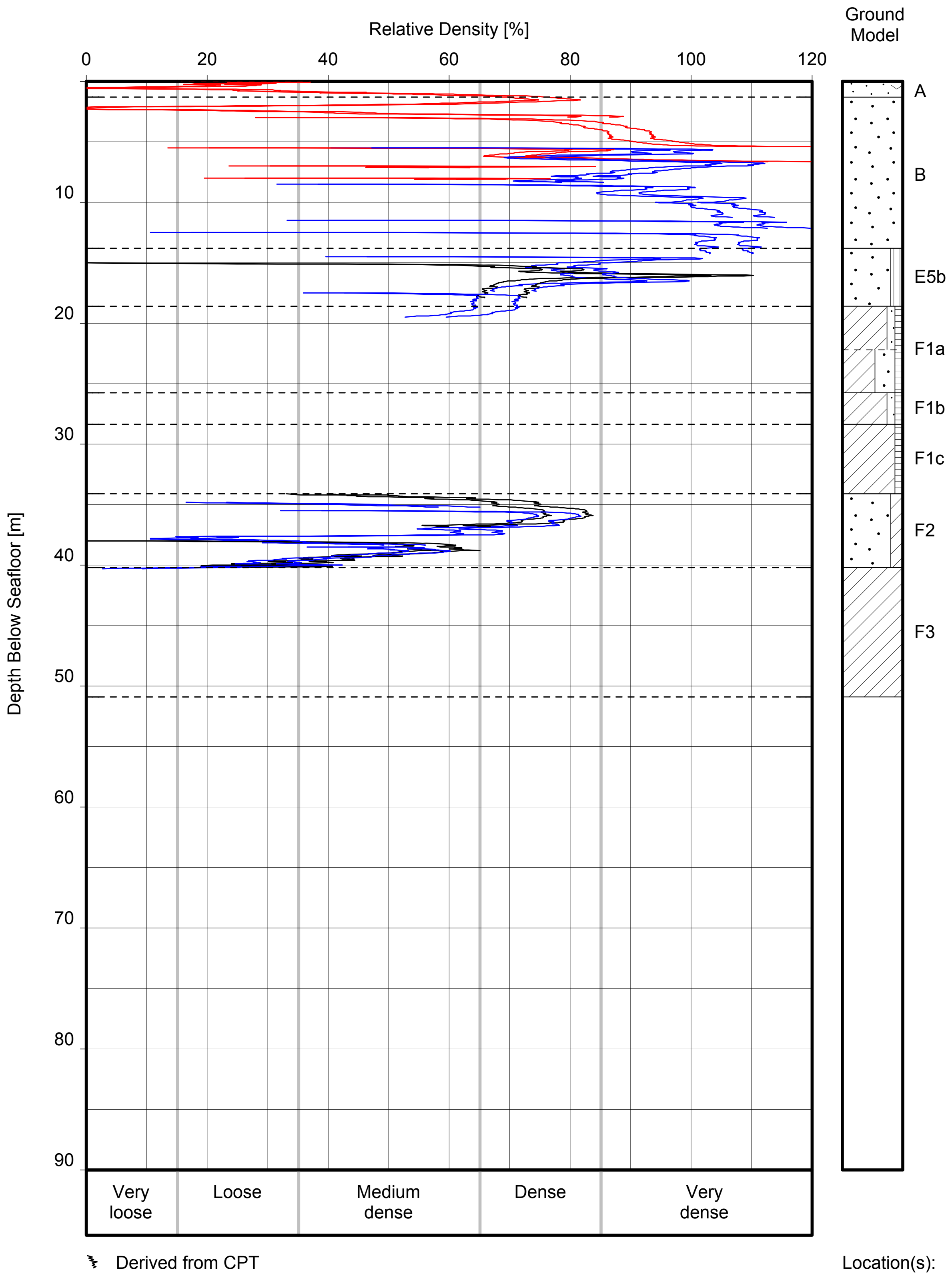


Location(s):
BH-WFS3-1
CPT_WFS3_1
CPT_WFS3_1A

Note(s):
- $K_0$ = 0.5 and $K_0$ = 1.0 are used to derive relative density from CPT

GeODin/6.Relative Density versus Depth 0-120 % (all UNITS, incl. GM).GLO/2015-12-09 10:48:03

**RELATIVE DENSITY VERSUS DEPTH**

BORSSELE WIND FARM ZONE, WFS III - DUTCH SECTOR, NORTH SEA

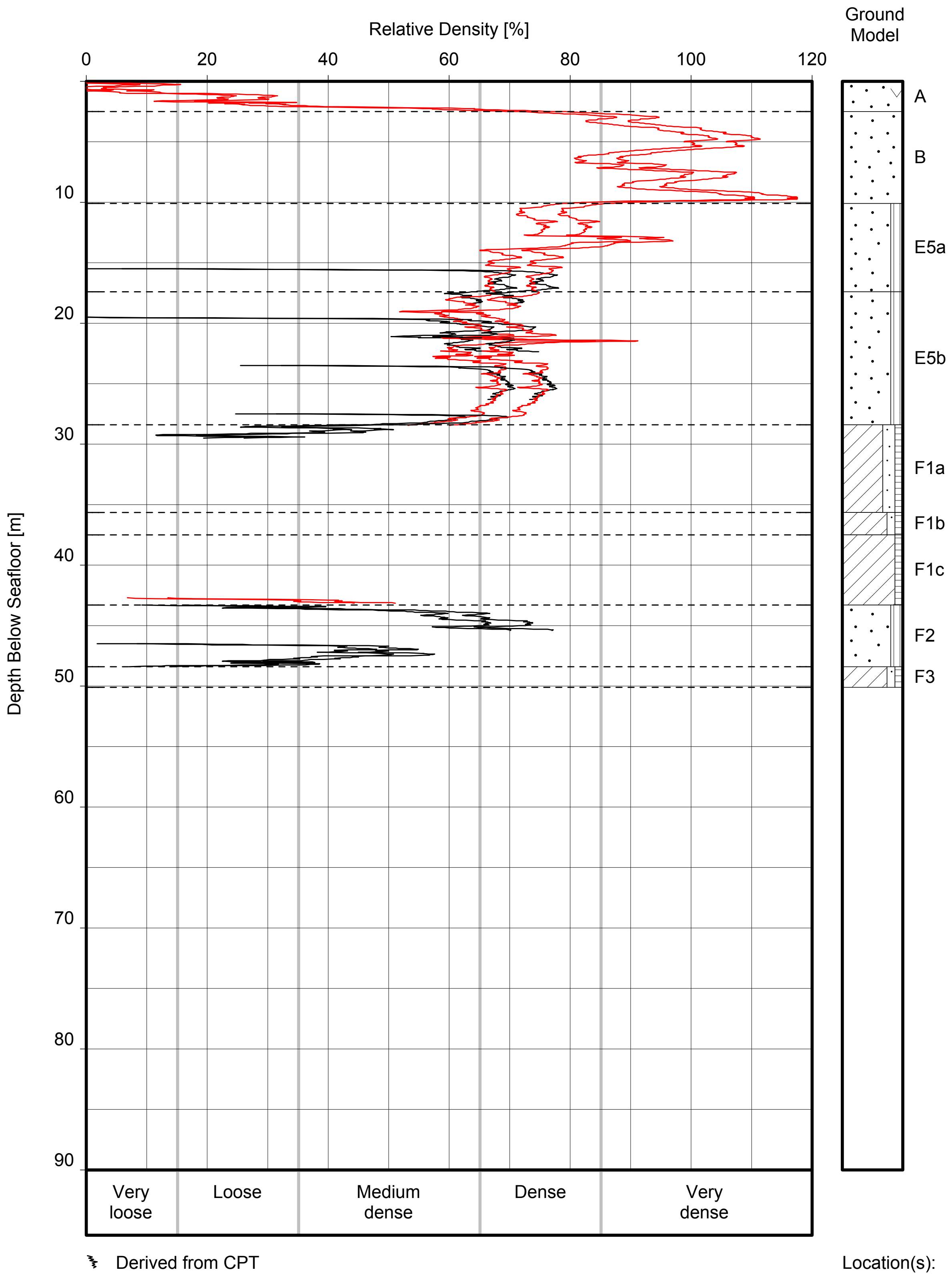


Location(s):
BH-WFS3-2
CPT_WFS3_2

Note(s):
- $K_0$ = 0.5 and $K_0$ = 1.0 are used to derive relative density from CPT

GeODin/6.Relative Density versus Depth 0-120 % (all UNITS, incl. GM).GLO/2015-12-09 10:51:18

**RELATIVE DENSITY VERSUS DEPTH**

BORSSELE WIND FARM ZONE, WFS III - DUTCH SECTOR, NORTH SEA

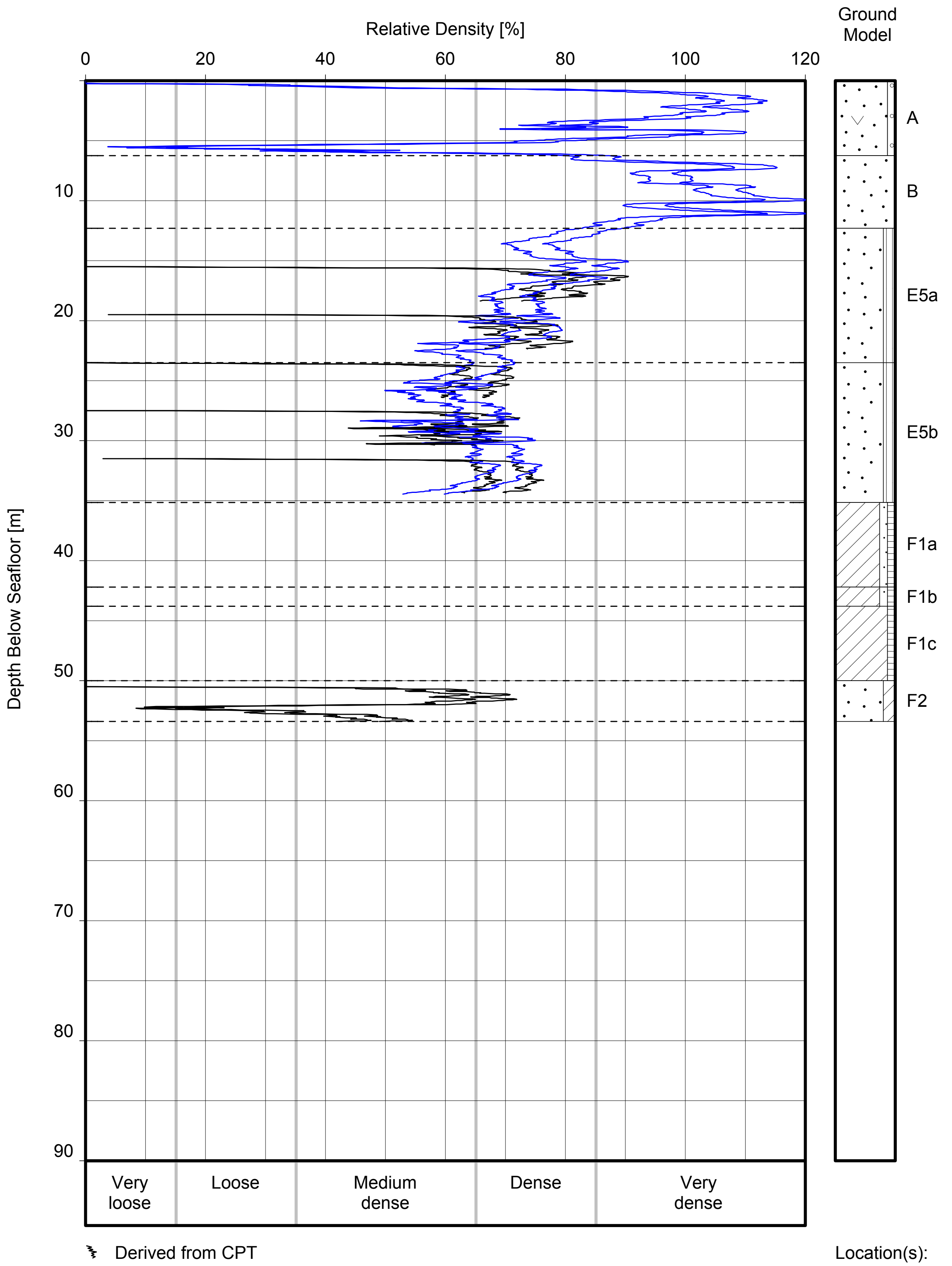


Note(s):
- $K_0$ = 0.5 and $K_0$ = 1.0 are used to derive relative density from CPT

GeODin/6.Relative Density versus Depth 0-120 % (all UNITS, incl. GM).GLO/2015-12-09 10:53:53

**RELATIVE DENSITY VERSUS DEPTH**

BORSSELE WIND FARM ZONE, WFS III - DUTCH SECTOR, NORTH SEA

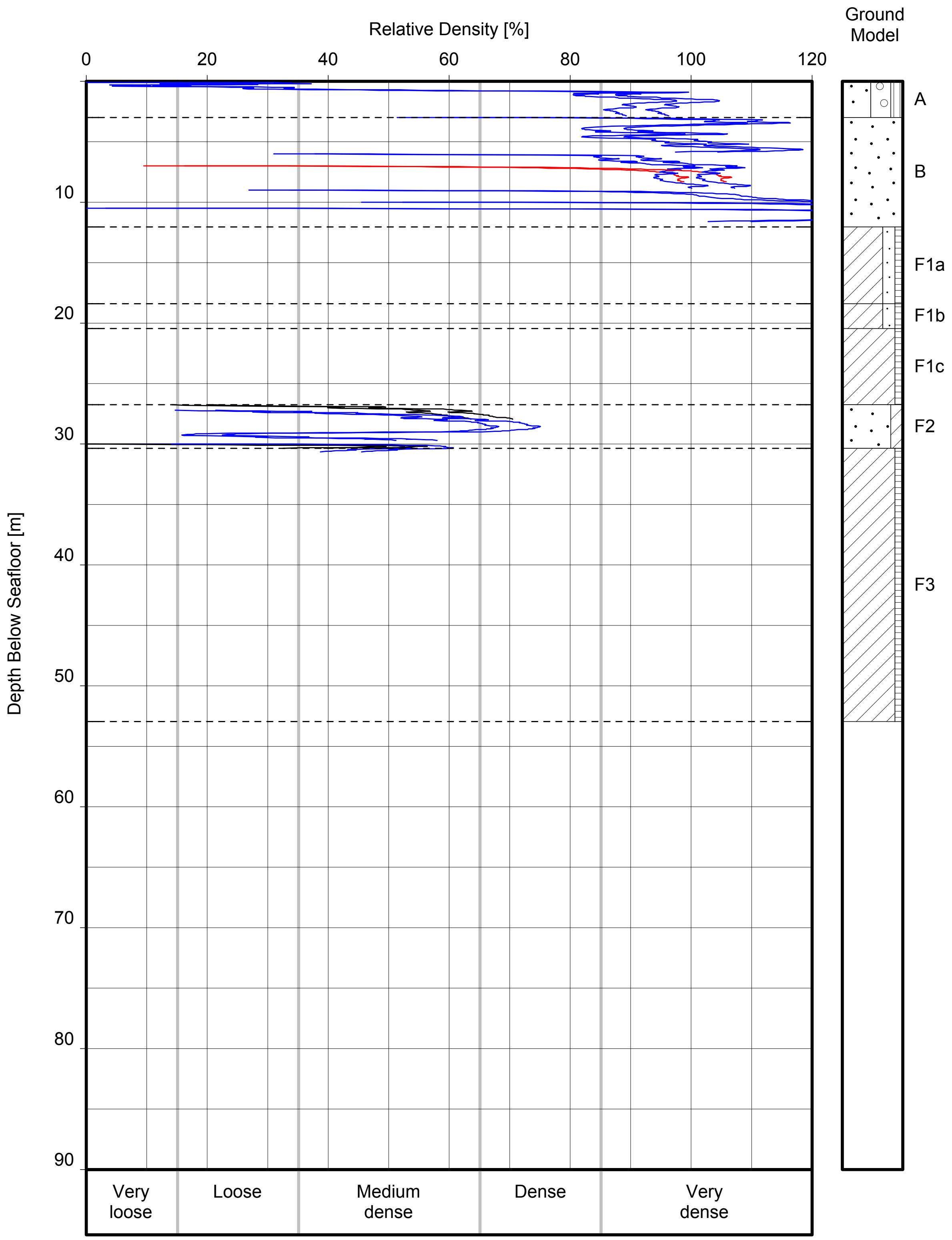


Derived from CPT

Location(s):
BH-WFS3-4A
BH-WFS3-4
CPT_WFS3_4

Note(s):
- $K_0$ = 0.5 and $K_0$ = 1.0 are used to derive relative density from CPT

GeODin/6.Relative Density versus Depth 0-120 % (all UNITS, incl. GM).GLO/2015-12-09 10:56:00

**RELATIVE DENSITY VERSUS DEPTH**

BORSSELE WIND FARM ZONE, WFS III - DUTCH SECTOR, NORTH SEA

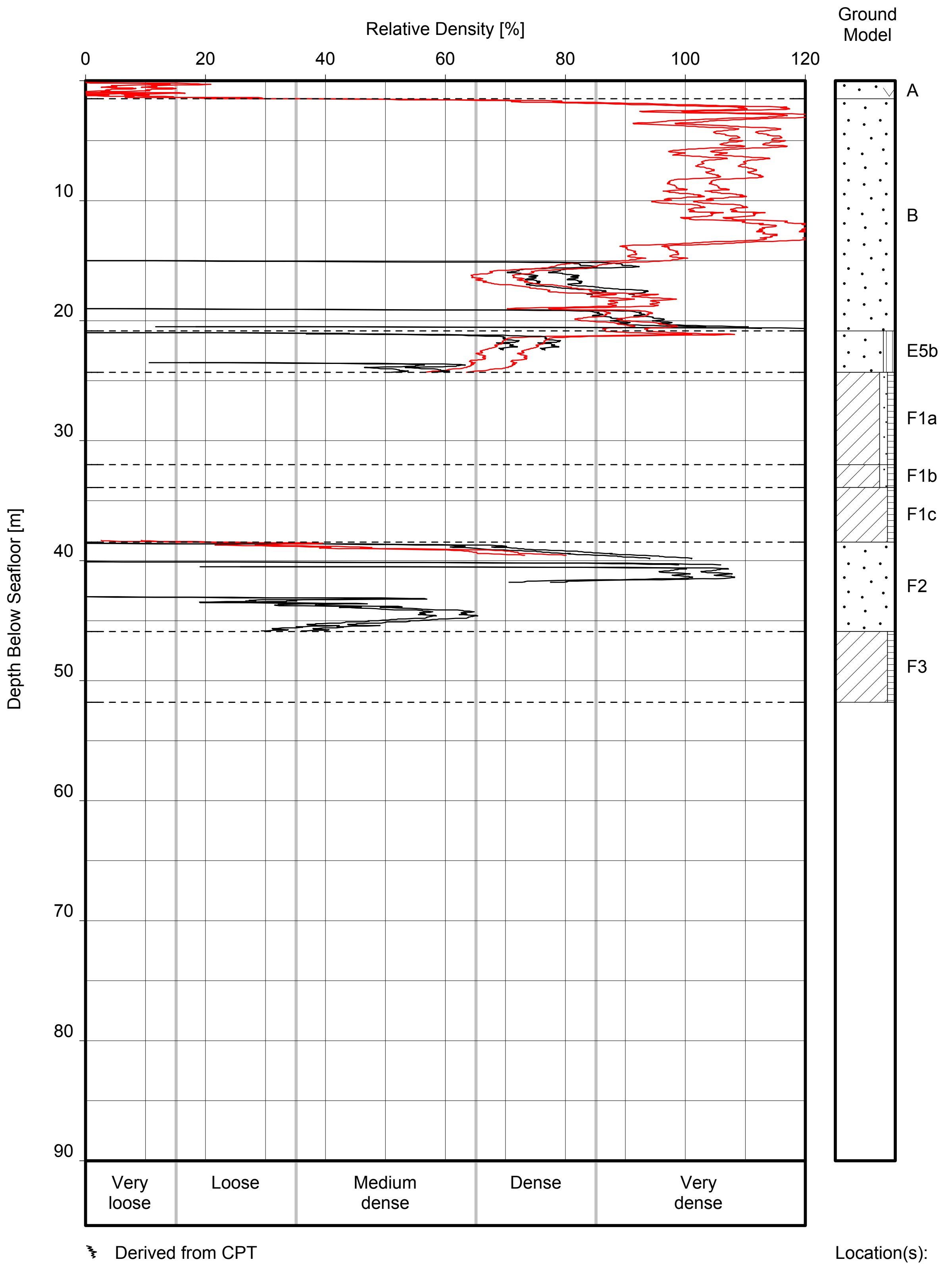


Note(s):
- $K_0$ = 0.5 and $K_0$ = 1.0 are used to derive relative density from CPT

GeODin/6.Relative Density versus Depth 0-120 % (all UNITS, incl. GM).GLO/2015-12-09 10:58:21

**RELATIVE DENSITY VERSUS DEPTH**

BORSSELE WIND FARM ZONE, WFS III - DUTCH SECTOR, NORTH SEA

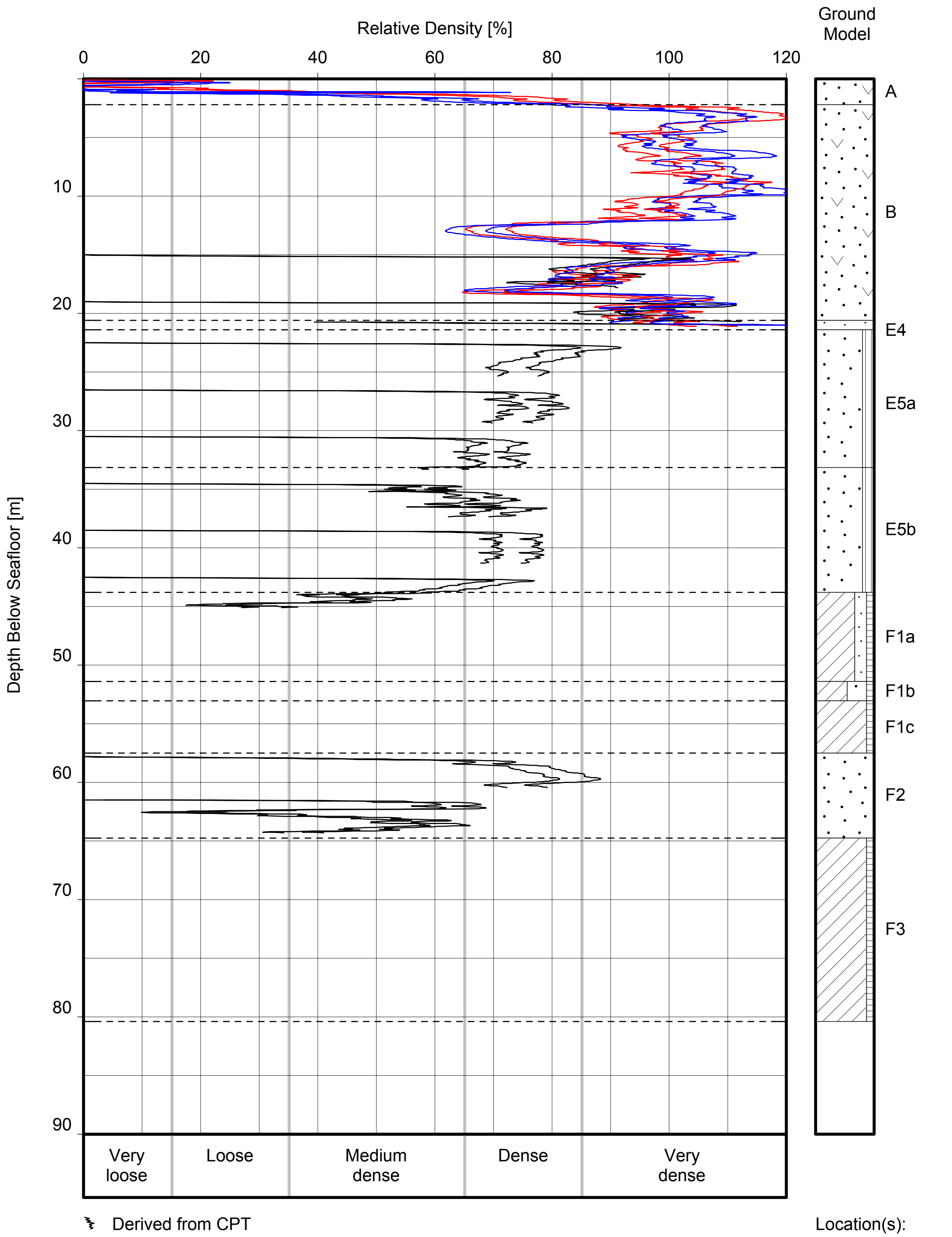


Location(s):
BH-WFS3-6
CPT_WFS3_6
CPT_WFS3_6A

Note(s):
- $K_0$ = 0.5 and $K_0$ = 1.0 are used to derive relative density from CPT

GeODin/6.Relative Density versus Depth 0-120 % (all UNITS, incl. GM).GLO/2015-12-09 11:20:13

**RELATIVE DENSITY VERSUS DEPTH**

BORSSELE WIND FARM ZONE, WFS III - DUTCH SECTOR, NORTH SEA

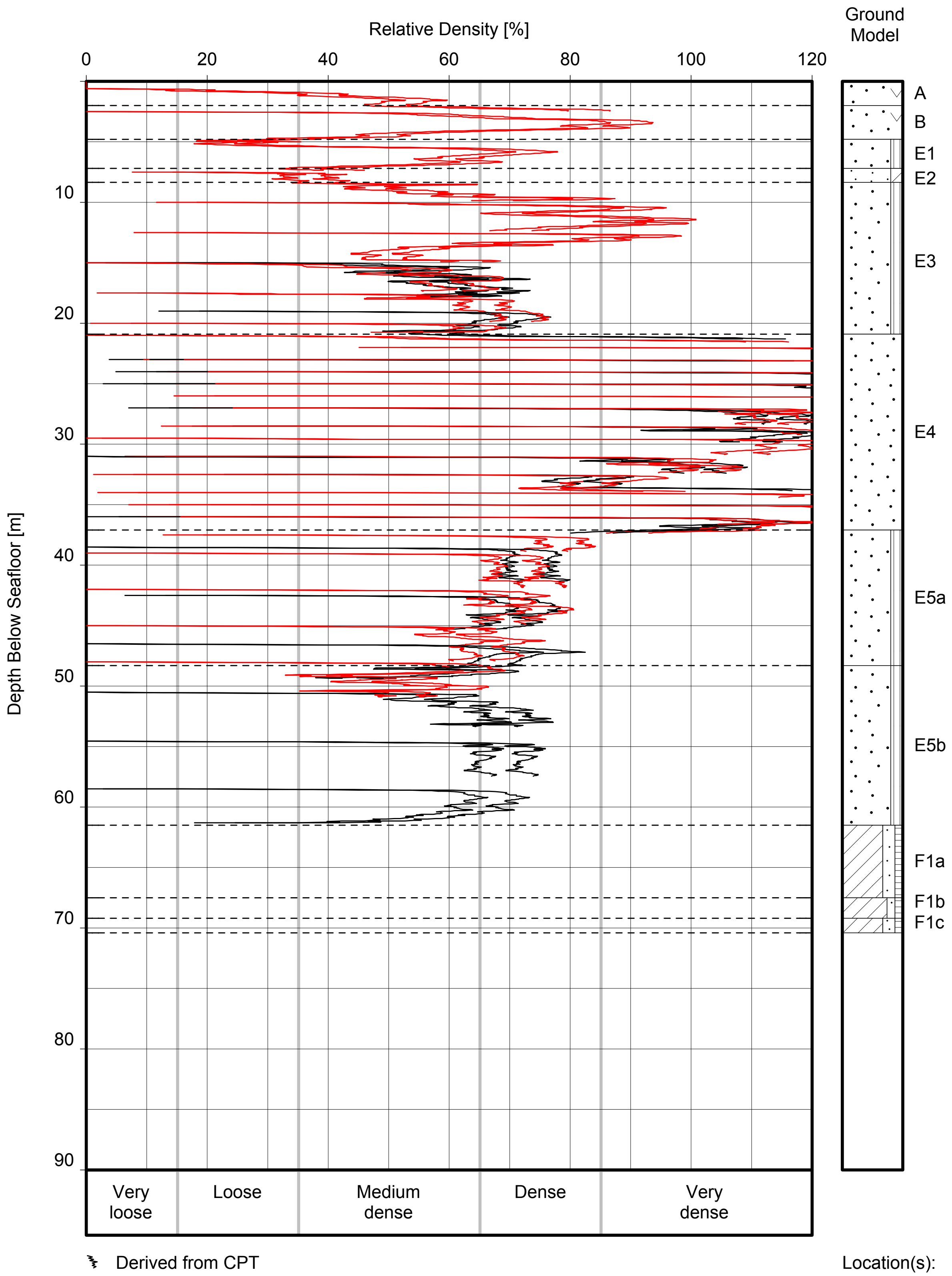


Location(s):
BH-WFS5-1
CPT_WFS5_1

Note(s):
- $K_0$ = 0.5 and $K_0$ = 1.0 are used to derive relative density from CPT

GeODin/6.Relative Density versus Depth 0-120 % (all UNITS, incl. GM).GLO/2015-12-09 11:22:37

**RELATIVE DENSITY VERSUS DEPTH**

BORSSELE WIND FARM ZONE, WFS III - DUTCH SECTOR, NORTH SEA

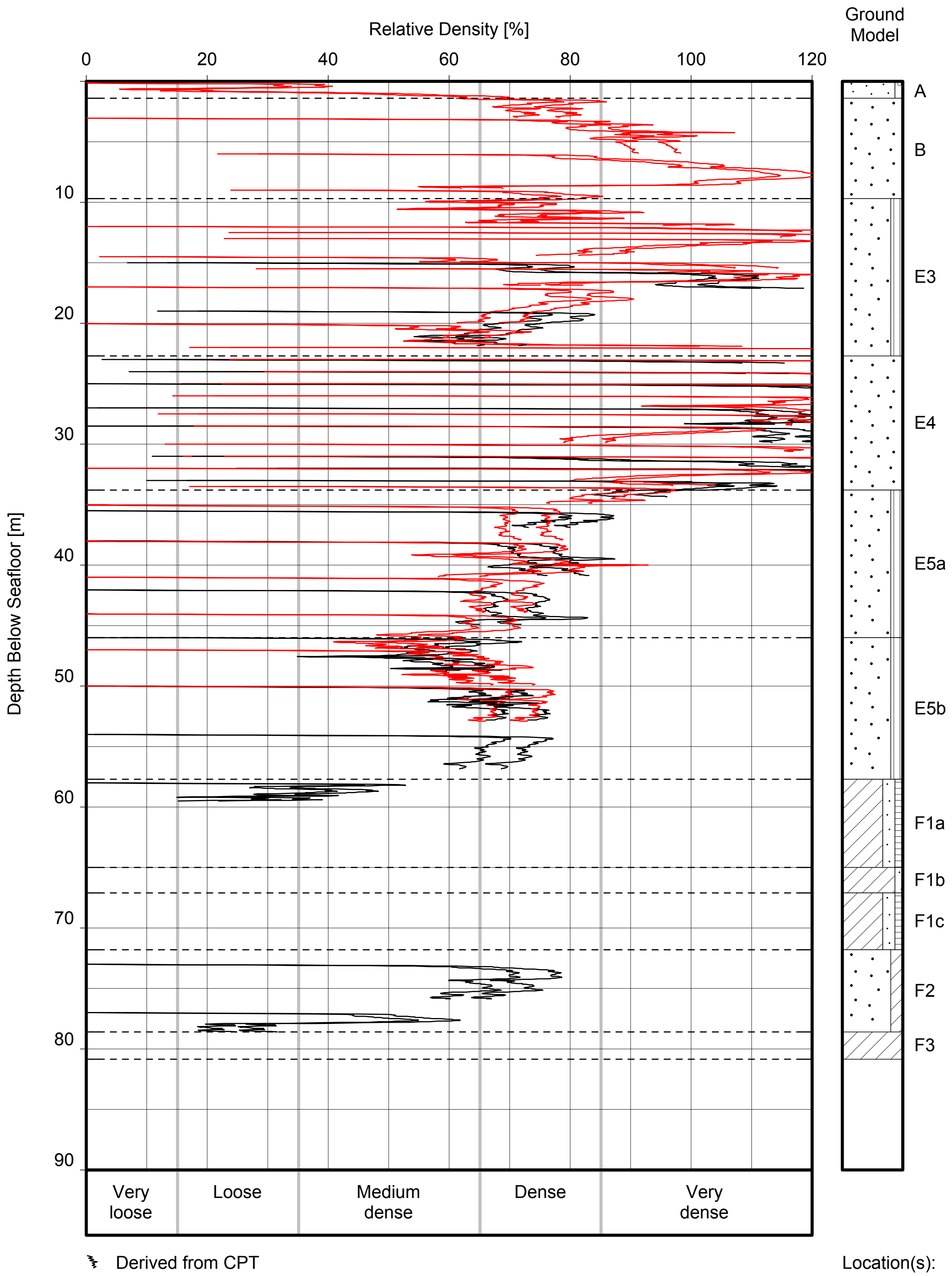


Location(s):
BH-SubStatB-1
CPT_SubStatB_1

Note(s):
- $K_0$ = 0.5 and $K_0$ = 1.0 are used to derive relative density from CPT

GeODin/6.Relative Density versus Depth 0-120 % (all UNITS, incl. GM).GLO/2015-12-09 11:25:11

## RELATIVE DENSITY VERSUS DEPTH

BORSSELE WIND FARM ZONE, WFS III - DUTCH SECTOR, NORTH SEA

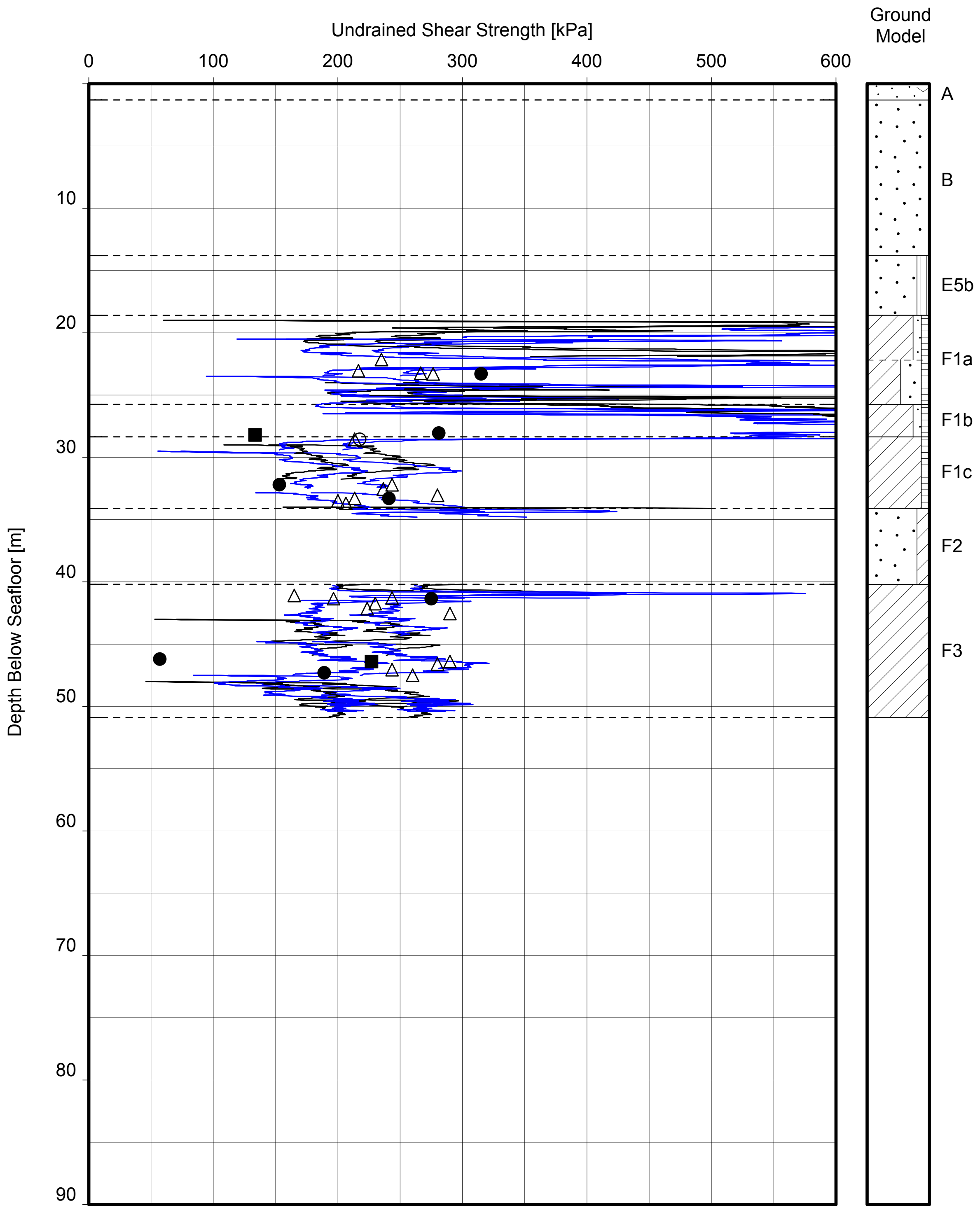


△ Pocket penetrometer
○ Torvane
▽ Fallcone
⊕ Laboratory vane

● UU-triaxial
■ CU-triaxial
◪ Direct simple shear
◆ In situ vane shear
Derived from CPT

Location(s):
BH-WFS3-1
CPT_WFS3_1
CPT_WFS3_1A

Note(s):
- $N_k$ = 15 and $N_k$ = 20 are used to derive $c_u$ from CPT

GeODin/7.Undrained Shear Strength versus Depth (all UNITS, incl. GM).glo/2015-12-09 10:48:18

**UNDRAINED SHEAR STRENGTH VERSUS DEPTH**

BORSSELE WIND FARM ZONE, WFS III - DUTCH SECTOR, NORTH SEA

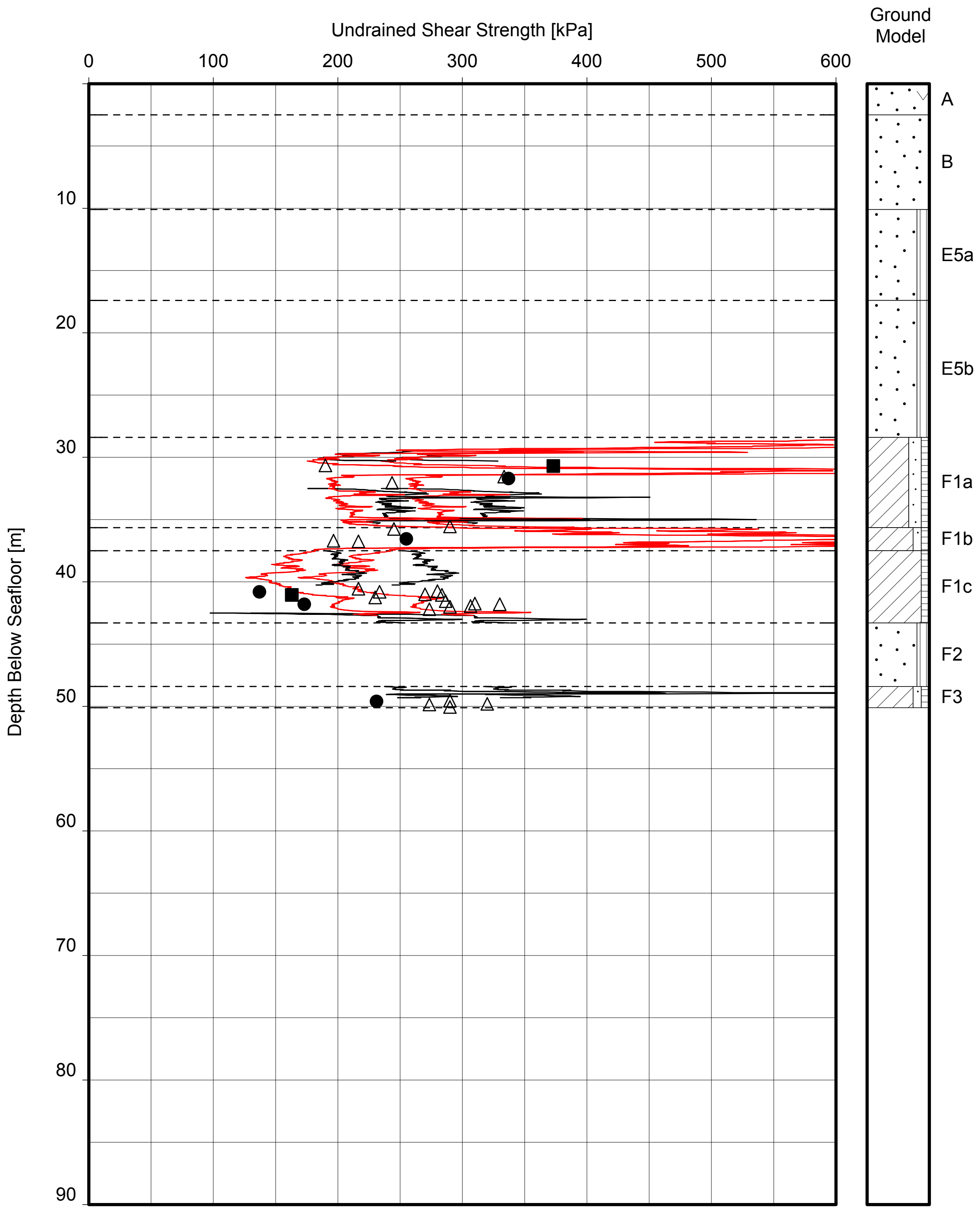


△ Pocket penetrometer
○ Torvane
▽ Fallcone
⊕ Laboratory vane

● UU-triaxial
■ CU-triaxial
◪ Direct simple shear
◆ In situ vane shear
Derived from CPT

Location(s):
BH-WFS3-2
CPT_WFS3_2

Note(s):
- $N_k$ = 15 and $N_k$ = 20 are used to derive $c_u$ from CPT

GeODin/7.Undrained Shear Strength versus Depth (all UNITS, incl. GM).glo/2015-12-09 10:52:05

**UNDRAINED SHEAR STRENGTH VERSUS DEPTH**

BORSSELE WIND FARM ZONE, WFS III - DUTCH SECTOR, NORTH SEA

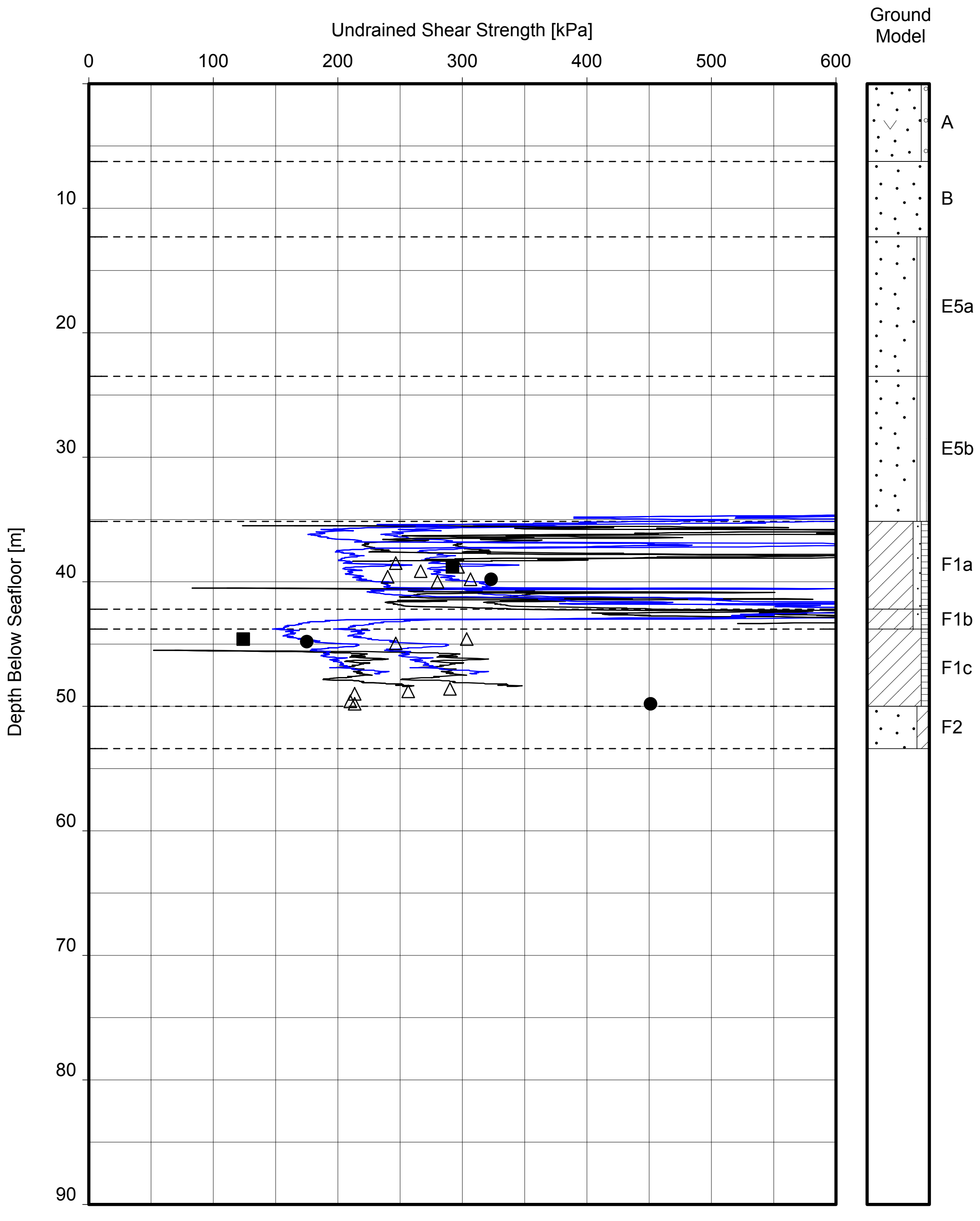


△ Pocket penetrometer
○ Torvane
▽ Fallcone
⊕ Laboratory vane
● UU-triaxial
■ CU-triaxial
◪ Direct simple shear
◆ In situ vane shear
Derived from CPT

Location(s):
BH-WFS3-3A
BH-WFS3-3
CPT_WFS3_3

Note(s):
- $N_k$ = 15 and $N_k$ = 20 are used to derive $c_u$ from CPT

GeODin/7.Undrained Shear Strength versus Depth (all UNITS, incl. GM).glo/2015-12-09 10:54:05

**UNDRAINED SHEAR STRENGTH VERSUS DEPTH**

BORSSELE WIND FARM ZONE, WFS III - DUTCH SECTOR, NORTH SEA

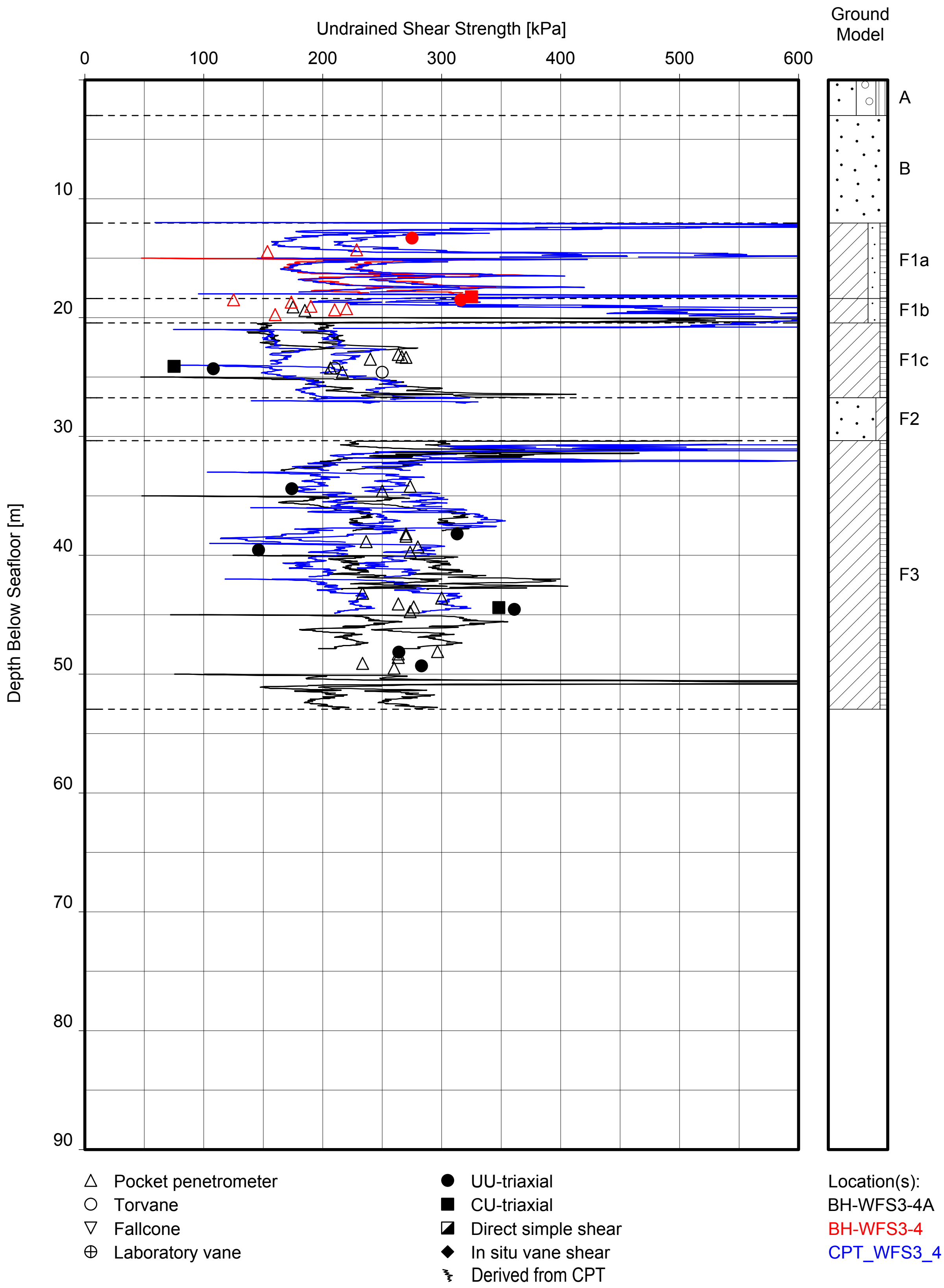


Note(s):
- $N_k$ = 15 and $N_k$ = 20 are used to derive $c_u$ from CPT

GeODin/7.Undrained Shear Strength versus Depth (all UNITS, incl. GM).glo/2015-12-09 10:56:17

**UNDRAINED SHEAR STRENGTH VERSUS DEPTH**

BORSSELE WIND FARM ZONE, WFS III - DUTCH SECTOR, NORTH SEA

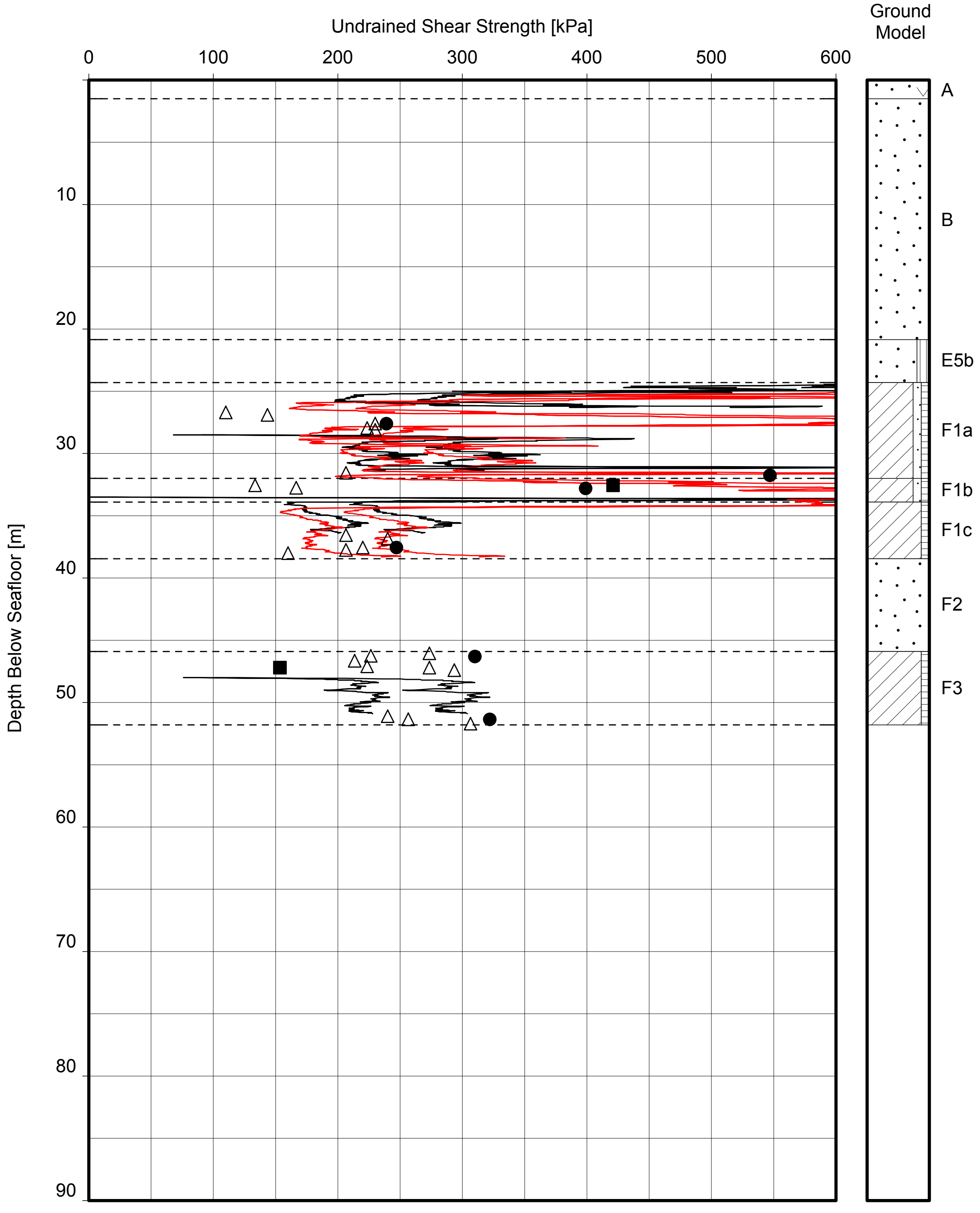


△ Pocket penetrometer
○ Torvane
▽ Fallcone
⊕ Laboratory vane

● UU-triaxial
■ CU-triaxial
Direct simple shear
◆ In situ vane shear
Derived from CPT

Location(s):
BH-WFS3-5
CPT_WFS3_5

Note(s):
- $N_k$ = 15 and $N_k$ = 20 are used to derive $c_u$ from CPT

GeODin/7.Undrained Shear Strength versus Depth (all UNITS, incl. GM).glo/2015-12-09 10:58:33

**UNDRAINED SHEAR STRENGTH VERSUS DEPTH**

BORSSELE WIND FARM ZONE, WFS III - DUTCH SECTOR, NORTH SEA

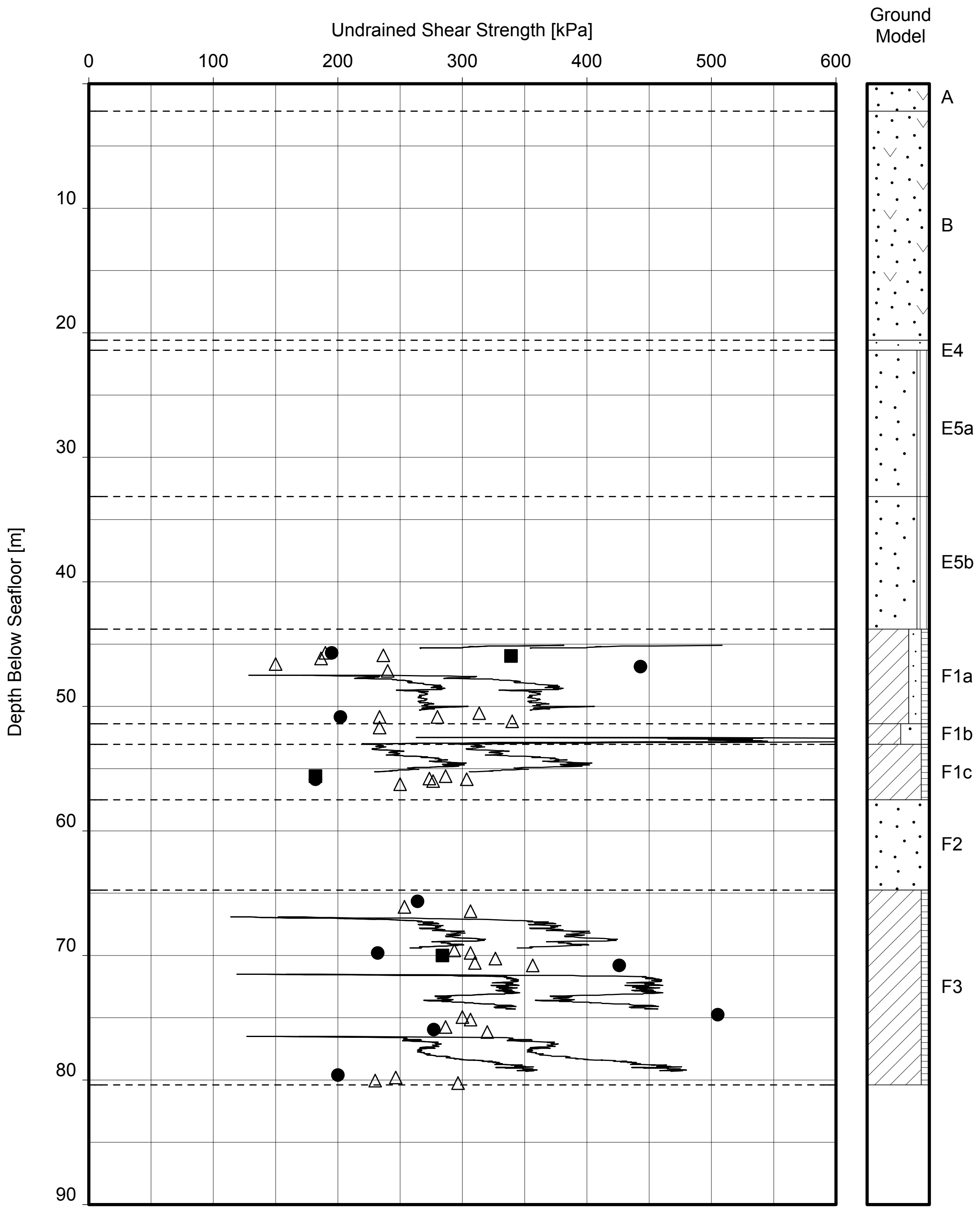


△ Pocket penetrometer
○ Torvane
▽ Fallcone
⊕ Laboratory vane
● UU-triaxial
■ CU-triaxial
◪ Direct simple shear
◆ In situ vane shear
Derived from CPT

Location(s):
BH-WFS3-6
CPT_WFS3_6
CPT_WFS3_6A

Note(s):
- $N_k$ = 15 and $N_k$ = 20 are used to derive $c_u$ from CPT

GeODin/7.Undrained Shear Strength versus Depth (all UNITS, incl. GM).glo/2015-12-09 11:20:29

**UNDRAINED SHEAR STRENGTH VERSUS DEPTH**

BORSSELE WIND FARM ZONE, WFS III - DUTCH SECTOR, NORTH SEA

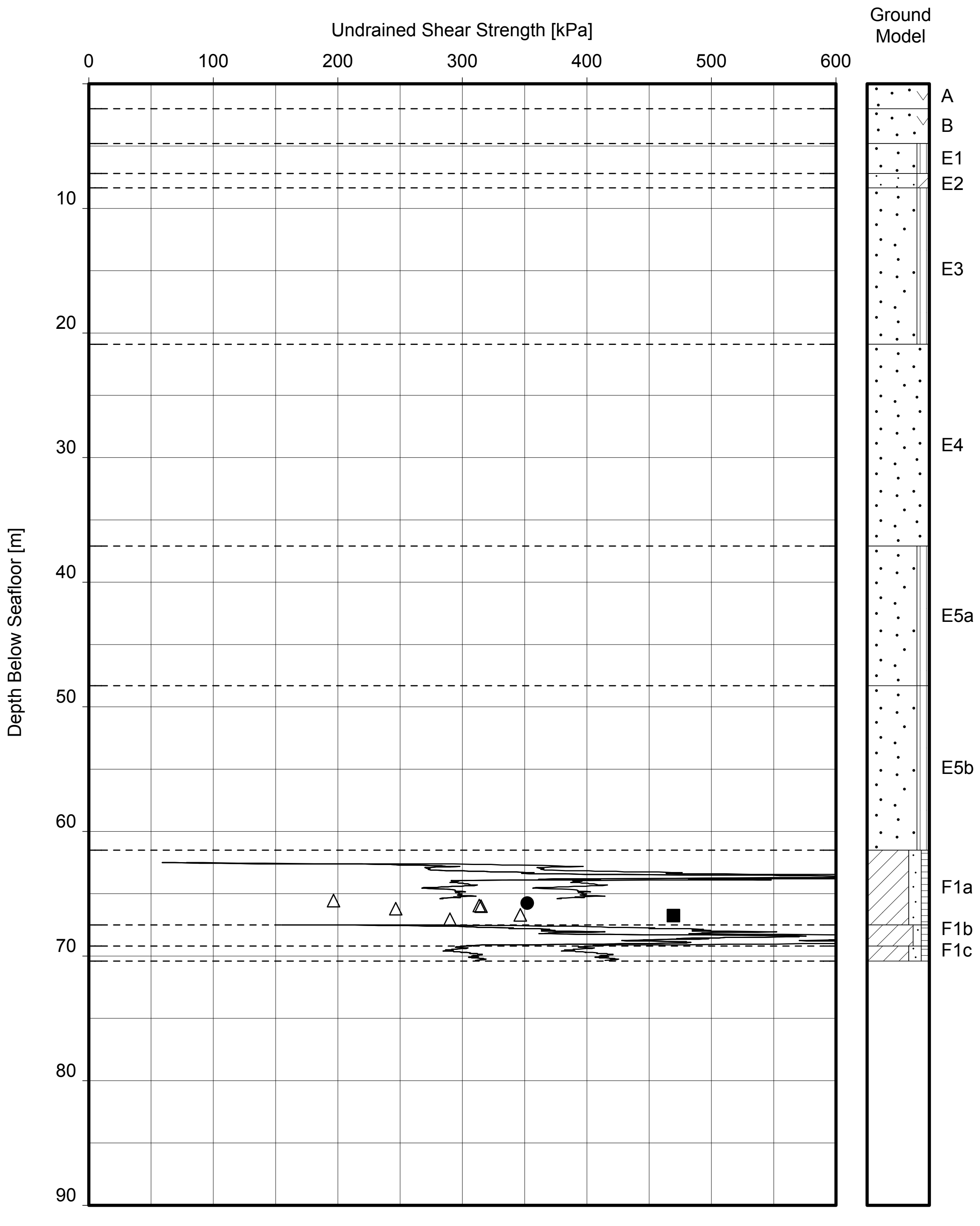


△ Pocket penetrometer
○ Torvane
▽ Fallcone
⊕ Laboratory vane
● UU-triaxial
■ CU-triaxial
◪ Direct simple shear
◆ In situ vane shear
Derived from CPT

Location(s):
BH-WFS5-1
CPT_WFS5_1

Note(s):
- $N_k$ = 15 and $N_k$ = 20 are used to derive $c_u$ from CPT

GeODin/7.Undrained Shear Strength versus Depth (all UNITS, incl. GM).glo/2015-12-09 11:23:08

**UNDRAINED SHEAR STRENGTH VERSUS DEPTH**

BORSSELE WIND FARM ZONE, WFS III - DUTCH SECTOR, NORTH SEA

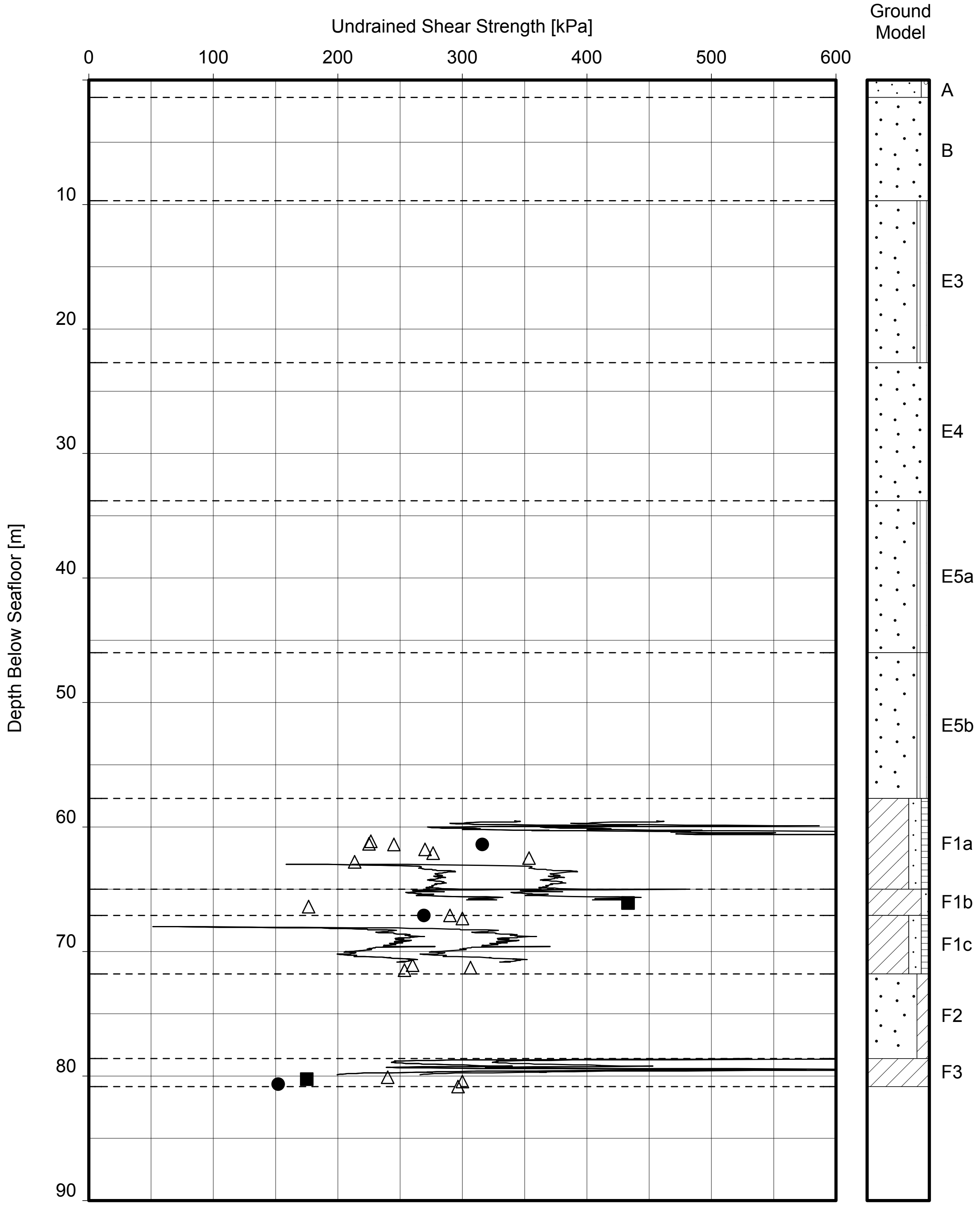


△ Pocket penetrometer
○ Torvane
▽ Fallcone
⊕ Laboratory vane
● UU-triaxial
■ CU-triaxial
◪ Direct simple shear
◆ In situ vane shear
Derived from CPT

Location(s):
BH-SubStatB-1
CPT_SubStatB_1

Note(s):
- $N_k$ = 15 and $N_k$ = 20 are used to derive $c_u$ from CPT

GeODin/7.Undrained Shear Strength versus Depth (all UNITS, incl. GM).glo/2015-12-09 11:25:30

**UNDRAINED SHEAR STRENGTH VERSUS DEPTH**

BORSSELE WIND FARM ZONE, WFS III - DUTCH SECTOR, NORTH SEA

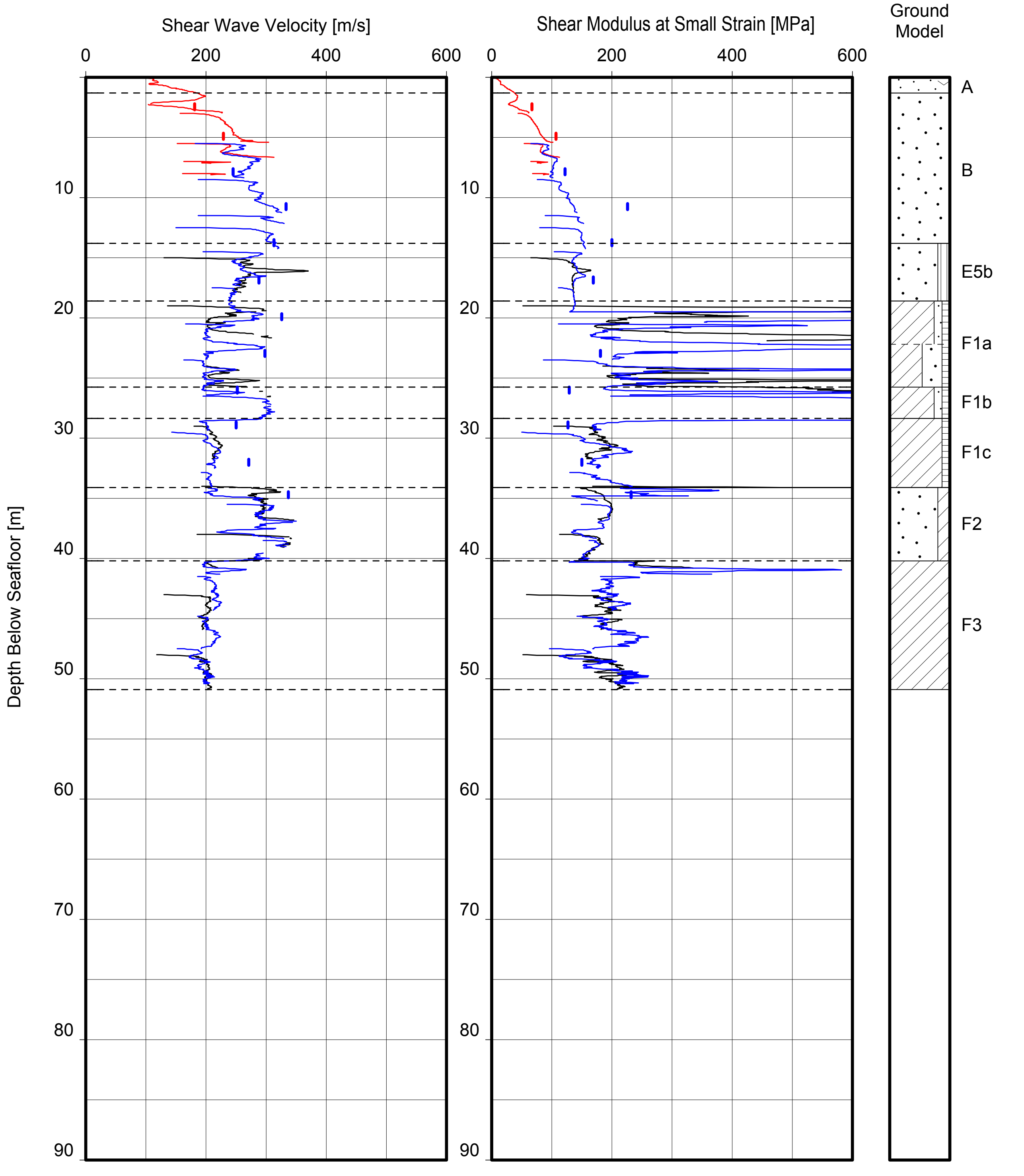


Shear wave velocity ($v_s$) measured in-between geophone array
Shear modulus at small strain ($G_{max}$) derived from $v_s$ measured
$v_s$ and $G_{max}$ derived from CPT

Location(s):
BH-WFS3-1
CPT_WFS3_1
CPT_WFS3_1A

Note(s):
- $v_s$ derived from CPT based on Robertson and Cabal (2010)
- $G_{max}$ for clays derived from CPT based on Mayne and Rix (1993)
- $G_{max}$ for sands derived from CPT based on Rix and Stokoe (1991)

GeODin/8.Shear Wave Velocity and Shear Modulus at Small Strain versus Depth (all UNITS, incl. GM).GLO/2015-12-09 11:28:54

**SHEAR WAVE VELOCITY AND SHEAR MODULUS AT SMALL STRAIN VERSUS DEPTH**

BORSSELE WIND FARM ZONE, WFS III - DUTCH SECTOR, NORTH SEA

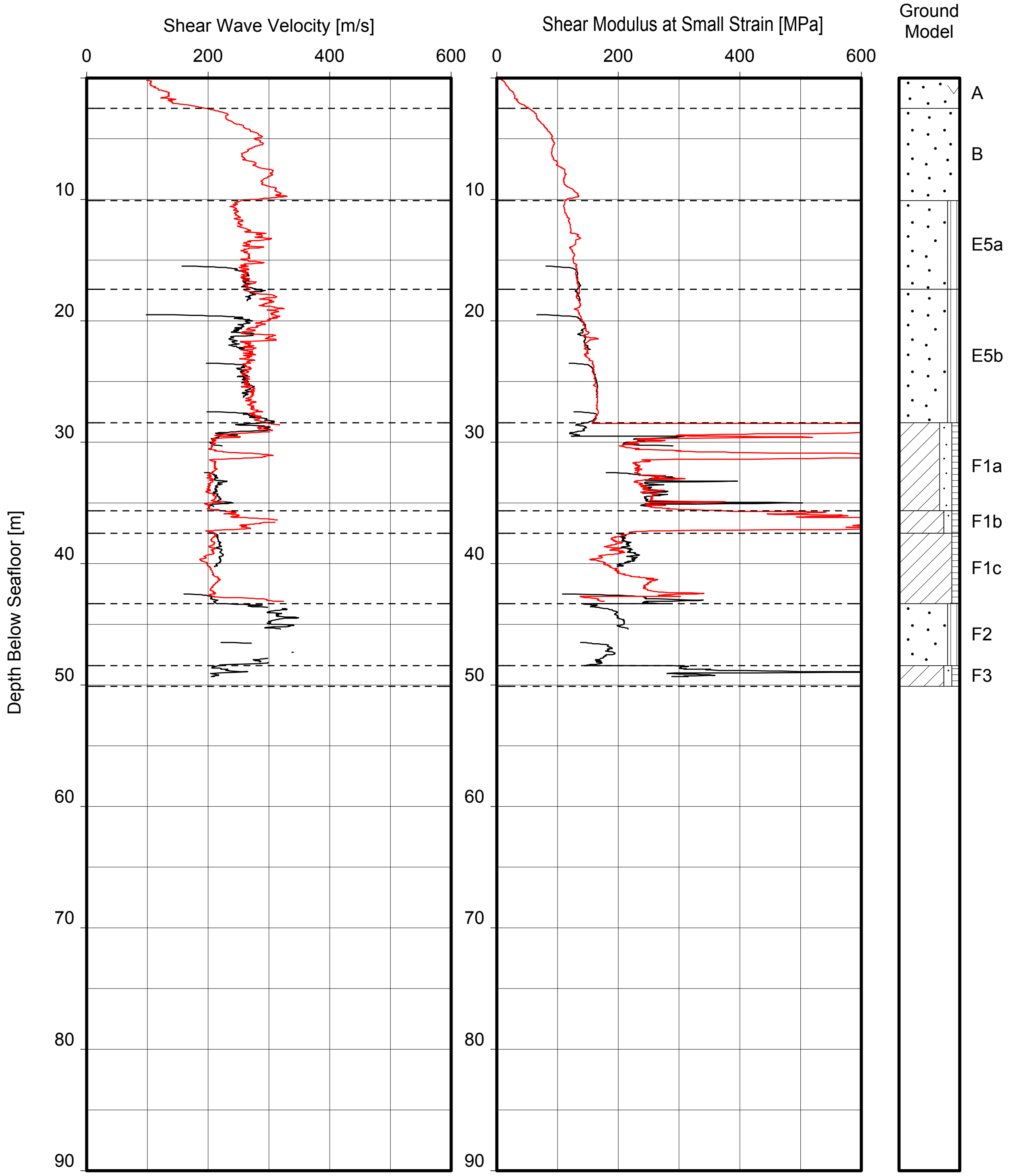


Shear wave velocity ($v_s$) measured in-between geophone array

Shear modulus at small strain ($G_{max}$) derived from $v_s$ measured

$v_s$ and $G_{max}$ derived from CPT

Location(s):
BH-WFS3-2
CPT_WFS3_2

Note(s):
- $v_s$ derived from CPT based on Robertson and Cabal (2010)
- $G_{max}$ for clays derived from CPT based on Mayne and Rix (1993)
- $G_{max}$ for sands derived from CPT based on Rix and Stokoe (1991)

GeODin/8.Shear Wave Velocity and Shear Modulus at Small Strain versus Depth (all UNITS, incl. GM).GLO/2015-12-09 11:29:16

**SHEAR WAVE VELOCITY AND SHEAR MODULUS AT SMALL STRAIN VERSUS DEPTH**

BORSSELE WIND FARM ZONE, WFS III - DUTCH SECTOR, NORTH SEA

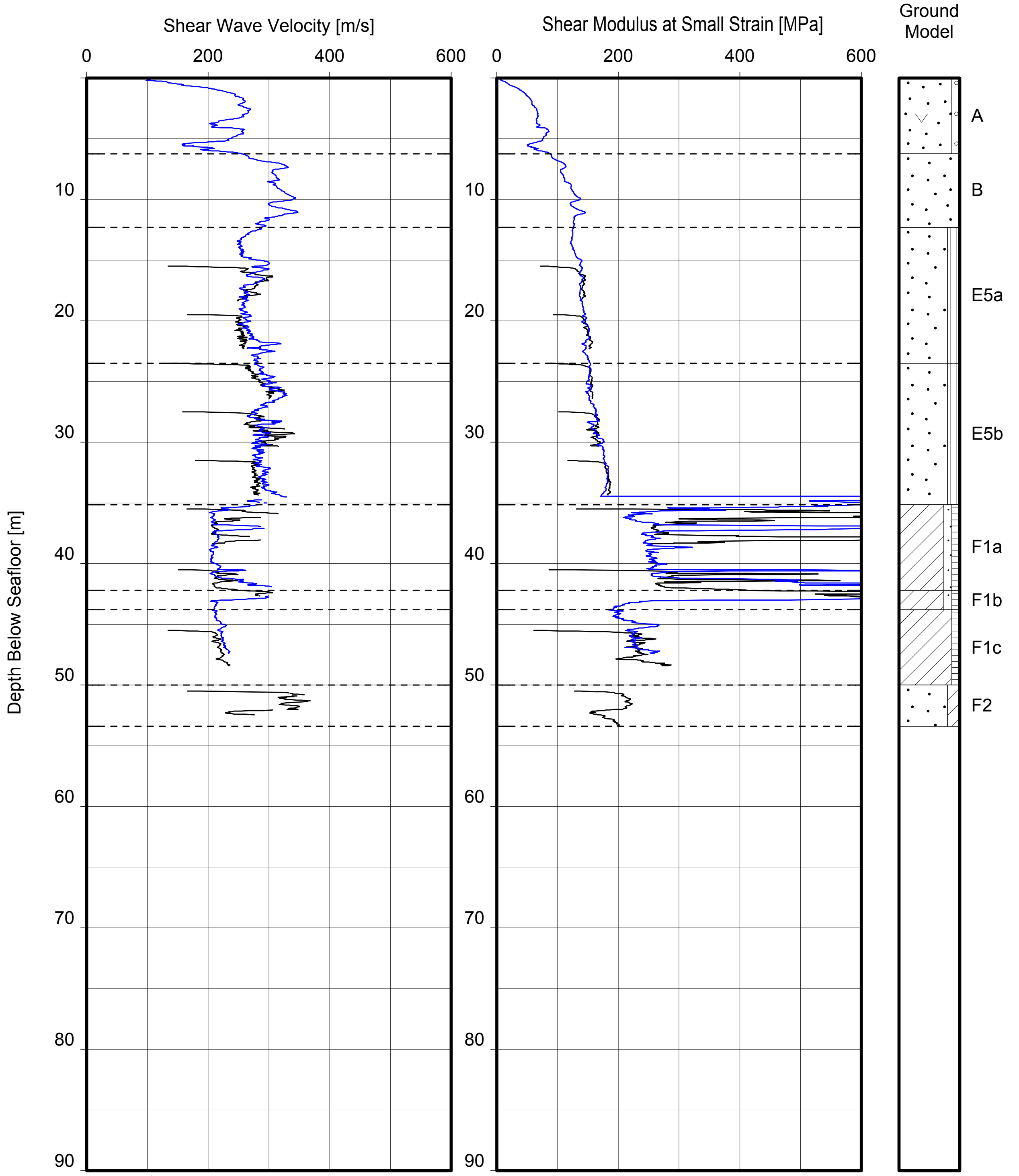


- Shear wave velocity ($v_s$) measured in-between geophone array
- Shear modulus at small strain ($G_{max}$) derived from $v_s$ measured
- $v_s$ and $G_{max}$ derived from CPT

Location(s):
BH-WFS3-3A
BH-WFS3-3
CPT_WFS3_3

Note(s):
- $v_s$ derived from CPT based on Robertson and Cabal (2010)
- $G_{max}$ for clays derived from CPT based on Mayne and Rix (1993)
- $G_{max}$ for sands derived from CPT based on Rix and Stokoe (1991)

GeODin/8.Shear Wave Velocity and Shear Modulus at Small Strain versus Depth (all UNITS, incl. GM).GLO/2015-12-09 11:29:38

**SHEAR WAVE VELOCITY AND SHEAR MODULUS AT SMALL STRAIN VERSUS DEPTH**

BORSSELE WIND FARM ZONE, WFS III - DUTCH SECTOR, NORTH SEA

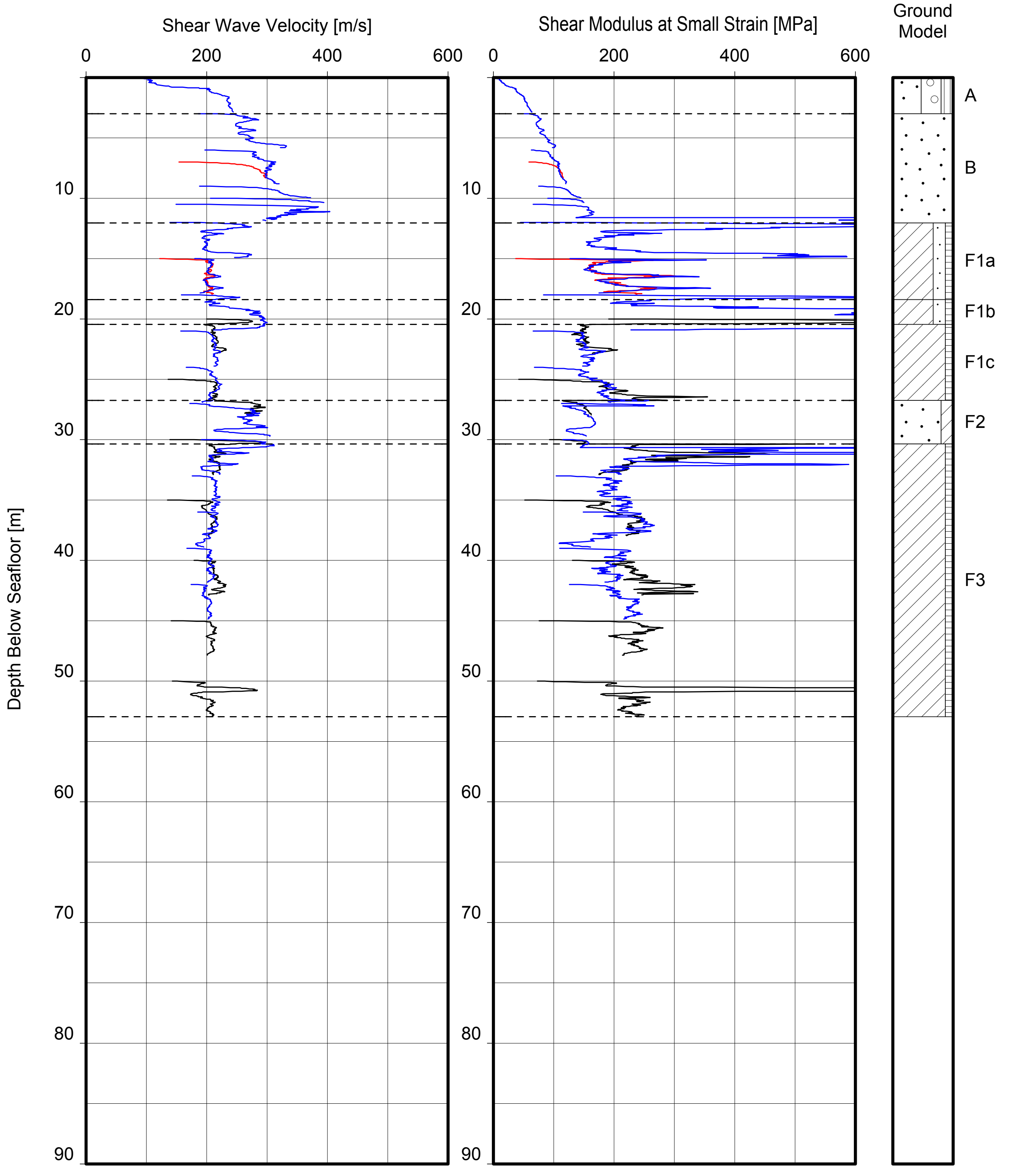


Shear wave velocity ($v_s$) measured in-between geophone array
Shear modulus at small strain ($G_{max}$) derived from $v_s$ measured
$v_s$ and $G_{max}$ derived from CPT

Location(s):
BH-WFS3-4A
BH-WFS3-4
CPT_WFS3_4

Note(s):
- $v_s$ derived from CPT based on Robertson and Cabal (2010)
- $G_{max}$ for clays derived from CPT based on Mayne and Rix (1993)
- $G_{max}$ for sands derived from CPT based on Rix and Stokoe (1991)

GeODin/8.Shear Wave Velocity and Shear Modulus at Small Strain versus Depth (all UNITS, incl. GM).GLO/2015-12-09 11:30:01

**SHEAR WAVE VELOCITY AND SHEAR MODULUS AT SMALL STRAIN VERSUS DEPTH**

BORSSELE WIND FARM ZONE, WFS III - DUTCH SECTOR, NORTH SEA

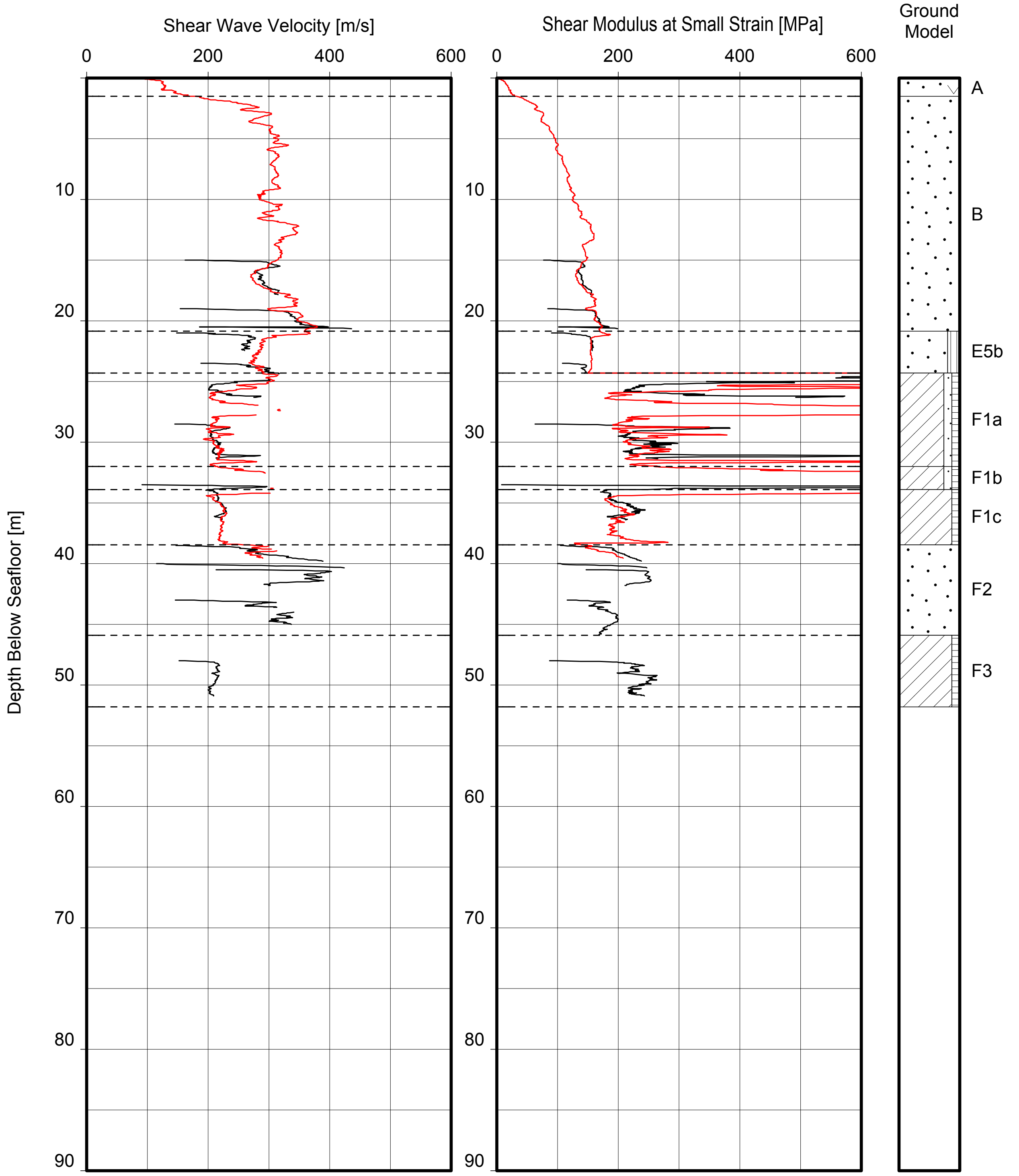


Shear wave velocity ($v_s$) measured in-between geophone array
Shear modulus at small strain ($G_{max}$) derived from $v_s$ measured
$v_s$ and $G_{max}$ derived from CPT

Location(s):
BH-WFS3-5
CPT_WFS3_5

Note(s):
- $v_s$ derived from CPT based on Robertson and Cabal (2010)
- $G_{max}$ for clays derived from CPT based on Mayne and Rix (1993)
- $G_{max}$ for sands derived from CPT based on Rix and Stokoe (1991)

GeODin/8.Shear Wave Velocity and Shear Modulus at Small Strain versus Depth (all UNITS, incl. GM).GLO/2015-12-09 11:30:20

## SHEAR WAVE VELOCITY AND SHEAR MODULUS AT SMALL STRAIN VERSUS DEPTH

BORSSELE WIND FARM ZONE, WFS III - DUTCH SECTOR, NORTH SEA

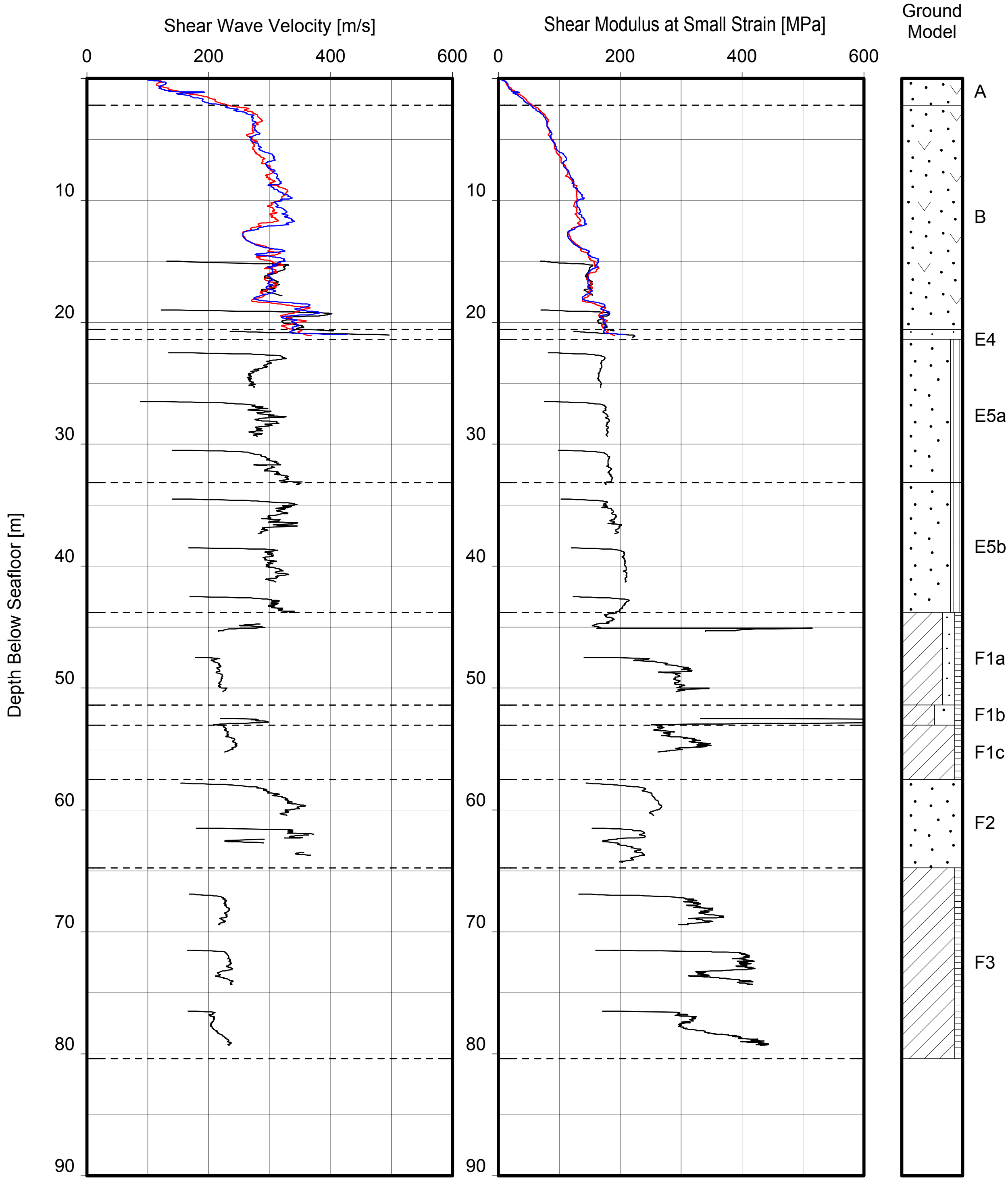


Shear wave velocity ($v_s$) measured in-between geophone array
Shear modulus at small strain ($G_{max}$) derived from $v_s$ measured
$v_s$ and $G_{max}$ derived from CPT

Location(s):
BH-WFS3-6
CPT_WFS3_6
CPT_WFS3_6A

Note(s):
- $v_s$ derived from CPT based on Robertson and Cabal (2010)
- $G_{max}$ for clays derived from CPT based on Mayne and Rix (1993)
- $G_{max}$ for sands derived from CPT based on Rix and Stokoe (1991)

GeODin/8.Shear Wave Velocity and Shear Modulus at Small Strain versus Depth (all UNITS, incl. GM).GLO/2015-12-09 11:30:44

## SHEAR WAVE VELOCITY AND SHEAR MODULUS AT SMALL STRAIN VERSUS DEPTH

BORSSELE WIND FARM ZONE, WFS III - DUTCH SECTOR, NORTH SEA

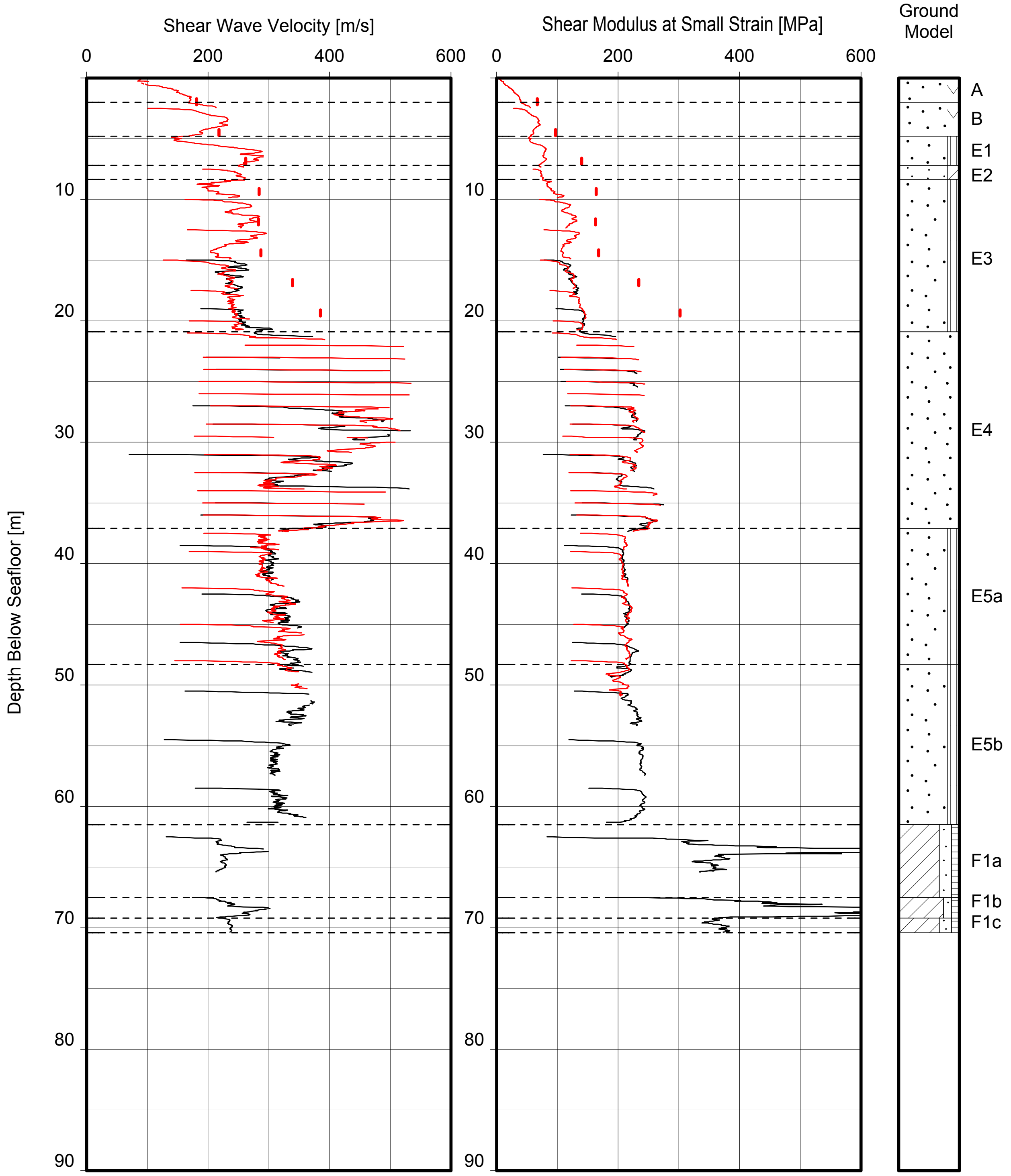


Shear wave velocity ($v_s$) measured in-between geophone array
Shear modulus at small strain ($G_{max}$) derived from $v_s$ measured
$v_s$ and $G_{max}$ derived from CPT

Location(s):
BH-WFS5-1
CPT_WFS5_1

Note(s):
- $v_s$ derived from CPT based on Robertson and Cabal (2010)
- $G_{max}$ for clays derived from CPT based on Mayne and Rix (1993)
- $G_{max}$ for sands derived from CPT based on Rix and Stokoe (1991)

GeODin/8.Shear Wave Velocity and Shear Modulus at Small Strain versus Depth (all UNITS, incl. GM).GLO/2015-12-09 11:31:02

**SHEAR WAVE VELOCITY AND SHEAR MODULUS AT SMALL STRAIN VERSUS DEPTH**

BORSSELE WIND FARM ZONE, WFS III - DUTCH SECTOR, NORTH SEA

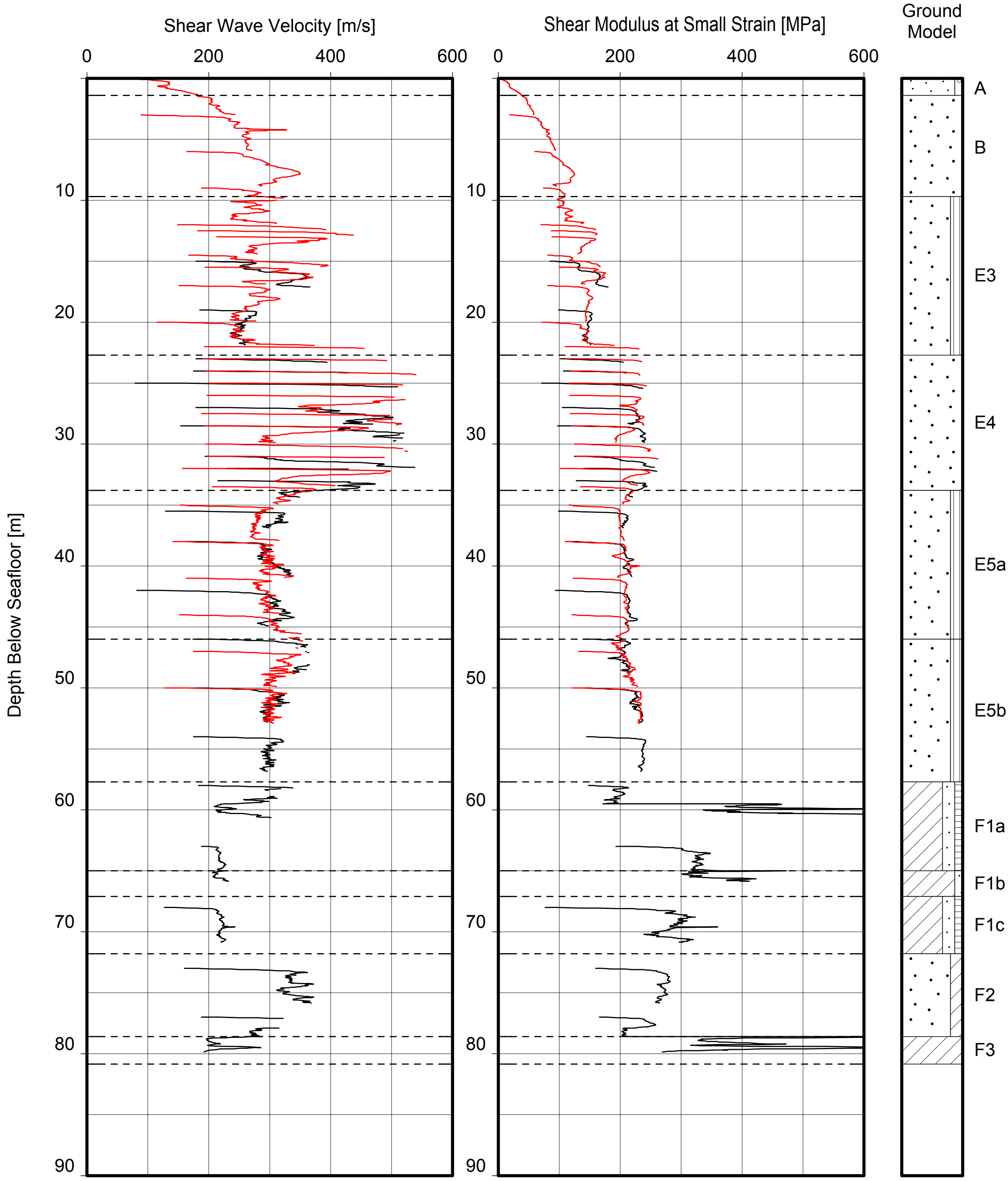


Shear wave velocity ($v_s$) measured in-between geophone array

Shear modulus at small strain ($G_{max}$) derived from $v_s$ measured

$v_s$ and $G_{max}$ derived from CPT

Location(s):
BH-SubStatB-1
CPT_SubStatB_1

Note(s):
- $v_s$ derived from CPT based on Robertson and Cabal (2010)
- $G_{max}$ for clays derived from CPT based on Mayne and Rix (1993)
- $G_{max}$ for sands derived from CPT based on Rix and Stokoe (1991)

GeODin/8.Shear Wave Velocity and Shear Modulus at Small Strain versus Depth (all UNITS, incl. GM).GLO/2015-12-09 11:28:23

**SHEAR WAVE VELOCITY AND SHEAR MODULUS AT SMALL STRAIN VERSUS DEPTH**

BORSSELE WIND FARM ZONE, WFS III - DUTCH SECTOR, NORTH SEA

**SECTION B: GEOTECHNICAL PARAMETERS – GROUPING PER GEOTECHNICAL UNIT**

**LIST OF PLATES IN SECTION B** Plate

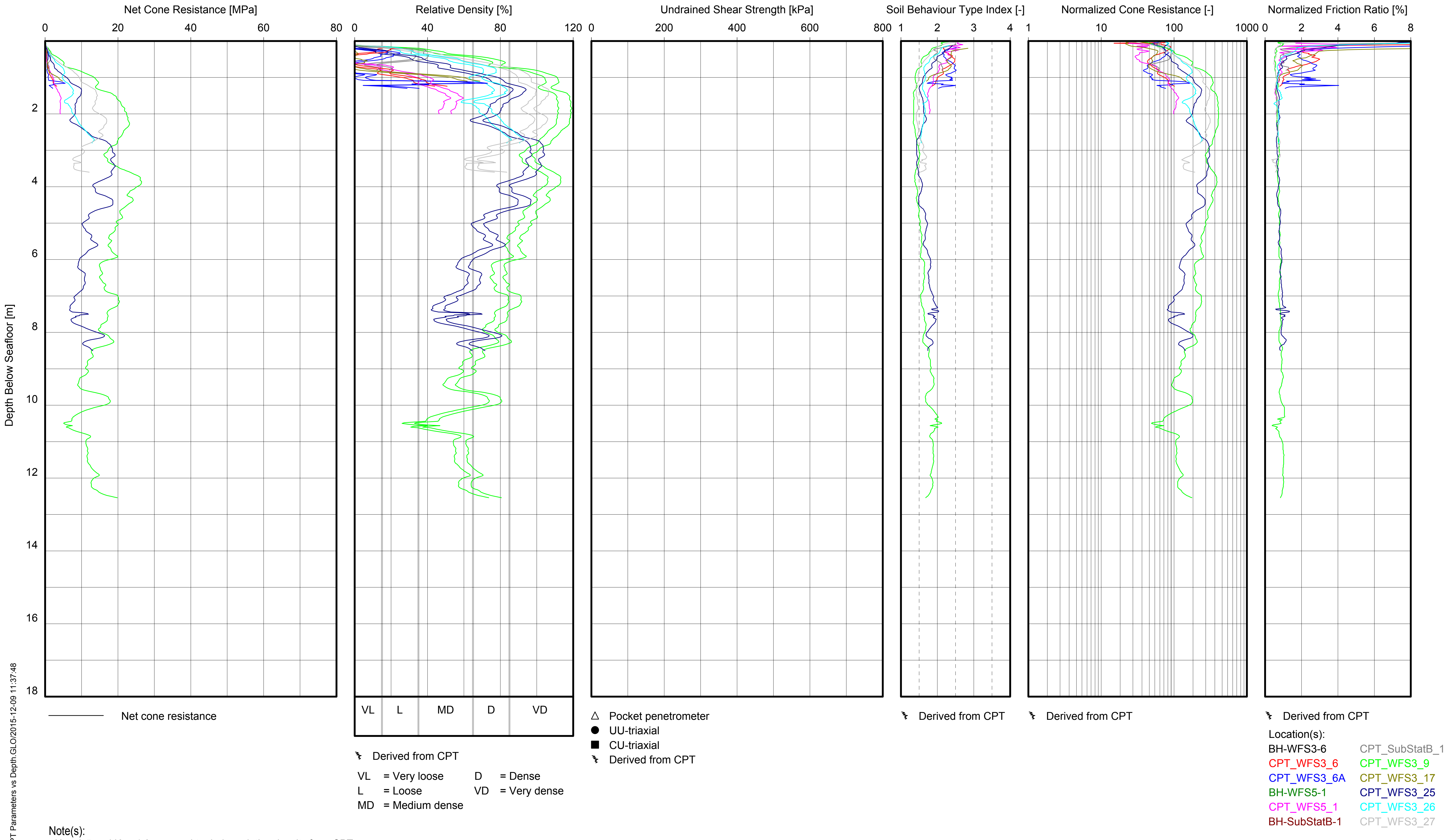


GeODin\1.CPT Parameters vs Depth.GLO/2015-12-09 11:37:48

Note(s):
- $K_0$ = 0.5 and $K_0$ = 1.0 are used to derive relative density from CPT
- $N_k$ = 15 and $N_k$ = 20 are used to derive $c_u$ from CPT
- Soil Behaviour Type Index is according to Robertson (2009), refer to Appendix 1, document titled "Cone Penetration Test Interpretation"

**CPT PARAMETERS AND STRENGTH DATA VERSUS DEPTH**

UNIT A

BORSSELE WIND FARM ZONE, WFS III - DUTCH SECTOR, NORTH SEA

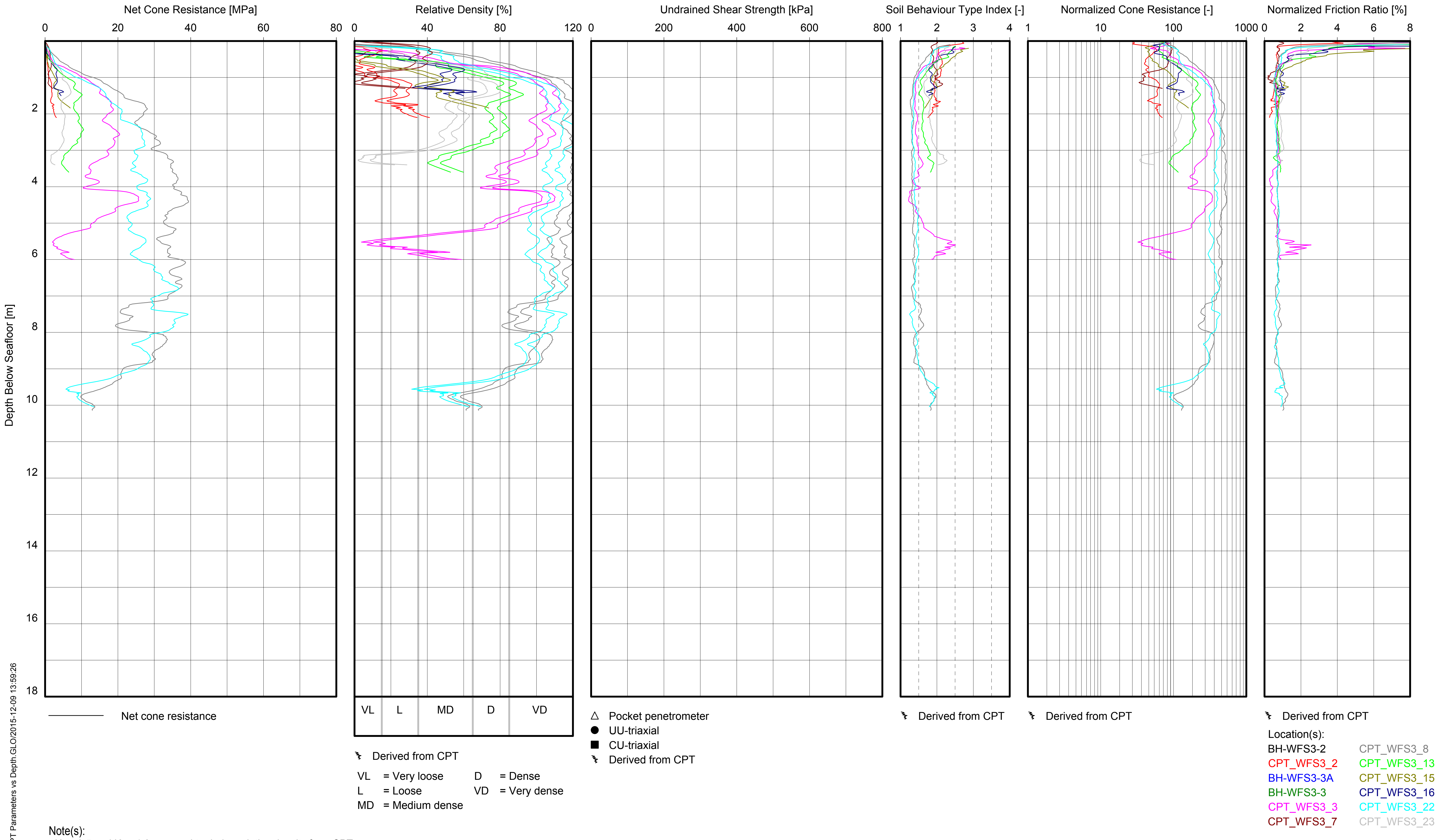


GeODin\1.CPT Parameters vs Depth.GLO/2015-12-09 13:59:26

Note(s):
- $K_0$ = 0.5 and $K_0$ = 1.0 are used to derive relative density from CPT
- $N_k$ = 15 and $N_k$ = 20 are used to derive $c_u$ from CPT
- Soil Behaviour Type Index is according to Robertson (2009), refer to Appendix 1, document titled "Cone Penetration Test Interpretation"

**CPT PARAMETERS AND STRENGTH DATA VERSUS DEPTH**

UNIT A

BORSSELE WIND FARM ZONE, WFS III - DUTCH SECTOR, NORTH SEA

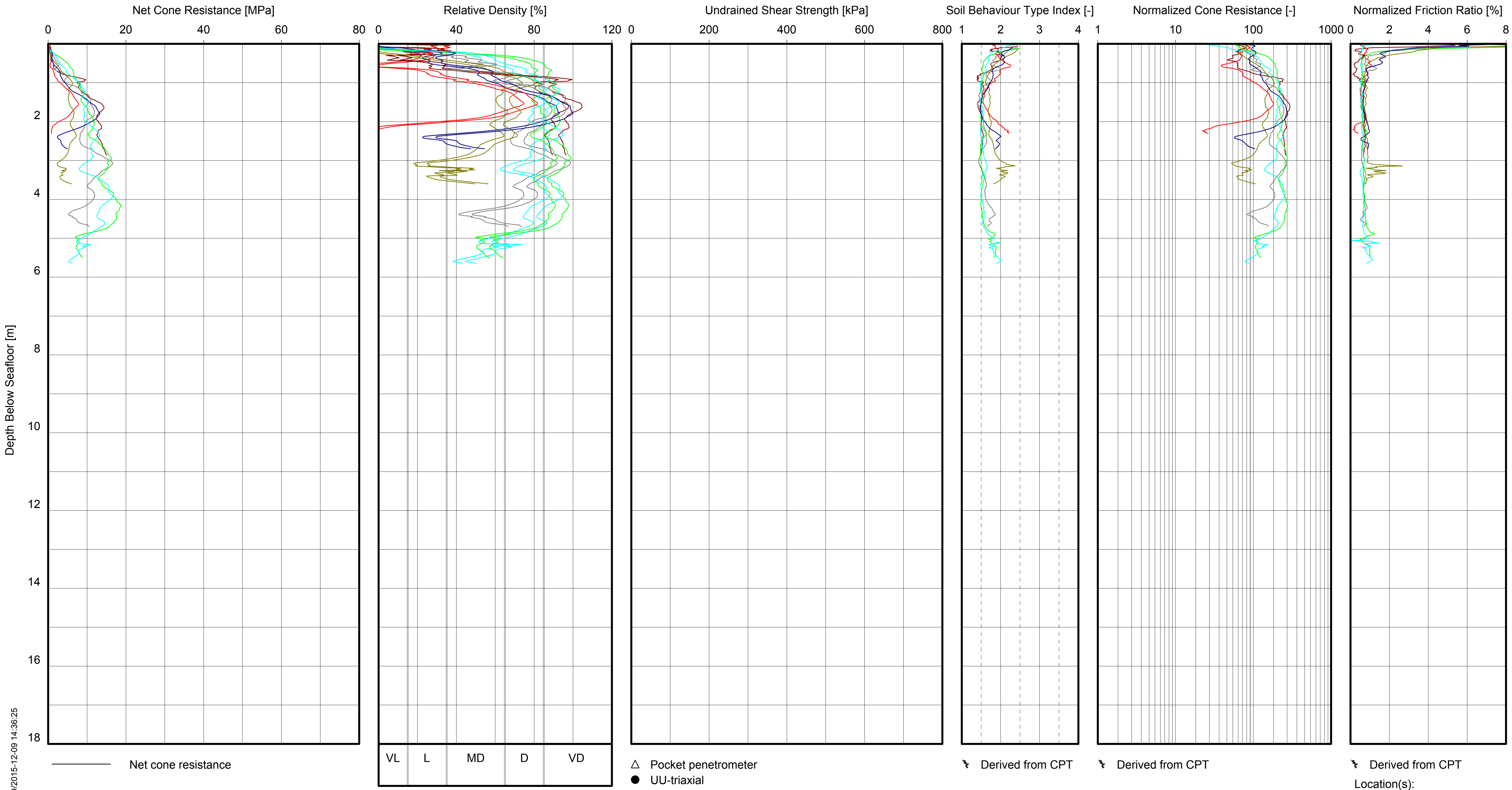


Net cone resistance

Derived from CPT

VL = Very loose
L = Loose
MD = Medium dense
D = Dense
VD = Very dense

△ Pocket penetrometer
● UU-triaxial
■ CU-triaxial
Derived from CPT

Derived from CPT

Derived from CPT

Derived from CPT

Location(s):

BH-WFS3-1
CPT_WFS3_1
CPT_WFS3_1A
BH-WFS3-4A
BH-WFS3-4
CPT_WFS3_4
CPT_WFS3_12
CPT_WFS3_18
CPT_WFS3_19
CPT_WFS3_20
CPT_WFS3_21

Note(s):
- $K_0$ = 0.5 and $K_0$ = 1.0 are used to derive relative density from CPT
- $N_k$ = 15 and $N_k$ = 20 are used to derive $c_u$ from CPT
- Soil Behaviour Type Index is according to Robertson (2009), refer to Appendix 1, document titled "Cone Penetration Test Interpretation"



**CPT PARAMETERS AND STRENGTH DATA VERSUS DEPTH**

UNIT A

BORSSELE WIND FARM ZONE, WFS III - DUTCH SECTOR, NORTH SEA

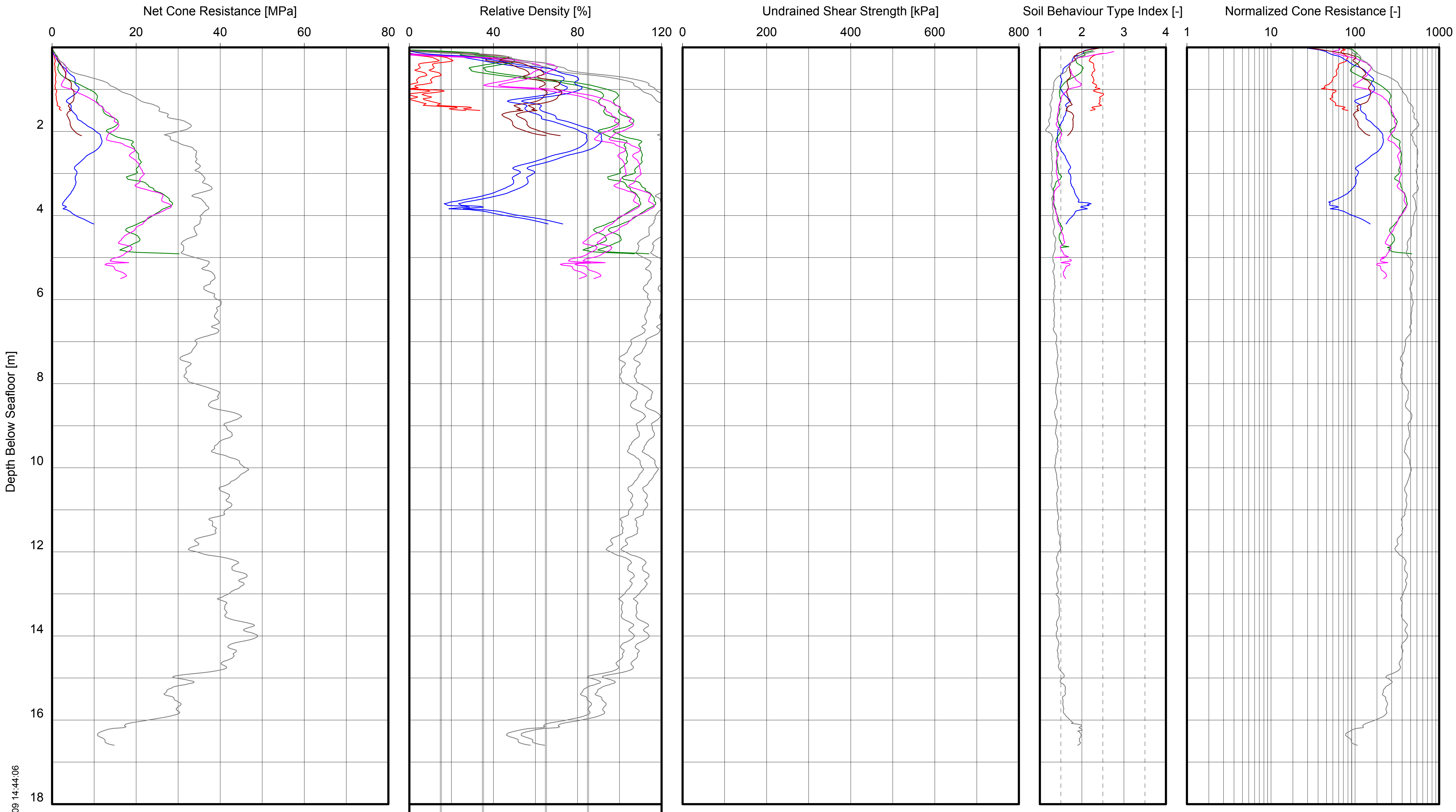


Net cone resistance

Derived from CPT

VL = Very loose
L = Loose
MD = Medium dense
D = Dense
VD = Very dense

△ Pocket penetrometer
● UU-triaxial
■ CU-triaxial
Derived from CPT

Derived from CPT

Derived from CPT

Derived from CPT

Location(s):
BH-WFS3-5
CPT_WFS3_5
CPT_WFS3_10
CPT_WFS3_11
CPT_WFS3_11A
CPT_WFS3_14
CPT_WFS3_24

GeODin\1.CPT Parameters vs Depth.GLO/2015-12-09 14:44:06

Note(s):
- $K_0$ = 0.5 and $K_0$ = 1.0 are used to derive relative density from CPT
- $N_k$ = 15 and $N_k$ = 20 are used to derive $c_u$ from CPT
- Soil Behaviour Type Index is according to Robertson (2009), refer to Appendix 1, document titled "Cone Penetration Test Interpretation"

**CPT PARAMETERS AND STRENGTH DATA VERSUS DEPTH**
UNIT A
BORSSELE WIND FARM ZONE, WFS III - DUTCH SECTOR, NORTH SEA

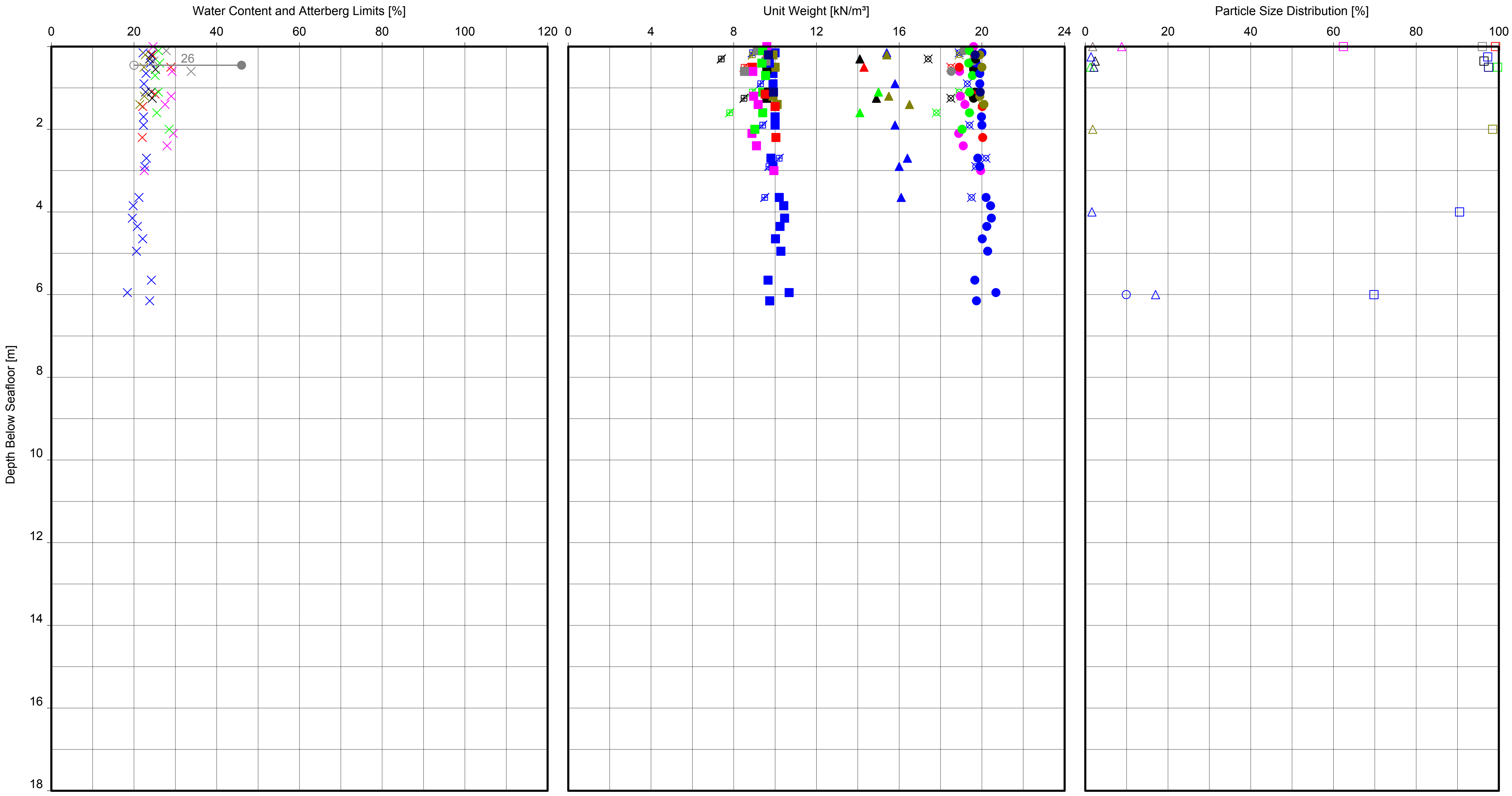


Water content
Plastic limit
Liquid limit
55 Plasticity index

Unit weight derived from water content and particle density
Unit weight derived from volume mass calculation
Submerged unit weight derived from water content and particle density
Submerged unit weight derived from volume mass calculation
Dry unit weight derived from volume mass calculation

Particle size by mass percentage <2 µm
Particle size by mass percentage <60 µm
Particle size by mass percentage <2000 µm

Location(s):
BH-WFS3-1
BH-WFS3-2
BH-WFS3-3
BH-WFS3-3A
BH-WFS3-4
BH-WFS3-4A
BH-WFS3-5
BH-WFS3-6
BH-WFS5-1
BH-SubStatB-1

Note(s):
- No dry unit weight is available for unit weight measurements by volume mass calculation on WAX samples.

GeODin/2:Water Content, Unit Weight And Particle Size Distribution vs Depth.GLO/2015-12-09 13:37:24

**WATER CONTENT, UNIT WEIGHT AND PARTICLE SIZE DISTRIBUTION VERSUS DEPTH**
UNIT A
BORSSELE WIND FARM ZONE, WFS III - DUTCH SECTOR, NORTH SEA

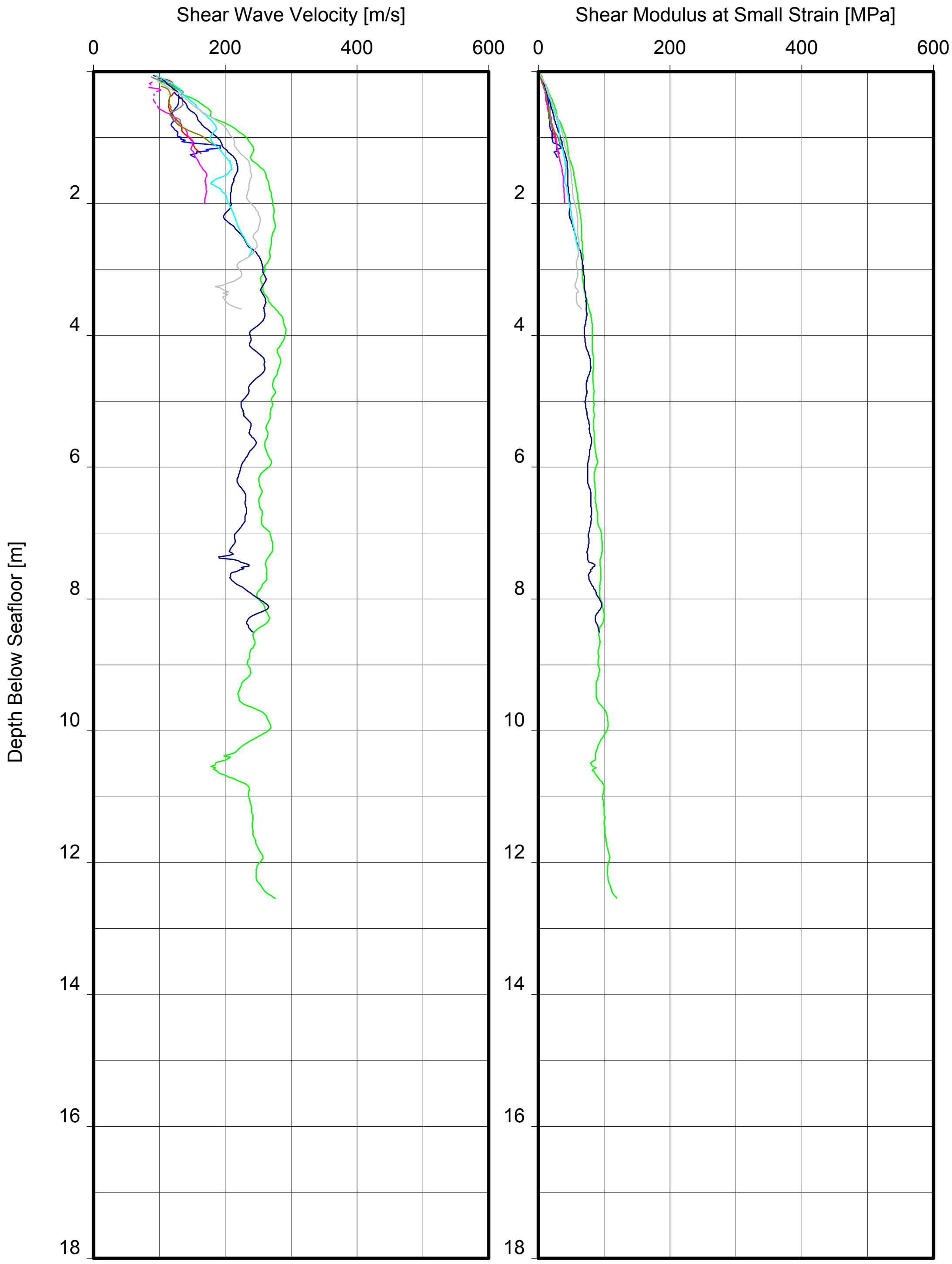


Shear wave velocity ($v_s$) measured in-between geophone array

Shear modulus at small strain ($G_{max}$) derived from $v_s$ measured

$v_s$ and $G_{max}$ derived from CPT

Location(s):

BH-WFS3-6
CPT_WFS3_6
CPT_WFS3_6A
BH-WFS5-1
CPT_WFS5_1
BH-SubStatB-1
CPT_SubStatB_1
CPT_WFS3_9
CPT_WFS3_17
CPT_WFS3_25
CPT_WFS3_26
CPT_WFS3_27

Note(s):

- $v_s$ derived from CPT based on Robertson and Cabal (2010)
- $G_{max}$ for clays derived from CPT based on Mayne and Rix (1993)
- $G_{max}$ for sands derived from CPT based on Rix and Stokoe (1991)

GeoDin/3.Shear Wave Velocity and Shear Modulus at Small Strain versus Depth (single UNIT, excl. GM).GLO/2015-12-10 09:25:13

**SHEAR WAVE VELOCITY AND SHEAR MODULUS AT SMALL STRAIN VERSUS DEPTH**

UNIT A

BORSSELE WIND FARM ZONE, WFS III - DUTCH SECTOR, NORTH SEA

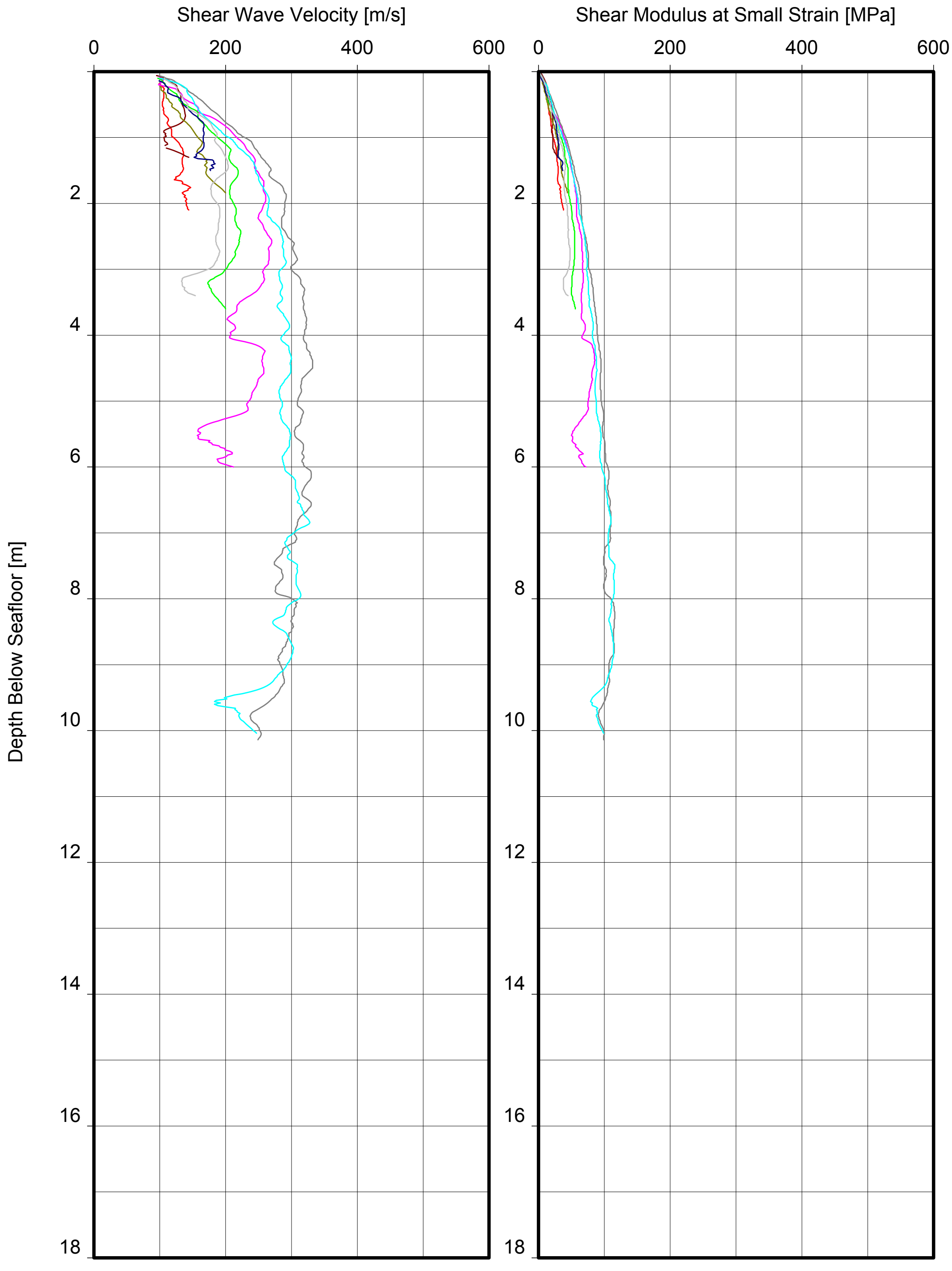


Shear wave velocity ($v_s$) measured in-between geophone array
Shear modulus at small strain ($G_{max}$) derived from $v_s$ measured
$v_s$ and $G_{max}$ derived from CPT

Location(s):
BH-WFS3-2
CPT_WFS3_2
BH-WFS3-3A
BH-WFS3-3
CPT_WFS3_3
CPT_WFS3_7
CPT_WFS3_8
CPT_WFS3_13
CPT_WFS3_15
CPT_WFS3_16
CPT_WFS3_22
CPT_WFS3_23

Note(s):
- $v_s$ derived from CPT based on Robertson and Cabal (2010)
- $G_{max}$ for clays derived from CPT based on Mayne and Rix (1993)
- $G_{max}$ for sands derived from CPT based on Rix and Stokoe (1991)

GeODin/3.Shear Wave Velocity and Shear Modulus at Small Strain versus Depth (single UNIT, excl. GM).GLO/2015-12-09 14:22:22

**SHEAR WAVE VELOCITY AND SHEAR MODULUS AT SMALL STRAIN VERSUS DEPTH**
UNIT A
BORSSELE WIND FARM ZONE, WFS III - DUTCH SECTOR, NORTH SEA

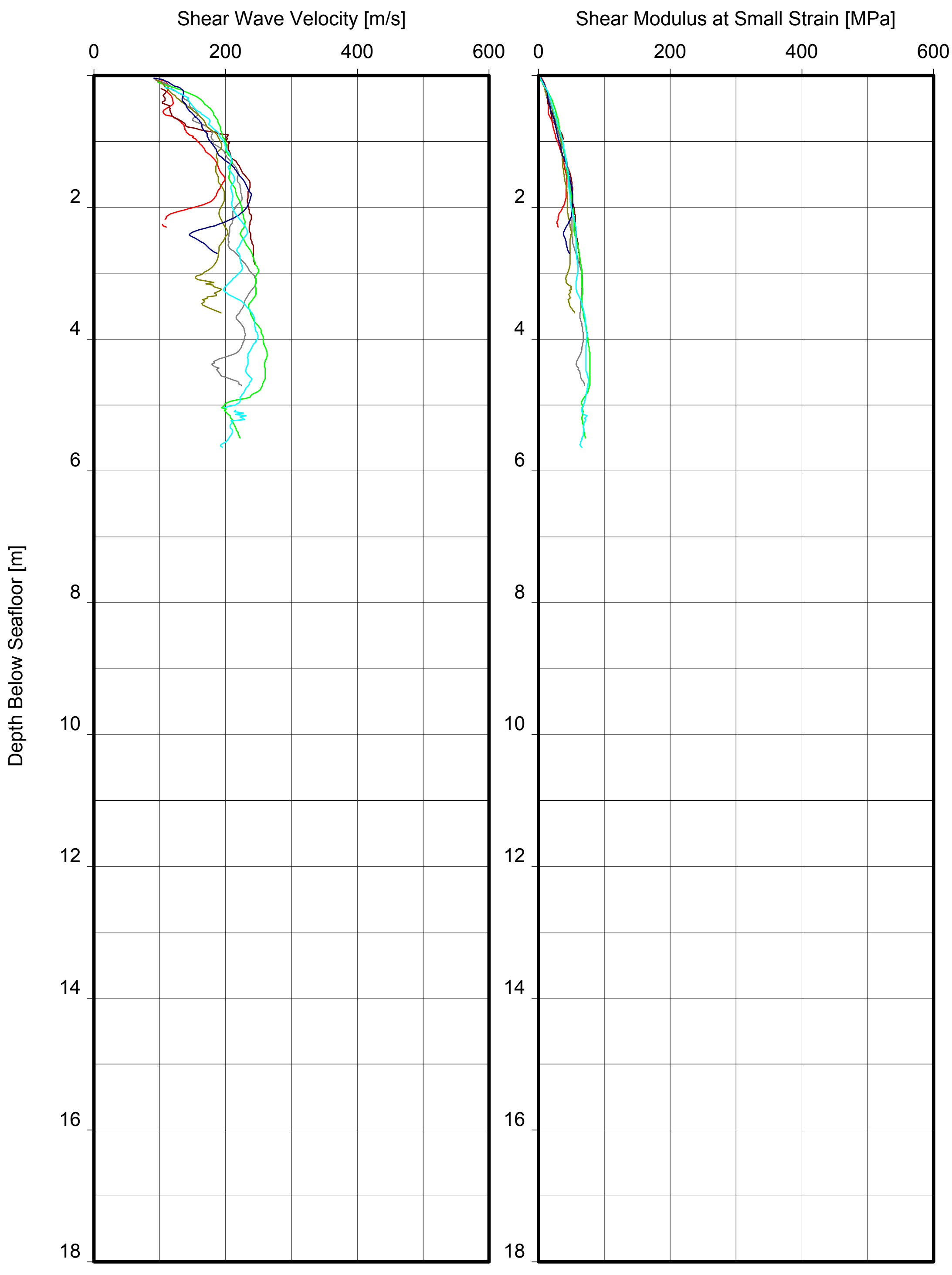


Shear wave velocity ($v_s$) measured in-between geophone array
Shear modulus at small strain ($G_{max}$) derived from $v_s$ measured
$v_s$ and $G_{max}$ derived from CPT

Location(s):
BH-WFS3-1
CPT_WFS3_1
CPT_WFS3_1A
BH-WFS3-4A
BH-WFS3-4
CPT_WFS3_4
CPT_WFS3_12
CPT_WFS3_18
CPT_WFS3_19
CPT_WFS3_20
CPT_WFS3_21

Note(s):
- $v_s$ derived from CPT based on Robertson and Cabal (2010)
- $G_{max}$ for clays derived from CPT based on Mayne and Rix (1993)
- $G_{max}$ for sands derived from CPT based on Rix and Stokoe (1991)

GeODin/3.Shear Wave Velocity and Shear Modulus at Small Strain versus Depth (single UNIT, excl. GM).GLO/2015-12-09 14:29:59

**SHEAR WAVE VELOCITY AND SHEAR MODULUS AT SMALL STRAIN VERSUS DEPTH**

UNIT A

BORSSELE WIND FARM ZONE, WFS III - DUTCH SECTOR, NORTH SEA

GeODin/3.Shear Wave Velocity and Shear Modulus at Small Strain versus Depth (single UNIT, excl. GM).GLO/2015-12-09 14:53:26

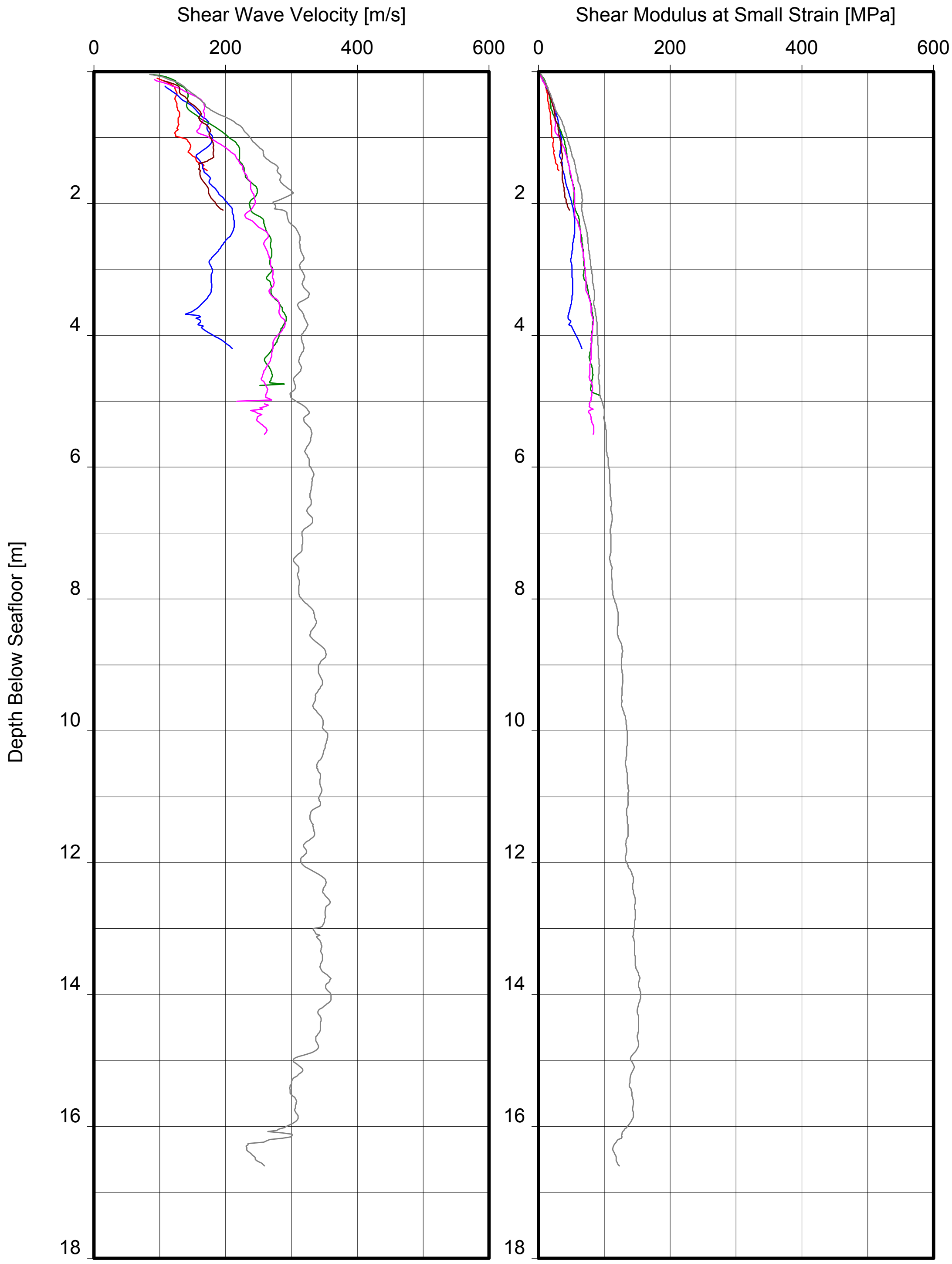


Shear wave velocity ($v_s$) measured in-between geophone array

Shear modulus at small strain ($G_{max}$) derived from $v_s$ measured

$v_s$ and $G_{max}$ derived from CPT

Location(s):

BH-WFS3-5

CPT_WFS3_5

CPT_WFS3_10

CPT_WFS3_11

CPT_WFS3_11A

CPT_WFS3_14

CPT_WFS3_24

Note(s):

- $v_s$ derived from CPT based on Robertson and Cabal (2010)
- $G_{max}$ for clays derived from CPT based on Mayne and Rix (1993)
- $G_{max}$ for sands derived from CPT based on Rix and Stokoe (1991)

**SHEAR WAVE VELOCITY AND SHEAR MODULUS AT SMALL STRAIN VERSUS DEPTH**

UNIT A

BORSSELE WIND FARM ZONE, WFS III - DUTCH SECTOR, NORTH SEA

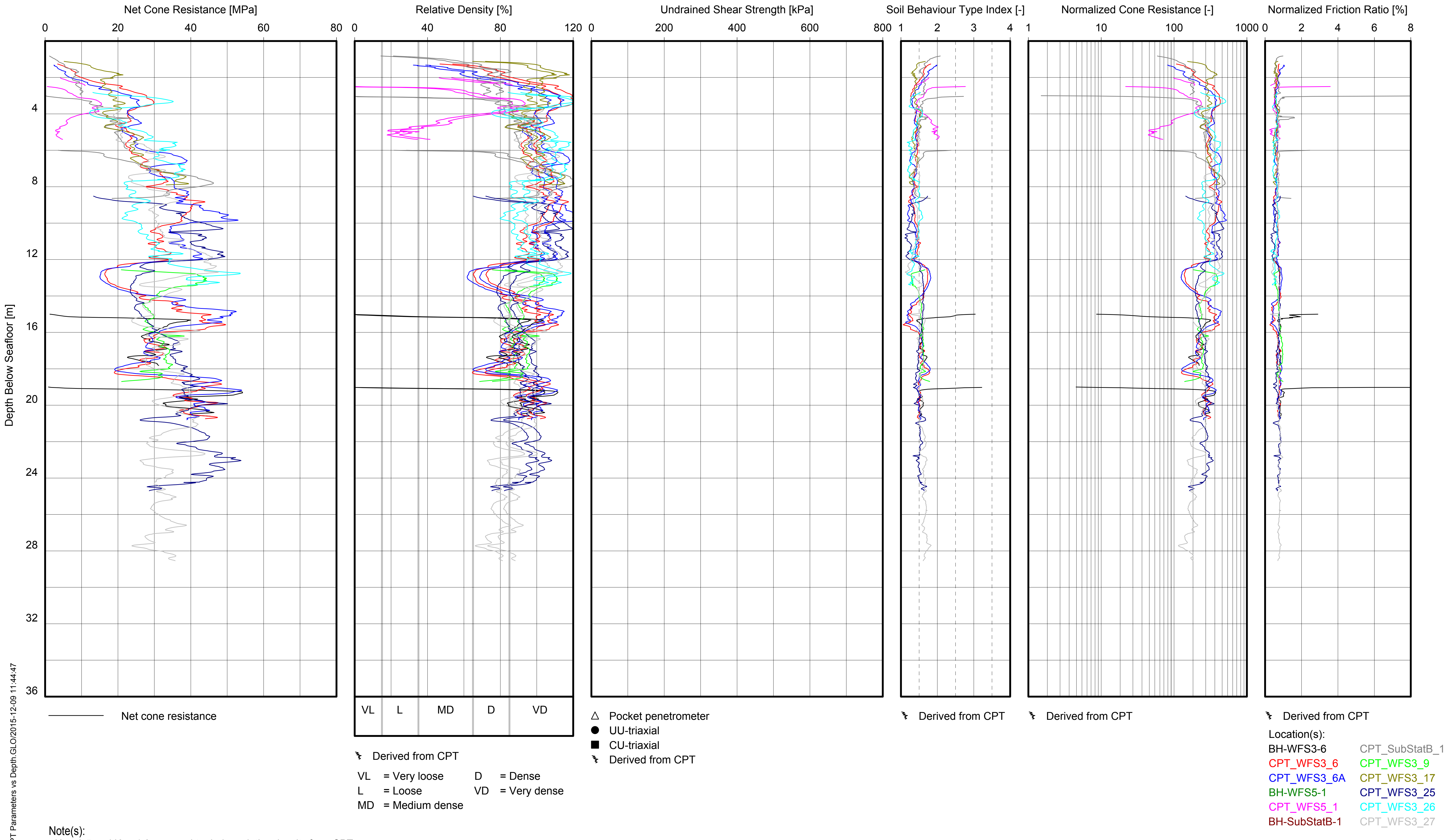


GeODin/1.CPT Parameters vs Depth.GLO/2015-12-09 11:44:47

Note(s):
- $K_0$ = 0.5 and $K_0$ = 1.0 are used to derive relative density from CPT
- $N_k$ = 15 and $N_k$ = 20 are used to derive $c_u$ from CPT
- Soil Behaviour Type Index is according to Robertson (2009), refer to Appendix 1, document titled "Cone Penetration Test Interpretation"

**CPT PARAMETERS AND STRENGTH DATA VERSUS DEPTH**
UNIT B
BORSSELE WIND FARM ZONE, WFS III - DUTCH SECTOR, NORTH SEA

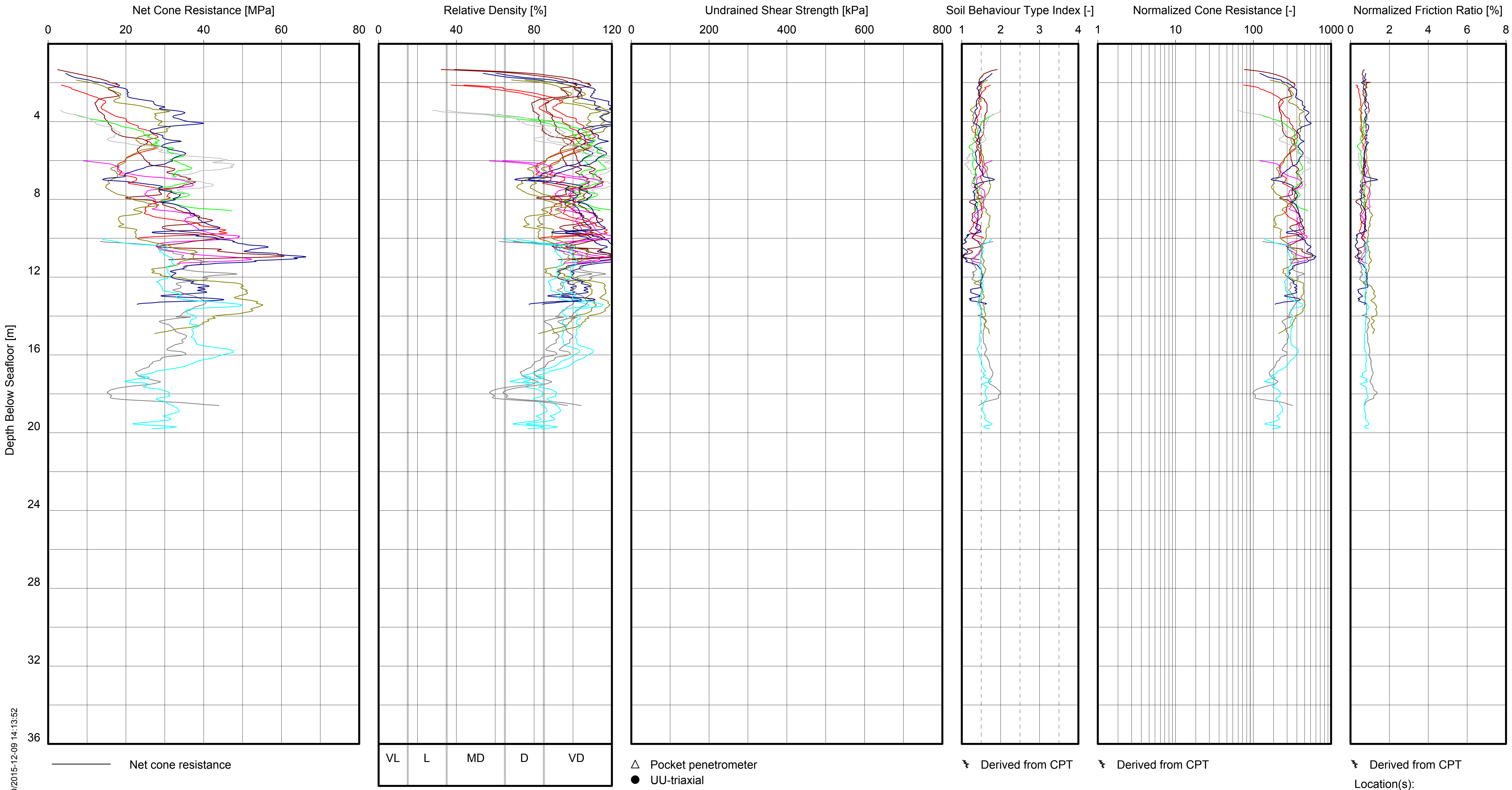


Net cone resistance

Derived from CPT

VL = Very loose
L = Loose
MD = Medium dense
D = Dense
VD = Very dense

△ Pocket penetrometer
● UU-triaxial
■ CU-triaxial
Derived from CPT

Derived from CPT

Derived from CPT

Derived from CPT

Location(s):

BH-WFS3-2, CPT_WFS3_2, BH-WFS3-3A, BH-WFS3-3, CPT_WFS3_3, CPT_WFS3_7, CPT_WFS3_8, CPT_WFS3_13, CPT_WFS3_15, CPT_WFS3_16, CPT_WFS3_22, CPT_WFS3_23

GeODin\1.CPT Parameters vs Depth.GLO/2015-12-09 14:13:52

Note(s):
- $K_0$ = 0.5 and $K_0$ = 1.0 are used to derive relative density from CPT
- $N_k$ = 15 and $N_k$ = 20 are used to derive $c_u$ from CPT
- Soil Behaviour Type Index is according to Robertson (2009), refer to Appendix 1, document titled "Cone Penetration Test Interpretation"

**CPT PARAMETERS AND STRENGTH DATA VERSUS DEPTH**
UNIT B
BORSSELE WIND FARM ZONE, WFS III - DUTCH SECTOR, NORTH SEA

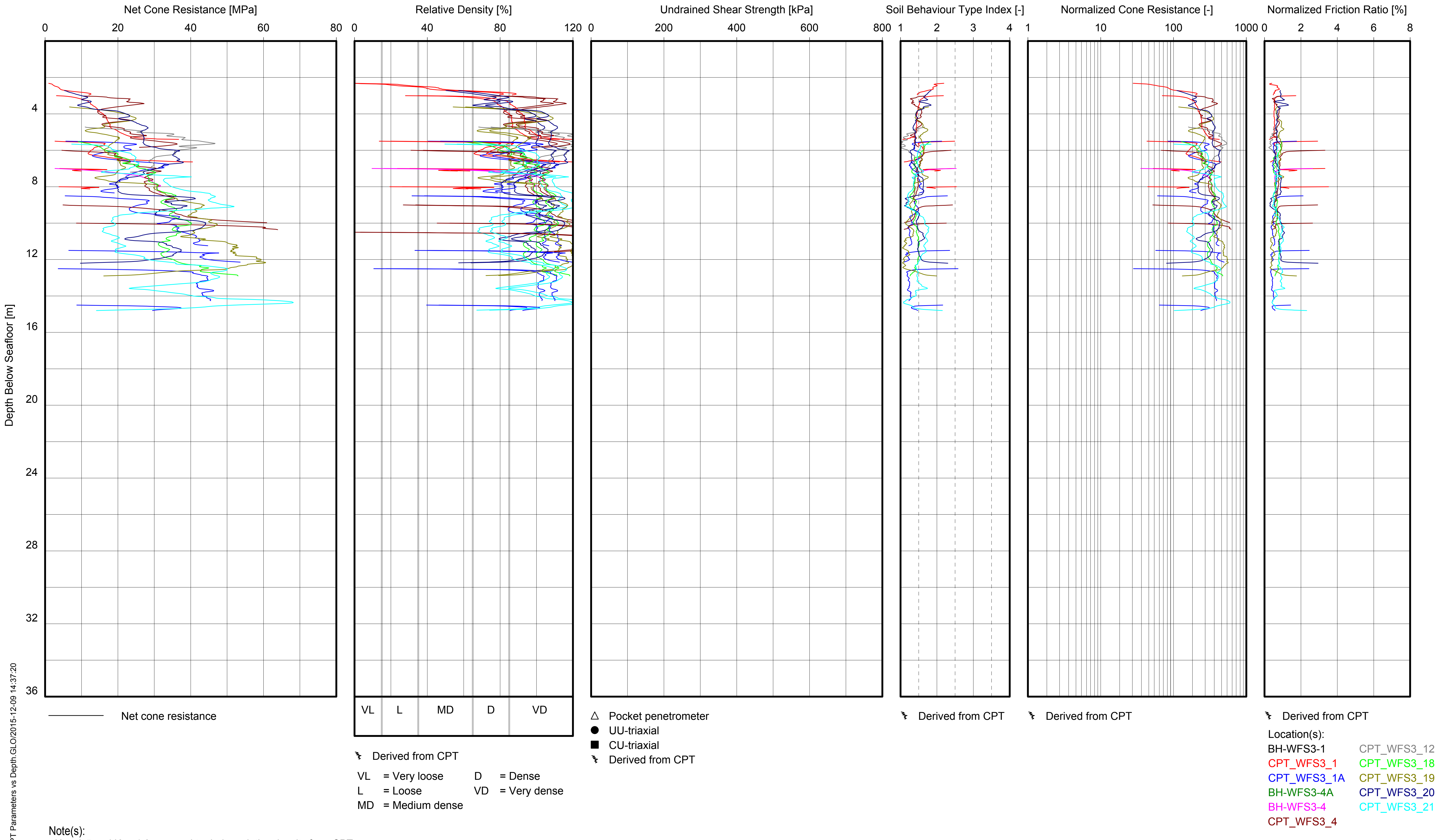


GeODin/1.CPT Parameters vs Depth.GLO/2015-12-09 14:37:20

Note(s):
- $K_0$ = 0.5 and $K_0$ = 1.0 are used to derive relative density from CPT
- $N_k$ = 15 and $N_k$ = 20 are used to derive $c_u$ from CPT
- Soil Behaviour Type Index is according to Robertson (2009), refer to Appendix 1, document titled "Cone Penetration Test Interpretation"

**CPT PARAMETERS AND STRENGTH DATA VERSUS DEPTH**

UNIT B

BORSSELE WIND FARM ZONE, WFS III - DUTCH SECTOR, NORTH SEA

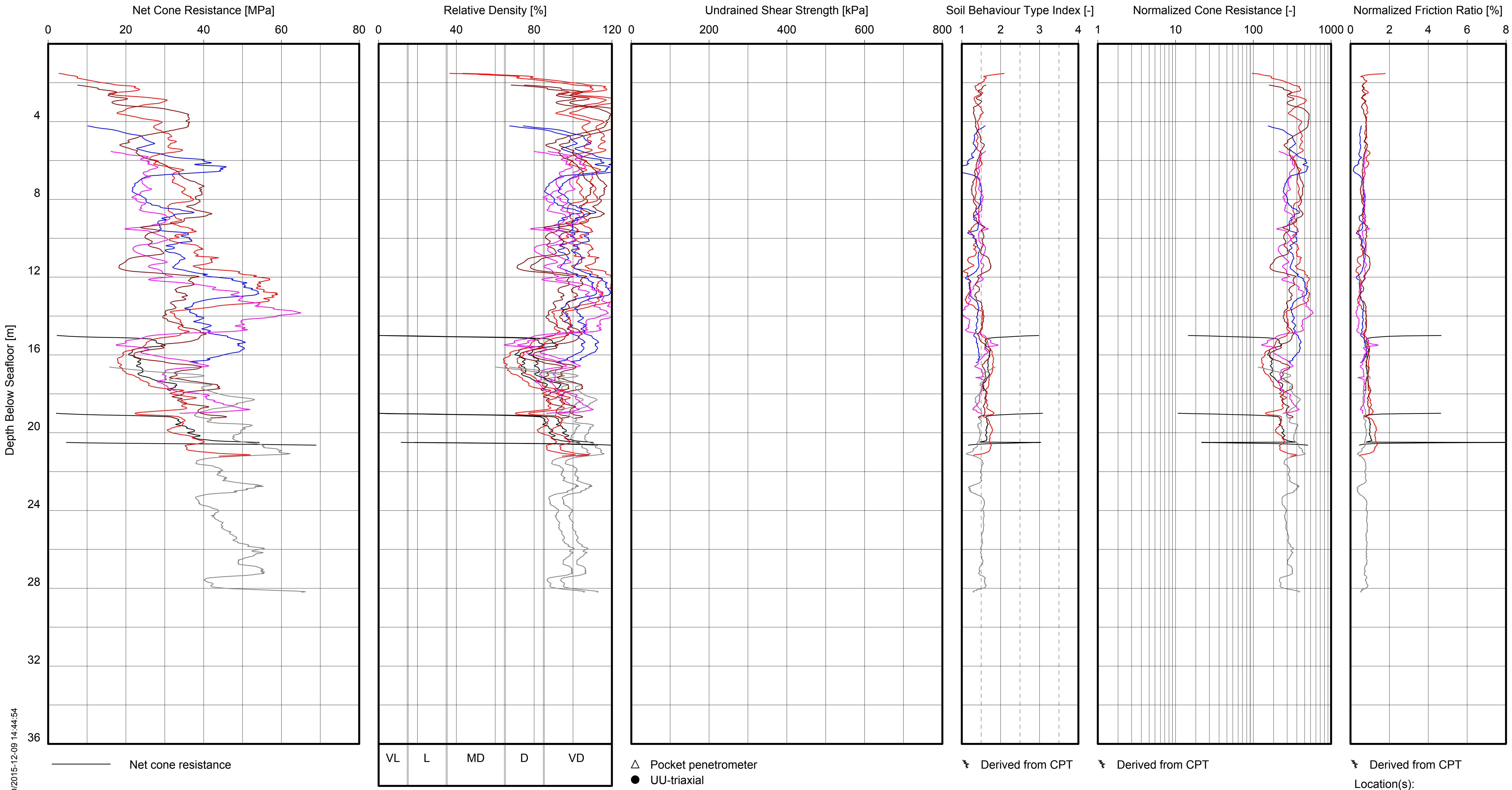


Net cone resistance

Derived from CPT

VL = Very loose
L = Loose
MD = Medium dense
D = Dense
VD = Very dense

△ Pocket penetrometer
● UU-triaxial
■ CU-triaxial
Derived from CPT

Derived from CPT

Derived from CPT

Derived from CPT

Location(s):
BH-WFS3-5
CPT_WFS3_5
CPT_WFS3_10
CPT_WFS3_11
CPT_WFS3_11A
CPT_WFS3_14
CPT_WFS3_24

Note(s):
- $K_0$ = 0.5 and $K_0$ = 1.0 are used to derive relative density from CPT
- $N_k$ = 15 and $N_k$ = 20 are used to derive $c_u$ from CPT
- Soil Behaviour Type Index is according to Robertson (2009), refer to Appendix 1, document titled "Cone Penetration Test Interpretation"

GeODin/1.CPT Parameters vs Depth.GLO/2015-12-09 14:44:54

**CPT PARAMETERS AND STRENGTH DATA VERSUS DEPTH**
UNIT B
BORSSELE WIND FARM ZONE, WFS III - DUTCH SECTOR, NORTH SEA

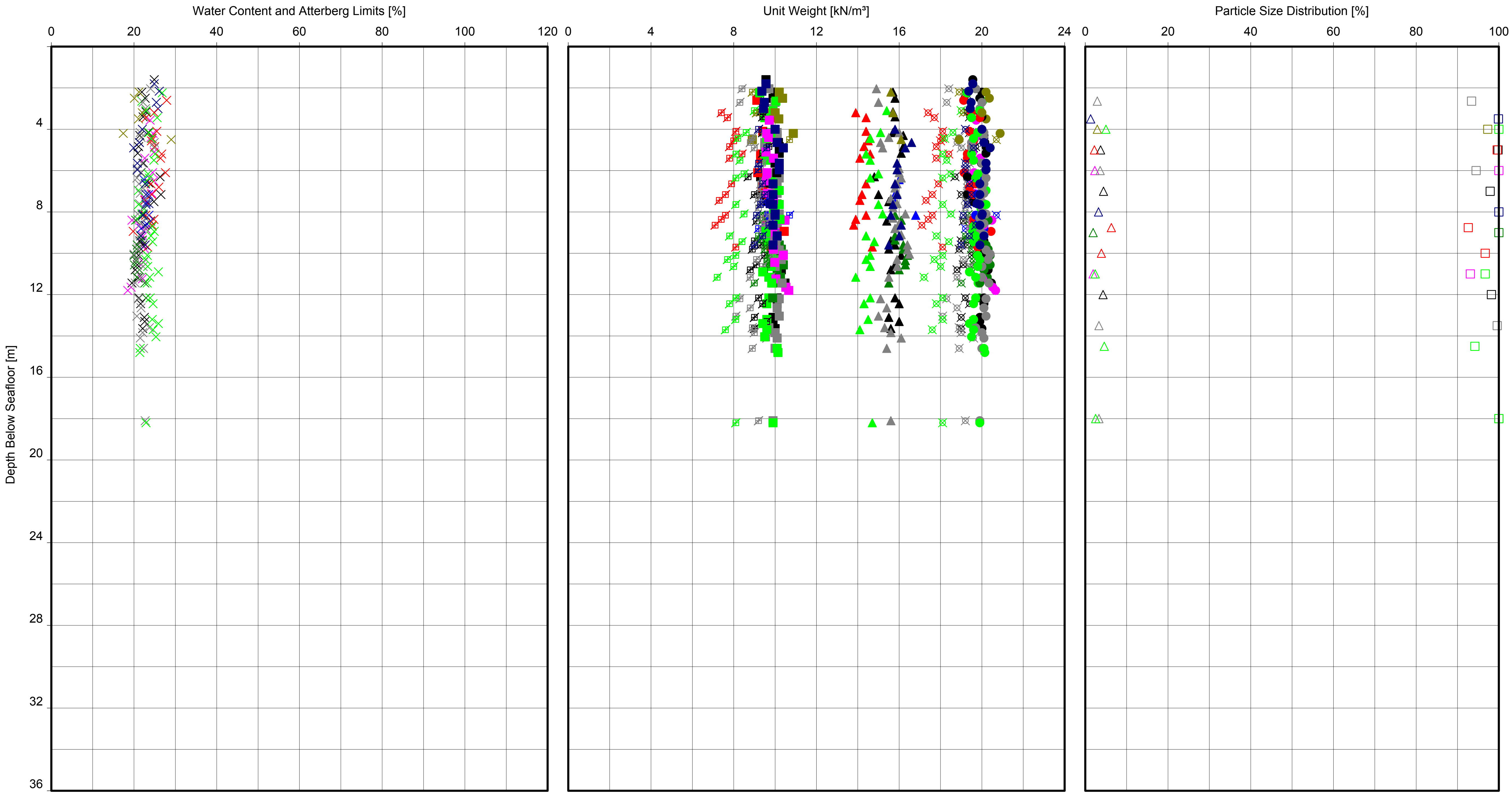


Water content
Plastic limit
Liquid limit
55 Plasticity index

Unit weight derived from water content and particle density
Unit weight derived from volume mass calculation
Submerged unit weight derived from water content and particle density
Submerged unit weight derived from volume mass calculation
Dry unit weight derived from volume mass calculation

Particle size by mass percentage <2 µm
Particle size by mass percentage <60 µm
Particle size by mass percentage <2000 µm

Location(s):
BH-WFS3-1
BH-WFS3-2
BH-WFS3-3
BH-WFS3-3A
BH-WFS3-4
BH-WFS3-4A
BH-WFS3-5
BH-WFS3-6
BH-WFS5-1
BH-SubStatB-1

Note(s):
- No dry unit weight is available for unit weight measurements by volume mass calculation on WAX samples.

GeODin/2.Water Content, Unit Weight And Particle Size Distribution vs Depth.GLO/2015-12-09 13:38:42

**WATER CONTENT, UNIT WEIGHT AND PARTICLE SIZE DISTRIBUTION VERSUS DEPTH**
UNIT B
BORSSELE WIND FARM ZONE, WFS III - DUTCH SECTOR, NORTH SEA

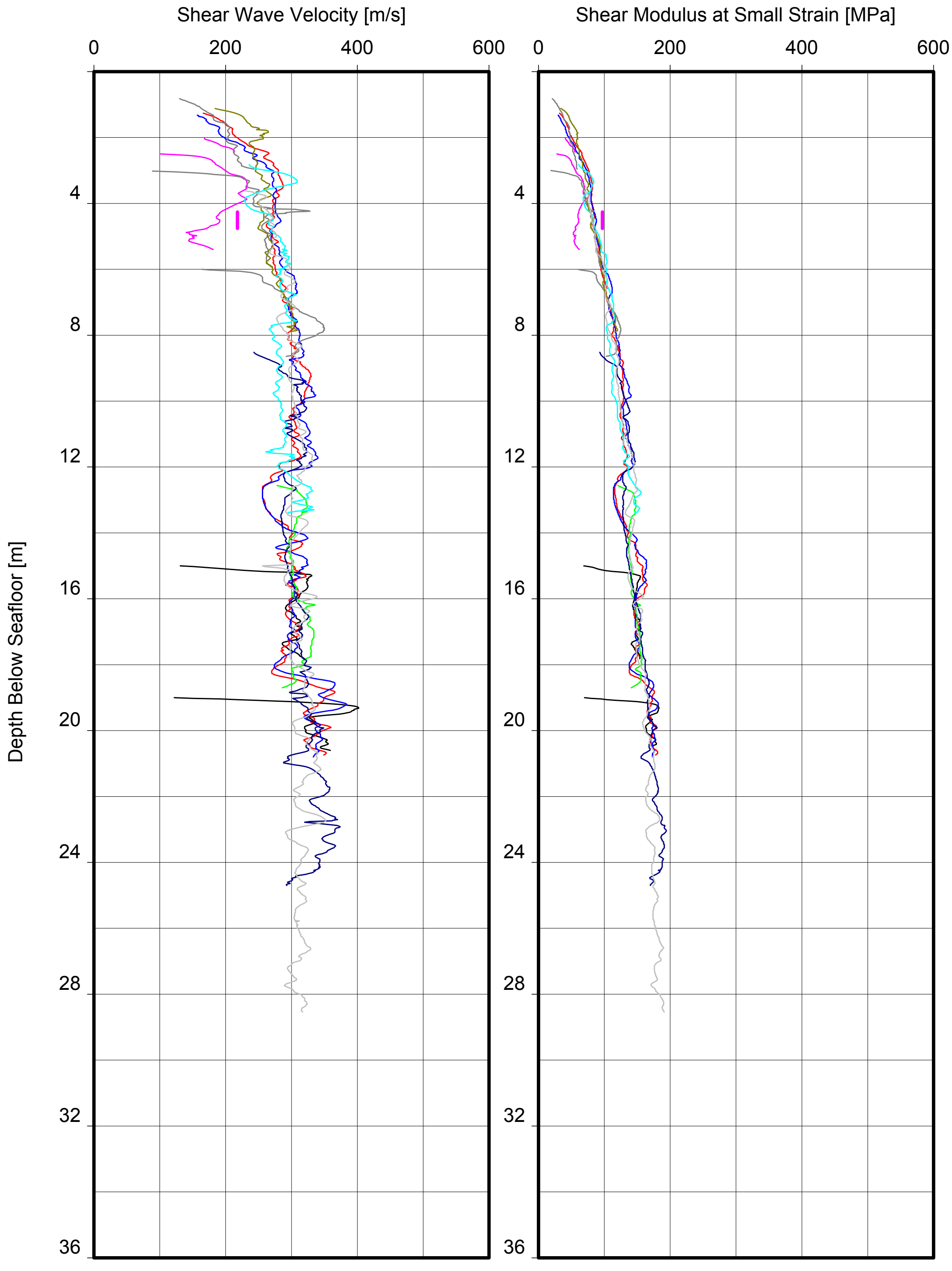


Shear wave velocity ($v_s$) measured in-between geophone array
Shear modulus at small strain ($G_{max}$) derived from $v_s$ measured
$v_s$ and $G_{max}$ derived from CPT

Location(s):
BH-WFS3-6
CPT_WFS3_6
CPT_WFS3_6A
BH-WFS5-1
CPT_WFS5_1
BH-SubStatB-1
CPT_SubStatB_1
CPT_WFS3_9
CPT_WFS3_17
CPT_WFS3_25
CPT_WFS3_26
CPT_WFS3_27

Note(s):
- $v_s$ derived from CPT based on Robertson and Cabal (2010)
- $G_{max}$ for clays derived from CPT based on Mayne and Rix (1993)
- $G_{max}$ for sands derived from CPT based on Rix and Stokoe (1991)

GeODin/3.Shear Wave Velocity and Shear Modulus at Small Strain versus Depth (single UNIT, excl. GM).GLO/2015-12-09 11:48:35

**SHEAR WAVE VELOCITY AND SHEAR MODULUS AT SMALL STRAIN VERSUS DEPTH**

UNIT B

BORSSELE WIND FARM ZONE, WFS III - DUTCH SECTOR, NORTH SEA

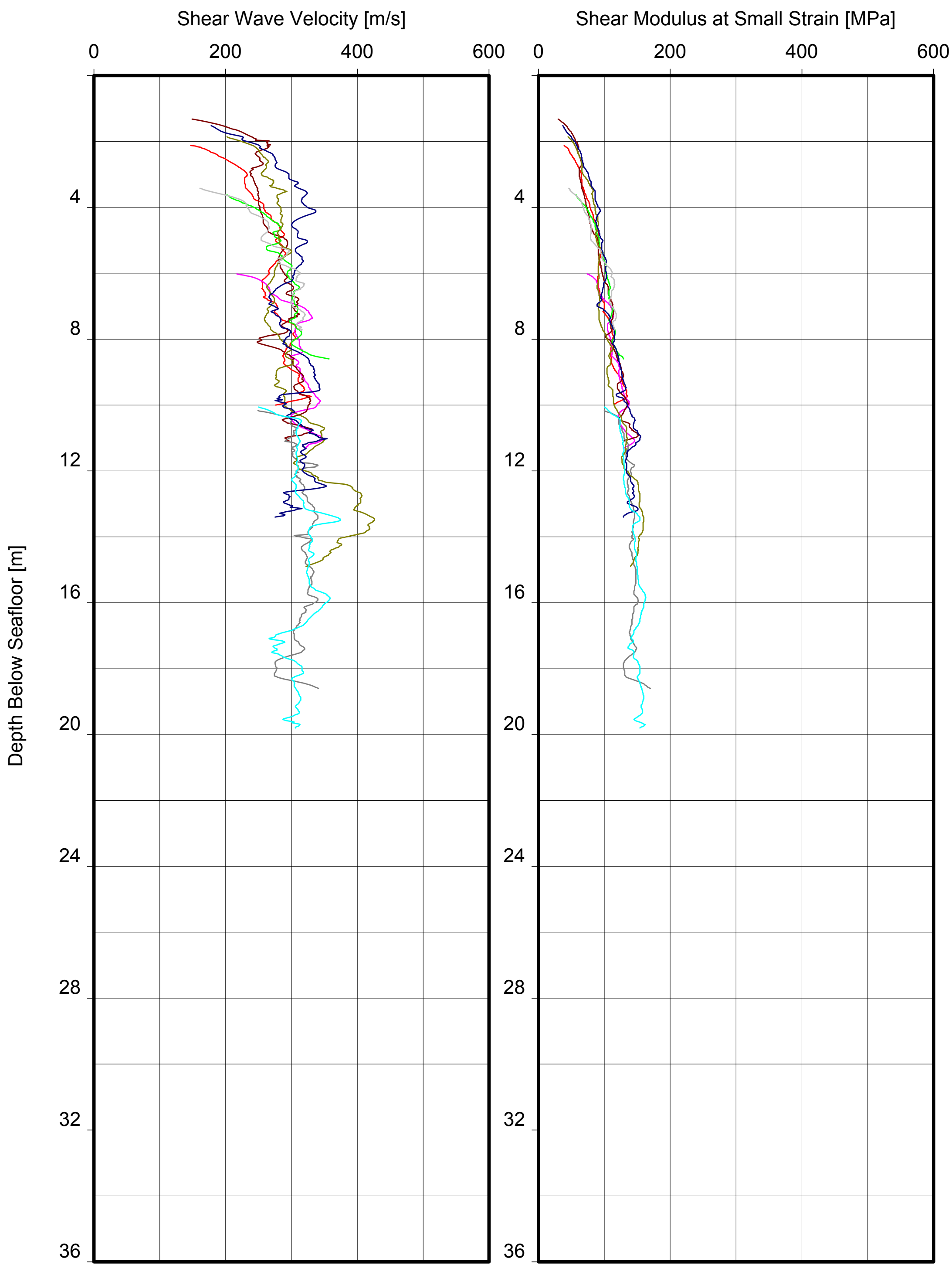


Shear wave velocity ($v_s$) measured in-between geophone array
Shear modulus at small strain ($G_{max}$) derived from $v_s$ measured
$v_s$ and $G_{max}$ derived from CPT

Location(s):
BH-WFS3-2
CPT_WFS3_2
BH-WFS3-3A
BH-WFS3-3
CPT_WFS3_3
CPT_WFS3_7
CPT_WFS3_8
CPT_WFS3_13
CPT_WFS3_15
CPT_WFS3_16
CPT_WFS3_22
CPT_WFS3_23

Note(s):
- $v_s$ derived from CPT based on Robertson and Cabal (2010)
- $G_{max}$ for clays derived from CPT based on Mayne and Rix (1993)
- $G_{max}$ for sands derived from CPT based on Rix and Stokoe (1991)

GeODin/3.Shear Wave Velocity and Shear Modulus at Small Strain versus Depth (single UNIT, excl. GM).GLO/2015-12-09 14:23:18

**SHEAR WAVE VELOCITY AND SHEAR MODULUS AT SMALL STRAIN VERSUS DEPTH**

UNIT B

BORSSELE WIND FARM ZONE, WFS III - DUTCH SECTOR, NORTH SEA

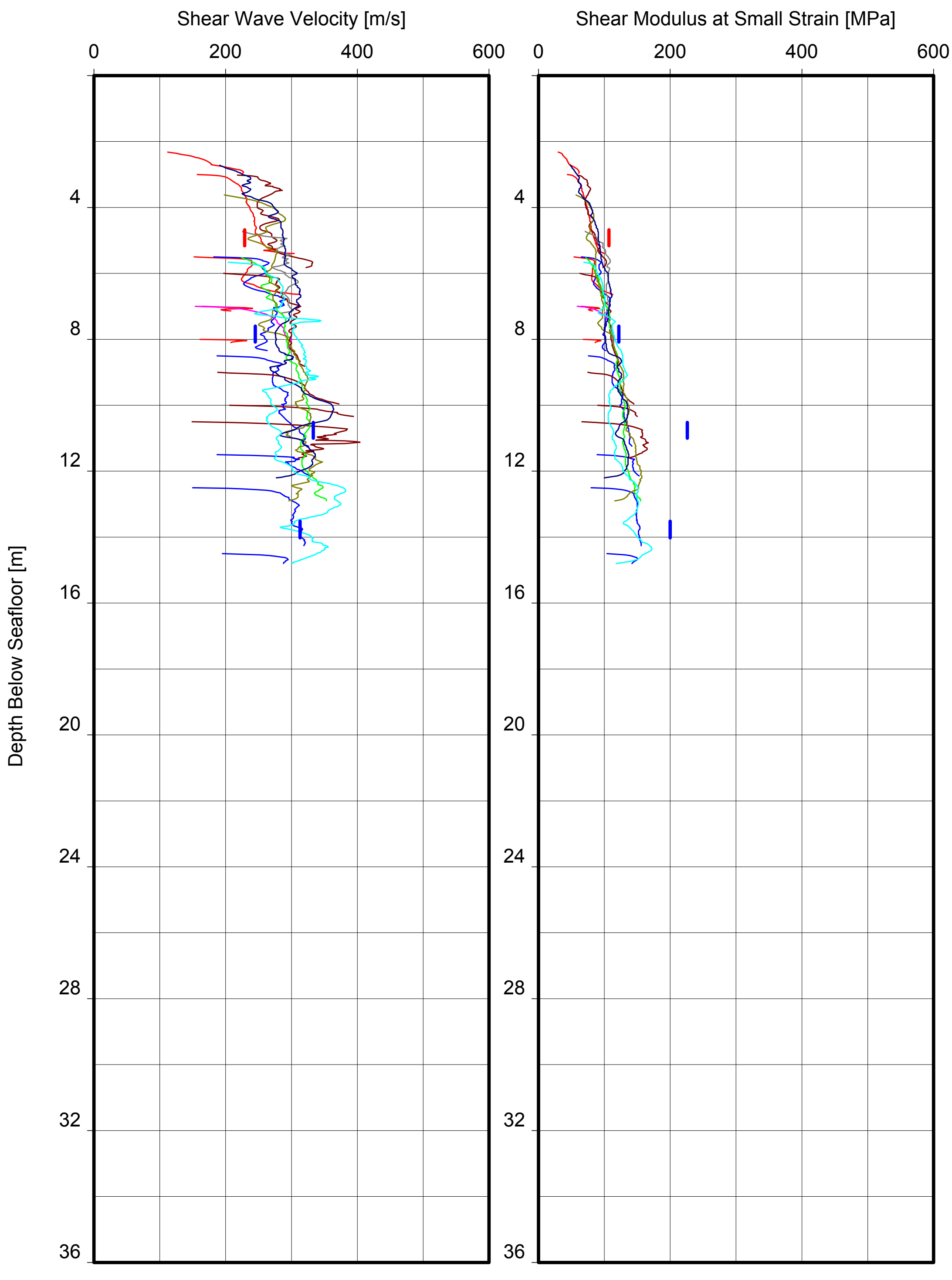


Shear wave velocity ($v_s$) measured in-between geophone array
Shear modulus at small strain ($G_{max}$) derived from $v_s$ measured
$v_s$ and $G_{max}$ derived from CPT

Note(s):
- $v_s$ derived from CPT based on Robertson and Cabal (2010)
- $G_{max}$ for clays derived from CPT based on Mayne and Rix (1993)
- $G_{max}$ for sands derived from CPT based on Rix and Stokoe (1991)

Location(s):
BH-WFS3-1
CPT_WFS3_1
CPT_WFS3_1A
BH-WFS3-4A
BH-WFS3-4
CPT_WFS3_4
CPT_WFS3_12
CPT_WFS3_18
CPT_WFS3_19
CPT_WFS3_20
CPT_WFS3_21

GeODin/3.Shear Wave Velocity and Shear Modulus at Small Strain versus Depth (single UNIT, excl. GM).GLO/2015-12-09 14:30:47

**SHEAR WAVE VELOCITY AND SHEAR MODULUS AT SMALL STRAIN VERSUS DEPTH**

UNIT B

BORSSELE WIND FARM ZONE, WFS III - DUTCH SECTOR, NORTH SEA

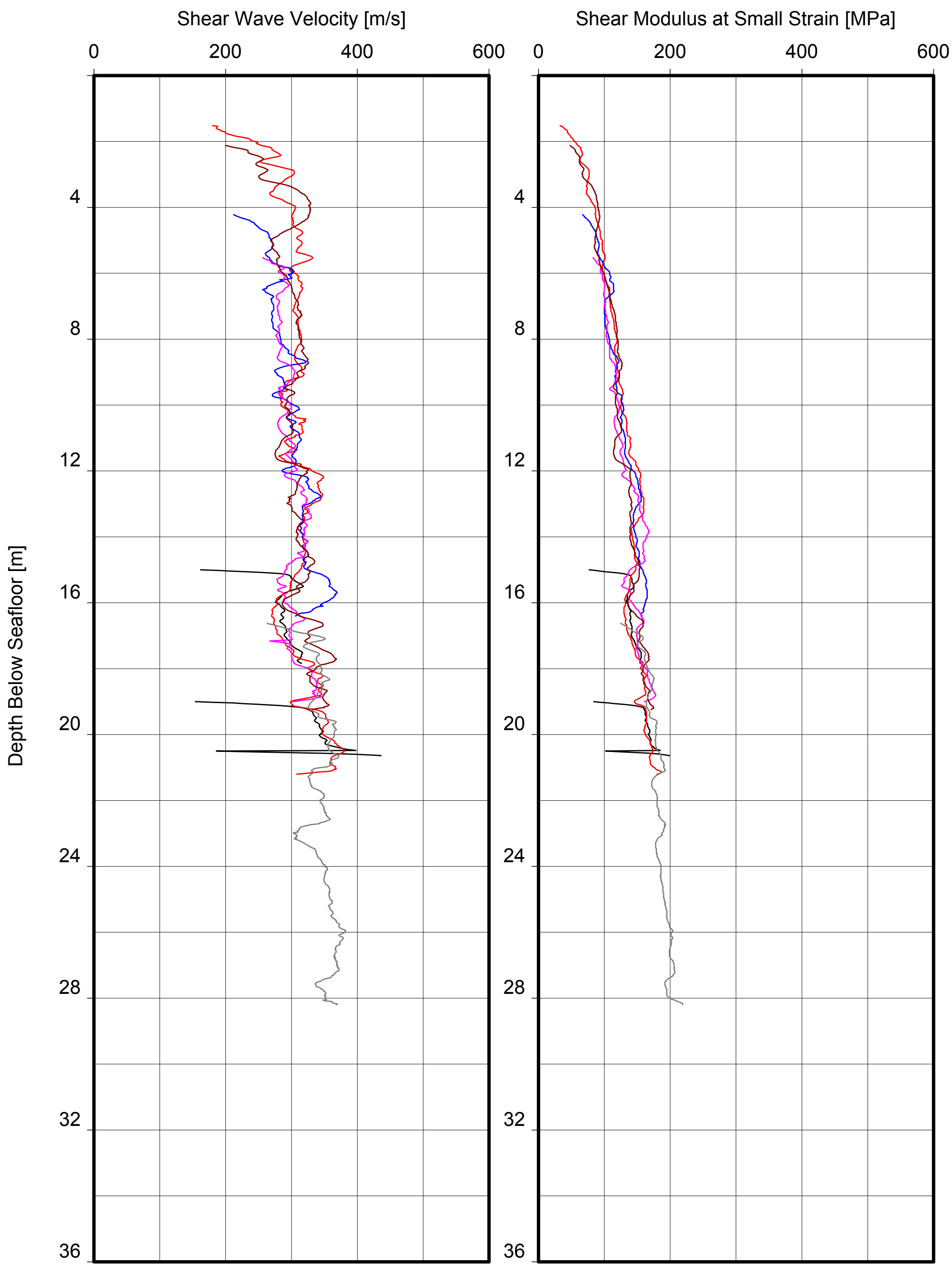


Shear wave velocity ($v_s$) measured in-between geophone array
Shear modulus at small strain ($G_{max}$) derived from $v_s$ measured
$v_s$ and $G_{max}$ derived from CPT

Location(s):
BH-WFS3-5
CPT_WFS3_5
CPT_WFS3_10
CPT_WFS3_11
CPT_WFS3_11A
CPT_WFS3_14
CPT_WFS3_24

Note(s):
- $v_s$ derived from CPT based on Robertson and Cabal (2010)
- $G_{max}$ for clays derived from CPT based on Mayne and Rix (1993)
- $G_{max}$ for sands derived from CPT based on Rix and Stokoe (1991)

GeODin/3.Shear Wave Velocity and Shear Modulus at Small Strain versus Depth (single UNIT, excl. GM).GLO/2015-12-09 14:52:55

**SHEAR WAVE VELOCITY AND SHEAR MODULUS AT SMALL STRAIN VERSUS DEPTH**

UNIT B

BORSSELE WIND FARM ZONE, WFS III - DUTCH SECTOR, NORTH SEA

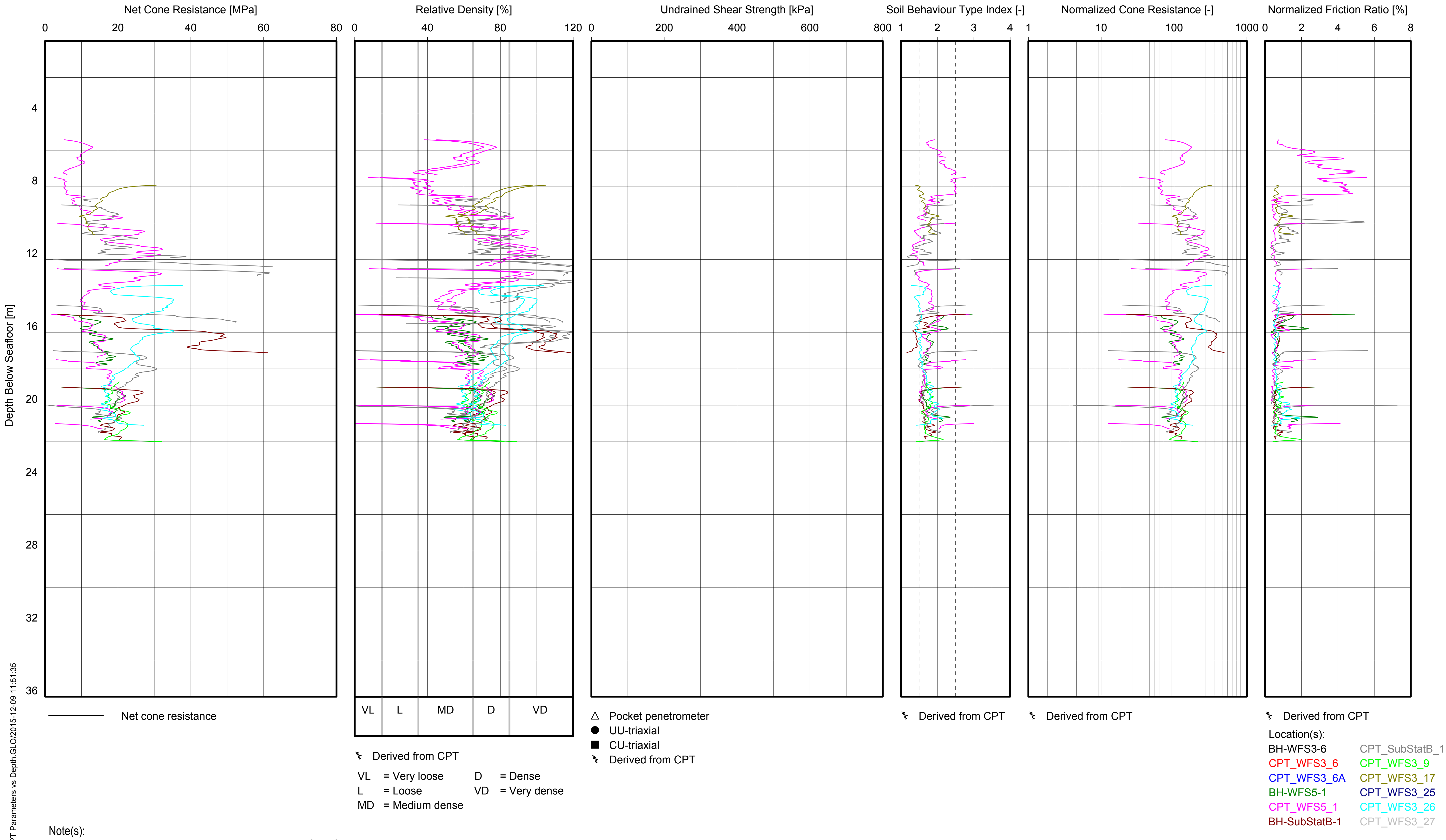


Note(s):
- $K_0$ = 0.5 and $K_0$ = 1.0 are used to derive relative density from CPT
- $N_k$ = 15 and $N_k$ = 20 are used to derive $c_u$ from CPT
- Soil Behaviour Type Index is according to Robertson (2009), refer to Appendix 1, document titled "Cone Penetration Test Interpretation"

GeODin/1.CPT Parameters vs Depth.GLO/2015-12-09 11:51:35

**CPT PARAMETERS AND STRENGTH DATA VERSUS DEPTH**

UNIT E1, E2 & E3

BORSSELE WIND FARM ZONE, WFS III - DUTCH SECTOR, NORTH SEA

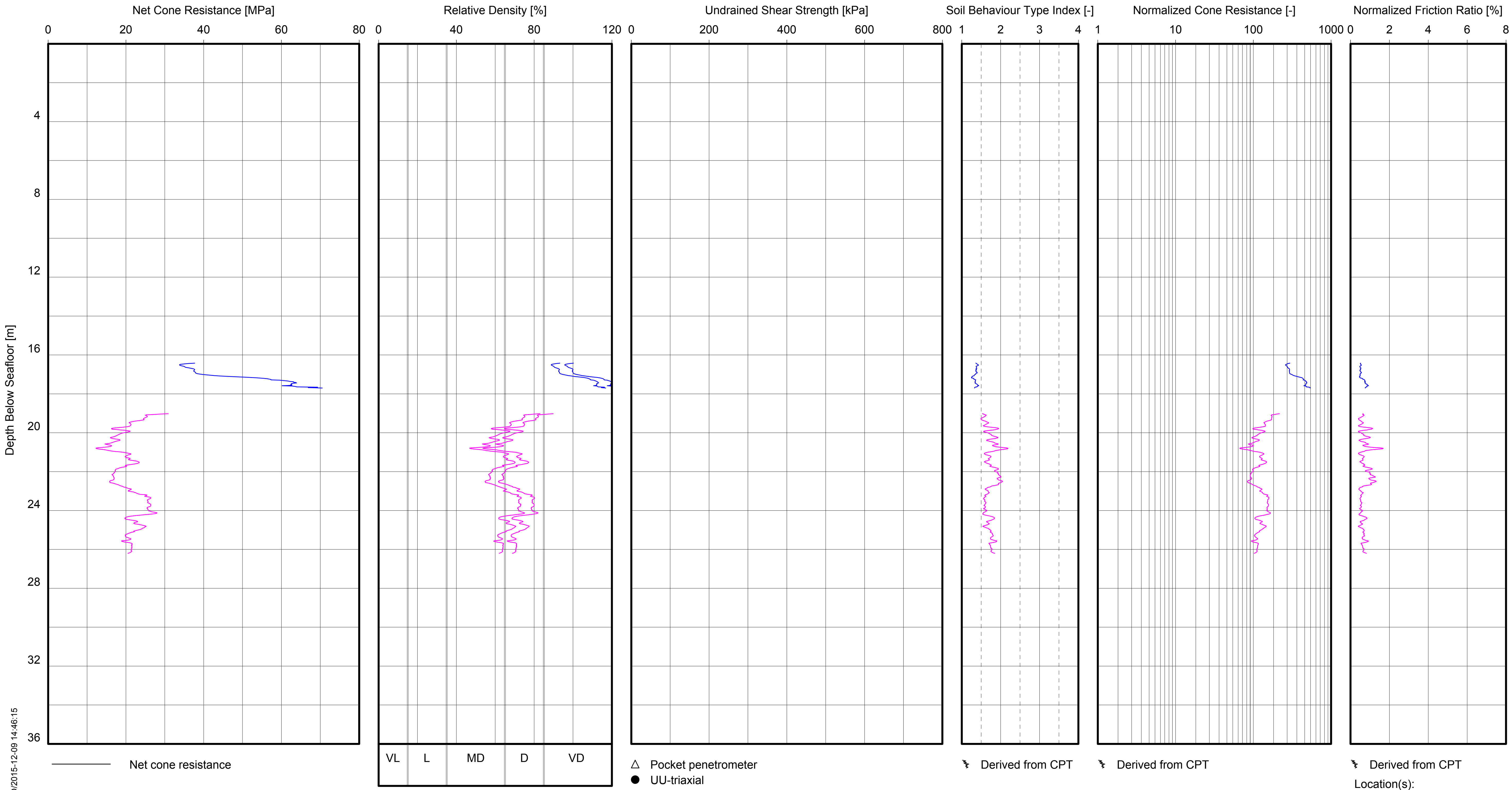


Net cone resistance

Derived from CPT

VL = Very loose
L = Loose
MD = Medium dense
D = Dense
VD = Very dense

Pocket penetrometer
UU-triaxial
CU-triaxial
Derived from CPT

Derived from CPT

Derived from CPT

Derived from CPT

Location(s):
BH-WFS3-5
CPT_WFS3_5
CPT_WFS3_10
CPT_WFS3_11
CPT_WFS3_11A
CPT_WFS3_14
CPT_WFS3_24

GeODin/1.CPT Parameters vs Depth.GLO/2015-12-09 14:46:15

Note(s):
- $K_0$ = 0.5 and $K_0$ = 1.0 are used to derive relative density from CPT
- $N_k$ = 15 and $N_k$ = 20 are used to derive $c_u$ from CPT
- Soil Behaviour Type Index is according to Robertson (2009), refer to Appendix 1, document titled "Cone Penetration Test Interpretation"

**CPT PARAMETERS AND STRENGTH DATA VERSUS DEPTH**
UNIT E1, E2 & E3
BORSSELE WIND FARM ZONE, WFS III - DUTCH SECTOR, NORTH SEA

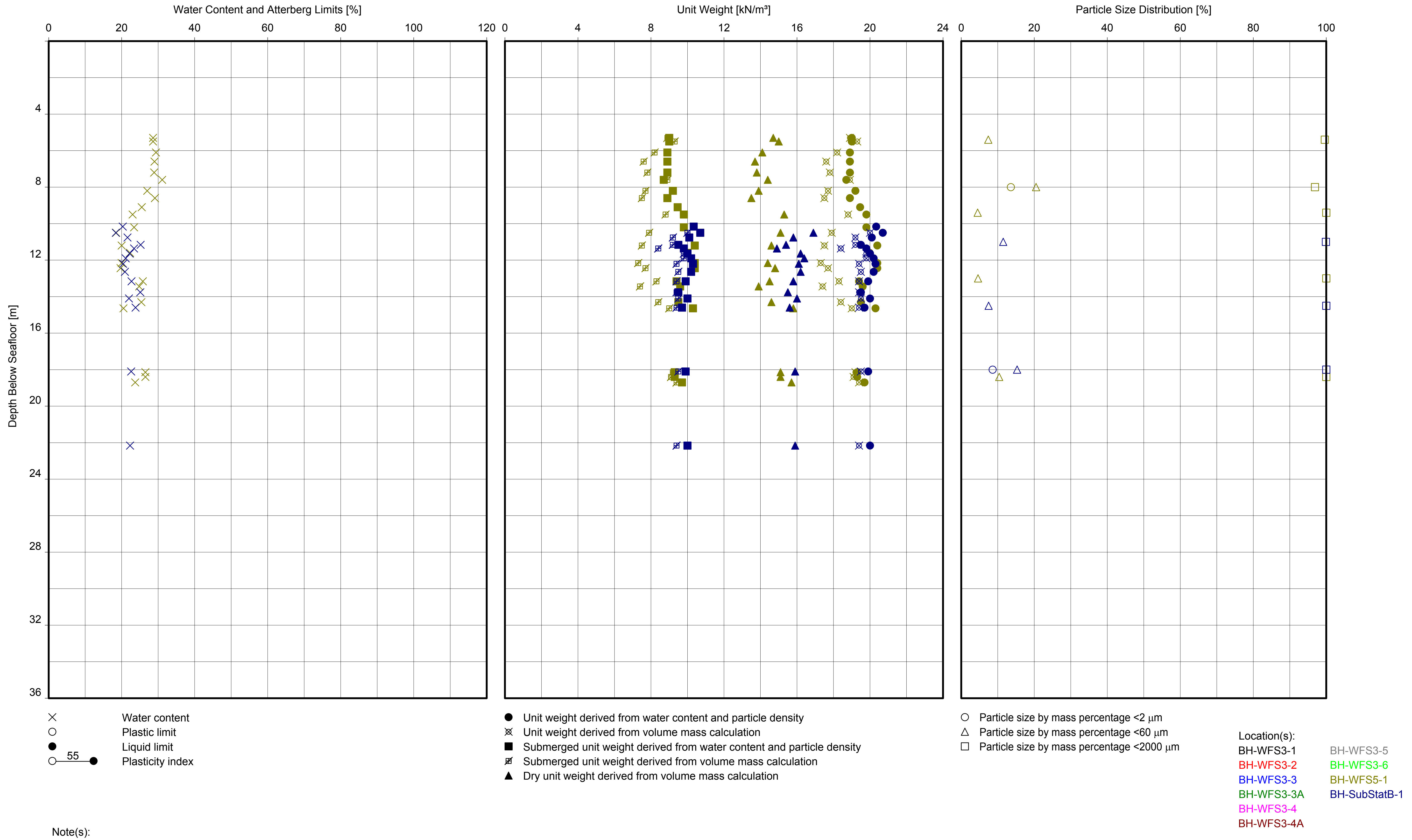


Note(s):
- No dry unit weight is available for unit weight measurements by volume mass calculation on WAX samples.

**WATER CONTENT, UNIT WEIGHT AND PARTICLE SIZE DISTRIBUTION VERSUS DEPTH**

UNIT E1, E2 & E3

BORSSELE WIND FARM ZONE, WFS III - DUTCH SECTOR, NORTH SEA

GeODin/2:Water Content, Unit Weight And Particle Size Distribution vs Depth.GLO/2015-12-09 13:40:12

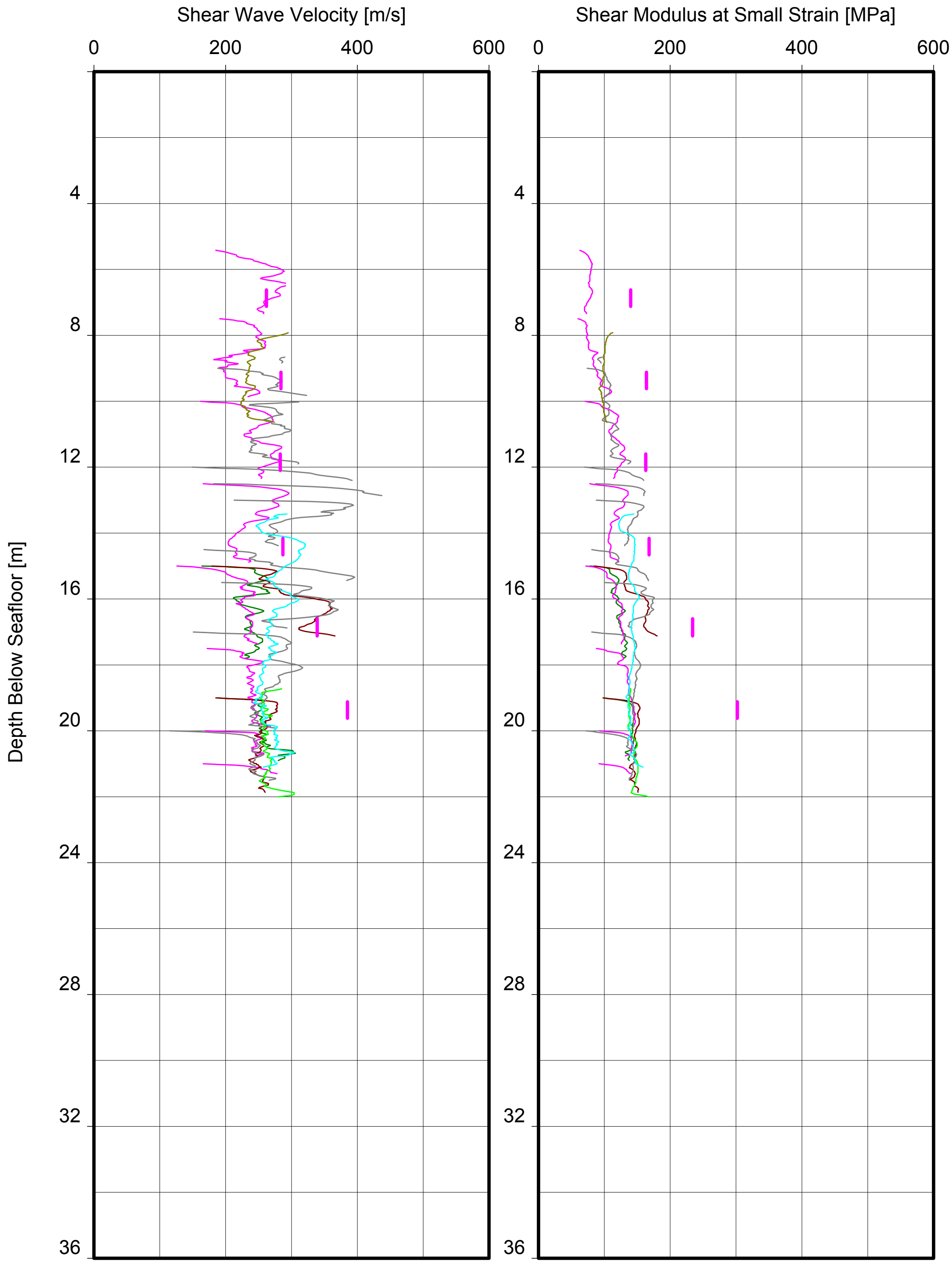


Shear wave velocity ($v_s$) measured in-between geophone array
Shear modulus at small strain ($G_{max}$) derived from $v_s$ measured
$v_s$ and $G_{max}$ derived from CPT

Location(s):
BH-WFS3-6
CPT_WFS3_6
CPT_WFS3_6A
BH-WFS5-1
CPT_WFS5_1
BH-SubStatB-1
CPT_SubStatB_1
CPT_WFS3_9
CPT_WFS3_17
CPT_WFS3_25
CPT_WFS3_26
CPT_WFS3_27

Note(s):
- $v_s$ derived from CPT based on Robertson and Cabal (2010)
- $G_{max}$ for clays derived from CPT based on Mayne and Rix (1993)
- $G_{max}$ for sands derived from CPT based on Rix and Stokoe (1991)

GeODin/3.Shear Wave Velocity and Shear Modulus at Small Strain versus Depth (single UNIT, excl. GM).GLO/2015-12-09 11:53:47

**SHEAR WAVE VELOCITY AND SHEAR MODULUS AT SMALL STRAIN VERSUS DEPTH**

UNIT E1, E2 & E3

BORSSELE WIND FARM ZONE, WFS III - DUTCH SECTOR, NORTH SEA

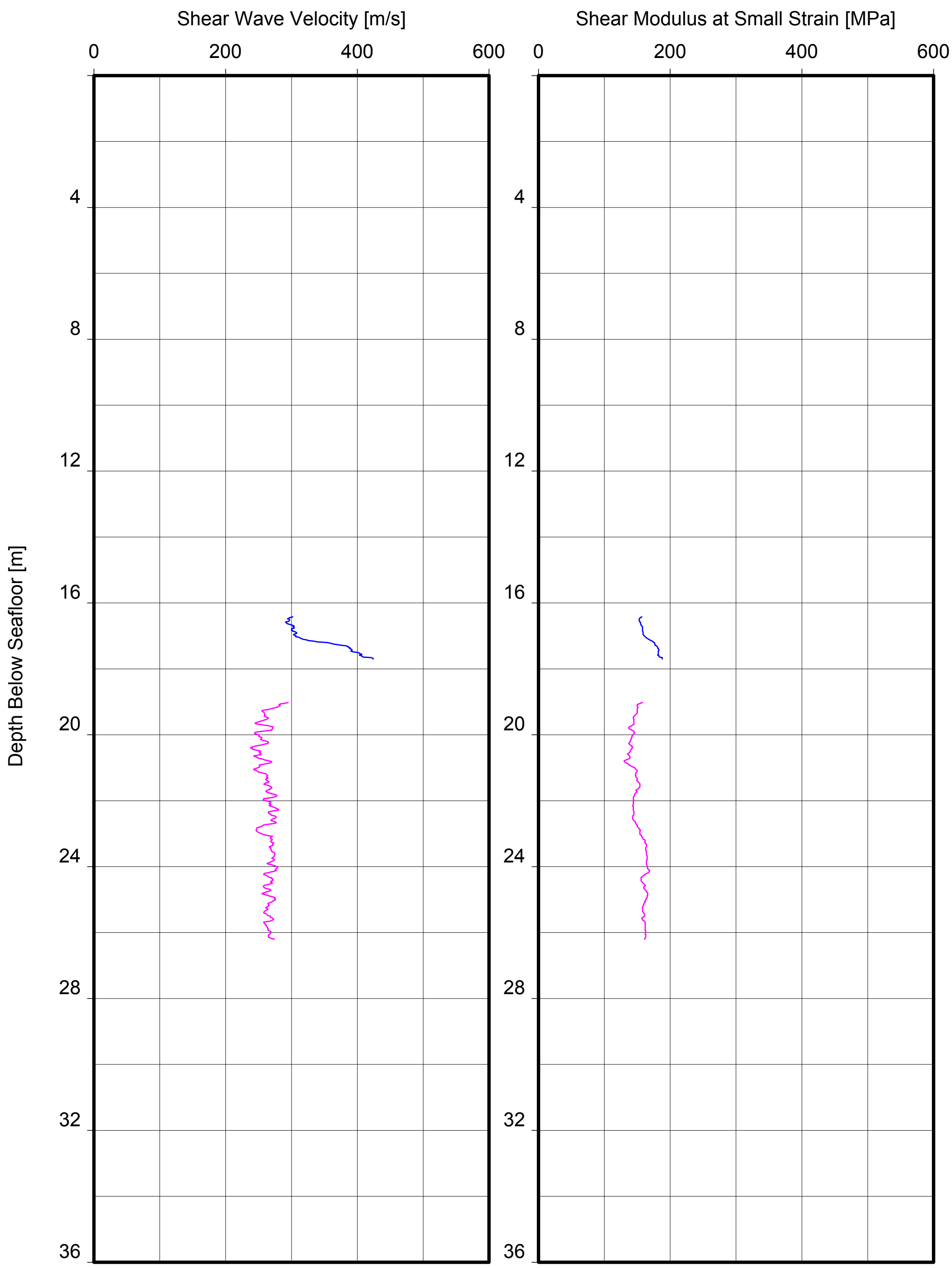


Shear wave velocity ($v_s$) measured in-between geophone array
Shear modulus at small strain ($G_{max}$) derived from $v_s$ measured
$v_s$ and $G_{max}$ derived from CPT

Location(s):
BH-WFS3-5
CPT_WFS3_24
CPT_WFS3_5
CPT_WFS3_10
CPT_WFS3_11
CPT_WFS3_11A
CPT_WFS3_14

Note(s):
- $v_s$ derived from CPT based on Robertson and Cabal (2010)
- $G_{max}$ for clays derived from CPT based on Mayne and Rix (1993)
- $G_{max}$ for sands derived from CPT based on Rix and Stokoe (1991)

GeODin/3.Shear Wave Velocity and Shear Modulus at Small Strain versus Depth (single UNIT, excl. GM).GLO/2015-12-09 14:52:18

**SHEAR WAVE VELOCITY AND SHEAR MODULUS AT SMALL STRAIN VERSUS DEPTH**

UNIT E1, E2 & E3

BORSSELE WIND FARM ZONE, WFS III - DUTCH SECTOR, NORTH SEA

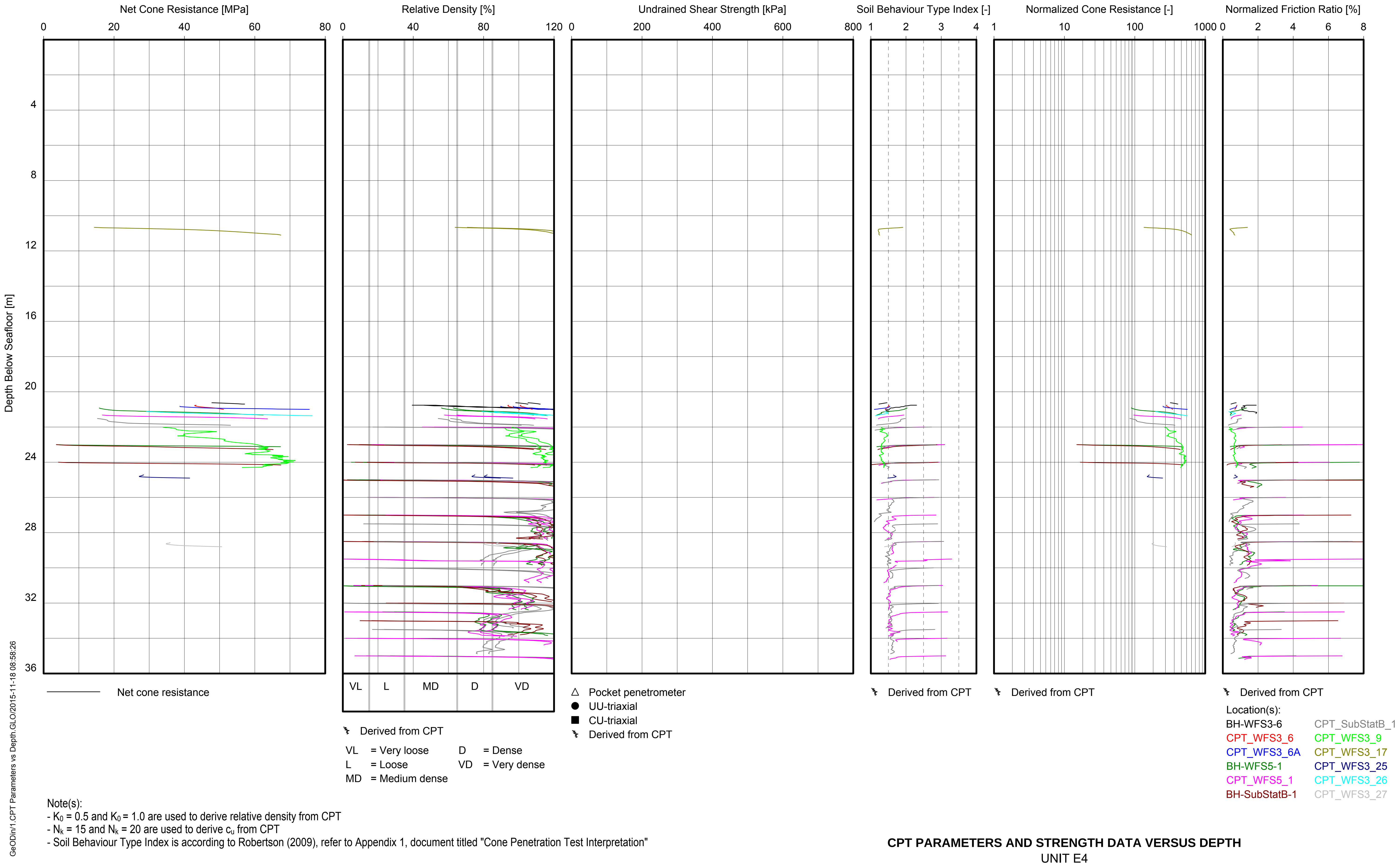


Note(s):
- $K_0$ = 0.5 and $K_0$ = 1.0 are used to derive relative density from CPT
- $N_k$ = 15 and $N_k$ = 20 are used to derive $c_u$ from CPT
- Soil Behaviour Type Index is according to Robertson (2009), refer to Appendix 1, document titled "Cone Penetration Test Interpretation"

**CPT PARAMETERS AND STRENGTH DATA VERSUS DEPTH**

UNIT E4

BORSSELE WIND FARM ZONE, WFS III - DUTCH SECTOR, NORTH SEA

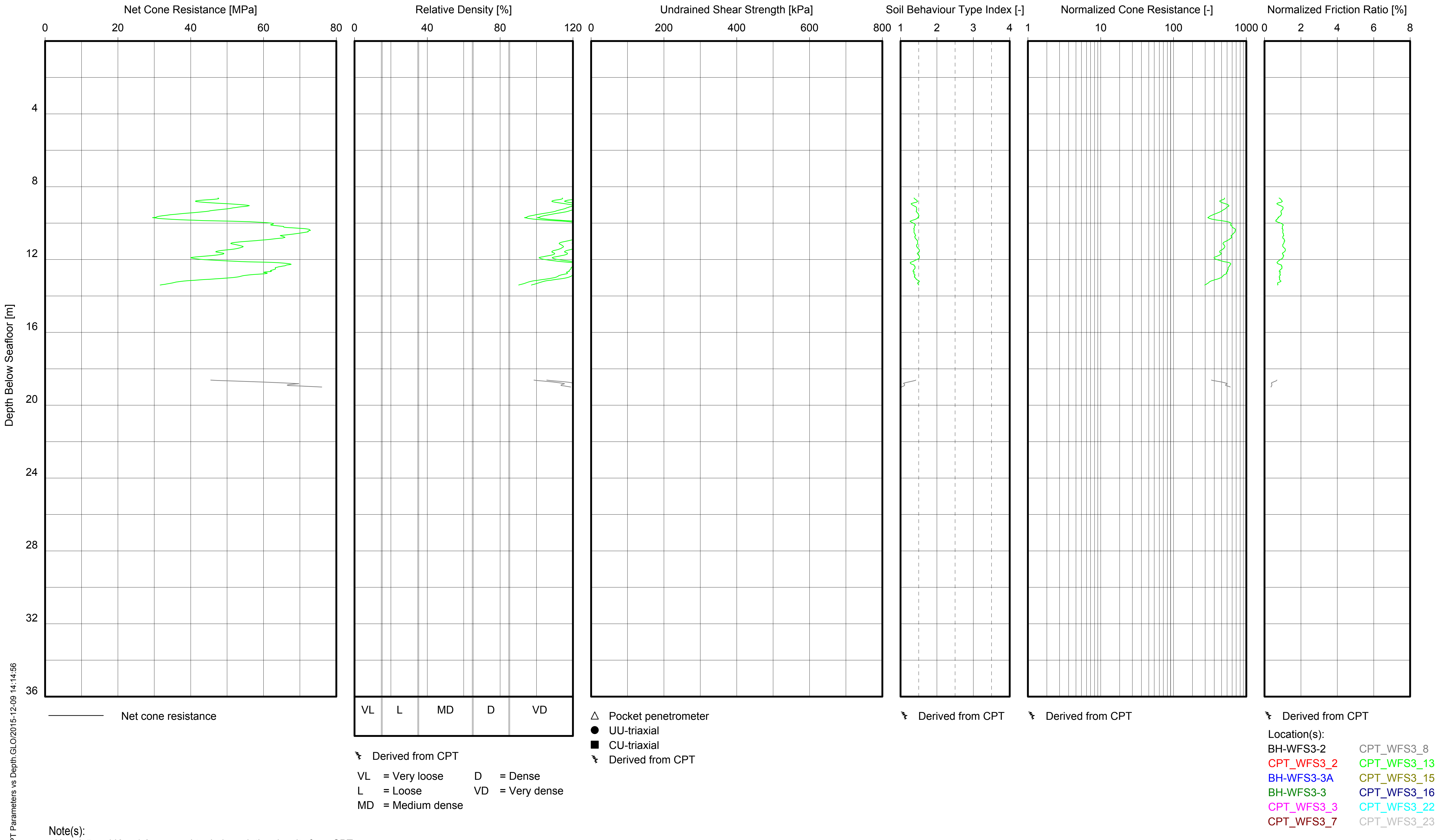


GeODin\1.CPT Parameters vs Depth.GLO/2015-12-09 14:14:56

Note(s):
- $K_0$ = 0.5 and $K_0$ = 1.0 are used to derive relative density from CPT
- $N_k$ = 15 and $N_k$ = 20 are used to derive $c_u$ from CPT
- Soil Behaviour Type Index is according to Robertson (2009), refer to Appendix 1, document titled "Cone Penetration Test Interpretation"

**CPT PARAMETERS AND STRENGTH DATA VERSUS DEPTH**
UNIT E4
BORSSELE WIND FARM ZONE, WFS III - DUTCH SECTOR, NORTH SEA

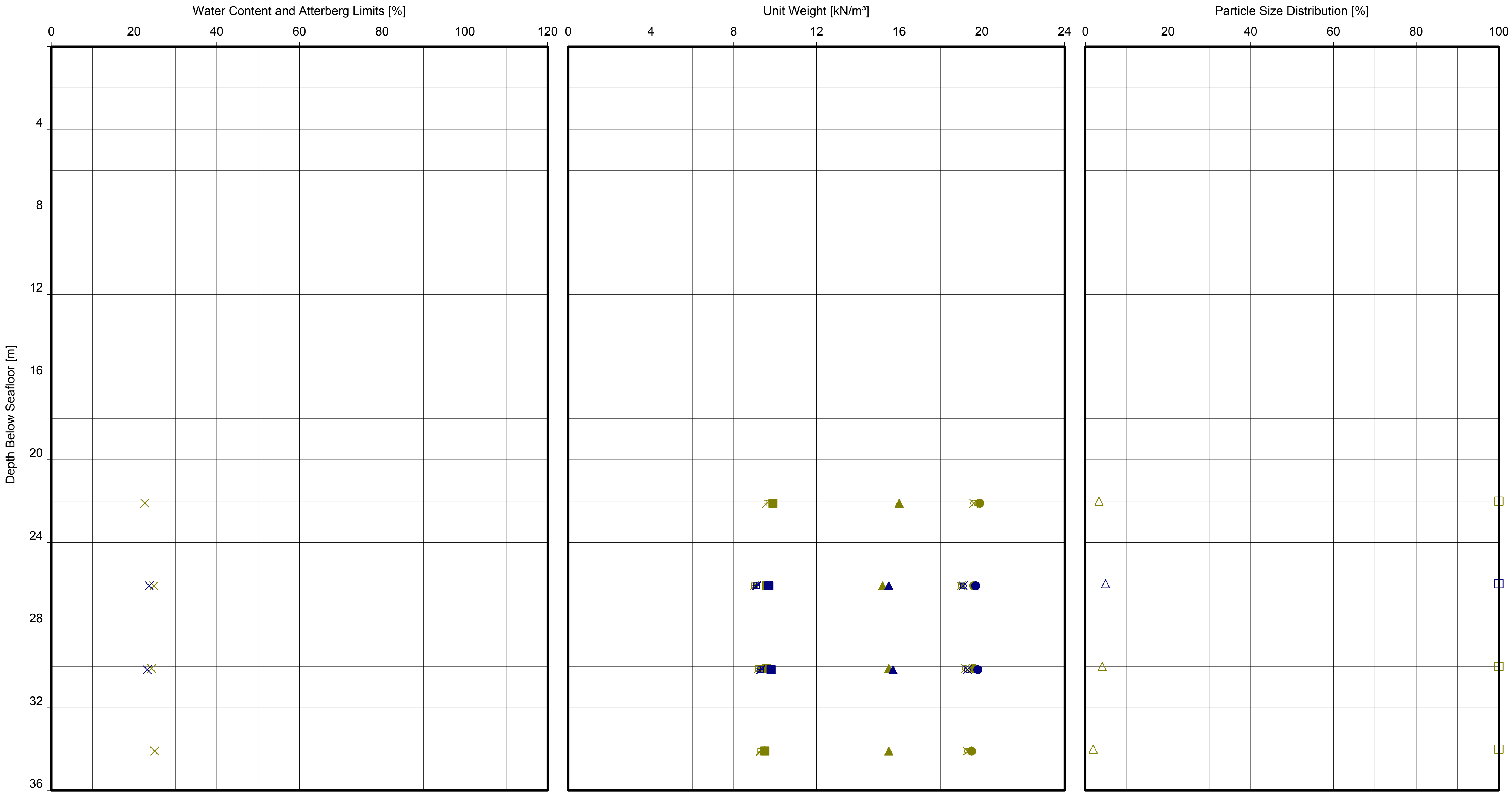


Water content
Plastic limit
Liquid limit
55
Plasticity index

Unit weight derived from water content and particle density
Unit weight derived from volume mass calculation
Submerged unit weight derived from water content and particle density
Submerged unit weight derived from volume mass calculation
Dry unit weight derived from volume mass calculation

Particle size by mass percentage <2 µm
Particle size by mass percentage <60 µm
Particle size by mass percentage <2000 µm

Location(s):
BH-WFS3-1
BH-WFS3-2
BH-WFS3-3
BH-WFS3-3A
BH-WFS3-4
BH-WFS3-4A
BH-WFS3-5
BH-WFS3-6
BH-WFS5-1
BH-SubStatB-1

Note(s):
- No dry unit weight is available for unit weight measurements by volume mass calculation on WAX samples.

GeODin/2.Water Content, Unit Weight And Particle Size Distribution vs Depth.GLO/2015-12-09 13:41:09

**WATER CONTENT, UNIT WEIGHT AND PARTICLE SIZE DISTRIBUTION VERSUS DEPTH**
UNIT E4
BORSSELE WIND FARM ZONE, WFS III - DUTCH SECTOR, NORTH SEA

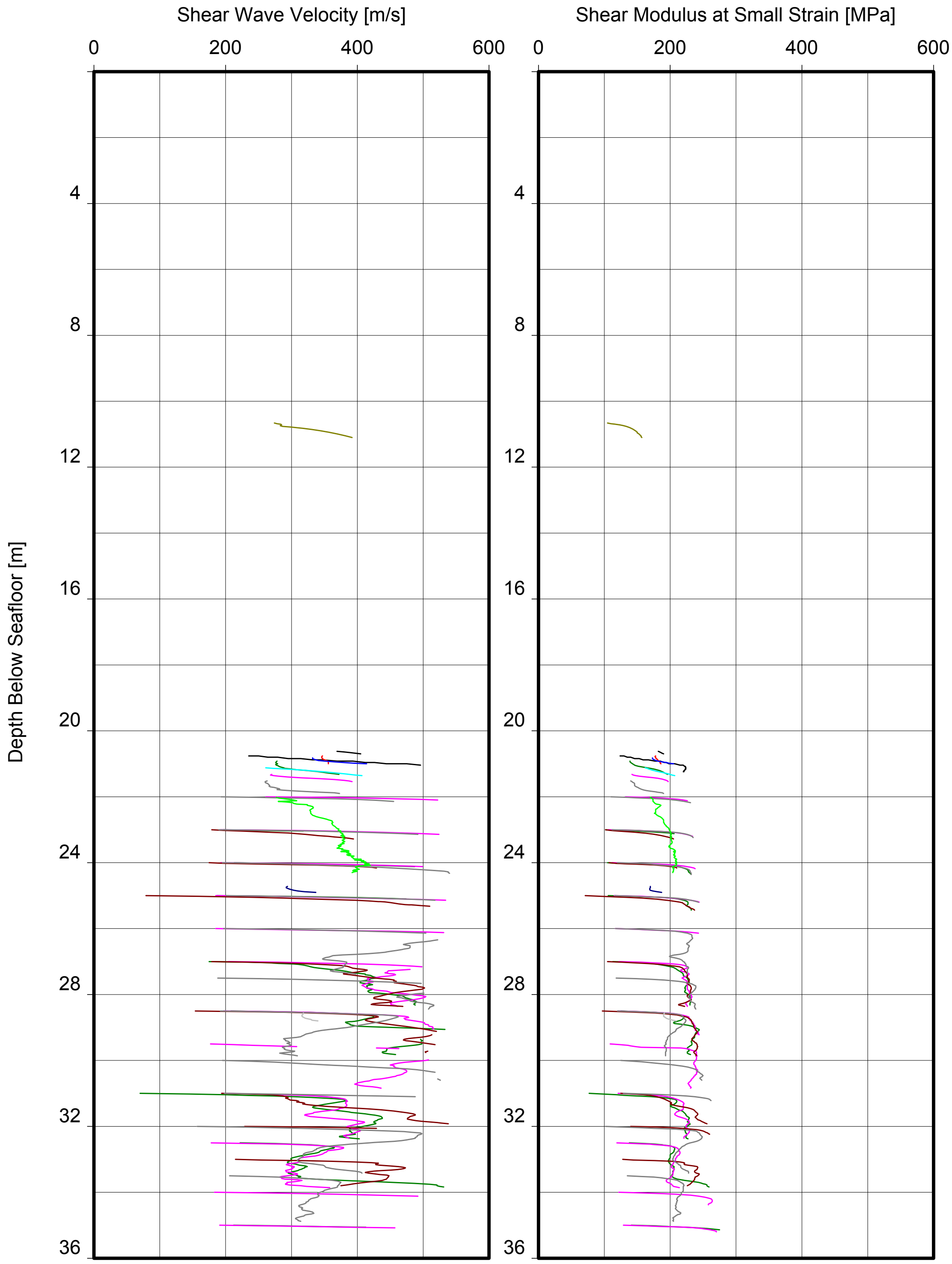


Shear wave velocity ($v_s$) measured in-between geophone array

Shear modulus at small strain ($G_{max}$) derived from $v_s$ measured

$v_s$ and $G_{max}$ derived from CPT

Location(s):

BH-WFS3-6, CPT_SubStatB_1, CPT_WFS3_6, CPT_WFS3_9, CPT_WFS3_6A, CPT_WFS3_17, BH-WFS5-1, CPT_WFS3_25, CPT_WFS5_1, CPT_WFS3_26, BH-SubStatB-1, CPT_WFS3_27

Note(s):
- $v_s$ derived from CPT based on Robertson and Cabal (2010)
- $G_{max}$ for clays derived from CPT based on Mayne and Rix (1993)
- $G_{max}$ for sands derived from CPT based on Rix and Stokoe (1991)

GeODin/3.Shear Wave Velocity and Shear Modulus at Small Strain versus Depth (single UNIT, excl. GM).GLO/2015-12-09 11:58:32

**SHEAR WAVE VELOCITY AND SHEAR MODULUS AT SMALL STRAIN VERSUS DEPTH**

UNIT E4

BORSSELE WIND FARM ZONE, WFS III - DUTCH SECTOR, NORTH SEA

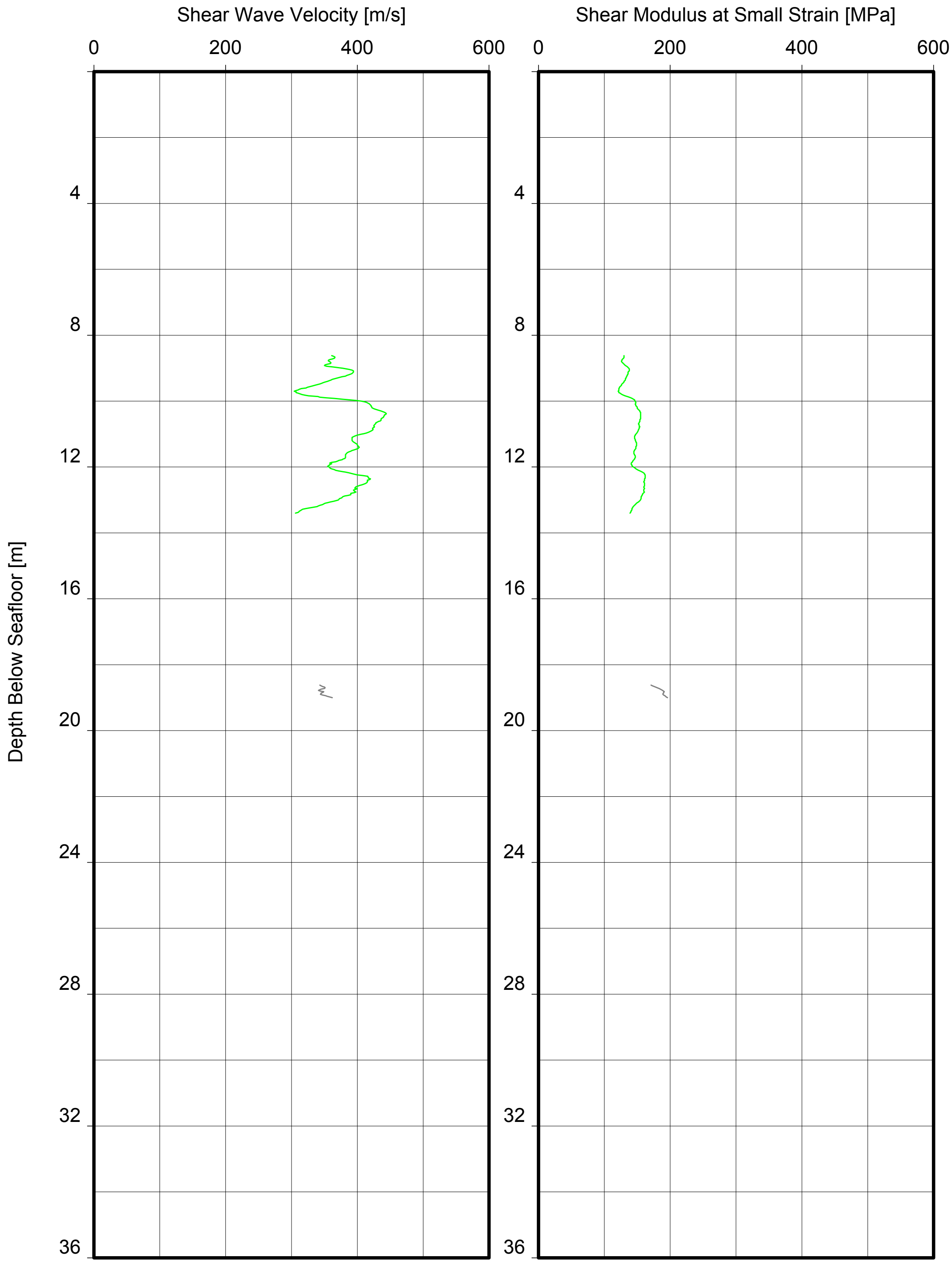


- Shear wave velocity ($v_s$) measured in-between geophone array
- Shear modulus at small strain ($G_{max}$) derived from $v_s$ measured
- $v_s$ and $G_{max}$ derived from CPT

Location(s):

BH-WFS3-2, CPT_WFS3_2, BH-WFS3-3A, BH-WFS3-3, CPT_WFS3_3, CPT_WFS3_7, CPT_WFS3_8, CPT_WFS3_13, CPT_WFS3_15, CPT_WFS3_16, CPT_WFS3_22, CPT_WFS3_23

Note(s):
- $v_s$ derived from CPT based on Robertson and Cabal (2010)
- $G_{max}$ for clays derived from CPT based on Mayne and Rix (1993)
- $G_{max}$ for sands derived from CPT based on Rix and Stokoe (1991)

GeODin/3.Shear Wave Velocity and Shear Modulus at Small Strain versus Depth (single UNIT, excl. GM).GLO/2015-12-09 14:24:05

**SHEAR WAVE VELOCITY AND SHEAR MODULUS AT SMALL STRAIN VERSUS DEPTH**

UNIT E4

BORSSELE WIND FARM ZONE, WFS III - DUTCH SECTOR, NORTH SEA

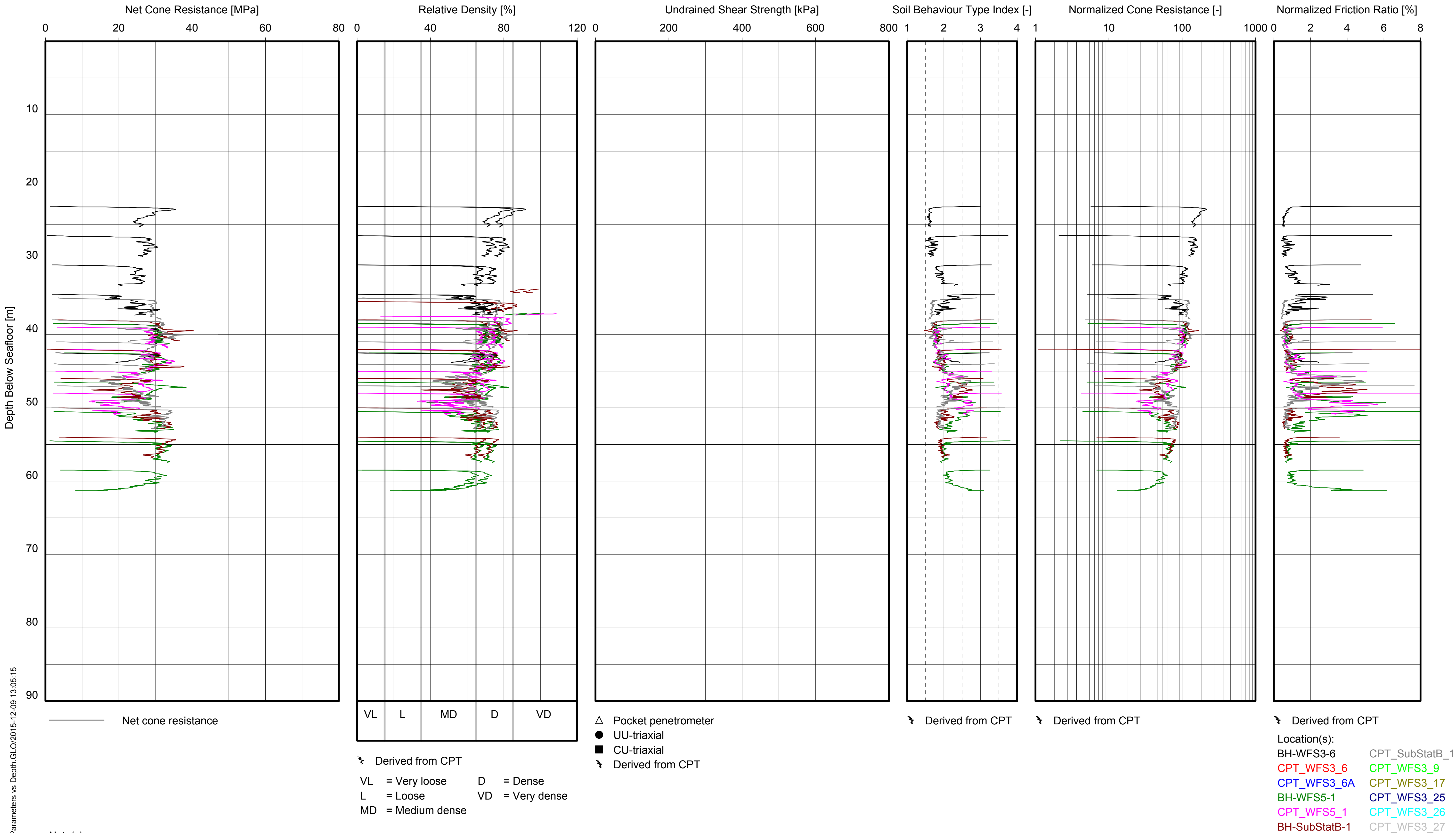


GeODin/1.CPT Parameters vs Depth.GLO/2015-12-09 13:05:15

Note(s):
- $K_0$ = 0.5 and $K_0$ = 1.0 are used to derive relative density from CPT
- $N_k$ = 15 and $N_k$ = 20 are used to derive $c_u$ from CPT
- Soil Behaviour Type Index is according to Robertson (2009), refer to Appendix 1, document titled "Cone Penetration Test Interpretation"

**CPT PARAMETERS AND STRENGTH DATA VERSUS DEPTH**

UNIT E5

BORSSELE WIND FARM ZONE, WFS III - DUTCH SECTOR, NORTH SEA

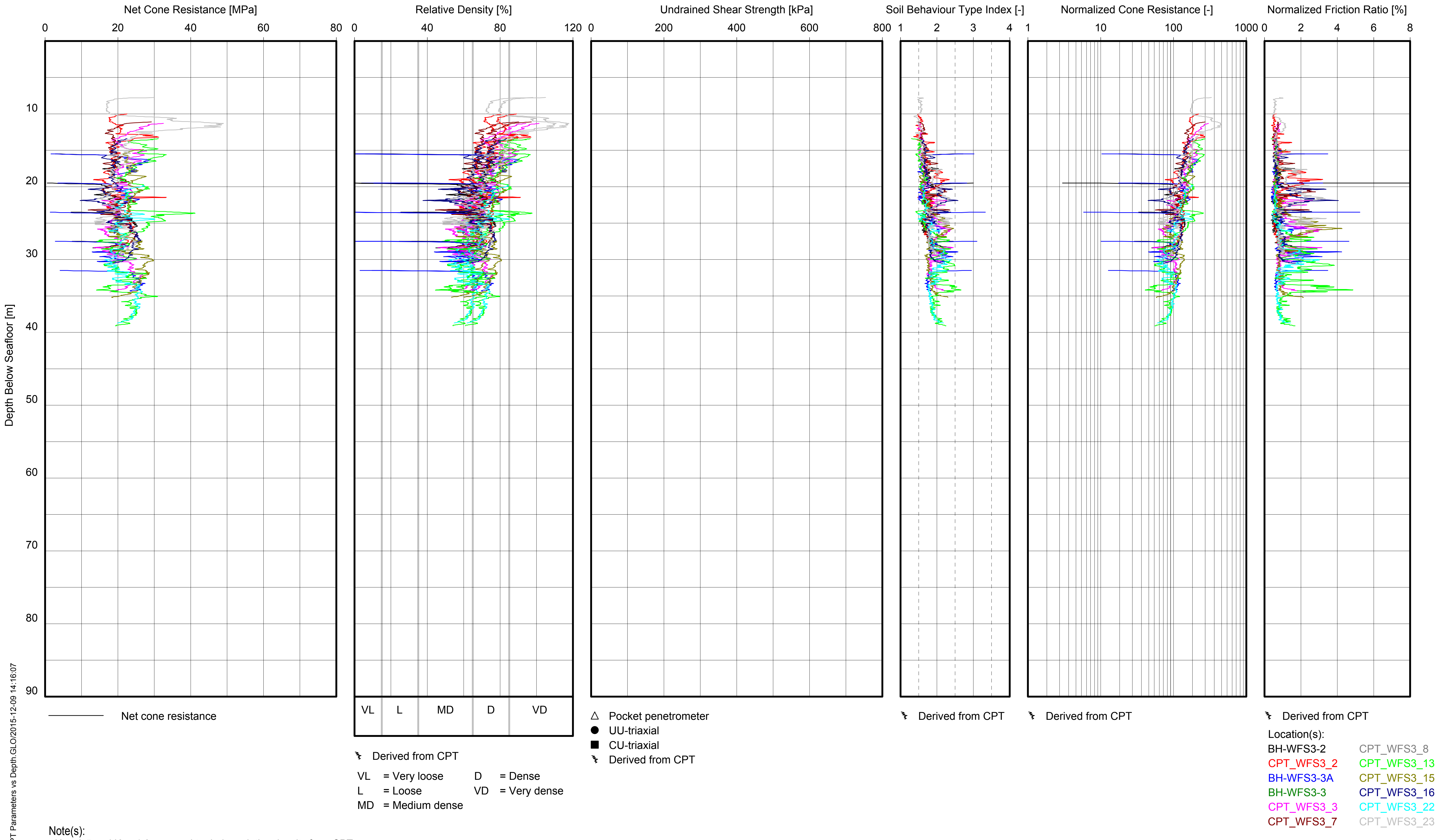


Note(s):
- $K_0$ = 0.5 and $K_0$ = 1.0 are used to derive relative density from CPT
- $N_k$ = 15 and $N_k$ = 20 are used to derive $c_u$ from CPT
- Soil Behaviour Type Index is according to Robertson (2009), refer to Appendix 1, document titled "Cone Penetration Test Interpretation"

GeODin/1.CPT Parameters vs Depth.GLO/2015-12-09 14:16:07

**CPT PARAMETERS AND STRENGTH DATA VERSUS DEPTH**

UNIT E5

BORSSELE WIND FARM ZONE, WFS III - DUTCH SECTOR, NORTH SEA

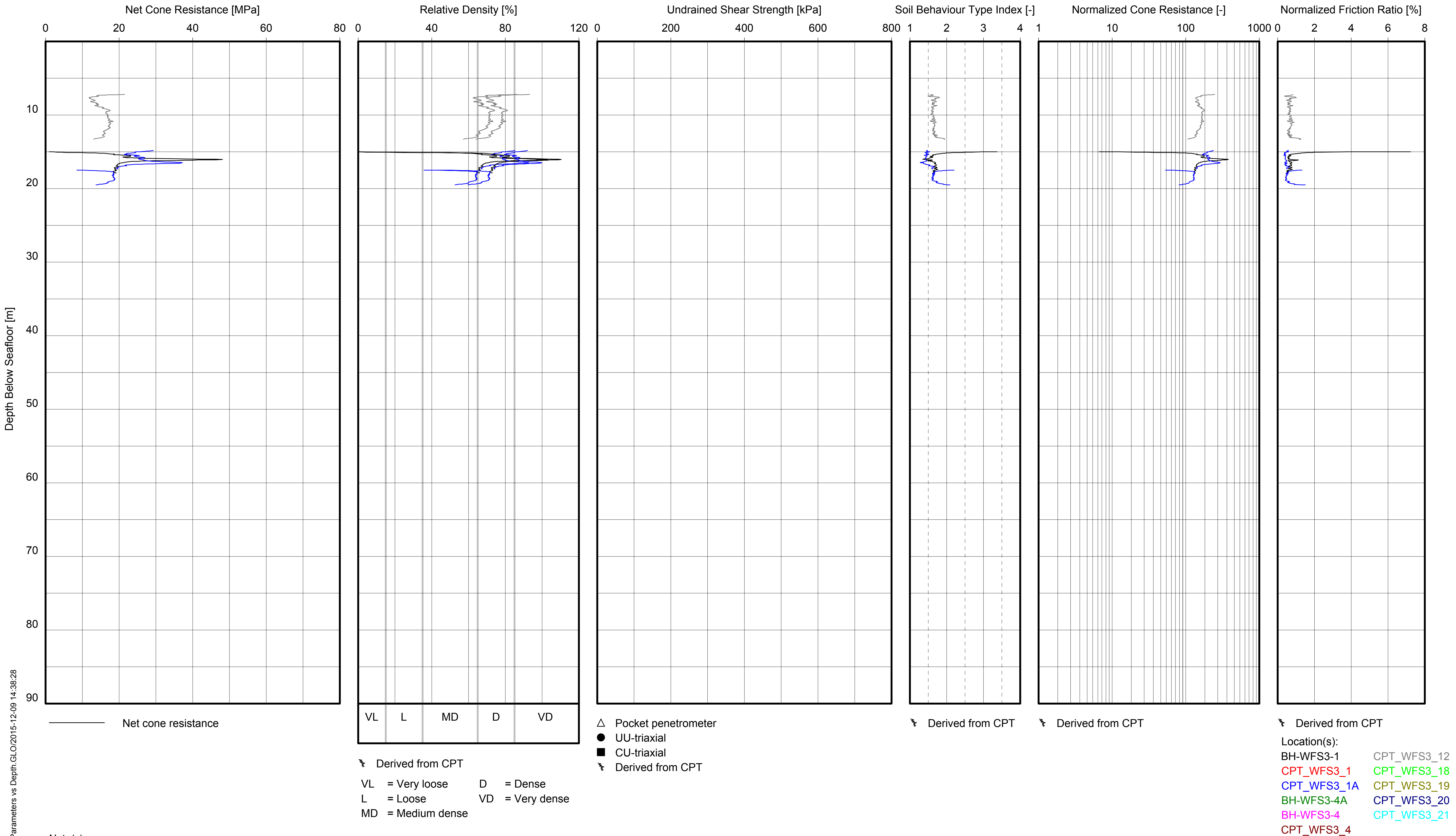


Note(s):
- $K_0$ = 0.5 and $K_0$ = 1.0 are used to derive relative density from CPT
- $N_k$ = 15 and $N_k$ = 20 are used to derive $c_u$ from CPT
- Soil Behaviour Type Index is according to Robertson (2009), refer to Appendix 1, document titled "Cone Penetration Test Interpretation"

GeODin/1.CPT Parameters vs Depth.GLO/2015-12-09 14:38:28

**CPT PARAMETERS AND STRENGTH DATA VERSUS DEPTH**
UNIT E5
BORSSELE WIND FARM ZONE, WFS III - DUTCH SECTOR, NORTH SEA

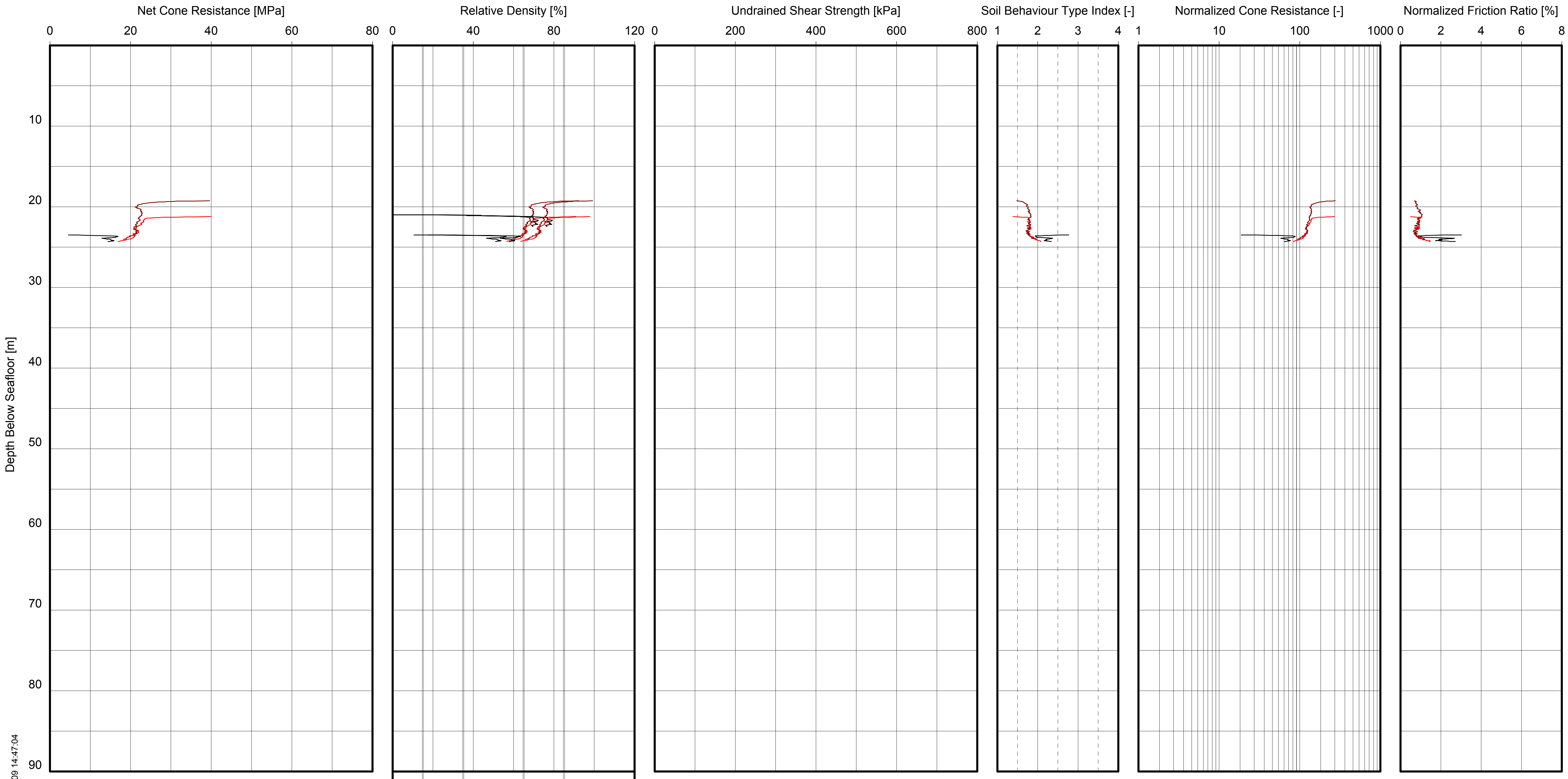


Net cone resistance

Derived from CPT

VL = Very loose
L = Loose
MD = Medium dense
D = Dense
VD = Very dense

△ Pocket penetrometer
● UU-triaxial
■ CU-triaxial
Derived from CPT

Derived from CPT

Derived from CPT

Derived from CPT

Location(s):
BH-WFS3-5
CPT_WFS3_5
CPT_WFS3_10
CPT_WFS3_11
CPT_WFS3_11A
CPT_WFS3_14
CPT_WFS3_24

GeODin\1.CPT Parameters vs Depth.GLO/2015-12-09 14:47:04

Note(s):
- $K_0$ = 0.5 and $K_0$ = 1.0 are used to derive relative density from CPT
- $N_k$ = 15 and $N_k$ = 20 are used to derive $c_u$ from CPT
- Soil Behaviour Type Index is according to Robertson (2009), refer to Appendix 1, document titled "Cone Penetration Test Interpretation"

**CPT PARAMETERS AND STRENGTH DATA VERSUS DEPTH**
UNIT E5
BORSSELE WIND FARM ZONE, WFS III - DUTCH SECTOR, NORTH SEA

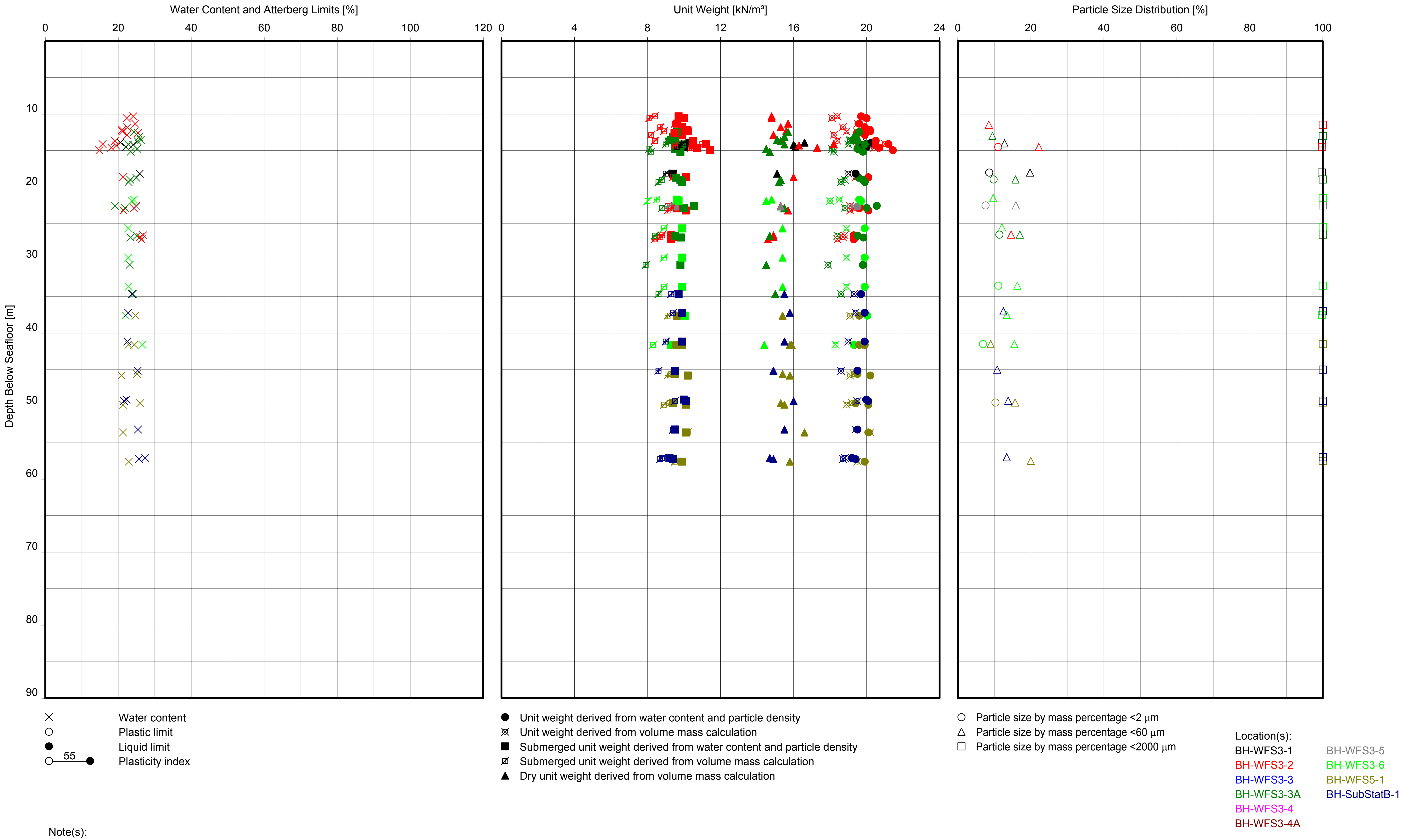


Note(s):
- No dry unit weight is available for unit weight measurements by volume mass calculation on WAX samples.

GeODin/2:Water Content, Unit Weight And Particle Size Distribution vs Depth.GLO/2015-12-09 13:42:33

**WATER CONTENT, UNIT WEIGHT AND PARTICLE SIZE DISTRIBUTION VERSUS DEPTH**

UNIT E5

BORSSELE WIND FARM ZONE, WFS III - DUTCH SECTOR, NORTH SEA

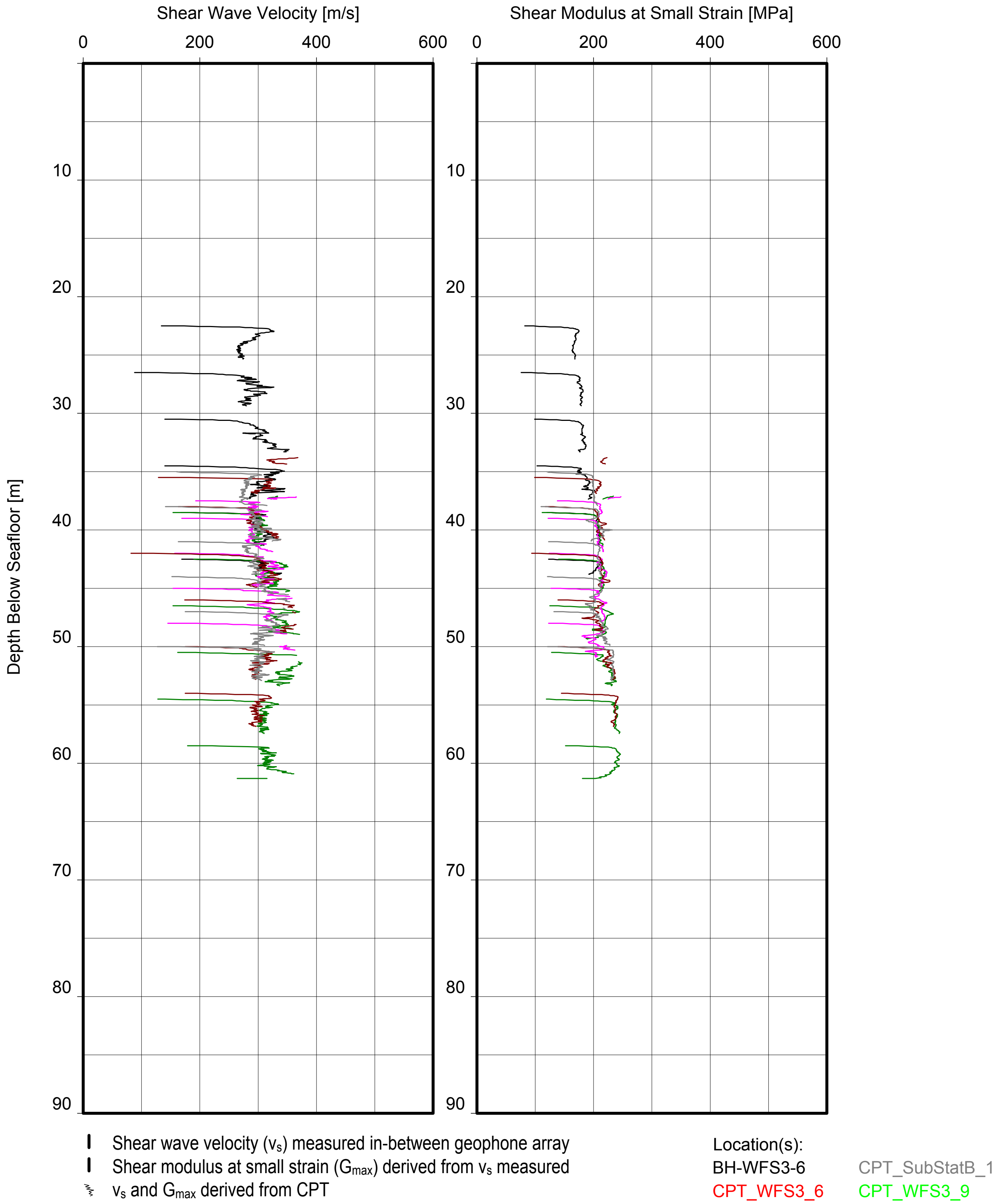


Note(s):
- $v_s$ derived from CPT based on Robertson and Cabal (2010)
- $G_{max}$ for clays derived from CPT based on Mayne and Rix (1993)
- $G_{max}$ for sands derived from CPT based on Rix and Stokoe (1991)

GeODin/3.Shear Wave Velocity and Shear Modulus at Small Strain versus Depth (single UNIT, excl. GM).GLO/2015-12-09 12:51:05

**SHEAR WAVE VELOCITY AND SHEAR MODULUS AT SMALL STRAIN VERSUS DEPTH**

UNIT E5

BORSSELE WIND FARM ZONE, WFS III - DUTCH SECTOR, NORTH SEA

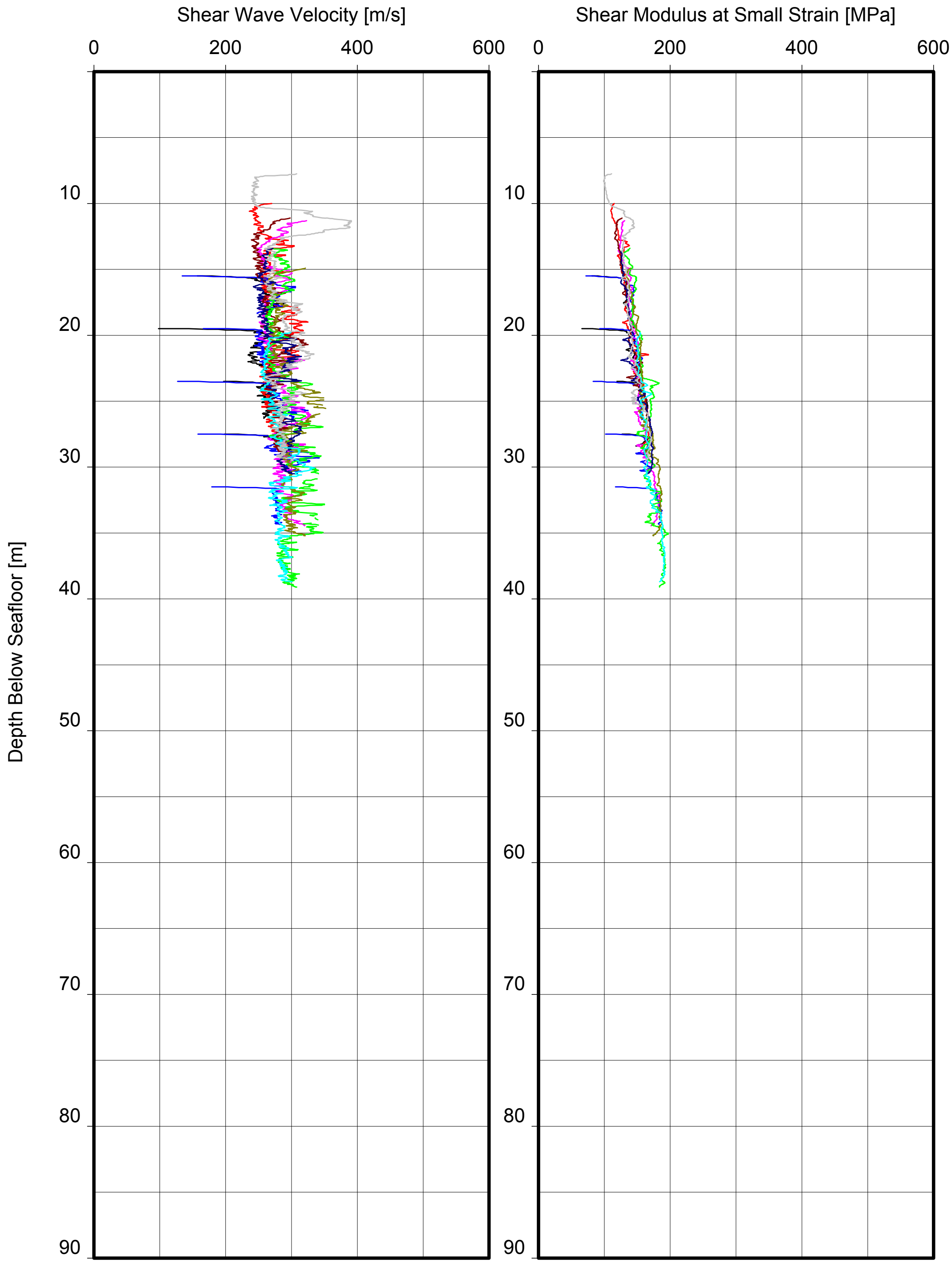


Shear wave velocity ($v_s$) measured in-between geophone array
Shear modulus at small strain ($G_{max}$) derived from $v_s$ measured
$v_s$ and $G_{max}$ derived from CPT

Location(s):
BH-WFS3-2
CPT_WFS3_2
BH-WFS3-3A
BH-WFS3-3
CPT_WFS3_3
CPT_WFS3_7
CPT_WFS3_8
CPT_WFS3_13
CPT_WFS3_15
CPT_WFS3_16
CPT_WFS3_22
CPT_WFS3_23

Note(s):
- $v_s$ derived from CPT based on Robertson and Cabal (2010)
- $G_{max}$ for clays derived from CPT based on Mayne and Rix (1993)
- $G_{max}$ for sands derived from CPT based on Rix and Stokoe (1991)

GeODin/3.Shear Wave Velocity and Shear Modulus at Small Strain versus Depth (single UNIT, excl. GM).GLO/2015-12-09 14:24:49

**SHEAR WAVE VELOCITY AND SHEAR MODULUS AT SMALL STRAIN VERSUS DEPTH**

UNIT E5

BORSSELE WIND FARM ZONE, WFS III - DUTCH SECTOR, NORTH SEA

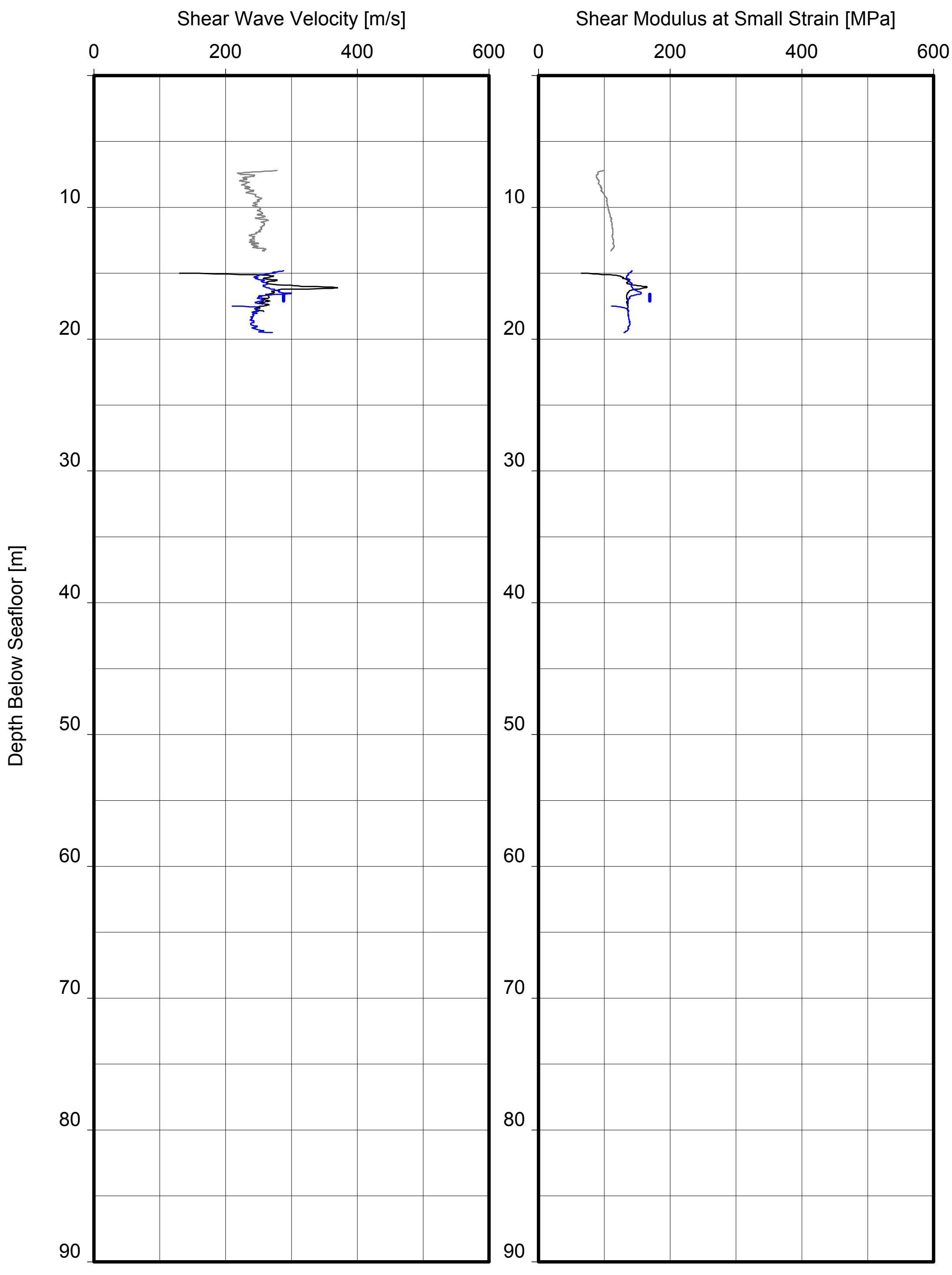


Shear wave velocity ($v_s$) measured in-between geophone array
Shear modulus at small strain ($G_{max}$) derived from $v_s$ measured
$v_s$ and $G_{max}$ derived from CPT

Location(s):
BH-WFS3-1
CPT_WFS3_1
CPT_WFS3_1A
BH-WFS3-4A
BH-WFS3-4
CPT_WFS3_4
CPT_WFS3_12
CPT_WFS3_18
CPT_WFS3_19
CPT_WFS3_20
CPT_WFS3_21

Note(s):
- $v_s$ derived from CPT based on Robertson and Cabal (2010)
- $G_{max}$ for clays derived from CPT based on Mayne and Rix (1993)
- $G_{max}$ for sands derived from CPT based on Rix and Stokoe (1991)

GeODin/3.Shear Wave Velocity and Shear Modulus at Small Strain versus Depth (single UNIT, excl. GM).GLO/2015-12-09 14:31:44

**SHEAR WAVE VELOCITY AND SHEAR MODULUS AT SMALL STRAIN VERSUS DEPTH**
UNIT E5
BORSSELE WIND FARM ZONE, WFS III - DUTCH SECTOR, NORTH SEA

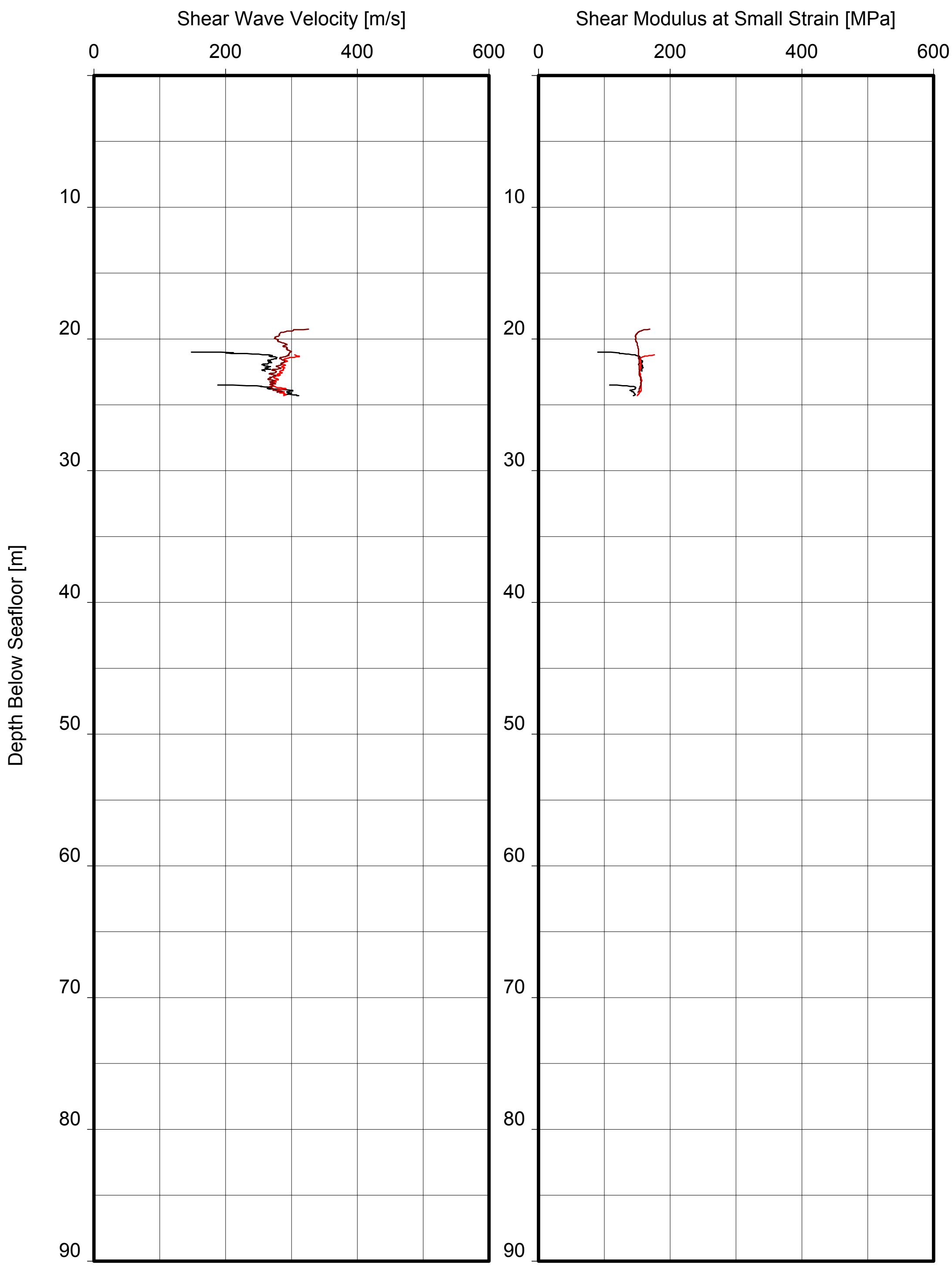


Shear wave velocity ($v_s$) measured in-between geophone array
Shear modulus at small strain ($G_{max}$) derived from $v_s$ measured
$v_s$ and $G_{max}$ derived from CPT

Location(s):
BH-WFS3-5
CPT_WFS3_5
CPT_WFS3_10
CPT_WFS3_11
CPT_WFS3_11A
CPT_WFS3_14
CPT_WFS3_24

Note(s):
- $v_s$ derived from CPT based on Robertson and Cabal (2010)
- $G_{max}$ for clays derived from CPT based on Mayne and Rix (1993)
- $G_{max}$ for sands derived from CPT based on Rix and Stokoe (1991)

GeODin/3.Shear Wave Velocity and Shear Modulus at Small Strain versus Depth (single UNIT, excl. GM).GLO/2015-12-09 14:51:06

**SHEAR WAVE VELOCITY AND SHEAR MODULUS AT SMALL STRAIN VERSUS DEPTH**

UNIT E5

BORSSELE WIND FARM ZONE, WFS III - DUTCH SECTOR, NORTH SEA

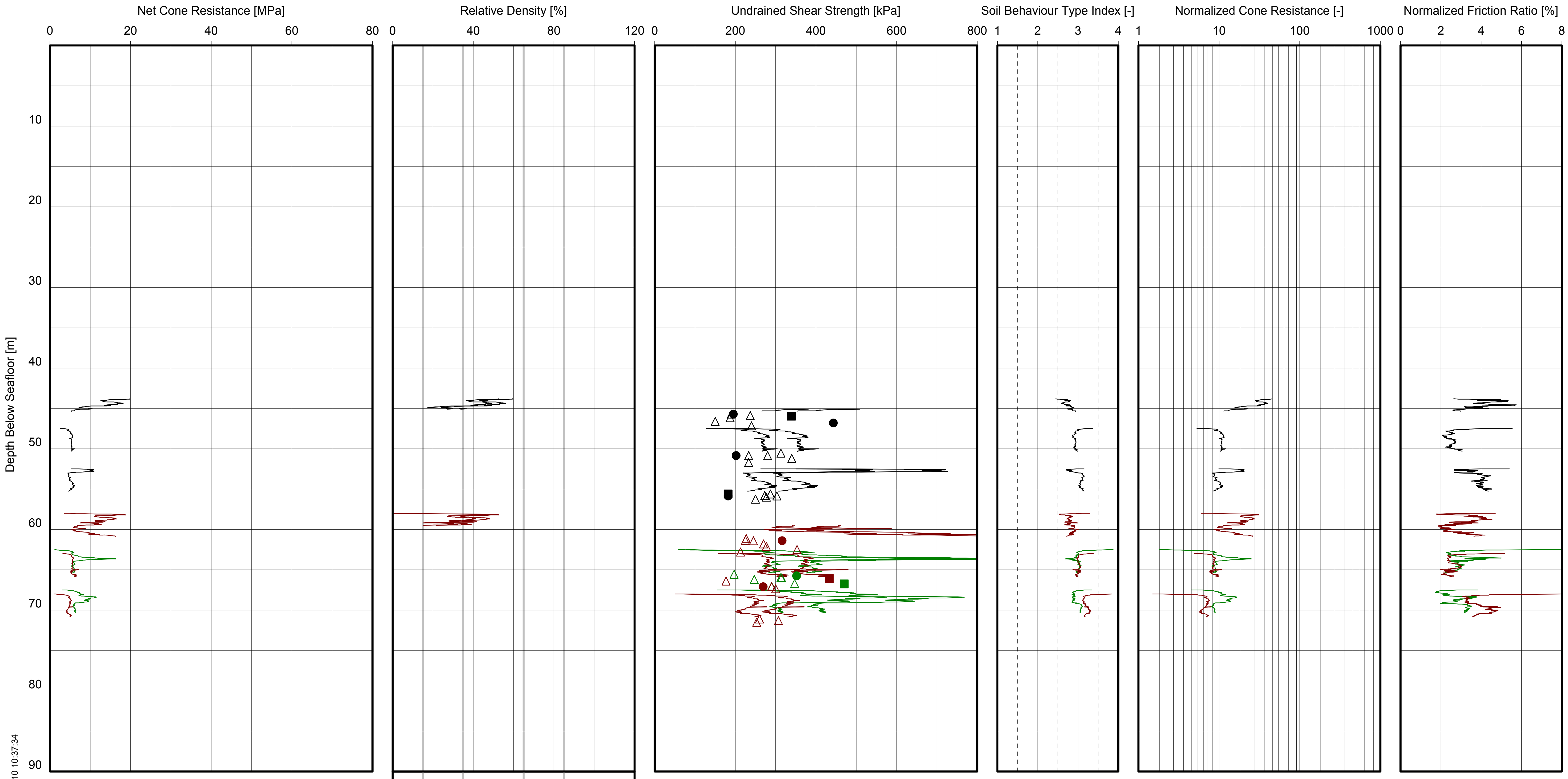


Net cone resistance

Derived from CPT

VL = Very loose
L = Loose
MD = Medium dense
D = Dense
VD = Very dense

Pocket penetrometer
UU-triaxial
CU-triaxial
Derived from CPT

Derived from CPT

Derived from CPT

Derived from CPT

Location(s):

BH-WFS3-6
CPT_WFS3_6
CPT_WFS3_6A
BH-WFS5-1
CPT_WFS5_1
BH-SubStatB-1
CPT_SubStatB_1
CPT_WFS3_9
CPT_WFS3_17
CPT_WFS3_25
CPT_WFS3_26
CPT_WFS3_27

GeODin\1.CPT Parameters vs Depth.GLO/2015-12-10 10:37:34

Note(s):
- $K_0$ = 0.5 and $K_0$ = 1.0 are used to derive relative density from CPT
- $N_k$ = 15 and $N_k$ = 20 are used to derive $c_u$ from CPT
- Soil Behaviour Type Index is according to Robertson (2009), refer to Appendix 1, document titled "Cone Penetration Test Interpretation"

**CPT PARAMETERS AND STRENGTH DATA VERSUS DEPTH**

UNIT F1

BORSSELE WIND FARM ZONE, WFS III - DUTCH SECTOR, NORTH SEA

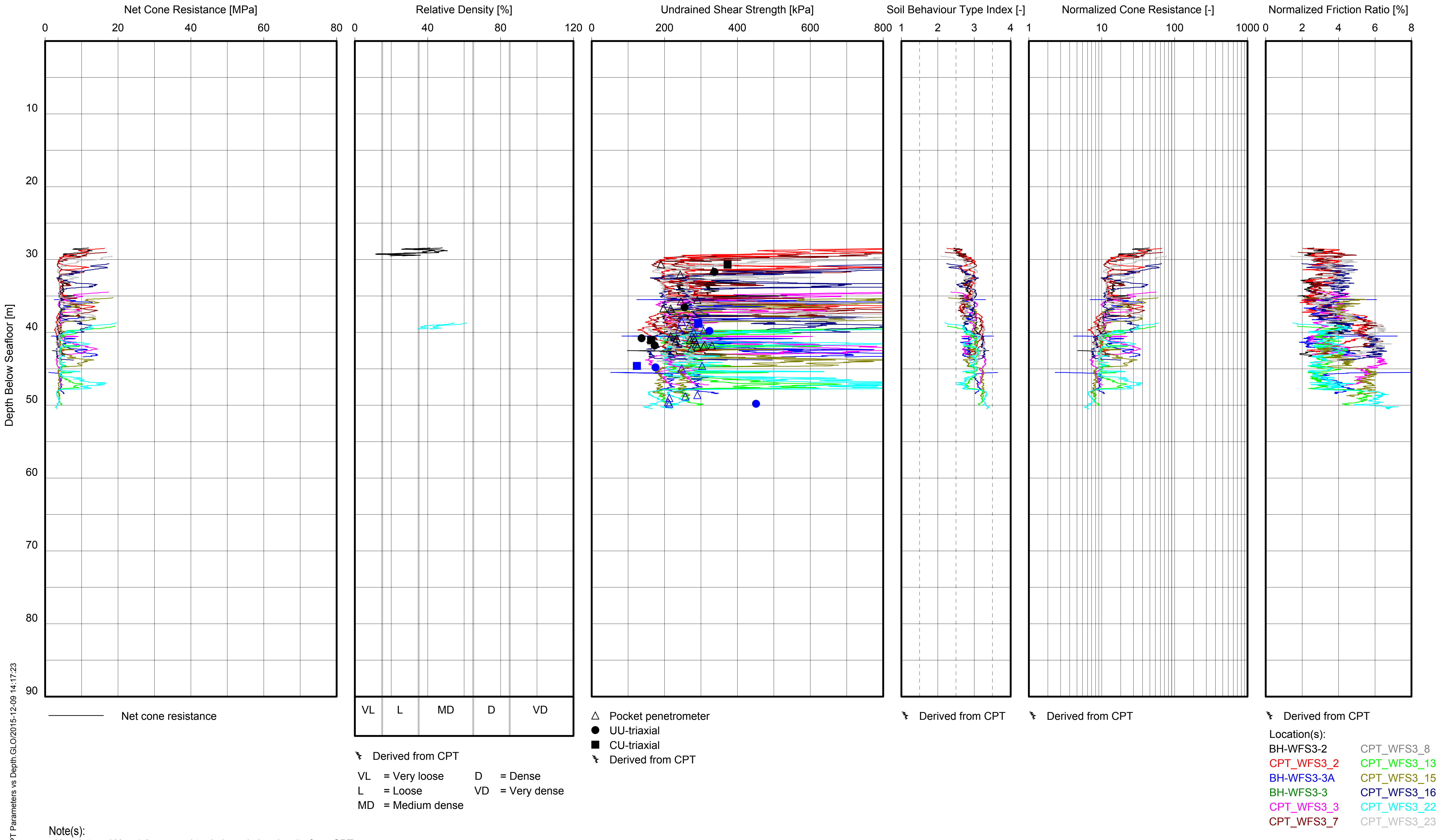


GeODin\1.CPT Parameters vs Depth.GLO/2015-12-09 14:17:23

Note(s):
- $K_0$ = 0.5 and $K_0$ = 1.0 are used to derive relative density from CPT
- $N_k$ = 15 and $N_k$ = 20 are used to derive $c_u$ from CPT
- Soil Behaviour Type Index is according to Robertson (2009), refer to Appendix 1, document titled "Cone Penetration Test Interpretation"

**CPT PARAMETERS AND STRENGTH DATA VERSUS DEPTH**
UNIT F1
BORSSELE WIND FARM ZONE, WFS III - DUTCH SECTOR, NORTH SEA

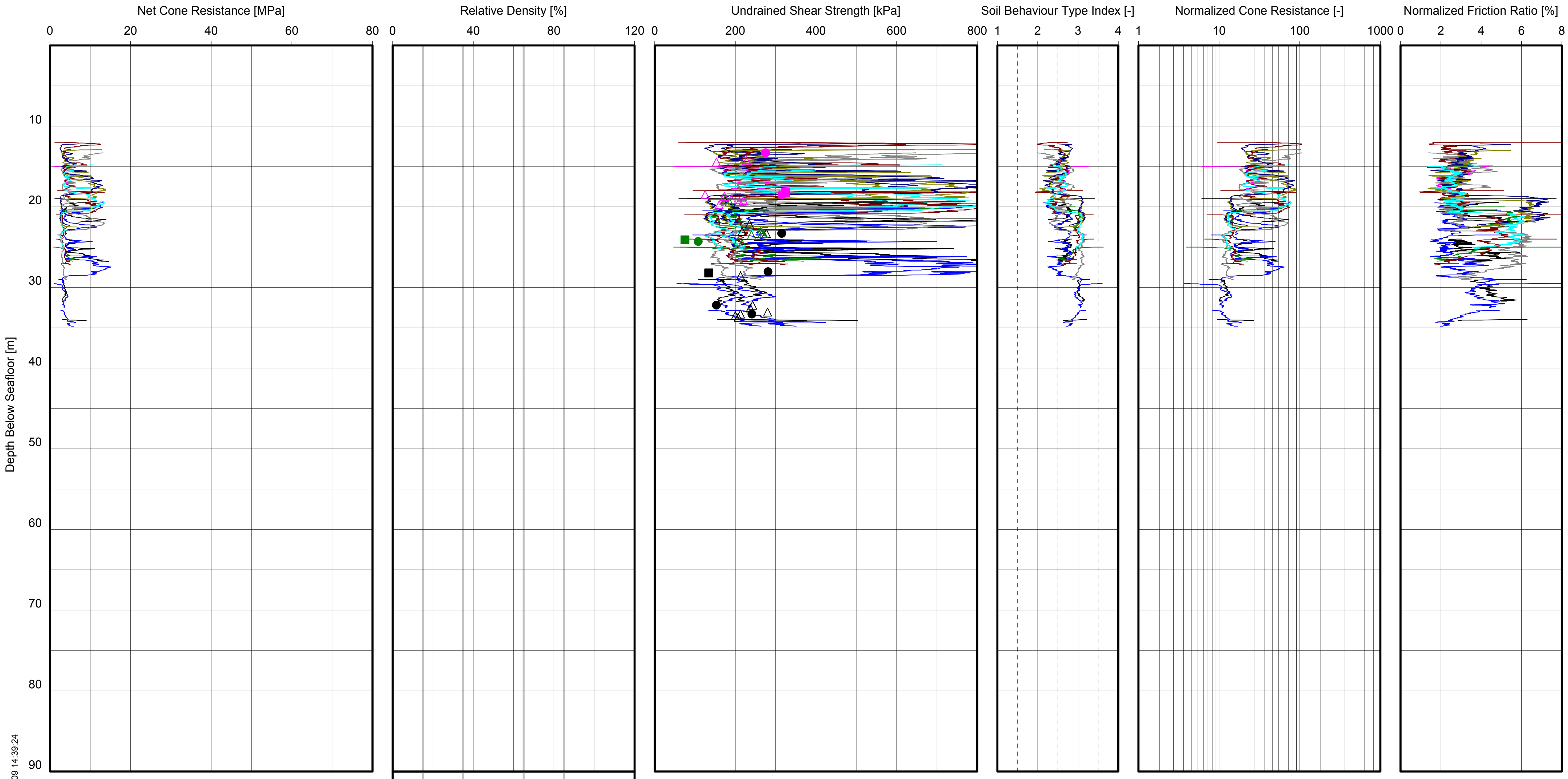


Net cone resistance

Derived from CPT

VL = Very loose
L = Loose
MD = Medium dense
D = Dense
VD = Very dense

Pocket penetrometer
UU-triaxial
CU-triaxial
Derived from CPT

Derived from CPT

Derived from CPT

Derived from CPT

Location(s):

BH-WFS3-1
CPT_WFS3_1
CPT_WFS3_1A
BH-WFS3-4A
BH-WFS3-4
CPT_WFS3_4
CPT_WFS3_12
CPT_WFS3_18
CPT_WFS3_19
CPT_WFS3_20
CPT_WFS3_21

GeODin/1.CPT Parameters vs Depth.GLO/2015-12-09 14:39:24

Note(s):
- $K_0$ = 0.5 and $K_0$ = 1.0 are used to derive relative density from CPT
- $N_k$ = 15 and $N_k$ = 20 are used to derive $c_u$ from CPT
- Soil Behaviour Type Index is according to Robertson (2009), refer to Appendix 1, document titled "Cone Penetration Test Interpretation"

**CPT PARAMETERS AND STRENGTH DATA VERSUS DEPTH**

UNIT F1

BORSSELE WIND FARM ZONE, WFS III - DUTCH SECTOR, NORTH SEA

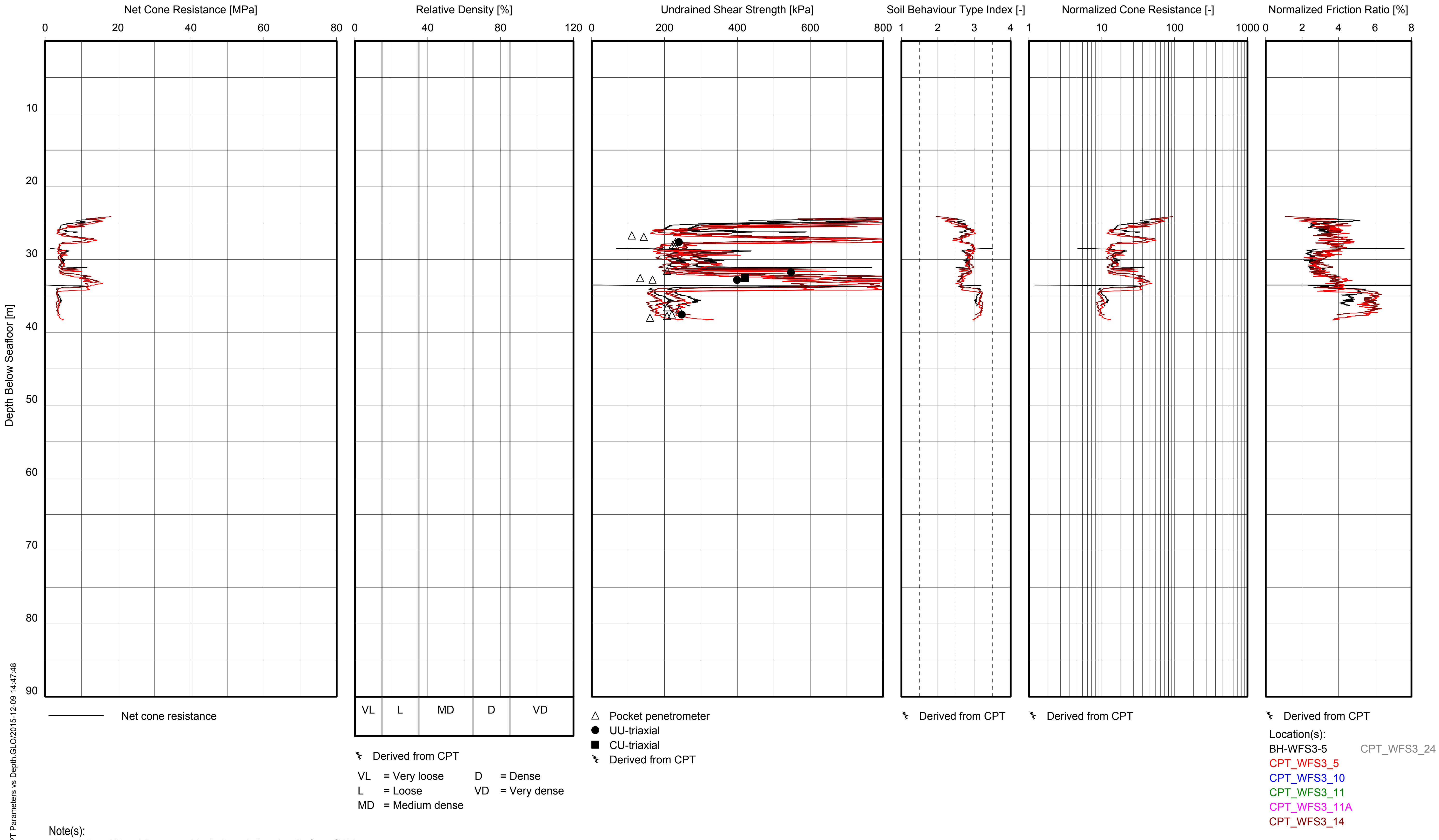


GeODin\1.CPT Parameters vs Depth.GLO/2015-12-09 14:47:48

Note(s):
- $K_0$ = 0.5 and $K_0$ = 1.0 are used to derive relative density from CPT
- $N_k$ = 15 and $N_k$ = 20 are used to derive $c_u$ from CPT
- Soil Behaviour Type Index is according to Robertson (2009), refer to Appendix 1, document titled "Cone Penetration Test Interpretation"

**CPT PARAMETERS AND STRENGTH DATA VERSUS DEPTH**

UNIT F1

BORSSELE WIND FARM ZONE, WFS III - DUTCH SECTOR, NORTH SEA

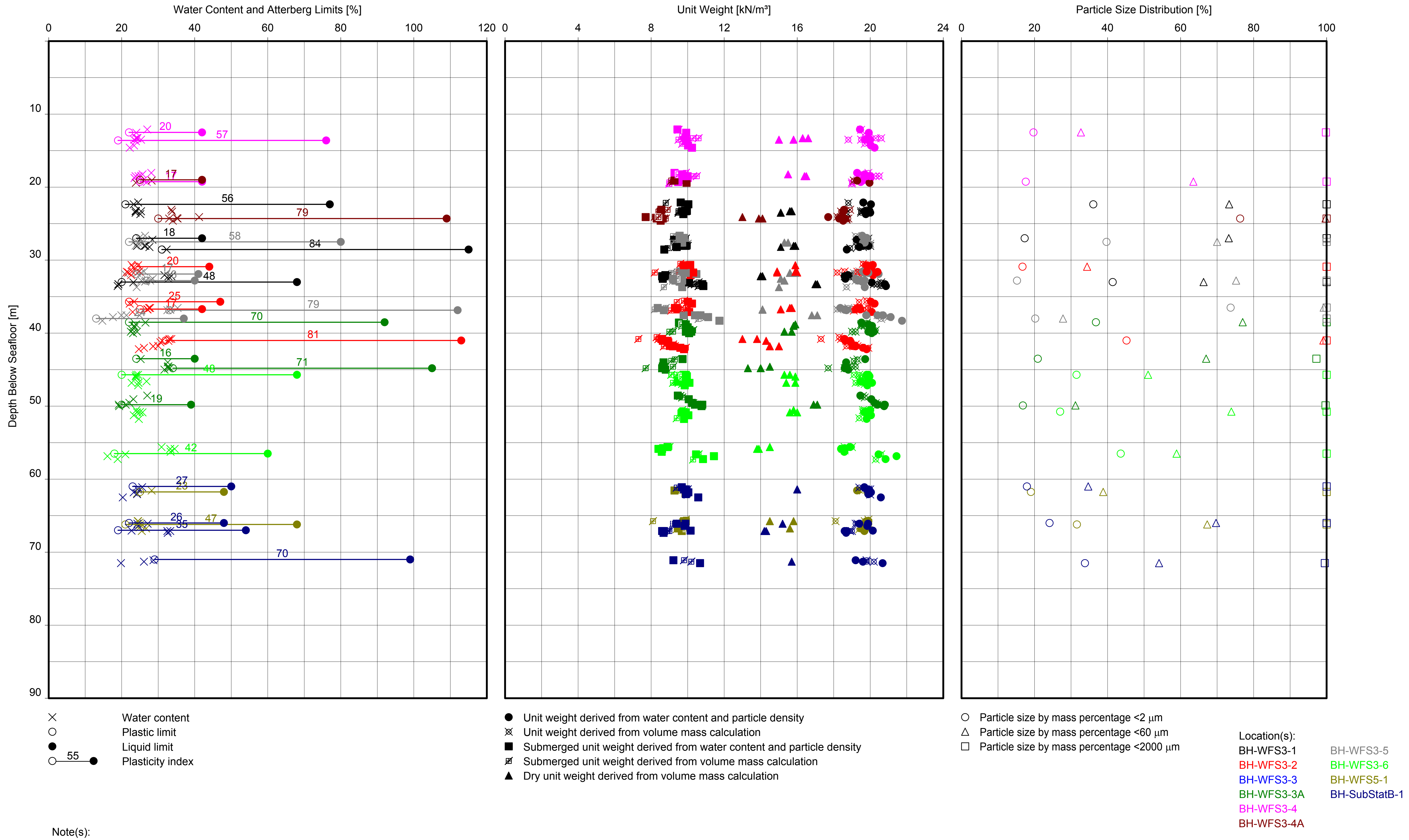


Note(s):
- No dry unit weight is available for unit weight measurements by volume mass calculation on WAX samples.

**WATER CONTENT, UNIT WEIGHT AND PARTICLE SIZE DISTRIBUTION VERSUS DEPTH**

UNIT F1

BORSSELE WIND FARM ZONE, WFS III - DUTCH SECTOR, NORTH SEA

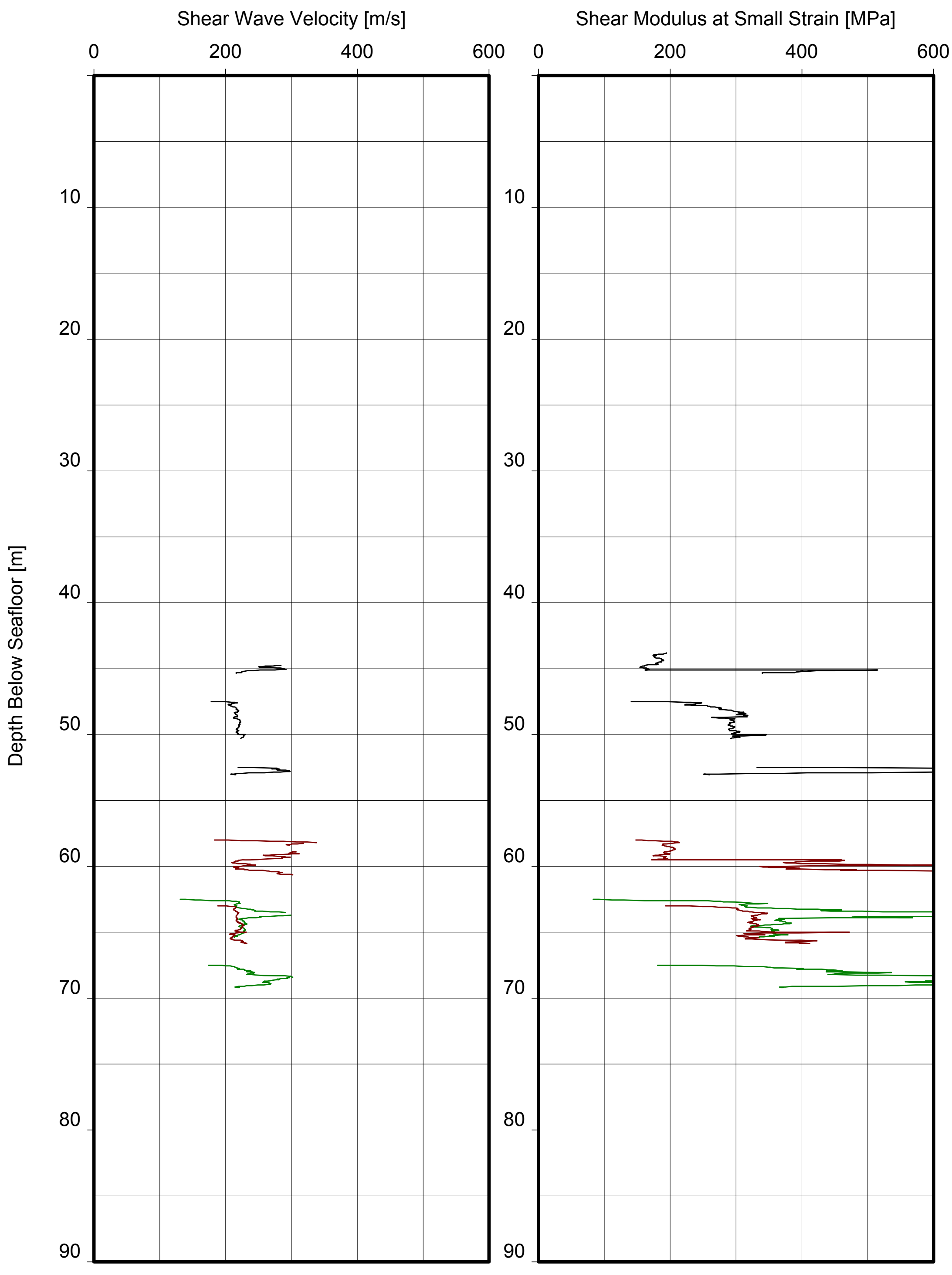


Shear wave velocity ($v_s$) measured in-between geophone array
Shear modulus at small strain ($G_{max}$) derived from $v_s$ measured
$v_s$ and $G_{max}$ derived from CPT

Location(s):
BH-WFS3-6
CPT_WFS3_6
CPT_WFS3_6A
BH-WFS5-1
CPT_WFS5_1
BH-SubStatB-1
CPT_SubStatB_1
CPT_WFS3_9
CPT_WFS3_17
CPT_WFS3_25
CPT_WFS3_26
CPT_WFS3_27

Note(s):
- $v_s$ derived from CPT based on Robertson and Cabal (2010)
- $G_{max}$ for clays derived from CPT based on Mayne and Rix (1993)
- $G_{max}$ for sands derived from CPT based on Rix and Stokoe (1991)

GeODin/3.Shear Wave Velocity and Shear Modulus at Small Strain versus Depth (single UNIT, excl. GM).GLO/2015-12-09 13:29:25

**SHEAR WAVE VELOCITY AND SHEAR MODULUS AT SMALL STRAIN VERSUS DEPTH**

UNIT F1

BORSSELE WIND FARM ZONE, WFS III - DUTCH SECTOR, NORTH SEA

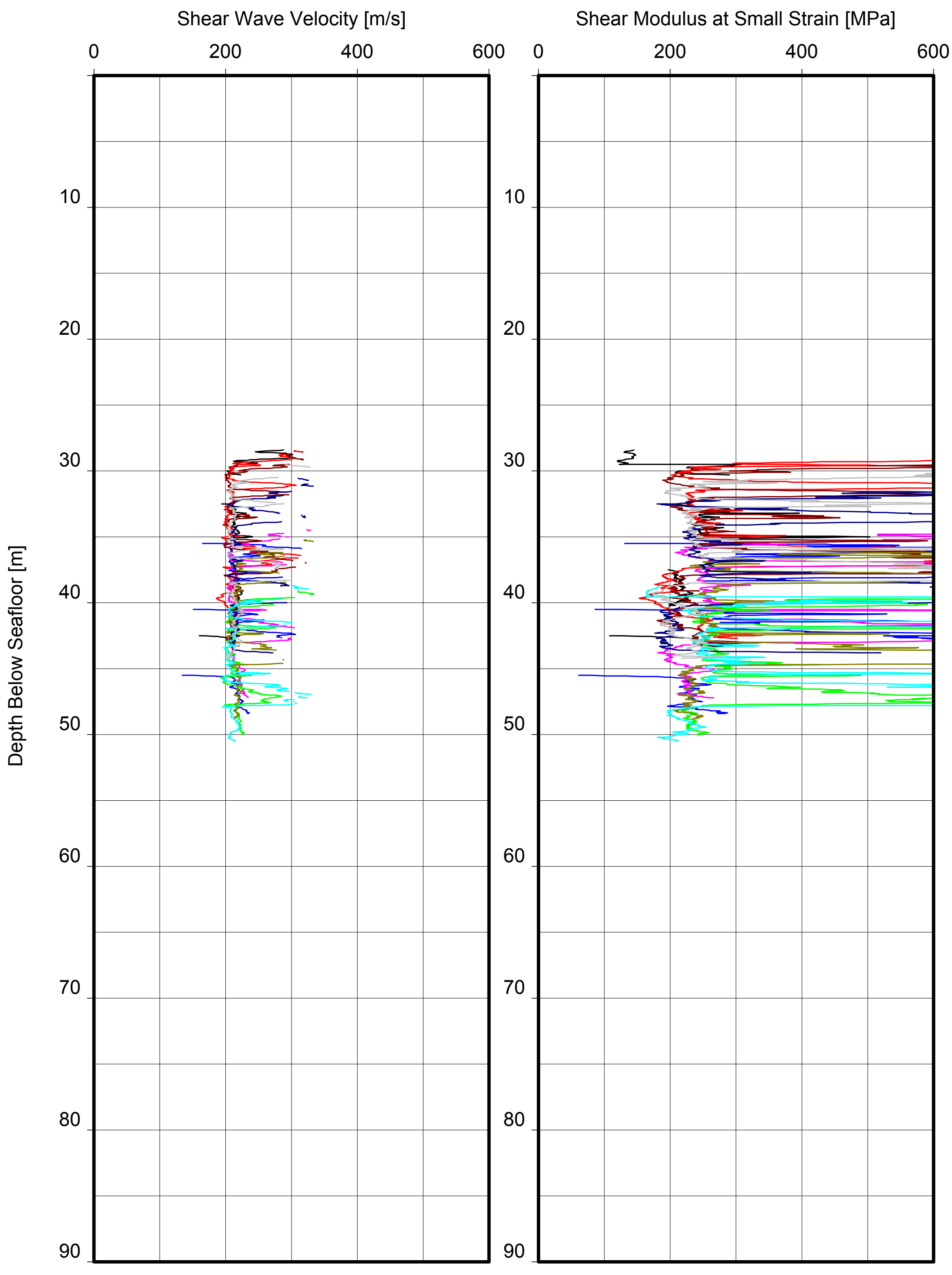


Shear wave velocity ($v_s$) measured in-between geophone array
Shear modulus at small strain ($G_{max}$) derived from $v_s$ measured
$v_s$ and $G_{max}$ derived from CPT

Location(s):
BH-WFS3-2
CPT_WFS3_2
BH-WFS3-3A
BH-WFS3-3
CPT_WFS3_3
CPT_WFS3_7
CPT_WFS3_8
CPT_WFS3_13
CPT_WFS3_15
CPT_WFS3_16
CPT_WFS3_22
CPT_WFS3_23

Note(s):
- $v_s$ derived from CPT based on Robertson and Cabal (2010)
- $G_{max}$ for clays derived from CPT based on Mayne and Rix (1993)
- $G_{max}$ for sands derived from CPT based on Rix and Stokoe (1991)

GeODin/3.Shear Wave Velocity and Shear Modulus at Small Strain versus Depth (single UNIT, excl. GM).GLO/2015-12-09 14:25:42

**SHEAR WAVE VELOCITY AND SHEAR MODULUS AT SMALL STRAIN VERSUS DEPTH**

UNIT F1

BORSSELE WIND FARM ZONE, WFS III - DUTCH SECTOR, NORTH SEA

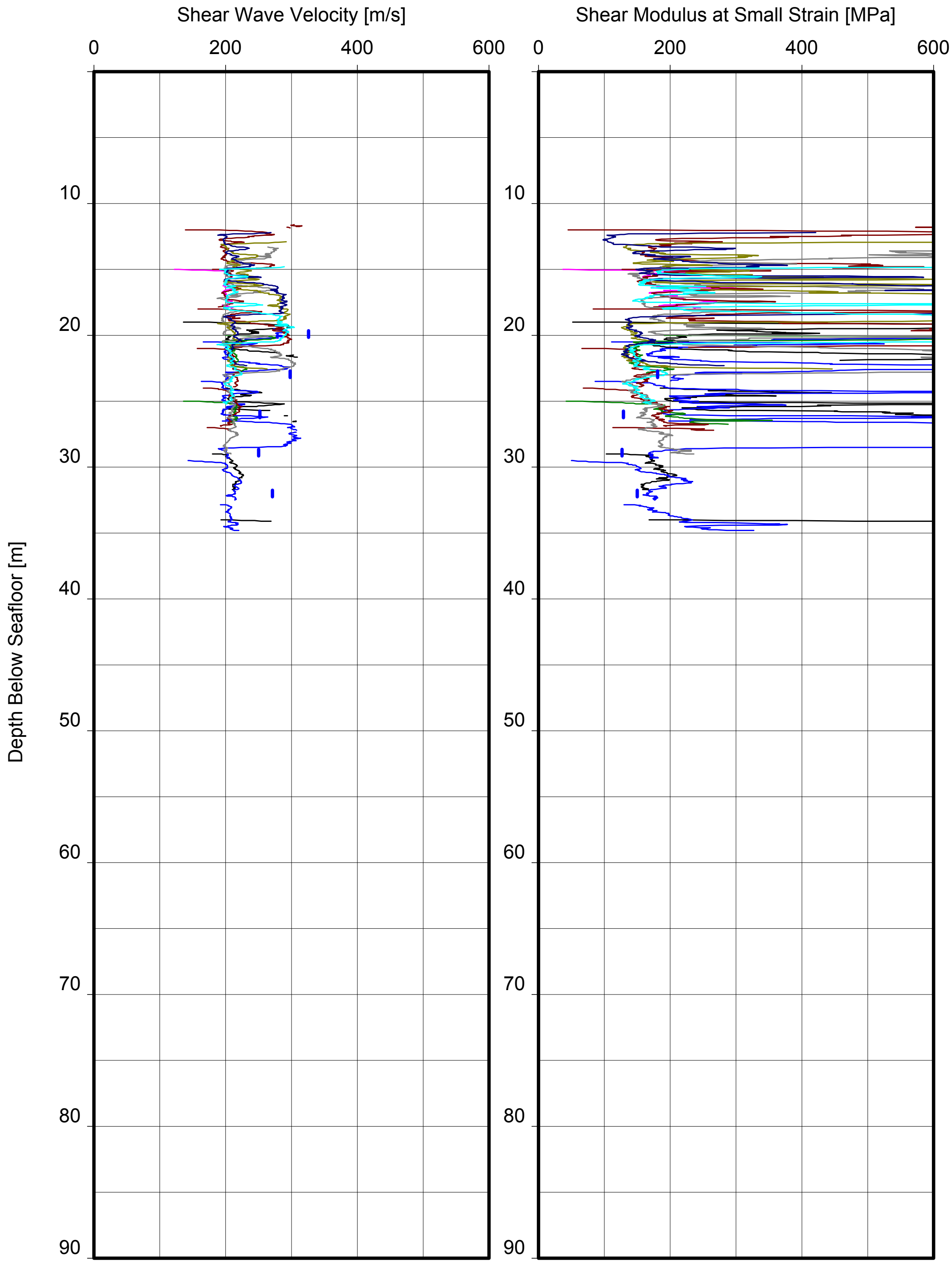


Shear wave velocity ($v_s$) measured in-between geophone array

Shear modulus at small strain ($G_{max}$) derived from $v_s$ measured

$v_s$ and $G_{max}$ derived from CPT

Location(s):

| | |
|---|---|
| BH-WFS3-1 | CPT_WFS3_12 |
| CPT_WFS3_1 | CPT_WFS3_18 |
| CPT_WFS3_1A | CPT_WFS3_19 |
| BH-WFS3-4A | CPT_WFS3_20 |
| BH-WFS3-4 | CPT_WFS3_21 |
| CPT_WFS3_4 | |

Note(s):
- $v_s$ derived from CPT based on Robertson and Cabal (2010)
- $G_{max}$ for clays derived from CPT based on Mayne and Rix (1993)
- $G_{max}$ for sands derived from CPT based on Rix and Stokoe (1991)

GeODin/3.Shear Wave Velocity and Shear Modulus at Small Strain versus Depth (single UNIT, excl. GM).GLO/2015-12-09 14:32:41

**SHEAR WAVE VELOCITY AND SHEAR MODULUS AT SMALL STRAIN VERSUS DEPTH**

UNIT F1

BORSSELE WIND FARM ZONE, WFS III - DUTCH SECTOR, NORTH SEA

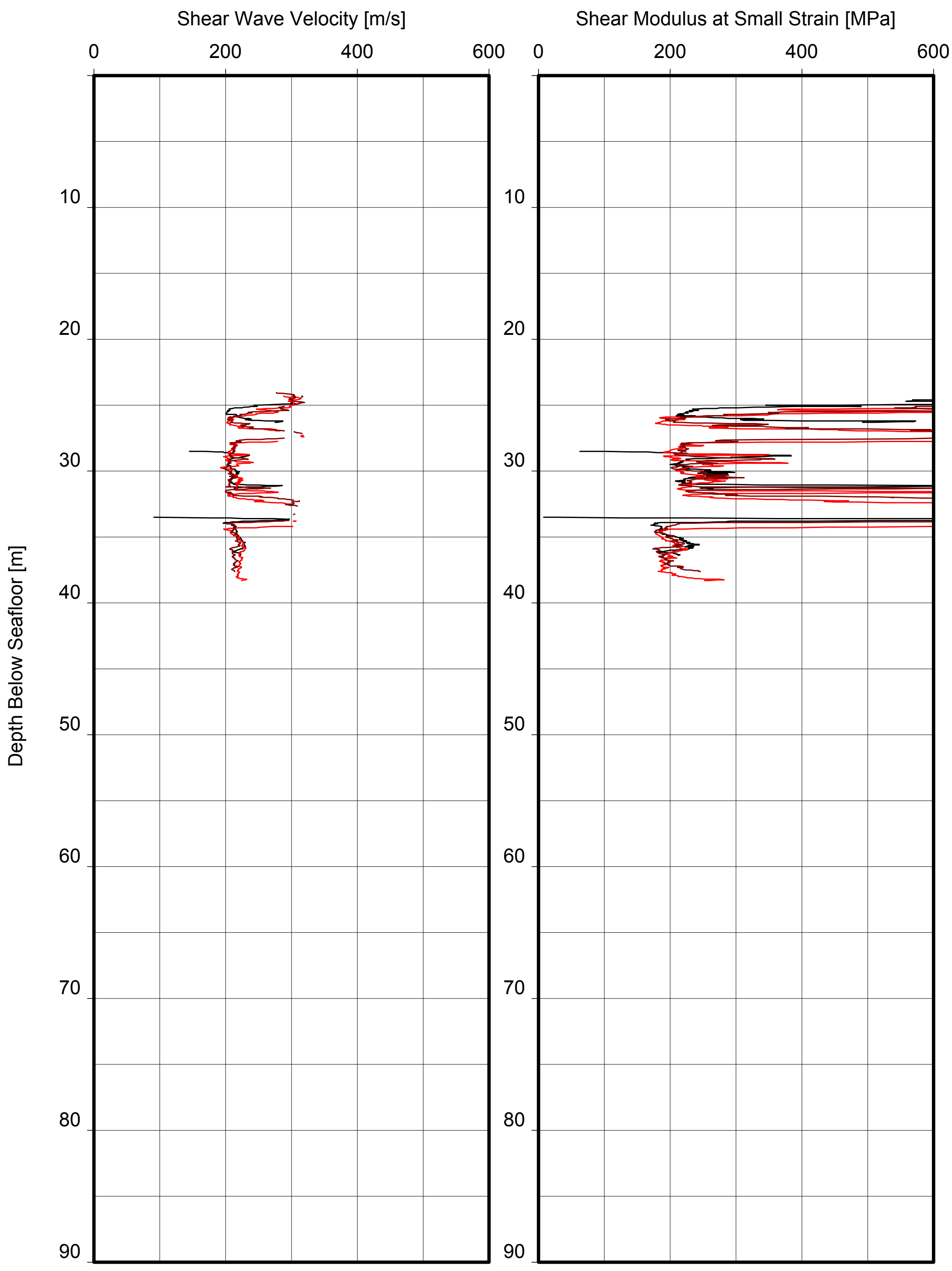


Shear wave velocity ($v_s$) measured in-between geophone array

Shear modulus at small strain ($G_{max}$) derived from $v_s$ measured

$v_s$ and $G_{max}$ derived from CPT

Location(s):
BH-WFS3-5
CPT_WFS3_5
CPT_WFS3_10
CPT_WFS3_11
CPT_WFS3_11A
CPT_WFS3_14
CPT_WFS3_24

Note(s):
- $v_s$ derived from CPT based on Robertson and Cabal (2010)
- $G_{max}$ for clays derived from CPT based on Mayne and Rix (1993)
- $G_{max}$ for sands derived from CPT based on Rix and Stokoe (1991)

GeODin/3.Shear Wave Velocity and Shear Modulus at Small Strain versus Depth (single UNIT, excl. GM).GLO/2015-12-09 14:50:29

**SHEAR WAVE VELOCITY AND SHEAR MODULUS AT SMALL STRAIN VERSUS DEPTH**

UNIT F1

BORSSELE WIND FARM ZONE, WFS III - DUTCH SECTOR, NORTH SEA

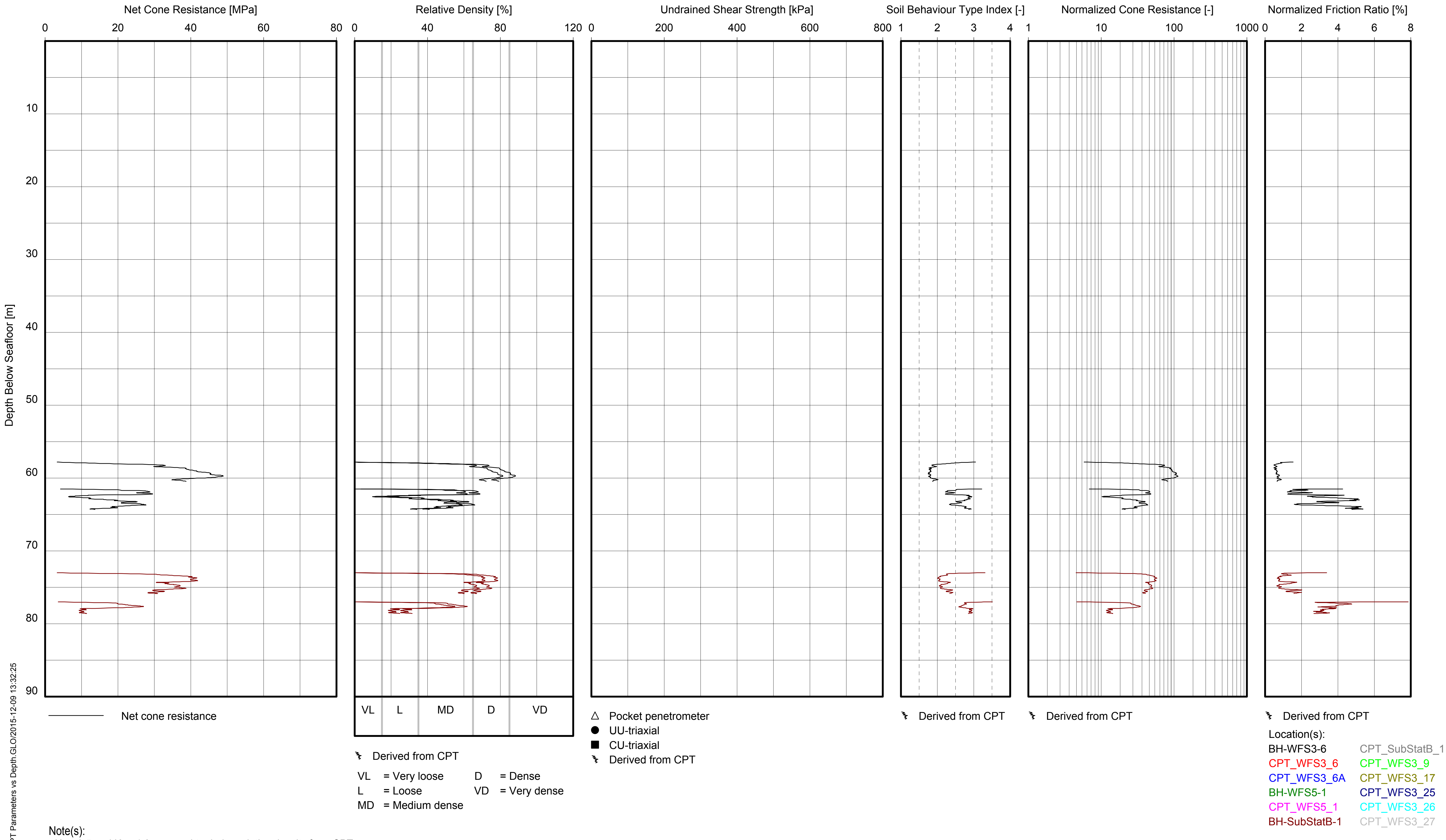


GeODin/1.CPT Parameters vs Depth.GLO/2015-12-09 13:32:25

Note(s):
- $K_0$ = 0.5 and $K_0$ = 1.0 are used to derive relative density from CPT
- $N_k$ = 15 and $N_k$ = 20 are used to derive $c_u$ from CPT
- Soil Behaviour Type Index is according to Robertson (2009), refer to Appendix 1, document titled "Cone Penetration Test Interpretation"

**CPT PARAMETERS AND STRENGTH DATA VERSUS DEPTH**
UNIT F2
BORSSELE WIND FARM ZONE, WFS III - DUTCH SECTOR, NORTH SEA

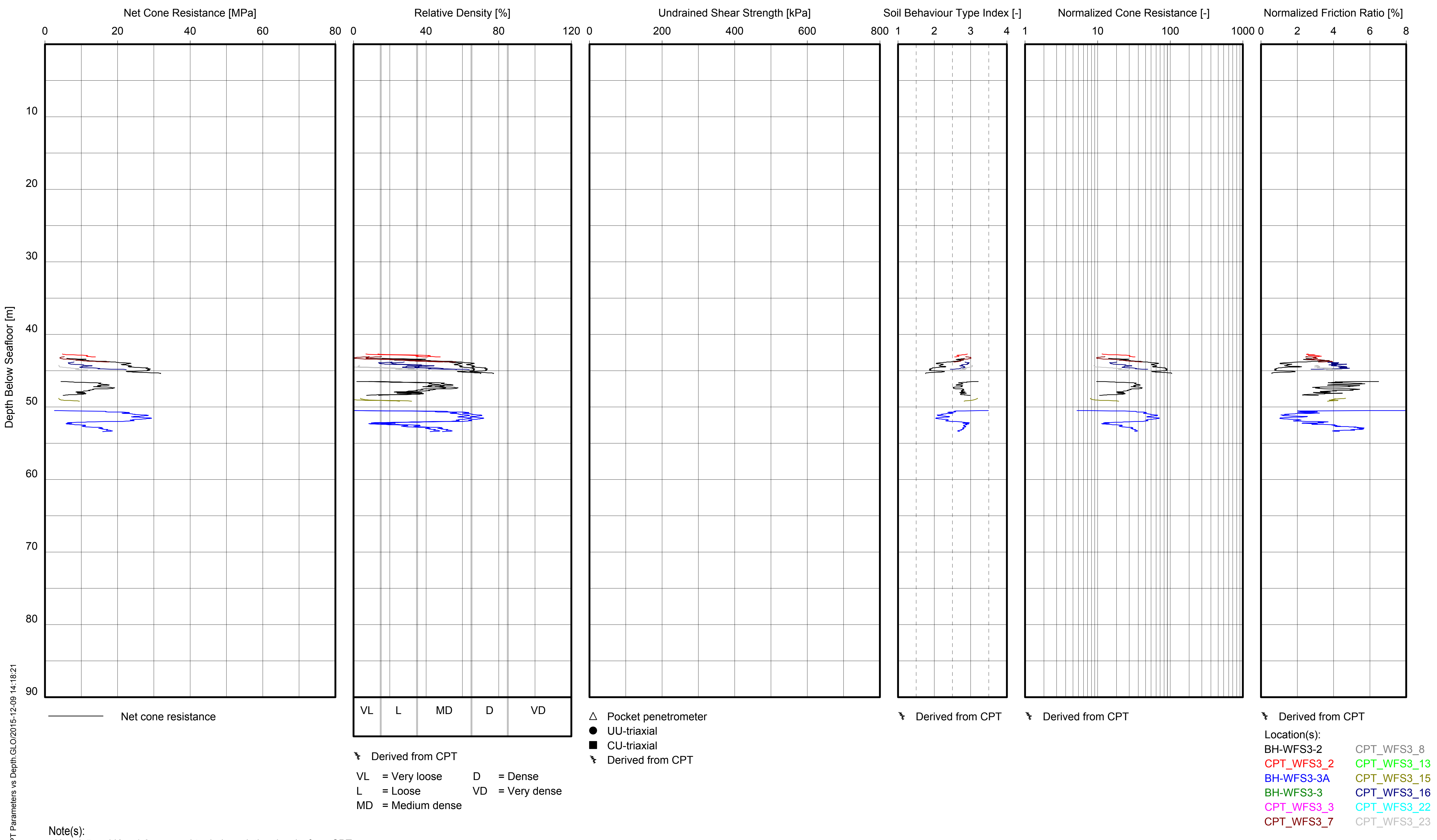


GeODin/1.CPT Parameters vs Depth.GLO/2015-12-09 14:18:21

Note(s):
- $K_0$ = 0.5 and $K_0$ = 1.0 are used to derive relative density from CPT
- $N_k$ = 15 and $N_k$ = 20 are used to derive $c_u$ from CPT
- Soil Behaviour Type Index is according to Robertson (2009), refer to Appendix 1, document titled "Cone Penetration Test Interpretation"

**CPT PARAMETERS AND STRENGTH DATA VERSUS DEPTH**
UNIT F2
BORSSELE WIND FARM ZONE, WFS III - DUTCH SECTOR, NORTH SEA

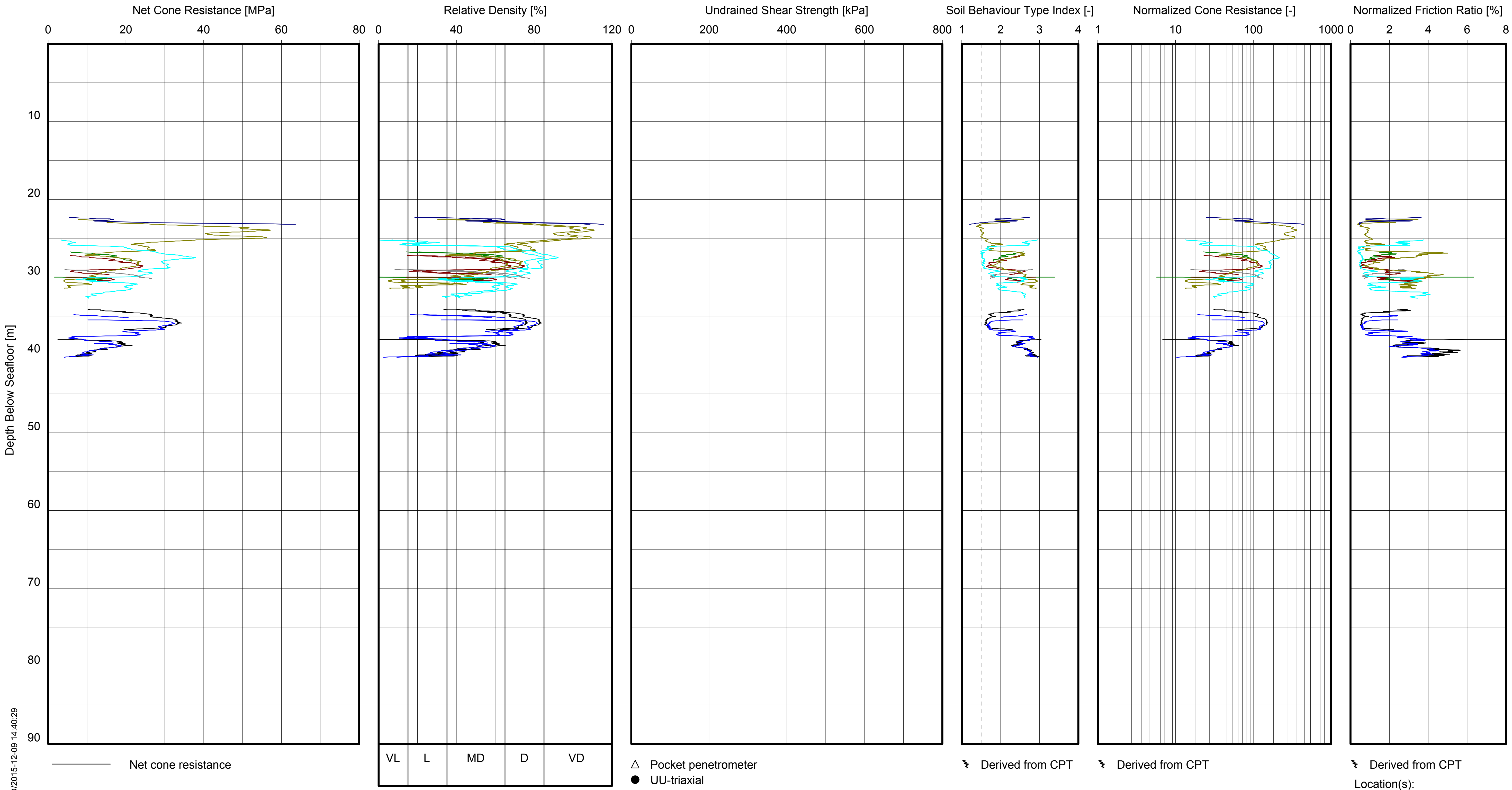


Net cone resistance

Derived from CPT

VL = Very loose
L = Loose
MD = Medium dense
D = Dense
VD = Very dense

△ Pocket penetrometer
● UU-triaxial
■ CU-triaxial
Derived from CPT

Derived from CPT

Derived from CPT

Derived from CPT

Location(s):

| | |
|---|---|
| BH-WFS3-1 | CPT_WFS3_12 |
| CPT_WFS3_1 | CPT_WFS3_18 |
| CPT_WFS3_1A | CPT_WFS3_19 |
| BH-WFS3-4A | CPT_WFS3_20 |
| BH-WFS3-4 | CPT_WFS3_21 |
| CPT_WFS3_4 | |

Note(s):
- $K_0$ = 0.5 and $K_0$ = 1.0 are used to derive relative density from CPT
- $N_k$ = 15 and $N_k$ = 20 are used to derive $c_u$ from CPT
- Soil Behaviour Type Index is according to Robertson (2009), refer to Appendix 1, document titled "Cone Penetration Test Interpretation"

GeODin/1.CPT Parameters vs Depth.GLO/2015-12-09 14:40:29

**CPT PARAMETERS AND STRENGTH DATA VERSUS DEPTH**
UNIT F2
BORSSELE WIND FARM ZONE, WFS III - DUTCH SECTOR, NORTH SEA

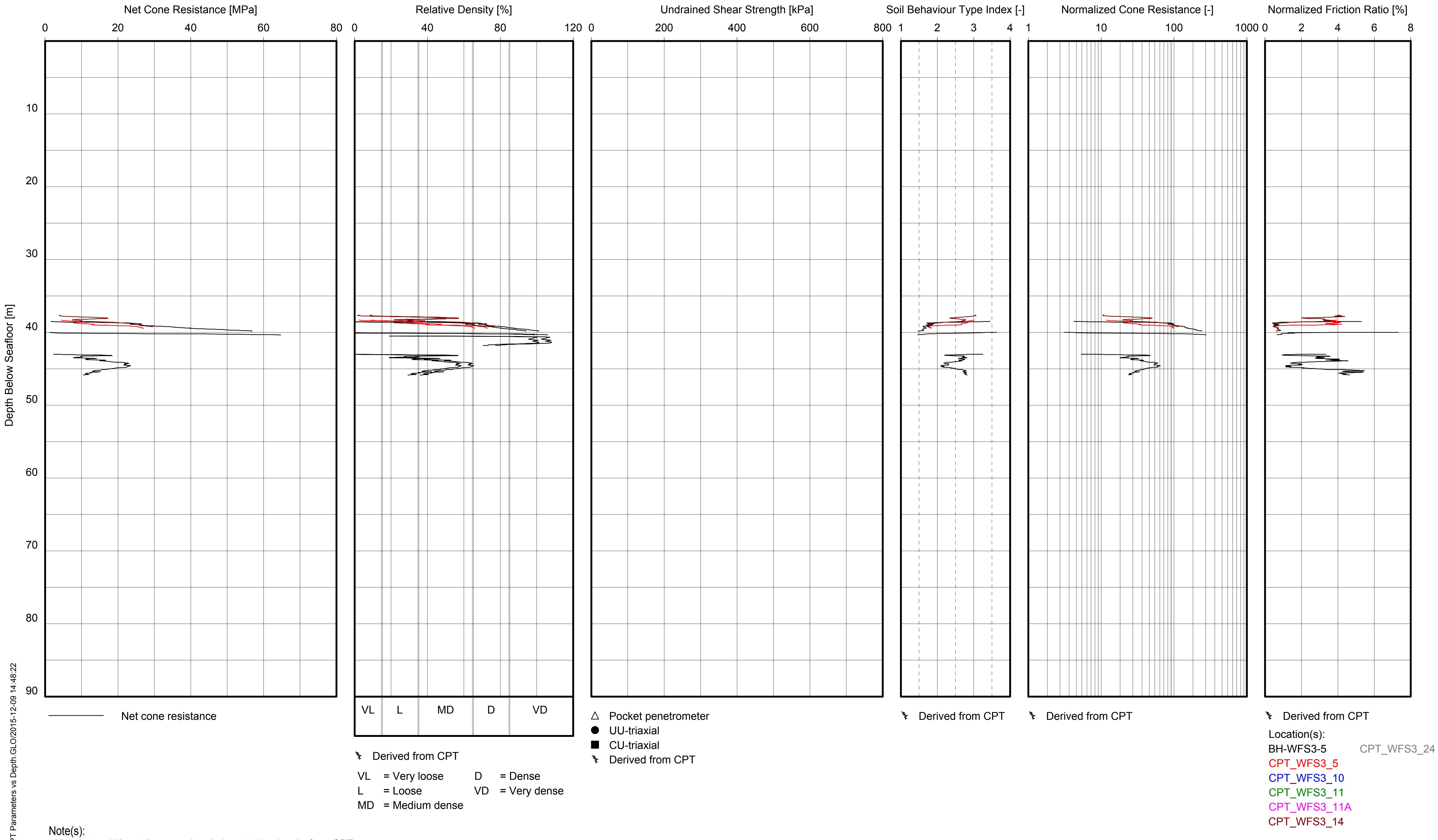


GeODin/1.CPT Parameters vs Depth.GLO/2015-12-09 14:48:22

Note(s):
- $K_0$ = 0.5 and $K_0$ = 1.0 are used to derive relative density from CPT
- $N_k$ = 15 and $N_k$ = 20 are used to derive $c_u$ from CPT
- Soil Behaviour Type Index is according to Robertson (2009), refer to Appendix 1, document titled "Cone Penetration Test Interpretation"

**CPT PARAMETERS AND STRENGTH DATA VERSUS DEPTH**

UNIT F2

BORSSELE WIND FARM ZONE, WFS III - DUTCH SECTOR, NORTH SEA

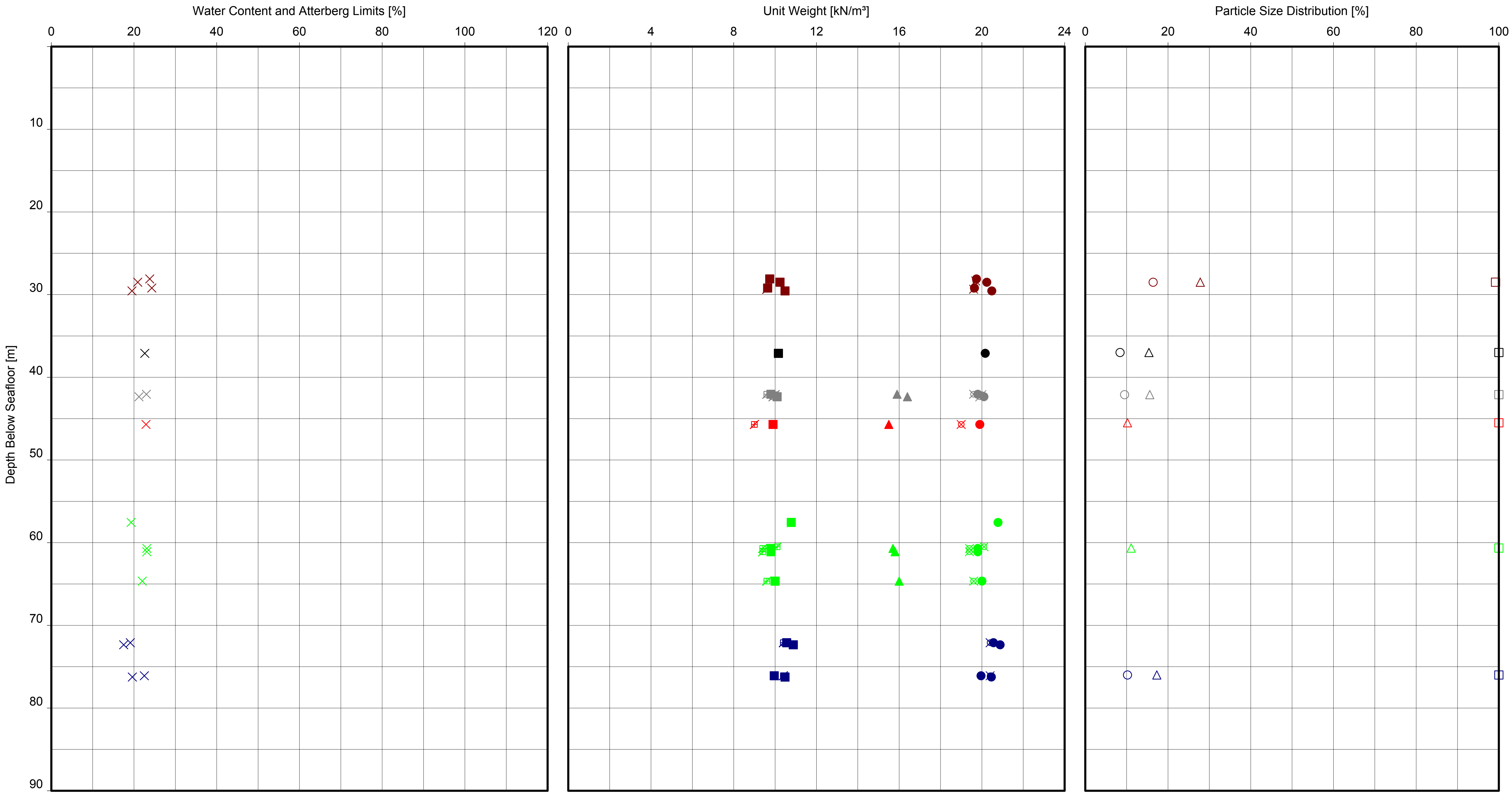


× Water content
○ Plastic limit
● Liquid limit
○—55—● Plasticity index

● Unit weight derived from water content and particle density
Unit weight derived from volume mass calculation
■ Submerged unit weight derived from water content and particle density
Submerged unit weight derived from volume mass calculation
▲ Dry unit weight derived from volume mass calculation

○ Particle size by mass percentage <2 µm
△ Particle size by mass percentage <60 µm
□ Particle size by mass percentage <2000 µm

Location(s):
BH-WFS3-1
BH-WFS3-2
BH-WFS3-3
BH-WFS3-3A
BH-WFS3-4
BH-WFS3-4A
BH-WFS3-5
BH-WFS3-6
BH-WFS5-1
BH-SubStatB-1

Note(s):
- No dry unit weight is available for unit weight measurements by volume mass calculation on WAX samples.

GeODin/2:Water Content, Unit Weight And Particle Size Distribution vs Depth.GLO/2015-12-09 13:50:44

**WATER CONTENT, UNIT WEIGHT AND PARTICLE SIZE DISTRIBUTION VERSUS DEPTH**
UNIT F2
BORSSELE WIND FARM ZONE, WFS III - DUTCH SECTOR, NORTH SEA

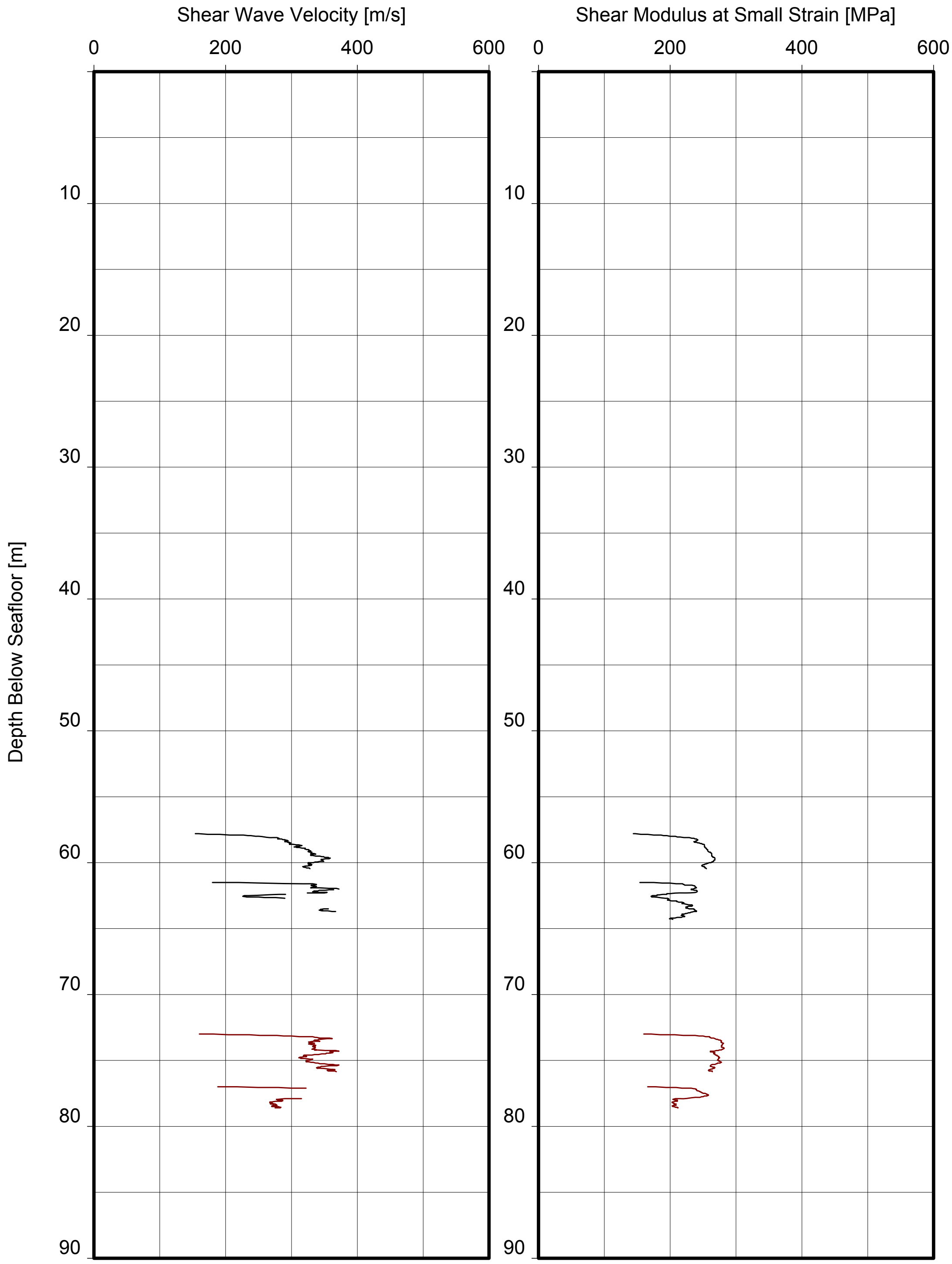


Shear wave velocity ($v_s$) measured in-between geophone array
Shear modulus at small strain ($G_{max}$) derived from $v_s$ measured
$v_s$ and $G_{max}$ derived from CPT

Location(s):
BH-WFS3-6
CPT_WFS3_6
CPT_WFS3_6A
BH-WFS5-1
CPT_WFS5_1
BH-SubStatB-1
CPT_SubStatB_1
CPT_WFS3_9
CPT_WFS3_17
CPT_WFS3_25
CPT_WFS3_26
CPT_WFS3_27

Note(s):
- $v_s$ derived from CPT based on Robertson and Cabal (2010)
- $G_{max}$ for clays derived from CPT based on Mayne and Rix (1993)
- $G_{max}$ for sands derived from CPT based on Rix and Stokoe (1991)

GeODin/3.Shear Wave Velocity and Shear Modulus at Small Strain versus Depth (single UNIT, excl. GM).GLO/2015-12-09 13:30:31

**SHEAR WAVE VELOCITY AND SHEAR MODULUS AT SMALL STRAIN VERSUS DEPTH**

UNIT F2

BORSSELE WIND FARM ZONE, WFS III - DUTCH SECTOR, NORTH SEA

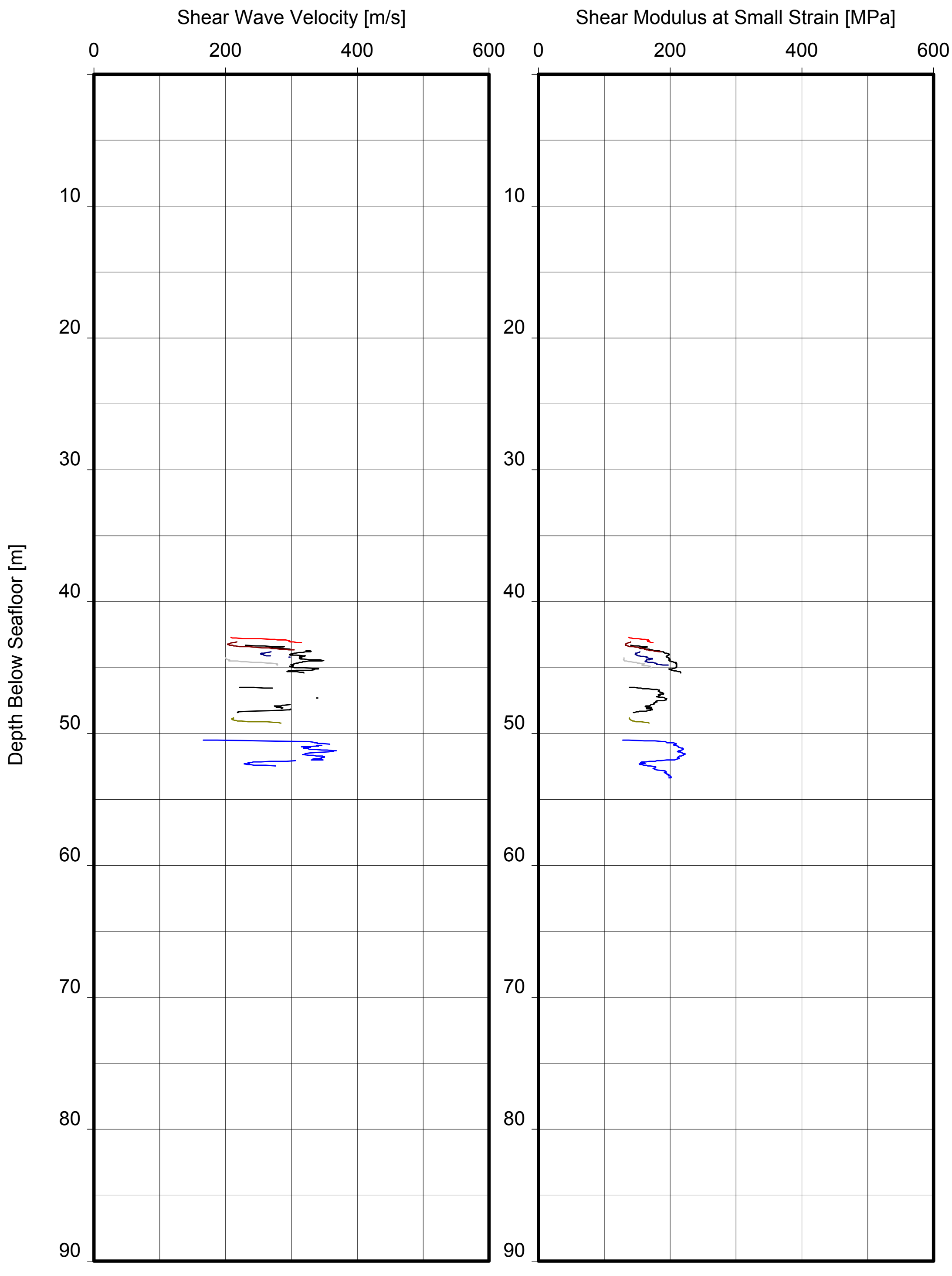


Shear wave velocity ($v_s$) measured in-between geophone array
Shear modulus at small strain ($G_{max}$) derived from $v_s$ measured
$v_s$ and $G_{max}$ derived from CPT

Location(s):
BH-WFS3-2
CPT_WFS3_2
BH-WFS3-3A
BH-WFS3-3
CPT_WFS3_3
CPT_WFS3_7
CPT_WFS3_8
CPT_WFS3_13
CPT_WFS3_15
CPT_WFS3_16
CPT_WFS3_22
CPT_WFS3_23

Note(s):
- $v_s$ derived from CPT based on Robertson and Cabal (2010)
- $G_{max}$ for clays derived from CPT based on Mayne and Rix (1993)
- $G_{max}$ for sands derived from CPT based on Rix and Stokoe (1991)

GeODin/3.Shear Wave Velocity and Shear Modulus at Small Strain versus Depth (single UNIT, excl. GM).GLO/2015-12-09 14:26:30

**SHEAR WAVE VELOCITY AND SHEAR MODULUS AT SMALL STRAIN VERSUS DEPTH**

UNIT F2

BORSSELE WIND FARM ZONE, WFS III - DUTCH SECTOR, NORTH SEA

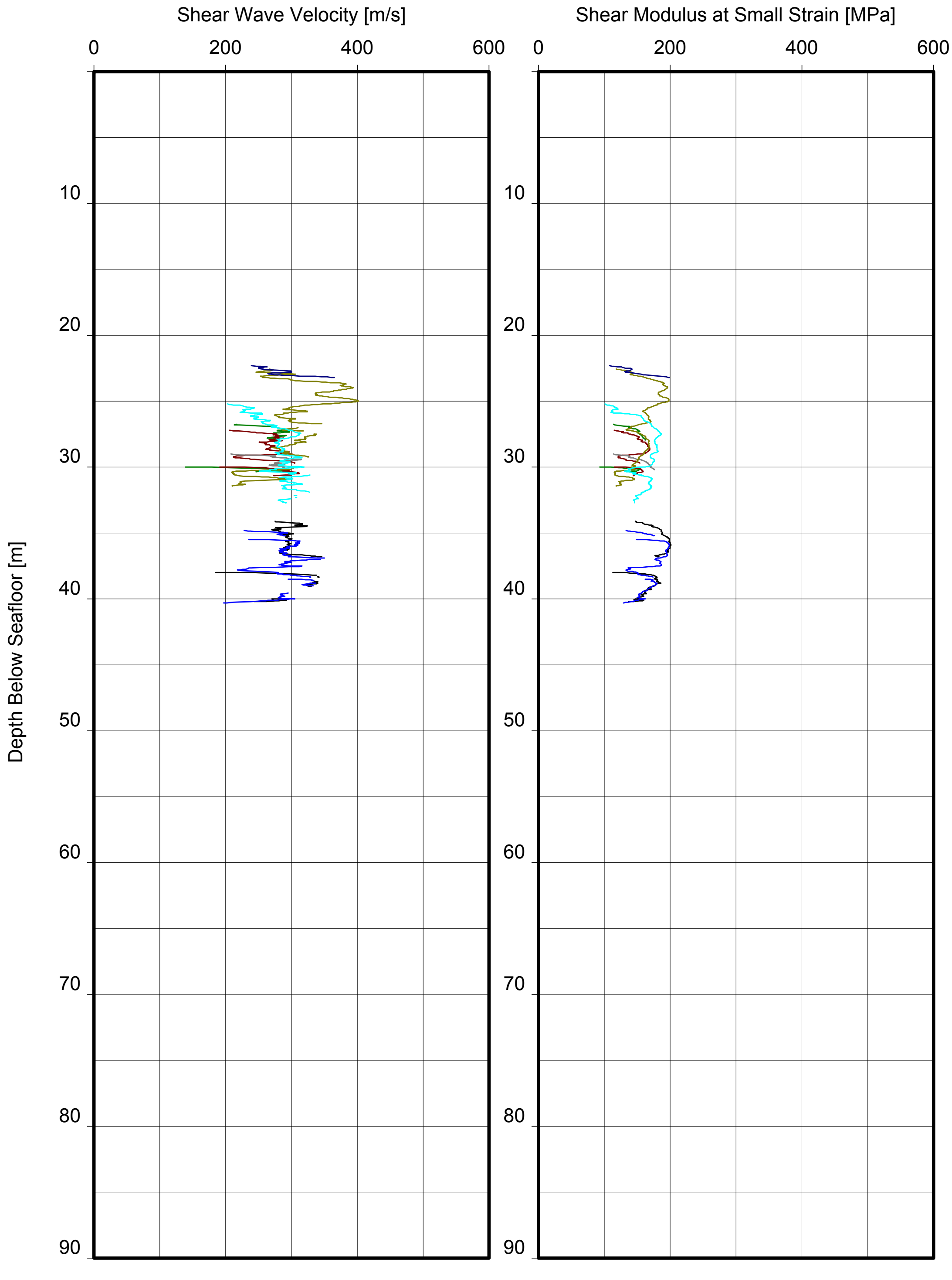


Shear wave velocity ($v_s$) measured in-between geophone array
Shear modulus at small strain ($G_{max}$) derived from $v_s$ measured
$v_s$ and $G_{max}$ derived from CPT

Location(s):
BH-WFS3-1
CPT_WFS3_1
CPT_WFS3_1A
BH-WFS3-4A
BH-WFS3-4
CPT_WFS3_4
CPT_WFS3_12
CPT_WFS3_18
CPT_WFS3_19
CPT_WFS3_20
CPT_WFS3_21

Note(s):
- $v_s$ derived from CPT based on Robertson and Cabal (2010)
- $G_{max}$ for clays derived from CPT based on Mayne and Rix (1993)
- $G_{max}$ for sands derived from CPT based on Rix and Stokoe (1991)

GeODin/3.Shear Wave Velocity and Shear Modulus at Small Strain versus Depth (single UNIT, excl. GM).GLO/2015-12-09 14:33:28

**SHEAR WAVE VELOCITY AND SHEAR MODULUS AT SMALL STRAIN VERSUS DEPTH**
UNIT F2
BORSSELE WIND FARM ZONE, WFS III - DUTCH SECTOR, NORTH SEA

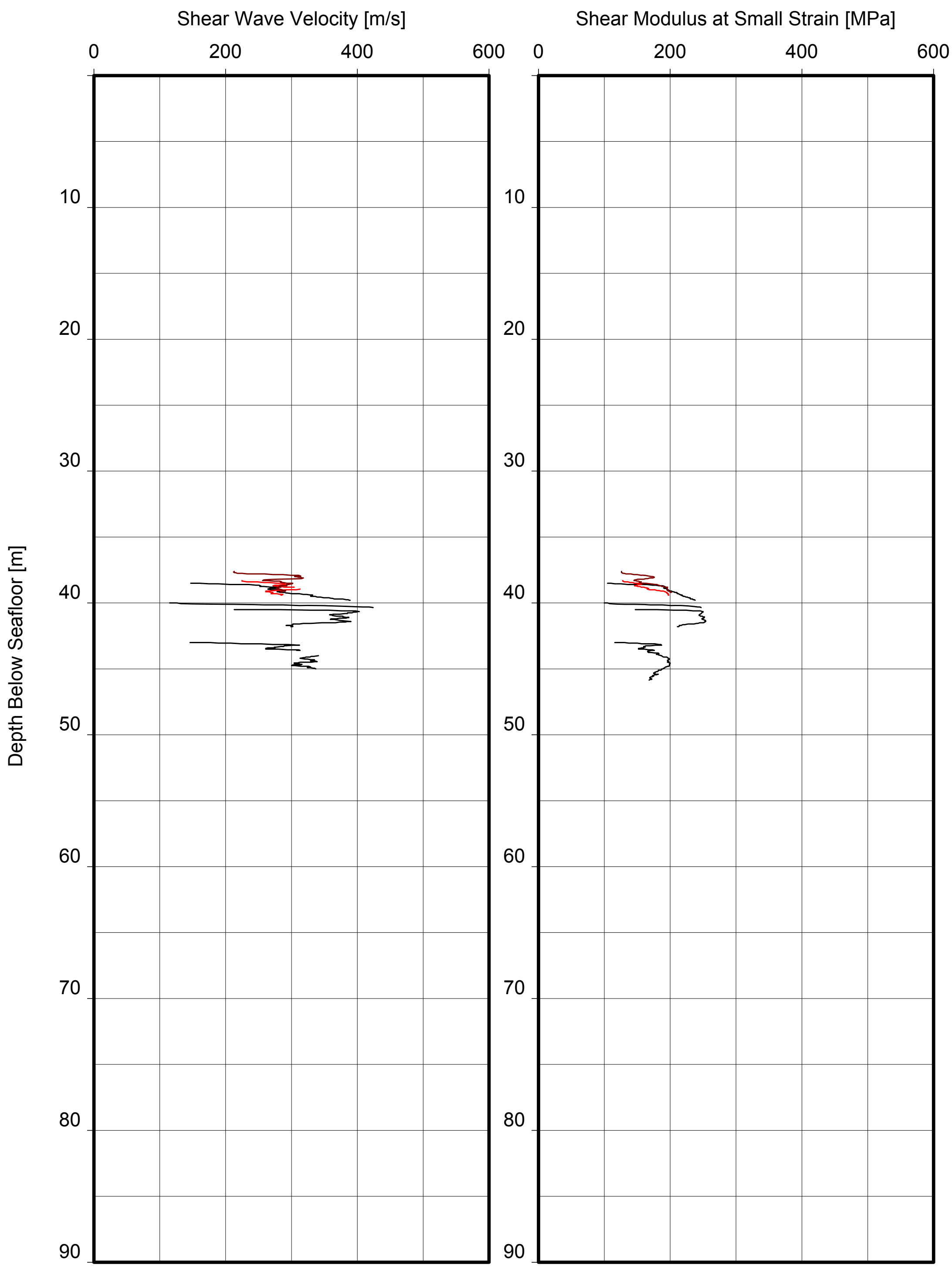


Shear wave velocity ($v_s$) measured in-between geophone array
Shear modulus at small strain ($G_{max}$) derived from $v_s$ measured
$v_s$ and $G_{max}$ derived from CPT

Location(s):
BH-WFS3-5
CPT_WFS3_5
CPT_WFS3_10
CPT_WFS3_11
CPT_WFS3_11A
CPT_WFS3_14
CPT_WFS3_24

Note(s):
- $v_s$ derived from CPT based on Robertson and Cabal (2010)
- $G_{max}$ for clays derived from CPT based on Mayne and Rix (1993)
- $G_{max}$ for sands derived from CPT based on Rix and Stokoe (1991)

GeODin/3.Shear Wave Velocity and Shear Modulus at Small Strain versus Depth (single UNIT, excl. GM).GLO/2015-12-09 14:49:51

**SHEAR WAVE VELOCITY AND SHEAR MODULUS AT SMALL STRAIN VERSUS DEPTH**

UNIT F2

BORSSELE WIND FARM ZONE, WFS III - DUTCH SECTOR, NORTH SEA

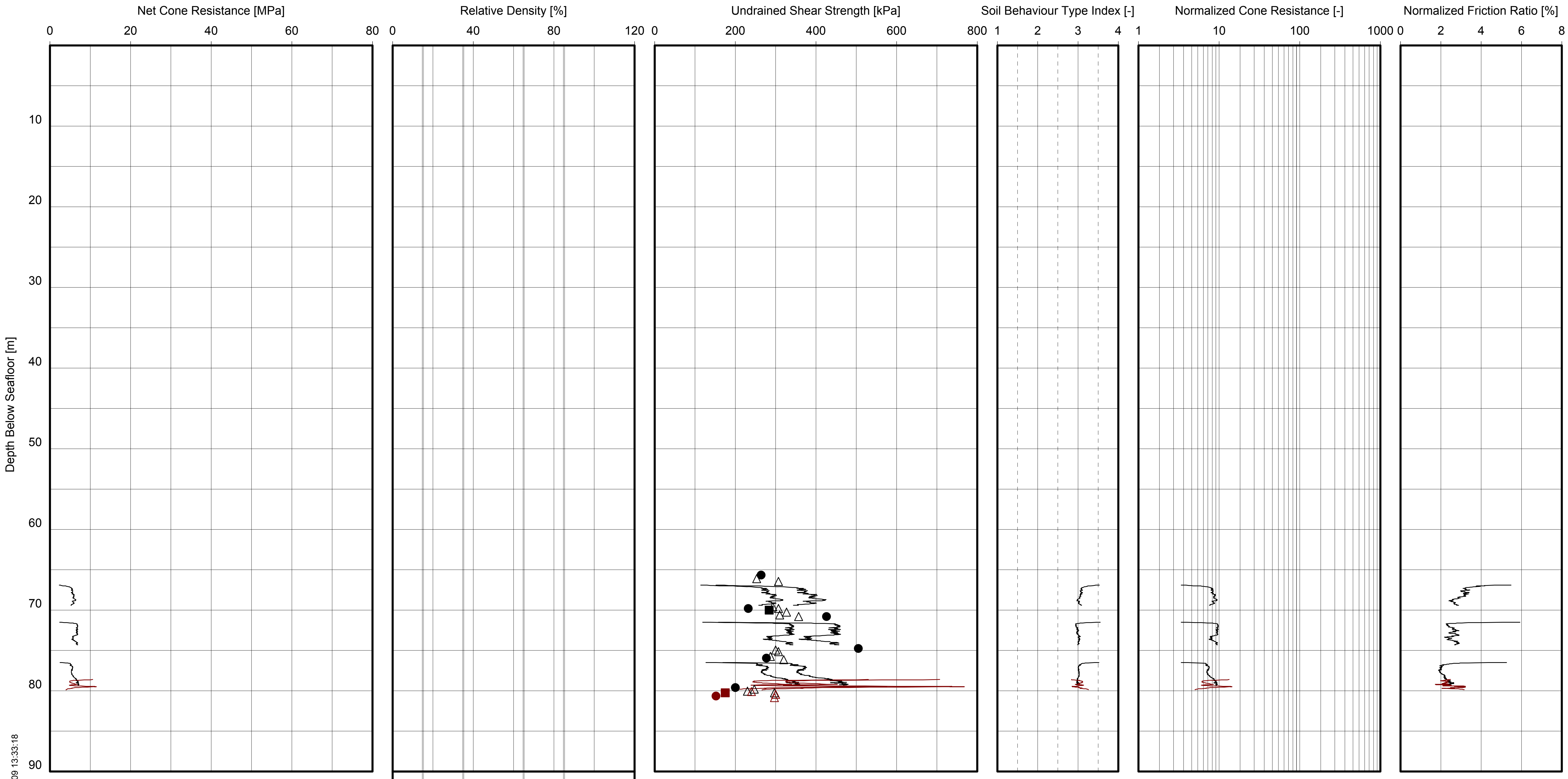


Net cone resistance

Derived from CPT

VL = Very loose
L = Loose
MD = Medium dense
D = Dense
VD = Very dense

Pocket penetrometer
UU-triaxial
CU-triaxial
Derived from CPT

Derived from CPT

Derived from CPT

Derived from CPT

Location(s):

BH-WFS3-6
CPT_WFS3_6
CPT_WFS3_6A
BH-WFS5-1
CPT_WFS5_1
BH-SubStatB-1
CPT_SubStatB_1
CPT_WFS3_9
CPT_WFS3_17
CPT_WFS3_25
CPT_WFS3_26
CPT_WFS3_27

Note(s):
- $K_0$ = 0.5 and $K_0$ = 1.0 are used to derive relative density from CPT
- $N_k$ = 15 and $N_k$ = 20 are used to derive $c_u$ from CPT
- Soil Behaviour Type Index is according to Robertson (2009), refer to Appendix 1, document titled "Cone Penetration Test Interpretation"

GeODin/1.CPT Parameters vs Depth.GLO/2015-12-09 13:33:18

**CPT PARAMETERS AND STRENGTH DATA VERSUS DEPTH**
UNIT F3
BORSSELE WIND FARM ZONE, WFS III - DUTCH SECTOR, NORTH SEA

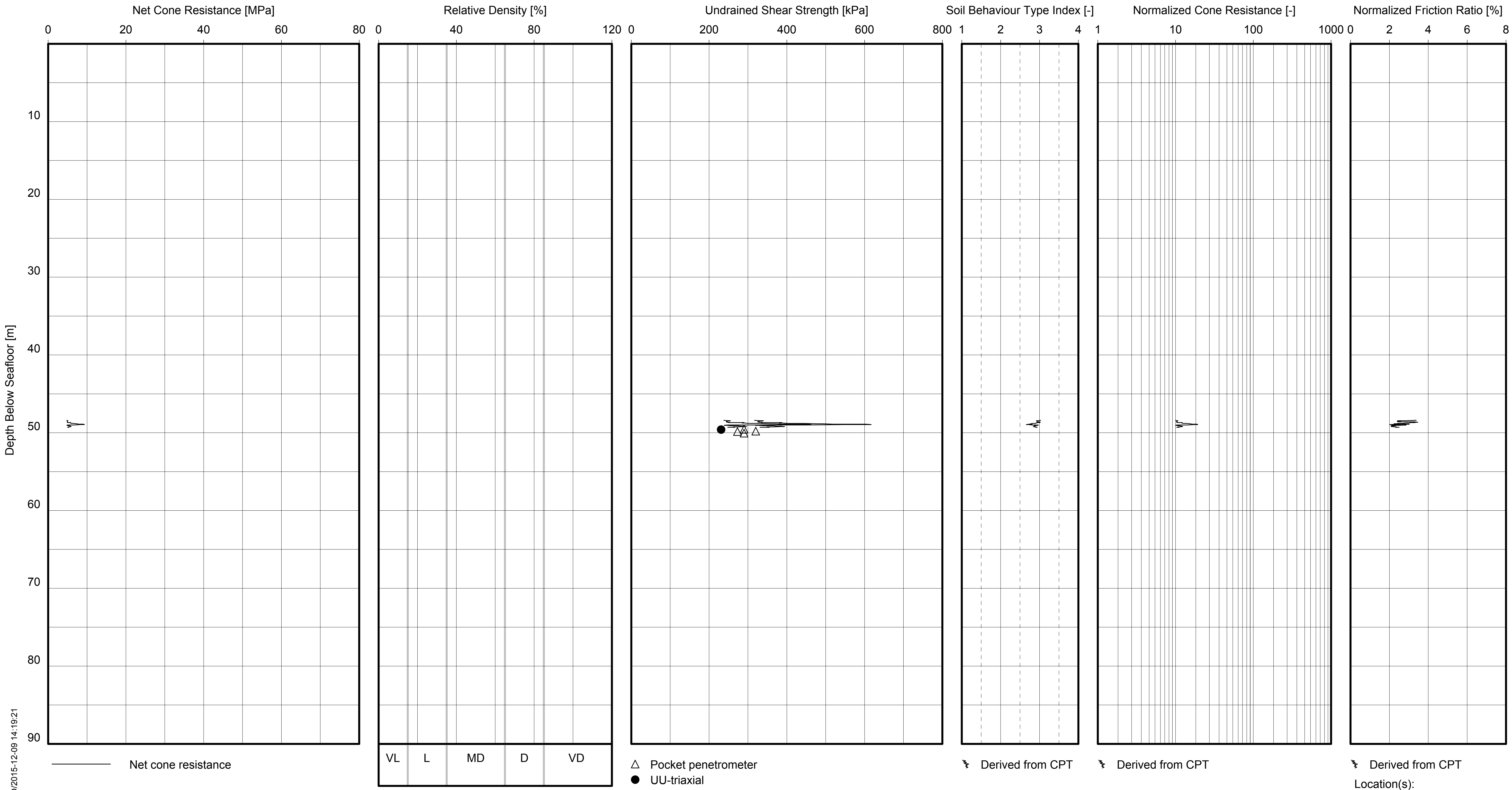


Net cone resistance

Derived from CPT

VL = Very loose
L = Loose
MD = Medium dense
D = Dense
VD = Very dense

Pocket penetrometer
UU-triaxial
CU-triaxial
Derived from CPT

Derived from CPT

Derived from CPT

Derived from CPT

Location(s):

BH-WFS3-2
CPT_WFS3_2
BH-WFS3-3A
BH-WFS3-3
CPT_WFS3_3
CPT_WFS3_7
CPT_WFS3_8
CPT_WFS3_13
CPT_WFS3_15
CPT_WFS3_16
CPT_WFS3_22
CPT_WFS3_23

GeODin\1.CPT Parameters vs Depth.GLO/2015-12-09 14:19:21

Note(s):
- $K_0$ = 0.5 and $K_0$ = 1.0 are used to derive relative density from CPT
- $N_k$ = 15 and $N_k$ = 20 are used to derive $c_u$ from CPT
- Soil Behaviour Type Index is according to Robertson (2009), refer to Appendix 1, document titled "Cone Penetration Test Interpretation"

**CPT PARAMETERS AND STRENGTH DATA VERSUS DEPTH**

UNIT F3

BORSSELE WIND FARM ZONE, WFS III - DUTCH SECTOR, NORTH SEA

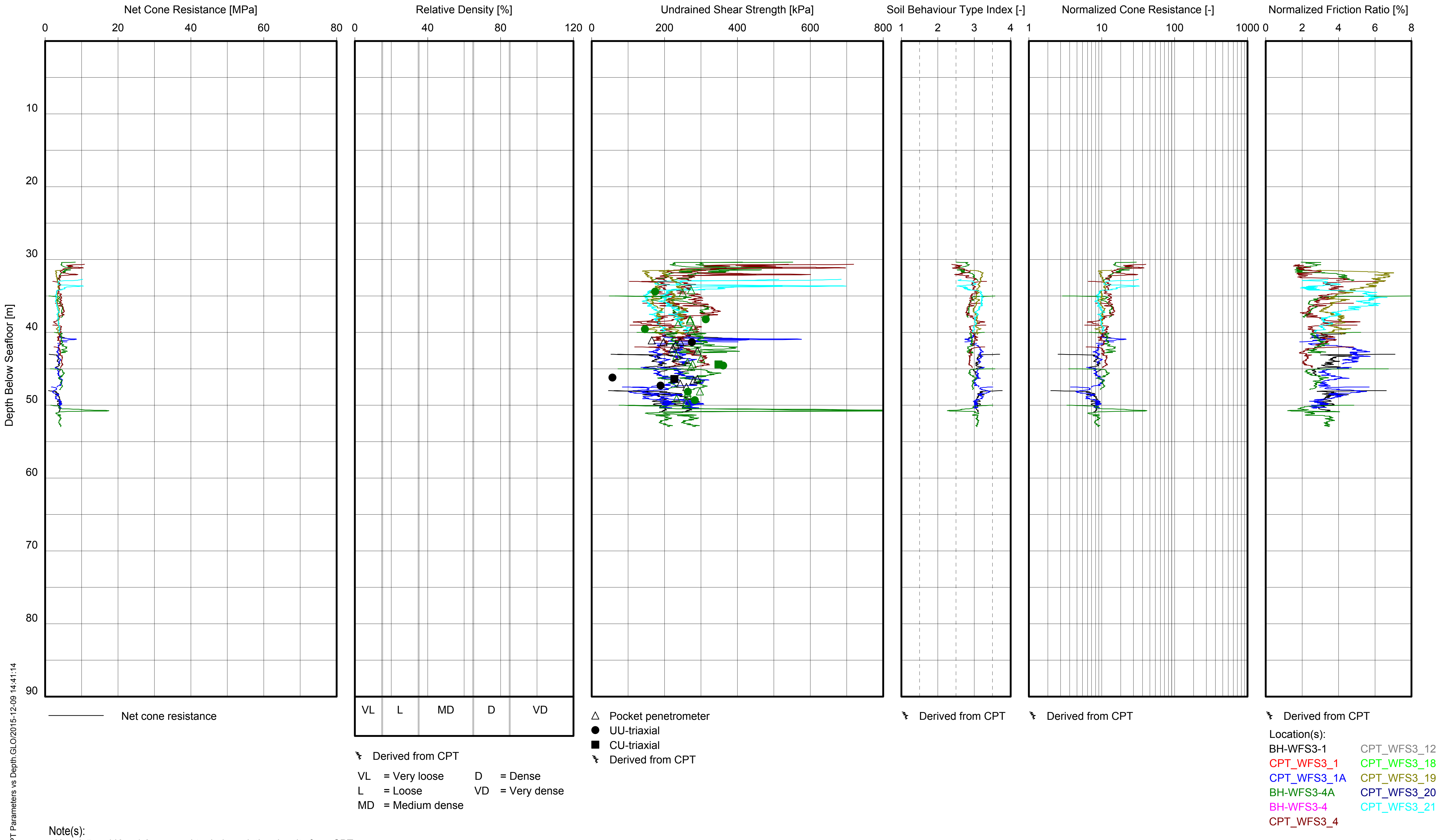


GeODin\1.CPT Parameters vs Depth.GLO/2015-12-09 14:41:14

Note(s):
- $K_0$ = 0.5 and $K_0$ = 1.0 are used to derive relative density from CPT
- $N_k$ = 15 and $N_k$ = 20 are used to derive $c_u$ from CPT
- Soil Behaviour Type Index is according to Robertson (2009), refer to Appendix 1, document titled "Cone Penetration Test Interpretation"

**CPT PARAMETERS AND STRENGTH DATA VERSUS DEPTH**
UNIT F3
BORSSELE WIND FARM ZONE, WFS III - DUTCH SECTOR, NORTH SEA

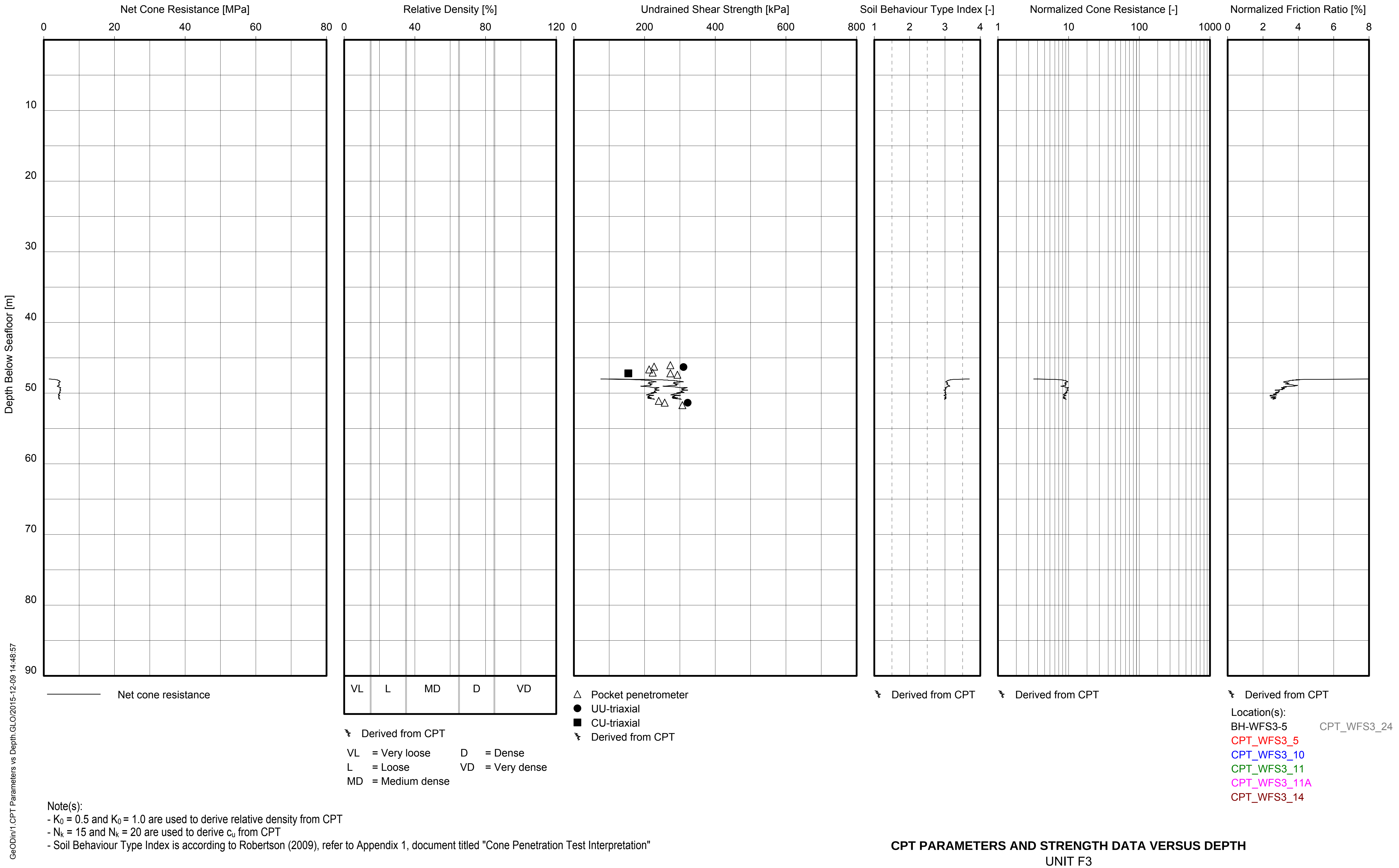


Note(s):
- $K_0$ = 0.5 and $K_0$ = 1.0 are used to derive relative density from CPT
- $N_k$ = 15 and $N_k$ = 20 are used to derive $c_u$ from CPT
- Soil Behaviour Type Index is according to Robertson (2009), refer to Appendix 1, document titled "Cone Penetration Test Interpretation"

**CPT PARAMETERS AND STRENGTH DATA VERSUS DEPTH**
UNIT F3
BORSSELE WIND FARM ZONE, WFS III - DUTCH SECTOR, NORTH SEA

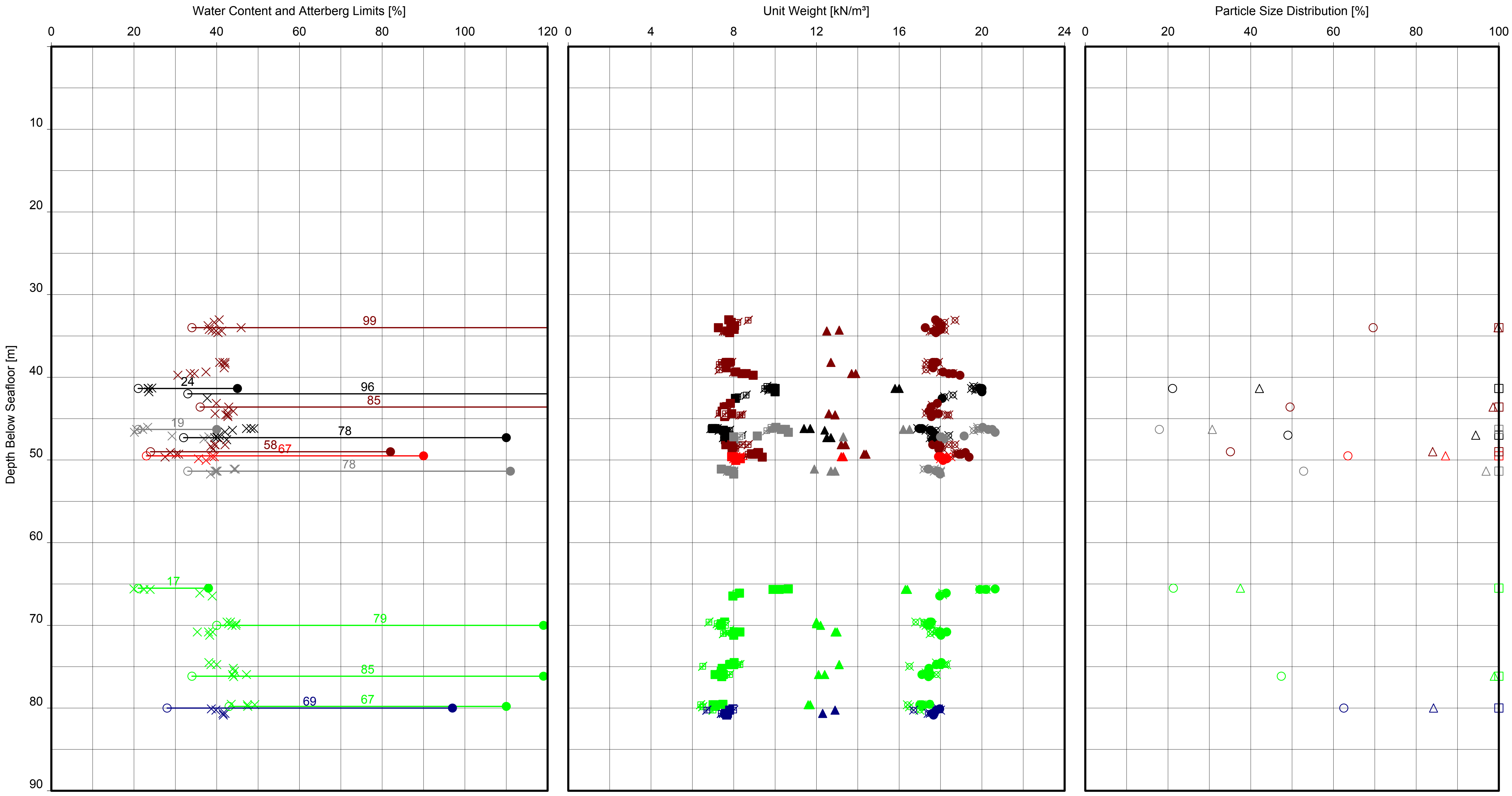


× Water content
○ Plastic limit
● Liquid limit
○—55—● Plasticity index

● Unit weight derived from water content and particle density
Unit weight derived from volume mass calculation
■ Submerged unit weight derived from water content and particle density
Submerged unit weight derived from volume mass calculation
▲ Dry unit weight derived from volume mass calculation

○ Particle size by mass percentage <2 µm
△ Particle size by mass percentage <60 µm
□ Particle size by mass percentage <2000 µm

Location(s):
BH-WFS3-1
BH-WFS3-2
BH-WFS3-3
BH-WFS3-3A
BH-WFS3-4
BH-WFS3-4A
BH-WFS3-5
BH-WFS3-6
BH-WFS5-1
BH-SubStatB-1

Note(s):
- No dry unit weight is available for unit weight measurements by volume mass calculation on WAX samples.

GeODin/2:Water Content, Unit Weight And Particle Size Distribution vs Depth.GLO/2015-12-09 13:52:32

**WATER CONTENT, UNIT WEIGHT AND PARTICLE SIZE DISTRIBUTION VERSUS DEPTH**
UNIT F3
BORSSELE WIND FARM ZONE, WFS III - DUTCH SECTOR, NORTH SEA

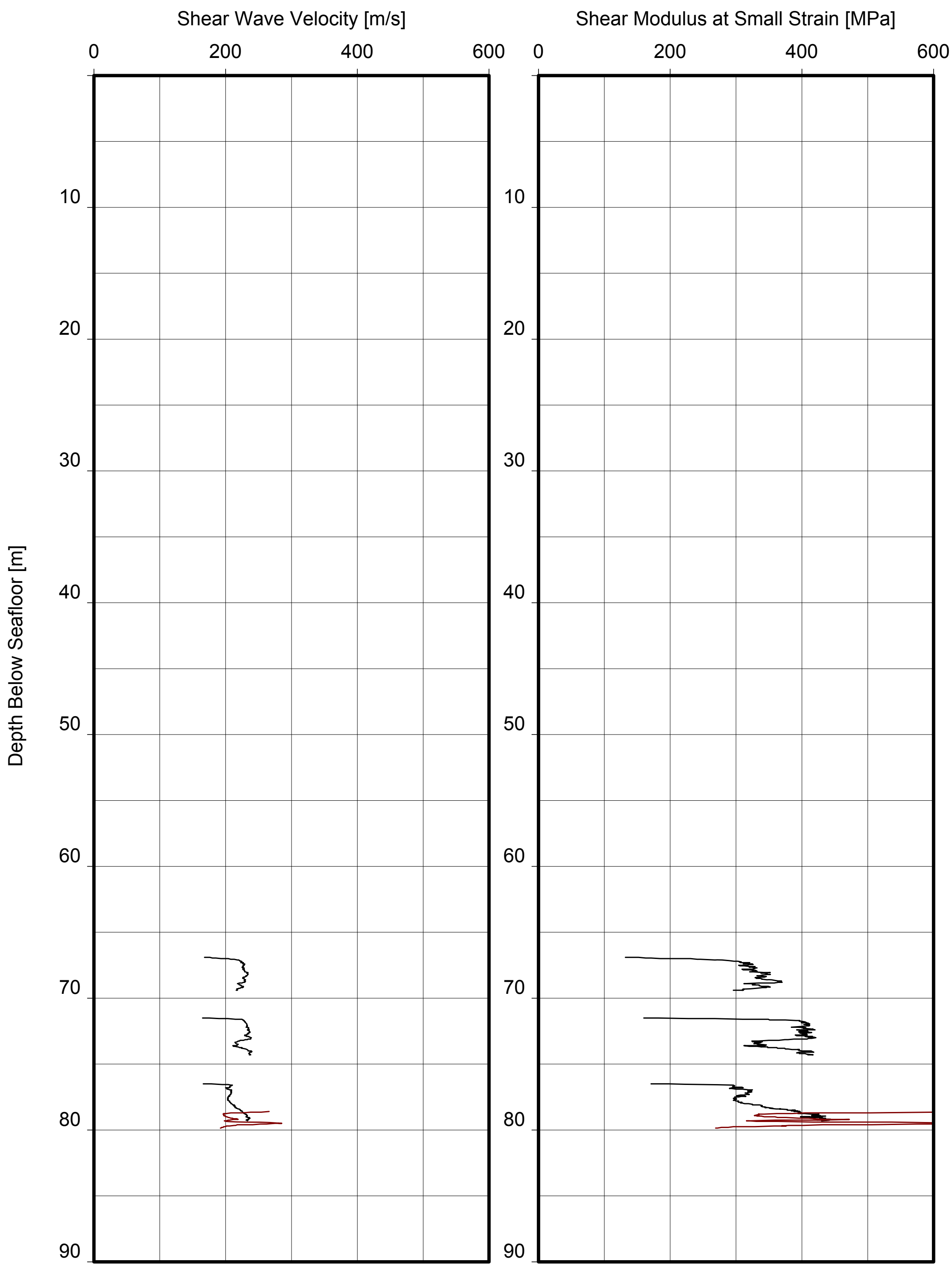


Shear wave velocity ($v_s$) measured in-between geophone array
Shear modulus at small strain ($G_{max}$) derived from $v_s$ measured
$v_s$ and $G_{max}$ derived from CPT

Location(s):
BH-WFS3-6
CPT_WFS3_6
CPT_WFS3_6A
BH-WFS5-1
CPT_WFS5_1
BH-SubStatB-1
CPT_SubStatB_1
CPT_WFS3_9
CPT_WFS3_17
CPT_WFS3_25
CPT_WFS3_26
CPT_WFS3_27

Note(s):
- $v_s$ derived from CPT based on Robertson and Cabal (2010)
- $G_{max}$ for clays derived from CPT based on Mayne and Rix (1993)
- $G_{max}$ for sands derived from CPT based on Rix and Stokoe (1991)

GeODin/3.Shear Wave Velocity and Shear Modulus at Small Strain versus Depth (single UNIT, excl. GM).GLO/2015-12-09 13:31:04

**SHEAR WAVE VELOCITY AND SHEAR MODULUS AT SMALL STRAIN VERSUS DEPTH**

UNIT F3

BORSSELE WIND FARM ZONE, WFS III - DUTCH SECTOR, NORTH SEA

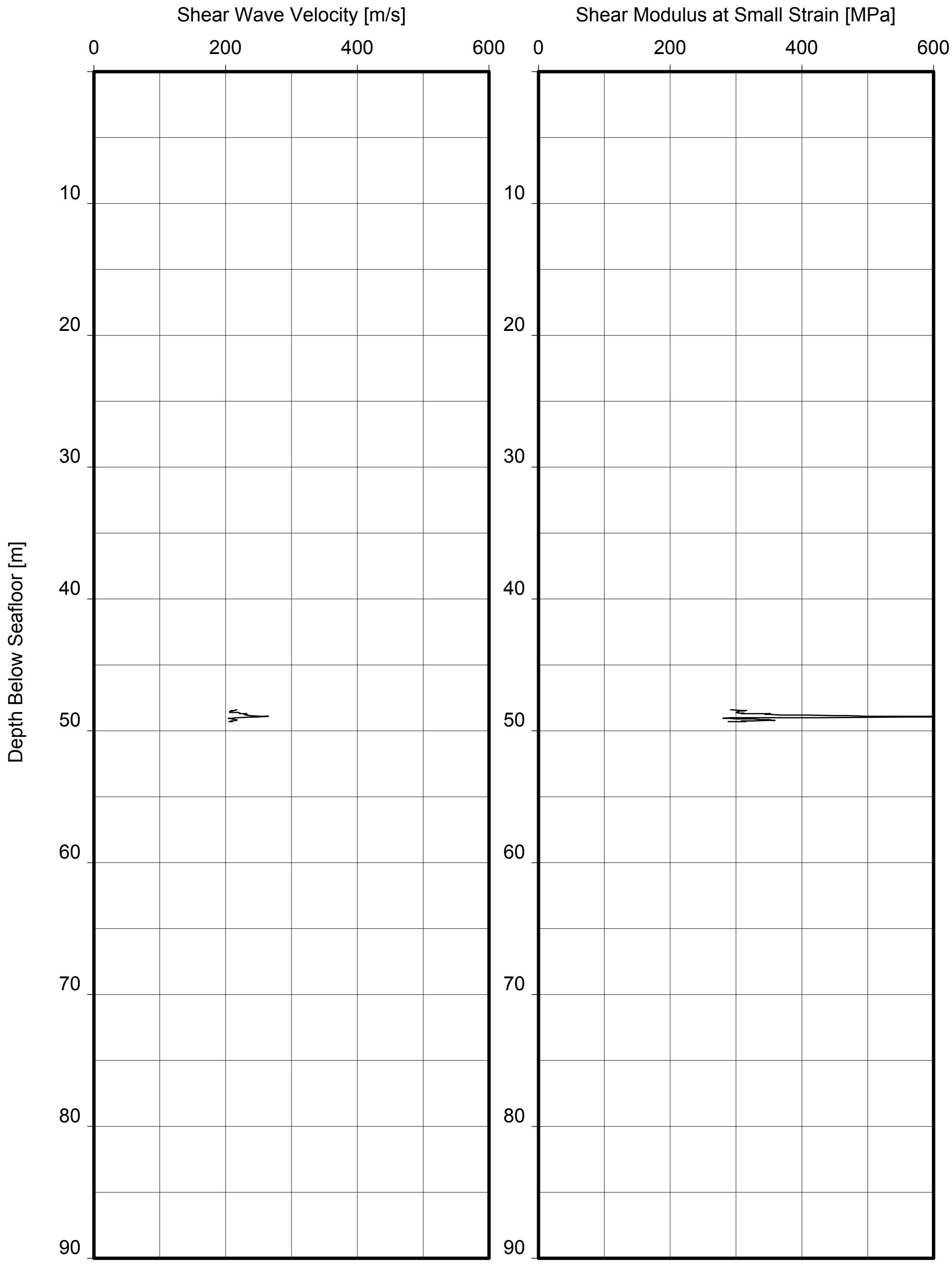


Shear wave velocity ($v_s$) measured in-between geophone array
Shear modulus at small strain ($G_{max}$) derived from $v_s$ measured
$v_s$ and $G_{max}$ derived from CPT

Location(s):
BH-WFS3-2
CPT_WFS3_2
BH-WFS3-3A
BH-WFS3-3
CPT_WFS3_3
CPT_WFS3_7
CPT_WFS3_8
CPT_WFS3_13
CPT_WFS3_15
CPT_WFS3_16
CPT_WFS3_22
CPT_WFS3_23

Note(s):
- $v_s$ derived from CPT based on Robertson and Cabal (2010)
- $G_{max}$ for clays derived from CPT based on Mayne and Rix (1993)
- $G_{max}$ for sands derived from CPT based on Rix and Stokoe (1991)

GeODin/3.Shear Wave Velocity and Shear Modulus at Small Strain versus Depth (single UNIT, excl. GM).GLO/2015-12-09 14:27:06

**SHEAR WAVE VELOCITY AND SHEAR MODULUS AT SMALL STRAIN VERSUS DEPTH**
UNIT F3
BORSSELE WIND FARM ZONE, WFS III - DUTCH SECTOR, NORTH SEA

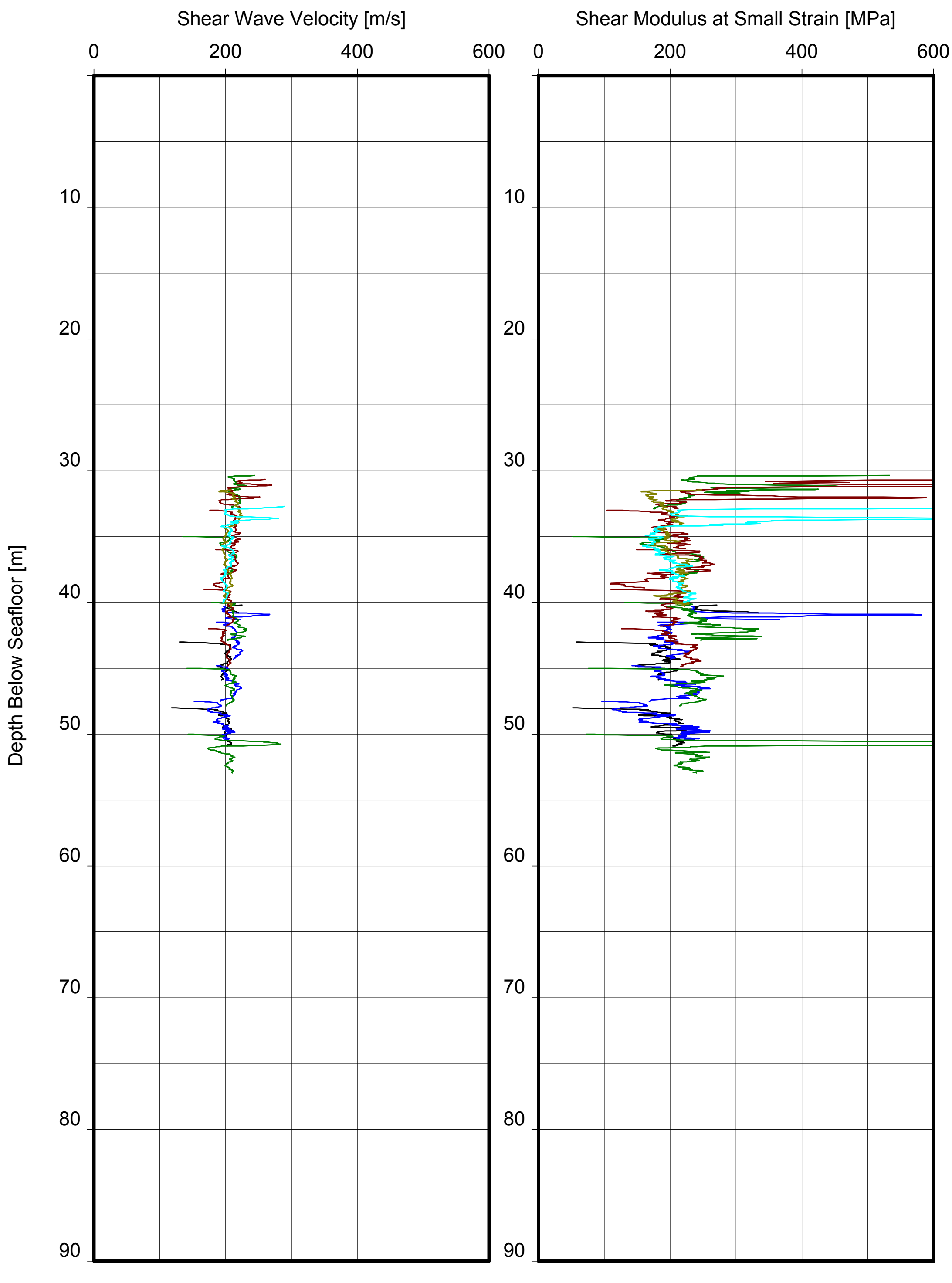


Shear wave velocity ($v_s$) measured in-between geophone array
Shear modulus at small strain ($G_{max}$) derived from $v_s$ measured
$v_s$ and $G_{max}$ derived from CPT

Location(s):
BH-WFS3-1
CPT_WFS3_1
CPT_WFS3_1A
BH-WFS3-4A
BH-WFS3-4
CPT_WFS3_4
CPT_WFS3_12
CPT_WFS3_18
CPT_WFS3_19
CPT_WFS3_20
CPT_WFS3_21

Note(s):
- $v_s$ derived from CPT based on Robertson and Cabal (2010)
- $G_{max}$ for clays derived from CPT based on Mayne and Rix (1993)
- $G_{max}$ for sands derived from CPT based on Rix and Stokoe (1991)

GeODin/3.Shear Wave Velocity and Shear Modulus at Small Strain versus Depth (single UNIT, excl. GM).GLO/2015-12-09 14:34:02

**SHEAR WAVE VELOCITY AND SHEAR MODULUS AT SMALL STRAIN VERSUS DEPTH**

UNIT F3

BORSSELE WIND FARM ZONE, WFS III - DUTCH SECTOR, NORTH SEA

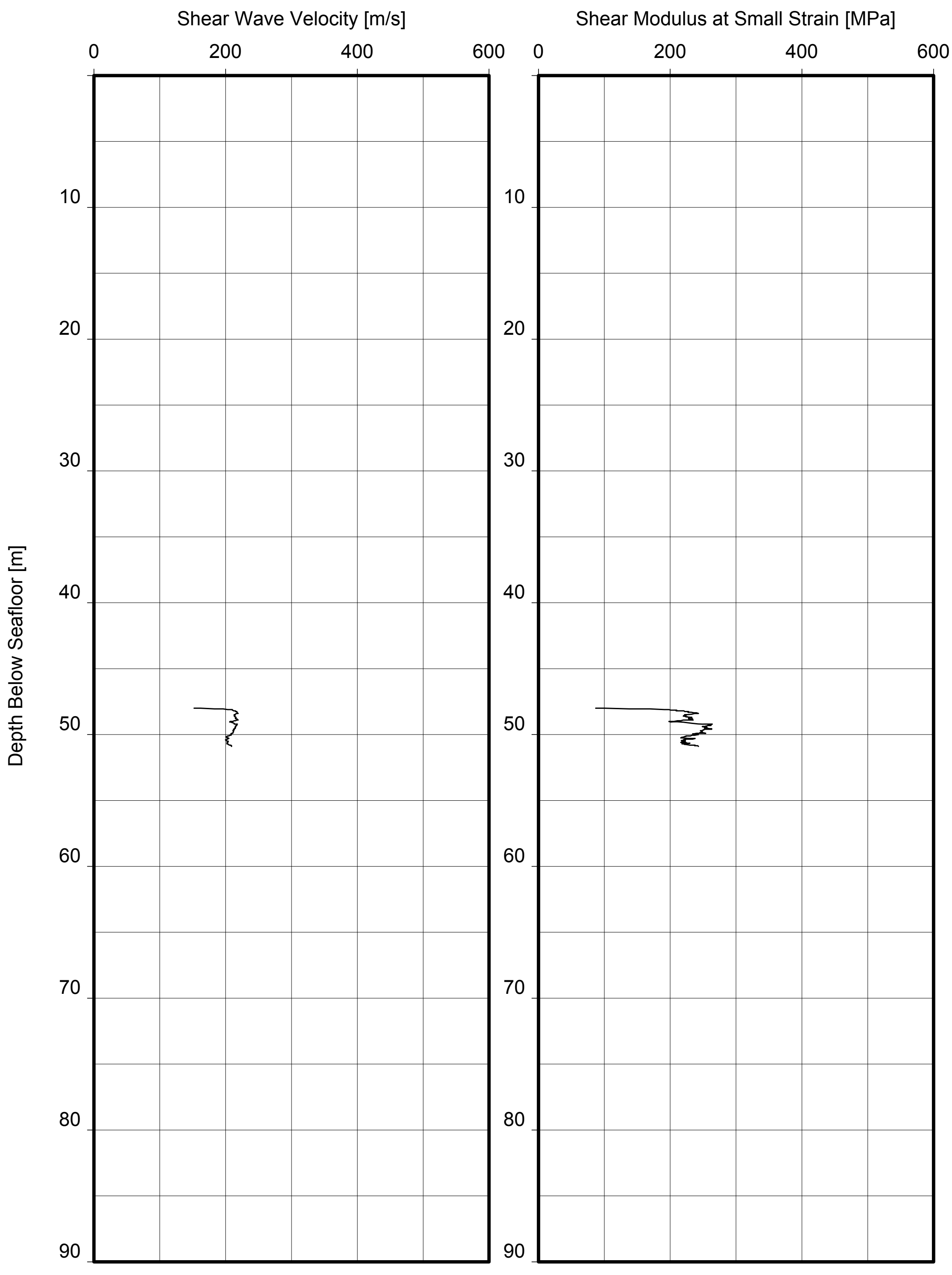


Shear wave velocity ($v_s$) measured in-between geophone array
Shear modulus at small strain ($G_{max}$) derived from $v_s$ measured
$v_s$ and $G_{max}$ derived from CPT

Location(s):
BH-WFS3-5
CPT_WFS3_5
CPT_WFS3_10
CPT_WFS3_11
CPT_WFS3_11A
CPT_WFS3_14
CPT_WFS3_24

Note(s):
- $v_s$ derived from CPT based on Robertson and Cabal (2010)
- $G_{max}$ for clays derived from CPT based on Mayne and Rix (1993)
- $G_{max}$ for sands derived from CPT based on Rix and Stokoe (1991)

GeODin/3.Shear Wave Velocity and Shear Modulus at Small Strain versus Depth (single UNIT, excl. GM).GLO/2015-12-09 14:49:28

**SHEAR WAVE VELOCITY AND SHEAR MODULUS AT SMALL STRAIN VERSUS DEPTH**

UNIT F3

BORSSELE WIND FARM ZONE, WFS III - DUTCH SECTOR, NORTH SEA

## SECTION C: GUIDELINES FOR USE OF REPORT

**CONTENTS** Reference

## INTRODUCTION

This document provides guidelines, recommendations and limitations regarding the use of information in this report.

The cost of geotechnical data acquisition, interpretation and monitoring is a small portion of the total cost of a construction project. By contrast, the costs of correcting a wrongly designed programme or mobilising alternative construction methods are often far greater than the cost of the original investigation. Attention and adherence to the guidelines and recommendations presented in this guide and in the geotechnical report can reduce delays and cost overruns related to geotechnical factors.

This guide applies equally to the use of geotechnical and multi-disciplinary project information and advice.

## REQUIREMENTS FOR QUALITY GEOTECHNICAL INFORMATION

Fugro follows ISO 9001 quality principles for project management and ISO 2394 for general principles on reliability for structures. Project activities usually comprise part of specific phases of a construction project. The quality plan for the entire construction project should incorporate geotechnical input in every phase - from the feasibility planning stages to project completion. The parties involved should do the following:

- Provide complete and accurate information necessary to plan an appropriate geotechnical site investigation.
- Describe the purpose(s), type(s) and construction methods of planned structures in detail.
- Provide the time, financial, personnel and other resources necessary for the planning, execution and follow-up of a site investigation programme.
- Understand the limitations and degree of accuracy inherent in the geotechnical data and engineering advice based upon these data.
- During all design and construction activities, be aware of the limitations of geotechnical data and geotechnical engineering analyses/advice, and use appropriate preventative measures.
- Incorporate all geotechnical input in the design, planning, construction and other activities involving the site and structures. Provide the entire geotechnical report to parties involved in design and construction.
- Use the geotechnical data and engineering advice for only the structures, site and activities which were described to Fugro prior to and for the purpose of planning the geotechnical site investigation or geotechnical engineering analysis programme.

## AUTHORITY, TIME AND RESOURCES NECESSARY FOR GEOTECHNICAL INVESTIGATIONS

Adequate designation of authority and accountability for geotechnical aspects of construction projects is necessary. This way, an appropriate investigation can be performed, and the use of the results by project design and construction professionals can be optimised.

Figure 1 illustrates the importance of the initial project phases for gathering adequate geotechnical information for a project. The initial phases, when site investigation requirements are defined and resources are allocated, are represented by more than 50% of the Quality Triangle (Figure 1). Decisions and actions made during these phases have a large impact of the outcome and thus the potential of the investigation to meet project requirements.

ISSUE 12

Figure 1: Quality of Geotechnical Site Investigation (adapted from SISG[1]).

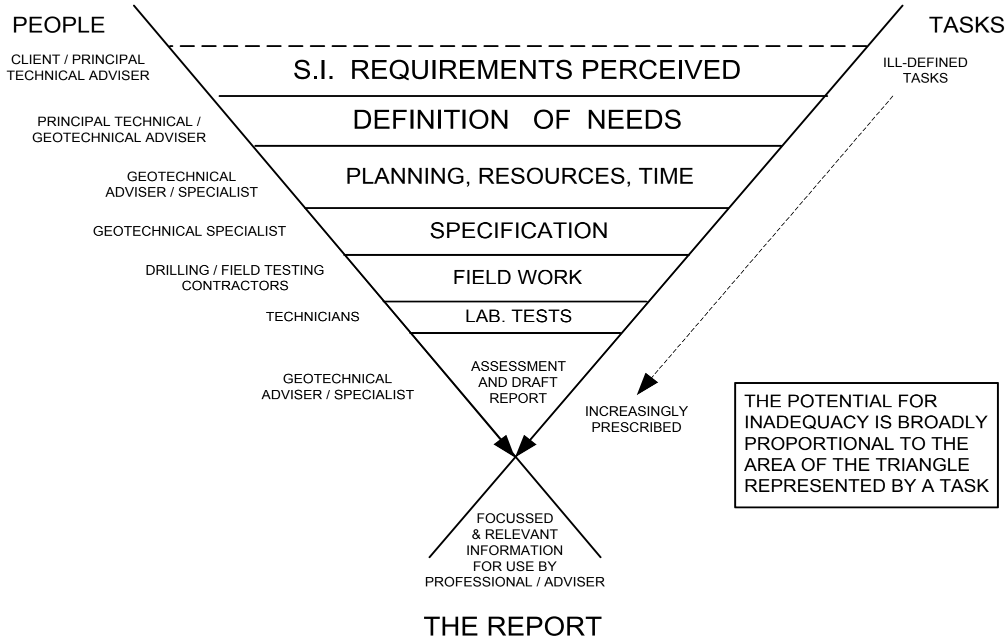


## DATA ACQUISITION AND MONITORING PROGRAMMES

Geotechnical investigations are operations of discovery. Investigation should proceed in logical stages. Planning should allow operational adjustments deemed necessary by newly available information. This observational approach permits the development of a sound engineering strategy and reduces the risk of discovering unexpected hazards during or after construction.

## GEOTECHNICAL INFORMATION – DATA TYPES AND LIMITATIONS

### 1. RELIABILITY OF SUPPLIED INFORMATION

Geotechnical engineering can involve the use of information and physical material that is publicly available or supplied by the Client. Examples are geodetic data, geological maps, geophysical records, earthquake data, earlier geotechnical logs and soil samples. Fugro endeavours to identify potential anomalies, but does not independently verify the accuracy or completeness of public or Client-supplied information unless indicated otherwise. This information, therefore, can limit the accuracy of the report.

### 2. COMPLEXITY OF GROUND CONDITIONS

There are hazards associated with the ground. An adequate understanding of these hazards can help to minimize risks to a project and the site. The ground is a vital element of all structures which rest on or in the ground. Information about ground behaviour is necessary to achieve a safe and economical structure. Often less is known about the ground than for any other element of a structure.

### 3. GEOTECHNICAL INVESTIGATION - SPATIAL COVERAGE LIMITATIONS

Geotechnical investigations collect data at specific test locations. Interpretation of ground conditions away from test locations is a matter of extrapolation and judgement based on geotechnical knowledge and experience, but actual conditions in untested areas may differ from predictions. For example, the interface between ground materials may be far more gradual or abrupt than a report indicates. It is not realistic to expect a geotechnical investigation to reveal or anticipate every detail of ground conditions. Nevertheless, an investigation can reduce the residual risk associated with unforeseen conditions to a tolerable level. If ground problems do arise, it is important to have geotechnical expertise available to help reduce and mitigate safety and financial risks.

---

1 Site Investigation Steering Group SISG (1993), "Site Investigation in Construction 2: Planning, Procurement and Quality Management", Thomas Telford, London.

4. ROLE OF JUDGEMENT AND OPINION IN GEOTECHNICAL ENGINEERING

Geotechnical engineering is less exact than most other design disciplines, and requires extensive judgement and opinion. Therefore, a geotechnical report may contain definitive statements that identify where the responsibility of Fugro begins and ends. These are not exculpatory clauses designed to transfer liabilities to another party, but they are statements that can help all parties involved to recognise their individual responsibilities and take appropriate actions.

**COMPLETE GEOTECHNICAL REPORT SHOULD BE AVAILABILE TO ALL PARTIES INVOLVED**

To prevent costly construction problems, construction contractors should have access to the best available information. They should have access to the complete original report to prevent or minimize any misinterpretation of site conditions and engineering advice. To prevent errors or omissions that could lead to misinterpretation, geotechnical logs and illustrations should not be redrawn, and users of geotechnical engineering information and advice should confer with the authors when applying the report information and/or recommendations.

**GEOTECHNICAL INFORMATION IS PROJECT-SPECIFIC**

Fugro's investigative programmes and engineering assessments are designed and conducted specifically for the Client described project and conditions. Thus this report presents data and/or recommendations for a unique construction project. Project-specific factors for a structure include but are not limited to:

- location
- size and configuration of structure
- type and purpose or use of structure
- other facilities or structures in the area.

Any factor that changes subsequent to the preparation of this report may affect its applicability. A specialised review of the impact of changes would be necessary. Fugro is not responsible for conditions which develop after any factor in site investigation programming or report development changes.

For purposes or parties other than the original project or Client, the report may not be adequate and should not be used.

**CHANGES IN SUBSURFACE CONDITIONS AFFECT THE ACCURACY / SUITABILITY OF THE DATA**

Ground is complex and can be changed by natural phenomena such as earthquakes, floods, seabed scour and groundwater fluctuations. Construction operations at or near the site can also change ground conditions. This report considers conditions at the time of investigation. Construction decisions should consider any changes in site conditions, regulatory provisions, technology or economic conditions subsequent to the investigation. In general, two years after the report date, the information may be considered inaccurate or unreliable. A specialist should be consulted regarding the adequacy of this geotechnical report for use after any passage of time.

## APPENDIX 1: DESCRIPTIONS OF METHODS AND PRACTICES

**CONTENTS** Reference



This appendix presents method statements and terminology that are generally familiar to expert users of the information.

## INTRODUCTION

Fugro employs a range of industry-standard systems for soil description, with additional refinements. The more important systems are:

- British Standard 5930 (BS, specifically Section 6 Paragraphs 41 to 43 on Description of soils) published in 1999.
- American Society for Testing and Materials (ASTM) Standards D 2487-11 (Classification of soils for Engineering Purposes) and D 2488-09a (Description and Identification of Soils – Visual-Manual Procedure).
- International Standard ISO 14688-1:2002 (Geotechnical Investigation and Testing - Identification and Classification of Soil: Identification and Description) and International Standard ISO 14688-2:2004 (Principles for a Classification).
- International Standard ISO 19901-8:2014 (Marine Soil Investigations).

The standards are similar, as they are (1) based on the Unified Classification System (Casagrande, 1948), (2) rely on a range of relatively simple visual and manual observations and (3) classify soils according to particle-size distribution and plasticity. Laboratory particle-size distribution and Atterberg limits tests are used to confirm the observations. In addition, the standards include organic soils characterization under soil particle type description.

Significant differences between the standards include the particle-size boundaries and the degree to which plasticity is used as a basis for description. Other differences include the format and order of the soil description.

This document describes a convention that is consistent with either the BS or ASTM standard, and that produces soil descriptions, which can be converted to the other standard. In addition, to describe calcareous soils, Fugro has integrated the carbonate classification system outlined by Clark and Walker (1977) with both British Standard and ASTM systems (Landva et al., 2007). No further information is given about the ISO standards.

British Standard and ASTM systems apply primarily to common terrestrial soils in temperate climates. However, construction activities in coastal areas and offshore can also encounter major carbonate soil deposits. The engineering characteristics of carbonate soil deposits can differ substantially from those of silica-based soil deposits, primarily because of cementation and differences in void ratios.

Appropriate description is necessary. A commonly accepted procedure for calcareous soil deposits is the Clark and walker system, originally developed for the Middle East. This considers particle size, carbonate content and material strength. The particle size classification fits both BS and ASTM system. The carbonate content is an additional feature and the material strength classification relates to common post-depositional alteration of calcareous soil.

This document does not include rock description or specific engineering geological classification systems, such as those for the detailed identification of peat, chalk or micaceous sand.

The main steps of the soil description system are:

1. Measure or estimate particle type as silica-based, organic, or calcareous.
2. For soils that are predominantly silica-based and organic, select BS 5930:1999 or ASTM D 2487 based on local geotechnical practice or project requirements, and follow the appropriate descriptive procedure. For calcareous soils, use the process described by Peuchen et al. (1999).
3. Measure or estimate the particle-size distribution and Atterberg limits (plasticity) for use in defining the principal and secondary soil fractions.
4. Measure or estimate soil strength according to one of the following: (1) relative density of coarse-grained soil, (2) consistency of fine-grained soil, (3) cementation of cemented soil, or (4) lithification of soil undergoing diagenesis.
5. Complete the description using the additional terms for the soil mass characteristics and other features such as bedding, colour, and particle shape.

## CALCAREOUS SOIL DESCRIPTION

The procedure considers particle size, carbonate content and material strength. The particle-size classification follows the Unified Soil Classification System. The carbonate content is an additional feature and the material strength classification relates to common post-depositional alteration of calcareous soil.

### PARTICLE TYPE

The first determinant for soil description is particle type using Table 1. It mainly differentiates between silica and carbonate soil compositions with organic content of less than 1% of the dry weight. Organic soils are further described in the soil description procedures for BS and ASTM (Table 4).

**TABLE 1 - PARTICLE TYPE**

| Clay soil | Other Soils | Carbonate Content (by dry weight) | Reaction with HCl (10%) |
|---|---|---|---|
| -- | Silica | < 10 % | In clays: no bubbles, or slowly forming bubbles. In sands: reaction often limited to some individual particles, or particle surface<br>Residue - Nearly all soil remaining |
| Calcareous | Calcareous silica | 10 to 50 | In clays: clearly visible, prolonged reaction and foaming. In sand: violent reaction<br>Residue - Large part of soil remaining |
| Carbonate | Siliceous carbonate | 50 to 90 | Violent reaction<br>Residue - Only small part of soil remaining |
| Carbonate | Carbonate | > 90 | Violent reaction<br>Residue - Hardly any soil remaining |

The description method does not distinguish between types of carbonate material, and assumes that non-carbonate particles are siliceous.

### CEMENTATION AND LITHIFICATION

Cementation is the process by which a binding material precipitates in the voids between the grains or minerals. Lithification is the process by which a soil is hardened due to pressure solution and transformation or new grain or mineral growth. Both processes contribute to the formation of rock.

The descriptions for cementation follow rock strength classification (Table 2) expressed as uniaxial compressive strength $\sigma_c$:

**TABLE 2 – CEMENTATION**

| Cementation | $\sigma_c$ [MPa] |
|---|---|
| Slightly cemented | 0.3 to 1.25 |
| Moderately cemented | 1.25 to 5.0 |
| Well cemented | 5.0 to 12.5 |

The term "well cemented" in Table 2 applies to soil, which also shows sublayers with little or no cementation. In case of further lithification, the soil description becomes a rock description using Table 3. The rock strength is only indicative.

ISSUE 25

**TABLE 3 - LITHIFICATION**

<table>
<tr><th rowspan="2">Carbonate content [%]</th><th colspan="6">Dominant fraction</th><th rowspan="2">$\sigma_c$ [MPa]</th></tr>
<tr><th>Clay</th><th>Silt</th><th>Sand</th><th>Gravel</th><th>Cobbles</th><th>Boulders</th></tr>
<tr><td colspan="8">incomplete lithification</td></tr>
<tr><td>< 10</td><td>CLAYSTONE</td><td>SILTSTONE</td><td>SANDSTONE</td><td>CONGLOMERATE</td><td colspan="2" rowspan="4">CONGLOMERATE or BRECCIA</td><td rowspan="4">0.3 to 12.5</td></tr>
<tr><td>10 to 50</td><td>Calcareous CLAYSTONE</td><td>Calcareous SILTSTONE</td><td>Calcareous SANDSTONE</td><td>Calcareous CONGLOMERATE</td></tr>
<tr><td>50 to 90</td><td>Clayey CALCILUTITE</td><td>Siliceous CALCISILTITE</td><td>Siliceous CALCARENITE</td><td>Conglomeratic CALCIRUDITE</td></tr>
<tr><td>> 90</td><td>CALCILUTITE</td><td>CALCISILTITE</td><td>CALCARENITE</td><td>CALCIRUDITE</td></tr>
<tr><td colspan="8">complete lithification</td></tr>
<tr><td>< 50</td><td>CLAYSTONE</td><td>SILTSTONE</td><td>SANDSTONE</td><td>GRAVEL CONGLOMERATE</td><td colspan="2" rowspan="2">CONGLOMERATE or BRECCIA</td><td rowspan="2">>12.5</td></tr>
<tr><td>> 50</td><td>Fine-grained Argillaceous LIMESTONE</td><td>Fine-grained Siliceous LIMESTONE</td><td>Medium grained LIMESTONE</td><td>Conglomeratic LIMESTONE</td></tr>
</table>

The Clark and Walker system does not include reef limestone (biolithite). **Reef limestone** represents an in situ accumulation of biological origin (e.g. coral reef) and consists largely of carbonate skeletal material of colonising organisms. The carbonate content normally exceeds 90%. Classification of strength follows rock description procedures.

## SOIL DESCRIPTION USING BS 5930:1999

In the following sections, each of the main characteristics is described in the order most commonly used for soil identification, with some portions of the text quoted (shown within quotation marks) or paraphrased from the BS 5930.

SOIL GROUP (BS)

The soil group subdivides the soils into very coarse, coarse, fine, and organic soils.

<u>Very coarse</u> soils consist of cobbles and boulders, with particles larger than 60 mm in diameter. These soil particles are rarely sampled using standard soil sampling techniques. They are described separately, and not included when determining the proportions of the other soil components.

The initial classification of silica soils as <u>coarse</u> or <u>fine</u> is based on the percentage of fine particles after the very coarse particles are removed. In BS 5930, the boundary between coarse (i.e. sands and gravels) and fines (i.e. silts and clays) is 0.060 mm (60 µm). When the soil contains approximately 35% or more fines, it is described as a fine soil; further classification of the fine soil as a clay or silt depends on the plasticity of the soil. When the soil contains less than about 35% fine material, it is usually described as a coarse soil. "The boundary between fine and coarse soils is approximate, as it depends on the plasticity of the fine fraction and the grading of the coarse fraction."

<u>Organic soils</u> contain usually small quantities of dispersed organic matter that can have a significant effect on soil plasticity. Organic soil descriptions in BS 5930 are based on an organic content by weight determined by loss on ignition. Where organic matter is present as a secondary constituent, the following terms are used:

**TABLE 4 - ORGANIC SOIL DESCRIPTIONS**

| Term | Organic content [% by weight] | Typical colour |
|---|---|---|
| Slightly organic clay or silt<br>Slightly organic sand | 2 to 5<br>1 to 3 | Grey<br>Same as mineral |
| Organic clay or silt<br>Organic sand | 5 to 10<br>3 to 5 | Dark grey<br>Dark grey |
| Very organic clay or silt<br>Very organic sand | > 10<br>> 5 | Black<br>Black |

Soils with organic contents up to approximately 30% by weight and water contents up to about 250% behave as mineral soils and are described using the terms given in the lower portion of Table 4.

Peat consists predominantly of plant remains, is usually dark brown or black, and has a distinctive smell. It is generally classified according to the degree of decomposition (fibrous, pseudo-fibrous, or amorphous) and strength (firm, spongy, or plastic). When encountered, reference can also be made to the classification given in ASTM Standard Procedure D 4427.

PRINCIPAL SOIL TYPE AND PARTICLE SIZE (BS)

**Coarse-Grained Soils**

The principal soil type in coarse-grained soils is sand if the dry weight of the sand fraction (0.06 mm to 2 mm particle sizes) exceeds that of the gravel fraction (2 mm to 60 mm particle sizes), and vice versa for gravel.

As an addition to the BS 5930 classification, coarse-grained soils are described as well-graded or poorly-graded based on the grain-size distribution curve, using the coefficient of uniformity ($C_U$) and, to a lesser extent, the coefficient of curvature ($C_C$), as follows:

– Sands with ≤12% fines are <u>well-graded</u> when $C_U \geq 6$ and $C_C$ is between 1 and 3.
– Sands are <u>poorly-graded</u> for other values of $C_U$ and $C_C$.
– Gravels with ≤12% fines are <u>well-graded</u> when $C_U \geq 4$ and $C_C$ is between 1 and 3.
– Gravels are <u>poorly-graded</u> for other values of $C_U$ and $C_C$.

For coarse-grained soils with fines contents > 12%, these terms are not used.

Sands and gravels are sub-divided into coarse, medium, and fine, as defined in Table 5.

**TABLE 5 - SIZE FRACTION DESCRIPTIONS FOR COARSE-GRAINED SOILS**

| Soil | Particle diameter range [mm] | | |
|---|---|---|---|
| | Coarse | Medium | Fine |
| Gravel | 60 to 20 | 20 to 6 | 6 to 2 |
| Sand | 2 to 0.6 | 0.6 to 0.2 | 0.2 to 0.06 |

**Fine-Grained Soils**

Fine-grained soils are classified as clay or silt according to the results of Atterberg limits tests. A fine-grained soil is classified as clay if:

$$I_P \geq 6 \text{ and } I_P \geq 0.73\,(w_L\text{-}20)$$

where:
$I_P$ = plasticity index [%]
$w_L$ = liquid limit [%]

Otherwise the dominant soil fraction is silt. The equation $I_P = 0.73\,(w_L-20)$ represents the "A-line" in a plasticity chart. The plasticity chart may also show a “U-line” defined as $I_P = 0.9\,(w_L-8)$ and $w_L \geq 16$, according to Casagrande (1948). The U-line represents an approximate upper limit of correlation between plasticity index and liquid limit for natural soils.

The following additional descriptors (as used in the ASTM soil description procedure) are added:

– Clays with liquid limits of 50% or higher are described as “fat.”
– Clays with liquid limits below 50% are described as “lean.”
– Silts with liquid limits of 50% or higher are termed “elastic silt.”
– Silts with liquid limits below 50% are simply “silts.”

The term “silty clay” is not used, since BS 5930 explicitly states that silt and clay “are to be mutually exclusive.”

### Particle Shape

The description of particle shape includes terms for form, angularity, and surface texture. These terms are the same for BS 5930 as for ASTM D 2488. Reference should be made to the corresponding ASTM section of this document.

COMPOSITE (SECONDARY) SOIL TYPES (BS)

BS 5930 defines procedures for assigning secondary soil fractions to coarse-grained soils that are identical for sand and gravel, except that the secondary soil type is sandy when the principal soil type is gravel and vice versa. For fine-grained soils (silt and clay) there is a single procedure for assigning secondary soil fractions. The ranges for the percentages of the secondary constituents are similar to, though different from, those defined by ASTM.

If the principal soil type is sand, secondary soil fractions may be gravelly and silty or clayey (e.g. silty sand). Similarly, if the principal soil type is clay, secondary soil fractions may be sandy or gravelly. Table 6 (from BS 5930) gives the terms to be used for ranges of secondary constituents.

**TABLE 6 - DESCRIPTIVE TERMS AND RANGES FOR SECONDARY CONSTITUENTS**

| Term | Principal soil type | Approximate proportion of secondary constituent | |
|---|---|---|---|
| | | Coarse soil | Fine soil |
| Slightly clayey or silty | SAND and/or GRAVEL | | < 5% |
| Clayey or silty | | | 5% to 20% |
| Very clayey or silty | | | > 20% (1) |
| Slightly sandy or gravelly | | < 5% | |
| Sandy or gravelly | | 5% to 20% | |
| Very sandy or gravelly | | > 20% | |
| Slightly sandy and/or gravelly | SILT or CLAY | < 35% | |
| Sandy and/or gravelly | | 35% to 65% | |
| Very sandy and/or gravelly | | > 65% (2) | |

**Notes**: (1) or can be described as fine soil depending on engineering behaviour
(2) or can be described as coarse soil depending on engineering behaviour.

COLOUR (BS)

Soil colours are described using the Munsell Soil Colour Charts (Gretag-Macbeth, 2000).

The Munsell colour is arranged according to three variables known as Hue, Value and Chroma. The Hue notation of a colour indicates its relation to red, yellow, green, blue and purple. The Value notation indicates the relative lightness. The Chroma notation indicates the intensity of the colour.

BEDDING/STRATIGRAPHY (BS)

Layers of different soil types within a stratum are called bedding units, and are described in terms of the unit thickness. In an otherwise homogeneous soil, these can be identified as bedding planes or as colour changes, and not necessarily as discontinuities.

Table 7 (from BS 5930) gives terms for bedding/stratigraphy.

**TABLE 7 - DESCRIPTIVE TERMS FOR BEDDING/STRATIGRAPHY**

| Stratified | Bedding | Interbedded | Thickness [mm] |
|---|---|---|---|
| Very thick beds | Very thick bedded | Very thickly interbedded | >2000 |
| Thick beds | Thickly bedded | Thickly interbedded | 600 to 2000 |
| Medium beds | Medium bedded | Medium interbedded | 200 to 600 |
| Thin beds | Thinly bedded | Thinly interbedded | 60 to 200 |
| Very thin beds | Very thinly bedded | Very thinly interbedded | 20 to 60 |
| Thick laminae | Thickly laminated | Thickly interlaminated | 6 to 20 |
| Thin laminae | Thinly laminated | Thinly interlaminated | <6 |

Strata with alternating or different beds or laminations can be described as interbedded or interlaminated. Where the soil types are approximately equal, both terms can be used (e.g. thinly interlaminated SAND and CLAY).

Partings are bedding surfaces that separate easily, and typically are laminae of no appreciable thickness. The spacing between partings is described in the same terms as for spacing of discontinuities (Table 8).

DISCONTINUITIES/STRUCTURE (BS)

Discontinuities include fissures and shear planes, and the descriptor refers to the mean spacing between such discontinuities in a soil mass. A soil is “fissured” when it breaks into blocks along unpolished discontinuities, and “sheared” when it breaks into blocks along polished discontinuities (which is equivalent to a slickensided soil). The spacing description ranges from extremely closely spaced (less than 20 mm) to very widely spaced (over 2000 mm). No other descriptive terms are used. An example would be: Firm grey very closely fissured fine sandy calcareous CLAY with many silt partings.

The spacing terms are also used for distances between partings, isolated beds or laminae, desiccation cracks, rootlets, etc.

**TABLE 8 - SPACING OF DISCONTINUITIES**

| **Term** | **Mean spacing range [mm]** |
|---|---|
| Very widely | Over 2000 |
| Widely | 600 to 2000 |
| Medium | 200 to 600 |
| Closely | 60 to 200 |
| Very closely | 20 to 60 |
| Extremely closely | Under 20 |

DENSITY/COMPACTNESS OF GRANULAR SOILS (BS)

Usually, soil description offers little evidence about the density condition of coarse-grained cohesionless (granular) soil samples. The reason for this is the substantial sampling disturbance incurred during conventional sampling operations such as push sampling, percussion sampling, and vibrocoring. Complementary investigation techniques, such as Cone Penetration Tests (CPT), are usually necessary. The strength of a cohesionless soil is normally measured as a function of its relative density (also termed compactness or density index). Relative density is the ratio of the difference between the void ratios of a cohesionless soil in its loosest state and existing natural state to the difference between its void ratio in the loosest and densest states.

Relative density (compactness) is referred to in BS 5930:1999 only in terms of N-values obtained by the Standard Penetration Test (which is not conducted in offshore site investigations). Rather than using SPT-based values, it is common practice to interpret relative density on the basis of CPT results. Ranges of relative density are given in Table 9. These ranges are in common use in the industry. They were originally given in Lambe and Whitman (1979) and in the API RP 2A guidelines generally used for offshore pile design. These terms also apply to cohesionless fine-grained soils.

**TABLE 9- RANGE OF RELATIVE DENSITY OF GRANULAR SOILS**

| **Term** | **Range of relative density [%]** |
|---|---|
| Very loose | Less than 15 |
| Loose | 15 to 35 |
| Medium dense | 35 to 65 |
| Dense | 65 to 85 |
| Very dense | Greater than 85 |

STRENGTH OF COHESIVE SOILS (BS)

The strength of cohesive soils is given in terms of undrained shear strength, using the terms and ranges given in Table 10, with an additional level to cover "very hard" soils.

**TABLE 10 - UNDRAINED SHEAR STRENGTH SCALE FOR COHESIVE SOILS (BS 5930:1999)**

| **Term** | **Undrained shear strength** | |
|---|---|---|
| | **[kPa]** | **[ksf]** (1) |
| Very soft | Less than 20 | Less than 0.4 |
| Soft | 20 to 40 | 0.4 to 0.8 |
| Firm | 40 to 75 | 0.8 to 1.5 |
| Stiff | 75 to 150 | 1.5 to 3.0 |
| Very stiff | 150 to 300 | 3.0 to 6.0 |
| Hard | 300 to 600 | 6.0 to 12.0 |
| Very hard (2) | Greater than 600 | Greater than 12.0 |

**Notes**: (1) Unit conversion added to table
(2) Added for global practice.

MINOR CONSTITUENTS (BS)

Percentages of minor constituents within the soil, such as shell or wood fragments, or small soil inclusions (such as partings or pockets), can be quantified using the terms "with trace", "with few", "with" and "with many" (in increasing order). These terms are usually added at the end of the main soil description (e.g. with many shell fragments, with silt pockets, etc.); exceptions are terms such as "shelly", which are more appropriate before the soil group name. For beds of material within a soil matrix, the terminology for spacing and thickness of beds is used. For individual particles of soil or material within a soil matrix, the terms "partings" and "pockets" are used.

SOIL ODOUR (BS)

Describing the odour from soil samples as they are retrieved or extruded on board ship can be useful. Terms used to describe the odour are $H_2S$, "musty", "putrid" and "chemical". It must be emphasised that soil odour descriptions are unlikely to be fully consistent, because of factors such as variations in sample handling, ambient conditions at time of sample description, and strong dependence on a person's ability to detect and identify odour.

## SOIL DESCRIPTION USING ASTM D 2487 AND D 2488

The identification and description of silica soils in the ASTM system consists primarily of a group name and symbol, which are based on the particle-size distribution and the Atterberg limits test results, and the results of other laboratory classification tests.

The main standard for soil description, D 2487 Classification of Soils for Engineering Purposes, is applicable to naturally-occurring soils passing a 3-in. (75-mm) sieve, and identifies three major soil types: coarse-grained, fine-grained, and highly organic soils. The major soil types are further subdivided into 15 specific basic soil groups.

An accompanying Standard, D 2488, outlines the Description and Identification of Soils using a Visual-Manual Procedure. This standard is used primarily in the field, where full particle-size distribution curves and Atterberg limits values are not available. It gives guidance for detailed descriptions of soil particles and soil conditions (e.g. colour, structure, strength, cementation, etc.), which are not included in D 2487.

Soil types with particles larger than 75 mm (i.e. cobbles and boulders) are not included in the Standards, but are identified.

SOIL TYPES (ASTM)

The initial classification of silica soils as coarse-grained or fine-grained is based on the percentage fines, expressed as the percentage of dry weight of the total sample after the very coarse particles are removed, as with BS 5930. However, ASTM has defined the coarse-fine boundary as 0.075 mm (75 µm).

The soil is coarse-grained (sand or gravel) if the percentage fines is 50% or less. Otherwise, the soil is fine-grained (silt or clay) – the classification is not based on plasticity.

Coarse-grained soils are classified further as either sand or gravel using the results of particle-size distribution tests.

Fine-grained soils are classified further as silt or clay on the basis of the liquid limit and plasticity index (from Atterberg limits tests).

The soil is an organic soil if it contains sufficient quantities of dispersed organic matter that it has an influence on the liquid limits of the fines component after oven-drying, as outlined in the BS Section. The definition of peat is similar to that in BS 5930 and it is generally classified according to the degree of decomposition and strength. When encountered, reference should be made to the classification given in ASTM D 4427.

SOIL GROUP NAME AND SYMBOL (ASTM)

**Coarse-Grained Soils**

For coarse-grained soils, the dominant soil fraction is sand if the dry weight of the sand fraction, i.e. particle sizes from 0.075 mm to 4.75 mm, exceeds that of the gravel fraction, i.e. particles ranging from 4.75 mm to 75 mm, and vice versa for gravel.

Coarse-grained soils with ≤12% fines are also described as well-graded or poorly-graded based on the particle-size distribution curve, using the coefficient of uniformity ($C_U$) and, to a lesser extent, the coefficient of curvature ($C_C$) as follows:
- Sands are well-graded when $C_U \geq 6$ and $C_C$ is between 1 and 3.
- Sands are poorly-graded for other values of $C_U$ and $C_C$.
- Gravels are well-graded when $C_U \geq 4$ and $C_C$ is between 1 and 3.
- Gravels are poorly-graded for other values of $C_U$ and $C_C$.

For coarse-grained soils with fines contents >12%, these terms are not used.

Sands and gravels are also sub-divided into coarse, medium, and fine, as defined in Table 11.

**TABLE 11 - SIZE FRACTION DESCRIPTIONS FOR COARSE-GRAINED SOILS**

| Soil | Particle diameter range [mm] | | |
|---|---|---|---|
| | Coarse | Medium | Fine |
| Gravel | 75 to 19 | - | 19 to 4.75 |
| Sand | 4.75 to 2.0 | 2.0 to 0.425 | 0.425 to 0.075 |

The predominant size fractions present are identified, and the absence of size range descriptors means that fine, medium, and coarse fractions are all present in roughly equal proportions.

**Fine-Grained Soils**

Fine-grained soils are classified as clay or silt according to the results of Atterberg limits tests. A soil is inorganic clay if: $I_P \geq 6$ and $I_P \geq 0.73(w_L\text{-}20)$

where:
$I_P$ = plasticity index [%]
$w_L$ = liquid limit [%]

The A-line and U-line in a plasticity chart are as described in the BS section.

Clays with liquid limit $w_L < 50$ and plasticity index $I_P > 7$ are further classified as lean clay, and given the group symbol "CL". Clays with liquid limits $w_L \geq 50$ are further classified as fat clay, and are given the group symbol "CH".

A soil is classified as a silt when it plots below the A-line or the plasticity index $I_P < 4$. Silts with liquid limit $w_L < 50$ are given the group symbol “ML”. Silts with liquid limits $w_L \geq 50$ are further classified as elastic silt, and are given the group symbol “MH”.

Soils are classified as silty clay where the liquid limit versus plasticity index plots on or above the A-line but where the plasticity index falls within the range $4 \leq I_P \leq 7$, i.e. the hatched zone in the lower left-hand corner of the plasticity chart. Silty clays are given the Group Symbol “CL-ML”.

### Organic Soils

For both clay and silt, or the fines component of a coarse-grained soil, the additional term organic applies if the ratio of the liquid limit of a sample (or the fines portion of the sample) after oven drying at 105° C to the liquid limit without oven drying is less than 0.75.

Organic soils are classified in a manner similar to that for inorganic soils for plots of the liquid limit (not oven dried) versus plasticity index with respect to the A-line. Organic clays and silts with liquid limit $w_L < 50$ are given the same group symbol “OL”. Organic clays and silts with liquid limits $w_L \geq 50$ are given the group symbol “OH”.

Coarse-grained soils containing fine organic material are described using the term “with organic fines”.

SECONDARY SOIL TYPE (ASTM)

Secondary soil type descriptions follow the ranges given in Table 12. No other terms are used, though combinations of these terms are.

**TABLE 12 - DESCRIPTIVE TERMS AND RANGES FOR SECONDARY CONSTITUENTS**

| Term | Principal soil type | Term | Approximate proportion of secondary constituent | |
|---|---|---|---|---|
| | | | Coarse soil | Fine soil |
| | SAND and/or GRAVEL(1) | | | < 5% |
| | SAND and/or GRAVEL(1) | with clay or silt | | 5% to 12% |
| Clayey or Silty | SAND and/or GRAVEL(1) | | | > 12% |
| | SAND and/or GRAVEL(1) | | <15% gravel or sand | |
| | SAND and/or GRAVEL(1) | with gravel or sand | ≥15% gravel or sand | |
| | SILT or CLAY | | < 15% | |
| | SILT or CLAY | with sand or gravel(1) | 15% to 29% | |
| Sandy and/or gravelly(1) | SILT or CLAY | | ≥30% | |

Note: (1) choice depends on which has higher percentage.

PARTICLE SHAPE (ASTM)

The description of particle shape includes references to form, angularity, and surface texture. These terms are normally used only for gravels, cobbles, and boulders, though in some cases for coarse sands.

The form (or shape) of coarse particles is described as flat, elongated, or both.

Flat: Width/Thickness > 3
Elongated: Length/Width > 3
Flat and elongated meets both criteria. These terms are not used if the criteria are not strictly met.

Angularity terms are usually only applied to particles gravel-size and larger (Table 13, from ASTM D 2488).

**TABLE 13 - ANGULARITY OF COARSE-GRAINED PARTICLES**

| Term | Criteria |
|---|---|
| Angular | Particles have sharp edges and relatively plane sides with unpolished surfaces |
| Subangular | Particles are similar to angular description but have rounded edges |
| Subrounded | Particles have nearly plane sides but have well-rounded corners and edges |
| Rounded | Particles have smoothly curved sides and no edges |

The surface texture of coarse particles are described as rough or smooth.

COLOUR (ASTM)

As noted for BS 5930 (BS section), soil colours are described using the Munsell Soil Colour Charts (Gretag-Macbeth, 2000).

SOIL ODOUR (ASTM)

The same descriptive terms suggested for BS 5930 (BS Section) are used with the ASTM Standards. It must be emphasised that soil odour descriptions are unlikely to be fully consistent, because of factors such as variations in sample handling, ambient conditions at time of sample description, and strong dependence on a person's ability to detect and identify odour.

STRENGTH OF COHESIVE SOILS (ASTM)

Descriptions of cohesive soil strength are not part of the ASTM classification system; however soil strength is incorporated whenever available from laboratory or in situ test results and interpretation. The boundaries for undrained shear strength ranges in current use in North American practice are given in Table 14. These boundaries are lower than those used with BS 5930.

**TABLE 14 - UNDRAINED SHEAR STRENGTH SCALE FOR COHESIVE SOILS (1)**

| **Term** | **Undrained shear strength** | |
|---|---|---|
| | **[kPa]** | **[ksf] (2)** |
| Very soft | Less than 12.5 | Less than 0.25 |
| Soft | 12.5 to 25 | 0.25 to 0.50 |
| Firm | 25 to 50 | 0.50 to 1.0 |
| Stiff | 50 to 100 | 1.0 to 2.0 |
| Very stiff | 100 to 200 | 2.0 to 4.0 |
| Hard | 200 to 400 | 4.0 to 8.0 |
| Very hard (3) | Greater than 400 | Greater than 8.0 |

**Notes**: 1) from Terzaghi and Peck (1967)
2) ksf used primarily for US projects
3) the upper boundary for "Hard", and the "Very hard" range have been added

DENSITY/COMPACTNESS OF GRANULAR SOILS (ASTM)

Tables of recommended values and descriptors for relative density are not provided in the ASTM Standards, but in practice relative density is often interpreted on the basis of cone penetration test results. The same ranges of relative density (compactness) as those recommended for use with BS 5930 (see BS Section) are used.

DISCONTINUITIES/STRUCTURE (ASTM)

Criteria for describing soil structure are provided in ASTM D 2488, and in Table 15 along with additional terms in use in the geotechnical industry.

**TABLE 15 - DESCRIPTIVE TERMS FOR SOIL STRUCTURE**

| **Term** | **Description** |
|---|---|
| Slickensided | Fracture or shear planes (or planes of weakness) that appears slick and glossy. |
| Fissured | Cohesive soil that breaks into blocks along unpolished planes (discontinuities), often filled with a different material. The fill material is noted. |
| Blocky | Cohesive soil that breaks into small angular lumps along polished planes (discontinuities) which resist further breakdown. |
| Gassy | Soil has a porous nature and there is evidence of gas, such as blisters. |
| Expansive | Visibly expands after sampling. Degree of expansion is estimated and noted. |
| Platy | A stratified appearance when the soil can be broken into thin horizontal plates. |
| Cemented | Material grains bound together forming an intact mass. |

The distance between the fissures, shear planes and expansion cracks is noted using the terms in Table 8.

BEDDING/STRATIGRAPHY (ASTM)

The terminology for bedding thickness and stratigraphic description used in North American offshore practice is more detailed than outlined in ASTM D 2488, and is different from BS 5930. In Table 16, the descriptive terms have been further defined and integrated with BS 5930 terminology.

**TABLE 16 - DESCRIPTIVE TERMS FOR BEDDING THICKNESS AND INCLUSIONS**

| Term | Bedding thickness | |
|---|---|---|
| | [mm] | [inch] |
| Pocket | Inclusion of material of different texture that is smaller than the diameter of the sample | |
| Parting | < 3 | 1/8 |
| Lamina | 3 to < 6 | 1/8 to < 0.25 |
| Laminated(1) | Alternating partings or laminae of different soil types in equal proportion | |
| Lens | 6 to < 20 | 0.25 to < 0.75 |
| Seam | 20 to < 76 | 0.75 to < 3 |
| Layer | Greater than 76 | Greater than 3 |
| Stratified(2) | Alternating lenses, seams or layers of different soil types in equal proportion | |
| Intermixed | Soil sample composed of pockets of different soil types, and laminated or stratified structure is not evident | |

Notes: (1) Equivalent to "Interlaminated" term used in BS 5930:1999
(2) Equivalent to "Interbedded" term used in BS 5930:1999.

MINOR CONSTITUENTS (ASTM)

Minor constituents within a soil, such as shell or wood fragments, or small quantities of soil particles (not secondary soil types), are typically more relevant to the site geology or to laboratory testing procedures than to soil behaviour. Since the terms and percentages are not defined in either BS 5930 or ASTM D 2487/8, the terms "with trace", "with few", "with", "with many" are used as a guide.

## WRITTEN SOIL DESCRIPTIONS

Although soils are classified in the order of the characteristics described in the preceding sections, written descriptions are given in a different order in both Standards. To bring as much consistency as possible to the soil descriptions, Fugro selected a single preferred order of terms, which most closely resembled the majority of the descriptions used in Fugro offices around the world.

In this description, the principal soil type is given last as the soil name, with most other terms written as adjectives. The principal soil type is given in upper-case.

The preferred order of terms for a soil description are:

1. Density/compactness/strength.
2. Discontinuities.
3. Bedding.
4. Colour.
5. Secondary (composite) soil types.
6. Particle shape.
7. Particle size.
8. PRINCIPAL SOIL TYPE.

with:

9. Minor constituents (can be inserted in front of the principal soil type, such as "shelly").
10. Soil odour.

For example: Firm closely-fissured dark olive grey sandy calcareous CLAY with few silt pockets. Where used, the Group Symbol is part of the soil description, e.g. loose poorly-graded fine to medium SAND with silt (SP-SM).

## PARTICULATE DEPOSITS

The geological origin of a single particle type allows the following descriptions (optional):

**Clastic**: sediment transported and deposited as grains of inorganic origin. Typical clastic particles are:
- quartz grains: clear or milky white and ranging from very angular to very rounded; commonly a frosted surface for wind-blown grains
- feldspar grains: varying in colour from milky white to light yellowish brown
- mica flakes: varying in colour from gold-coloured to dark brown
- dark mineral grains: usually of igneous or metamorphic origin with undetermined mineralogy
- silicate grains: undetermined mineralogy
- rock fragments: including fragments of carbonate rock
- debris: deposit of rock fragments of a variety of particle sizes which may include sand and finer fractions; typical examples are rock debris and coral debris.

**Organic**: remains of plants and animals that consists mainly of carbon compounds

**Bioclastic**: sediment transported and deposited as grains of organic origin. Examples of bioclastic particles are:
- Calcareous algae: crustal or nodular growths or erect and branching forms produced by lime-secreting algae; microstructures include layered, rectangular structures and internal fine tube-like structures.
- Foraminifera: hard sediment test (external skeleton) consisting of calcite or aragonite and produced by unicellular organisms; commonly less than 1 mm in diameter, multi-chambered and intact.
- Sponge spicules: spicules of siliceous sponges in a variety of rayed shapes; dimensions ranging from less than 1 mm to over 1 cm in length but usually less than 1 mm in width.
- Corals: commonly consisting of small fibres set perpendicular to the walls and septal surfaces; mainly aragonite composition for relatively recent forms; conversion of aragonite to calcite for earlier corals, usually with consequent loss of original structural details.
- Echinoids: hard part of echinoids consisting of a plate or skeletal element forming a single crystal of calcite; five-rayed internal symmetry for spines of echinoids; typical widths ranging from several mm to a few cm.
- Bryozoans: chambered cell-like structures that are considerably coarser than those of calcareous algae; either aragonite or calcite composition; possible cell in-fill consisting of clear calcite and/or micrite.
- Bivalves and Gastropods: Mollusk shells, chiefly of aragonite composition; inner layer of aragonite protected by an outer layer of calcite for some bivalve shells and gastropods.

**Oolitic**: sediment consisting of solid, round or oval, highly polished and smooth coated grains, which may or may not have a nucleus. The coating consists of chemically precipitated aragonite, possibly converted to calcite. Ooliths have concentric structures and may also have radial structures. The grains are generally less than 2 mm diameter.

**Pelletal**: sediment consisting of well-rounded grains of ellipsoidal shape and no specific internal structure. The composition is clay to silt-sized carbonate material, which is probably the excretion product of sediment eating organisms. Pellets may have an oolitic crust. The grains are generally less than 2 mm diameter.

## STRUCTURE OF NON PARTICULATE DEPOSITS

**Reef**: soil or rock formed by in situ accumulation or build-up of carbonate material by colonial organisms such as polyps (coral), algae (algal mats or balls) and sponges.

**Orthochemical**: orthochemical components precipitated during or after deposition. These components can include: (1) pyrite spherulites and grains, (2) crystal euhedra of anhydride or gypsum, (3) replacement patches and nodular masses of anhydrite and gypsum. Single grains are rare.

## GEOLOGICAL INFORMATION

Specific geological terms can assist the geotechnical soil description by providing information on stratigraphy, origin (genesis) or regional significance (optional). Examples are:

- time stratigraphy, such as Eemian and Pleistocene
- lithostratigraphy, such as Yarmouth Roads Formation
- depositional environment, such as Marine, Glacio-lacustrine and Residual Soil
- regional significance, such as Chalk and Mud.

## REFERENCES

ASTM International (2011), “Standard Practice for Classification of Soils for Engineering Purposes (Unified Soil Classification System)", ASTM D2487-11.

ASTM International (2009), “Standard Practice for Description and Identification of Soils (Visual-Manual Procedure)", ASTM D2488-09a.

ASTM International (2007), “Standard Classification of Peat Samples by Laboratory Testing”, ASTM D4427-07.

BSI British Standards Institution (1999), "Code of Practice for Site Investigations", British Standard BS 5930:1999.

Casagrande, A. (1948), “Classification and Identification of Soils”, Proceedings of the American Society of Civil Engineers, Vol. 73, No. 6, pp. 783-810.

Clark, A.R. and Walker, B.F. (1977), "A Proposed Scheme for the Classification and Nomenclature for use in the Engineering Description of Middle Eastern Sedimentary Rocks", Géotechnique, Vol. 27, No. 1, pp. 94-99.

Gretag-Macbeth (2000), “Munsell Soil Color Charts”, Year 2000 revised washable ed., Gretag-Macbeth, New Windsor.

ISO International Organization for Standardization (2002), "Geotechnical Investigation and Testing - Identification and Classification of Soil - Part 1: Identification and Description", International Standard ISO 14688-1:2002.

ISO International Organization for Standardization (2004), "Geotechnical Investigation and Testing - Identification and Classification of Soil - Part 2: Principles for a Classification", International Standard ISO 14688-2:2004.

ISO International Organization for Standardization (2014), “Petroleum and Natural Gas Industries - Specific Requirements for Offshore Structures – Part 8: Marine Soil Investigations”, International Standard ISO 19901-8:2014.

Landva, J., Remijn, M. and Peuchen, J. (2007), "Note on Geotechnical Soil Description", in Offshore Site Investigation and Geotechnics: Confronting New Challenges and Sharing Knowledge: Proceedings of the 6th International Conference, 11–13 September 2007, London, UK, Society for Underwater Technology, London, pp. 505-514.

Peuchen, J., De Ruijter, M. and Goedemoed, S. (1999), "Commercial Characterisation of Calcareous Soils", in Al-Shafei, K.A. (Ed.), Engineering for Calcareous Sediments: Proceedings of the Second International Conference on Engineering for Calcareous Sediments, Bahrain, 21-24 February 1999, Vol. 1, A.A. Balkema, Rotterdam, pp. 113-121.

## TESTING PRACTICE

GENERAL

This document summarises geotechnical laboratory test methods for soil.

Fugro strives to arrange testing in registered laboratories with formal accreditation. This document summarises test methods used by Fugro geotechnical laboratories in the Netherlands. Test methods used by on-site laboratories and other office laboratories are often identical or generally equivalent.

Laboratory tests are carried out in general accordance with standards published by ASTM International (ASTM), British Standards Institution (BSI) and International Organization for Standardization (ISO). Note that ISO (2014) refers mainly to test procedures published in other documents, with some additional recommendations. In-house test procedures adopted for some tests are generally based on published recommendations for which no standards are available. Detailed work instructions and calibration details are available for inspection at the laboratory.

Some of the laboratory tests allow various optional procedures. These procedures are not applicable, unless specifically agreed.

Soil parameter values can vary with temperature. Tests are generally conducted at laboratory temperatures of around 20$^{o}$C. Any tests conducted at specific temperatures and any corrections for temperature are explicitly reported.

Laboratory test results show depth defined as vertical distance between ground surface or seafloor and top of the laboratory test specimen, unless indicated otherwise.

SAMPLE REQUIREMENTS

The feasibility of a particular laboratory test relates to the sampling practice and sample handling for a particular soil and depends on factors such as soil type, available amount of sample material and sample quality. Usually, a reasonable estimate of test feasibility is possible at the time of sampling. A further refinement is possible in the laboratory prior to testing and, in some cases, only after testing. The limitations of feasibility estimates may lead to rejection of samples for testing upon inspection in the laboratory or may result in appropriate comments on test results after completion of testing.

The adopted classification system for sample quality is according to BSI (2015) and ISO (2006, 2014). The classification system recognises 5 classes on the basis of feasibility of specific geotechnical identification and laboratory tests. A summary of these classes is as follows:
Class 1: undisturbed: strength, stiffness and consolidation
Class 2: undisturbed: permeability, unit weight, boundaries of strata - fine
Class 3: disturbed: water content
Class 4: disturbed: particle size analysis, Atterberg limits, boundaries of strata - broad
Class 5: disturbed: sequence of layers
The higher class includes the laboratory tests of the lower class.

An indication of intact (undisturbed) sample quality may be obtained from re-compression of a test specimen, for example in an oedometer or triaxial cell. Table 1 presents a method recommended by ISO (2014) based on $\Delta e/e_0$. Here, $\Delta e$ represents the change in void ratio $\Delta e$ from an initial laboratory value ($e_0$) at atmospheric conditions to the specimen void ratio upon re-compression to in situ stress conditions.

**TABLE 1 - INTACT SAMPLE QUALITY** - $\Delta e/e_0$

| **Overconsolidation Ratio** | $\Delta e/e_0$ | | | |
|---|---|---|---|---|
| | **1** (very good to excellent) | **2** (good to fair) | **3** (poor) | **4** (very poor) |
| 1 to 2 | < 0.04 | 0.04 to 0.07 | 0.07 to 0.14 | > 0.14 |
| 2 to 4 | < 0.03 | 0.03 to 0.05 | 0.05 to 0.10 | > 0.10 |

ISSUE 42

The presented criteria are based on tests on marine clays in the depth range 4 m to 25 m, with plasticity index in the range 6% to 43%, water content 20% to 67% and overconsolidation ratios of 1 to 4. The criteria must be used with caution for soils outside this range.

Table 2 presents an alternative indication of intact (undisturbed) sample quality according to Terzaghi et al. (1996). Here, volumetric strain is derived from an initial laboratory specimen volume and the specimen volume upon re-compression to in situ stress conditions. The criteria apply to clays with an overconsolidation ratio of less than about 3 to 5. Parameters such as effective preconsolidation pressure $\sigma'_p$ and undrained shear strength $c_u$ preferably require laboratory specimen with SQD equal to B or better (DeGroot et al., 2005).

**TABLE 2 – INTACT SAMPLE QUALITY - SDQ**

| Volumetric Strain $\varepsilon_v$ [%] | SDQ |
|---|---|
| < 1 | A |
| 1 to 2 | B |
| 2 to 4 | C |
| 4 to 8 | D |
| > 8 | E |
| **Note**: SDQ: Sample Quality Designation | |

The $\Delta e/e_0$ and $\varepsilon_v$ criteria represent a simplification, as they ignore important soil changes during the process of sampling and sample handling up to specimen preparation in a geotechnical laboratory. This simplification avoids interpretation anomalies related to uncertainties in laboratory values for soil unit weights, water contents and density of solid particles.

The $\Delta e/e_0$ and $\varepsilon_v$ criteria assume no-gas within the pore water. Gas can cause an increase in void ratio when recovering samples to surface. The result is a correspondingly larger change in void ratio when returning a specimen back to the estimated effective stress conditions in situ. In such case, it is likely that the undrained shear strength would be less affected than soil stiffness, as the void ratio in situ has been partially restored. Changes in soil fabric remain.

Values for $\Delta e/e_0$ and $\varepsilon_v$ should exclude secondary consolidation. In practice, no correction for secondary consolidation will be applied. This practice underestimates undisturbed sample quality, particularly for incremental loading oedometer tests with 24 hour load increments and longer.

## GEOTECHNICAL INDEX TESTING

### WATER CONTENT

The water content is determined by drying selected moist/wet soil material for at least 18 hours to a constant mass in a 110°C drying oven. The difference in mass before and after drying is used as the mass of the water in the test material. The mass of material remaining after drying is used as the mass of the solid particles. The ratio of the mass of water to the measured mass of solid particles is the water content of the material. This ratio can exceed 1 (or 100%).

Test references: ASTM D2216-10, BS 1377: Part 2: 1990, ISO/TS 17892-1:2014, ISO 19901-8:2014

### UNIT WEIGHT – VOLUME-MASS CALCULATION

Measurement of volume and mass of a soil sample allows calculation of unit weight. For fine-grained (cohesive) soils, a soil specimen is generally obtained from a standard steel cylinder with cutting edge, which is pushed manually into the extruded soil sample. Preference is given to a 100 ml cylinder (area ratio of 12%), but a volume of 33.3 ml (area ratio of 21%) may be used when insufficient homogeneous sample is available. If possible, a specimen of coarse-grained (non-cohesive) soil is obtained by selecting a part of a cylindrical soil sample, trimming the end surfaces, and measuring height and diameter. This method also applies to fine-grained specimens selected for strength and/or stiffness (e.g. triaxial and oedometer) tests.

Unit weight $\gamma$ (kN/m$^3$) refers to unit weight of the soil specimen at the water content at the time of test.

The method excludes correction for pore water salinity r (contains dissolved solids), in situ pressure and temperature. The diagram below provides an indication of error in calculated submerged unit weight $\gamma'$ versus submerged unit weight corrected for salinity, $\gamma'^*$ (Kay et al., 2005). Typical seawater salinity is 35 g salt per kg seawater (r = 0.035). Correction for salinity is optional.

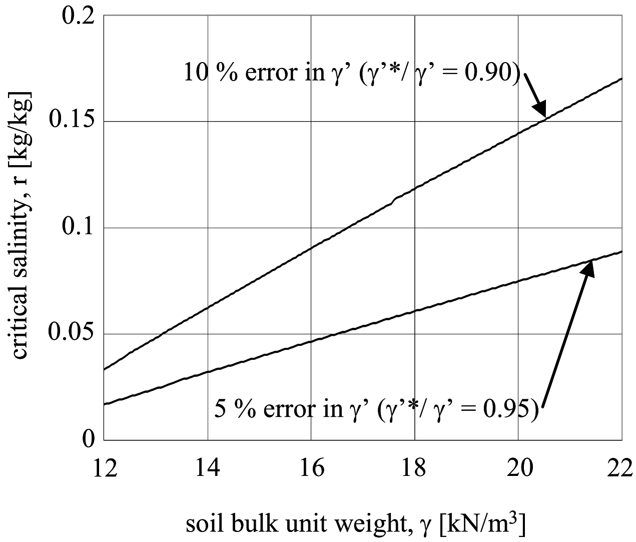


Optionally, dry unit weight $\gamma_d$, is calculated from the mass of oven-dried soil and the initial specimen volume.

Test references: BS 1377: Part 2: 1990, ASTM D7263-09, ISO 19901-8:2014

UNIT WEIGHT – DERIVED FROM WATER CONTENT

Water content (w) measurement allows estimation of soil unit weight ($\gamma$) on fully saturated samples. This practice requires input on density of solid particles ($\rho_s$) and presumes saturation of non-saline pore water.

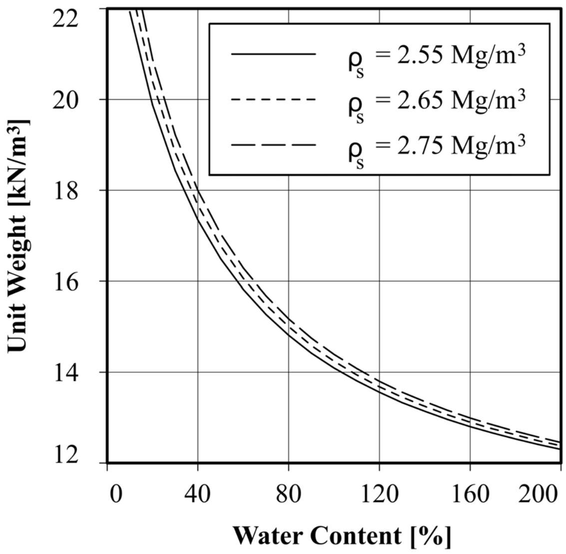


Correction for (high) pore water salinity (contains dissolved solids) is optional.

Test reference: In-house

## DENSITY OF SOLID PARTICLES – CONVENTIONAL PYCNOMETER

The density of the solid particles of an oven-dried soil sample is determined by means of a stoppered-bottle pycnometer, using distilled water. The method is considered applicable to solid particles that are not soluble in water. For soils with a high organic content, a different liquid may be selected. Soils with high pore water salinity (contain dissolved solids) require use of a gas pycnometer. This is optional.

Test references: BS 1377: Part 2: 1990, ASTM D854-14, ISO 19901-8:2014

## GRAIN SHAPE

Grain shape is determined by microscopic comparison of both grain roundness and sphericity with standard grain shapes. The standard shapes are presented together with the test results.

Test reference: In-house

## PARTICLE SIZE ANALYSIS

Particle size analysis can be performed by means of sieving and/or hydrometer readings. Sieving is carried out for particles that would be retained on a 0.063 mm (ISO and BS) or 0.075 mm (ASTM) sieve, while additional hydrometer readings may be carried out when a significant fraction of the material passes a 0.063 mm (0.075 mm) sieve.

In a sieve analysis, the mass of soil retained on each sieve is determined, and expressed as a percentage of the total mass of the sample. Prior to sieving, samples are treated with a dispersing agent (sodium hexameta-phosphate), rinsed on a 0.063 mm (0.075 mm) sieve and dried.

The hydrometer method allows measurement of the density of a suspension consisting of fine-grained soil particles and distilled water, to which a dispersion agent is added. This suspension is mixed using a high speed stirrer. Testing is performed in a thermostatically controlled water bath (25° ± 0.5°). The particle size is calculated according to Stokes' Law for a single sphere, on the basis that particles of a particular diameter were at the surface of the suspension at the beginning of sedimentation and had settled to the level at which the hydrometer is measuring the density of the suspension. These calculations require a value for the density of solid particles. Generally, a value of 2.65 t/m$^3$ is assumed. When other values are used, this is included in the laboratory report. The hydrometer results for selected particle sizes are presented as a percentage of the total mass of the soil sample.

Particle size is presented on a logarithmic scale so that two soils having the same degree of uniformity are represented by curves of the same shape regardless of their positions on the particle size distribution plot. The general slope of the distribution curve may be described by the coefficient of uniformity $C_u$, where $C_u = D_{60}/D_{10}$, and the coefficient of curvature $C_c$, where $C_c = (D_{30})^2/D_{10} \times D_{60}$. $D_{60}$, $D_{30}$, and $D_{10}$ are effective particle sizes indicating that 60%, 30%, and 10% respectively of the particles (by weight) are smaller than the given effective size.

Combined presentation of results from hydrometer readings and sieving normally requires data harmonising in the area of overlap, i.e. near the 0.06 mm particle size.

Test references: ISO/TS 17892-4:2004, BS 1377: Part 2: 1990, ASTM D422-63 (2007)e2, ISO 19901-8:2014

## PERCENTAGE FINES

The Percentage Fines test identifies the proportions of fine grained (< 0.06 mm for BS/ISO and < 0.075 mm for ASTM) and coarse-grained (> 0.06 mm) particle sizes of a soil sample by wet sieving through a 0.063 mm (0.075 mm) sieve. Prior to sieving, the sample is treated with a dispersing agent. The Percentage Fines is defined as the ratio of dry mass of soil passing the 0.063 mm (0.075 mm) sieve to the dry mass of the total soil sample, expressed as a percentage.

Test references: ISO/TS 17892-4:2004, BS 1377: Part 2: 1990, ASTM D422-63 (2007)e2, ISO 19901-8:2014

## ATTERBERG LIMITS

Atterberg limits are determined on soil specimens with a particle size of less than 0.425 mm. If necessary, coarser material is removed by dry sieving. The Atterberg limits refer to arbitrarily defined boundaries between the liquid and plastic states (Liquid Limit, $w_L$), and between the plastic and brittle states (Plastic Limit, $w_P$) of fine grained soils. They are expressed as water content, in percent.

The liquid limit is defined as the water content at which a part of soil is placed in a standard cup and cut by a groove of standard dimensions will flow together at the base of the groove, when the cup is subjected to 25 standard shocks. The one-point liquid limit test is usually carried out. Distilled water may be added during soil mixing to achieve the required consistency.

The plastic limit is defined as the water content at which a soil can no longer be deformed by rolling into 3 mm diameter threads without crumbling.

The range of water contents over which a soil behaves plastically is the Plasticity Index, $I_P$. This is the difference between the liquid limit and the plastic limit ($w_L$-$w_P$).

Test references: BS 1377: Part 2: 1990, ASTM D4318-10e1, ISO 19901-8:2014

## MINIMUM INDEX UNIT WEIGHT

The minimum index unit weight ($\gamma_{dmin}$) of cohesionless soil is determined from the mass of oven-dry material that is deposited by slowly withdrawing a soil-filled funnel from a standard mould of either 70 ml or 550 ml volume.

Test reference: In-house

## MAXIMUM INDEX UNIT WEIGHT - IMPACT COMPACTION

The maximum index unit weight ($\gamma_{dmax}$) of cohesionless soil is determined from the mass of oven-dry, compacted soil in a standard mould. The soil is compacted in 5 layers, with each layer being subjected to respectively 5, 10, 20, 40 and 80 blows from a standard, hand-held hammer.

Equipment dimensions are as follows. Preference is given to the large mould, but application depends on size of sample.

| | | **70.5 ml mould** | **554 ml mould** |
|---|---|---|---|
| Hammer mass | [g] | 185 | 750 |
| Drop height | [mm] | 300 | 390 |
| Cross-sectional area | [$mm^2$] | 1006 | 38,500 |

Reference: In-house, DGI Product Sheet #000 96-07-02

ISSUE 42

## MAXIMUM INDEX UNIT WEIGHT – VIBRATING HAMMER

The maximum index unit weight ($\gamma'_{dmax}$) is obtained by compacting soil that has been passed through a 4 mm sieve into a mould at a range of water contents. The first sample is thoroughly mixed with water, to produce a soil with a 4% water content, and then compacted in three equal layers using a vibrating hammer for a period of 10 seconds per layer. The top section of the mould is removed and the sample levelled in the bottom section of the mould. The unit weight of the sample is calculated and a representative portion of soil is removed for water content determination.



The test is repeated at four further water contents. By determining the dry unit weight achieved at each water content, a maximum dry unit weight may be estimated. There is evidence of breakdown of crushable particles during a test.

Equipment dimensions are as follows:
- Volume of mould: 96.4 ml
- Hammer: Milwaukee heavy duty 545S
  - 1300 W nominal / 650 W release
  - rotation/min: 300
  - hammer force: 8.5 J
  - mass: 6.7 kg

Test reference: In-house

## GEOCHEMICAL TESTING

### ORGANIC MATTER CONTENT – DICHROMATE OXIDATION METHOD

An oven-dried (50°C) soil sample is mixed with potassium dichromate solution and left for 30 min to allow the oxidation of organic matter to proceed. The solution is titrated with a ferrous sulphate solution (to determine the amount of excess potassium dichromate). The organic matter content is defined as the ratio of the total volume of potassium dichromate solution used to oxidize the organic matter in the soil sample to the mass of the initial dried soil sample (Walkley and Black's method). It is expressed as a percentage.

Note: soils containing sulphides or chlorides have been found to yield inaccurate (too high) organic matter content measurements using this procedure.

Test references: BS 1377: Part 3: 1990:3

### ORGANIC MATTER CONTENT – LOSS ON IGNITION

An oven-dried (105°C) soil sample is heated to 550°C for 2 hours. The mass is measured before and after heating. The organic matter content is defined as the ratio of the mass loss due to heating to the original mass of the dried soil sample, and is expressed as a percentage.

Note: the mass loss on ignition test is reliable for (1) sandy soils that contain little or no clay and no carbonate and (2) peats and organic clays containing more than 10% organic matter.

Test references: BS 1377: Part 3: 1990:4, ASTM D2974-14, NEN 5754, ISO 19901-8:2014

### CARBONATE CONTENT – GAS VOLUME

The carbonate content is determined by drying selected soil material to a constant mass in a 110°C drying oven, and measuring the volume of dissipated carbon dioxide ($CO_2$) upon reaction of the soil with hydrochloric acid (HCl). The carbonate content is calculated from calibration values, and expressed as a percentage of dry mass of the original soil.

Test reference: ISO 10693:2004, ISO 19901-8:2014

### CARBONATE CONTENT - GAS PRESSURE

The carbonate content is determined by using a dried or a natural soil specimen and measuring the pressure of dissipated carbon dioxide ($CO_2$) upon reaction of the soil with hydrochloric acid (HCl). The carbonate content is calculated from the mass of the specimen and the pressure increase after reaction by comparison with calibration values. For a natural soil, a correction factor is applied to correct for water content. Carbonate content is expressed as a percentage of dry mass of the original soil.

Test reference: ASTM D4373-14, ISO 19901-8:2014

### WATER-SOLUBLE SULPHATE CONTENT – GRAVIMETRIC METHOD

The water-soluble sulphate content of a soil sample is determined on a test portion that has been sieved and crushed through a 2 mm sieve and oven dried to 110°C. The test portion is mixed with distilled water to prepare a 2:1 water:soil extract.

In the gravimetric method, barium chloride solution is added to the water:soil extract and the precipitated barium sulphate is collected, dried and weighted. The sulphate content is then calculated from the mass of the material used in the analysis and the mass of the barium sulphate precipitated. BS presents the results in $SO_3$ [g/l] and AASTHO in $SO_4$ [mg/kg].

If a 2:1 water:soil extract is prepared, one can convert sulphites ($SO_3$) into sulphates ($SO_4$) by multiplying $SO_3$ by a factor 1.2. For extractions other than a 2:1 the multiplying factor is different.

Test reference: BS 1377: Part 3:1990, AASHTO T290-95-UL (2007)

WATER-SOLUBLE CHLORIDE CONTENT – MOHR'S METHOD

The water-soluble chloride content of a soil sample is determined on a test portion that has been sieved and crushed through a 2 mm sieve and oven dried to 110°C. The test portion is mixed with distilled water to prepare a 2:1 water:soil extract.

In the Mohr's method chloride ion will precipitate with silver nitrate. The chloride reacts with the silver ion before any silver chromate forms, due to the lower solubility of silver nitrate. The potassium chromate indicator reacts with excess silver ion to form a red silver chromate precipitate. The end point is the appearance of the first permanent orange colour. The chloride content is expressed as a percentage by mass of dry soil.

This test method is suitable for analysing solutions with a pH between 6.0 and 8.5.

Test reference: BS 1377: Part 3: 1990, AASHTO T291-94-UL (2008)

**PERMEABILITY TESTING**

CONSTANT HEAD PERMEABILITY: TRIAXIAL CELL

The effect of stress level on the coefficient of permeability may be estimated from constant head tests in a triaxial cell – flexible wall permeameter. The specimen is compacted in a split mould by tamping of thin layers of moist soil to the required initial density, and subsequently mounted in the triaxial cell. Filter screens or porous disks are placed at both ends of the specimen. The required stress level is applied and saturation is achieved by flushing with $CO_2$ gas followed by controlled flow of de-aired water and the application of backpressure. The degree of saturation is checked by the pore water pressure response to small variations in cell pressure. A hydraulic gradient is applied and the rate of flow is recorded for various time steps. The permeability is calculated in accordance with Darcy's equation for laminar flow.

References: BS 1377: Part 6: 1990, ASTM D5084-10, ISO 19901-8:2014

**COMPRESSIBILITY TESTING**

OEDOMETER - INCREMENTAL LOADING

The oedometer test covers determination of the rate and magnitude of consolidation of a laterally restrained soil specimen, which is axially loaded in increments of constant stress until the excess pore water pressures have dissipated for each increment. Normally, each load increment is maintained for 24 hours.

The test is generally carried out on undisturbed (intact) cohesive specimens using a consolidometer (oedometer) apparatus, which is placed in a thermostatically controlled room (10°C). Selection of mounting method depends on soil characteristics. Soils that show a tendency to swell, such as peat or overconsolidated clays, are mounted dry. Moist sponges are placed in the oedometer cell to retain sample moisture conditions. Other samples are usually mounted using the wet mounting method. Distilled water is added to the cell when loads are applied to the loading arm. When required, the initial load is increased to prevent swell.

Key parameters that can be obtained from this test are the preconsolidation pressure $\sigma'_p$ and the coefficient of consolidation $c_v$. The preconsolidation pressure is estimated using the graphical Casagrande construction. The root time method or the log time method is used for determination of $c_v$. Other parameters that may be derived from this test are the compression index $C_c$, the coefficient of volume compressibility $m_v$ and the vertical permeability $k_v$.

Test references: ASTM D2435/D2435M -11, BS 1377: Part 5: 1990, ISO 19901-8:2014

OEDOMETER - CONSTANT RATE OF STRAIN

The Constant Rate of Strain (CRS) oedometer test covers determination of the rate and magnitude of consolidation of a laterally restrained soil specimen when it is drained axially and subjected to controlled deformation loading. The rate of deformation is selected so that excess pore water pressures are between 3% and 20% of the applied axial stress. Drainage of pore water is permitted from the top of the specimen and pore water pressures are measured at the bottom of the specimen. The test is generally carried out on undisturbed (intact) cohesive specimens using a consolidometer, in a thermostatically controlled room (20°C).

Key parameters that can be obtained from this test are the preconsolidation pressure $\sigma'_p$ and the coefficient of consolidation $c_v$ as a function of axial stress. The preconsolidation pressure is estimated using the graphical Casagrande procedure, while the coefficient of consolidation is determined analytically from the measurements of axial stress, strain and excess pore water pressure. Other parameters that may be derived from this test are the compression index $C_c$, the coefficient of volume compressibility $m_v$ and the coefficient of vertical permeability $k_v$.

Test reference: ASTM D4186/D4186M-12, ISO 19901-8:2014

**STRENGTH INDEX TESTING**

TORVANE AND POCKET PENETROMETER

The torvane and pocket penetrometer are small hand-held instruments for rapid strength index testing of fine grained (cohesive) soils. The torvane test is carried out by pressing a standard vane into the soil and measuring the minimum torque required to rotate the vane. The vane size can be selected to suit the expected torque up to an equivalent undrained shear strength of the soil of 250 kPa. The undrained shear strength is correlated to the measured torque by vane size and torvane spring constant.

The pocket penetrometer test consists of pressing a small solid cylinder into the soil, to a specified penetration. The maximum force required for penetration is correlated to the undrained shear strength. The size of the cylinder can be selected so that undrained shear strength readings of up to 900 kPa can be taken.

Test reference: ISO 22475-1:2006, ISO 19901-8:2014

FALL CONE

The fall cone is a rapid index test for determining undrained shear strength of undisturbed or remoulded specimens of cohesive soil. The test consists of suspending a standard cone of a specified mass and apex angle vertically over and just touching the surface of the specimen. Subsequently, the cone is released and penetrates into the sample under its self-weight. The depth of penetration for the selected cone is correlated to the undrained shear strength of the soil. Several correlations exist. The cone size and shape can be selected to suit the expected undrained shear strength of the specimen.

Reference: ISO/TS 17892-6, ISO 19901-8:2014

HAND VANE

The hand vane allows index testing for undrained shear strength of cohesive soil. The tool is similar to the laboratory miniature vane except for reduced control: manual penetration and rotation of the vane.

Several different measurements of undrained shear strength are possible:
a) Intact: undisturbed undrained shear strength as measured on an intact specimen.
b) Intact–residual: measured post-peak during initial shearing of an intact specimen.
c) Intact–vane-remoulded: measured after multiple rotations of the hand vane after completion of the intact test.
d) Hand-remoulded: steady state (post-peak if exists) resistance of a hand-remoulded test specimen.
e) Hand-remoulded–cane-remoulded: steady state resistance of a hand-remoulded specimen measured after applying multiple vane rotations.

Different values of the remoulded shear strength are often obtained from the different measurement methods.

A specimen may be tested in the sample tube in which it was taken, in a block sample or in a mould after removal from a sampler. The test apparatus consists of a rectangular vane with a short push rod for penetration into the soil. The vane is then slowly rotated by hand and the maximum torsional moment is recorded. Various vane sizes can be selected depending on the consistency of the specimen. Calculation of undrained shear strength is based on a cylindrical failure surface for which uniform stress distributions are assumed. The equation for undrained shear strength is as follows:

$$c_U = \frac{T_{max}}{\pi D^2 \left( \frac{1}{2} H + \frac{1}{6} D \right)}$$

where:

| | | |
|---|---|---|
| $c_u$ | = peak undrained shear strength | [kPa] |
| $T_{max}$ | = maximum torsional moment | [kNm] |
| D | = vane diameter | [m] |
| H | = vane height | [m] |

Test reference: in-house

LABORATORY MINIATURE VANE

The laboratory miniature vane test allows determination of undrained shear strength of cohesive soil. CEN (2007) classifies the laboratory miniature vane as a strength index test.

Several different measurements of undrained shear strength are possible:

a) Intact: undisturbed undrained shear strength as measured on an intact specimen.
b) Intact–residual: measured post-peak during initial shearing of an intact specimen.
c) Intact–vane-remoulded: measured after multiple rotations of the vane after completion of the intact test.
d) Hand-remoulded: steady state (post-peak if exists) resistance of a hand-remoulded test specimen.
e) Hand-remoulded–vane-remoulded: steady state resistance of a hand-remoulded specimen measured after applying multiple vane rotations.

Different values of the remoulded shear strength are often obtained from the different measurement methods.

A specimen may be tested in the sample tube in which it was taken or in a mould after extrusion from the sample tube. The sample tube or mould is mounted in the test apparatus and a rectangular vane is lowered into the soil. The vane is then rotated at 10°/min (BS 1377) or at 60°/min to 90°/min (ASTM D4648) and the maximum torsional moment is recorded. A continuous record of rotation versus torsional moment can also be made if required (optional). Various vane sizes can be selected depending on the consistency of the specimen. Calculation of undrained shear strength is based on a cylindrical failure surface for which uniform stress distributions are assumed. The equation for undrained shear strength is as follows:

$$c_U = \frac{T_{max}}{\pi D^2 \left( \frac{1}{2} H + \frac{1}{6} D \right)}$$

where:

| | | |
|---|---|---|
| $c_u$ | = peak undrained shear strength | [kPa] |
| $T_{max}$ | = maximum torsional moment | [kNm] |
| D | = vane diameter | [m] |
| H | = vane height | [m] |

Test references: BS 1377: Part 7: 1990, ASTM D4648/D4648M-13, ISO 19901-8:2014

UNCONSOLIDATED UNDRAINED TRIAXIAL (UU)

This type of test is usually performed on undisturbed (intact) samples of cohesive soils. Depending on the consistency of the cohesive material, the test specimen is prepared by trimming the sample or by pushing a mould into the sample. A latex membrane with a thickness of approximately 0.2 mm is placed around the specimen. A lateral confining pressure of 600 kPa to 1000 kPa is maintained during axial compression loading of the specimen. Some test procedures consider lateral confining pressures that are equivalent to total in situ vertical stress. Consolidation and drainage of pore water during testing is not allowed. The test is deformation controlled (strain rate of 60%/h), single stage, and stopped when an axial strain of 15% or 20% is achieved. The deviator stress is calculated from the measured load assuming that the specimen deforms as a right cylinder.

The presentation of test results includes a plot of deviator stress versus axial strain. The undrained shear strength, $c_u$, is taken as half the maximum deviator stress. The stress at 15% or 20% strain is used to calculate undrained shear strength if a maximum stress has not been reached earlier.

To determine strength sensitivity, the test may be repeated on remoulded (compacted) specimens. When possible, the tested undisturbed specimen is kneaded in the membrane, and then reshaped in a mould prior to testing. Stiff to hard specimens are cut into pieces, and reconstituted (compacted) by tamping the pieces in layers into a mould, until the original specimen dimensions are obtained. The sensitivity is the ratio of shear strength of undisturbed soil to shear strength of remoulded soil, $c_u/c_{u;r}$.

Test references: ASTM D2850-03a (2007), BS 1377: Part 7: 1990 (Clause 8), ISO 19901-8:2014

## STRENGTH TESTING

### RING SHEAR - SOIL/STEEL INTERFACE

Ring shear interface tests are performed on remoulded or reconstituted (compacted) soils to infer the residual friction angle, also called the constant volume friction angle ($\delta_{cv}$), on a soil-steel interface.

The ring shear apparatus enables an annular specimen of soil, 5 mm thick with internal and external diameters of 70 mm and 100 mm, respectively, to be subjected to rotational shear.

First, the sample is consolidated to selected stress conditions. Then, it is sheared at a rate of 500 mm/min (fast shear), followed by 50 mm/min, up to a relative displacement of at least one metre. The sample is then resting for a period of 24h and after that is again consolidated to its selected stress conditions. Finally, the sample is sheared at a slower rate of 0.018 mm/min under drained conditions.

The presentation of the test results includes a plot of stress ratio and angle of shearing resistance versus displacement, both for fast and slow shear.

Test reference: BS 1377: Part 7: 1990, Jardine et al. (2005) (Appendix A), ISO 19901-8:2014

### DIRECT SIMPLE SHEAR (DSS)

Simple shear tests provide a simulation of the plane strain mode of shearing for undisturbed (intact), remoulded or reconstituted (compacted) specimens. Key features of the DSS test are essentially constant horizontal dimensions of the specimen in the direction of shear, and a constant volume during shear to simulate undrained behaviour for a saturated test specimen. A constant volume is achieved by maintaining a constant specimen height. A constant specimen height is achieved by varying the normal load applied to the specimen or by fixing the vertical loading ram in place.

The direct simple shear test is carried out on a cylindrical specimen of 66 mm diameter and 16 mm to 19 mm height depending on the test apparatus. Lateral confinement of the specimen is provided by a membrane in combination with a stack of brass shearing washers, or by a reinforced membrane. There are no facilities for applying back pressure and control of drainage.

The stress state within a test specimen is insufficiently uniform to allow fundamental processing of test results. Nevertheless, data are commonly presented by shear stresses and strains for the horizontal plane and by equivalent pore pressures.

The peak horizontal shear stress is inferred as the undrained shear strength.

Test reference: ASTM D6528-07, ISO 19901-8:2014

DIRECT SHEAR – SOIL/SOIL INTERFACE

Direct shear testing (or shear box testing) is a method for determining drained soil resistance (angle of internal friction, φ') for cohesionless and cohesive soils.

The soil to be tested is placed in a split mould, with internal dimensions of 60 mm by 60 mm. A porous stone and loading plate are placed on top of the specimen and a normal load is applied to the specimen. The sample is then sheared, by displacing the top half of the split mould relative to the bottom half, at a rate of displacement preventing significant excess pore water pressures to be generated. During the test, horizontal displacement, load and vertical displacement are recorded.

On completion of the first stage, the specimen is removed from the mould and the unit weight and water content are determined. Two further tests may then be performed, at the same unit weight, but with increased normal loads.

The test results are presented in the form of graphs of horizontal displacement versus shear stress and normal stress versus maximum shear stress.

Test reference: BS1377: Part 7: 1990, ISO 19901-8:2014

CONSOLIDATED UNDRAINED TRIAXIAL (CIU AND CAU)

The consolidated undrained triaxial test offers the opportunity to derive both undrained and drained strength parameters for undisturbed (intact) or remoulded (compacted) specimens. Specimens are generally prepared by trimming cohesive samples to the required dimensions. The wet mounting method is used, which includes use of wet porous disks and a water-filled drainage system.

Test procedures include specimen saturation, consolidation and compression loading. For cohesive soils, filter paper strips are attached to the specimen circumference to promote drainage during consolidation. Saturation is obtained by incrementing cell pressure and back pressure. The degree of saturation is checked by the pore water pressure response to small variations in cell pressure.

In case of isotropic consolidation (CIU) the specimen is usually consolidated to a stress level equivalent to the mean in situ stress estimated for the appropriate sample depth. For anisotropic consolidation (CAU), the specimen is consolidated to the estimated vertical and horizontal effective stresses. Various consolidation stages may be adopted to simulate the consolidation history and the effects of the expected loading sequence.

Specimen shearing is carried out under conditions of constant axial strain rate, while monitoring axial load and pore water pressure. A strain rate of 4%/h is generally applied, except when consolidation was slow, in which case a smaller strain rate is applied. The deviator stress is calculated from the measured load assuming the specimen deforms as a right cylinder. The shearing stage is terminated on the basis of effective principal stress ratio (ratio of effective axial stress to effective lateral stress $\sigma'_1/\sigma'_3$), or when an axial strain of 15% or 20% is reached. The CIU test may consist of three consolidation and shearing stages of increasing stress level. These stages may be performed on a single specimen or on three separate specimens.

The presentation of test results includes stress-strain data, effective stress paths, pore water pressures and shear strength parameters. Stress paths may be presented in terms of a mean effective stress (p' or s') and the principal stress difference or deviator stress (q or t) as follows:

- Cambridge p'-q space and ASTM p'-q space, with p' defined as $(\sigma'_1+2\sigma'_3)/3$ and q as $\sigma_1-\sigma_3$;
- BSI (1990) s'-t space, with s' defined as $(\sigma'_1+\sigma'_3)/2$ and t as $(\sigma_1-\sigma_3)/2$.

The undrained shear strength is defined as half the deviator stress at failure, $c_u = q/2$ and is reported for the following failure criteria:

1) maximum deviator stress
2) maximum stress ratio q/p'.

The stress at 15% or 20% strain is used to calculate undrained shear strength when a maximum stress has not been reached. A secant angle of internal friction, φ', is determined from q = Mp' where M = (6sinφ')/(3-sinφ') or sin φ' = 3M/(6+M) for compression conditions. This definition assumes a zero effective cohesion intercept and may be applied to $M_{max}$ but also to other values of M and corresponding values of q and p'. Similarly, sin φ' = t/s'. For tests with three shearing stages, angles of internal friction may be determined for each stage separately, and from a straight line approximation of the failure points of the three stages. The latter method also provides a value for effective cohesion intercept c'.

Test references: NEN 5117, ASTM D4767-11, BS 1377: Part 8: 1990 (Clause 4, 5, 6, 7), ISO 19901-8:2014

CONSOLIDATED DRAINED TRIAXIAL (CID AND CAD)

Consolidated drained triaxial compression tests are generally performed on samples of cohesionless soils. The specimen of dry soil is prepared in the rubber membrane on the base of the triaxial cell, without the use of side drains. Soil particles larger than 20% of the diameter of the specimen are removed. Specimens are prepared by tamping thin layers of soil to a density approximating the estimated in situ dry density. To saturate the specimen, $CO_2$ gas is used to expel the air and subsequently de-aired water is used to expel the $CO_2$ gas. The specimen is further saturated by incrementing cell pressure and back pressure, until the pore pressure response to a cell pressure increment (B-factor) indicates saturation is complete. The specimen is then isotropically or anisotropically consolidated (CID and CAD respectively).

After consolidation the sample is sheared by applying axial load at a sufficiently slow rate to permit drainage (usually 6%/h). The lateral confining pressure is kept constant during each loading stage. Pore pressure measurements are made at the bottom to check if the test is fully drained. The deviator stress is calculated from the measured load assuming the specimen deforms as a right cylinder. The CID test may have three consolidation and loading stages of increasing pressure performed on either a single specimen or on three separate specimens. The CAD test is limited to a single shearing stage. A shearing stage is terminated on the basis of effective stress ratio (ratio of effective axial stress to effective lateral stress, $\sigma'_1/\sigma'_3$), or when an axial strain of 15% or 20% is reached.

Results include stress-strain data, stress paths, and volumetric/shear strain of each loading stage. Stress paths may be presented in terms of a mean effective stress (p' or s') and the principal stress difference or deviator stress (q or t) as follows:

- Cambridge p'-q space and ASTM p'-q space, with p' defined as $(\sigma'_1+2\sigma'_3)/3$ and q as $\sigma_1-\sigma_3$;
- BSI (1990) s'-t space, with s' defined as $(\sigma'_1+\sigma'_3)/2$ and t as $(\sigma_1-\sigma_3)/2$.

A secant angle of internal friction, φ', is determined from q = Mp' where M = (6sinφ')/(3-sinφ') or sin φ' = 3M/(6+M) for compression conditions. This definition assumes zero effective cohesion intercept and may be applied to $M_{max}$ but also to other values of M and corresponding values of q and p'. Similarly, sin φ' = t/s'. For tests with three shearing stages, angles of internal friction may be determined for each stage separately, and from a straight line approximation of the failure points of the three stages. The latter method also provides a value for effective cohesion intercept c'.

Test reference: ASTM D7181-11; BS 1377: Part 8: 1990 (Clause 4, 5, 6, 8), ISO 19901-8:2014

## REFERENCES

American Association of State and Highway Transportation Officials, 2007. *T290-95-UL Standard Method of Test for Determining Water-Soluble Sulfate Ion Content in Soil*. Washington, D.C., AASHTO

American Association of State and Highway Transportation Officials, 2008. *AASHTO T291-94-UL Standard Method of Test for Determining Water-Soluble Chloride Ion Content in Soil*. Washington, D.C., AASHTO

ASTM International, 1963. *ASTM D422-63(2007) Standard Test Method for Particle-Size Analysis of Soils*. West Conshohocken: ASTM International.

ASTM International, 2014. *ASTM D854-14 Standard Test Methods for Specific Gravity of Soil Solids by Water Pycnometer.* West Conshohocken: ASTM International.

ASTM International, 2010. *ASTM D2216-10 Standard Test Methods for Laboratory Determination of Water (Moisture) Content of Soil and Rock by Mass.* West Conshohocken: ASTM International.

ASTM International, 2011. *ASTM D2435/D2435M-11 Standard Test Methods for One-dimensional Consolidation Properties of Soils Using Incremental Loading.* West Conshohocken: ASTM International.

ASTM International, 2003. *ASTM D2850-03a(2007)Standard Test Method for Unconsolidated-Undrained Triaxial Compression Test on Cohesive Soils.* West Conshohocken: ASTM International.

ASTM International, 2014. *ASTM D2974-14 Standard Test Methods for Moisture, Ash, and Organic Matter of Peat and Other Organic Soils.* West Conshohocken: ASTM International.

ASTM International, 2012. *ASTM D4186/D4186M-12 Standard Test Method for One-dimensional Consolidation Properties of Saturated Cohesive Soils using Controlled-strain Loading.* West Conshohocken: ASTM International.

ASTM International, 2010. *ASTM D4318-10e1 Standard Test Methods for Liquid Limit, Plastic Limit, and Plasticity Index of Soils.* West Conshohocken: ASTM International.

ASTM International, 2014. *ASTM D4373-14 Standard Test Method for Rapid Determination of Carbonate Content of Soils.* West Conshohocken: ASTM International.

ASTM International, 2013. *ASTM D4648/D4648M-13 Standard Test Method for Laboratory Miniature Vane Shear Test for Saturated Fine-grained Clayey Soil.* West Conshohocken: ASTM International.

ASTM International, 2011. *ASTM D4767-11 Standard Test Method for Consolidated Undrained Triaxial Compression Test for Cohesive Soils.* West Conshohocken: ASTM International.

ASTM International, 2010. *ASTM D5084-10 Standard Test Methods for Measurement of Hydraulic Conductivity of Saturated Porous Materials Using a Flexible Wall Permeameter.* West Conshohocken: ASTM International.

ASTM International, 2007. *ASTM D6528-07 Standard Test Method for Consolidated Undrained Direct Simple Shear Testing of Cohesive Soils.* West Conshohocken: ASTM International.

ASTM International, 2011. *ASTM D7181-11 Standard Test Method for Consolidated Drained Triaxial Compression Test for Soils.* West Conshohocken: ASTM International.

ASTM International, 2009. *ASTM D7263-09 Standard Test Methods for Laboratory Determination of Density (Unit Weight) of Soil Specimens.* West Conshohocken: ASTM International.

British Standards Institution, 1990. *BS 1377:1990 British Standard Methods of Test for Soils for Civil Engineering Purposes.* London: BSI. (Parts 1-9, with Amendments)

British Standards Institution, 2015. *BS 5930:2015 Code of practice for ground investigations*. London: BSI.

DeGroot, D.J., Poirier, S.E. and Landon, M.M. 2005. Sample Disturbance - Soft Clays. *Studia Geotechnica et Mechanica,* Vol. 27, No. 3-4, pp. 91-105.

Danish Geotechnical Institute (DGI), *Minimum Index Void Ratio, $e_{min}$ (Danish Method).* DGI Product Sheet #000 96-07-02.

International Organization for Standardization, 2004. *ISO 10693:2004 Soil quality - Determination of Carbonate Content - Volumetric Method.* Geneva: ISO.

International Organization for Standardization, 2004. *ISO/TS 17892-1:2014 Geotechnical Investigation and Testing - Laboratory Testing of Soil - Part 1: Determination of Water Content.* Geneva: ISO.

International Organization for Standardization, 2004. *ISO/TS 17892-4:2004 Geotechnical Investigation and Testing – Laboratory Testing of Soil - Part 4: Determination of Particle Size Distribution.* Geneva: ISO.

International Organization for Standardization, 2006. *ISO 22475-1:2006 Geotechnical Investigation and Testing - Sampling Methods and Groundwater Measurements - Part 1: Technical Principles for Execution.* Geneva: ISO.

International Organization for Standardization, 2014. *ISO 19901-8:2014 Petroleum and Natural Gas Industries - Specific Requirements for Offshore Structures – Part 8: Marine Soil Investigations.* Geneva: ISO.

Jardine, R., Chow, F.C., Overy, R.F. and Standing, J.R. 2005. *ICP Design Methods for Driven Piles in Sands and Clays*. London: Thomas Telford.

Kay, S., Goedemoed, S.S. and Vermeijden, C.A. 2005. Influence of Salinity on Soil Properties. In Gourvenec, S. and Cassidy, M. Eds., *Frontiers in Offshore Geotechnics ISFOG 2005: Proceedings of the First International Symposium on Frontiers in Offshore Geotechnics, University of Western Australia, Perth, 19-21 September 2005,* London: Taylor & Francis, pp. 1087-1093.

Lunne, T., Berre, T., Andersen, K.H., Strandvik, S. and Sjursen, M. 2006. Effects of Sample Disturbance and Consolidation Procedures on Measured Shear Strength of Soft Marine Norwegian Clays. *Canadian Geotechnical Journal*, Vol. 43, No. 7, pp. 726-750.

Nederlands Normalisatie-instituut, 1991. NEN 5117 Geotechnics - Determination of the Shear Resistance and Deformation Parameters of Soil - Triaxial Test.Delft: NEN. (With Amendment NEN 5117/A1, May 1997) (in Dutch)

Terzaghi, K. 1943, 1946. *Theoretical Soil Mechanics*.New York: Wiley.

## INTRODUCTION

This document presents a summary of interpretation methods for Cone Penetration Test (CPT) results. The project-specific selection of methods depends on the agreed project requirements. Some of the methods suit computer-based interpretation of CPT data records.

Interpretation of Cone Penetration Test results helps provide parameters for geotechnical models. Conventional models are typically based on plasticity theory for ultimate limit states, and on elasticity theory and consolidation theory for serviceability limit states. Features of these geotechnical models are:

– analysis of either drained (sand model) behaviour or undrained (clay model) behaviour for plasticity models
– analysis for the ultimate limit state differs from that for the serviceability limit state.

CPT interpretation methods are mostly based on empirical correlations with limited theoretical backing. Data integration with other, complementary investigation techniques (such as drilling, sampling and laboratory testing) improves confidence levels.

The interpretation techniques discussed below are subject to limitations such as:

– The majority of interpretation methods apply to "conventional" sands and clays. Conventional methods may not be appropriate for silts, sand/clay/gravel mixtures, varved or layered soils, gassy soils, underconsolidated soils, peats, carbonate soils, cemented soils and residual soils. These non-conventional soils warrant a more specific approach.
– Empirical correlations use reference parameters such as the undrained shear strength determined from a laboratory single-stage Isotropically Consolidated Undrained triaxial test (CIU) on an undisturbed specimen obtained by means of push sampling techniques (Van der Wal et al., 2010). The reference parameter may not be appropriate for the selected geotechnical model, and adjustment may be necessary. Also, adjustment for test conditions may be necessary, for example in situ temperature versus laboratory temperature.
– The cone penetration test offers limited direct information on serviceability limit states (deformation), as the penetration process imposes large strains in the surrounding soil. In comparison to ultimate limit states, better complementary data will usually be required.
– CPT interpretation techniques are often indirect. Usually, interpretation requires estimates of various other parameters. This is consistent with an integrated geotechnical investigation approach. Inevitably, this approach also includes some redundancy of data.
– Drained or undrained behaviour for the geotechnical analysis at hand may or may not coincide with respectively drained or undrained behaviour during fixed-rate penetration testing. This interpretation difficulty remains largely unresolved at this time.
– The interpretations apply to conditions as encountered at the time of the geotechnical investigation. Geological, environmental and construction/operational factors may alter as-found conditions.

ISSUE 28

## PENETRATION BEHAVIOUR

Soil behaviour during cone penetration testing shows large displacements in the immediate vicinity of the penetrometer, and small elastic displacements further away from the penetrometer. Density/structure, stiffness and in situ stress conditions significantly affect the measured parameters.

The measured cone resistance ($q_c$) includes hydrostatic water pressures as well as stress-induced pore pressures. The pore pressures are usually negligible for clean sand because the ratio of effective stress to pore pressure is high. This ratio is, however, low for penetration into clay. Knowledge of pore pressures around the penetrometer can thus be important. CPT parameters that take account of pore pressure effects include total cone resistance ($q_t$), net cone resistance ($q_n$) and pore pressure ratio ($B_q$). These parameters can be calculated if Piezo-cone Penetration Test (PCPT or CPTU) data are available. The influence of pore pressures on sleeve friction $f_s$ is relatively small. It is common to ignore this influence. Calculation of friction ratio $R_f$ (defined as $f_s/q_c$) includes no allowance for pore pressure effects.



The penetration rate with respect to soil permeability determines whether soil behaviour is primarily undrained, drained or partially drained. In general, soil behaviour during cone penetration testing is drained in clean sand (no measurable pore pressures as a consequence of soil displacements) and undrained in clay (significant pore pressure changes). Partially drained behaviour occurs in soils with intermediate permeability, such as sandy silt. The following sections mostly consider interpretation of drained soil behaviour (sand) and undrained soil behaviour (clay).

## SOIL BEHAVIOUR IDENTIFICATION

Identification of soil stratigraphy in terms of general soil behaviour (and to a lesser degree soil type) is a more important feature of CPT than other investigation technique.

Figures 1 to 3 show soil behaviour identification according to procedures given by Robertson (2009) and Ramsey (2002). Robertson (2009) represents an update of Robertson (1990), by exchange of $Q_t$ with $Q_{tn}$. The procedures consider a normalised soil behaviour classification that provides general guidance on likely soil type (silty sand for example) and a preliminary indication of parameters such as angle of internal friction $\varphi'$, overconsolidation ratio (OCR) and clay sensitivity ($S_t$). The procedures require piezo-cone test data:

$$Q_{tn} = [(q_t - \sigma_{vo})/P_a]\,(P_a/\sigma'_{vo})^n \qquad Q_t = \frac{q_t - \sigma_{vo}}{\sigma'_{vo}} \qquad F_r \text{ or } nR_f = \frac{f_s}{q_t - \sigma_{vo}}100\% \qquad B_q = \frac{u - u_0}{q_t - \sigma_{vo}}$$

where:

$Q_{tn}$ = normalised cone resistance with variable stress exponent
$Q_t$ = normalised cone resistance
$q_t$ = corrected cone resistance
$\sigma_{vo}$ = total in situ vertical stress
$\sigma'_{vo}$ = effective in situ vertical stress
$P_a$ = atmospheric pressure
$n$ = stress exponent
$f_s$ = measured sleeve friction
$u$ = measured pore pressure
$u_0$ = theoretical hydrostatic pore pressure.

Zhang et al. (2002) defined stress exponent n as follows:

$$n = 0.381\,(I_c) + 0.05\,(\sigma'_{vo} / P_a) - 0.15 \text{ where } n \leq 1$$

Robertson and Wride (1998) defined soil behaviour type index $I_c$ (Figure 3) as follows:

$$I_c = [(3.47 - \log Q_{tn})^2 + (\log F_r + 1.22)^2\,]^{0.5}$$

Soils with $I_c < 2.5$ are generally cohesionless, coarse grained, where cone penetration is generally drained and soils with $I_c > 2.7$ are generally cohesive, fine grained, where cone penetration is generally undrained (Robertson, 1990). Cone penetration in soils with $2.5 < I_c < 2.7$ is often partially drained.

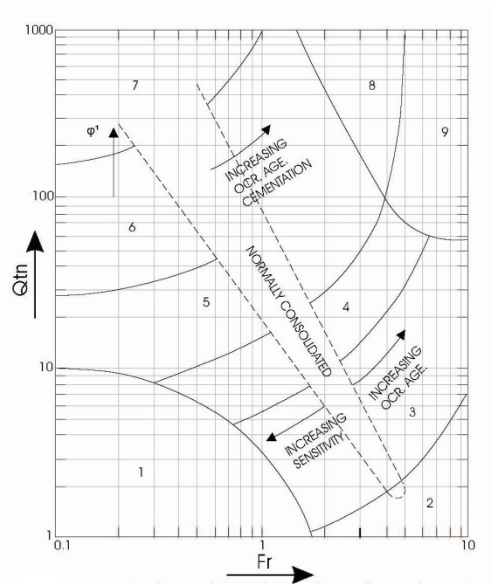


1. Sensitive, fine grained
2. Organic soils - peats
3. Clays- clay to silty clay
4. Silt mixtures – clayey silt to silty clay
5. Sand mixtures – silty sand to sandy silt
6. Sands – clean sand to silty sand
7. Gravelly sand to sand
8. Very stiff sand to clayey sand*
9. Very stiff, fine grained*

(*) Heavily overconsolidated or cemented

**Figure 1, Classification chart Robertson (2009)**

ISSUE 28

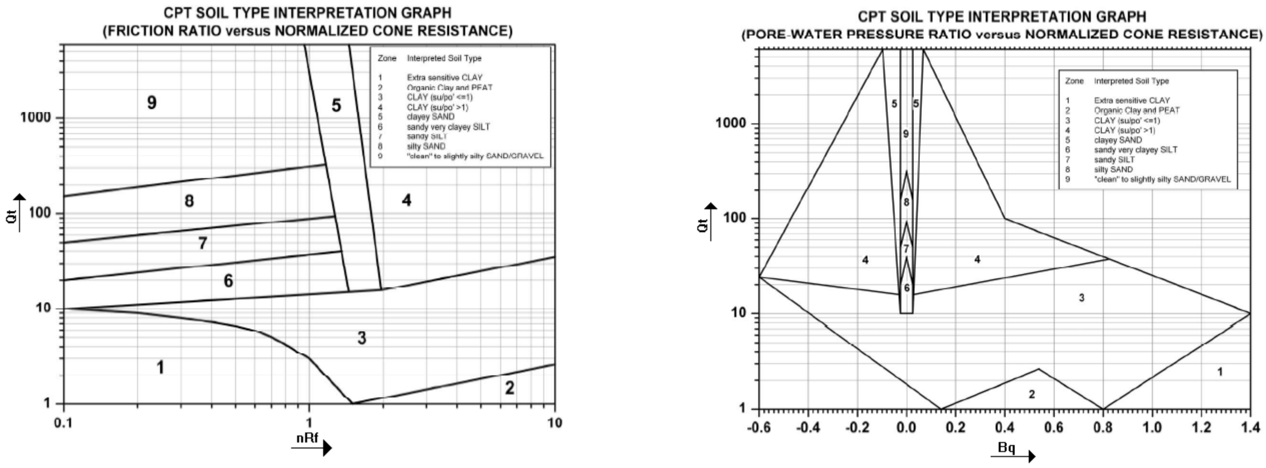


1. Extra sensitive clay
2. Organic clay and peat
3. Clay ($c_u/\sigma'_{vo}$ <= 1)
4. Clay ($c_u/\sigma'_{vo}$ > 1)
5. Clayey sand
6. Sandy very clayey silt
7. Sandy silt
8. Silty sand
9. "Clean" sand/gravel

**Figure 2, Classification charts Ramsey (2002)**

Classification is only possible for certain combinations of $Q_{tn}$, $Q_t$ , $F_r$, $nR_f$ and $B_q$, as shown below.

| Classification Limits | |
|---|---|
| **Robertson** | **Ramsey** |
| $1 \le Q_{tn} \le 1000$<br>$0.1 \le F_r \le 10$<br>$-0.2 \le B_q \le 1.4$ | $1 \le Q_t \le 6000$<br>$0.1 \le nR_f \le 10$<br>$-0.6 \le B_q \le 1.4$ |

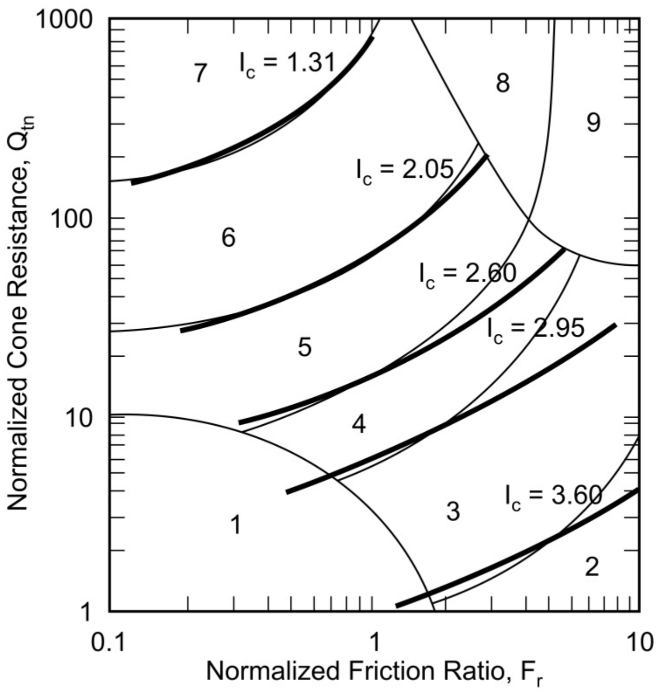


**Figure 3, Soil behaviour type index $I_c$ superimposed on Robertson (2009) classification chart**

Figure 4 presents a classification chart for friction cone data according to Robertson (2010). This procedure requires no pore pressure input. A non-normalised soil behaviour type index, $I_{SBT}$ applies:

$$I_{SBT} = [(3.47 - \log(q_c/P_a))^2 + (\log R_f + 1.22)^2]^{0.5}$$

$I_{SBT}$ is similar to $I_c$. Values for $I_{SBT}$ and $I_c$ are typically comparable for effective in situ vertical stress between 50 kPa and 150 kPa.

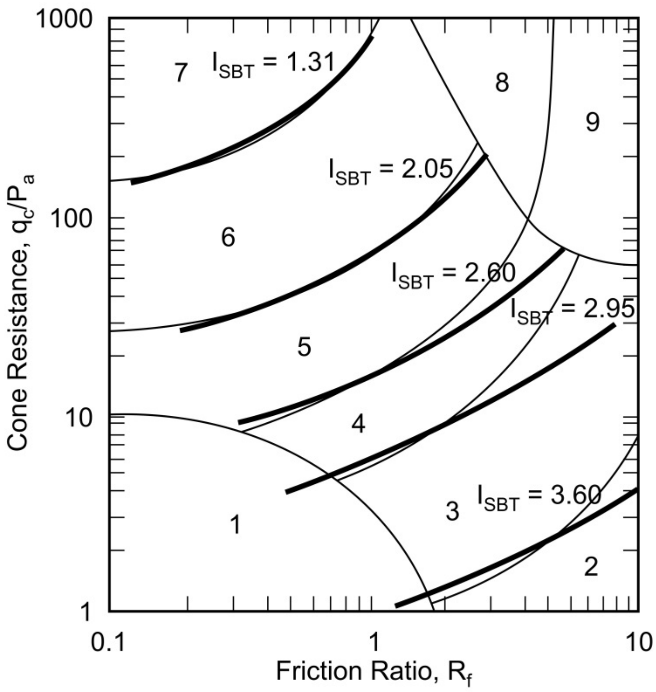


**Figure 4, Robertson (2010) classification chart including $I_{SBT}$**

## SAND MODEL

### Unit Weight – Sand

Unit weight of uncemented (silica) sand, silt and clay soils may be derived according to Mayne et al. (2010):

$$\gamma = 1.95\,\gamma_w \left(\frac{\sigma'_{vo}}{P_a}\right)^{0.06} \left(\frac{f_t}{P_a}\right)^{0.06}$$

where total unit weight $\gamma$ and unit weight of water $\gamma_w$ are in kN/m$^3$ and effective in situ vertical stress $\sigma'_{vo}$ is in kPa. The symbol $f_t$ refers to sleeve friction corrected for pore pressures acting on the end areas of the friction sleeve, with units in kPa. Atmospheric pressure $P_a$ is in kPa.

### In Situ Stress Conditions - Sand

A knowledge of in situ stress conditions is required for estimation of parameters such as relative density $D_r$ and angle of internal friction of a sand deposit $\varphi'$. The effective in situ vertical stress $\sigma'_{vo}$ may be calculated with a reasonable degree of accuracy but the effective in situ horizontal stress $\sigma'_{ho} = K_o\sigma'_{vo}$ is generally unknown. Usually, it is necessary to consider a range of conditions for $K_o$ (coefficient of earth pressure at rest). The range considers overconsolidation as inferred from a geological assessment, pre-consolidation pressures of intermediate clay layers and/or theoretical limits of $K_o$.

Geological factors concerning overconsolidation include ice loading, soil loading and groundwater fluctuations. Possible subdivisions for these factors are mechanical, cyclic and ageing consolidation.

ISSUE 28

$K_o$ may be directly correlated to Overconsolidation Ratio (OCR), as follows:

$$K_o = 0.4\ \sqrt{(OCR)}$$

Mayne and Kulhawy (1982) investigated mechanical overconsolidation of reconstituted laboratory specimens for over 170 different soils. A $K_0$ OCR correlation requiring effective angle of internal friction as input was found to provide a reasonable match. It can be shown that the $K_o = 0.4\ \sqrt{(OCR)}$ equation provides similar statistics to the Mayne and Kulhawy correlation.

No laboratory study can fully capture in situ behaviour. Particularly, $K_o$ may be underestimated if effects such as ageing and cyclic loading are relevant.

In general, in situ $K_o$ values are limited to the range $K_o = 0.5$ to $K_o = 1.5$. For many situations, $K_o$ values are believed to be relatively low at greater depths (say $K_o < 1$ for depths exceeding 50 m). Jamiolkowski et al. (2003) recommend using a limiting value $K_o = 1$ in practice.

**Relative Density - Sand**

Procedures for estimation of in situ density condition (loose, dense, etc.) consist of:
(a) Estimation of in situ stress conditions $\sigma'_{vo}$ and $\sigma'_{ho}$
(b) Empirical correlation of relative density $D_r$ (or density condition) with $q_c$, $\sigma'_{vo}$ and $\sigma'_{ho}$.

Estimation of stress conditions has been discussed above.

Common relationships between $q_c$ and $D_r$ are based on Cone Penetration Tests carried out in sand samples reconstituted in laboratory calibration chamber tests. Such tests are carried out as part of general geotechnical research projects and are subject to a number of limitations, such as:

- soil type dependence
- inaccuracies in determination of laboratory $D_r$
- limited range of stress levels and $K_o$ values
- sample preparation and soil stress history simplifications.

Jamiolkowski et al. (2003) proposes the following relationship between $q_c$ and $D_r$ for normally and overconsolidated silica (dry) sands:

$$D_{r(dry)} = \frac{1}{2.96} \ln \left[ \frac{\frac{q_c}{P_a}}{24.94 \left( \frac{\sigma'_{vo} \left( \frac{1+2K_o}{3} \right)}{P_a} \right)^{0.46}} \right]$$

and for saturated sands:

$$D_{r(sat)} = \left( \frac{-1.87 + 2.32 \ln \frac{q_c}{(P_a * \sigma'_{v0})^{0.5}}}{100} + 1 \right) \frac{D_r(dry)}{100}$$

where relative density $D_r$ is a fraction. The correlation for saturated sands results in relative densities that can be up to about 10% higher compared to the correlation for dry sands.

Determination of laboratory minimum and maximum index dry unit weights ($\gamma_{dmin}$ and $\gamma_{dmax}$) forms the basis for the relative density concept (loose, dense sand, etc.). As yet, there is no internationally agreed procedure. Hence, laboratory test procedure dependence applies. Also, it is unlikely that any of the procedures consistently provide the "lowest" $\gamma_{dmin}$ or the "highest" $\gamma_{dmax}$. In situ soil unit weights may therefore fall outside laboratory ranges. The relative density concept is necessary to provide a link between field investigations and laboratory testing on reconstituted specimens, as undisturbed sampling of sands is expensive.

Calibration chamber test results apply to a limited range of stress conditions only; typically:

$$50\ \text{kPa} < \sigma'_{vo} < 400\ \text{kPa}$$
$$0.4 < K_o < 1.5$$

Sample preparation for laboratory chamber tests is usually by means of dry pluviation. Soil stress history application is by mechanical overconsolidation.

### Angle of Internal Friction - Sand

The effective shear strength parameter $\varphi'$ is not a true constant. It depends on factors such as density, stress level, shearing mode and mineralogy. There is evidence that overconsolidation ratio, method of deposition and in situ stress anisotropy is less important.

Correlation of angle of internal friction $\varphi'$ to cone resistance $q_c$ may be done at various levels of sophistication. Simple procedures rely on a conservative assessment of soil behaviour classification. A more sophisticated empirical correlation consists of:
(a) Estimation of in situ stress conditions $\sigma'_{vo}$ and $\sigma'_{ho}$
(b) Estimation of relative density $D_r$
(c) Empirical correlation of angle of internal friction $\varphi'$ with $D_r$, $\sigma'_{vo}$ and $\sigma'_{ho}$.

Estimation of stress conditions and relative density has been discussed above.

The empirical procedure proposed by Bolton (1986 and 1987) is used for estimation of $\varphi'$. This correlation applies to clean sands and considers peak secant angle of internal friction in Isotropically Consolidated Drained triaxial compression (CID) of reconstituted sand. This procedure requires estimation of the dilatancy index and the critical state angle of internal friction.

Kulhawy and Mayne (1990) determined an equation based upon 20 data sets obtained from calibration chamber tests. This equation is almost identical to the empirical formula determined earlier by Trofimenkov (1974) which was based on mechanical cone data. Mayne (2007) validated the use of total cone resistance $q_t$ instead of cone resistance $q_c$ used in the equation from Kulhawy and Mayne (1990).

$$\varphi' = 17.6 + 11.0 \log\left(\left(\frac{q_t}{P_a}\right) / \left(\frac{\sigma'_{vo}}{P_a}\right)^{0.5}\right) \qquad \text{(Mayne, 2007)}$$

### Undrained Shear Strength - Sand

Undrained shear strength of cohesionless soil can be important for assessment of cyclic mobility and liquefaction potential. Geotechnical procedures other than the conventional limit state models are employed.

### Compressibility - Sand

Correlations between CPT data and compressibility parameters are indicative only. Further developments in interpretation techniques may offer improvement in the future.

Elasticity theory is commonly employed for analysis of drained soil deformation behaviour. Secant moduli are adopted. A common guideline is an empirical correlation given by Baldi et al. (1989). The correlation is for silica-based sand and considers cone resistance $q_c$, in situ stress conditions and secant Young's modulus for drained stress change E'. The ratio of $E'/q_c$ typically ranges from about 3 to 5 for recently deposited normally consolidated sands up to about $E'/q_c$ = 6 to 25 for overconsolidated sands. The correlation has been inferred from laboratory conditions; including CPT tests in a calibration chamber and conventional triaxial compression tests on reconstituted sand samples. It takes account of the degree of deformation and overconsolidation. In this regard, it is noted that secant deformation moduli are strongly dependent on strain level: the elastic modulus increases with decreasing strain to an upper limit at about $10^{-4}$% strain.

For estimation of initial (small strain) or dynamic shear moduli, ratios of $G_{max}/q_c$ of between about 4 and 20 are considered, in accordance with Baldi et al. (1989).The basis for this correlation is similar to that of secant Young's modulus, except that laboratory resonant column tests serve as reference instead of triaxial compression tests. Results of limited in situ seismic cross-hole and downhole tests provide an approximate check of this correlation.

ISSUE 28

**Constrained Modulus M - Sand**

Kulhawy and Mayne (1990) derived two formulas for the determination of the constrained modulus for both normally consolidated and overconsolidated sands by indicating that the modulus is a function of relative density. The determination of relative density can be done with, for example, the methods indicated previously.

$$M = q_c * 10^{1.09-0.0075D_r} \quad \text{(Normally consolidated sands, Kulhawy and Mayne, 1990)}$$

$$M = q_c * 10^{1.78-0.0122D_r} \quad \text{(Overconsolidated sands, Kulhawy and Mayne, 1990)}$$

where $D_r$ is in %, and $q_c$ and M in kPa respectively.

**Shear Wave Velocity $v_s$ – Sand**

If no in situ measurements of shear wave velocities ($v_s$) are available, then empirical correlation with CPT parameters may be considered. Hegazy and Mayne (2006) published a statistical correlation derived from 73 sites worldwide representing a range of soil types including sands, clays, soil mixtures and mine tailings (Figure 5). The correlation considers a normalized cone resistance ($q_{c1N\_hm}$) and a soil behaviour type index ($I_{c\_hm}$) as follows:

$$v_s = 0.0831 q_{c1N\_hm} (\sigma'_{vo} / P_a)^{0.25} \, e^{(1.786 \, I_{c\_hm})} \quad \text{(Hegazy and Mayne, 2006)}$$

where shear wave velocity $v_s$ is in m/s and $q_{c1N\_hm}$ and $I_{c\_hm}$ are dimensionless. Calculations for $q_{c1N\_hm}$ and $I_{c\_hm}$ require iteration, and consider measured cone resistance $q_c$ or corrected cone resistance $q_t$, measured sleeve friction $f_s$, total in situ vertical stress $\sigma_{vo}$, effective in situ vertical stress $\sigma'_{vo}$ and atmospheric pressure $P_a$.

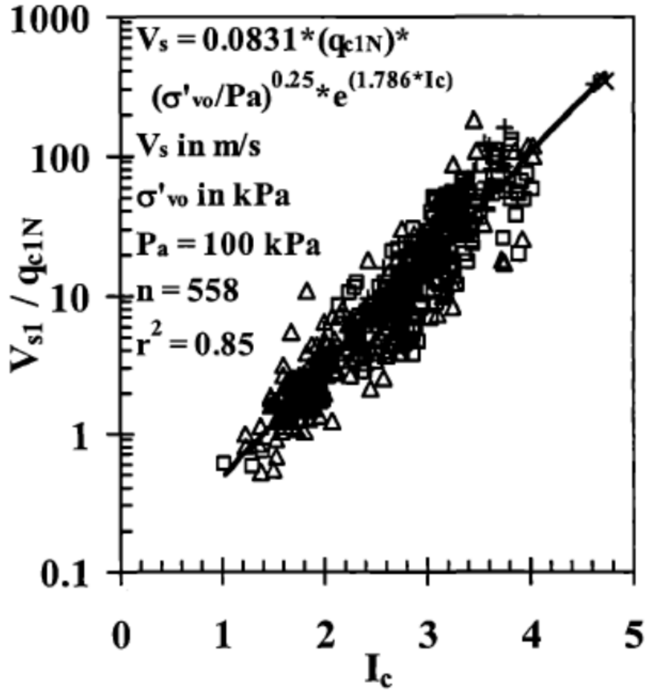


**Figure 5, $v_s$ – $q_c$ correlation according to Hegazy and Mayne (2006)**

Robertson and Cabal (2010) present a $v_s$ correlation incorporating net cone resistance $q_n$ (= $q_t - \sigma_{vo}$) and soil behaviour type index ($I_c$) as defined by Robertson and Wride (1998):

$$v_s = [\alpha_{vs}(q_t - \sigma_{v0})/P_a]^{0.5} \text{ where } \alpha_{vs} = 10^{(0.55 I_c + 1.68)} \quad \text{(Robertson and Cabal, 2010)}$$

where shear wave velocity $v_s$ is in m/s and total cone resistance $q_t$, total in situ vertical stress $\sigma_{vo}$ and atmospheric pressure $P_a$ are in kPa. The method can be applied to a wide range of soil behaviour types, notably uncemented Holocene to Pleistocene age soils. Older deposits could have a higher shear wave velocity. Exceptions are Zones 1, 8 and 9 of Robertson (1990 and 2009).

Baldi et al. (1989) derived a correlation between shear wave velocity $v_s$ and cone resistance $q_c$ for uncemented silica sands. This correlation is based on data from CPT, cross-hole and Seismic Cone Penetration Tests (SCPT) performed in quaternary deposits of the predominantly silica Po river sand and Gioia Tauro sand with gravel.

$$v_s = 277 q_c^{0.13} \sigma'_{vo}{}^{0.27} \qquad \text{(Baldi et al., 1989)}$$

where shear wave velocity $v_s$ is in m/s and cone resistance $q_c$ and effective in situ vertical stress $\sigma'_{vo}$ are in MPa.

Shear wave velocity may be normalised according to Robertson and Cabal (2010):

$$v_{s1} = v_s \cdot (P_a / \sigma'_{vo})^{0.25} \qquad \text{(Robertson and Cabal, 2010)}$$

**Shear Modulus $G_{max}$ - Sand**

Interpretation of low-strain shear modulus can be considered by using the modified correlation proposed by Rix and Stokoe (1991) in which data from calibration test measurements is compared to the correlation obtained between $G_{max}$ and $q_c$ by Baldi et al. (1989).

$$G_{max} = 1634 (q_c)^{0.25} (\sigma'_{vo})^{0.375} \qquad \text{(Rix and Stokoe, 1991)}$$

where $G_{max}$, $q_c$ and $\sigma'_{vo}$ are in kPa.

**CLAY MODEL**

**Unit Weight – Clay**

Empirical correlation between unit weight of clay and CPT parameters is as described in "Unit Weight – Sand" above.

**In Situ Stress Conditions - Clay**

Similar to sand, a knowledge of in situ stress conditions is generally necessary for estimation of other parameters such as consistency (soft, stiff, etc.) of a clay deposit and compressibility.

Calculation of the effective in situ vertical stress $\sigma'_{vo}$ is reasonably accurate. A more approximate estimate applies to the effective in situ horizontal stress $\sigma'_{ho}$, or, more particular, $K_o$ as $\sigma'_{ho} = K_o \sigma'_{vo}$.

Direct correlations for interpretation of the coefficient of earth pressure at rest $K_o$ are uncommon.

For normally consolidated clays and silts, $K_{onc}$ may be correlated with angle of internal friction, in accordance with Jaky (1944), or more simply in accordance with Mayne and Kulhawy (1982). The reference angle of internal friction is that obtained from a straight-line approximation of the Mohr-Coulomb failure envelope determined from Isotropically Consolidated Undrained (CIU) triaxial compression tests on undisturbed specimens.

For overconsolidated clays, $K_{ooc}$ may be correlated with angle of internal friction and overconsolidation ratio, in accordance with Mayne and Kulhawy (1982). The plasticity index together with OCR may also be used for preliminary estimates of $K_{ooc}$ as indicated by Brooker and Ireland (1965).

$$K_o = (1 - \sin\varphi') OCR^{\sin\varphi'} \qquad \text{(Mayne and Kulhawy, 1982)}$$

**Overconsolidation Ratio - Clay**

Overconsolidation ratio is defined as: OCR = $\sigma'_p/\sigma'_{vo}$ where $\sigma'_p$ is the pre-consolidation pressure considered to correspond with the maximum vertical effective stress to which the soil has been subjected, and $\sigma'_{vo}$ is the current effective in situ vertical stress. The pre-consolidation pressure approximates a stress level where relatively small strains are separated from relatively large strains occurring on the virgin compression stress range. The reference OCR is usually based on laboratory oedometer tests carried out on undisturbed samples, and may thus be influenced by factors such as sample disturbance, strain rate effects and

interpretation procedure.
Various analytical and semi-empirical models for interpretation of pre-consolidation pressure from piezo-cone test data are available. Sandven (1990) presents a summary. The procedures are mostly "experimental" and as yet uncommon in practice. Chen and Mayne (1996) presented a direct correlation between net cone resistance and overconsolidation ratio for 205 clay sites around the world, as follows:

$$OCR = 0.317\ Q_t \qquad \text{(Chen and Mayne, 1996)}$$

The overconsolidation ratio may also be inferred from a geological assessment and from undrained strength ratios.

Geological factors concerning overconsolidation have been discussed under "in situ stress conditions - sand". An empirical procedure for estimation of OCR based on undrained strength ratio $c_u/\sigma'_{vo}$ is given by Wroth (1984). The procedure uses the strength rebound parameter $\Lambda$. Guidance for selection of $\Lambda$ and normally consolidated undrained strength ratio is given by Mayne (1988). Historically, much use has also been made of the Skempton (1957) relationship between normally consolidated undrained strength ratio and plasticity index $I_p$. This equation is useful for preliminary estimates, considering that $I_p$ probably relates to $\varphi'$ in some complex manner.

**Undrained Shear Strength - Clay**

No single undrained shear strength exists. The in situ undrained shear strength $c_u$ depends on factors such as mode of failure, stress history, anisotropy, strain rate and temperature.

Various theoretical and empirical procedures are available to correlate $q_c$ with $c_u$. Theoretical approaches use bearing capacity, cavity expansion or steady penetration solutions, all of which require a number of simplifying assumptions. Empirical approaches are more common in engineering practice because of difficulties in realistic soil modelling. An empirical correlation for soft to stiff, intact and relatively homogeneous clays is given by Battaglio et al. (1986) as follows:

$$c_u = (q_c - \sigma_{vo})/N_c$$

where $c_u$, $\sigma_{vo}$ and $q_c$ are in kPa. $N_c$ is an empirical factor that ranges between 10 and 25, with the higher $N_c$ factors applying to clays with a relatively low plasticity index, and vice versa. The reference undrained shear strength is that determined from in situ vane test results. The term $\sigma_{vo}$ (total in situ vertical stress) becomes insignificant for stiff clays at shallow depth so that the equation reduces to $c_u = q_c/N_c$.

For specific design situations, a different $c_u$ reference strength should be used. For example, offshore axial pile capacity predictions in accordance with API (2014) recommend $c_u$ to be based on undrained triaxial compression tests, which are likely to yield lower $c_u$ values than in situ vane tests. A site-specific or regional approach should generally be preferred. For example, $N_c$ factors of 15 to 20 have been commonly used for firm to hard North Sea clays. They give reasonable strength estimates for $c_u$ values determined from pocket penetrometer, torvane and Unconsolidated Undrained triaxial tests (UU) on Shelby tube samples obtained by hammer sampling and push sampling techniques. Lower $N_c$ factors are generally appropriate for soft clays and higher factors for heavily overconsolidated clays.

If piezo-cone test data are available, then improved correlations are feasible because of the pore pressure information. Empirical correlations of piezo-cone test results with CIU undrained shear strengths are given by Rad and Lunne (1988), as follows:

$$c_u = q_n/N_k$$

$N_k$ ranges typically between 8 and 30 with the higher $N_k$ factors applying to heavily overconsolidated clays.

Low et al. (2010) recommend $N_k$ = 10 to 14 with a mean value of 12 for correlation with laboratory triaxial compressive strength and $N_k$ = 11.5 to 15.5 with a mean value of 13.5 for correlation with average undrained shear strength defined as the average of laboratory triaxial compression, simple shear and triaxial extension. These recommendations apply to high plasticity, normally consolidated to slightly overconsolidated clays with $q_n$ values of typically less than 1.5 MPa.

ISSUE 28

**Clay Sensitivity**

The sensitivity of a clay ($S_t$) is the ratio of undisturbed undrained shear strength to remoulded undrained shear strength. Sensitivity may be assessed from the CPT friction ratio $R_f$, in accordance with Schmertmann (1978):

$$S_t = N_s/R_f$$

where $N_s$ is a correlation factor typically ranging between 5 and 10. The correlation is expected to be inaccurate for sensitive clays where uncertainty in very low values for sleeve friction may dominate results.

The reference $S_t$ value is often taken to be that determined from undisturbed and remoulded laboratory unconsolidated undrained triaxial tests. This reference $S_t$ value may differ from that determined from other tests, for example laboratory miniature vane tests. This is partly related to the definition of sensitivity. For vane tests, several measurements of undrained shear strength are possible:

- Intact (I) = undisturbed undrained shear strength as measured on an intact/undisturbed specimen.
- Intact-Residual (I-R) = measured post peak during initial shearing of the intact specimen.
- Intact-Vane Remoulded (I-VR) = measured after multiple-quick rotations of the vane after completion of the intact test.
- Hand Remoulded (HR) = steady state (post-peak if exists) resistance of hand remoulded test specimen.
- Hand Remoulded – Vane Remoulded (HR-VR) = steady state resistance of hand remoulded specimen measured after applying multiple-quick vane rotations.

Skempton and Northey (1952) present a correlation of sensitivity and laboratory liquidity index $I_L$. This correlation may allow a check on CPT-based interpretation of sensitivity.

**Effective Shear Strength Parameters - Clay**

Measurement of pore water pressures during penetration testing has led to development of interpretation procedures for estimation of effective stress parameters of cohesive soils. Background information may be found in Sandven (1990). Currently available procedures are evaluated to be "experimental" and are as yet not commonly adopted.

In general, CPT interpretation of effective shear strength parameters for clay and silt relies on soil behaviour-type classification.

It is noted that significant silt and sand fractions in a clay deposit will increase $\varphi'$, while a significant clay fraction in silt will decrease $\varphi'$.

Masood and Mitchell (1993) provide an equation for the determination of $\varphi'$ by combining sleeve friction with the Rankine earth-pressure theory. The equation is based on the following assumptions:

- Unit adhesion between soil and sleeve is negligible.
- Friction angle between soil and sleeve = $\varphi'/3$.
- Lateral earth pressure coefficient during penetration is equal to the Rankine coefficient of lateral earth pressure under passive conditions.

$$\frac{f_s}{\sigma'_{vo}} = \tan^2(45° + \frac{\varphi'}{2})\tan(\frac{\varphi'}{3}) \qquad \text{(Masood and Mitchell, 1993)}$$

Mayne (2001) proposed an approximation of the Masood and Mitchell equation, as follows:

$$\varphi' = 30.8\left[\log(\frac{f_s}{\sigma'_{vo}}) + 1.26\right] \qquad \text{(Mayne, 2001)}$$

Mayne (2001) also proposed the following approximation of friction angle $\varphi'$ based on pore pressure ratio $B_q$ and the cone resistance number $N_m$ (Senneset, Sandven and Janbu, 1989):

$$\varphi' = 29.5B_q^{0.121}(0.256 + 0.336B_q + \log N_m) \qquad \text{(Mayne, 2001)}$$

where

$$N_m = \frac{q_t - \sigma_{vo}}{\sigma'_{vo} + a}$$

where the cone resistance number $N_m$ is dimensionless, total cone resistance $q_t$, total in situ vertical stress $\sigma_{v0}$ and effective in situ vertical stress $\sigma'_{v0}$ are in kPa.

Senneset et al. (1989) use the attraction value [a] as a function of soil type. In general the attraction value ranges from 5 to > 50 for both sands and clays and may be estimated directly from CPT results. The correlation is valid if the angle of plastification β is zero. In general a plastification angle of zero applies to medium sands and silts, sensitive clays and highly compressible clays.

**Compressibility – Clay**

Correlations between CPT data and compressibility parameters are viewed as indicative only, as discussed for sand compressibility.

The use of elasticity theory is common for analysis of undrained soil deformation behaviour. The adopted procedure is as follows:
(a) Estimation of undrained shear strength $c_u$ from CPT data, as outlined above.
(b) Estimation of secant Young's moduli for undrained stress change $E_u$ in general accordance with correlations based on $c_u$, as presented by Ladd et al. (1977).

Laboratory undrained triaxial tests carried out on undisturbed clay specimen form the basis for the $E_u$ versus $c_u$ correlations. Typical $E_u/c_u$ ratios at a shear stress ratio of 0.3 range between about 300 and 900 for normally consolidated clays and $E_u/c_u$ = 100 to 300 for heavily overconsolidated clay. Higher $E_u/c_u$ ratios would apply to lower shear stress ratios, and vice versa.

Mitchell and Gardner (1976) present an approximate correlation of cone resistance with constrained modulus M (or coefficient of volume compressibility $m_v$, where $M = 1/m_v$). Typical ratios of $M/q_c$ range between 1 and 8 for silts and clays. Refinements include $q_c$ ranges and soil type (silt, clay, low plasticity, high plasticity, etc.). The correlation relies on the results of conventional laboratory oedometer tests carried out on undisturbed clay and silt samples. The constrained modulus can also be related (approximately) to secant Young's modulus E' and shear modulus G'.

It is noted that laboratory soil stiffness may differ from in situ stiffness because of inevitable sampling disturbance (in particular soil structure disturbance). In general, this implies that laboratory stiffness will usually be less than in situ stiffness.

ISSUE 28

**Constrained Modulus M**

Kulhawy and Mayne (1990) correlated constrained modulus M in clays with net cone resistance data. This relationship is based on data from 12 different test sites, with constrained moduli up to 60 MPa. The published standard deviation is 6.7 MPa.

$$M = 8.25\, q_n \qquad \text{(Kulhawy and Mayne, 1990)}$$

**Shear Wave Velocity $v_s$ – Clay**



Hegazy and Mayne (2006) and Roberson and Cabal (2010) present empirical correlations between shear wave velocity and CPT parameters for a wide range of soils including clays, as described in “Shear Wave Velocity $v_s$ – Sand” above. The Hegazy and Mayne correlation is sensitive to use of $q_c$ or $q_t$. It should be used with caution for soils showing undrained or partially drained CPT response.

Mayne and Rix (1995) derived a correlation between shear wave velocity $v_s$ and cone resistance $q_c$ for intact and fissured clays. A database from Mayne and Rix (1993) was used including 31 different clay sites.

$$v_s = 1.75 q_c^{0.627} \qquad \text{(Mayne and Rix, 1995)}$$

where shear wave velocity $v_s$ is in m/s and cone resistance $q_c$ is in kPa.

**Shear Modulus $G_{max}$**

Mayne and Rix (1993) determined a relationship between $G_{max}$ and $q_c$ by studying 481 data sets from 31 sites all over the world. $G_{max}$ ranged between about 0.7 MPa and 800 MPa.

$$G_{max} = 2.78\, q_c^{1.335} \qquad \text{(Mayne and Rix, 1993)}$$

where $G_{max}$ and $q_c$ are in kPa.

## REFERENCES

American Petroleum Institute, 2014. *API RP 2A-WSD, 22nd Edition Planning, designing and constructing fixed offshore platforms - Working Stress Design*. Washington, D.C.: API.

Baldi, G., Bellotti, R., Ghionna, V.N., Jamiolkowski, M. and Lo Presti, D.C.F. 1989. Modulus of Sands from CPT's and DMT's. In *Proceedings of the Twelfth International Conference on Soil Mechanics and Foundation Engineering, Rio de Janeiro, 13-18 August 1989, Vol. 1,* Rotterdam: Balkema, pp. 165-170.

Battaglio, M., Bruzzi, D., Jamiolkowski, M. and Lancellotta, R. 1986. Interpretation of CPT's and CPTU's, 1st Part: Undrained Penetration of Saturated Clays. In *Field Instrumentation and In-Situ Measurements: Proceedings of the 4th International Geotechnical Seminar, 25-27 November 1986, Singapore, Nanyang Technological Institute,* Singapore, pp. 129-143.

Bolton, M.D. 1986. The Strength and Dilatancy of Sands. *Géotechnique,* Vol. 36, No. 1, pp. 65-78.

Bolton, M.D. 1987. Author's Reply to Discussion of The Strength and Dilatancy of Sands. *Géotechnique,* Vol. 37, No. 2, pp. 225-226.

Brooker, E.W. and Ireland, H.O. 1965. Earth Pressures at Rest Related to Stress History. *Canadian Geotechnical Journal*, Vol. 2, No. 1, pp. 1-15.

Chen, B.S.Y. and Mayne, P.W. 1996. Statistical Relationships between Piezocone Measurements and Stress History of Clays. *Canadian Geotechnical Journal*, Vol. 33, No. 3, pp. 488-498.

Hegazy, Y.A. and Mayne, P.W. 2006. A Global Statistical Correlation between Shear Wave Velocity and Cone Penetration Data. In Puppala, A.J. et al. Eds. *Site and Geomaterial Characterization: Proceedings of Sessions of GeoShanghai, June 6-8, 2006, Shanghai, China,* Reston: American Society of Civil Engineers, Geotechnical Special Publication, No. 149, pp. 243-248.

Jaky, J. 1944. The Coefficient of Earth Pressure at Rest. *Magyar Mérnök és Epitész Egylet Közlönye,* Vol. 78, No. 22, pp. 355-358. (in Hungarian).

Jamiolkowski, M., Lo Presti, D.C.F. and Manassero, M. 2003. Evaluation of Relative Density and Shear Strength of Sands from CPT and DMT. In Germaine, J.T., Sheahan, T.C. and Whitman, R.V. Eds. *Soil Behavior and Soft Ground Construction: Proceedings of the Symposium, October 5-6, 2001, Cambridge, Massachusetts,* Reston: American Society of Civil Engineers, Geotechnical Special Publication, No. 119, pp. 201-238.

Kulhawy, F.H. and Mayne, P.W. 1990. *Manual on Estimating Soil Properties for Foundation Design.* Palo Alto: Electric Power Research Institute EPRI, EPRI Report, EL-6800.

Ladd, C.C., Foott, R., Ishihara, K., Schlosser, F. and Poulos, H.G. 1977. Stress-deformation and Strength Characteristics. In *Proceedings of the Ninth International Conference on Soil Mechanics and Foundation Engineering, 1977, Tokyo, Vol. 2,* Tokyo: Japanese Society of Soil Mechanics and Foundation Engineering, pp. 421-494.

Low, H.E., Lunne, T., Andersen, K.H., Sjursen, M.A., Li, X. and Randolph, M.F. 2010. Estimation of Intact and Remoulded Undrained Shear Strengths from Penetration Tests in Soft Clays. *Géotechnique,* Vol. 60, No. 11, pp. 843-859.

Masood, T. and Mitchell, J.K. 1993. Estimation of In Situ Lateral Stresses in Soils by Cone-Penetration Test. *Journal of Geotechnical Engineering*, Vol. 119, No. 10, pp. 1624-1639.

Mayne, P.W. 1988. Determining OCR in Clays from Laboratory Strength. *Journal of Geotechnical Engineering*, Vol. 114, No. 1, pp. 76-92.

Mayne, P.W. 2001. *Geotechnical Site Characterization Using Cone, Piezocone, SCPTu, and VST*. Atlanta: Georgia Institute of Technology.

Mayne, P.W. 2007. In-Situ Test Calibrations for Evaluating Soil Parameters. In Tan, T.S., Phoon, K.K., Hight, D.W. and Leroueil, S. Eds. *Characterisation and Engineering Properties of Natural Soils Volume 3.* London: Taylor & Francis, pp. 1601-1652.

Mayne, P.W. and Kulhawy, F.H. 1982. $K_o$ - OCR Relationships in Soil. *Journal of the Geotechnical Engineering Division,* Vol. 108, No. GT6, pp. 851-872.

Mayne, P.W. and Rix, G.J. 1993. $G_{max}$-$q_c$ Relationships for Clays. *Geotechnical Testing Journal,* Vol. 16, No. 1, pp. 54-60.

Mayne, P.W. and Rix, G.J. 1995. Correlations between Shear Wave Velocity and Cone Tip Resistance in Natural Clays. *Soils and Foundations,* Vol. 35, No. 2, pp. 107-110.

Mayne, P.W., Peuchen, J. and Bouwmeester, D. 2010. Soil Unit Weight Estimated from CPTu in Offshore Soils. In Gourvenec, S. and White, D. Eds., *Frontiers in Offshore Geotechnics II: Proceedings of the 2nd International Symposium on Frontiers in Offshore Geotechnics, Perth, Australia, 8-10 November 2010,* Boca Raton: CRC Press, pp. 371-376.

Mitchell, J.K. and Gardner, W.S. 1976. In *Situ Measurement of Volume Change Characteristics. In Proceedings of the Conference on In Situ Measurement of Soil Properties, June 1-4, 1975, Raleigh, North Carolina: Specialty Conference of the Geotechnical Engineering Division, ASCE, Vol. II,* New York: American Society of Civil Engineers, pp. 279-345.

Rad, N.S. and Lunne, T. 1988. Direct Correlations between Piezocone Test Results and Undrained Shear Strength of Clay. In De Ruiter, J. Ed., *Penetration Testing 1988: Proceedings of the First International Symposium on Penetration Testing, ISOPT-1, Orlando, 20-24 March 1988, Vol. 1*, Rotterdam: Balkema, pp. 911-917.

Ramsey, N. 2002. A Calibrated Model for the Interpretation of Cone Penetration Tests CPTs) in North Sea Quaternary Soils. In Cook, M. et al. Eds., *Offshore Site Investigation and Geotechnics: 'Diversity and Sustainability': Proceedings of an International Conference Held in London, UK, 26-28 November 2002,* London: Society for Underwater Technology, pp. 341-356.

Rix, G.J. and Stokoe, K.H. 1991. Correlation of Initial Tangent Modulus and Cone Penetration Resistance. In Huang, A.B. Ed. *Calibration Chamber Testing: Proceedings of the First International Symposium on Calibration Chamber Testing ISOCCTI, Potsdam, New York, 28-29 June 1991,* New York: Elsevier Science, pp. 351-362.

Robertson, P.K. 1990. Soil Classification Using the Cone Penetration Test. *Canadian Geotechnical Journal*, Vol. 27, No. 1, pp. 151-158.

Robertson, P.K. 2009. Performance Based Earthquake Design Using the CPT. In Kokusho, T., Tsukamoto, Y. and Yoshimine, M. Eds. *Performance-Based Design in Earthquake Geotechnical Engineering – from Case History to Practice: Proceedings of the International Conference on Performance-Based Design in Earthquake Geotechnical Engineering IS-Tokyo 2009), 15-18 June 2009,* Boca Raton: CRC Press, pp. 3-20.

Robertson, P.K. and Cabal, K.L. 2010. *Guide to Cone Penetration Testing for Geotechnical Engineering*. 4th ed., Signal Hill: Gregg Drilling & Testing.

Robertson, P.K. 2010. Soil Behaviour type from the CPT: an update. In *2nd International Symposium on Cone Penetration Testing, Huntington Beach, CA, Vol.2.* pp 575-583.

Robertson, P.K. and Wride (Fear), C.E. 1998. Evaluating Cyclic Liquefaction Potential Using the Cone Penetration Test. *Canadian Geotechnical Journal*, Vol. 35, No. 3, pp. 442-459.

Robertson, P.K., Woeller, D.J. and Finn, W.D.L. 1992. Seismic Cone Penetration Test for Evaluating Liquefaction Potential under Cyclic Loading. *Canadian Geotechnical Journal*, Vol. 29, No. 4, pp. 686-695.

Sandven, R. 1990. *Strength and Deformation Properties of Fine Grained Soils Obtained from Piezocone Tests.* Thesis, Norwegian Institute of Technology, Department of Civil Engineering, Trondheim.

Schmertmann, J.H. 1978. *Guidelines for Cone Penetration Test Performance and Design.* U.S. Department of Transportation, Federal Highway Administration, Washington, Report FHWA-TS-78-209.

Senneset, K., Sandven, R. and Janbu, N. 1989. *The Evaluation of Soil Parameters from Piezocone Tests.* Geotechnical Division, Norwegian Institute of Technology, University of Trondheim, Trondheim, Preprint National Research Council, Transportation Research Board 68th Annual Meeting, January 22-26, 1989, Washington, D.C.

Skempton, A.W. 1957. Discussion on Airport Paper No. 35: The Planning and Design of the New Hong Kong Airport. *ICE Proceedings,* Vol. 7, p. 306.

Skempton, A.W. and Northey, R.D. 1952. The Sensitivity of Clays. *Géotechnique,* Vol. 3, No. 1, pp. 30-53.

Trofimenkov, J.G. 1974. Penetration Testing in USSR: State-of-the-Art Report. In *Proceedings of the European Symposium on Penetration Testing ESOPT, Stockholm, June 5-7, 1974, Vol. 1,* Stockholm: National Swedish Building Research, pp. 147-154.

Van der Wal, T., Goedemoed, S. and Peuchen, J. 2010. Bias Reduction on CPT-based Correlations. In *CPT'10: 2nd International Symposium on Cone Penetration Testing, Huntington Beach, CA: Conference Proceedings.*

Wroth, C.P. 1984. The Interpretation of In Situ Soil Tests. *Géotechnique,* Vol. 34, No. 4, pp. 449-489.

Zhang, G., Robertson, P.K. and Brachman, R.W.I. 2002. Estimating Liquefaction induced Ground Settlements from CPT for Level Ground. *Canadian Geotechnical Journal*, Vol. 39, No. 5, pp.1168-1180.

## INTRODUCTION

Site characterisation may be defined as a fit-for-purpose model of seabed conditions at a geographical location in a sea or ocean. Seabed is the ground below seafloor, including pore fluid and gas. The model is fundamental to managing ground risks and optimizing opportunities. The model is a prediction and a reduction of reality:

- Providing sound information with which to define and assess the suitability of a site for proposed facilities
- Detecting and assessing the possible effects of geohazards and changes in seabed conditions with time
- Choosing parameter values for assessment of limit states and assess the feasibility of building/ installing, operating and/or decommissioning a structure.

Other terms used in practice for (parts of) site characterisation include integrated study, integrated geosciences, desk study, seabed characterisation.

Site characterisation can also refer to the activities required to create the model of seabed conditions (e.g. Evans, 2010; Peuchen, 2014).

The terms seabed and seafloor are according to ISO (2003):

- Seabed comprises materials below the sea in which a structure is founded, whether of soils such as sand, silt or clay, cemented materials or, of rock
- Seafloor is defined as the interface between the sea and the seabed.

This document focuses on offshore projects. Site characterisation is an integral part of offshore structure design and operation according to reliability principles covered by standards and codes of practice; for instance API (2000, 2009 and 2011), BWEA (2011), CEN (2004 and 2011); ISO (2002, 2003, 2004, 2009, 2012 and 2013), Osborne et al. (2011) and SNAME (2008).

The following sections provide further information.

## SITE HAZARDS

### TYPES OF HAZARDS, RISK AND MITIGATION

Site hazards may be grouped into:

- natural geohazards
- man-made hazards.

Natural geohazards are commonly referred to as geohazards or geological hazards. They are about past geological processes and events have shaped the seafloor and seabed. Some of these processes may still be active today. The resulting seafloor topography, and geological and geotechnical conditions within the seabed can be hazardous when installing offshore structures including infrastructure (e.g. Clayton and Power, 2002; OGP, 2009; API, 2011).These processes.

Man-made hazards include shipwrecks, fallen objects, seafloor debris and unexploded ordnance. Within the context of this document, man-made hazards exclude accidental events such as vessel impact, sabotage, well drilling problems and fishing activities.

In relation of offshore activities, geohazards can be defined as local and/or regional site and soil conditions having a potential of developing into a condition (e.g. irregular seafloor topography) or process (e.g. currents, submarine slides) that could cause loss of life or damage to health, environments and/or assets. The event-triggering sources can be ongoing geological processes or human induced changes (OGP, 2009). Figure 1 presents a schematic overview of offshore geohazards.

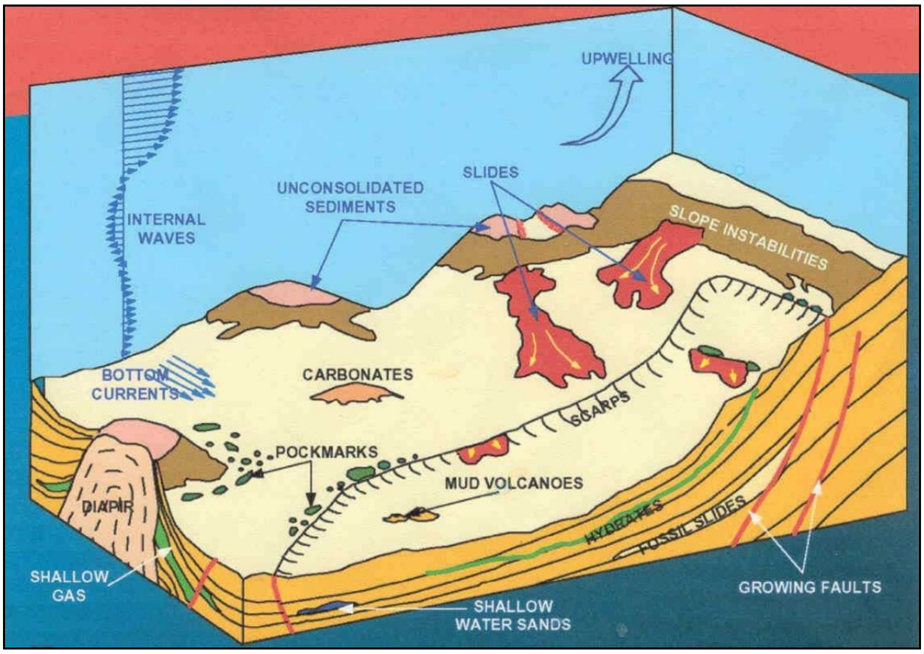


**Figure 1: Offshore natural geohazards in deep water settings (modified after Campbell et al., 1986)**

The damage potential of site hazards can range from, for example, local effects on pipelines and subsea structures to complete loss of all installations in a license areas and 3rd party losses (OGP, 2009).

The table below presents an overview of potential impacts and/or consequence associated with natural geohazards (and man-made hazards) occurring offshore.

**Table 1: Potential Impact/Consequence Associated with Site Hazards**

| Impact / Consequence | Natural Geohazards and Man-made Hazards | | | | | | | | | | | | | | | |
|---|---|---|---|---|---|---|---|---|---|---|---|---|---|---|---|---|
| | Irregular Seafloor Topography | Seafloor Bedforms | Seafloor Outcrops and Hard Seafloor | Soil Liquefaction | Shallow Gas & Gassy Soils | Gas Hydrates | Gas and Fluid Seepage | Diapirs (e.g. Mud /Salt) and Mud Volcanoes | Earthquakes | Faults | Tsunami | Slope Failure | Submarine Mass Movement | Wind, Waves and Currents | Seafloor Scour and Sediment Mobility | Man-Made Hazards |
| Uneven support (foundation instability) | | x | | | | x | | | | x | x | | | | x | |
| Loss of support (structural stresses) | | | | x | | | x | | x | | x | x | x | | | |
| Spanning (pipeline & flowlines) | x | x | x | | | | | | | x | | | | | | |
| Increased foundation settlements, reduced access | | | | x | x | | | | | | | | | | | |
| Burial / embedment leading to additional loading and reduced access | | x | | x | | | | | | | | | x | | x | |
| Reduced soil strength and bearing resistance | | | | x | x | | x | | | | | | | | | |

| Impact / Consequence | Natural Geohazards and Man-made Hazards | | | | | | | | | | | | | | | |
|---|---|---|---|---|---|---|---|---|---|---|---|---|---|---|---|---|
| | Irregular Seafloor Topography | Seafloor Bedforms | Seafloor Outcrops and Hard Seafloor | Soil Liquefaction | Shallow Gas & Gassy Soils | Gas Hydrates | Gas and Fluid Seepage | Diapirs (e.g. Mud /Salt) and Mud Volcanoes | Earthquakes | Faults | Tsunami | Slope Failure | Submarine Mass Movement | Wind, Waves and Currents | Seafloor Scour and Sediment Mobility | Man-Made Hazards |
| Lateral loading of structure leading to overstressing of foundation / structure components | | | | | | | | | x | | x | x | x | x | | x |
| Structure displacement and structural damage | | | | x | | | | | x | x | x | x | x | | | x |
| Increased potential for soil liquefaction | | | | | x | x | x | | x | | x | | | x | | |
| Increased potential for shallow soil instability and submarine sliding | | | | | x | x | x | x | x | | x | | | x | x | |
| Foundation and structure installation difficulties | x | x | x | | x | x | x | | | | | | | | | x |
| Steel abrasion, gouging and denting; excessive wear trenching equipment | | | x | | | | | | | | | | | | | |
| Gas and fluid migration (excess pore pressures) | | | | | x | x | x | x | | x | x | | | x | | |
| Corrosion of steel structures, pipelines, flowlines | | | | | x | | x | x | | | | | | | | |
| Well (borehole) instability | | | | | x | x | x | | | x | | | | | | |
| Mud losses (well/borehole drilling) | | | | | | | | | | x | | | | | | |
| Damage to casing string and pile foundations | | | | | | | | | | x | | | | | | |
| Presence of environmentally protected chemosynthetic communities | | | | | x | | x | x | | | | | | | | |
| Explosions leading to changed site conditions | | | | | | | | | | | | | | | | x |

Site hazards can generally not be treated on a statistical basis applying solely historical data. The nature of a hazard is often site and time dependent. In addition, natural geohazards are often interrelated. This may be due to a common trigger mechanism (e.g. earthquake, slope failure), or that one geohazard occurrence or process forms a trigger for other geohazards.

For instance:

- Earthquakes will induce dynamic actions on a structure and may induce elevated pore pressures leading to increased susceptibility to soil liquefaction;
- Slope failures and their deposits may result in irregular seafloor topography;
- Mud and salt diapirs are commonly associated with radial fault patterns, and continuous diapirism may result in (shallow) slope failures.

Table 2 highlights some relations between natural geohazards.

**Table 2: Related Offshore Natural Geohazards**

| | Irregular Seafloor Topography | Seafloor Bedforms | Seafloor Outcrops and Hard Seafloor | Soil Liquefaction | Shallow Gas & Gassy Soils | Gas Hydrates | Gas and Fluid Seepage | Diapirs (e.g. mud /salt) and Mudvolcanoes | Earthquakes | Faults | Tsunamis | Slope Failure | Submarine Mass Movement | Wind, Waves and Currents | Seafloor Scour and Sediment Mobility |
|---|---|---|---|---|---|---|---|---|---|---|---|---|---|---|---|
| Irregular Seafloor Topography | | x | x | | | | | | | x | | x | x | x | x |
| Seafloor Bedforms | x | | | | | | | | | | | | | x | x |
| Seafloor Outcrops and Hard Seafloor | x | | | | x | | x | x | | | | x | | | x |
| Soil Liquefaction | | | | | x | x | x | x | x | | | | | x | |
| Shallow Gas & Gassy Soils | | | x | x | | x | x | x | | x | | x | x | | |
| Gas Hydrates | | | | x | x | | x | | | | | x | x | | |
| Gas and Fluid Seepage | | | x | x | x | x | | x | | x | | x | x | | |
| Diapirs (e.g. mud /salt) and Mudvolcanoes | | | x | x | x | | x | | | x | | x | | | |
| Earthquakes | | | | x | | | | | | x | x | x | x | | |
| Faults | x | | | | x | | x | x | x | | x | x | x | | |
| Tsunamis | | | | | | | | | x | x | | x | x | x | x |
| Slope Failure | x | | x | | x | x | x | x | x | x | x | | x | x | x |
| Submarine Mass Movement | x | | | | x | x | x | | x | x | x | x | | x | x |
| Wind, Waves and Currents | x | x | | x | | | | | | | x | x | x | | x |
| Seafloor Scour and Sediment Mobility | x | x | x | | | | | | | | x | x | x | x | |

Assessment of hazard probability of occurrence and frequency can be based on geomechanical modelling taking into account uncertainty in modelling of site conditions, soil parameter values, ongoing geological processes, actions and applied analysis methods (Clayton and Power, 2002; OGP, 2009).

The risk of a site hazard is the sum of the product of the probability of a hazard event affecting a structure and damage consequence. The damage consequence can depend on factors such as structure robustness and vulnerability. The information in this document covers the nature of hazards and their potential implications, not the risk. Power et al. (2005) and Galavazi et al. (2006) describe risk analysis methodology.

Risk mitigation can include avoidance (e.g. a certain standoff distance to avoid structure interaction) and design for robustness.

## IRREGULAR SEAFLOOR

Seafloor morphology can be irregular as a result of past or present geological processes. Human activities can also affect the seafloor topography. Irregular seafloor may be caused by (or be associated with) a number of natural and man-made phenomena. These include:

- Canyons and channels
- Boulders (e.g. drop stones)
- Spudcan footprints
- Anchor scars
- Trawl marks and scars
- Drill cuttings.

The scale of morphological features varies (e.g. scour marks, submarine canyons). The impact can differ per structure type and geometry.

## SEABED SCOUR AND SEDIMENT MOBILITY

Seabed scour relates to the erosion of seabed sediments. Such erosion can occur under normal metocean conditions or can be enhanced as a result of a structure or multiple structures interrupting a natural flow regime above seafloor, thereby increasing flow velocities. Scour can be enhanced or initiated by secondary processes such as rocking of a structure.

Especially non-cohesive sandy (and silty) sediments are susceptible to scour. Erosion and transport of fine sand can start at a flow velocity in excess of 0.2 m/s. Local scour pits (or scour holes) can form shortly after installation of a structure. Their dimensions will usually vary in time depending on the flow regime.

Scour can occur in any water depth (from shoreline to deep sea). The flow regime due to wave- and tidal-influence is generally stronger in shallow water than in deep water (Soulsby, 1997; Sumer & Fredsoe, 2002). In general, tide- and wave-action, in combination with fluvial discharge of fresh water determine the natural flow regime in coastal areas. Deepwater bottom current activity may result from density differences between water masses and from global thermohaline ocean circulation. Resulting sedimentary accumulations are known as contourite drifts (Faugeres et al., 1999).

Seafloor variation can usually be characterized as some combination of the following Whitehouse (1998):

- Local scour and sedimentation; usually a steep sided scour pit around a structure or structural element
- Global (or general) scour; a (shallow) scoured basin of large extent around a structure, possibly due to overall structure effects, multiple structure interaction, or wave-soil-structure interaction
- Overall seabed movement; erosion, deposition, bedform migration that would also occur in the absence of a structure (i.e. regional scour).

## SEAFLOOR BEDFORMS

A seafloor bedform is a morphological feature formed by interaction of wave-action and (tidal-) currents and cohesionless sediment (i.e. sand/silt). Bedforms are typically found on sandy areas of continental shelves.

Bedforms can be grouped into:

- Ripples: wave length about 0.3 m to 0.6 m, height up to 0.05 m
- Mega ripples: wave length 0.3 m to 1 m, height 0.05 m to 0.2 m
- Sand waves (dunes): wave length 30 m to several hundreds of metres, height between 1 m to 2 m and 10 m to15 m
- Sand banks: wave length 1 km to tens of km, width 0.5 km up to 10 km, height up to tens of metres.

A characteristic of bedforms is their mobility. Sand waves tend to move slowly (metre per year) or flex their crests with tidal currents. Ripples tend to be more mobile, in the order of a metre per day (Morelissen et al., 2003).

For structure design it is important to identify which part of the seabed and/or the bedforms is actually mobile. The rate at which bedforms recover after having been modified by, for example, cable trenching mainly depends on sediment transport rate and supply of sediment.

## SEAFLOOR OUTCROPS AND HARD SEAFLOOR

Seafloor outcrops and hard seafloor ground conditions commonly include:

- Shell and coral banks, reefs, which are common in shallow waters in the tropical zones.
- Local patches of cemented soil (e.g. hard ground, cap rock). Examples are authigenic carbonates around pockmarks, Kurkar ridges (cemented aeolian dunes) in the eastern Mediterranean Sea, beach rocks (cemented beach sediments) in the Caribbean Sea, sabkha deposits (evaporitic-tidal floodplain deposits) in the Arabian/Persian Gulf and Gulf of Suez.
- Crust composed of precipitated metalsulphides associated with hydrothermal activity (e.g. black and white smokers) in vicinity of tectonic plate boundaries and faults.
- Outcrops of rock. Examples are pre-Quaternary sand- and limestone beds offshore West Africa, sedimentary and metamorphic rocks exposed in the Irish Sea.

It should be noted that seafloor outcrops and hard seafloor may have environmental protection status or legislative implications.

Cementation of soil may result from sub-marine cementation processes. Cementation may also have resulted from past sub-aerial exposure of a continental shelf during low sea level stands under arid climate conditions. Cementation generally occurs in carbonate-rich and hyper-saline environments.

## DIAPIRS AND MUD VOLCANOES

A diapir is a domal upwelling of sediment, rock or salt that forms in response to tectonic forces, density differences and high overburden pressures. Diapirs can pierce through a stratigraphic overburden and create an envelope of overconsolidated soils, deformed rock and sediments around a diaper core (e.g. salt). Generally, a circular dome-shaped topographic feature develops when a diapir approaches the seafloor. Diapirs are commonly associated with radial faulting patterns and locally increased seafloor slopes.

Salt diapirs are known to be present in, for example, the Gulf of Mexico, offshore Brazil and West Africa, and the North Sea.

Mud diapirs and mud volcanoes are usually associated with rapidly-deposited sediments and in situ pore pressure conditions significantly higher than hydrostatic (overpressured). Additionally, high vertical and horizontal stresses typically apply, caused by faulting, folding and uplift processes.

Mud diapirs and mud volcanoes occur mostly in (historic) delta areas: Nile Delta (offshore Egypt), Absheron Ridge (offshore Azerbaijan, Caspian Sea), Makran Ridge (offshore Iran, Arabian Sea), Niger Delta (offshore Nigeria).

Release of pressure is commonly provided by faults and folding of the strata. Sediments mixed with over-pressured fluid and gas (mud) migrate upward through the stratigraphic overburden in vertical columnar zones (diapirs). Usually the over-pressured muds enter fault planes, thus causing diapirism along faults. A mud volcano can form when a mud diapir breaks the seafloor.

In general, mud volcanoes are conical, as tall as 65 m and up to 2 km across. The size and shape of a mud volcano depends on the frequency of expulsion and the type of material ejected. This can be unconsolidated soils, overconsolidated material, fractured rock (e.g. breccia), oil, gas and water (Snead, 1972; Newton et al., 1980; Delisle et al., 2002; Delisle, 2004; Delisle, 2005). Not all offshore mud volcanoes are active. Eruptions are believed to be episodic.

## SHALLOW GAS & GASSY SOILS

Gas may be present (trapped) in the seabed (e.g. gassy soils). Shallow gas can comprise a mixture of different gases, such as carbon dioxide, hydrogen sulphide, ethane and methane. In general, the gases originate from bacterial decay of organic matter (biogenic gases) within a few metres of the seafloor. Gas may also come from sources much deeper in the stratigraphy and migrate upwards through pores and cracks in the soil and rock (petrogenic gases).

Shallow gas may be present dissolved in pore water, as free gas in gas-filled voids or bubbles, and as gas hydrates. Over time, gas in soil may increase the in-situ pore pressures and result in excess pore pressures.

Migration of gas in soil can result in accumulation of gas in seabed below a foundation. Shallow gas in the pore water can have a serious effect on foundation behaviour.

In addition, shallow gas can be toxic to humans, can combust and explode.

Soil property measurements on geotechnical samples containing shallow gas may not be representative of in situ properties.

GAS HYDRATES

Gas hydrates are ice-like crystalline solids composed of water molecules surrounding a molecule of gas, generally methane. Gas hydrates can only form when gas is over-saturated in water. Gas hydrates are stable under high pressure and low temperature conditions, and may be present at seafloor and in shallow sediments, generally in deep water environments in excess of 500 m below Mean Sea Level (Rastogi et al., 1999; Von Rad et al., 2000).

Stable gas hydrate acts as cement and increases strength and rigidity of soil.

Natural gas hydrates are regarded as a geohazard when they dissociate, start “melting”. Both water and gas are released into soil when gas hydrates dissociate. This can result in formation of “gassy soils”. The addition of water and gas may decrease soil strength and form a weak layer (Orange and Breen, 1992; Judd and Hovland, 2007). Gas hydrate dissociation may be initiated by human activities, e.g. flow of “hot” hydrocarbons through well production casings, pipelines and flowlines.

Gas hydrates may for as a result of human activity. Gas hydrates can be a by-product of hydrocarbon production, forming hydrate plugs in the wellbore, around leaking joints and in pipelines. If a deep water exploration or production well is leaking, gas introduced into the shallow soils may react with water molecules to form hydrate layers or nodules.

GAS AND FLUID SEEPAGE

Gas and fluid seepage at seafloor is commonly associated with pockmarks. Pockmarks are roughly circular or conical depressions in the seafloor, generally 1 m to 350 m wide and up to 35 m deep (Newton et al., 1980; Von Rad et al., 2000; Judd and Hovland, 2007).

Pockmarks form by disruption of a pore pressure environment. This disruption may be triggered by natural or human causes, and can form on time scales of less than a year. Pockmarks can be intermittently active over long periods of time or can grow with explosive eruption events. The sediments in a pockmark are generally variable and may be overconsolidated.

When gas seeps continue over a long period of time, biological processes may cause cementation of the seabed sediments. Formation of authigenic carbonates can take place around the seeps (Judd and Hovland, 2007; Ding, 2008). In some cases, unique ecological habitats form in and around pockmarks. Such habitats may be protected by environmental legislation.

Authigenic carbonates may form thin crusts of weakly cemented sediments (hard grounds). They can be continuous over distances of several hundreds of metres (Von Rad et al., 2000). Locally more massive, competent layers of authigenic carbonates can be present as hard cemented layers or ‘lenses’. They may form large build-ups and seafloor mounts (Judd and Hovland, 2007).

Apart from natural seeps, gas seepage may also be induced by drilling activities (e.g. geotechnical drilling, hydrocarbon exploration drilling). The drilling process may cause fracturing of soil and rock, when drilling mud pressures exceed the fracture pressure of the soil or rock (i.e. hydraulic fracturing). These fractures may form pathways for fluid and gas migration into the wellbore and up to seafloor. A wellbore or leaking well casing may form a pathway to the surrounding rock and soil formations, introducing gas into sand layers in the shallow subsurface. Overtime, the introduced gas may affect the geotechnical properties of a soil and have serious effects on foundation behaviour.

Drilling-induced fluid flows (e.g. shallow water flows) occur when a pressurised sand body (aquifer) encapsulated in clay is penetrated by the drilling process. Shallow water flows are common offshore large river deltas, such as the Mississippi Delta (Gulf of Mexico) and the Nile Delta (offshore Egypt). The sandbodies are commonly derived from sediment deposition out of turbidity currents.

EARTHQUAKES

An earthquake, or seismic event, occurs after stresses in the earth's crust that have gradually built up, are suddenly released by movements along a fault. The movement generates seismic waves which propagate away from the earthquake epicentre. Most earthquakes occur along tectonic plate boundaries.

The location, magnitude and frequency (recurrence) of earthquakes cannot be reliably predicted. The probability of seismic events can be assessed on the basis of historic records of earthquake activity.

Seismic impact depends on geotechnical conditions at the site and structure design. Seismic activity may induce faulting, soil liquefaction, slope failure, and tsunamis.

SOIL LIQUEFACTION

Two types of liquefaction may be distinguished:
- gravitational (sometimes called static or flow) liquefaction, usually occurring in submerged slopes;
- cyclic liquefaction, usually generated through strong cyclic forces.

Soil liquefaction or cyclic mobility represents a decrease of soil strength and stiffness caused by an increase in pore water pressure in saturated soil. Soil liquefaction usually occurs in response to sudden change in stress condition, causing it to behave like a liquid. Examples of cyclic and dynamic actions include earthquake shaking, storm wave loading, structure displacements upon cyclic load application, pile installation by driving and vortex vibrations due to fluid flow around a structure.

Liquefaction potential can be significant for loose cohesionless soils present close to ground surface (seafloor) and below the water table. Dense sands, loose unsaturated sands and some sensitive cohesive materials can also liquefy under some conditions. In addition, the presence of gas in loose sands can change soil behaviour and may potential for liquefaction (Grozic, 2003).

FAULTS

A fault is a planar fracture or discontinuity in a volume of soil or rock along which significant vertical and/or horizontal displacement has occurred (Figure 2) (i.e. faulting). Fault zones are areas where multiple fractures and faults occur in close proximity, with similar moment direction.

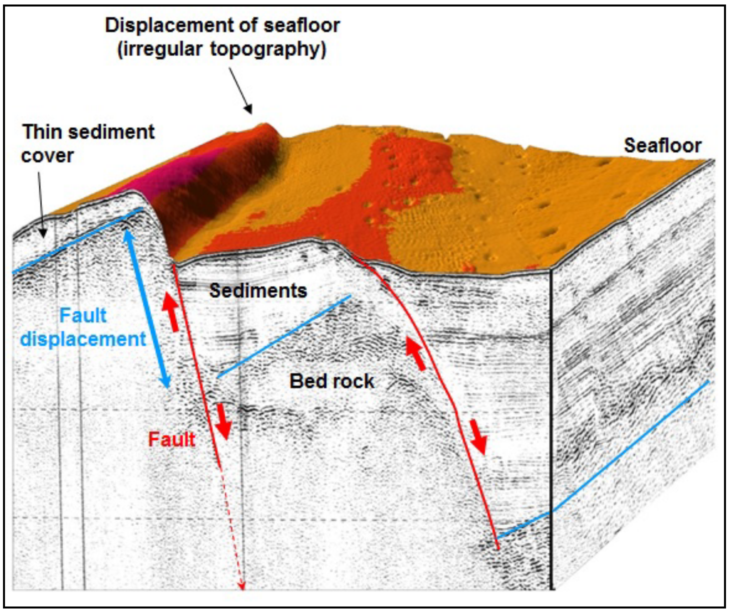


**Figure 2: Surface and subsurface expression of fault displacement**

Faults can be associated with:

- Tectonic activity (e.g. at tectonic plate boundaries, earthquake zones);
- Laterally variable soil subsidence and compaction;
- Soil contractions (e.g. polygonal faulting in North Sea and West African seabed sediments);
- Diapirism (e.g. radial faulting);
- Slope failure (e.g. headwall scarp, failure planes, tension cracks).

Movement along the fault plane (and hence soil displacement) is a semi-continuous process acting on time scales ranging from years to millions of years. Faults are commonly considered to be in-active if there has been no observed movement or evidence of seismic activity during the last 10,000 years. In this case a faults can be covered by a uniform layer of soil (i.e. without a clear discontinuity surface being present). Depending on crustal stresses and changes therein, apparently in-active faults may be reactivated causing further soil displacements and even seismic events.

Faults may result in a displaced, stepped seafloor and/ or irregular linear topographic features on the seafloor (e.g., headwall scarps). In addition, stratigraphic sequences are displaced in the seabed.

Deep-seated faults, with lengths of 100's to 1000's of metres, may be associated with earthquakes. The build-up of stresses due to differential movement in the earth's crust may be released along these deep-seated faults, whereby large amounts of energy move through rock and soils in the form of pressure waves and shear waves. These deep-seated, earthquake generating, faults are sometimes referred to as seismic faults.

TSUNAMIS

A tsunami (or surge wave) is a series of ocean waves of long wave lengths, which are created when a large volume of water is suddenly displaced by a submarine earthquake, landslide or volcanic eruption (Figure 3). In the open ocean, tsunami waves travel at high speeds (in excess of 800 km/h) with heights of, say, less than 0.05 m. As they approach the coast, the velocity decreases (to approximately 50 km/h) and the wave height increases up to several metres or tens of metres. At the coastline, the force of a tsunami wave can cause loss of life, damage to buildings and infrastructure, large scale erosion (scour) and flooding of low-lying areas.

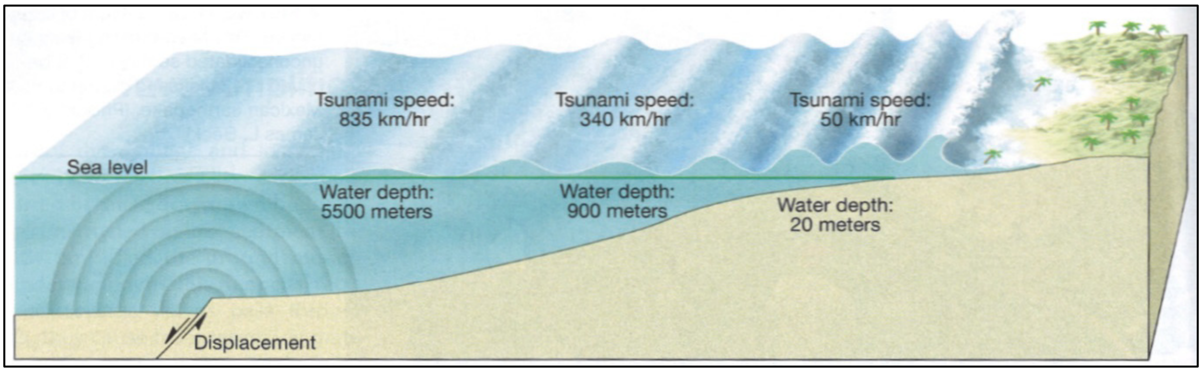


**Figure 3 Tsunami generated by fault displacement offshore**

SLOPE FAILURE

Slope failure occurs when downslope driving forces acting on seabed exceed resistance. In general, slope failure results in the down-slope movement of a soil mass (see section titled Submarine Mass Movements). Slopes may be unstable at any water depth.

Slopes may develop due to tectonics, high sedimentation rates or incision and erosion by seafloor currents and flows.

Slope failure can be triggered by earthquakes, strong currents, storms (wave actions), tsunamis, volcanism and human activity (Hampton et al., 1996; Mulder and Cochonat, 1996; Locat and Lee, 2005; Judd and Hovland, 2007; Rogers and Goodbred, 2010).

Usually, a combination of two or more factors influence slope failure, e.g. presence of shallow gas and an earthquake (Orange and Breen, 1992; Judd and Hovland, 2007). Slopes can be unstable due to low shear strength and overpressured strata (e.g. shallow gas). Seabed may fail on slight slopes as little as 0.5˚ (Hampton et al., 1996; Judd and Hovland, 2007).

Failure scarps and oversteepened slopes are commonly associated with past slope failures. Past slope failures may be reactivated if a trigger (e.g. pore pressure build-up, earthquake) is present. The seafloor morphology resulting from a slope failure may be irregular and undulating (see section titled Irregular Seafloor Topography).

SUBMARINE MASS MOVEMENTS

A submarine mass movement is a displacement of seabed material driven directly by gravity or other body forces, rather than stresses associated with fluid flow. The deposits of submarine mass movements are commonly referred to as mass transport deposits, MTDs.

Submarine mass movements commonly follow from slope failures and include the following processes (Figure 4) (Lee et al., 2007):

– Slides:
    - Translational slide
    - Rotational slide
– Mass flows:
    - Debris flow
    - Debris avalanche
    - Mud flow
    - Liquefaction flow
    - Turbidity current

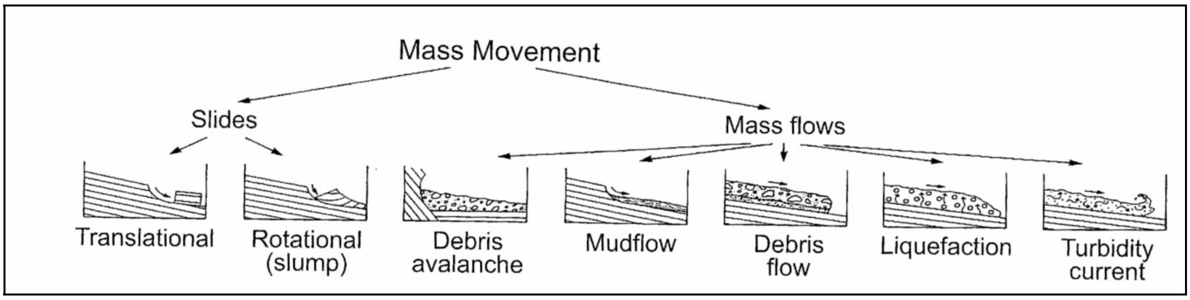


**Figure 4: Submarine mass movement classification (after Lee et al., 2007)**

Slides are movements of essentially rigid, undeformed masses along discrete failure/slip planes. If slip occurs along a planar surface the slide is referred to as a <u>translational slide</u>. If slip occurs along a curved failure plane and the rigid mass shows rotation, the slide is referred to as <u>rotational</u>.

If moving sediments take a form of viscous fluid, the feature is referred to as mass flow or gravity flow. Mass flow deposits show considerable internal deformation with many invisible or short-lived internal slip surfaces. Submarine slides can become mass flows as the failed material progressively disintegrates, gets entrained with surrounding water and moves downslope.

<u>Debris flows</u> are mass flows in which sediments are heterogeneous and may include larger clasts supported by a fine-grained soil matrix. <u>Mud flows</u> involve predominantly fine-grained (mud) sediments. <u>Turbidity currents</u> involve downslope transport of a relatively dilute suspension of sediment grains that are supported

by an upward component of fluid turbulence. Turbidity currents often evolve from disintegration and dilution of debris and mud flows. Liquefaction flows occur when loosely packed sandy sediments collapse under environmental conditions (e.g. cyclic actions by waves or earthquakes; see section titled Soil Liquefaction. Debris avalanches occur where slides collapse and disintegrate into smaller pieces. They move rapidly without following pre-existing channels or valleys.

The potential impact of submarine mass movements on a structure depends upon the location or orientation of the structure in relation to the movement direction (Figure 5).

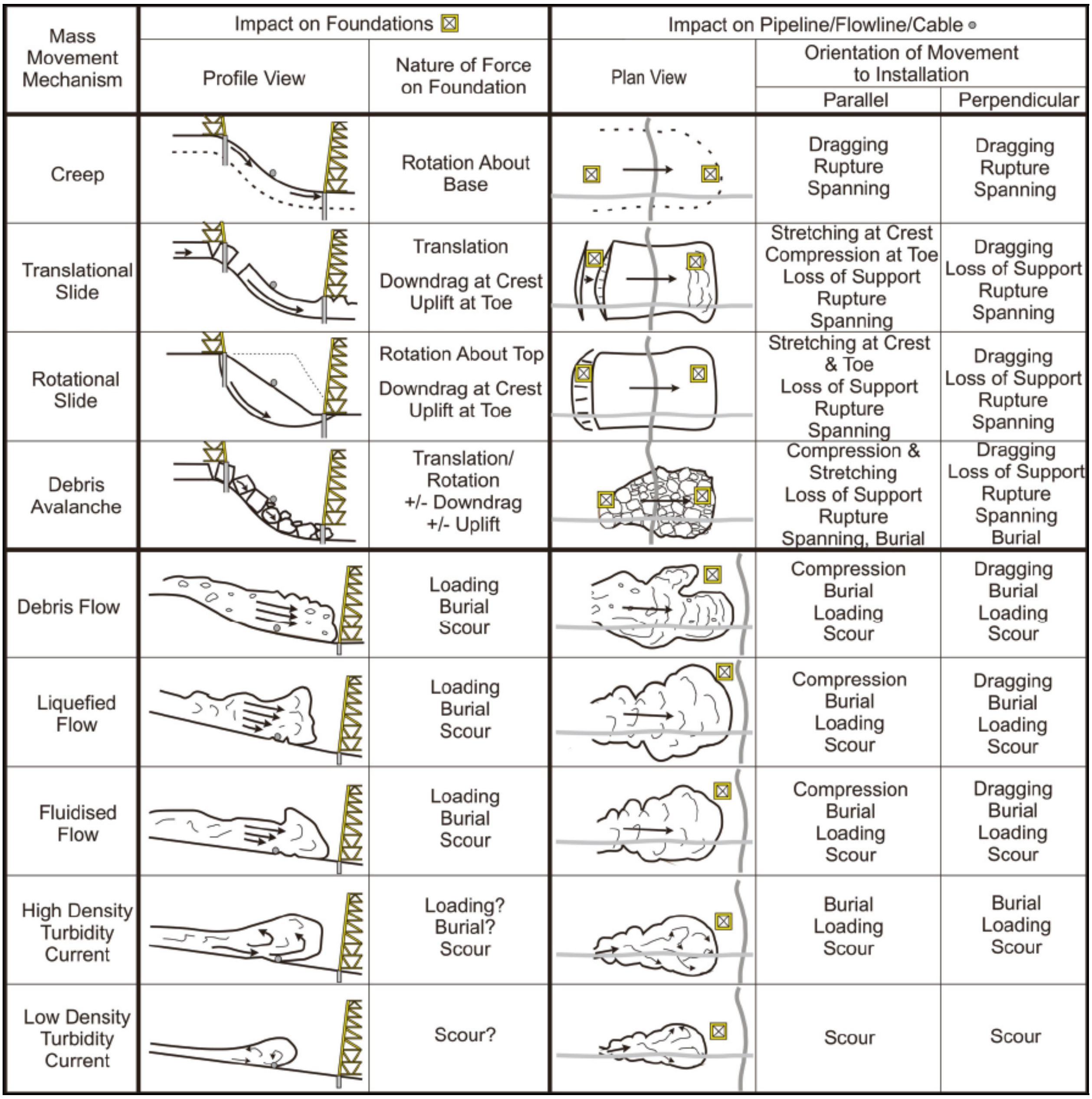

| Mass Movement Mechanism | Impact on Foundations: Profile View | Impact on Foundations: Nature of Force on Foundation | Impact on Pipeline/Flowline/Cable: Plan View | Orientation of Movement to Installation: Parallel | Orientation of Movement to Installation: Perpendicular |
|---|---|---|---|---|---|
| Creep | | Rotation About Base | | Dragging Rupture Spanning | Dragging Rupture Spanning |
| Translational Slide | | Translation<br>Downdrag at Crest Uplift at Toe | | Stretching at Crest Compression at Toe Loss of Support Rupture Spanning | Dragging Loss of Support Rupture Spanning |
| Rotational Slide | | Rotation About Top<br>Downdrag at Crest Uplift at Toe | | Stretching at Crest & Toe Loss of Support Rupture Spanning | Dragging Loss of Support Rupture Spanning |
| Debris Avalanche | | Translation/ Rotation +/- Downdrag +/- Uplift | | Compression & Stretching Loss of Support Rupture Spanning, Burial | Dragging Loss of Support Rupture Spanning Burial |
| Debris Flow | | Loading Burial Scour | | Compression Burial Loading Scour | Dragging Burial Loading Scour |
| Liquefied Flow | | Loading Burial Scour | | Compression Burial Loading Scour | Dragging Burial Loading Scour |
| Fluidised Flow | | Loading Burial Scour | | Compression Burial Loading Scour | Dragging Burial Loading Scour |
| High Density Turbidity Current | | Loading? Burial? Scour | | Burial Loading Scour | Burial Loading Scour |
| Low Density Turbidity Current | | Scour? | | Scour | Scour |

**Figure 5: Potential impacts of submarine mass movements on platform foundation and pipeline (modified after Thomas et al., 2009)**

WIND, WAVES, CURRENTS AND TIDES

Periods of extreme weather conditions, such as (tropical) storms, monsoons, peak wind, waves and current regimes, can cause lateral and cyclic actions on the seafloor and any seabed-supported structure. In addition, adverse weather conditions may complicate structure installation activities.

Peak wave and (seafloor/bottom) current regimes can also cause changes in seafloor conditions due to scour and burial (i.e. sediment remobilisation), winnowing of seafloor sediments (i.e. removal of fine/clay-size materials) and development of irregular seafloor topography.

Tidal variation and atmospheric pressure fluctuations as a result of storms are known to change pore pressures conditions in the seabed, potentially creating circumstances leading to soil failure and liquefaction.

Estimation of environmental actions is relatively inaccurate. It normally involves statistical data for a specific geographic region and various procedures for modelling the interaction of a structure and its environment.

MAN-MADE HAZARDS

Human activities and anthropogenic (i.e. man-made/man-induced) features, debris or obstructions can have an adverse effect on an offshore structure.

Seafloor features and objects have been left by human activities since the dawn of mankind. Ship wrecks can form archaeological sites, war graves, enhance ecological diversity and may be restricted areas.

In addition, offshore energy activities, such as drilling, (jack-up) platform installation and decommissioning and resulting footprints may alter seafloor topography and/or potentially alter seabed conditions (e.g. drill spoils, gas charging as a result leaking exploration wells).

Commonly encountered man-made hazards include:
- Unexploded ordnance (UXO);
- Existing energy facilities (e.g. fixed platforms, pipelines, manifolds, wellheads, power cables etc.);
- Telecommunication cables;
- Ship wrecks;
- Fallen objects (e.g. shipping containers).

These hazards may complicate structure installation and design if not identified at an early stage.

## REFERENCES

API American Petroleum Institute (2011), "Geotechnical and Foundation Design Considerations: ISO 19901-4:2003 (Modified), Petroleum and Natural Gas Industries - Specific Requirements for Offshore Structures, Part 4 - Geotechnical and Foundation Design Considerations", ANSI/API Recommended Practice 2GEO, First Edition.

API American Petroleum Institute (2009), "Design, Construction, Operation, and Maintenance of Offshore Hydrocarbon Pipelines (Limit State Design)", API Recommended Practice 1111, 4th Edition. (With Errata, May 2011)

API American Petroleum Institute (2000), "Recommended Practice for Planning, Designing and Constructing Fixed Offshore Platforms - Working Stress Design", API Recommended Practice 2A-WSD (RP 2A-WSD), 21st Edition. (With Errata and Supplement 1, December 2002, Errata and Supplement 2, October 2005, and Errata and Supplement 3, March 2008)

BWEA (2011), "Guidelines for the Selection and Operation of Jack-ups in the Marine Renewable Energy Industry: Industry Guidance Aimed at Jack-up Operators, Developers and Contractors", BWEA, London.

Campbell, K.J., Hooper, J.R. and Prior, D.B. (1986), "Engineering Implications of Deepwater Geologic and Soil Conditions, Texas-Louisiana Slope", in Eighteenth Annual Offshore Technology Conference, May 5-8, 1986, Houston, Texas: Proceedings, Vol. 1, OTC Paper 5105, pp. 225-232.

CEN European Committee for Standardization (2004), "Eurocode 7: Geotechnical Design - Part 1: General Rules", EN 1997-1:2004. (With Corrigendum EN 1997-1:2004/AC, February 2009).

CEN European Committee for Standardization (2011), “Petroleum and Natural Gas Industries - Pipeline Transportation Systems (ISO 13623:2009 Modified)”, European Standard EN 14161:2011.

Clayton, C. and Power, P. (2002), "Managing Geotechnical Risk in Deepwater", in Cook, M. et al. (Eds.), Offshore Site Investigation and Geotechnics: 'Diversity and Sustainability': Proceedings of an International Conference Held in London, UK, 26-28 November 2002, Society for Underwater Technology, London, pp. 425-443.

Delisle, G. (2004), “The Mud Volcanoes of Pakistan”, Environmental Geology, Vol. 46, No. 8, pp. 1024-1029. Mud Volcanoes, Geodynamics and Seismicity: Proceedings of the NATO Advanced Research Workshop

Delisle, G. (2005), “Mud Volcanoes of Pakistan: an Overview”, in Martinelli, G. and Panahi, B. (Eds.), Series. IV. Earth and Environmental Sciences, Vol. 51, Springer, Dordrecht, pp. 159-169. on Mud Volcanism, Geodynamics and Seismicity, Baku, Azerbaijan, 20-22 May 2003, NATO Science

Delisle, G., Von Rad, U., Andruleit, H., Von Daniels, C.H., Tabrez, A.R. and Inam, A. (2002), "Active Mud Vol. 91, No. 1, pp. 93-110. Volcanoes On- and Offshore Eastern Makran, Pakistan", International Journal of EarthSciences, Vol. 91, No. 1, pp. 93-110.

Ding, F. (2008), "Near-surface Sediment Structures at Cold Seeps and their Physical Control on Seepage: a Geophysical and Geological Study in the Southern Gulf of Mexico and at the Frontal Makran Accretionary Prism/Pakistan", Dissertation, Universität Bremen.

Evans, T.G. (2010), “A Systematic Approach to Offshore Engineering for Multiple-project Developments in Geohazardous Areas. In S. Gourvenec & D. White (eds), Frontiers in offshore geotechnics II; Proceedings of the 2nd international Symposium on Frontiers in Offshore Geotechnics, Perth, Australia, 8-10 November 2010: 3-32. Boca Raton: CRC Press.

Faugères, J.-C., Stow, D.A.V., Imbert, P. and Viana, A. (1999), "Seismic features diagnostic of contourite drifts", Marine Geology, Vol. 162, No. 1, pp. 1-38

Galavazi, M.A., Moore, R., Lee, M., Brunsden, D. and Austin, B. (2006), "Quantifying the impact of deepwater geohazards", 2006 Offshore Technology Conference, 1-4 May, Houston, OTC Paper 18083

Grozic, J.L.H. (2003), “Liquefaction Potential of Gassy Marine Sands”, in Locat, J. and Mienert, J. (Eds.), Submarine Mass Movements and Their Consequences, Kluwer Academic Publishers, Dordrecht, pp. 37-45.

Hampton, M.A., Lee, H.J. and Locat, J. (1996), "Submarine Landslides", Review of Geophysics, Vol. 34, No. 1, pp. 33-59.

ISO International Organization for Standardization (2013), “Petroleum and Natural Gas Industries - General Requirements for Offshore Structures”, International Standard ISO 19900:2013.

ISO International Organization for Standardization (2002), "Geotechnical Investigation and Testing - Identification and Classification of Soil - Part 1: Identification and Description", International Standard ISO 14688-1:2002.

ISO International Organization for Standardization (2004), "Geotechnical Investigation and Testing - Identification and Classification of Soil - Part 2: Principles for a Classification", International Standard ISO 14688-2:2004.

ISO International Organization for Standardization (2003), "Petroleum and Natural Gas Industries - Specific Requirements for Offshore Structures - Part 4: Geotechnical and Foundation Design Considerations", International Standard ISO 19901-4:2003.

ISO International Organization for Standardization (2009), “Petroleum and Natural Gas Industries - Pipeline Transportation Systems”, International Standard ISO 13623:2009.

ISO International Organization for Standardization (2012), “Petroleum and Natural Gas Industries - Site Specific Assessment of Mobile Offshore Units - Part 1: Jack-ups”, International Standard ISO 19905-1:2012.

Judd, A.G. and Hovland, M. (2007), "Seabed Fluid Flow: the Impact on Geology, Biology, and the Marine Environment", Cambridge University Press, Cambridge.

Lee, H.J., Locat, J., Desgagnés, P., Parsons, J.D., McAdoo, B.G., Orange, D.L., Puig, P., Wong, F.L., Dartnell, P. and Boulanger, E. (2007), "Submarine Mass Movements on Continental Margins", in Nittrouer, C.A. et al. (Eds.), Continental Margin Sedimentation: from Sediment Transport to Sequence Stratigraphy, Blackwell Publishing Ltd, Oxford, Special Publication of the International Association of Sedimentologists, No. 37, pp. 213-274.

Locat, J. and Lee, H.L. (2005), "Subaqueous Debris Flows", in Jakob, M. and Hungr, O. (Eds.), Debris-flow Hazards and Related Phenomena, Springer-Verlag, Berlin, Springer-Praxis Books in Geophysical Sciences, pp. 203-245.

Morelissen, R., Hulscher, S., Knaapen, M.A.F., Németh, A.A. and Bijker, R. (2003), "Mathematical Modelling of Sand Wave Migration and the Interaction with Pipelines", Coastal Engineering, Vol. 48, No. 3, pp. 197-209.

Mulder, T. and Cochonat, P. (1996), “Classification of Offshore Mass Movements”, Journal of Sedimentary Research, Vol. 66, No. 1, pp. 43-57.

Newton, R.S., Cunningham, R.C. and Schubert, C.E. (1980), “Mud Volcanoes and Pockmarks: Seafloor Engineering Hazards or Geological Curiosities?”, in Twelfth Annual Offshore Technology Conference, May 5-8, Houston, Texas: Proceedings, OTC Paper 3729.

OGP (2009) “Geohazards from seafloor instability and mass flow”, Report No. 425, dated December 2009.

OGP (2013) “Guidelines for the conduct of offshore drilling hazard site surveys”, Report No. 373-18-1, Issue 1.2, dated April 2013.

Osborne, J.J., Teh, K.L., Houlsby, G.T., Cassidy, M.J., Bienen, B. and Leung, C.F. (2011), "InSafeJIP: Improved Guidelines for the Prediction of Geotechnical Performance of Spudcan Foundations during Installation and Removal of Jack-up Units: Joint Industry-funded Project", RPS Energy, Woking, Report No. EOG0574-Rev1c.

Parker, E.J., Traverso, C., Moore, R., Evans, T. and Usher, N. (2008), “Evaluation of Landslide Impact on Deepwater Submarine Pipelines”, OTC.08: Proceedings 2008 Offshore Technology Conference, -8 May, Houston, Texas, USA, OTC Paper 19459.

Power, P.T., Galavazi, M.A. and Wood, G. (2005), "Geohazards need not be: redefining project risk", Offshore Technology Conference 2-5 May 2005, Houston, Texas, U.S.A., OTC Paper 17634, 7 pp.

Rastogi, A., Deka, B., Budhiraja, I.L. and Agarwal, G.C. (1999), "Possibility of Large Deposits of Gas Hydrates in Deeper Waters of India", Marine Georesources & Geotechnology, Vol. 17, No. 1, pp. 49-63.

Rogers, K.G. and Goodbred, S.L. (Jr.) (2010), "Mass Failures Associated with the Passage of a Large Tropical Cyclone over the Swatch of No Ground Submarine Canyon (Bay of Bengal)", Geology, Vol. 38, No. 11, pp. 1051-1054.

Skipp, B.O. and Mallard, D.J. (1995), "Site Investigations with Earthquakes in Mind", in Elnashai, A.S. (Ed.),European Seismic Design Practice: Research and Application: Proceedings of the Fifth SECED Conference on European Seismic Design Practice, Chester, United Kingdom, 26-27 October 1995, A.A. Balkema, Rotterdam, pp. 151-161.

SNAME Society of Naval Architects and Marine Engineers (2008), "Recommended Practice for Site Specific Assessment of Mobile Jack-up Units", First Edition – May 1994 (Revision 3 – August 2008), Technical & Research Bulletin, 5-5A.

Snead, R.E. (1972), "Mud Volcanoes of the Makran Coast", Explorers Journal, Vol. 50, No. 1, pp. 22-28.

Soulsby, R. (1997), "Dynamics of marine sands: A manual for practical applications", Thomas Telford Ltd., London, XXI, 249 p.

Sumer, B.M. and Fredsøe, J. (2002), "The mechanics of scour in the marine environment", World Scientific, Singapore, XIII, 536 p. (Advanced Series on Ocean Engineering; Vol. 17).

Thomas, S., Hooper, J.R. and Clare, M. (2009), "Constraining Geohazards to the Past: Impact Assessment of Submarine Mass Movements on Seabed Developments", Mosher, D.C. et al. (Eds.), Submarine Mass Movements and their Consequences: 4th International Symposium, Springer, Dordrecht, Advances in Natural and Technological Hazards Research, Vol. 28, pp. 387-398.

Von Rad, U., Berner, U., Delisle, G., Doose-Rolinksi, H., Fechner, N., Linke, P., Lückge, A., Roeser, H.A., Schmaljohann, R., Wiedicke, M. and SONNE 122/130 Scientific Parties (2000), "Gas and Fluid Venting at the Makran Accretionary Wedge off Pakistan", Geo-Marine Letters, Vol. 20, No. 1, pp. 10-19.

Wells, D.L. and Coppersmith, K.J. (1994), "New Empirical Relationships among Magnitude, Rupture Length, Rupture Width, Rupture Area, and Surface Displacement", Bulletin of the Seismological Society of America, Vol. 84, No.4, pp.974-1002.

Whitehouse, R. (1998), "Scour at marine structures: a manual for practical applications", Thomas Telford Ltd., London, XIX, 198 p.

Yuan, F., Wang, L., Guo, Z. and Shi, R. (2012), "A Refined Analytical Model for Landslide or Debris Flow Impact on Pipelines. Part I: Surface Pipelines", Applied Ocean Research, Vol. 35, pp. 95-104.

## INTRODUCTION

A geotechnical design situation or a re-assessment of an existing structure requires geotechnical analysis, including evaluation of hazards and verification of relevant limit states. Geotechnical analysis follows design philosophies included in standards and codes of practice, where available. All consider that the resistance (or capacity) of a geotechnical system must be greater than the actions (demands or loads) on the system for an acceptable or required level of safety or reliability (ISO 2394, 2015).

## HAZARD EVALUATION

Hazards are situations or events with potential to cause damage (ISO 2000, 2013). Hazard evaluation typically includes classification, estimation of probability of occurrence and measures for countering the hazard. Examples of hazards are abnormal environmental events, accidental events, geohazards and man-made site hazards. Note that event probability differs from risk, where risk is defined as the product of probability and consequence.

In many geotechnical situations, hazard evaluation will not be complete and exact. It will be necessary to draw on so-called tacit expert knowledge. This means senior expertise, with access to geotechnical knowledge and experience. Judgement and opinion are inevitable and a senior expert or a team of senior experts is more likely to arrive at a correct understanding and an appropriate way forward. Judgement is qualitative and subjective. Table 1 shows probability expressions intended for a context of approximate and subjective probability of the occurrence of a hazardous event or phenomena during a defined exposure period (Peuchen et al., 2015).

**Table 1. Expressions for approximate and subjective probability**

| Term | Verbal descriptor | Approximate probability for exposure period |
|---|---|---|
| Negligible | unlikely, although the possibility cannot be ruled out completely | 0 to 0.01 |
| Low | not probable, although uncertain | 0.01 to 0.1 |
| High | credible, possibility can be described with reasonable confidence by known physical conditions or processes | 0.1 to 1 |

Measures for countering a hazard include source elimination, avoidance, implementation of a barrier, minimising consequences and design for the hazard.

## LIMIT STATES

Limit states may be grouped into Ultimate Limit States (ULS, for example structure stability), Serviceability Limit States (SLS, for example for avoiding excessive settlement), Fatigue Limit States (FLS) and Accidental Limit States (ALS). Verification of a limit state usually involves one or more of the following approaches:
- calculation models
- prescriptive measures
- experimental models and load tests
- observational method.

Features of a calculation model include:
- method of analysis typically including simplifications and modification of the results where necessary to improve accuracy or to allow for uncertainty and systematic error
- actions, such as (a sequence of) imposed loads or imposed displacements
- geometrical data, such as the shape of a geotechnical structure, geometry of the ground surface, water levels and interfaces between ground strata
- characteristic values of geotechnical parameters of ground (soil, rock, pore fluid, pore gas) and other materials
- limiting values of, for example, deformations and vibrations
- partial factors or safety factors.

The common analytical models rely on semi-empirical and direct methods of analysis.

Prescriptive measures generally involve (1) conventional and conservative details in the design and (2) attention to specification and control of materials, workmanship, protection and maintenance procedures. Their use is often applicable where calculation models are not available or not necessary. Examples are prescriptive measures for ensuring durability against chemical attack or frost action.

Experimental models and load tests can help to justify a design approach. Important considerations for evaluation of the results include differences in ground conditions, time effects and scale effects.

Prediction of geotechnical behaviour is often difficult. The observational method allows carefully planned monitoring during construction and includes planned contingency measures where necessary. Assessment of the monitoring results takes place at appropriate stages.

## DESIGN PHILOSOPHIES

Design philosophies typically incorporate geotechnical calculation models and corresponding (partial) factors. These partial factors or safety factors may vary depending on the specific design scenario.

Design philosophies for the ULS may be grouped as follows:
1. Working Stress Design (WSD) or Allowable Stress Design (ASD).
2. Partial Factor Design (PFD) or Limit State Design (LSD).
    a. Factored material properties.
    b. Factored resistance.

The WSD method uses global safety factors applied to characteristic values (or ultimate values) of resistance.

The PFD methods use partial action factors and partial factors applied to resistance. The partial action factors are applied to characteristic or representative values of actions. This results in design values for actions. The factored material properties and factored resistance methods differ by their calculation of resistance. The method for factored material properties applies partial material factors to characteristic values of material properties such as undrained shear strength of soil. The factored values are then used in the calculation model to obtain a design value for resistance (factored resistance). The factored resistance method uses characteristic values of material properties in the calculation model and then applies a partial resistance factor to obtain a design value for resistance. An additional factor $\gamma_d$ can be considered to account for model uncertainty or other uncertainties not covered by other partial factors (ISO, 2013).

API Recommended Practice RP 2A-WSD (API, 2014) is an example of the WSD approach. Eurocode 7 Geotechnical Design (CEN, 2004; 2007), ISO 19900 (2013), ISO 19901-4 (2003) and API RP 2GEO Geotechnical and Foundation Design Considerations (API, 2011 and 2014) provide design principles according to the PFD approaches.

Design philosophies for the ALS, SLS and FLS are similar. Global safety factors and partial factors will differ from the ULS.

## GEOTECHNICAL PARAMETER VALUES

### DESIGN PROCESS

Assignment of geotechnical parameter values or soil property values is according to the following steps:
1. Site characterisation and stratigraphic schematisation.
2. Evaluation of derived values of geotechnical parameters.
3. Selection of characteristic values of geotechnical parameters and application in a calculation model.

The selection of characteristic values of geotechnical parameters takes place within the context of a calculation model and thus includes consideration of limit states, actions, geometry, limiting values and partial factors or safety factors. Divorcing the selection of characteristic values from the actual use and evaluation of a calculation model may lead to errors.

## STRATIGRAPHIC SCHEMATISATION

General site characterisation is necessary before selection of geometrical data for the ground and before evaluation of the results of specific tests and observations. Such site characterisation comprises a general assessment of the character and basic constituents of the ground (soil and rock classification) and their possible change in time.

Typical parameters for soil classification include particle size distribution, water content, carbonate content, Atterberg limits, unit weight, relative density and undrained shear strength. Typical parameters for rock classification include mineralogy, water content, unit weight and uni-axial compressive strength.

Stratigraphic schematisation depends on the nature of the actions, geometrical quantities of the structure that interacts with the ground, volume of ground that represents the domain of influence with respect to the limits state, spatial ground variability, simplification of ground conditions, e.g. undrained versus drained foundation response.

Two competing factors apply to spatial ground variability: (1) the spatial averaging of properties over a potential failure surface, which reduces the coefficient of variation of property values (i.e. with respect to that for the location under consideration) and (2) the tendency for a failure surface to follow the path of least resistance.

Stratigraphic schematisation can include evaluation of:

- basic parameters such as undrained shear strength and relative density on the basis of derived values of geotechnical parameters (refer following section)
- geological and hydro-geological setting
- results of a geophysical survey
- hazards such as potential instability of the ground
- water levels
- aggressiveness of ground and ground water.

## DERIVED VALUES OF GEOTECHNICAL PARAMETERS

A derived value of a geotechnical parameter or coefficient is obtained from test results by theory, correlation or empiricism. In situ test and laboratory test measurements and other relevant data provide a basis for obtaining derived values of geotechnical parameters.

Laboratory test standards often specify procedures for obtaining derived values, in particular where it is possible to obtain a derived value by means a of a conversion model or theory. Such derived values are thus part of the laboratory test report. An example is the unconsolidated undrained triaxial compression test. Normalised load and displacement data are the basic measured values. The measured values and the use of theory allow the calculation of a derived value of undrained shear strength by consideration of principal stress conditions and a theoretical deformation model.

Standards for in situ tests usually require reporting of (normalised) measured values only. Examples of measured values are cone resistance and sleeve friction for a Cone Penetration Test (CPT). Measured values can serve as input for some calculation models that rely on empirical relationships. An example is the use of CPT cone resistance for the calculation of axial pile resistance. A more common approach is to obtain derived values of geotechnical parameters from in situ tests on the basis of empiricism or (simplified) theory or a combination thereof. Evaluation of derived values of geotechnical parameters will usually comprise undrained shear strength ($c_u$) and relative density ($D_r$) according to a single interpretation method, where appropriate.

Many empirical correlations and theoretical interpretation models are available for obtaining specific derived values of geotechnical parameters from the results of laboratory and in situ tests. Evaluation of various sets of derived values by engineering judgement or statistical methods can be considered, whereby one method is selected as reference.

Measured values and derived values may be represented by low estimate, best estimate and high estimate values. In statistical terms, a best estimate value aims to represent a mean value of a geotechnical parameter for a stratum or multiple soil layers. Low and high estimates aim for the quantile associated with the 5% fractile. Comments are as follows:

- Low, best and high estimates usually consider a reference method or procedure, if values from multiple methods or procedures are combined. This is because a test result or a derived value can depend on the method(s) selected to obtain the parameter value. For example, a value of undrained shear strength derived from a triaxial test can depend on the sampling method, sample handling practice, laboratory test procedure and whether undrained shear strength is derived from maximum deviator stress or maximum principal stress ratio.
- Low, best and high estimates can include judgement and opinion, particularly for a limited quantity or absence of test results and derived values. This implies that outliers may be ignored and that a bias may be introduced relative to the available data. Judgement and opinion consider physically credible values, comparison of data with results from other tests and *a priori* knowledge such as geological setting and comparable experience.
- A wide spread of data can indicate spatial variability of soil. This means that averaging of test results and derived values can obscure a weaker or stronger zone.
- A calculation model can require specific schematisation of soil stratigraphy and model-specific selection of parameter values. This is not covered by low, best and high estimates.

CHARACTERISTIC VALUES OF GEOTECHNICAL PARAMETERS

A characteristic value of a geotechnical parameter represents a ***cautious estimate*** for the value affecting the occurrence of a limit state (CEN, 2004). The selection of a characteristic value takes account of possible differences between derived values of geotechnical parameters and geotechnical parameters representative of the behaviour of a geotechnical structure. Reasons for differences can include non-homogeneity of the ground, extent of the zone governing a particular limit state, uncertainties in geometrical data and analytical model, time effects, brittle or ductile response of the ground, influence of construction activities.

Characteristic values may be lower values, which are less than the most probable value, or upper values, which are greater. Each calculation requires the most unfavourable combination of lower and/or upper values for independent geotechnical parameters.

Statistical methods may be appropriate for selection of a characteristic value (Hicks, 2013; Baecher and Christian, 2003). Usually, they should allow for incorporation of a-priori knowledge of comparable experience with geotechnical parameters, for example by Bayesian methods, as necessary. Selection of a statistical characteristic value is typically such that the calculated probability of a worse value governing the occurrence of a limit state is not greater than 5%. Variance reduction methods may be applied where appropriate.

In principle, spatial ground variability affects:

- The mean ($X_m$), Standard Deviation (SD) and probability density function (pdf) of the ground property for the location under consideration, including any depth trend.
- The scale of fluctuation (θ) of the ground property, which is the distance over which the property values are significantly correlated; the scale of fluctuation in the (near) horizontal plane is often much larger than in the vertical direction, i.e. $\theta_h >> \theta_v$, for example due to the process of deposition.
- The limit state under consideration, particularly relating to the geometrical quantities of the structure that interacts with the ground, the nature of the applied actions and the volume of ground that represents the domain of influence with respect to the limit state.

The pdf required for the characteristic value should take account of the spatial variability of ground property values and the limit state under consideration, and thus may differ considerably from the underlying pdf for the location under consideration (Figure 1). If the domain of influence is represented by the dimension D, the characteristic value will be a function of the ratio θ/D and will generally lie within the following limits:

- For relatively large values of θ/D, there may be considerable uncertainty regarding the property value governing the structure response. Specifically, although the occurrence of the limit state will generally be governed by the "local" mean, there will be uncertainty about what that mean actually is. The characteristic value may then be represented by the 5 percentile of the underlying pdf. (Figure 1a)

- For intermediate values of θ/D, the characteristic value may be estimated from a pdf with a reduced variance to account for averaging of properties. However, account should also be taken of any apparent reduction in the property mean due to the tendency for failure to follow the path of least resistance. (Figure 1b)
- For small values of θ/D, there is considerable averaging of property values over potential failure surfaces and the response of the structure may be reasonably represented by a cautious estimate of the mean over the failure surface. For the assumption of a normal distribution of X, this is equivalent to a cautious estimate of $X_m$, the mean of the underlying distribution. (Figure 1c)

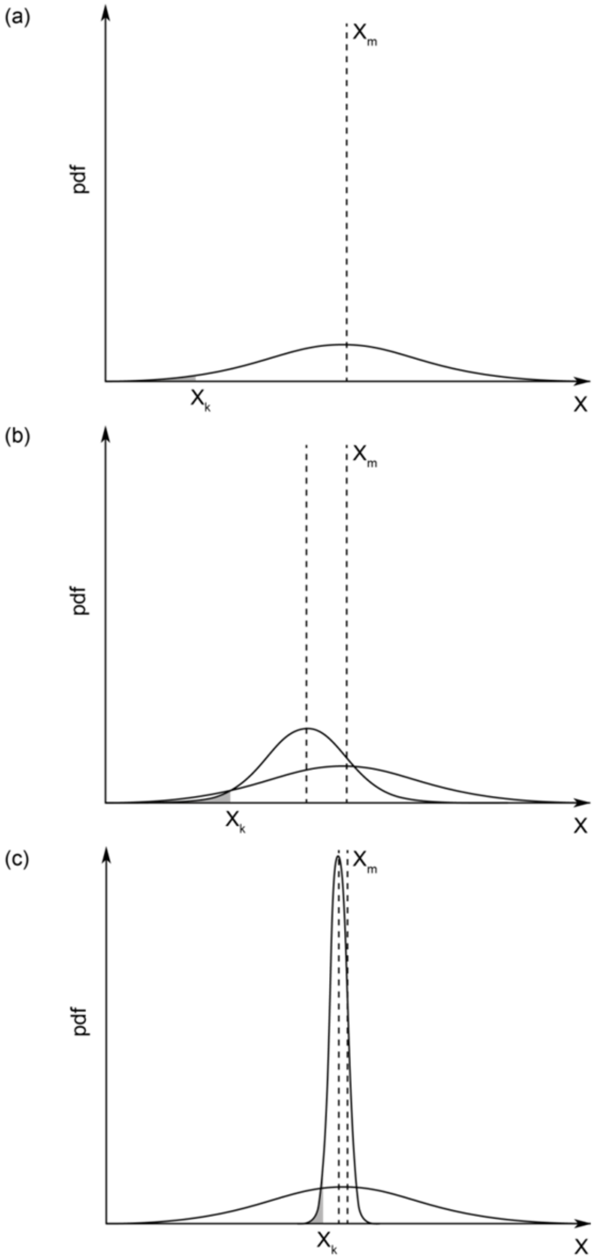


**Figure 1. Estimation of characteristic value and pdf (after Hicks, 2013): (a) $X_k$ based on underlying pdf (for large θ/D); (b) $X_k$ based on modified pdf (for intermediate θ/D); (c) $X_k$ based on modified pdf (for small θ/D)**



## REFERENCES

API American Petroleum Institute (2014), "Recommended Practice for Planning, Designing and Constructing Fixed Offshore Platforms - Working Stress Design", API Recommended Practice 2A-WSD (RP 2A-WSD), 22nd Edition.

API American Petroleum Institute (2011), "Geotechnical and Foundation Design Considerations: ISO 19901-4:2003 (Modified), Petroleum and Natural Gas Industries - Specific Requirements for Offshore Structures, Part 4 - Geotechnical and Foundation Design Considerations", ANSI/API RP 2GEO, First Edition (with addendum, 2014).

Baecher, G.B., and Christian, J.T. (2003), "Reliability and Statistics in Geotechnical Engineering", John Wiley and Sons, London and New York.

CEN European Committee for Standardization (2004), "Eurocode 7: Geotechnical Design - Part 1: General Rules", European Standard EN 1997-1:2004. (With Corrigendum EN 1997-1:2004/AC, February 2009).

CEN European Committee for Standardization (2007), "Eurocode 7 - Geotechnical Design – Part 2: Ground Investigation and Testing", European Standard EN 1997-2:2007. (With Corrigendum EN 1997-2:2007/AC, June 2010).

Hicks, M.A. (2013), "An Explanation of Characteristic Values of Soil Properties in Eurocode 7", in P. Arnold, G.A. Fenton, M.A. Hicks, T. Schweckendiek and B. Simpson (Eds.), Modern Geotechnical Design Codes of Practice: Implementation, Application and Practice. IOS Press, pp. 36-45.

ISO International Organization for Standardization (2015), "General Principles on Reliability for Structures", International Standard ISO 2394:2015.

ISO International Organization for Standardization (2003), "Petroleum and Natural Gas Industries - Specific Requirements for Offshore Structures - Part 4: Geotechnical and Foundation Design Considerations", International Standard ISO 19901-4:2003.

ISO International Organization for Standardization (2013), "Petroleum and Natural Gas Industries - General Requirements for Offshore Structures", International Standard ISO 19900:2013.

ISO International Organization for Standardization (2000), "Petroleum and Natural Gas Industries – Offshore Production Installations – Guidelines on Tools and Techniques for Hazard Identification and Risk Assessment", International Standard ISO 17776:2000.

Peuchen, J., Meijninger, B. and Drummen, T. (2015), "Reassessment of Geotechnical Conditions after an Offshore Well Incident", Proceedings of the XVI ECSMGE: Geotechnical Engineering for Infrastructure and Development, ICE Publishing, 2015, pp. 195-206.

| Symbol | Unit | Quantity |
|---|---|---|
| I - GENERAL | | |
| L | m | Length |
| B | m | Width |
| D | m | Diameter |
| d | m | Depth |
| h | m | Height or thickness |
| z | m | Penetration or depth below reference level (usually ground surface) |
| A | $m^2$ | Area |
| V | $m^3$ | Volume |
| W | kN | Weight |
| t | s | Time |
| v | m/s | Velocity |
| a | $m/s^2$ | Acceleration |
| g | $m/s^2$ | Acceleration due to gravity ($g = 9.81\ m/s^2$) |
| m | kg | Mass |
| $\rho$ | $kg/m^3$ | Density |
| $\pi$ | - | Mathematical constant (= 3.14159) |
| e | - | Base of natural logarithm (= 2.71828) |
| ln | - | Natural logarithm |
| log | - | Logarithm base 10 |
| II - STRESS AND STRAIN | | |
| $P_a$ | kPa | Atmospheric pressure |
| u | MPa | Pore water pressure |
| $u_o$ | MPa | Hydrostatic pore pressure relative to seafloor or phreatic surface |
| $\sigma$ | kPa | Total stress |
| $\sigma'$ | kPa | Effective stress |
| $\tau$ | kPa | Shear stress |
| t | kPa | Shear stress in s'-t space [= $(\sigma'_1 - \sigma'_3)/2$] or [= $(\sigma_1 - \sigma_3)/2$] |
| $\sigma_1,\sigma_2,\sigma_3$ | kPa | Principal stresses |
| $\sigma'_{ho}$ | kPa | Effective in situ horizontal stress |
| $\sigma_{vo}$ | kPa | Total in situ vertical stress relative to ground surface or phreatic surface |
| $\sigma'_{vo}$ | kPa | Effective in situ vertical stress (or $p'_o$) |
| $\sigma'_h$ | kPa | Effective horizontal stress |
| $\sigma'_v$ | kPa | Effective vertical stress |
| $r_u$ | - | Pore pressure ratio [= $u/\sigma_{vo}$] |
| p' | kPa | Mean effective stress [= $(\sigma'_1 + \sigma'_2 + \sigma'_3)/3$] |
| q | kPa | Principal deviator stress [= $\sigma'_1 - \sigma'_3$] or [= $\sigma_1 - \sigma_3$] |
| s' | kPa | Mean effective stress in s'-t space [= $(\sigma'_1 + \sigma'_3)/2$] |
| $\varepsilon$ | - | Linear strain |
| $\varepsilon_1,\varepsilon_2,\varepsilon_3$ | - | Principal strains |
| $\varepsilon_v$ | - | Volumetric strain |
| $\gamma$ | - | Shear strain |
| $\nu$ | - | Poisson's ratio |
| $\nu_u$ | - | Poisson's ratio for undrained stress change |
| $\nu_d$ | - | Poisson's ratio for drained stress change |
| E | MPa | Modulus of linear deformation (Young's modulus) |
| $E_u$ | MPa | Modulus of linear deformation (Young's modulus for undrained stress change) |
| $E_d$ | MPa | Modulus of linear deformation (Young's modulus for drained stress change) |
| G | MPa | Modulus of shear deformation (shear modulus) |
| $G_{max}$ | MPa | Shear modulus at small strain |
| $I_r$ | - | Rigidity index [= $G/\tau_{max}$ or $G/s_u$] |
| K | MPa | Modulus of compressibility (bulk modulus) |
| M | MPa | Constrained modulus [= $1/m_v$] |
| $\mu$ | - | Coefficient of friction |
| $\eta$ | kPa.s | Coefficient of viscosity |

| Symbol | Unit | Quantity |
|---|---|---|

III - PHYSICAL CHARACTERISTICS OF GROUND

**(a) Density and Unit weights**

| | | |
|---|---|---|
| $\gamma$ | kN/m$^3$ | Unit weight of ground (or bulk unit weight or total unit weight) |
| $\gamma_d$ | kN/m$^3$ | Unit weight of dry ground |
| $\gamma_s$ | kN/m$^3$ | Unit weight of solid particles |
| $\gamma_w$ | kN/m$^3$ | Unit weight of water |
| $\gamma_{pf}$ | kN/m$^3$ | Unit weight of pore fluid |
| $\gamma_{dmin}$ | kN/m$^3$ | Minimum index (dry) unit weight |
| $\gamma_{dmax}$ | kN/m$^3$ | Maximum index (dry) unit weight |
| $\gamma'$ or $\gamma_{sub}$ | kN/m$^3$ | Unit weight of submerged ground |
| $\rho$ | Mg/m$^3$ [= t/m$^3$] | Density of ground |
| $\rho_d$ | Mg/m$^3$ [= t/m$^3$] | Density of dry ground |
| $\rho_s$ | Mg/m$^3$ [= t/m$^3$] | Density of solid particles |
| $\rho_w$ | Mg/m$^3$ [= t/m$^3$] | Density of water |
| $D_r$ | -, % | Relative density [= $I_D = \gamma_{dmax} (\gamma_d - \gamma_{dmin})/\gamma_d(\gamma_{dmax} - \gamma_{dmin}) = (e_{max} - e)/(e_{max} - e_{min})$] |
| v | - | Specific volume [= 1+e] |
| e | - | Void ratio |
| $e_o$ | - | Initial void ratio |
| $e_{max}$ | - | Maximum index void ratio |
| $e_{min}$ | - | Minimum index void ratio |
| $I_D$ | -, % | Density index [= $D_r$] |
| $R_D$ | -, % | Dry density ratio [= $\gamma_d/\gamma_{dmax}$] |
| n | -, % | Porosity |
| w | % | Water content |
| $S_r$ | % | Degree of saturation |
| r | -, g/kg | Salinity of pore fluid [= ratio of mass of salt to mass of pore fluid] |
| R | g/l | Salinity of fluid [= ratio of mass of salt to volume of distilled water] |
| s | g/l | Salinity of fluid [= ratio of mass of salt to volume of fluid] |
| S | g/kg | Salinity of seawater [= ratio of mass of salt to mass of seawater] |

**(b) Consistency**

| | | |
|---|---|---|
| $w_L$ | % | Liquid limit |
| $w_P$ | % | Plastic limit |
| $I_P$ | % | Plasticity index [= $w_L - w_P$] |
| $I_L$ | % | Liquidity index [= $(w - w_P)/(w_L - w_P)$] |
| $I_C$ | % | Consistency index [= $(w_L - w)/(w_L - w_P)$] |
| A | -, % | Activity [= ratio of plasticity index to percentage by weight of clay-size particles] |

**(c) Particle size**

| | | |
|---|---|---|
| D | mm | Particle diameter |
| $D_n$ | mm | n percent diameter [n% < D] |
| $C_u$ | - | Uniformity coefficient [= $D_{60}/D_{10}$] |
| $C_c$ | - | Curvature coefficient [= $(D_{30})^2/D_{10}D_{60}$] |

**(d) Dynamic Properties**

| | | |
|---|---|---|
| $v_p$ | m/s | P-wave velocity (compression wave velocity) |
| $v_s$ | m/s | S-wave velocity (shear wave velocity) |
| $v_{s1}$ | m/s | S-wave velocity normalised to 100 kPa in situ vertical stress |
| D | -, % | Damping ratio of ground |

| Symbol | Unit | Quantity |
|---|---|---|

**(e) Hydraulic properties**

| | | |
|---|---|---|
| k | m/s | Coefficient of permeability |
| $k_v$ | m/s | Coefficient of vertical permeability |
| $k_h$ | m/s | Coefficient of horizontal permeability |
| i | - | Hydraulic gradient |

**(f) Thermal and Electrical properties**

| | | |
|---|---|---|
| T | °C | Temperature |
| k | W/(m·K) | Thermal conductivity |
| $a_L$ | 1/°C | Thermal expansion coefficient (linear) |
| $\alpha$ | $m^2/s$ | Thermal diffusion coefficient |
| $\rho$ | Ω.m | Electrical resistivity |
| K | S/m | Electrical conductivity |

**(g) Magnetic properties**

| | | |
|---|---|---|
| B | T | Magnetic flux density (or magnetic induction) |

**(h) Radioactive properties**

| | | |
|---|---|---|
| $\gamma$ | CPS | Natural gamma ray |

IV - MECHANICAL CHARACTERISTICS OF GROUND

**(a) Cone Penetration Test (CPT)**

| | | |
|---|---|---|
| $q_c$ | MPa | Cone resistance |
| $q_{c1}$ | MPa | Cone resistance normalised to 100 kPa effective in situ vertical stress |
| $f_s$ | MPa | Sleeve friction |
| $f_t$ | MPa | Sleeve friction corrected for pore pressures acting on the end areas of the friction sleeve |
| $R_f$ | % | Ratio of sleeve friction to cone resistance |
| $R_{ft}$ | % | Ratio of sleeve friction to corrected cone resistance ($f_s/q_t$ or $f_t/q_t$) |
| $u_1$ | MPa | Pore pressure at the face of the cone |
| $u_2$ | MPa | Pore pressure at the cylindrical extension above the base of the cone or in the gap between the friction sleeve and the cone |
| $u_2$* | MPa | Pore pressure $u_2$, but derived rather than measured |
| $u_3$ | MPa | Pore pressure immediately above the friction sleeve or in the gap above the friction sleeve |
| K | - | Adjustment factor for ratio of pore pressure at $u_1$ to $u_2$ location |
| $q_n$ | MPa | Net cone resistance |
| $q_t$ | MPa | Corrected cone resistance (or total cone resistance) |
| $B_q$ | - | Pore pressure ratio |
| $Q_t$ | - | Normalized cone resistance [= $q_n/\sigma'_{vo}$] |
| $Q_{tn}$ | - | Normalized cone resistance with variable stress exponent |
| $F_r$ | % | Normalized friction ratio [= $f_t/q_n$] |
| $N_c$ | - | Cone factor between $q_c$ and $s_u$ |
| $N_k$ | - | Cone factor between $q_n$ and $s_u$ |
| $I_c$ | - | Soil behaviour type index index (for $Q_{tn}$ and $F_r$) |
| $I_{SBT}$ | - | Soil behaviour type index (for $q_c$ and $R_f$) |

**(b) Standard Penetration Test (SPT)**

| | | |
|---|---|---|
| N | Blows/0.3 m | SPT blowcount |
| $N_{60}$ | Blows/0.3 m | SPT blowcount normalised to 60% energy |
| $N_{1,60}$ | Blows/0.3 m | SPT blowcount normalised to 60% energy and to 100 kPa effective in situ vertical stress |

| Symbol | Unit | Quantity |
|---|---|---|
| **(c) Strength of soil** | | |
| $s_u$ | kPa | Undrained shear strength (or $c_u$) |
| $s_u/\sigma'_{vo}$ | - | Undrained strength ratio |
| $\kappa$ | kPa/m | Rate of increase of undrained shear strength with depth (linear) |
| c' | kPa | Effective cohesion intercept |
| $\varphi'$ | °(deg) | Effective angle of internal friction |
| $\varphi'_{cv}$ | °(deg) | Effective angle of internal friction at large strain |
| $\varepsilon_{50}$ | % | Strain at 50% of peak deviator stress (or $\varepsilon_c$) |
| $E_{50}$ | MPa | Young's modulus at 50% of peak deviator stress |
| $s_{u;r}$ | kPa | Undrained shear strength of remoulded soil |
| $s_{u;ar}$ | kPa | Undrained shear strength of aged remoulded soil |
| $s_R$ | kPa | Undrained residual shear strength |
| $S_t$ | - | Sensitivity [= $s_u/s_{u;r}$ or $s_u/s_R$] |
| $T_x$ | - | Thixotropy strength ratio [$T_x(t) = s_{u;ar}(t)/s_{u;r}$] |
| $\sigma'_c$ | kPa | Effective consolidation pressure |
| M | - | Gradient of critical state line when projected onto a constant volume plane |
| A | - | Pore pressure coefficient for anisotropic pressure increment |
| B | - | Pore pressure coefficient for isotropic pressure increment |
| **(d) Strength of rock** | | |
| $I_{s(50)}$ | MPa | Point load strength index |
| $\sigma_c$ | MPa | Uni-axial compressive strength |
| **(e) Consolidation (one dimensional)** | | |
| $\sigma'_p$ | kPa | Effective preconsolidation pressure (or effective vertical yield stress in situ) |
| $\sigma^*_{ve}$ | kPa | Effective vertical stress on ICL at $e_0$ |
| $\sigma'_{vy}$ | kPa | Effective vertical yield stress in situ (or effective preconsolidation pressure) |
| $C_c$ | - | Compression index |
| $C^*_c$ | - | Intrinsic compression index [= $e^*_{100} - e^*_{1000}$] |
| $C_s$ | - | Swelling index (or re-compression) |
| CR | - | Primary compression ratio [= $C_c/(1+e_0)$] |
| RR | - | Recompression ratio [= $C_s/(1+e_0)$] |
| $e_0$ | - | Void ratio at $\sigma'_{vo}$ |
| $e_L$ | - | Void ratio at liquid limit $w_L$ |
| $e^*_{100}$ | - | Void ratio at $\sigma'_v$ = 100 kPa during one-dimensional intrinsic compression |
| $e^*_{1000}$ | - | Void ratio at $\sigma'_v$ = 1000 kPa during one-dimensional intrinsic compression |
| $C_\alpha$ | - | Coefficient of secondary compression (primary compression) |
| $C_{\alpha s}$ | - | Coefficient of secondary compression (swelling/re-compression) |
| $c_v$ | $m^2/s$ | Coefficient of consolidation |
| H | m | Drainage path length |
| ICL | - | Intrinsic compression line (Burland 1990) |
| $I_v$ | - | Void index [= $(e_0 - e^*_{100})/C^*_c$] |
| $m_v$ | $m^2/MN$ | Coefficient of volume compressibility |
| M | MPa | Constrained modulus [= $1/m_v$] |
| p | kPa | Vertical pressure |
| OCR | - | Overconsolidation ratio [= $\sigma'_p/\sigma'_{vo}$] |
| SCC | - | Sedimentation compression curve |
| SCL | - | Sedimentation compression line (Burland 1990) |
| $S_\sigma$ | - | Stress sensitivity [= $\sigma'_{vy}/\sigma^*_{ve}$] |
| YSR | - | Yield stress ratio [= $\sigma'_{vy}/\sigma'_{vo}$] |

V - GEOTECHNICAL DESIGN

### (a) Partial factors

| | | |
|---|---|---|
| $\gamma_d$ | - | Factor related to model uncertainty or other circumstances |
| $\gamma_f$ | - | Partial action factor (load factor) |
| $\gamma_m$ | - | Partial material factor (partial safety factor) |
| $\gamma_R$ | - | Partial resistance factor (partial safety factor) |

### (b) Seismicity

| | | |
|---|---|---|
| $a_g$ | $m/s^2$ | Effective peak ground acceleration (design ground acceleration) |
| $d_g$ | m | Peak ground displacement |
| $\alpha$ | - | Acceleration ratio [= $a_g/g$] |
| $\tau_c$ | kPa | Seismic shear stress |

### (c) Compaction

| | | |
|---|---|---|
| $\rho_{dmax}$ | $Mg/m^3$ [= $t/m^3$] | Maximum dry density |
| $\rho_{max}$ | $Mg/m^3$ [= $t/m^3$] | Maximum density |
| $w_{opt}$ | % | Optimum moisture content |

### (d) Earth pressure

| | | |
|---|---|---|
| $\delta$ | °(deg) | Angle of interface friction (between ground and foundation) |
| K | - | Coefficient of lateral earth pressure |
| $K_a$ | - | Coefficient of active earth pressure |
| $K_{ac}$ | - | Coefficient of active earth pressure for total stress analysis |
| $K_p$ | - | Coefficient of passive earth pressure |
| $K_{pc}$ | - | Coefficient of passive earth pressure for total stress analysis |
| $K_o$ | - | Coefficient of earth pressure at rest |
| $K_{onc}$ | - | $K_o$ for normally consolidated soil |
| $K_{ooc}$ | - | $K_o$ for overconsolidated soil |

### (e) Foundations

| | | |
|---|---|---|
| A | $m^2$ | Total foundation area |
| A' | $m^2$ | Effective foundation area |
| B' | m | Effective width of foundation |
| $E_s$ | $MN/m^3$ | Modulus of subgrade reaction |
| k | MPa/m | Rate of change of modulus of subgrade reaction $E_s$ with depth z |
| L' | m | Effective length of foundation |
| H | MN | Horizontal external force or action |
| V | MN | Vertical external force or action |
| M | MN.m | External moment |
| T | MN.m | External torsion moment |
| Q | MN | Total vertical resistance of a foundation/pile |
| $Q_p$ | MN | End-bearing of pile |
| $Q_s$ | MN | Shaft resistance of pile |
| $q_p$ | MPa | Unit end-bearing |
| $q_{lim}$ | MPa | Limit unit end-bearing |
| f | kPa | Unit skin friction (or $q_s$) |
| $f_{lim}$ | kPa | Limit unit skin friction |
| p | MN/m | Lateral resistance per unit length of pile |
| $p_{lim}$ | MN/m | Limit lateral resistance per unit length of pile |
| s | m | Settlement |
| t | MN/m | Skin friction per unit length of pile |
| y | mm | Lateral pile deflection |
| z | mm | Axial pile displacement |
| $\alpha$ | - | Adhesion factor between ground and foundation (= $f/s_u$) |
| $\beta$ | - | Adhesion factor between ground and foundation (= $f/\sigma'_v$ or $f/\sigma'_{vo}$) |

| Symbol | Unit | Quantity |
|---|---|---|
| $\delta$ | °(deg) | Angle of interface friction (between ground and foundation) |
| $\delta_{cv}$ | °(deg) | Constant volume or critical-state angle of interface friction (between ground and foundation) |
| $N_c, N_q, N_\gamma$ | - | Bearing capacity factors |
| $K_c, K_q, K_\gamma$ | - | Bearing capacity correction factors for inclined forces or actions, foundation shape and depth of embedment |
| $i_c, i_q, i_\gamma$ | - | Bearing capacity correction factors for external force inclined from vertical shape |
| $s_c, s_q, s_\gamma$ | - | Bearing capacity correction factors for foundation shape |
| $d_c, d_q, d_\gamma$ | - | Bearing capacity correction factors for foundation embedment |

**Signs**:
- A "prime" applies to effective stress.
- A "bar" above a symbol relates to average properties.
- A "dot" above a symbol denotes derivative with respect to time.
- The prefix "$\Delta$" denotes an increment or a change.
- A “star” after a symbol denotes value corrected for pore fluid salinity.

BIBLIOGRAPHY

Burland, J.B. (1990), “On the Compressibility and Shear Strength of Natural Clays”, Géotechnique, Vol. 40, No. 3, pp. 329-378.

CEN European Committee for Standardization (2004), "Eurocode 7: Geotechnical Design - Part 1: General Rules", European Standard EN 1997-1:2004.

CEN European Committee for Standardization (2007), “Eurocode 7 - Geotechnical Design – Part 2: Ground Investigation and Testing”, European Standard EN 1997-2:2007 and Corrigenda.

DNV Det Norske Veritas (1992), “Foundations”, Classification Notes No. 30.4.

ISO International Organization for Standardization (2013), “Petroleum and Natural Gas Industries - General Requirements for Offshore Structures”, International Standard ISO 19900:2013.

ISO International Organization for Standardization (2003), "Petroleum and Natural Gas Industries - Specific Requirements for Offshore Structures - Part 4: Geotechnical and Foundation Design Considerations", International Standard ISO 19901-4:2003.

ISO International Organization for Standardization (2004), "Geotechnical Investigation and Testing - Identification and Classification of Soil - Part 2: Principles for a Classification", International Standard ISO 14688-2:2004.

ISSMFE Subcommittee on Symbols, Units, Definitions (1978), “List of Symbols, Units and Definitions”, in Proceedings of the Ninth International Conference on Soil Mechanics and Foundation Engineering, 1977, Tokyo, Vol. 3, Japanese Society of Soil Mechanics and Foundation Engineering, Tokyo, pp. 156-170.

ISRM Commission on Terminology, Symbols and Graphic Representation (1970), "List of Symbols”.

Noorany, I. (1984), “Phase Relations in Marine Soils”, ASCE Journal of Geotechnical Engineering, Vol. 110, No. 4, pp. 539-543.

ISSUE 43

Contacts
Netherlands Enterprise Agency (RVO.nl)
Croeselaan 15 | 3521 BJ | Utrecht
P.O. Box 8242 | 3503 RE | Utrecht
www.rvo.nl / http://english.rvo.nl

Netherlands Enterprise Agency (RVO.nl) | January 2016